- **Applications for Waterwells, Monitoring Wells, Mining Boreholes, Geotechnical Boreholes, and Oil and Gas Recovery Wells**

- **Direct and Reverse Circulation**

- **Shallow and Deep Drilling Operations**

Air and Gas Drilling Manual

William C. Lyons / Bayum Guo
Frank A. Seidel

AIR AND GAS DRILLING MANUAL

This page intentionally left blank.

AIR AND GAS DRILLING MANUAL
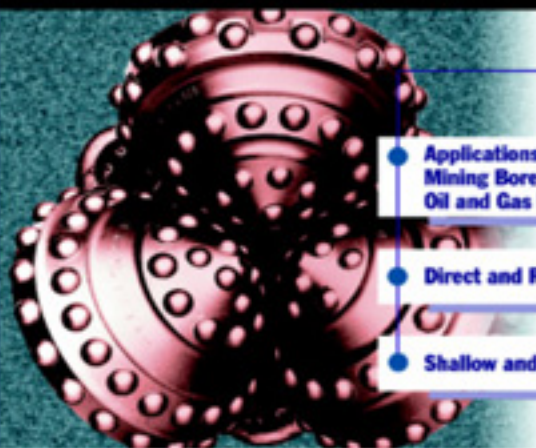
Engineering Applications for Water Wells, Monitoring Wells, Mining Boreholes, Geotechnical Boreholes, and Oil and Gas Recovery Wells

Second Edition

William C. Lyons, Ph.D., P.E.
New Mexico Institute of Mining and Technology
Socorro, New Mexico

Boyun Guo, Ph.D.
University of Louisiana
Lafayette, Louisiana

Frank A. Seidel, B.S.
Burlington Resources
Farmington, New Mexico

McGraw-Hill

A Division of The McGraw-Hill Companies

All trademarks are trademarks of their respective owners. Rather than put a trademark symbol after every occurrence of a trademarked name, we use names in an editorial fashion only, and to the benefit of the trademark owner, with no intention of infringement of the trademark. Where such designations appear in this book, they have been printed with initial caps.

McGraw-Hill eBooks are available at special quantity discounts to use as premiums and sales promotions, or for use in corporate training programs. For more information, please contact George Hoare, Special Sales, at george_hoare@mcgraw-hill.com or (212) 904-4069.

This page intentionally left blank.

Contents

This page intentionally left blank.

Preface

This is the second edition of the *Air and Gas Drilling Manual*. The first edition of this book was published in 1984 by Gulf Publishing company of Houston, Texas. The first edition of the book was written primarily for the oil and gas recovery drilling industry. This first edition had moderate success and was sold out of the initial printing by the late 1980's. However, in the early 1990's underbalanced drilling became an important technology for oil and gas recovery drilling and completions. Also, at about this same time air and gas drilling technology became an important environmental tool for monitoring and cleanup operations. These events have prompted our effort to create the second edition of the *Air and Gas Drilling Manual*.

The second edition of the *Air and Gas Drilling Manual* is written as an engineering practice book for engineers and earth scientists who are engaged in planning and carrying out shallow and deep air and gas drilling operations. The first objective of this book is to give engineers and earth scientists general knowledge of air and gas drilling operations and a calculation methodology that can be used for planning future operations. Also the results of this methodology can be used to assist in carrying out a successful drilling operation. The book contains many illustrative examples that demonstrate the calculation methodology. The calculations are easily understood by any technically trained individual with a basic understanding of rotary drilling. The basic equations are derived and presented for use in both the English units and in SI units.

This book is an excellent companion for two popular drilling specialty books already in the market today. For those engineers and scientists interested in shallow direct and reverse circulation drilling, this book describes the detailed calculations required to support the equipment and field techniques given in the *Handbook of Ground Water Development* by the Roscoe Moss Company (a John Wiley Publication). Likewise, for those engineers interested in deep underbalanced direct circulation drilling, this book describes the detailed calculations required to support the equipment and field techniques given in the *Underbalanced Drilling Manual* (a Gas Research Institute publication).

This book covers both direct and reverse circulation operations. Also, the book covers all aspects of air and gas drilling technology (i.e., air or gas drilling, aerated fluids drilling, and stable foam drilling). The secondary objective of this text is to give oil and gas recovery drilling engineers knowledge of some important technologies that have been used for decades in shallow drilling operations.

vii

Likewise, it is to give shallow drilling operations engineers and scientists knowledge of some important technologies used in deep drilling operations.

The original illustrative example calculations have been carried using the commercial software package MathCad. The authors feel this software provided a very convenient calculation vehicle for demonstrating the solution techniques. However, there are a several other commercial software packages that can accomplish these solutions (e.g., MS Excel, MatLab).

The preparation of this book has been underway since 1997 and has required the cooperation of engineers and scientists in many operating and service companies. Specifically, the authors would like to especially thank the management and personnel of San Juan Division of Burlington Resources, Phillips Petroleum Company, OXY USA, Chevron USA, Patterson Resources, Oil Tools International, Mountain Air Drilling, Symbol Incorporated, and MI Air Drilling.

There were many individual who assisted in the preparation of this book. Much of the art work used in this book was prepared by Anna Edwards, Ann Gardner, and Georgia Eaton. Many of the figures and tables were prepared by Tanya Cases, Adrienne Garcia, Ryan Robinson, and Julie Seaman. Many of the illustrative example calculations were carried out by Dr. Lyons' students at the New Mexico Institute of Mining and Technology. In particular, we would like to thank Heru Danardatu who assisted in preparing many of the most difficult calculations.

The draft manuscript was read by three engineering graduates from the New Mexico Institute of Mining and Technology who have been in industry or practice for the past two decades. These individuals were Allen Hains, Chris Russell, and Robert Schwering. These individuals gave the authors many important and valuable suggestions. The authors would like to give our very special thanks to Laurie Barr who was willing to read the initial drafts of nearly all of chapters in the manuscript. She had to suffer through the many spelling and grammatical errors that the three engineer authors made during the initial preparation.

The authors would like to thank the editors and staff at McGraw-Hill Company and especially Sponsoring Editors Ken McCombs and Bob Esposito for their encouragement and assistance during the preparation of this manuscript and Senior Editing Supervisor Frank Kotowski Jr. for his expert conversion of the manuscript into this book.

The authors would like to encourage comments on the book from engineers and scientists in industry and practice. We also apologize for any errors that might be still lurking in the manuscript. We know our book is not perfect, but we also know that this edition is completed.

William C. Lyons
Boyun Guo
Frank A. Seidel

List of Symbols

a = eccentricity, ft

a_a = constant

A_b = cross-sectional area of the inside of the blooey line, ft^2

A_{bi} = cross-sectional area of the single drill bit orifice, ft^2

A_{dci} = cross-sectional area of inside of the drill collars, ft^2

a_i = constant

A_n = total cross-sectional area of flow through drill bit nozzles, ft^2

A_o = total cross-sectional area of flow through the drill bit open orifices, ft^2

A_{tn} = total nozzle flow area, ft^2

c = clearance volume ratio

C = fluid flow loss coefficient for drill bit orifices or nozzles

D = inside diameter (or hydraulic diameter) of the pressure conduit, ft

$dı$ = inside diameter of drill pipe body lumped geometry in openhole section, in

$Dı$ = inside diameter of drill pipe body lumped geometry in openhole section, ft

d_1 = outer diameter of the rotary cylinder, ft

d_2 = inside diameter of the cylindrical housing, ft

D_{ani} = annulus inside diameter, ft

d_{ani} = annulus inside diameter, in

D_{ano} = annulus outside diameter, ft

d_{ano} = annulus outside diameter, in

d_b	= inside diameter of blooey line, in
D_b	= inside diameter of the blooey line, ft
D_{bi}	= drill bit single orifice diameter, ft
D_c	= approximate diameter of the rock cutting particle, ft (m)
d_c	= inside diameter of the casing at the tope of the well, in
D_{cl}	= diameter to the centerline of the nozzles, ft
d_{cl}	= diameter to the centerline of the nozzles, in
D_e	= equivalent single orifice inside diameter, ft
d_h	= drill bit diameter, in
D_h	= inside diameter of the borehole, ft
D_{hy}	= hydraulic diameter for annular cross-section, ft
D_{io}	= inside diameter of the outer tube of the dual wall pipe, ft
D_n	= inside diameter of each nozzle, ft
d_n	= inside diameter of each nozzle, in
D_o	= inside diameter of open orifices, ft
d_o	= inside diameter of open orifices, in
D_{oi}	= outside diameter of the innertube of the dual wall pipe, ft
D_{op}	= diameter of open orifice, ft
d_{op}	= diameter of open orifice, in
D_p	= outside diameter of the drill pipe, ft
d_p	= outside diameter of the drill pipe, in
D_{pp}	= inside diameter of air hammer bit passage, ft
d_{pp}	= inside diameter of air hammer bit passage, in
D_{sp}	= inside diameter of shank passage, ft
d_{sp}	= inside diameter of shank passage, in
D_{sp}	= inside diameter of the drive shaft passage, ft
d_{sp}	= inside diameter of the drive shaft passage, in
D_{sr}	= inside diameter of the surface return flow line, ft
e_{av}	= average absolute surface roughness, ft

e_{avo}	= average absolute surface roughness of the annulus, ft
e_{oh}	= openhole outer wall absolute surface roughness, ft
e_p	= absolute surface roughness of commercial pipe, 0.00015 ft
f	= Fanning friction factor
F	= axial tension force (or load), lb
F_a	= maximum allowable design axial tension force, lb
f_{ac}	= Fanning friction factor for flow in the cased section of the annulus
f_b	= Fanning friction factor for the blooey line
F_c	= hoisting capacity of rotary drill rig, lb
FS	= factor of safety
f_{sr}	= Fanning friction factor for flow in the surface return flow line
F_y	= drill pipe tension force to produce material yield, lb
g	= acceleration of gravity, 32.2 ft/sec^2
H	= total depth of borehole, ft
h	= reference depth, ft
HP_b	= drive shaft horsepower developed at any drive shaft speed, hp
k	= ratio of specific heats for the gas (for air $k = 1.4$ and for natural gas $k = 1.28$)
K_a	= average drilling rate, ft/hr
K_b	= buoyancy factor
KE	= kinetic energy per unit volume, ft-lb/ft^3
KE_a	= kinetic energy per unit volume for air drilling, ft-lb/ft^3
KE_{ai}	= kinetic energy per unit volume of the gas above the drill bit inside the drill pipe, ft-lb/ft^3
KE_{bh}	= kinetic energy per unit volume at the bottom of the borehole in the annulus, ft-lb/ft^3
KE_m	= kinetic energy per unit volume for drilling mud, ft-lb/ft^3
KE_{sfake}	= kinetic energy per unit volume in the annulus, ft-lb/ft^3
K_t	= minor loss factor for the T turn at the top of the annulus

K_{Tee} = minor loss flow resistance coefficient for the Tee

K_v = minor loss factor for the valves in the blooey line

L = length of a cubic foot of the compressed air in the drill collars prior to
the stop, ft

l = length of the cylinder, ft

L_{anp} = length of the annulus passage, ft

l_{anp} = length of the annulus passage, in

L_b = length of the blooey line, ft

L_c = length of drill collars, ft

L_d = nozzle depth along the periphery of the stator, ft

l_d = nozzle depth along the periphery of the stator, in

ln = exponential logarithm

log = natural logarithm

L_{op} = length of orifice passages, ft

l_{op} = length of orifice passages, in

L_p = length of drill pipe, ft

L_{pp} = length of piston passages, ft

l_{pp} = length of piston passages, in

L_{sp} = length of shank passage, ft

l_{sp} = length of shank passage, in

L_{sp} = length of the drive shaft passage, ft

l_{sp} = length of the drive shaft passage, in

L_{sr} = length of the surface return flow line, ft

L_t = nozzle throat opening, ft

l_t = nozzle throat opening, in

m = number of vanes

MOP = margin of overpull

m_w = mole weight of gas, lb/lb-mole

N = drill string (drill bit) speed, rpm

n	= number of equal diameter orifices
N_m	= drill bit speed of the motor, rpm
N_p	= estimated number of piston cycles, strike/minute
$\mathbf{N_R}$	= classic expression for Reynolds number
N_{rb}	= runaway speed of the drive shaft, rpm
$\mathbf{N_{Rl}}$	= Reynolds number for the volumetric flow rate derived for the laminar flow terminal velocity equation
N_{rr}	= theoretical runaway speed of the rotor, rpm
$\mathbf{N_{Rsfa}}$	= Reynolds number of foam exiting the cased annulus and starts into the Tee
$\mathbf{N_{Rsfbp}}$	= Reynolds number of foam flow upstream of the back pressure valve
$\mathbf{N_{Rsr}}$	= Reynolds number of the aerated drilling fluid exiting the surface return flow line
n_s	= number of compression stages in the multistage compressor
P	= fluid pressure, lb/ft^2 abs
P_{ac}	= pressure in the annulus at the bottom of the cased section of the borehole, lb/ft^2
p_{ac}	= pressure in the annulus at the bottom of the cased section of the borehole, psia
P_{ai}	= pressure above the bit inside the drill string, lb/ft^2 abs
P_{am}	= pressure above the motor cavity, lb/ft^2 abs
p_{am}	= pressure above the motor cavity, psia
P_{at}	= atmospheric pressure, lb/ft^2 abs
p_{at}	= atmospheric pressure, psia
P_{bca}	= pressure at bottom of casing in annulus, lb/ft^2 abs
P_{bdca}	= pressure at bottom of drill collars in the annulus, lb/ft^2 abs
P_{bdci}	= pressure at bottom of drill collars inside the drill string, lb/ft^2 abs
P_{bdpa}	= pressure at bottom of drill pipe in annulus, lb/ft^2 abs
P_{bdpi}	= pressure at the bottom of drill pipe inside the drill string, lb/ft^2 abs
P_{bh}	= bottomhole pressure in the annulus, lb/ft^2 abs

P_{bm} = pressure at the bottom of the motor cavity, lb/ft^2 abs

p_{bm} = pressure at the bottom of the motor cavity, psia

P_{bp} = back pressure, lb/ft^2 abs

p_{bp} = back pressure, psia

P_{cdci} = pressure due to the stop action of the air hammer, lb/ft^2 abs

p_{cdci} = pressure due to the stop action of the air hammer, psia

p_{d2} = approximated derated output pressure, psia

P_e = pressure at top of the annulus, lb/ft^2 abs

P_g = gas pressure, lb/ft^2 abs

p_i = input pressure, psia

P_i = pressure entering the first stage of the compressor, lb/ft^2 abs (N/m^2 abs)

P_{iab} = pressure inside drill bit above the nozzles, lb/ft^2 abs

p_{iab} = pressure inside drill bit above the nozzles, psia

P_{ias} = pressure above the turbine stator, lb/ft^2 abs

p_{ias} = pressure above the turbine stator, psia

P_{in} = injection pressure, lb/ft^2 abs

P_{mav} = average pressure in the motor, lb/ft^2 abs

p_{mav} = average pressure in the motor, psia

p_o = output pressure, psia

P_o = pressure exiting the last stage of the compressor, lb/ft^2 abs (N/m^2 abs)

P_{pl} = pipeline pressure, lb/ft^2 abs

p_{pl} = pipeline pressure, psia

PR = power ratio

p_r = reference atmospheric pressure, psia

P_s = surface pressure at the top of the annulus, lb/ft^2 abs

p_{sat} = saturation pressure of air at the annulus bottomhole conditions, psia

p_{sr} = pressure at the entrance end of the line, psia

P_{sr} = pressure at the entrance of the surface return flow line, lb/ft^2 abs

p_{Tee} = pressure upstream of the Tee at the top of the annulus, psia

P_{Tee}	= pressure upstream of the Tee at the top of the annulus, lb/ft^2 abs
Pv	= flow work, ft-lb/lb
Q_{ai}	= volumetric flow rate of the gas above the drill bit inside the drill pipe, ft^3/sec
Q_{bh}	= volumetric flow rate of the gas at the bottom of the borehole in the annulus, ft^3/sec
q_f	= total volume of fuel consumption rate, gal/hr
q_{fw}	= approximate volumetric flow rate of formation water, gal/hr (bbl/hr)
Q_g	= gas volumetric flow rate, ft^3/sec
Q_{ga}	= volumetric flow rate of gas exiting the cased annulus and starts into the Tee, ft^3/sec
Q_{gbh}	= volumetric flow rate of the gas at the bottomhole pressure and temperature conditions, ft^3/sec
q_i	= input volumetric flow rate, ft^3/min
Q_i	= volumetric flow rate entering the first stage of the compressor, ft^3/sec (m^3/sec)
q_{iw}	= flow rate of injected water, gal/hr
Q_m	= volumetric flow rate of drilling mud, ft^3/sec
Q_{mav}	= average volumetric flow rate of air through the motor cavity, ft^3/sec
q_{mav}	= average volumetric flow rate of air through the motor cavity, gal/min
q_s	= volumetric flow rate, cfm
Q_w	= volumetric flow rate of water, ft^3/sec
q_w	= volumetric flow rate of water, gal/min
R	= gas constant for API standard dry air, 53.36 ft-lb/lb-°R
R$_a$	= gas constant for API standard dry air, 53.36 ft-lb/lb-°R
r_c	= total fixed compression ratio across two stage compressor
r_s	= compression ratios for each stage
r_{sb}	= first stage compressor ratio
r_{sp}	= fixed compression ratio for single-stage primary

r_{st}	= fixed compression ratio
$\mathbf{R_u}$	= universal gas constant, 1,545.4 ft-lb/lb-mole-°R
s	= displacement, in^3
S_g	= specific gravity of the particular gas used
S_s	= specific gravity of the solid rock cuttings
S_{wf}	= specific gravity of the formation water
T	= absolute temperature at any position in the annulus, °R
T	= applied torque to the top of the drill string, ft-lb
t	= vane thickness, ft
T_{at}	= absolute atmospheric temperature, °R
t_{at}	= atmospheric temperature, °F
T_{av}	= average temperature of the borehole over the depth interval, °R
T_{avc}	= average absolute over the depth to the bottom of the cased section of the borehole, °R
T_{avo}	= average temperature of the openhole section of the borehole, °R
T_{bh}	= bottomhole temperature, R
T_c	= absolute temperature at the bottom of the casing, °R
T_g	= absolute gas temperature, °R
t_h	= geothermal temperature at depth, °F
T_i	= input gas temperature, °R (K)
$Torque_b$	= torque developed by the motor at any drive shaft speed, ft-lb
$Torque_{sb}$	= stall torque of the drive shaft, ft-lb
$Torque_{sr}$	= stall torque of the turbine motor, ft-lb
T_{pl}	= absolute pipeline temperature, °R
t_{pl}	= pipeline temperature, °F
T_r	= absolute reference temperature, °R
t_r	= reference temperature, °F
V	= average velocity in the annulus, ft/sec

V_{ai} = velocity of the gas above the drill bit inside the drill pipe, ft/sec

V_{bh} = velocity of the gas at the bottom of the borehole in the annulus, ft/sec

V_c = critical concentration velocity, ft/sec

V_{dci} = approximate velocity of compressed air inside the drill collars, ft/sec

V_f = average velocity of the fluid, ft/sec

V_{ml} = total velocity of the fluid, ft/sec

V_n = velocity of the gas exiting the nozzle, ft/sec

Vol_c = compressed volume of the compressed air in the drill collars after the stop, ft^3

V_{sfa} = average velocity of foam exiting the cased annulus and starts into the Tee, ft/sec

V_{sfake} = average velocity of foam above the drill collar annulus section flowing around the drill pipe body, ft/sec

V_{sfbp} = average velocity of foam upstream of the back pressure valve, ft/sec

V_{sr} = average velocity of the aerated drilling fluid exiting the end of the surface return flow line, ft/sec

V_t = terminal velocity of the rock cuttings particle, ft/sec

V_{Tee} = approximate velocity of foam flow downstream of the Tee and valves, ft/sec

V_{tl} = terminal velocity for laminar flow conditions, ft/sec

w_c = weight per unit length of drill collars, lb/ft

w_p = weight per unit length of drill pipe, lb/ft

$\dot{w}$ = weigh rate of flow through the compressor, lb/sec (N/sec)

$\dot{w}_f$ = total weight of fuel consumption per hour, lb/hr

$\dot{w}_{fw}$ = weight rate of flow of formation water, lb/sec

$\dot{w}_g$ = weigh rate of flow of the gas, lb/sec

$\dot{w}_{iw}$ = weight rate of flow of injected water , lb/sec

$\dot{w}_m$ = weight rate of flow of drilling mud, lb/sec

$\dot{w}_s$ = weight rate of flow of rock cuttings solids, lb/sec

$\dot{w}_t$ = total weigh rate of flow, lb/sec

$\dot{w}_w$ = weight rate of flow of the incompressible fluid, lb/sec

$\dot{W}_{as}$ = actual shaft power, hp

$\dot{W}_{asb}$ = actual shaft horsepower required by each compressor, hp

$\dot{W}_{asp}$ = actual shaft horsepower, hp

$\dot{W}_{ast}$ = total actual shaft horsepower needed by the combined primary and booster compressor system, hp

$\dot{W}_i$ = derated input horsepower available, hp

$\dot{W}_s$ = time rate of shaft work done, ft-lb/sec

$\dot{W}_{sb}$ = theoretical shaft horsepower required by this compressor, hp

$\dot{W}_{sp}$ = theoretical shaft horsepower required by the primary compressor, hp

$\dot{W}_t$ = total actual shaft horsepower by both the compressor and the hydraulic pump, hp

$\dot{W}_{td}$ = horsepower required at the top drive system, hp

Ws = total shaft work, ft-lb/lb

β = geothermal gradient constant, °F/ft

ΔL_c = distance the air flow is compressed inside the drill collars above the hammer, ft

ΔP_b = pressure change through the drill bit, lb/ft^2

ΔP_{Tee} = approximate pressure change through two valves and Tee, lb/ft^2

ε_m = mechanical efficiency

ε_v = volumetric efficiency

Γ	= foam quality
Γ_{bh}	= foam quality at the bottom of the annulus
Γ_{bp}	= foam quality at the top of the annulus upstream from the back pressure valve
Γ_{sfa}	= foam quality exiting the cased annulus and starts into the Tee
Γ_{sfbh}	= foam quality at the bottom of the annulus
γ	= specific weigh of the, lb/ft^3
γ_{ah}	= approximate specific weigh of air inside the drill collars entering the air hammer, lb/ft^3
γ_{ai}	= specific weight of air above the drill bit inside the drill pipe, lb/ft^3
γ_{bh}	= specific weight of the air at bottomhole pressure and temperature conditions, lb/ft^3
γ_{bp}	= specific weigh of the gas (air) upstream of the back pressure valve, lb/ft^3
γ_{cdci}	= new specific weight of compressed air in the drill collars, lb/ft^3
γ_f	= specific weight of the incompressible drilling fluid, lb/ft^3 (N/m^3)
γ_g	= specific weight of the gas, lb/ft^3
γ_{ga}	= approximate specific weight of gas exiting the cased annulus and starts into the Tee, lb/ft^3
γ_{gi}	= specific weight of gas entering the drill string, lb/ft^3
γ_m	= specific weigh of the drilling mud (fluid), lb/ft^3
γ_{mav}	= average specific weight of air in the motor cavity, lb/ft^3
γ_{mix}	= specific weight of the mixture of air (or other gas), incompressible fluid, and rock cuttings, lb/ft^3
γ_{mixai}	= mixture specific weight above the drill bit inside the drill string, lb/ft^3
γ_{mixbh}	= mixture specific weight at the bottom of the annulus, lb/ft^3
γ_s	= specific weight of the solid rock cuttings, lb/ft^3 (N/m^3)

γ_{sfa} = specific weigh of foam exiting the cased annulus and starts into the Tee, lb/ft^3

γ_{sfbp} = specific weigh of foam upstream of the back pressure valve, lb/ft^3

γ_{Tee} = approximate specific weight at the Tee, lb/ft^3

γ_w = specific weight of the incompressible fluid, lb/ft^3

κ = penetration rate, ft/sec

κ_{max} = actual sustainable maximum drilling rate, ft/hr

μ_e = effective absolute viscosity, lb-sec/ft^2 (n-sec/m^2)

μ_g = absolute viscosity of the air at atmospheric conditions, lb-sec/ft^2

μ_m = absolute viscosity of the drilling mud, cps

μ_{mp} = absolute plastic viscosity of the drilling mud, lb-sec/ft^2

μ_{sf} = absolute viscosity of the stable foam, lb-sec/ft^2

μ_{sfa} = absolute viscosity of foam exiting the cased annulus and starts into the Tee, lb-sec/ft^2

μ_{sfbp} = absolute viscosity of the foam just upstream of the back pressure valve, lb-sec/ft^2

μ_w = absolute viscosity of the water (and surfactant), lb-sec/ft^2

v = kinematic viscosity of the drilling fluid, ft^2/sec

v_{avi} = kinematic viscosity of mixture entering the drill string, ft^2/sec

v_{el} = effective kinematic viscosity for laminar conditions, ft^2/sec

v_g = kinematic viscosity of the gas, ft^2/sec

v_{gi} = kinematic viscosity of gas entering the drill string, ft^2/sec

v_m = kinematic viscosity of the drilling mud, ft^2/sec

v_{sfa} = kinematic viscosity of foam exiting the cased annulus and starts into the Tee, ft^2/sec

v_{sfbp} = kinematic viscosity of foam upstream of the back pressure valve, ft^2/sec

v_{sr} = average kinematic viscosity at the exit end of the surface return flow line, ft^2/sec

v_w = kinematic viscosity of he incompressible fluid, ft^2/sec

ρ_g = density of the gas, lb-sec^2/ft^4

ρ_{gi} = density of gas entering the drill string, lb-sec^2/ft^4

ρ_m = drilling mud density, lb-sec^2/ft^4 (slugs/ft^3)

ρ_{mixbh} = density of the stable foam at eh bottomhole pressure and temperature, lb-sec^2/ft^4

ρ_{sfa} = density of foam exiting the case annulus and starts into the Tee, lb-sec^2/ft^4

ρ_{sfake} = density of foam in the annulus, lb-sec^2/ft^4

ρ_{sfbp} = density of foam upstream of the back pressure valve, lb-sec^2/ft^4

ρ_w = density of incompressible fluid, lb-sec^2/ft^4

τ_p = period of a single cycle of the piston, sec

This page intentionally left blank.

List of Abbreviations

°C	= degrees Celsius		gals	= gallons
°F	= degrees Fahrenheit		Hg	= mercury
°F/ft	= degrees Fahrenheit per foot		IADC	= International Association of Drilling Contractors
°R	= degrees Rankin		ID	= inside diameter
acfm	= actual cubic feet per minute		in	= inch or inches
acfm	= actual cubic feet per minute		KE	= kinetic energy per unit volume
AISI	= American Iron and Steel Institute		KOP	= kick off point
API	= American Petroleum Institute		lb/ft	= pounds per foot
ASME	= American Society of Mechanical Engineers		lb/ft^2, abs	= pounds per square foot, absolute
bbl/hr	= barrels per hour		lb/ft^3	= pounds per cubic foot
BHA	= bottomhole assembly		lb/gal	= pounds per gallon
BOP	= blowout preventor		lb/hp-hr	= pounds per horsepower hour
cfm	= cubic feet per minute		lb/lb-mole	= pounds per pounds mole
cps	= centipoises		lb/sec	= pounds per second
dP	= differential pressure		lbs	= pounds
DTH	= down the hole		$lb\text{-}sec/ft^2$	= pound seconds per square foot
EU	= external upset		m/hr	= meters per hour
FS	= factor of safety		m/sec	= meters per second
ft	= foot or feet		m^3/sec	= cubic meters per second
ft/hr	= feet per hour		Max.	= maximum
ft/lb	= foot pounds		Min.	= minimum
ft/sec	= feet per second		mm	= millimeters
ft^2/sec	= square feet per second		MOP	= margin-of-overpull
ft^3/min	= cubic feet per minute		MWD	= measure-while-drilling
ft^3/sec	= cubic feet per second		N/m^2, abs	= newtons per square meter, absolute
$ft\text{-}lb/ft^3$	= foot pounds per cubic foot		N/m^3	= Newton per cubic meter
ft-lb/lb	= foot pounds per pound		$N\text{-}sec/m^2$	= Newton seconds per square meter
ft-lb/lb-°R	= foot pounds per pounds degrees Rankin		OD	= outside diameter
ft-lb/sec	= foot pounds per second		PDC	= polycrystalline diamond compact
gal/bbl	= gallons per barrel			
gal/hr	= gallons per hour			
gal/min	= gallons per minute			

ppg	= pounds per gallon
psi	= pounds per square inch
psia	= pounds per square inch atmosphere
psig	= pounds per square inch gauge
p-v	= pressure-volume
rpm	= rotations per minute
scfm	= standard cubic feet per minute
SI	= Systeme Internationale d'Units
$slugs/ft^3$	= slugs per cubic foot
TD	= total depth
Ten.	= tension
US	= United States
WOB	= weight on bit
Yd.	= yield

This page intentionally left blank.

Part 1: Basic Technology

This page intentionally left blank.

This engineering practice book has been prepared for engineers, earth scientists, and technicians who work in modern rotary drilling operations. The book derives and illustrates engineering calculation techniques associated with air and gas drilling technology. Since this book has been written for a variety of professionals and potential applications, the authors have attempted to minimize the use of field equations. Also the technical terminology used in the book should be easily understood by all those who study this technology. In nearly all parts of the book, equations are presented that can be used with any set of consistent units. Although most of the example calculations use English units, a reader can easily convert to the Systeme Internationale d'Units (SI units) using the tables in Appendix A.

Air and gas drilling technology is the utilization of compressed air or other gases as a rotary drilling circulating fluid to carry the rock cuttings to the surface that are generated at the bottom of the well by the advance of the drill bit. The compressed air or other gas (e.g., nitrogen or natural gas) can be used by itself, or can be injected into the well with incompressible fluids such as fresh water, formation water, or formation oil. There are three distinct operational applications for this technology: air or gas drilling operations (using only the compressed air or other gas as the circulating fluid), aerated drilling operations (using compressed air or other gas mixed with an incompressible fluid), and stable foam drilling operations (using the compressed air or other gas with an incompressible fluid to create a continuous foam circulating fluid).

Air and gas drilling operations have in the past been a small segment of industrial drilling. In water well drilling operations and environmental monitoring well drilling operations, fresh water and fresh water drilling muds have been the drilling fluid of choice. The drilling of deep oil and gas wells where bottomhole pore pressures can be very large, water based and oil based weighted drilling muds have been the circulation fluids of choice. Only in the mining industry has drilling with compressed air been a standard operation competitive with drilling muds. In the mining industry, the drilling of shallow test boreholes with compressed air began shortly after portable air compressors became available.

Pneumatic conveying represents the first use of moving air to transport entrained solids in the flowing stream of air. This air stream was created by steam powered fans that were the direct outgrowth of the industrial revolution of the early sixteenth century. Pneumatic conveying was accomplished on an industrial scale by the late 1860's [1]. The need for higher pressure flows of air and other gases led to the first reliable industrial air compressors (stationary) in the late 1870's [2]. Again, these early compressors were steam powered. After the development of the internal combustion engines, portable reciprocating and rotary compressors were possible. These portable compressors were first utilized in the late 1880's by an innovative mining industry to drill in mine pneumatic percussion boreholes and shaft pilot boreholes [2].

After their development, portable compressor technology revolutionized many industries.

1.1 Rotary Drilling

Rotary drilling is a method used to drill deep boreholes in rock formations of the earth's crust. This method is comparatively new, having been first developed by a French civil engineer, Rudolf Leschot, in 1863 [3]. The method was initially used to drill water wells using fresh water as the circulation fluid. Today this method is the only rock drilling technique used to drill deep boreholes (greater than 3,000 ft). It is not known when air compressors were first used for the drilling of water wells, but it is known that deep petroleum and natural gas wells were drilled utilizing portable air compressors in the 1920's [4]. Pipeline gas was used to drill a natural gas well in Texas in 1935 using reverse circulation techniques [5].

Today rotary drilling is used to drill a variety of boreholes. Most water wells and environmental monitoring wells drilled into bedrock are constructed using rotary drilling. In the mining industry rotary drilling is used to drill ore body test boreholes and pilot boreholes for guiding larger shaft borings. Rotary drilling techniques are used to drill boreholes for water, oil, gas, and other fluid pipelines that need to pass under rivers, highways, and other natural and man-made obstructions. Most recently, rotary drilling is being used to drill boreholes for fiber optics and other telecommunication lines in obstacle ridden areas such as cites and industrial sites. The most sophisticated application for rotary drilling is the drilling of deep boreholes for the recovery of natural resources such as crude oil, natural gas, and geothermal steam and water. Drilling boreholes for fluid resource recovery requires boreholes drilled to depths of 3,000 ft to as much as 20,000 ft.

Rotary drilling is highly versatile. The rotary drilling applications given above require the drilling of igneous, metamorphic, and sedimentary rock. However, the

deep drilling of boreholes for the recovery of crude oil and natural gas are almost exclusively carried out in sedimentary rock.   Boreholes for the recovery of geothermal steam and water are constructed in all three rock types.   The rotary drilling method requires the use of a rock cutting or crushing drill bit.   Figure 1-1 shows a typical mill tooth tri-cone roller cone bit.   This type of drill bit uses more of a crushing action to advance the bit in the rock (see Chapter 3 for more details). This type of bit is used primarily in the drilling of sedimentary rock.

Figure 1-1: Mill tooth 7 7/8 inch tri-cone roller cutter bit IADC Code 126 (courtesy of Reed Rock Bit Company).

To advance the drill bit in rock requires the application of an axial force on the bit (to push the bit into the rock face), torque on the bit (to rotate the bit against the resistance of the rock face), and circulating fluid to clear the rock cuttings away from the bit as the bit generates more cuttings with its advance (see Figure 1-2).
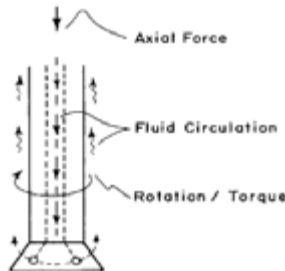

Figure 1-2: The three necessary components for rotary drilling.

Rotary drilling is carried out with a variety of drilling rigs. These can be small "single" rigs, or larger "double" and "triple" rigs. Today most of the land rotary drilling rigs are mobile units with folding masts. A single drilling rig has a vertical space in its mast for only one joint of drill pipe. A double drilling rig has a vertical space in its mast for two joints of drill pipe and a triple drilling rig space for three joints. Table 1-1 gives the API length ranges for drill collars and drill pipe [6].

Table 1-1: API length ranges for drill collars and drill pipe.

Ranges	Minimum Length (ft)	Maximum Length (ft)
Range 1	18	22
Range 2	27	30
Range 3	38	45

Figure 1-3 shows a typical single drilling rig. Such small drilling rigs are highly mobile and are used principally to drill shallow (less than 3,000 ft in depth) water wells, environmental monitoring wells, mining related boreholes, and other geotechnical boreholes. These single rigs are usually self-propelled. The self-propelled drilling rig in Figure 1-3 is a George E. Failing Company Star 30K. These rigs typically use Range 1 drill collars and drill pipe.

Figure 1-3: Typical self-propelled single drilling rig (courtesy of George E. Failing Company).

Single rigs can be fitted with either an on-board air compressor, or an on-board mud pump. Some of these rigs can accommodate both subsystems. These rigs have either a dedicated prime mover on the rig deck, or have a power-take-off system which allows utilization of the truck motor as a prime mover for the drilling rig equipment (when the truck is stationary). These small drilling rigs provide axial force to the drill bit through the drill string via a chain or cable actuated pull-down system, or hydraulic pull-down system. A pull-down system transfers a portion of the weight of the rig to the top of the drill string and then to the drill bit. The torque and rotation at the top of the drill string is provided by a hydraulic tophead drive (similar to power swivel systems used on larger drilling rigs) which is moved up and down the mast (on a track) by the chain drive pull-down system. Many of these small single drilling rigs are capable of drilling with their masts at a 45° angle to the vertical. The prime mover for these rigs is usually diesel fueled.

Figure 1-4 shows a typical double drilling rig. Such drilling rigs are also mobile and can be self-propelled or trailer mounted. Figure 1-5 shows the schematic of a self-propelled double drilling rig.

Figure 1-4: Typical trailer mounted drilling rig (courtesy of George E. Failing Company).

The trailer mounted drilling rig in Figure 1-4 is a George E. Failing Company SS-40. These double rigs have the capability to drill to depths of approximately 10,000 ft and are used for oil and gas drilling operations, geothermal drilling operations, deep mining and geotechnical drilling operations, and water wells. Double rigs typically use Range 2 drill collars or drill pipe. These rigs are fitted

with an on-board prime mover which operates the rotary table, drawworks, and mud pump. The axial force on the drill bit is provided by drill collars. The torque and rotation at the top of the drill string is provided by the kelly and the rotary table. The double drilling rigs have a "crows nest" or "derrick board" nearly midway up the mast. This allows these rigs to pull stands of two drill collar joints or two drill pipe joints. These rigs can carry out drilling operations using drilling mud (with the on-board mud pump) or using compressed air or gas drilling fluids (with external compressors). A few of these drilling rigs are capable of drilling with their masts at a 45° angle to the vertical. The prime mover for these rigs is usually diesel fueled, but can easily be converted to propane or natural gas fuels.

Triple drilling rigs are available in a variety of configurations. Nearly all of these drilling rigs are assembled and erected from premanufactured sections. The vertical tower structure on these drilling rigs are called derricks. The smaller triple land rigs can drill to approximately 20,000 ft and utilize Range 2 drill collars and drill pipe. Very large triple drilling rigs are used on offshore platforms. These rigs can utilize Range 3 drill collars and drill pipe.
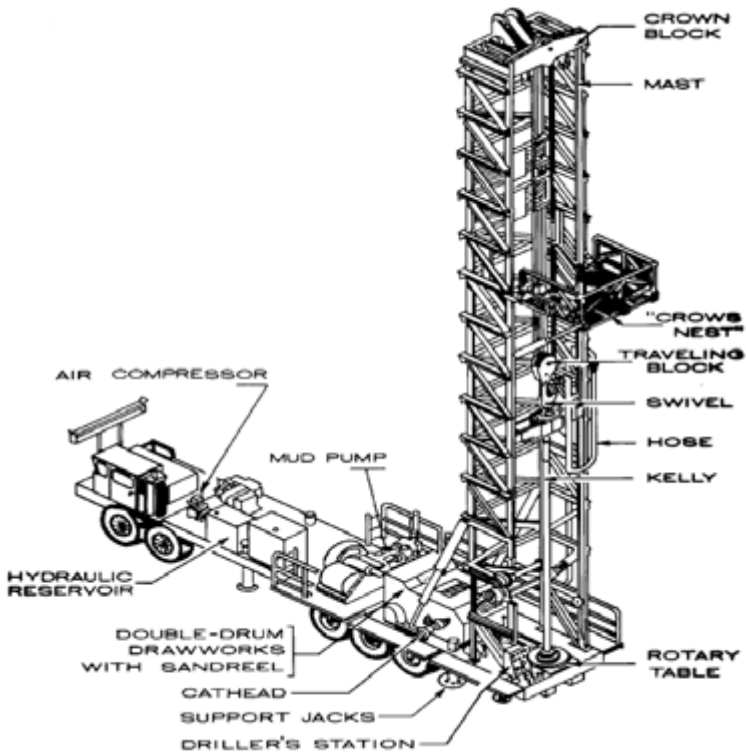

Figure 1-5: Typical self-propelled double drilling rig schematic layout.

The schematic layout in Figure 1-5 shows a typical self-propelled double drilling rig. This example rig is fitted with a mud pump for circulating drilling mud. There is a vehicle engine that is used to propel the rig over the road. The same engine is used in a power-take-off mode to provide power to the rotary table, drawworks, and mud pump. For this rig, this power-take-off engine operates a hydraulic pump which provides fluid to hydraulic motors to operate the rotary table, drawworks, and mud pump. The "crows nest" on the mast indicates that the rig is capable of drilling with a stand of two joints of drill pipe. This drilling rig utilizes a rotary table and a kelly to provide torque to the top of the drill string. The axial force on the bit is provided by the weight of the drill collars at the bottom of the drill string (there is no chain pull-down capability for this drilling rig). This example schematic shows a rig with on-board equipment that can provide only drilling mud or treated water as a circulate fluid. The small air compressor at the front of the rig deck is to operate the pneumatic controls of the rig. However, this rig can easily be fitted for air and gas drilling operations. This type of drilling rig (already fitted with a mud pump), would require an auxiliary hook up to external air compressor(s) to carry out an air drilling operation. Such compressor systems and associated equipment for air drilling operations are usually provided by a subcontractor specializing in these operations.

1.2 Circulation Systems

Two types of circulation techniques can be used for either a mud drilling system or an air or gas drilling system. These are direct circulation and reverse circulation.

1.2.1 *Direct Circulation*

Figure 1-6 shows a schematic of a rotary drilling, direct circulation mud system that would be used on a typical double (and triple) drilling rig. Direct circulation requires that the drilling mud (or treated water) flow from the slush pump (or mud pump), through the standpipe on the mast, through the rotary hose, through the swivel and down the inside of the kelly, down the inside of the drill pipe and drill collars, through the drill bit (at the bottom of the borehole) into the annulus space between the outside of the drill string and the inside of the borehole. The drilling mud entrains the rock bit cuttings and then flows with the cuttings up the annulus to the surface where the cuttings are removed from the drilling mud by the shale shaker; the drilling mud is returned to the mud tanks (where the slush pump suction side picks up the drilling mud and recirculates the mud back into the well). The slush pumps used on double (and triple) drilling rigs are positive displacement piston type pumps.

For single drilling rigs, the drilling fluid is often treated fresh water in a pit dug in the ground surface and lined with an impermeable plastic liner. A heavy duty hose is run from the suction side of the on-board mud pump (see Figure 1-5) to the mud pit. The drilling water is pumped from the pit, through the pump, through an on-board pipe system, through the rotary hose, through the hydraulic tophead drive, down the inside of the drill pipe, and through the drill bit to the bottom of the well. The drilling water entrains the rock cuttings from the advance of the bit and carries the cuttings to the surface via the annulus between the outside of the drill pipe and

the inside of the borehole. At the surface the drilling fluid (water) from the annulus with entrained cuttings is returned to the pit where the rock cuttings are allowed to settle out to the bottom. The pumps on single drilling rigs are small positive displacement reciprocating piston or centrifugal type.
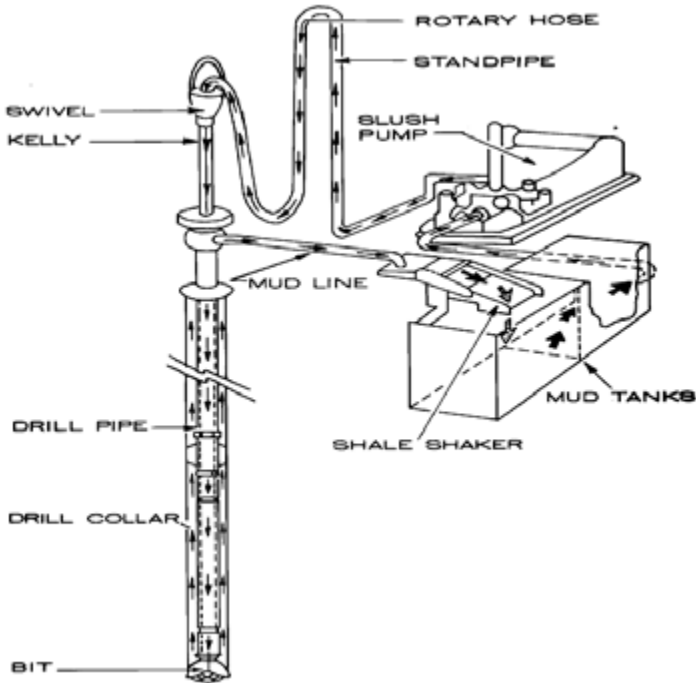
Figure 1-6: Direct circulation mud system.

Figure 1-7 shows a detailed schematic of a direct circulation compressed air drilling system that would be used on a typical double or triple drilling rig. Direct circulation requires that atmospheric air be compressed by the compressor and then forced through the standpipe on the mast, through the rotary hose, through the swivel and down the inside of the kelly, down the inside of the drill pipe and drill collars, through the drill bit (at the bottom of the borehole) into the annulus space between the outside of the drill string and the inside of the borehole. The compressed air entrains the rock bit cuttings and then flows with the cuttings up the annulus to the surface where the compressed air with the entrained cuttings exit the circulation system via the blooey line. The compressed air and cuttings exit the blooey line into a large pit dug into the ground surface (burn pit). These pits are lined with an impermeable plastic liner.

If compressed natural gas is to be used as a drilling fluid, a gas pipeline is run from a main natural gas pipeline to the drilling rig. Often this line is fitted with a booster compressor. This allows the pipeline natural gas pressure to be increased (if higher pressure is needed) before the gas reaches the drilling rig standpipe.
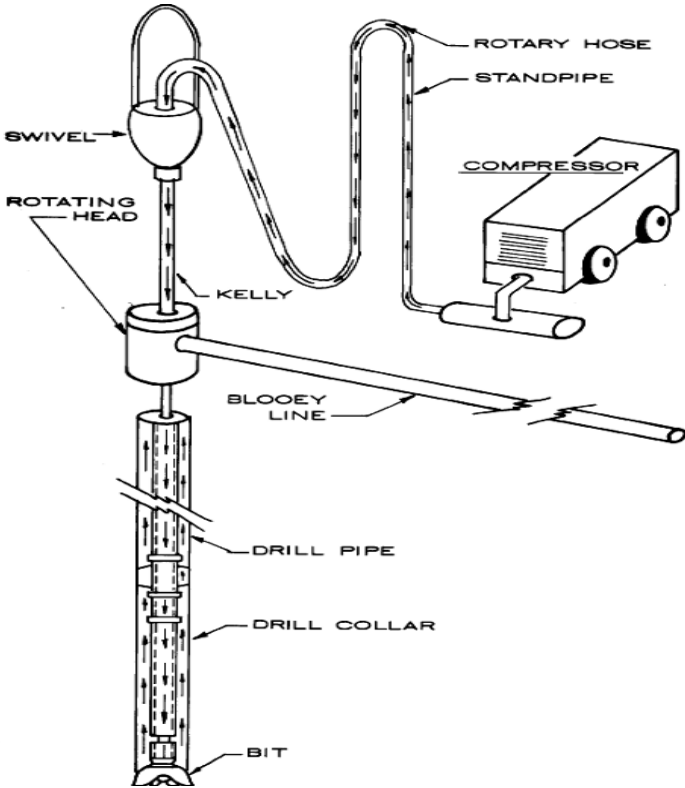
Figure 1-7: Direct circulation air system.

1.2.2 *Reverse Circulation*

Rotary drilling reverse circulation (either using drilling mud and/or compressed air or gas) can be a useful alternative to direct circulation methods. The reverse circulation technique is particularly useful for drilling relatively shallow large diameter boreholes. In a typical reverse circulation operation utilizing drilling mud, the drilling mud (or treated water) flows from the slush pump (or mud pump) to the top of the annulus between the outside of the drill string and the inside the borehole, down the annulus space to the bottom of the borehole. At the bottom of the borehole the drilling mud entrains the rock bit cuttings and flows through the large orifice in the drill bit and then upward to the surface through the inside of the drill

string. At the surface the cuttings are removed from the drilling mud by the shale shaker and the drilling mud is returned to the mud tanks (where the slush pump suction side picks up the drilling mud and recirculates the mud back to the well).

   Reverse circulation can also be carried out using air and gas drilling techniques. Figure 1-8 shows a typical application of reverse circulation using compressed air as the drilling fluid (or mist, unstable foam) [7]. This example is a dual tube (or dual drill pipe) closed reverse circulation system. The closed system is characterized by an annulus space bounded by the inside of the outer tube and the outside of the innertube. This is a specialized type of reverse circulation and is usually limited to small single and double drilling rigs with top head rotary drives. Dual tube and dual drill pipe are available from a number of manufacturers in the United States and elsewhere in world (see Chapter 3 for drill pipe details).
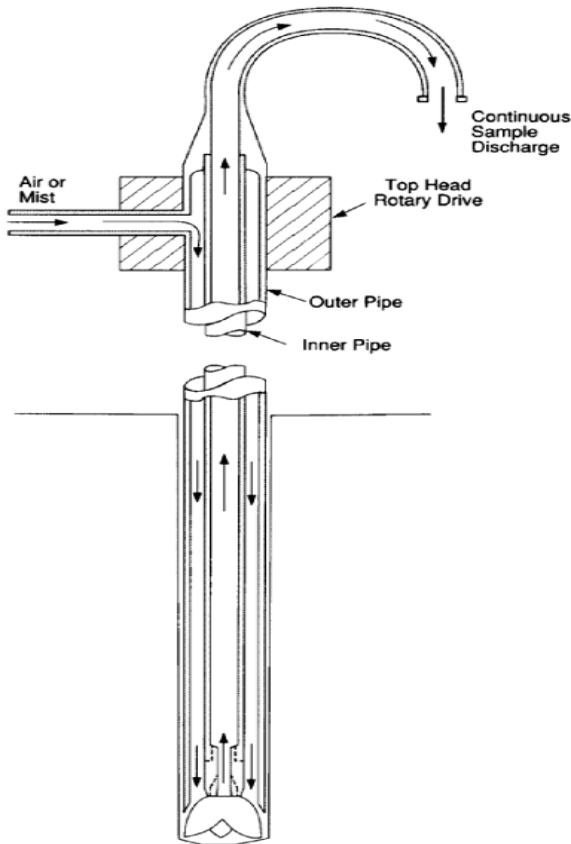

Figure 1-8: Dual tube (or dual drill pipe) closed reverse circulation operation.

Reverse circulation drilling operations require specially fabricated drill bits. Figure 1-9 shows a schematic of the interior flow channel of a tri-cone rotary drill bit designed for reverse circulation. These drill bits utilize typical roller cutter cones exactly like those used in direct circulation drill bits (see Figure 1-1). These bits, however, have a large central channel opening that allows the circulation fluid flow with entrained rock cuttings to flow from the bottom of the borehole to the inside of the drill string and then to the surface.
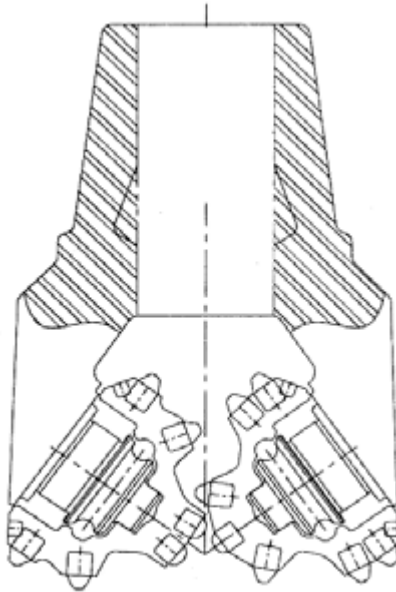
Figure 1-9: Schematic of the internal flow channel of a tri-cone roller cutter bit designed for reverse circulation operations (courtesy of Smith International Incorporated).

Most tri-cone drill bits with a diameter of 5 3/4 inches or less are designed with the central flow channel as shown in Figure 1-9 above. Figure 1-1 showed the typical tri-cone drill bit for direct circulation operations. These direct circulation drill bits usually have three orifices that can be fitted with nozzles. Tri-cone roller cutter drill bits for reverse circulation operations are available in diameters from 4 1/2 inches to 31 inches. The larger diameter bits for reverse circulation operations are usually custom designed and fabricated. Dual wall pipe reverse circulation operations require special skirted drill bits (see Chapter 3 for details). These skirted drill bits are also custom designed for the particular drilling operation. Most reverse circulation tri-cone bits are manufactured by companies that specialize in geotechnical and mining drilling equipment.

1.3 Comparison of Mud and Air Drilling

The direct circulation model is used to make some important comparisons between mud drilling and air and gas drilling operations.

1.3.1 *Advantages and Disadvantages*

There are some very basic advantages and disadvantages to mud drilling and air drilling operations.   The earliest recognized advantage of air and gas drilling technology was the increase in drilling penetration rate relative to mud drilling operations. Figure 1-10 shows a schematic of the various drilling fluids (the top four comprise air and gas drilling technology) and how these drilling fluids affect drilling penetration rate. The drilling fluids in Figure 1-10 are arranged with the lightest at the top of the list and the heaviest at the bottom.   In general, the lighter the drilling fluid the greater the drilling penetration rate (the arrow points upward for increasing penetration rate).   The lighter the fluid column in the annulus (with entrained rock cuttings) the lower the confining pressure on the rock bit cutting face. This lower confining pressure allows the rock bit to be more easily advanced into the rock (see Chapter 3 for more details).

Improved Penetration Rate

increasing

Air and Gas

Unstable Foam

Stable Foam

Aerated Mud

Mud

Figure 1-10: Improved penetration rate.

Figure 1-11 shows a schematic of the various drilling fluids and their respective potential for avoiding formation damage. Formation damage is an important issue in fluid resource recovery (e.g., water well, environmental monitoring, well drilling operations, oil and natural gas, and geothermal fluids). The lighter the fluid column in the annulus (with entrained rock cuttings), the lower the potential for formation damage (arrow points upward to increasing avoidance of formation damage). Formation damage occurs when the fluid column pressure at the bottom of borehole is higher than the pore pressure of the resource fluid (oil, gas, or water) in the rock formations. This higher bottomhole pressure forces the drilling fluid (with entrained rock cutting fines) into the exposed fractures and pore passages in the drilled rock formations.   These fines plug these features in the immediate region around the borehole. This damage is called a "skin effect".   This skin effect damage restricts

later formation fluid flows to the borehole, thus, reducing the productivity of the well.

Ability to Not Cause Formation Damage

Increasing

Air and Gas

Unstable Foam
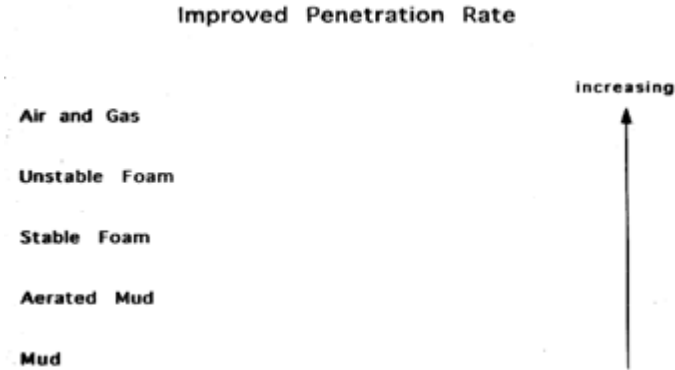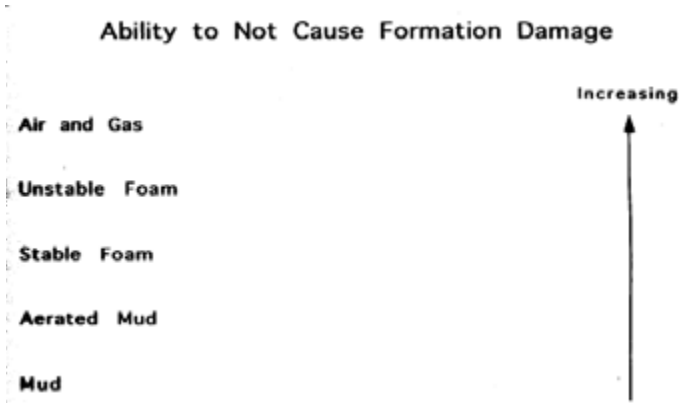
Stable Foam

Aerated Mud

Mud

Figure 1-11: Formation damage avoidance.

Figure 1-12 shows a schematic of the various drilling fluids and their respective potential for avoiding loss of circulation. Loss of circulation occurs when drilling with drilling muds or treated water through rock formations that have fractures or large interconnected pores or vugs. If these features are sufficiently large and are not already filled with formation fluids, then as drilling progresses the drilling fluid that had been flowing to the surface in the annulus can be diverted into these fractures or pore structures. This diversion can result in no drilling fluid (with entrained rock cuttings) returning to the surface. The rock cuttings are left in the borehole and consolidate around the lower portion of the drill string and the drill bit.   If this situation is not identified quickly, the drill string will begin to torque-up in the borehole and mechanical damage to the drill string will occur. Such damage can sever the drill string and result in a fishing job to retrieve the portion of the drill string remaining in the borehole.

For deep oil and natural gas recovery wells, loss of circulation can result in even more catastrophic situations. If drilling fluids are lost to thief formations, the fluid column in the annulus can be reduced resulting in a lower bottomhole pressure. This low bottomhole pressure can cause a high pressure oil and/or natural gas kick, or geothermal fluid kick (a slug of formation fluid) to enter the annulus. Such kicks must be immediately and carefully circulated out of the annulus (to the surface) otherwise an uncontrolled blowout of the well could occur. Here again heavier drilling fluids are generally more prone to loss of circulation (arrow points upward to increasing loss of circulation avoidance).

Figure 1-13 shows a schematic of the various drilling fluids and their respective potential for use in geologic provinces with high pore pressures.   High pore pressures are encountered in oil, natural gas, and geothermal drilling operations. New discoveries of oil, natural gas, or geothermal fluid deposits are usually highly

pressured. In order to safely drill boreholes to these deposits heavily weighted drilling muds are utilized. The heavy fluid column in the annulus provides the high bottomhole pressure needed to balance (or overbalance) the high pore pressure of the deposit.

Ability to Drill in Loss of Circulation Zones

Air and Gas

Unstable Foam

Stable Foam

Aerated Mud

Mud
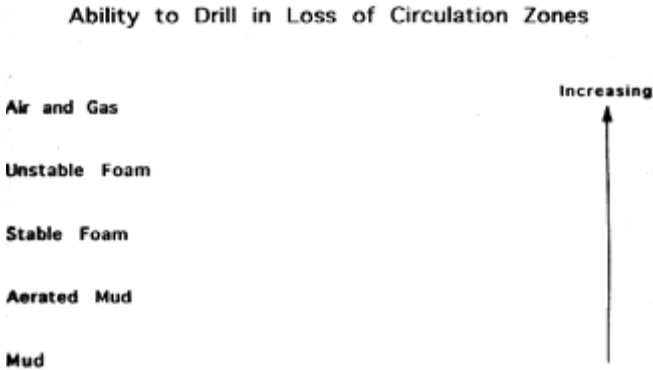
Increasing ↑

Figure 1-12: Loss of circulation avoidance.

Figure 1-13 also shows that the heavier the drilling fluid column in the annulus the more useful the drilling fluid is for controlling high pore pressure (the arrow points downward to increasing capability to control high pore pressure). There are limits to how heavy a drilling mud can be. As was discussed above, too heavy a drilling mud results in overbalanced drilling and this can result in formation damage. But there is a greater risk to overbalanced drilling. If the drilling mud is too heavy the rock formations in the openhole section can fracture. These fractures could result in a loss of the circulating mud which could result in a blowout.

Ability to Drill in High Pore Pressure Zones

Air and Gas

Unstable Foam

Stable Foam

Aerated Mud

Mud

↓

Increasing

Figure 1-13: Controlling high pore pressure.

In the past decade it has been observed that drilling with a circulation fluid that has a bottomhole pressure slightly below that of the pore pressure of the fluid deposit gives near optimum results. This type of drilling is denoted as underbalanced drilling. Underbalanced drilling allows the formation to produce fluid as the drilling progresses. This lowers or eliminates the risk of formation damage and eliminates the possibility of formation fracture and loss of circulation. In general, if the pore pressure of a deposit is high, an engineered adjustment to the drilling mud weight (with additives) can yield the appropriate drilling fluid to assure underbalanced drilling. However, if the pore pressure is not unusually high then air and gas drilling techniques are required to lighten the drilling fluid column in the annulus.

Figure 1-14 shows a schematic of the various drilling fluids and their respective potential for keeping formation water out of the drilled borehole. Formation water is often encou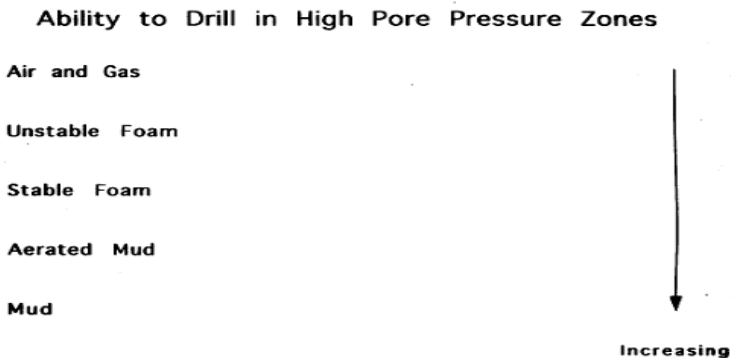ntered when drilling to a subsurface target depth. This water can be in fracture and pore structures of the rock formations above the target depth. If drilling mud is used as the circulating fluid, the pressure of the mud column in the annulus is usually sufficient to keep formation water from flowing out of the exposed rock formations in the borehole. The lighter drilling fluids have lower bottomhole pressure, thus, the lower the pressure on any water in the exposed fracture or pore structures in the drilled rock formations. Figure 1-14 shows that the heavier drilling fluids have a greater ability to cope with formation water flow into to the borehole (the arrow points downward to increasing control of formation water).

Ability to Cope with Formation Water

Air and Gas

Unstable Foam

Stable Foam

Aerated Mud

Mud

Increasing
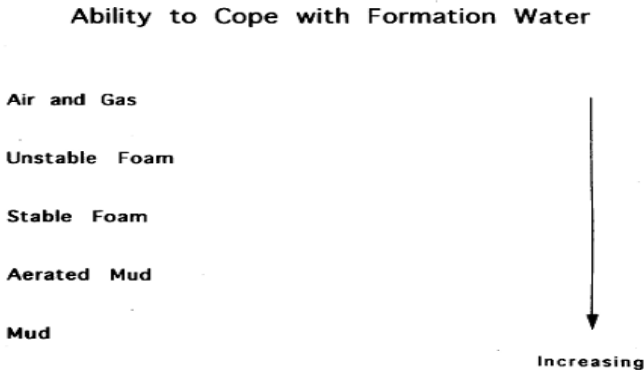
Figure 1-14: Control of the inflow of formation water.

1.3.2 *Flow Characteristics*

A comparison is made of the flow characteristics of mud drilling and air drilling in an example deep well. A schematic of this example well is shown in Figure 1-15. The well is cased from the surface to 7,000 ft with API 8 5/8 inch diameter, 28.00 lb/ft nominal, casing. The well has been drilled out of the casing shoe with a 7 7/8 inch diameter drill bit. The comparison is made for drilling at 10,000 ft. The drill string in the example well is made up of (bottom to top), 7 7/8 inch diameter drill bit, ~ 500 ft of 6 3/4 inch outside diameter by 2 13/16 inch inside diameter

drill collars, and ~ 9,500 ft of API 4 1/2 inch diameter, 16.60 lb/ft nominal, EU-S135, NC 50, drill pipe.
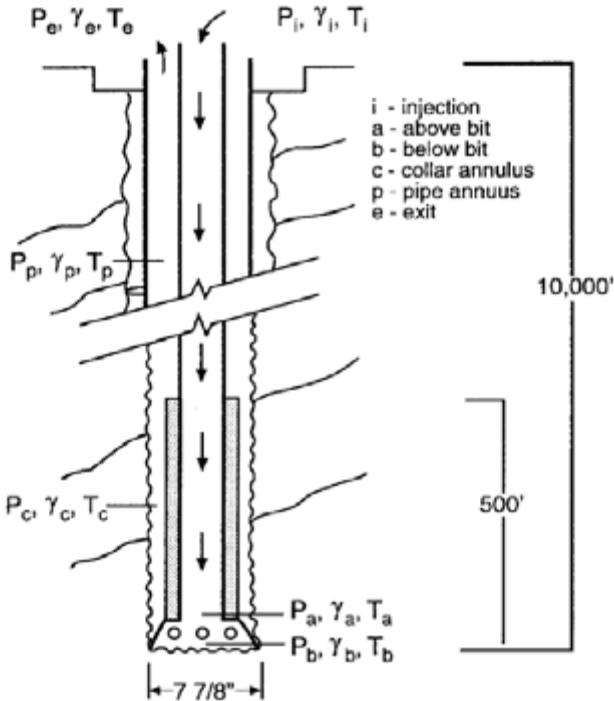
Figure 1-15: Comparison example well and drill string.

The mud drilling hydraulics calculations are carried out assuming the drilling mud weight is 10 lb/gal (75 lb/ft^3), the Bingham mud yield is 10 lb/100 ft^2, and the plastic viscosity is 30 centipose. The drill bit is assumed to have three 13/32 inch diameter nozzles and the drilling mud circulation flow rate is 300 gals/minute. Figure 1-16 shows the plots of the pressures in the incompressible drilling mud as a function of depth. In the figure is a plot of the pressure inside the drill string. The pressure is approximately 1,400 psig at injection and 6,000 psig at the bottom of the inside of the drill string just above the bit nozzles. Also in the figure is a plot of the pressure in the annulus. The pressure is approximately 5,440 psig at the bottom of the annulus just below the bit nozzles and 0 psig at the top of the annulus at the surface.

The pressures in Figure 1-16 reflects the hydrostatic weight of the column of drilling mud and the resistance to fluid flow from the inside surfaces of the drill

string and the surfaces of the annulus. This resistance to flow results in pressure losses due to friction. The total losses due to friction are the sum of pipe wall, openhole wall, and drill bit orifice resistance to flow. This mud drilling example shows a drilling string design which has a open orifice or large diameter nozzle openings in the drill bit. This is reflected by the approximate 700 psi loss through the drill bit. Smaller diameter nozzles would yield higher pressure losses across the drill bit and higher injection pressures at the surface.
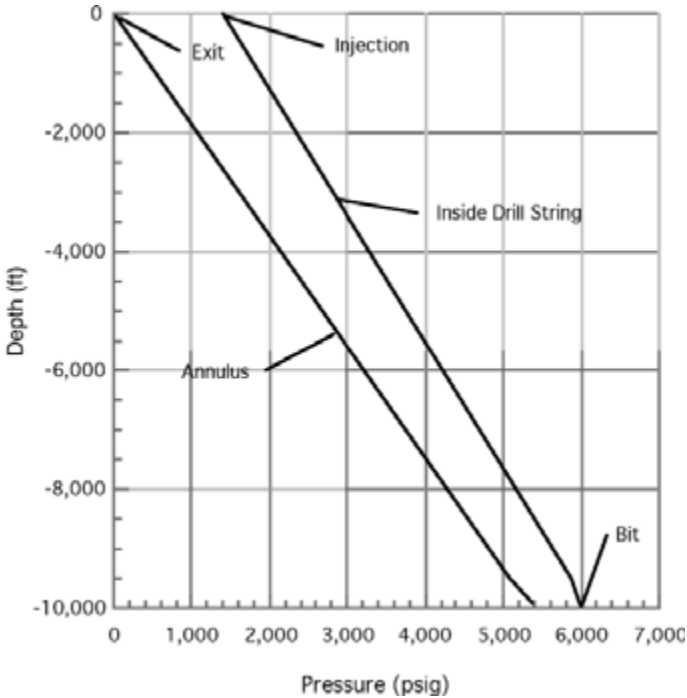
Figure 1-16: Mud drilling pressures versus depth.

The air drilling calculations are carried out assuming the drilling operation is at sea level. There are two compressors capable of 1,200 scfm each, so the total volumetric flow rate to the drill string is 2,400 scfm. The drill bit is assumed to have three open orifices (~0.80 inches diameter). Figure 1-17 shows the plots of the pressures in the compressible air as a function of depth. In the figure is a plot of the

pressure inside the drill string.   The pressure is approximately 260 psia at injection and 270 psia at the bottom of the inside of the drill string just above the bit orifices. Also in the figure is a plot of the pressure in the annulus.   The pressure is approximately 260 psia at the bottom of the annulus just below the bit orifices and 14.7 psia at the end of the blooey line at the surface (top of the annulus).

As in the mud drilling example, the pressures in Figure 1-17 reflects the hydrostatic weight of the column of compressed air and the resistance to air flow from the inside surfaces of the drill string and the surfaces of the annulus.   This resistance to flow results in pressure losses due to friction. In this example the fluid is compressible. Considering the flow inside the drill string, the hydrostatic weight of the column dominates the flow (relative to friction losses) and this results in the injection pressure at the surface being less than the pressure at the bottom of the drill string (inside the drill string above the bit open orifices).
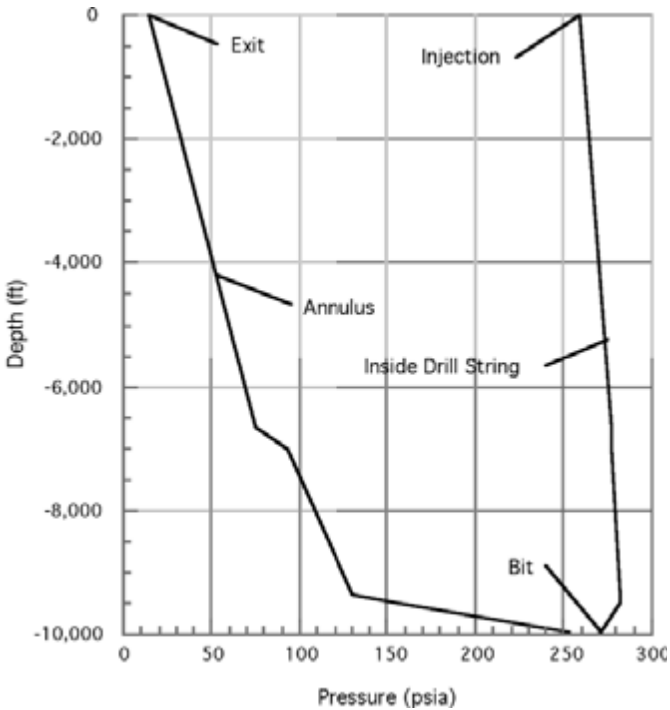
Figure 1-17: Air drilling pressures versus depth.

Figure 1-18 shows the plots of the temperature in the incompressible drilling mud as a function of depth. The geothermal gradient for this example is 0.01˚F/ft. Subsurface earth is nearly an infinite heat source. The drilling mud in a mud drilling circulation system is significantly more dense than compressed air or other gases. Thus, as the drilling mud flows down the drill string and up through the annulus to the surface, heat is transferred from the rock formations through the surfaces of the borehole, through the drilling mud in the annulus, through the steel drill string to the drilling mud inside. It is assumed that the drilling mud is circulated into the top of the drill string at 60˚F.
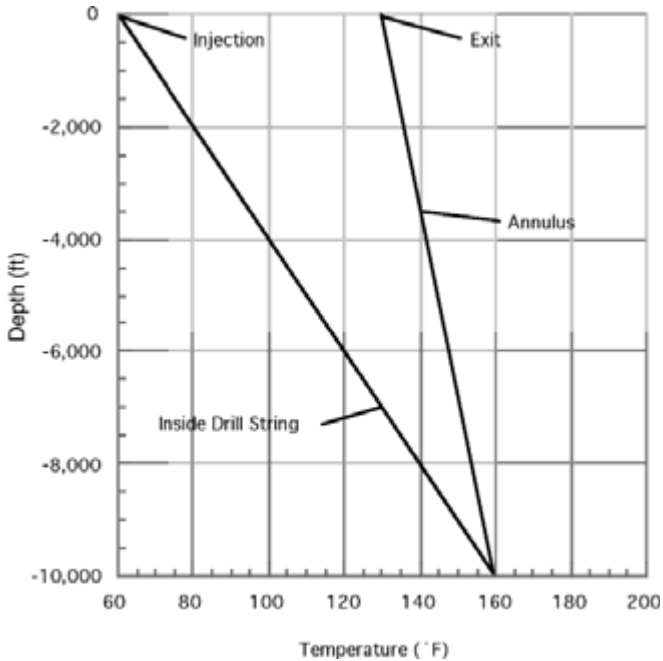
Figure 1-18: Mud drilling temperature versus depth.

As the drilling mud flows down the inside of the drill string the drilling mud heats up as heat flows from the higher temperature rock formations and drilling mud in the annulus. At the bottom of the well the drilling mud temperature reaches the bottomhole temperature of 160˚F. The drilling mud flowing up the annulus (usually laminar flow conditions) is heated by the geothermal heat in the rock formation.

The heated drilling mud flowing in the annulus heats the outside of the drilling string and this in turn heats the drilling mud flowing down the drill string. Because of its good heat storage capabilities, the drilling mud exits the annulus with a temperature greater than the injection temperature but less than the bottomhole temperature. In this example, the temperature of the drilling mud exiting the annulus is approximately 130°F.

Figure 1-19 shows the plots of the temperature in the compressible air drilling fluid as a function of depth. The compressed air drilling fluid is significantly less dense than drilling mud. Thus, compressed air has poor heat storage qualities relative to drilling mud. Also, compressed air flowing in the drilling circulation system is flowing rapidly and therefore the flow is turbulent inside the drill string and in the annulus. Turbulent flow is very efficient in transferring heat from the surface of the borehole to the flowing air in the annulus and in the inside the drill string. Assuming the compressed air entering the top of the drill string is at 60°F the heat rapidly transfers to heat (or cool) the air flow in the well. Under these conditions the compressed air exiting the annulus has approximately the same temperature as the air entering the top of the drill string.
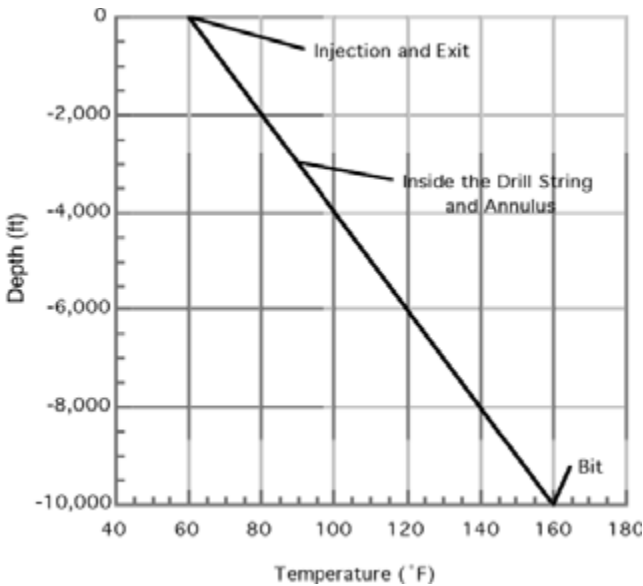
Figure 1-19: Air drilling temperature versus depth.

Figure 1-19 shows that the temperature of the compressed air at any position in the borehole is approximately the geothermal temperature at that depth. Thus, the temperature of the flowing air at the bottom of the hole is the bottomhole temperature of 160°F. There is some local cooling of the air as it exits the open orifices of the drill bit at the bottom of the hole. This cooling effect is more pronounced if nozzles are used in the drill bit (when using a downhole motor). This cooling effect is known as the Joule-Thomson effect and can be estimated [8]. However, it is assumed that this effect is small and that the air flow returns very quickly to the bottomhole geothermal temperature.

Figure 1-20 shows the plot of the specific weight of drilling mud for this example calculation. The drilling mud is incompressible and, therefore, the specific weight is 75 lb/ft^3 (or 10 lb/gal) at any position in the circulation system. There is some slight expansion of the drilling mud due to the increase in temperature as the drilling mud flows to the bottom of the well. This effect is quite small and is neglected in these engineering calculations.
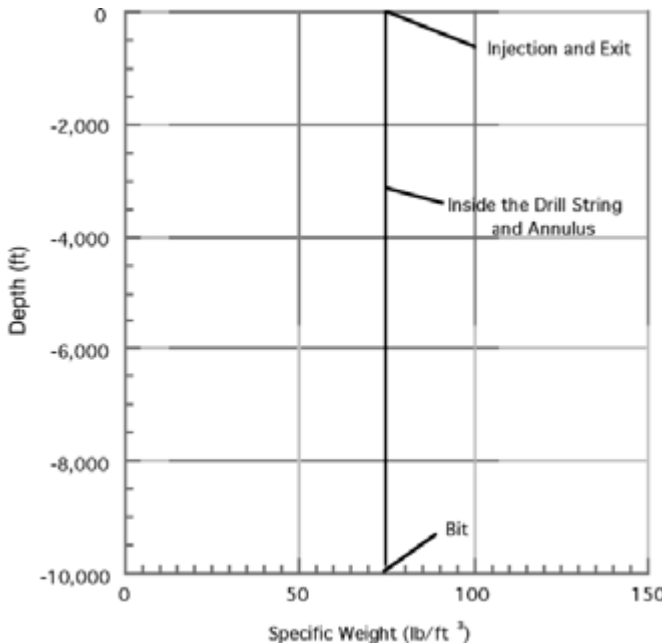
Figure 1-20: Mud drilling specific weight versus depth.

Figure 1-21 shows the plot of the specific weight of the compressed air in this example. The compressed air is injected into the top of the drill string at a specific weight of 1.3 lb/ft^3 (at a pressure of 260 psia and temperature of 60°F). As the air flows down the drill string the pressure remains approximately the same. At the bottom of the drill string the specific weight is 1.2 lb/ft^3 (at a pressure of 270 psia and a temperature of 160°F). The compressed air exits the drill bit orifices into the bottom of the annulus (bottom of the well) with a specific weight of 1.1 lb/ft^3 (at a pressure of 260 psia and a temperature of 160°F).
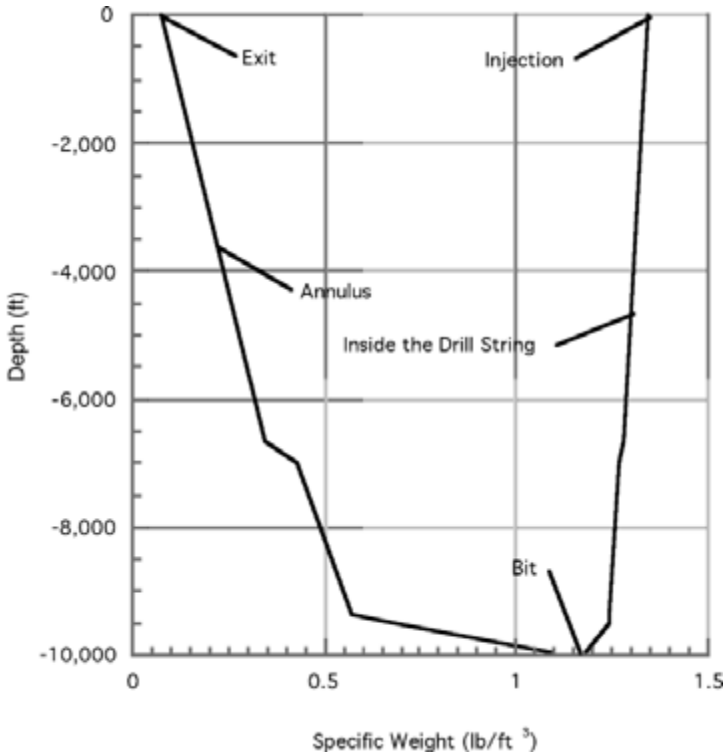
Figure 1-21: Air drilling specific weight versus depth.

As the compressed air flows to the surface through the annulus it decompresses as it flows to the low atmospheric pressure at the surface. At the surface the air exits

the annulus (via the blooey line) with a specific weight of 0.0763 lb/ft³.   The surface atmosphere for this example is assumed to be API Mechanical Equipment Standards standard atmospheric conditions (dry air, pressure of 14.696 psia and a temperature of 60°F) [9].   This figure shows a typical friction resistance dominated drill string flow (as opposed to hydrostatic column weight dominated).   This type of flow has a drill string injection pressure at the top that is higher than the pressure above the drill bit at the bottom.   Friction dominated flow results when the drill bit is run with no nozzles.

Figure 1-22 is the concluding plot of these example calculations.   This shows the side-by-side comparison of the annulus velocities of the drilling mud and the compressed air as they flow to the surface.   It is the power of these return flows up the annulus that keeps the rock cuttings entrained and moving to the surface at a rate that allows the drill bit to be safely advanced.

The drilling mud flows in the annulus around the drill collars with an average velocity of about 7.6 ft/sec.   The drilling mud slows to an average velocity of about 3.0 ft/sec in the annulus around the drill pipe.

For the air drilling case, the compressed air flows in the annulus with an average velocity of about 30 ft/sec around drill collars.   The velocity increases up the annulus to about 125 ft/sec at the exit to the annulus.

It is instructive to compare the power (per unit volume) of example flows at the positions in the annulus where the power is likely the lowest.   For both of these examples the lowest power is just above the drill collars in the annulus around the bottom of the drill pipe.   The kinetic energy per unit volume, KE, is [1, 10]

$$KE \ = \ \frac{1}{2} \ \rho \ V^2 \tag{1-1}$$

where KE is the kinetic energy per unit volume (ft-lb/ft³),
ρ is the specific weight of the fluid (lb-sec²/ft⁴),
V is the average velocity of the fluid (ft/sec).
The density of the fluid, ρ, is

$$\rho \ = \ \frac{\gamma}{g} \tag{1-2}$$

where γ is the specific weight of the fluid (lb/ft³),
g is the acceleration of gravity (32.2 ft/sec²).
For the mud drilling example the specific weight of the drilling mud in the annulus just above the drill collars is 75 lb/ft³.   Using these values in Equation 1-2 the density of the drilling mud is

$$\rho_m \ = \ \frac{75.0}{32.2}$$

$$\rho_m \ = \ 2.33 \ \frac{lb - sec^2}{ft^4}$$

The average velocity of the drilling mud at this position is approximately 3.0 ft/sec. Using these values in Equation 1-1, the kinetic energy per unit volume for the drilling mud example becomes

$$KE_m = \frac{1}{2} (2.33) (3.0)^2$$

$$KE_m = 10.5 \frac{ft-lb}{ft^3}$$
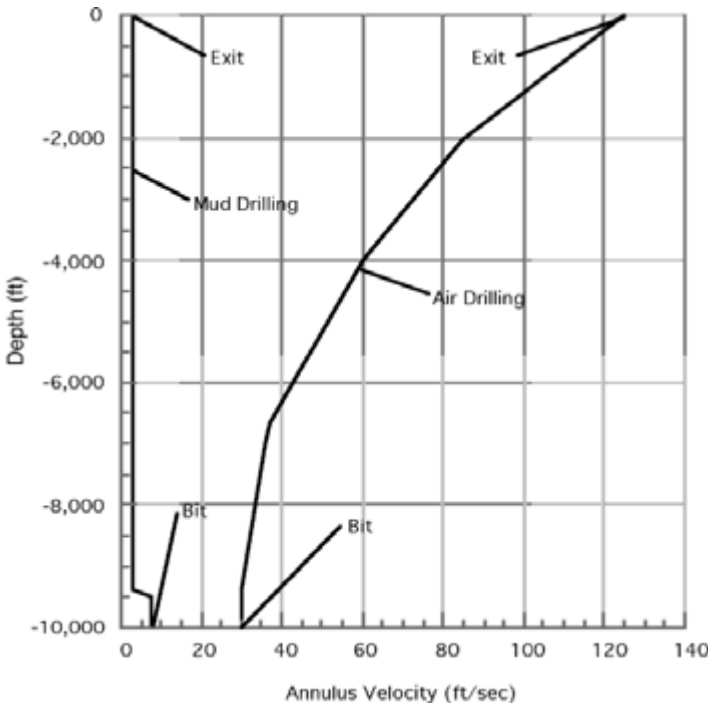
Figure 1-22: Annulus velocities for drilling mud and compressed air.

For the air drilling example the specific weight of the compressed air in the annulus just above the drill collars is 0.688 lb/ft³. Using these values in Equation 1-2 the density of the compressed air is

$$\rho_a = \frac{0.688}{32.2}$$

$$\rho_a = 0.0214 \ \frac{lb-sec^2}{ft^4}$$

The average velocity at this position is approximately 30 ft/sec. Using these values in Equation 1-1, the kinetic energy per unit volume for the air drilling example becomes

$$KE_a = \frac{1}{2} \ (0.0214) \ (30.0)^2$$

$$KE_a = 9.6 \ \frac{ft-lb}{ft^3}$$

The kinetic energy per unit volume values of the two example flows (drilling mud and compressed air) are nearly the same at the position in the annulus where it would be expected that the rock cuttings carrying capacity of the fluids are a minimum. The flow kinetic energy per unit volume of the mud drilling fluid does not change as the drilling mud flows to the surface in the annulus (uniform cross-sectional area). The flow kinetic energy per unit volume of the compressed air on the other hand increases exponentially as it seeks atmospheric conditions at the exit to the annulus. This is because the compressed air has stored internal energy and as it starts up the annulus and resistance to flow decreases (i.e., lower hydrostatic head) this internal energy is converted to velocity.

References

1. Marcus, R. D., et al., *Pneumatic Conveying of Solids*, Chapman and Hall, 1990.

2. Singer, C., et al., *A History of Technology*, Vol. 4, Oxford Press, 1958.

3. Singer, C., et al., *A History of Technology*, Vol. 5, Oxford Press, 1958.

4. Singer, C., et al., *A History of Technology*, Vol. 6, Oxford Press, 1958.

5. Personal communication with H. J. Gruy, February 5, 1997.

6. *API Recommended Practice for Drill Stem Design and Operating Limits*, API RP7G, 16th Edition, August 1998.

7. Roscoe Moss Company, *Handbook of Ground Water Development*, Wiley, 1990.

8. Burghardt, M. D., *Engineering Thermodynamics with Applications*, Harper and Row, 1982.

9. *API Specifications for the Internal-Combustion Reciprocating Engines for Oil-Field Service*, API Std. 7B-11C, Ninth Edition, 1994.

10. Angel, R. R., "Volumetric Requirements for Air or Gas Drilling," *Petroleum Transactions, AIME*, Vol. 210, 1957.

This page intentionally left blank.

Air and gas drilling operations require some special surface equipment not normally used in rotary mud drilling operations. Shallow drilling operations usually have this specialized equipment incorporated into the single rotary drilling rig design. For the deeper drilling operations that use double and triple rotary drilling rigs, this specialized surface equipment is usually provided by an air and gas drilling equipment contractor. These contractors supply the rotary drilling contractor (the drilling rig) with the necessary surface equipment to convert the mud drilling rig to an air and gas drilling rig. The rotary drilling contractor and the air and gas drilling contractor are usually contracted by an operating company.

2.1 Drilling Location

Nearly all air and gas drilling operations are land operations. Figure 2-1 shows a typical air drilling location plan for the drilling rig and the other important surface equipment [1]. The plan in this figure shows the location of the drilling rig (borehole directly below the rotary table). This is a typical triple drilling rig configuration. The drilling rig floor is larger and, therefore, it is easier to show the important features of an air drilling operation with this type of rig. This rig is a typical mud rotary drilling rig that has been set up to drill with compressed air as the circulating fluid. The rig is powered by two prime movers on the rig floor. These prime movers provide their power to the rig equipment through the compound (a chain drive transmission system). The prime mover on a triple rotary drilling rig like that shown in Figure 2-1 is limited to operating either the rotary table or the

drawworks (hoist system), but not both simultaneously [2]. The development of the hydraulic top head rotary drive, which replaces the rotary table on most single and some double drilling rigs, allows the prime mover to simultaneously operate the rotary action and the hoist system. These smaller hydraulic top head rotary drive rigs use rig weight (via pull-down systems) to put axial force on the bit.

Figure 2-1 shows the primary compressors (low pressure) that supply compressed air to a flow line between the compressors and the rig standpipe. In this example there are two primary compressors supplying the rig. These compressors intake air from the atmosphere and compress the air in several stages of mechanical compression. These primary compressors are positive displacement fluid flow machines, either reciprocating piston, or rotary compressors (see Chapter 4 for more details). These primary compressors are usually capable of an intake rate of about 1,200 acfm (actual cubic feet per minute) of atmospheric air and output air at pressures up to approximately 300 psig. These primary compressors expel their compressed air into the flow line to the standpipe of the drilling rig. This flow line is usually an API 2 7/8 inch (OD) line pipe (or an ASME equivalent), or larger [3]. Downstream along this flow line from the primary compressors is the booster compressor. This booster compressor is a reciprocating piston compressor. The booster compressor is used to increase the flow pressure from the primary compressors to pressures up to approximately 1,000 psig. In most drilling operations the injection pressure is less than 300 psig and, therefore, the booster compressor is commonly used only for special drilling operations such as directional drilling with a downhole motor.

Downstream from the booster compressor are liquid pump systems that allow water to be injected into the compressed air flow to the rig. Also solids can be injected into the compressed air flow. This is accomplished by injecting the solids into a small water tank, then the water with the entrained solids are injected into the air flow.

Along the flow line leading from the compressors to the drilling rig standpipe is an assembly of pressure gauges, temperature gauges, valves, and a volumetric flow rate meter [3]. This instrumentation is critical in successfully controlling air drilling operations. Also along this flow line is a safety valve. This flow line safety valve acts in the similar manner as the safety valves on each of the compressors in releasing pressure in the event the pressure exceeds safe limits. Also on the flow line is a valve allowing the compressed air flow to be diverted either to the atmosphere or to primary and secondary jets in the blooey line.

The blooey line runs from the top of the annulus to the burn pit and allows the compressed air with the entrained rock cuttings to exit the circulating system to the atmosphere. The blooey line is about 100 to 200 ft in length. Usually the blooey line is an API 8 5/8 inch (OD) casing or larger [4]. However, some blooey line systems are fabricated with two smaller diameter parallel lines. As shown in Figure 2-1, the exit (to the atmosphere) of the blooey line expels the air with the rock cuttings into a burn pit. For oil and natural gas drilling operations, a pilot flame is placed at the exit of the blooey line. This ignites any oil or natural gas produced at the bottom of the well and exiting the blooey line with the circulating air. The mud tanks (pits) are maintained at air and gas drilling operation locations in the event high bottomhole pressure forces conversion to mud drilling.
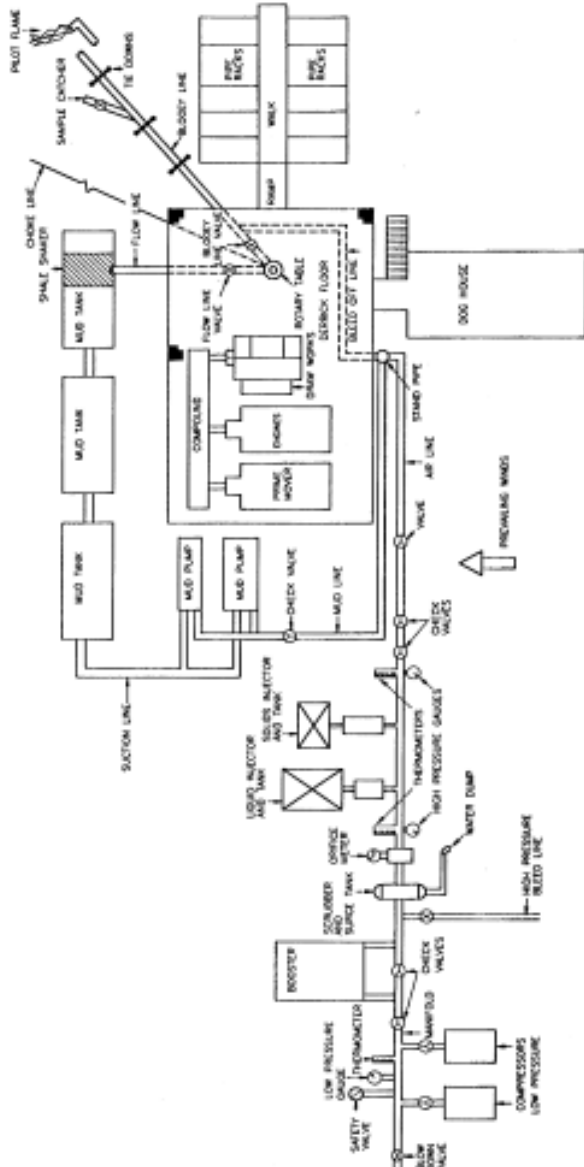
Figure 2-1: Drilling rig location plan for air drilling operations [1].

Note that Figure 2-1 shows a drilling location that is oriented so that the blooey line exit is downwind of the prevailing wind over the site. This keeps dust or smoke from blowing across the location.

2.2 Flow Line to the Rig

The flow line to the standpipe of the drilling rig acts as a manifold collecting the compressed air outputs from the primaries. These flow lines are API 2 7/8 inch (OD), or 3 1/2 inch (OD) steel line pipe (or ASME equivalent) [5]. The valves in the flow line at the booster compressor allow the air flow from the primaries to be diverted to the booster when high compression of the air is needed. When higher compression is not needed the booster compressor is isolated with the check valves in the flow line to the rig.

2.2.1 *Bleed-Off Line*

The bleed-off line allows pressure to be released throughout the flow line to the rig and inside the standpipe, rotary hose, kelly, and the drill pipe to the depth of the first float valve (see Figure 2-1). The bleed-off line is usually run to the blooey line and exits into that line.   The bleed-off line is generally used when drill pipe connections are made, replacing the drill bit (making round trips), and for other operations where the well is opened to the atmosphere.

2.2.2 *Scrubber*

The scrubber removes excess water in the compressed air flow in the flow line. If the humidity of the atmospheric air is high, then as the air is compressed in the compressors much of the water will return to the liquid state. Dry air drilling operations require the removal of this water before the compressed air is injected into the well.   The scubber is incorporated into a surge tank.   The water in the compressed air flow is collected in the bottom of the surge tank as the air flows through this tank and is vented from time to time to eliminate the water from the line.

2.2.3 *Water Injection Pump*

Unstable foam (mist) drilling operations require the injection of water into the compressed air flow before the air is injected into the well.   The water injection pump injects water, chemical corrosion inhibitors, and liquid foamers into the compressed air flow line. Figure 2-2 shows a skid mounted water injection pump for air and gas drilling operations. These skid mounted water injection pumps are used for the deep drilling operations. These pumps are capable of injecting up to 20 bbl/hr (at 42 gal/bbl) into the air or gas flow to the well.

The smaller drilling rigs have on-board water injection pumps. These smaller rig water injection pumps have capabilities from 10 to 25 gal/min. The small water injection pump carries out the same objective on these smaller rigs as the skid mounted water pump for the larger double and triple drilling rigs. The injection of water and appropriate chemicals and foamer is a vital option for air and gas drilling operations. Very few air and gas drilling operations are carried out without some water, chemical additives, and foam producing additives being injected.

Figure 2-2: Water injection pump (courtesy of Mountain Air Drilling Services).

2.2.4 *Solids Injector*

The solids injector is used to inject hole drying and hole stabilizing powders into the well to dry water seeping into the well from water-bearing rock formations. Other solids are often injected to reduce torque between the drill string and the borehole. These torque reduction solids are often necessary when drilling highly deviated and horizontal boreholes.

2.2.5 *Valves*

Both manually and remotely operated valves are located along the flow line to the rig. These valves are usually the gate or ball type. These valves cannot be operated in a partially open position. The abrasive nature of the compressed air flow in the flow line would erode the gate or ball of the valve and render the valve ineffective in the closed position. At strategic locations along the flow line are check valves. These special mechanical valves allow compressed air flow in only one direction (toward the standpipe). These check valves are spring loaded and the force of the flow allows the mechanism (flapper-gate or ball) to open in correct direction of flow. If the flow is reversed, the mechanism is forced closed by the spring and the force of the reverse flow.

2.2.6 *Gauges*

Each of the compressors is equipped with independent gauges to assess its operating performance. In addition to the compressor gauges are those placed along the flow line. A low pressure gauge is placed downstream of the primary compressors but upstream of the booster compressor. This gauge allows assessment of the performance of the primaries. A high pressure gauge is placed downstream of the booster compressor to assess the performance of the primaries and booster when high pressure compressed air is required. Pressure gauges are also placed upstream and downstream of the water injection pump and the solids injector. These gauges allow assessment of the performance of these injection systems. All these gauges must be high quality gas gauges. Most drilling rig floors are equipped with a mud

pressure gauge. For air drilling operations this mud gauge must be replaced with a high quality gas gauge having the appropriate pressure range.

2.2.7 *Volumetric FlowRate Meters*

No driller would carry out a mud drilling operation without knowing the volumetric flow rate of mud being circulated to the well. The volumetric flow rate from a mud pump can be easily assessed by either counting strokes per minute of the mud pump (and knowing the capacity of the pump in gallons per stroke and then calculating the output of the pump in gallons per minute), or by providing the rig floor with an accurate volumetric flow rate gauge.

The volumetric flow rate of air (or other gases) to the well is vital knowledge for a successful drilling operation and its knowledge must also be made available to the rig personnel. Volumetric flow rate of air (or other gases) is referenced to the atmospheric conditions of the air entering the primary compressor. At sea level locations the volumetric flow rate is given as standard cubic feet per minute (scfm). At locations above sea level the volumetric flow rate is given as actual cubic feet per minute (acfm).

There are two techniques for determining the air volumetric flow rate from the primary compressors (or natural gas from a pipeline). A gas production orifice plate with associated recording system can be used in the flow line downstream of the compressors and scrubber, but upstream from the water injection pump. Figure 2-3 shows a simple schematic of an orifice plate with a differential pressure gauge to measure the difference between the pressure upstream and downstream of the plate. Chapter 9 gives detailed orifice plate example calculations for determining volumetric flow rate from flow line pressure gauge readings.
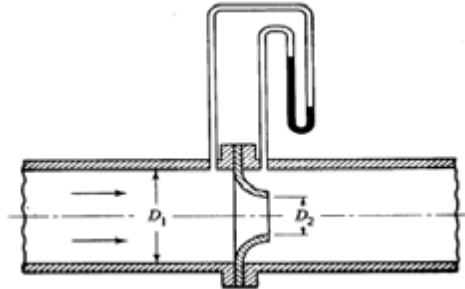
Figure 2-3: Schematic of orifice plate and manometer differential pressure gauge.

The other volumetric flow rate metering device is the gas turbine flow meter. Figure 2-4 shows this type of flow meter. Figure 2-5 shows the placement of this type of flow meter in an ASME 2 inch nominal diameter steel pipe (or API 2 3/8 inch (OD) line pipe). Figure 2-6 shows the digital readout that accompanies the turbine flow meter. The turbine and read-out need to be correlated for the flow gas specific gravity and the location atmospheric conditions. The digital read-out can also be wired to the rig floor to allow the driller and other rig personnel to assess the operation of the compressors.
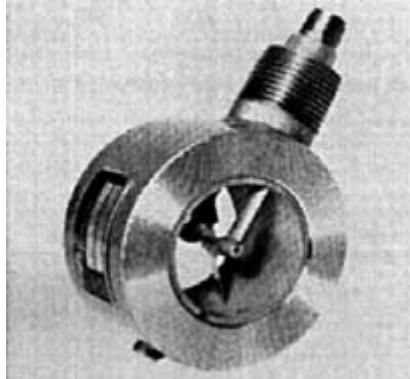
Figure 2-4: Turbine flow meter (courtesy of Halliburton Energy Services, Incorporated).
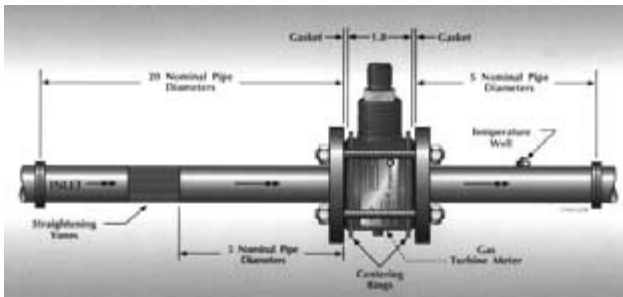
Figure 2-5: Installation of the turbine flow meter in ASME 2 inch nominal diameter pipe (courtesy of Halliburton Energy Services, Incorporated).

Figure 2-6: Digital display for the turbine flow meter (courtesy of Halliburton Energy Services, Incorporated).

2.3 Wellhead Equipment

All air and gas drilling operations require the use of a rotating head (or similar air or gas flow diverter) which is installed below the rotary table.   The blowout preventer (BOP) stack is always used when subsurface overpressured dangerous gases or fluids might be encountered while drilling (i.e., oil and natural gas drilling operations, and geothermal drilling operations).   Figure 2-7 shows schematics of three typical wellhead assemblies for double and triple drilling rigs set up for air and gas drilling operations to recover oil and natural gas, or geothermal fluids [6].

Typical BOP Stacks
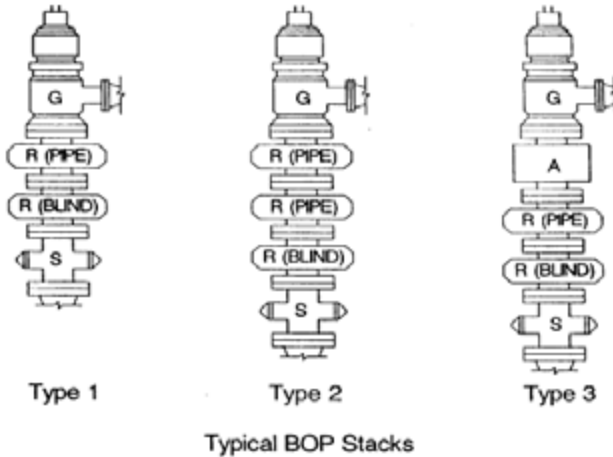
Figure 2-7: Typical wellhead assemblies for an air and gas drilling operation (G denotes a rotating head, A denotes an annular blowout preventer, R denotes pipe or blind rams, and S denotes the drilling spool).

2.3.1 *Rotating Head*

The rotating head or a similar air flow diverter was developed for use in air and gas drilling operations to keep air or gas with entrained rock cuttings from flowing to the drilling rig floor through the rotary table kelly bushings.   Diverting this drilling fluid flow from the drilling rig floor is mandatory for all air and gas drilling operations.   Even on small drilling rigs the air exiting the annulus (direct circulation) must be diverted in order to provide a safe work space for the rig operators. These diverter devices were developed with the introduction of air and gas drilling operations in the early 1930's.

The right side of the rotating heads shown in Figure 2-7 shows the vent to the blooey line. Figure 2-8 shows a low pressure rotating head.   This rotating head is capable of diverting a 500 psig air or gas flow while rotating at 100 rpm (and 1,000 psig with no rotation). This rotating head is made up (via the flange fitting on the bottom of the head) to the top of a BOP stack or the top of a casing spool and casing. The BOP stack is incorporated in the wellhead assembly when overpressured dangerous gases or fluids may be encountered in the drilling operation

(see Figure 2-7).   Typically the BOP is used for all deep wells.   The type of rotating head shown in Figure 2-8 is used with large drilling rigs.   Direct circulation or reverse circulation drilling operations can be carried out with these rotating heads. This particular rotating head is available in a 8.25 inch bore design (Model 8000) and a 9.00 inch bore design (Model 9000).

Figure 2-8: Low pressure rotating head (courtesy Williams Tool Company).

Figure 2-9 shows an exploded view of the four major sections of the rotating head.   The top three sections are the internal sections of the head and are easily removed in the field from the fourth (bottom) section (the bowl or main housing and quick-lock clamp assembly).   The top section in the figure is the kelly driver with lugs on its side that lock into the bearing assembly shown below it.   The bearing assembly has bearings and bearing seals that allow the inside of this assembly to rotate with the drill string and its outside to seal inside the non-rotating housing (i.e., the bowl and quick-lock clamp assembly).   Attached to the bottom of the bearing assembly is the stripper rubber (or flexible packer).   The stripper rubber is designed to fit tightly around and rotate with the kelly, the drill pipe, the drill pipe tool joints, and any crossover subs in the drill string. Any air or gas pressure in the annulus of the well acts to force the stripper rubber to fit more tightly around the kelly and drill string.

In order to place the drill string and kelly into the well, the quick-lock clamp must be unlocked and the three rotating internal sections lifted to the rig floor.   The drill bit with the drill collars are placed in the well through the open rotating head. The internal sections of the rotating head are fitted over the bottom tool joint of the drill pipe.   The bottom drill pipe joint is lowered into the well and the internal sections placed into the rotating head and the quick-lock clamp locked.   This secures the rotating head for drilling operations.   Drill pipe can be lowered into the well through the rotating head as the drill bit is advanced. The kelly drive (together with the kelly bushing) fits snugly around the kelly and allows the internal rotating sections of the head to rotate with the rotation of the drill string.   If it is anticipated that a well will be making large volumes of natural gas, the bottomhole assembly of

the drill string is designed to allow the stripper rubber to be stripped over the drill collars to the drill bit.

The procedures for placing the drill string into a well and removing it from the well must be carefully followed when a well is making natural gas or geothermal steam or hot water (or any other dangerous gases or fluids). There are other operations performed by a drilling rig that involve the use of the rotating head and that must be carefully carried out if a well is making gas or geothermal steam (e.g., placing a casing string or a liner string in a well).
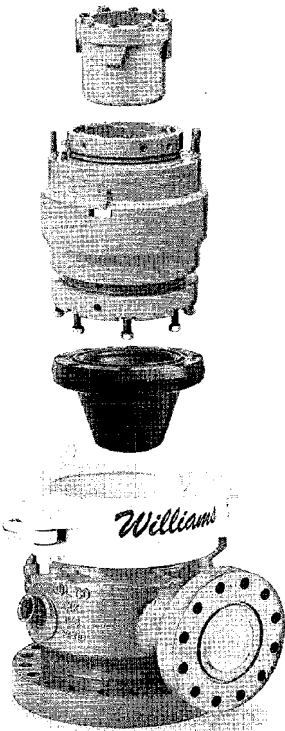
Figure 2-9: Rotating internal parts of the rotating head (courtesy of Williams Tool Company).

Figure 2-10 shows a cut-a-way view of a typical rotating head. This figure shows the rotating head in the drilling position with the kelly inside the head. The kelly drive section has a kelly bushing which can be changed to accommodate various kelly designs. The spindle subassembly rotates with the drill string. The spindle housing subassembly (which does not rotate) seats into the main body

housing of the head and seals to prevent air or gas from passing to the rig floor. The stripper rubber (flexible packer) diverts the air or gas with entrained rock cuttings to the outlet (to the blooey line). The flexible stripper rubber is forced by air (or gas) flow pressure against the outer surface of the kelly or drill pipe. There are other seals between the rotating assembly and the spindle housing. Together all these sealing agents divert the air or gas flow (with entrained rock cuttings) to the blooey line and away from passage to the rig floor (see Figure 2-10).
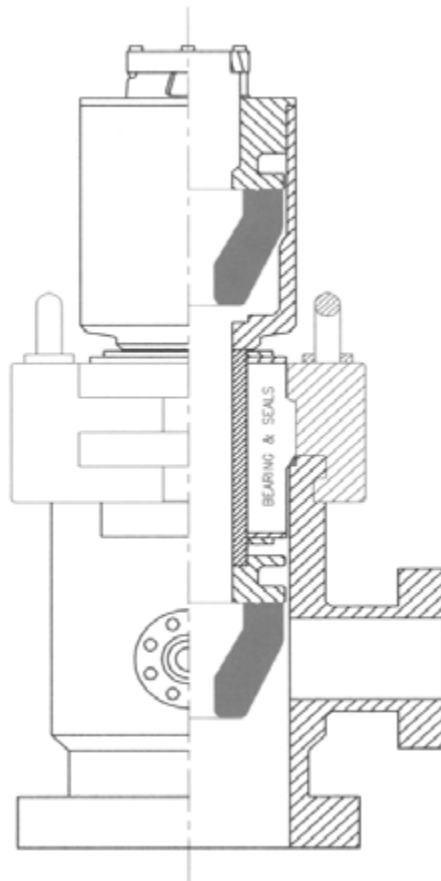
Figure 2-10: Cut-a-way view of a rotating head with dual stripper rubbers (courtesy of Williams Tool Company).

Although the rotating head was originally developed for air and gas drilling operations, this device was adapted for use in geothermal drilling operations and

later for use in underbalanced drilling operations to recover oil and natural gas. These recent applications have encouraged the development of rotating heads capable of operating at higher pressures and temperatures. High pressure heads are used in underbalanced drilling operations where light weight drilling mud (or other drilling fluids) is used to drill through pressured oil or natural gas rock formations. The light weight drilling mud (or other drilling fluids) allows oil and gas to flow into the well bore as the drill bit advances into the rock formation. When these reservoir fluids are circulated to the surface they impose high pressures on the wellhead equipment. These higher pressure heads are capable of operating at pressures up to approximately 1,500 psig (while rotating the drill string at about 100 rpm) and up to approximately 3,000 psig (for the non-rotating drill string). The high temperature rotating heads are generally used in geothermal drilling operations. Most of these heads can operate with steam and hot water flows at temperatures up to about 500˚F. High temperature rotating heads usually have a high pressure capability.

Rotating heads are also used in air and gas drilling operations where subsurface high overpressured oil, natural gas, or geothermal fluids are not expected. These are deep water well, deep monitoring well, deep mining borehole, and deep geotechnical borehole drilling operations where double and triple drilling rigs are required. These rotating heads are used to keep air or gas (in this case nitrogen) flow with entrained rock cuttings from flowing to the rig floor (for direct circulation). But many of these non-oil, natural gas, or geothermal recovery drilling operations utilize reverse circulation. Reverse circulation requires that the compressed air or gas be injected into the "outlet" of the rotating head to the annulus space of the borehole (see Figure 2-10). In this situation the rotating head still keeps the air or gas from flowing to the rig floor.

Air and gas drilling operations using small single drilling rigs drill only shallow (usually less than 1,000 ft in depth) water wells, monitoring wells, mining boreholes, and geotechnical boreholes (see Figure 1-3). Some of the air drilling operations on these small rigs use direct circulation, but most utilize reverse circulation. These small single drilling rigs usually have hydraulic top head rotary drives. The rig "floor" (the break-out platform) on these small rigs is protected from cuttings returns by a rubber seal around the drill string and a flexible skirt around the edge of the floor (skirt not shown in figure). When direct circulating, the air returning up the annulus (with the entrained rock cuttings) is kept from coming through the rig floor by the rubber seal around the drill string. The operator at the control panel is protected only by the skirt around the edge of the floor. The drilling cuttings are allowed to accumulate on the surface of the ground around the top of the borehole where the skirt slows the air flow and allows the cuttings to be dropped out.

Reverse circulation provides a useful way for dealing with the return flow of compressed air and entrained rock cuttings from the borehole. The compressed air is injected into the annulus of the borehole via a sealed fitting at the top of the annulus, or a dual drill pipe annulus fitting. After circulating through the bit, the air with entrained rock cuttings exits the borehole through the inside of the drill string, then flows through the top head rotary drive, and then through the rotary hose. The air with the cuttings can be diverted to a pit away from the rig with a hose extension, or the hose extension run to a cyclone separator where cuttings samples

can be obtained for analysis. Air drilling operations using small single drilling rigs are generally safer for the operators and more environmentally clean when utilizing reverse circulation. More details on reverse circulation operations will be given in Chapter 9 and 10.

2.3.2 *Blowout Prevention Stack*

Blowout prevention equipment was developed for use in drilling deep wells for the recovery of oil and natural gas. Later this unique oil and gas industry equipment was adapted for use in drilling deep geothermal wells. Natural deposits of oil and gas exist in porous rock formations deep in the earth's crust. These deposits were created by millions of years of sediment burial and confinement by geologic structures. Over time, increased sedimentary burial created high pressures and temperatures in these deposits. Most newly discovered oil and natural gas deposits have static pressures up to about 8,000 psi and temperatures of about 300°F. There are a few abnormally pressured natural gas deposits that have static pressures as high as 16,000 psi. These pressures, although found in deposits at depths of 10,000 ft or greater, are quite dangerous to drilling rig personnel and the environment. Blowout prevention equipment (or the BOP stack) were developed to provide protection of surface from these high pressured deposits.

A blowout occurs when oil and/or natural gas deposits are allowed to flow uncontrollably to the atmosphere at the surface. The first line of defense against the dangers of these high pressure deposits is weighted drilling mud. Water based and oil based drilling muds can be designed so that their specific weights are sufficiently high to provide bottomhole pressures that are slightly higher than the static pressure of the deposits when the drill bit penetrates the host rock formation. When drilling exploratory wells it is not possible to precisely know the static pressure in target oil or natural gas deposits. Therefore, geologic and engineering judgment must be used to estimate the static pressures that might be encountered. These estimates are used to design the weighted drilling mud. But even after the first exploratory wells have been successfully drilled and the oil or gas field is being developed with follow-on development wells, surprises in deposit pressures can occur. When too light a drilling mud is used and a high pressure deposit is drilled, the well will receive a liquid or gas "kick." A kick is a slug of formation liquid and/or gas that has flowed from the formation into the annulus of the well bore. The kick is composed of fluids that have lower specific weights than the heavily weighted drilling muds. Therefore, the kick will "float" in the drilling mud and rise rapidly to the surface. If the kick is mostly natural gas, the gas will expand as it moves up the drill string annulus to the surface. The surface wellhead equipment is the second line of defense against a blowout. The wellhead equipment in the form of the BOP stack must be engineered so that it is capable of containing the high pressure of this gas when it reaches the top of the annulus. This BOP stack must contain this gas pressure while the slug is circulated under control to the surface and expelled from the annulus via a flow line to a remote burn area where the slug can be safely burned off.

The BOP stack can be composed of two types of preventers; 1) the ram-type blowout preventer and, 2) the annular-type preventer. The ram-type preventer can be a blind (shear) ram and or a pipe ram. The blind ram is capable of sealing the well completely by compressing the drill pipe from two sides and failing the pipe steel

structure in a manner to prevent the well fluids from escaping to the surface through either the inside of the drill pipe or around the outside of the drill pipe. This vise like action of the two rams essentially forces the pipe to deform between the two rams. The pipe ram acts in a somewhat similar manner as the blind ram. Except the pipe ram has a geometric shape on the end of the rams that conform to the outside surface of the drill pipe. Thus the pipe ram seals against the outside of the drill pipe and prevents well fluids from escaping to the surface around the outside of the drill pipe. The pipe ram does not fail the pipe structure, therefore, drilling mud can be circulated down the inside of the drill pipe to safely allow the kick to be circulated to the surface.

Figure 2-11 shows a cut-a-way view of a twin ram-type blowout preventer. A typical twin preventer will have a pipe ram on the top and a blind ram on the bottom. The cut-a-way shows the bottom blind ram. In the event of a blowout, the pipe ram would be used to seal the well and allow the slug in the annulus to be safely circulated to the surface. In the event that the pipe ram cannot seal the well for the safe circulation of the slug, the blind ram can be actuated to seal the well. These rams can be actuated manually or hydraulically. Figure 2-11 shows the blind rams on the bottom are set up to be actuated manually.
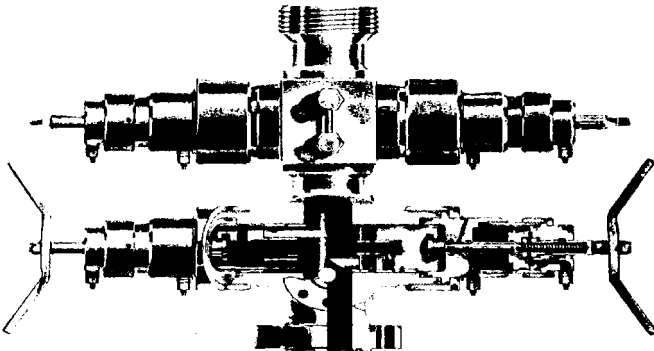
Figure 2-11: Typical twin ram-type blowout preventer (courtesy of Bowen Tools, Incorporated).

This twin ram-type blowout preventer is flange connected (made up) to the top of the well casing. The bottom of the casing spool is threaded (or welded) to the top of the casing. The top of the spool is flange connected to the bottom flange fitting of the twin ram-type blowout preventer.

Figure 2-7 shows a Type 1 BOP stack which utilizes only the twin ram-type blowout preventer for well control. This BOP stack is fitted with a rotating head flange connected to the top of the twin ram blowout preventer. This is the standard well control set up for air or gas drilling operations directed toward the recovery of oil and natural gas deposits with static bottomhole pressures of the order of 3,000 psi or less. Figure 2-7 shows a Type 2 BOP stack which utilizes three ram-type blowout preventers for well control. This BOP stack is configured with two pipe

rams on the top and a blind ram on the bottom. The two pipe rams allow some flexibility in carrying out well control when drilling deep wells with a tapered drill string and when placing a liner string in an air or gas drilled well. This BOP stack is fitted with a rotating head flange connected to the top pipe ram blowout preventer. This stack can be configured for the recovery of oil and natural gas deposits with static bottomhole pressures of up to 5,000 psi.

The annular-type blowout preventer can also be used in a BOP stack (see Type 3 in Figure 2-7). An annular preventer is hydraulically operated. Figure 2-12 shows a cut-a-way view of a typical annular preventer. The closing of the preventer is actuated by hydraulic pressure. This hydraulic pressure forces the operating piston upward against a pusher plate (see Figure 2-12). The pusher plate in turn displaces (compresses) an elastomer donut inward to close and seal on the outer surface of drill pipe, drill collar, casing, or liner. Utilizing an annular preventer in conjunction with ram blowout preventers greatly increases well control flexibility and general rig safety when drilling with air and gas drilling fluids. The Type 3 BOP stack in Figure 2-7 is configured with twin ram-type blowout preventer on the bottom (pipe ram on top and blind ram on the bottom), an annular preventer flange connected to the top of the twin ram preventer, and a rotating head flange connected to the top of the annular preventer. This BOP stack can be configured for the recovery of oil and natural gas deposits with static bottomhole pressures of up to 10,000 psi.
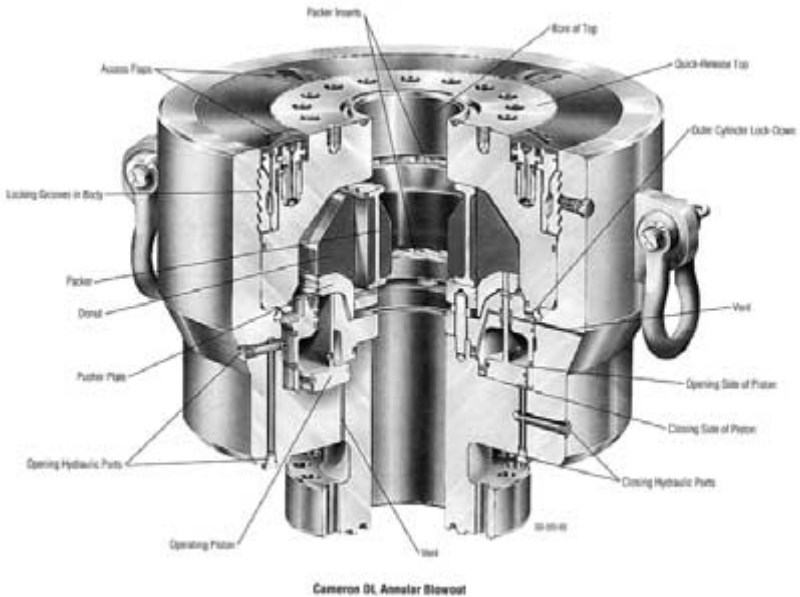
Figure 2-12: Typical annular blowout preventer (courtesy of Cooper Corporation).

Figure 2-13 shows a schematic of a more recent innovation in BOP stack design. This configuration is a variation of the standard Type 3 shown in Figure 2-7. Figure 2-13 shows the addition of a pipe ram below the drilling spool. This BOP configuration has evolved for use in underbalanced drilling and completion operations. Underbalanced drilling operations allow the oil and natural gas fluids to continue to be produced by the reservoir formation as the rock is penetrated by the advance of the drill bit. In order for underbalanced drilling operations to be successful, the oil and natural gas formations must be allowed to flow even when connections are being made, during liner operations, or during well completion operations (after drilling operations). The addition of the pipe ram below the drilling spool increases BOP flexibility to accommodate these operations. With the drill string or tubing string in the well and with the upper pipe ram closed, drilling on completions fluids with entrained formation fluids can be safely circulated to the surface through the choke line (attached to the drilling spool). The bottom pipe ram provides a back-up well control device during these operations [7 and 8].
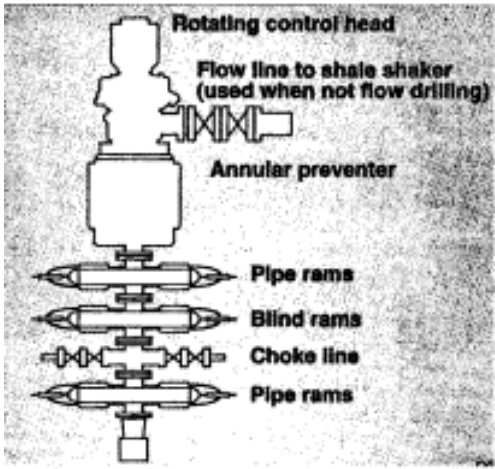
Figure 2-13: Schematic of recent BOP stack design for underbalanced drilling operations.

2.4 Flow Line from Rig

Air and gas drilling operations require a variety of flow line designs from the drilling rig. Drilling operations using compressed air or other compressed gases require the use of large inside diameter flow lines. These return flow lines should be designed not to choke the air or gas flow as it exits the circulating system. This line is known as the "blooey line" which derives its name from the sound made when a slug of formation water is ejected from the line with high velocity air or gas (see Figure 2-1). Aerated drilling operations require return flow lines that are similar to those of conventional mud drilling operations since volumetric flow rates are very similar. These return lines are usually longer in length than the conventional mud return flow lines. The air in the returning aerated fluid with entrained rock cuttings

is released to the atmosphere as the fluid exits the flow line. Foam drilling return flow lines are large diameter pipelines and are unique in that they must be equipped with valves to allow the choking of the return flows.

2.4.1 *Blooey Line*

Figure 2-1 shows the blooey line exiting from the drilling rig annulus for direct circulation operations. Blooey lines (or equivalent) are required for all air and gas drilling operations and are needed to keep drilling rock dust and cuttings away from the drilling rig and rig personnel. Blooey lines must be secured to the ground surface with tie-downs (see Figure 2-1). The high velocity of the air or gas flow from the well will interact with the flexible blooey line to set up an aerodynamic flutter situation which is very similar to the motion of a water hose on the ground when the water valve is turned on. This flutter situation can result in high dynamic forces and resulting blooey line movement.   This potential movement must be constrained along its length by tie-downs to the ground.

The blooey line should be designed with a inside cross-sectional area greater (by a factor of ~1.1) than the annulus cross-sectional area at the top of the well.   In general this is not practical when drilling the shallow larger diameter borehole sections.   This requirement applies to the drilling of the deep smaller diameter borehole sections. Therefore, the inside diameter of the blooey line, d_b(inches), should be approximately

$$d_b \ge \left[1.1 \left(d_c^2 - d_p^2\right)\right]^{0.5} \tag{2-1}$$

where d_c is the inside diameter of the casing at the top of the well (inches) and d_p is the outside diameter of the drill pipe at the top of the well (inches).

The typical length of the blooey line for large drilling rigs is from 100 ft to 300 ft. This line is run from the annulus to a burn pit (see Figure 2-1).   The air or natural gas drilling fluid with the entrained rock cuttings flows from the annulus down the blooey line and exits at the burn pit. The rock cuttings are dropped in the burn pit and any natural gas is ignited by the pilot flame at the blooey line exit.

In some operations the single blooey line is replaced by two parallel smaller diameter lines.   In this situation the inside cross-sectional area of the two lines should also be designed to be greater (by a factor of ~1.1) than the annulus cross-sectional area at the top of the well.

All blooey lines should be equipped with two high pressure gate valves. These valves are located on the horizontal blooey line at its entrance (just downstream from the Tee turn where the return flow from the annulus turns to horizontal flow in the blooey line). Figure 2-13 shows these two valves on the horizontal flow line (blooey line) just below the rotating (control) head. During drilling operations these valves are in the full open position to prevent erosion. These valves are an added safety feature allowing the well to be closed when the surface pressure in the well is low.   But the valves can also be used to carry out some rudimentary well testing operations (e.g., static wellhead pressure, wellhead flowing pressure and volumetric flow rate, etc.).

2.4.2 *Burn Pit*

Figures 2-1 and 2-14 show the burn pit at the exit end of the blooey line. The burn pit should always be located away from the standard mud drilling reserve pit (water storage for an emergency mud drilling operation). This design of pit location prevents any hydrocarbon liquids from flowing into the reserve pit, thus, preventing reserve pit fires near the rig. The burn pit is located downwind from the drilling rig. Such a location keeps the smoke and any dust from the drilling operation from blowing back over the drilling rig. The burn pit must be lined with an impermeable layer of commercial clay to prevent contamination of surrounding soil and ground water. Usually the burn pit is designed with a high berm (~6 ft) at one side of the pit (opposite the exit from the blooey line). This berm prevents high velocity rock particles and liquid slugs from passing over the burn pit. The burn pit is part of the drilling site location preparation.
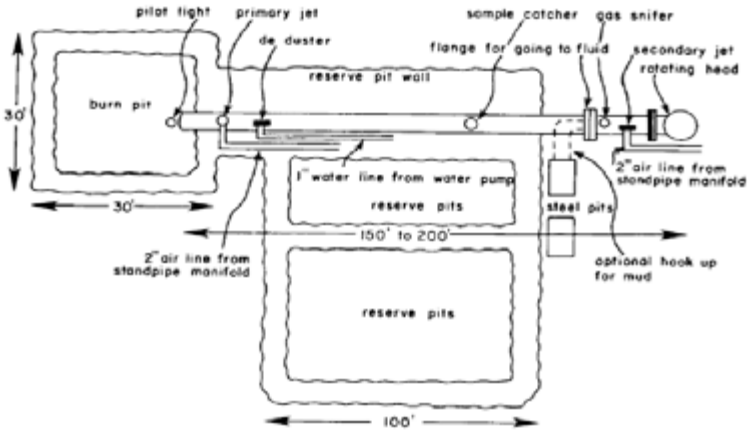
Figure 2-14: Schematic of burn pit, reserve pit, and blooey line plan [3].

2.4.3 *Primary and Secondary Jets*

Figure 2-14 shows the exit positions in the blooey line of the primary and secondary jet flow lines from the compressors. Figure 2-15 shows the high pressure vent lines from the compressor for the primary and secondary jet flow lines. These jet flow line installations in the blooey line are only required for drilling operations directed toward the recovery of oil, natural gas, or geothermal gas products.

Primary and secondary jets are incorporated into the blooey line to allow the safe venting of the top of the wellhead when the well is producing natural gas or other dangerous gas. These lines allow for the direct discharge of compressed air from the compressors into the blooey line. This discharge into the closed blooey provides jet pumping action which forces any gas venting from an atmosphere exposed wellhead to flow to the blooey line and exit this line at the burn pit. Figure 2-15 shows the surface layout of the flow line from the compressors to the standpipe. This figure shows the high pressure vent flow lines to the primary and

secondary jets. The primary jet positioned near the exit end of the blooey line and the secondary jet near the entrance end of the blooey line just downstream of the tee from the annulus (see Figure 2-14).
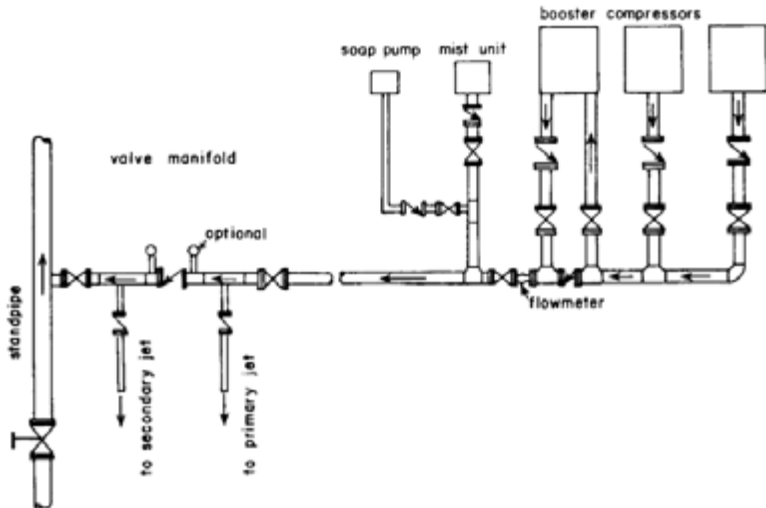
Figure 2-15: High pressure vent lines to the primary and secondary jets[3].

2.4.4 *Sample Catcher*

Sample catchers are usually required for any air and gas drilling operation. The sample catcher allows small rock cutting samples to be obtained from a well during the drilling operation. The sample catcher is installed in the body of the blooey line usually near the entrance to the blooey line (see Figure 2-14). Figure 2-16 shows a typical sample catcher design. This design has a small diameter (2 inch nominal diameter or smaller) transport pipe welded through the blooey line body. A short section of this small pipe protrudes into the flow stream inside the blooey line. Inside the blooey line there is a short section of angle iron welded to the small transport pipe. This angle iron directs the cuttings into the small transport pipe. Outside the blooey line there is a gate valve on the small pipe to allow discharge of sample rock cuttings.   Since the flow of air or gas up the annulus is at high velocities (of the order of 50 ft/sec to 80 ft/sec), cuttings sampling can be accurately correlated to subsurface rock formations being drilled.

The securing of rock cuttings from the depths is an essential practice when drilling deep boreholes. At the drilling location, these rock cuttings samples can be studied under a microscope and analyzed to ascertain chemical and physical properties. Knowledge of the rock characteristics and properties allows geologists and drilling engineers to identify the rock formations being penetrated as the drill bit

is advanced. This information allows the drilling operation to accurately drill to a subsurface target area.
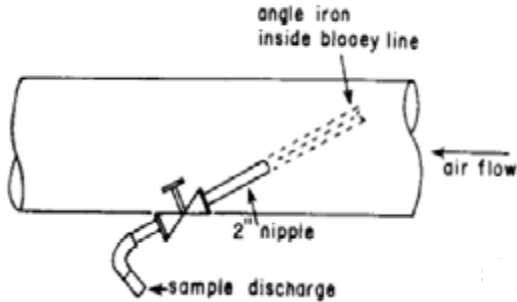
Figure 2-16: Typical sample catcher designs [3].

2.4.5 *De-Duster*

De-dusters are usually required for any air or gas drilling operation. Figure 2-14 shows the location of the de-duster near the exit end of the blooey line.   Figure 2-17 shows a typical de-duster design. The de-duster is a small diameter pipe (2 inch nominal diameter or smaller) water system located inside the blooey line. A pump supplies the system with water. The water is sprayed on the dry rock dust particles that exit the line. This reduces or eliminates the dust clouds that are typical of dry air or natural gas drilling operations.
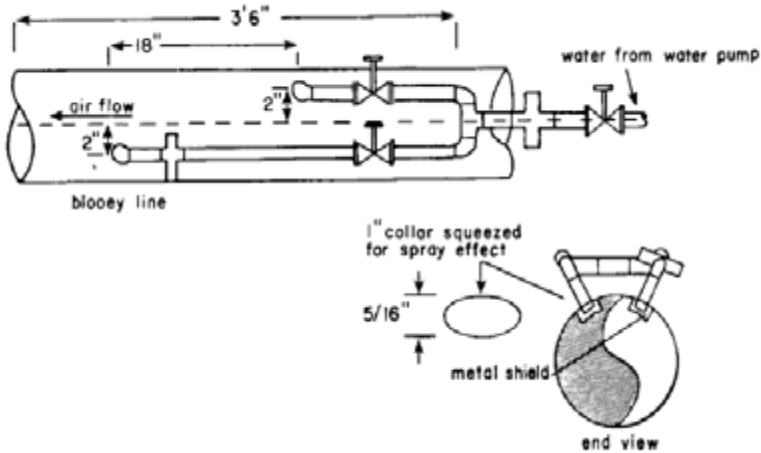
Figure 2-17: Typical de-duster design [3].

2.4.6 *Gas Detector*

Gas detectors (gas sniffers) are used only in air drilling operations directed at the recovery of oil and natural gas. Figure 2-14 shows the position of the gas detector on the blooey line. This detector can detect very small quantities of hydrocarbons that might enter the blooey line from the annulus. As the drill bit is advanced and hydrocarbon producing formations are drilled, the hydrocarbons are entrained in the return air flow to the surface with entrained rock cuttings. The detector alerts the drilling rig crew that hydrocarbons are in the annulus. This alert allows rig personnel to take safety precautions against subsurface and surface fires or explosions.

2.4.7 *Pilot Light*

Figures 2-1 and 2-14 show a pilot light at the end of the blooey line. Pilot lights are used only in air or gas drilling operations directed at the recovery of oil and natural gas. The pilot light is a small open flame (propane or natural gas) maintained at the end of the blooey line to ignite and burn any hydrocarbons that might exit the line as the drilling operation progresses. Many new air and gas drilling operations are equipped with electric igniters instead of open flame pilot lights.

References

1. Mitchell, B. J., Personal communication, November 1982.

2. Moore, W. W., *Fundamentals of Rotary Drilling*, Energy Publications, 1981.

3. Hook, R. A., Cooper, L. W., and Payne, B. R., "Air, Mist and Foam Drilling: A Look at Latest Techniques: Parts I and II," *World Oil*, April and May 1977.

4. "Bulletin on Performance Properties of Casing, Tubing, and Drill Pipe," *API Bul 5C2*, Twentieth Edition, May 31, 1987.

5. "API Specification for Line Pipe," *API Spec 5L*, Thirty-Fourth Edition, May 31, 1984.

6. "API Recommended Practices for Blowout Prevention Equipment Systems for Drilling Wells," *API RP 53*, First Edtion, February 1976.

7. Bourgoyne, A. T., "Rotating Control Head Applications Increasing," *Oil and Gas Journal*, October 9, 1995.

8. Hannegan, D. M., "RCHs Lower Cost, Boost Productivity," *The American Oil and Gas Reporter*, April 1996.

This page intentionally left blank.

Three

Downhole Equipment

Air and gas drilling operations require some special subsurface equipment and drilling methods that are not normally used in rotary mud drilling operations. Deep direct circulation operations use rotary drill strings that are similar to those used in mud drilling. But even these drill strings are equipped with downhole tools unique to air and gas drilling operations.

Larger diameter shallow and intermediate depth wells are usually drilled with reverse circulation techniques. These techniques and their associated equipment are virtually unknown to those who drill deep small diameter wells.

3.1 Rotary Drill String

There are two general types of drill strings used in air and gas drilling operations. The standard drill string discussed below is used almost exclusively for deep direct circulation operations. The dual wall pipe drill string is used exclusively for intermediate and shallow depth reverse circulation operations.

3.1.1 *Standard Drill String*

Figure 3-1 shows a schematic of a standard rotary drill string used to drill deep boreholes with direct circulation. Such a drill string would be used on large drilling rigs. At the bottom of the drill string is the drill bit. The drill bit is threaded (made-up) to a bit sub. The drill bit has a male thread or threaded pin pointing up. The bit sub is a short thick wall pipe that has a female thread or threaded box on both ends. Above the bit sub are the drill collars. Each of the drill collars and most

of the remainder of the components in the drill string are designed with a threaded pin down and a threaded box up. The bit sub is used to protect the bottom threads of the bottom drill collar from the wear caused by the frequent drill bit changes that are typical for all deep drilling operations. A drill collar is a thick wall pipe that provides the weight or vertical axial force on the drill bit allowing the drill bit to be advanced as it is rotated (see Figure 1-2). Usually there are a number of drill collars in a drill string. The number of drill collars in a drill string depends on how much weight-on-bit (WOB) is required to allow the drill bit to be advanced efficiently (drill string design will be discussed in Section 3.6). The drill collar lengths are in accordance with the range designations of Table 1-1 [1].
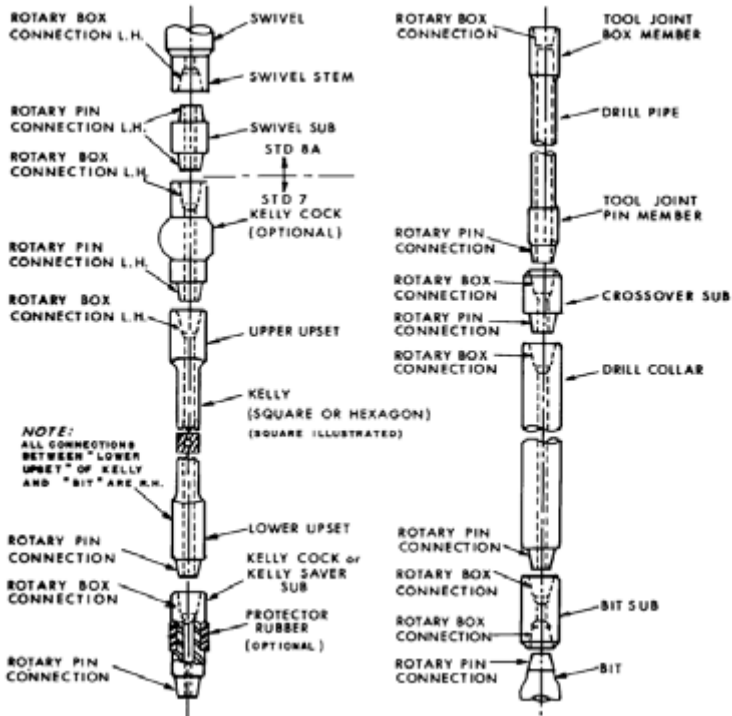
Figure 3-1: Standard rotary drill string for direct circulation.

Generally the drill collars in a drill string have the same thread design. Above the drill collars are the drill pipe joints. The drill pipe joint lengths are also in accordance with the range designations of Table 1-1. The threads of the drill collar connections are usually not the same as the threads of the drill pipe joint connections (tool joints). Therefore, a special crossover sub must be used to mate the drill collars to the drill pipe. The crossover sub is a short thick walled pipe with a threaded pin down (with the drill collar threads) and a threaded box up (with the drill

pipe threads). The number of drill pipe joints is determined by the depth of the borehole to be drilled. Only the drill collars can be placed in compression (to place weight on the bit). The drill pipe joints are always kept in tension [1].

All of the threaded connections in drill strings are API threaded shoulder connections. There are a variety of these connections and they will be discussed in detail in Sections 3.3 and 3.4. Figure 3-2 shows a typical API threaded shoulder connection for a drill pipe. As can be seen, the connection has matching flat shoulders on the pin and on the box. When a pin and box are made up, the flat surfaces of the shoulders mate against each other and seal to form a strong structure that is also leak proof. The shouldered connection protects the thinner walled body of the drill pipe and the threads inside the connection from damage when the drill string (and the connection) are flexed when bent in a deviated borehole [2].
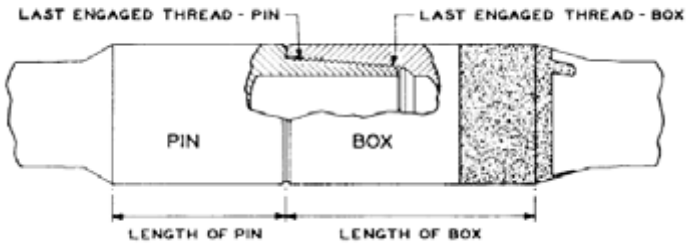
Figure 3-2: Cutaway of a made-up API shouldered connection.

At the top of the drill pipe section is the kelly cock (or saver) sub. The kelly cock sub is another crossover sub. But this sub is used to protect the bottom threads of the kelly. Even if the threads at the bottom the kelly are the same as the drill pipe threads, this special crossover sub is usually used. As drilling progresses additional elements of drill pipe are added to the top of the drill string. The kelly is a special type of drill pipe with a square or hexagon outer surface. The rotary table grips the outside of this pipe and provides the torque to the drill string to make it rotate. Thus, as additional drill pipe are added to the drill string as the bit advances in the borehole, drill pipe must be disconnected and a new pipe joint added. The bottom threaded box of the kelly save takes the wear of these repeated connections of drill pipe. All of the threaded components below the top threaded connection of the kelly are right hand threads. The rotary table rotates to the right (clockwise from the top view of the table). This rotation tightens the right hand threads below the table.

At the top of the kelly is a left-hand thread connection (threaded box). As drilling progresses, the rotary table, in addition to providing torque to rotate the drill string, also allows the kelly to slide through the table allowing the borehole to be deepened. Since the torque is applied along the square or hexagon outer surfaces of the kelly, the left hand thread at the top of the kelly is tightened by the inertial drag of the non-rotating components above the kelly. All of the components above the kelly are left hand thread connections. Above the kelly is a kelly cock sub (optional). The kelly cock is a special valve that allows the sealing off of the inside of the drill string in a blowout event during oil or natural gas drilling operations.

The kelly cock sub has a threaded pin connection down and a threaded box connection up. Above the kelly cock sub is a swivel sub. The swivel sub protects the swivel and has a threaded pin connection down and a threaded pin up. Above the swivel sub is the swivel. The bottom of the swivel has a threaded box connection down. The swivel is split into two sections, a rotating section on the bottom and a non-rotating section on the top (see Figure 1-5). The non-rotating section of the swivel is held in the mast by the traveling block and hoisting system. A sealed bearing allows the bottom section of the swivel to rotate while the top section is held by the traveling block. The swivel allows the circulation fluid (drilling mud or compressed air or natural gas) to flow through the swivel to the rotating drill string.

For direct circulation, the circulation fluid flows down the inside of the drill string to the drill bit, flows through the drill bit orifices (or nozzles), entrains the rock cuttings from the drill bit, and flows up the annulus between the outside surface of the drill string and the inside surface of the borehole.

3.1.2 *Dual Wall Pipe Drill String*

Intermediate and shallow depth large diameter wells can be drilled with direct circulation techniques. But reverse circulation techniques are more efficient and are the preferred techniques. The drilling industry has developed some very unique downhole tools for reverse circulation air drilling operations. Figure 3-3 shows a schematic configuration of a rotary reverse circulation operation using dual wall drill pipe.

Reverse circulation techniques are not restricted to air drilling operations. Reverse circulation techniques often use standard drill string like that shown in Figure 3-1. In the past two decades there has been a dramatic increase in the use of air drilling reverse circulation techniques for drilling water wells, monitoring wells, geotechnical boreholes, and other shallow (i.e., less than 3,000 ft) wells. The increased use of reverse circulation techniques has been encouraged by the development of new technologies. One of these innovations is the development of dual wall drill pipe.

Rotary dual wall pipe reverse circulation operations must be used on drilling rigs equipped with hydraulic rotary top drive systems (for single drilling rigs) or with hydraulic power swivel systems (for double and triple drilling rigs) to rotate the drill string. Dual wall pipe is quite rigid and has a much higher weight per unit length than standard single wall drill pipe. Thus, dual wall pipe can be used like drill collars (the lower portion of the drill string can be placed in compression). The dual wall drill string in Figure 3-3 is shown rotating a tri-cone drill bit. The top drive system rotates the entire drill string. The tri-cone drill bits used in reverse circulation operations have the same cutting structures as tri-cone bits used in direct circulation operations. However, the reverse circulation bits are fabricated to allow the compressed air to flow from the annulus between the two walls of the dual wall pipe to the bit rock cutting face. At the bottom of the well the air flow entrains the rock cuttings and flows to the surface through a large center orifice in the drill bit that leads to the inside of the inner pipe of the dual wall pipe. The drill bit used in a dual wall pipe reverse circulation operation is selected to have a diameter that is slightly larger than the outside diameter of the dual wall pipe. Thus, the outside

annulus between the inside of the borehole and the outside of the dual wall pipe is kept quite small.   This outer micro annulus together with a skirt structure on the drill bit itself (see Figure 1-9) restrict the return flow to the surface of air and entrained rock cuttings to the inside of the inner pipe [3].
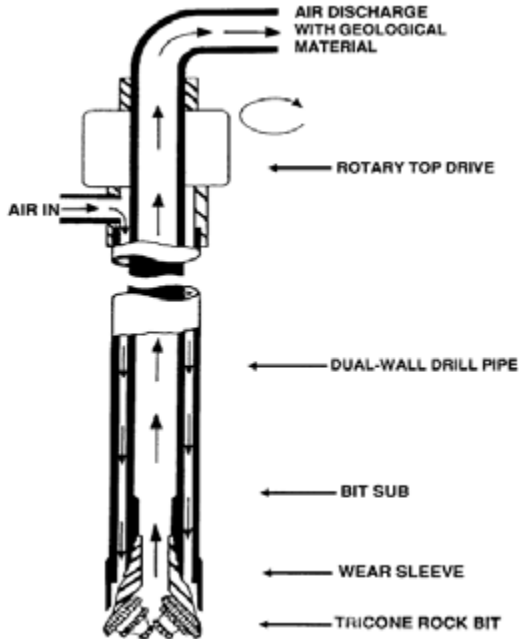
Figure 3-3: Dual wall pipe drill string for reverse circulation operations (courtesy of Foremost Industries Incorporated).

The drill string for a dual wall pipe reverse circulation air drilling operations is rather simple. These specially fabricated reverse circulation drill bits have a threaded box connection. The bit sub has a threaded pin connection down and threaded box connection up. The bottom threaded pin connection (of the bottom dual wall pipe joint in the drill string) is made up to the top connection of the bit sub.   Additional dual wall pipe are made up to each other and the top threaded box connection of the top pipe is made up a special side inlet sub (shown in Figure 3-4). This sub allows compressed air to be injected into the dual wall pipe annulus through the non-rotating outer section of the sub. The return flow of air and entrained rock cuttings from the inside of the inside pipe flows up through the rotating inner section of the sub to and through the rotary top drive.

The side inlet sub acts as the "first swivel" for the dual wall pipe drill string. This first swivel accommodates the injection of air into the circulation system while allowing the air and entrained rock cuttings to pass through. The "second swivel," which is the rotary top drive, is above the side inlet sub.   This second swivel

provides torque and the rotation of the drill string while allowing the air and entrained rock cuttings to return to the surface.

Figure 3-4: Side inlet sub for dual wall pipe reverse circulation operations (courtesy of Holte Manufacturing Company).

The threaded pin and box connections on most dual wall pipe are shouldered connections. Most manufactures of this type of pipe do not use API thread profiles. The threaded connections for dual wall pipe will be discussed in Section 3.4.

3.1 Drill Bits

There are three basic types of rotary drill bits. These are drag bits, roller cutter bits, and air hammer bits.

3.2.1 *Drag Bits*

Drag bits have fixed cutter blades or elements that are integral with the body of the bit. The earliest drag bits were simply steel cutter blades rigidly attached to a steel body that is made up to the bottom of the drill string. Later natural diamonds were used as the cutter elements. A diamond drill bit has natural diamonds that are embedded in a tungsten carbide matrix body that is made up to the bottom of the drill string. The most recent development in drag bit technology is the polycrystalline diamond compact (PDC) bit. These drill bits have specially designed diamond cutter elements bonded to small tungsten carbide studs. These studs in turn are embedded in a steel body that is made up to the bottom of the drill

string. Drag bits have no moving parts. Their cutting mechanism is a scrapping action that is best used to drill rock formations that fail structurally in a plastic mode (e.g., soft, firm and medium-hard, non-abrasive rock formations). The modern drag bits require incompressible liquid circulation fluids to keep the diamonds from being damaged by excessive heat. Thus, these modern drag bits have very limited applications in air and gas drilling operations.

3.2.2 *Roller Cutter Bits*

Roller cutter bits use a crushing action to remove rock from the cutting face and advance the drill bit. The weight or axial force that is applied to the drill bit is transferred to the tooth or teeth on the bit. These teeth are pointed (mill tooth bit) or rounded (insert tooth bit) and the force applied is sufficient to fail the rock in shear and tension and cause particles of the rock to separate from the cutting face. The drill bits are designed to remove a layer of rock with each successive rotation of the bit. Figure 3-5a shows the tooth of a tri-cone bit being forced against the rock face. Figure 3-5b shows the rock particles created by the failure of the rock face due to the "crushing" action of the tooth. The circulation fluid entrains these rock cuttings and carries them away from the rock face.
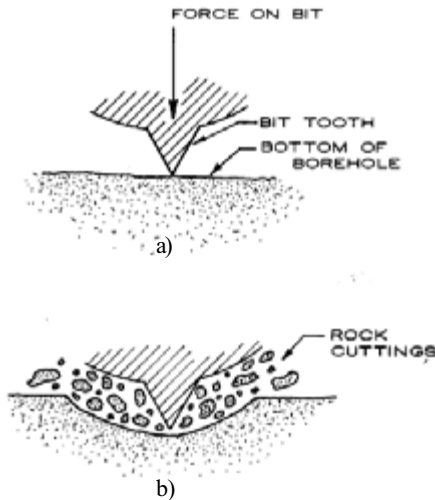
Figure 3-5: The rock crushing action of a tooth of a roller cutter drill bit, a) prior to failure of rock, and b) after failure of rock.

The roller cutter element(s) of a drill bit has a series of teeth that are designed to crush rock over the entire rock face after a single rotation of the drill bit. The repeated crushing action of the teeth in conjunction with the circulation fluid allow rock particles at the rock face to be continuously removed and the drill bit advanced.

When this crushing action takes place at the bottom of a well filled with drilling mud, the hydrostatic pressure due to the fluid column compresses the rock face and

places the rock face and the rock material in the immediately vicinity of the rock face in compression. This makes the crushing action less efficient and ultimately reduces the overall drilling rate of the drill bit (for a given WOB).

When this crushing action takes place at the bottom of a well filled only with compressed air, there is little hydrostatic pressure on the rock face. Further, the drilling process has removed a column of rock (above the rock face) from an semi-infinite block of pre-stressed rock. The in-situ pre-existing stresses that were in this block of rock prior to the drilling operation and the vertical cylindrical void of the new borehole create a thin tension stress field in the rock material just below the rock face (see Figure 3-6). This makes the crushing action very efficient and ultimately increases the overall drilling rate of the drill bit (for a given WOB).
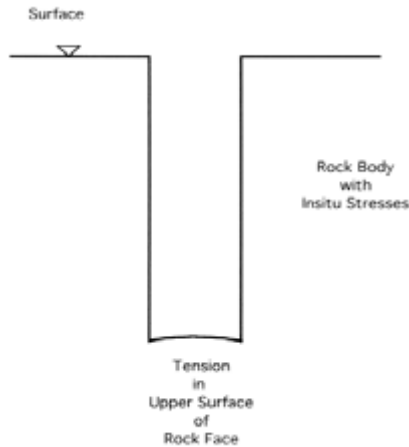
Figure 3-6: Schematic of tension rock face at bottom of borehole.

The above argument explains why the drilling rate for an air and gas drilling operation is approximately two to four times greater than that of a similar mud drilling operation (given similar geology and drilling parameters).

There are four styles of roller cutter drill bits. These are quad-cone drill bits, tri-cone drill bits, dual-cone bits, and single cone bits. Quad-cone drill bits and dual-cone drill bits are used for special mud drilling operations and have little application in air and gas drilling. Tri-cone drill bits are used extensively in air and gas drilling operations.

Tri-Cone Bits

The most widely used roller cutter bit is the tri-cone drill bit. The tri-cone drill bit has three roller cutter cones. Each of these cones has a series of teeth that crushes rock on the rock face as they roll over the face when the drill string (and thus the drill bit) is rotated. Figure 3-7 shows a schematic of the configuration of the tri-cone bit.   Figure 3-7a shows a cross-section view of a cone (for a soft rock

formation). Figure 3-7b shows the three roller cones at the bottom of a borehole. This latter schematic shows the offset of the cones. The offset is the degree the cones of the bit are designed to depart from a true rolling action on the rock face. Offset indicates that two or more cones of the bits do not have their centerlines of rotation passing through the center of bit rotation. Figure 3-7b shows a bit with no cone centerline passing through the center of the bit rotation [4].

SOFT FORMATION CONE DESIGN

a

OFFSET

b
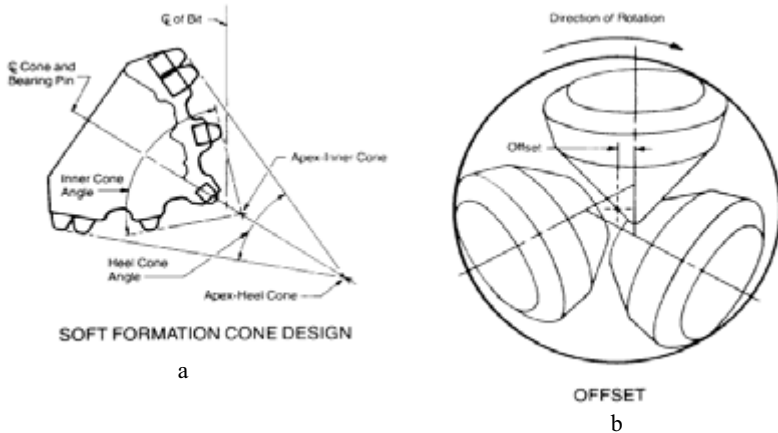
Figure 3-7: Schematic of the three cones of the tri-cone bit on the bottom of the borehole, a) cross-section of cone, and b) top view of action of the three cones during rotation [4].

Tri-cone drill bits can be used to drill a wide variety of rock formations. Figure 1-1 in Chapter 1 shows a typical mill tooth tri-cone drill bit. These drill bits are used to drill soft to medium rock formations. The "mill tooth" term refers to the fact that the teeth on the cones are machined into the cone as an integral part of the cone. Figure 3-8 shows a typical insert tri-cone drill bit. The "insert" term for this bit refers to the fact that the teeth are tungsten carbide studs that are inserted (shrink fit) into holes drilled in the cone material. The insert tri-cone drill bits are used to drill medium to hard rock formations.

Most tri-cone drill bits are manufactured to be used with drilling mud. But most manufactures produce a few of their drill bit styles for air drilling operations. These tri-cone drill bits are designed with special internal air passages to provide the bit bearings with the appropriate cooling from the less dense compressed air or natural gas. Figure 3-9 shows a cut-a-way of a tri-cone drill bit used for air operations.

Tri-cone drill bits used for air and gas drilling are usually designed with increased gauge protection (relative to their mud drilling counterparts). This gauge protection allows air bits to drill long abrasive sections without appreciable loss of gauge. However, it should be noted that some gauge loss will always occur in hard abrasive formations. It is good practice to design the well profile (i.e., borehole diameters and associated casing diameters) in such a manner that long sections having hard abrasive formations can be drilled with either the drill bit diameter

sequence of 6 inch, 6 1/8 inch , 6 1/4 inch, 6 1/2 inch, 6 3/4 inch, or the sequence of 7 1/8 inch, 7 3/8 inch, 7 5/8 inch, and 7 7/8 inch, or the sequence of 8 3/8 inch, 8 1/2 inch, 8 3/4 inch, 9 inch.   Using one of these drill bit diameter sequences allows anticipation of loss of gauge. The top of a long hard abrasive section can be drilled with a 6 1/2 inch diameter drill bit and when there is a bit change, followed by a 6 1/4 inch diameter drill bit, and then near the bottom of the section followed by a 6 1/8 inch diameter drill bit for the last bit change.

Figure 3-8: Insert tooth 7 7/8 inch diameter tri-cone roller cutter bit IADC Code 517 (courtesy of Reed Rock Bit Company).

Most air or natural gas drilling operations use insert tri-cone drill bits.   Even though previous drilling operations with mud may have shown that a mill tooth bit had been successful in drilling a particular rock formation, the mechanics of the rock cuttings creation process at the bottom of the air borehole require that an insert bit be used in order to generate smaller rock cuttings.   The smaller the rock cuttings generated by the drill bit, the more efficient the rock cutting creation and transport of cuttings particles from the bottom of the borehole.

Nearly all tri-cone drill bits are equipped to accept nozzle inserts in three open orifice flow channels in the drill bit body. Nozzles of various sizes (in 32nds of an inch) are extensively used in mud drilling operations. Standard practice for vertical direct circulation air or natural gas rotary drilling operations is to use tri-cone drill bits with open orifices (i.e., no nozzles). Thus, for well planning calculations (to be discussed in Chapters 8 to 11) it is important to ascertain from the drill bit manufacturer the open orifice minimum inside diameters for the drill bits to be used in the operation.

There are special reverse circulation tri-cone drill bits. These are fabricated using the same mill tooth and insert tooth cone designs as the direct circulation drill bits discussed above. Figure 1-9 shows the schematic of the inside flow channel of a reverse circulation tri-cone drill bit. This large orifice allows the return flow of drilling fluid and entrained rock cuttings to flow from the annulus through the large orifice in the bit body to the inside of the drill string. These reverse circulation drill bits are manufactured by geotechnical and mining equipment companies.
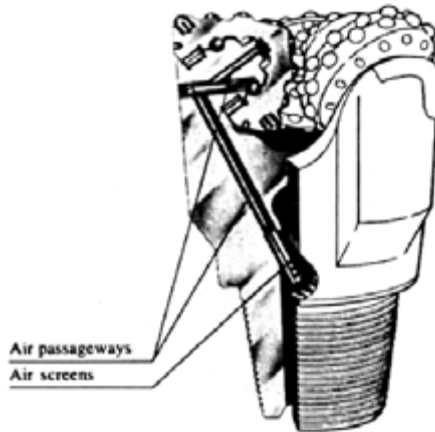
Figure 3-9: Cutaway of the interior of a tri-cone drill bit (courtesy of Reed Rock Bit Company).

Single Cone Bits

There are single cone or "monocone" drill bits. Unlike tri-cone drill bits that drill by a crushing action, the single cone bits drill by a scraping action. Thus, the single cone drill bits utilize wear resistant tungsten carbide inserts in the cutting structure. These drill bits are most effective in smaller diameters (~ 2 3/4 inch to 6 1/8 inch) and, with the appropriate cutting structure, are suitable for drilling soft as well as medium and hard rock formations.

The principal advantage of the single cone drill bits is the large size of the support bearing of the cone and the tungsten carbide inserts in the small drill bit diameters. Small diameter tri-cone drill bits are very fragile and subject to pinching and bearing damage if forced into an out of gauge borehole or used to ream an out of gauge borehole. These single cone drill bits are not subject to pinching and other damage when used to ream out of gauge boreholes. It is therefore good drilling practice to use single cone drill bits to drill small diameter sections in deep wells.

Figure 3-10 shows a typical single cone drill bit. Single cone drill bits are also equipped to accept nozzle inserts in three open orifice flow channels in the drill bit body. But like the tri-cone drill bits used for air and gas drilling operations, it is standard practice to use single cone drill bits with open orifices (i.e., no nozzles).

Thus, for well planning calculations (to be discussed in Chapters 8 to 10) it is important to ascertain from the drill bit manufacturer the open orifice minimum inside diameters for the drill bits to be used in the operation.

Figure 3-10: Single cone roller cone drill bit (courtesy Rock Bit International Incorporated).

3.2.3 *Air Hammer Bits*

Percussion air hammers have been used for decades in shallow air drilling operations. These shallow operations have been directed at the drilling of water wells, monitoring wells, geotechnical boreholes, and mining boreholes. In the past decade, however, the percussion air hammers have seen increasing use in drilling deep oil and natural gas wells. Percussion air hammers have a distinct advantage over roller cutter bits in drilling abrasive, hard rock formations.

The use of percussion air hammers (or down-the-hole air hammers) is an acceptable option to using rotating tri-cone or single cone drill bits for air and gas drilling operations. The air hammer utilizes an internal piston (or hammer) that is actuated by the compressed air (or other gas) flow inside the drill string. The internal piston moves up and down in a chamber under the action of air pressure applied either below or above the piston through ports in the inside of the air hammer. In the downward stroke, the hammer strikes the bottom of the upper end of the drill bit shaft (via a coupling shaft) and imparts an impact load to the drill bit. The drill bit in turn transfers this impact load to the rock face of the bit. This impact load creates a crushing action on the rock face very similar to that discussed above at the beginning of Section 3.2.2. But in this situation, the crushing action is

dynamic and is more effective than the quasi-static crushing action of tri-cone and single cone drill bits. Therefore, air hammer drilling operations require far less WOB as comparable drilling operations using tri-cone or single cone drill bits.

The air hammer is made up to the bottom of the drill string and at the bottom of the air hammer is the air hammer bit. The air hammer drill string must be rotated just like a drill string that utilizes tri-cone or single cone drill bits. The rotation of the drill string allows the inserts (i.e., tungsten carbide studs) on the bit face to move to a different location on the rock face surface. This rotation allows a different position on the rock face to receive the impact load as the upper end of the hammer bit is struck by the hammer. In direct circulation operations, air flow passes through the hammer section, through the drill bit channel and orifices to the annulus. As the air passes into the annulus, the flow entrains the rock cuttings and carries the cuttings to the surface in the annulus. Direct circulation air hammers are available in a wide variety of outside housing diameters (3 inches to 16 inches). These air hammers drill boreholes with diameters from 3 5/8 inches to 17 1/2 inches.

There are also reverse circulation air hammers. These unique air hammers allow air pressure in the annulus to actuate the hammer via ports in the outside housing of the hammer. The reverse circulation air hammer bits are designed with two large orifices in the bit face that allow the return air flow with entrained rock cuttings to flow to the inside of the drill string and then to the surface. Reverse circulation air hammers are available in larger outside housing diameters (6 inches to 24 inches). These air hammers drill boreholes with diameters from 7 7/8 inches to 33 inches.

Figure 3-11 shows two typical air hammer bits that would be used with direct circulation air hammers. The larger bit (standing on its shank end) is an 8 5/8 inch

Figure 3-11: Two typical air hammer bits with concave face (8 5/8 inch diameter bit on end, 6 inch diameter on side) (courtesy of Rock Bit International Incorporated).

diameter concave bit. The smaller bit (laying on its side) is a 6 inch diameter concave bit.

There are five air hammer bit cutting face designs. Figure 3-12a shows the profile of the drop center bit and Figure 3-12b shows the profile of the concave bit. Figure 3-13a shows the profile of the step gauge bit and Figure 3-13b shows the profile of the double gauge bit. Figure 3-14 shows the profile of the flat face bit. These five bit cutting face designs are applicable for a variety of drilling applications from non-abrasive, soft rock formations to highly abrasive, very hard rock formations. The application of these five face designs are shown in Figure 3-15.
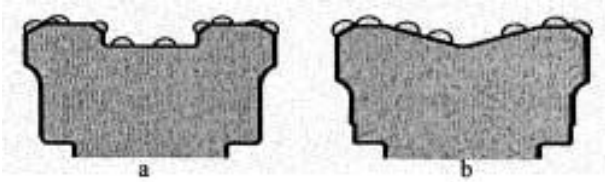
Figure 3-12: Air hammer bit face profile designs, a) drop center bit, and b) concave bit (courtesy AB Sandvik Rock Tools).
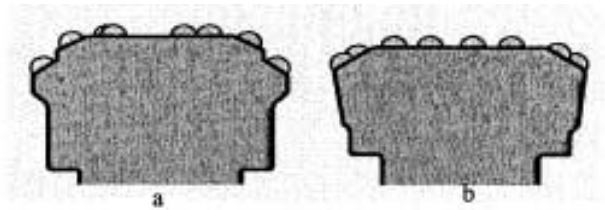
Figure 3-13: Air hammer bit face profile designs, a) step gauge bit, and b) double gauge bit (courtesy AB Sandvik Rock Tools).
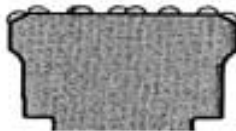
Figure 3-14: Air hammer bit face profile design, flat face bit (courtesy AB Sandvik Rock Tools).

In the past the air hammer manufactures have provided the air hammer bits for their specific air hammers. This practice insured compatibility of bit with hammer housing. The increased air hammer use in drilling deep oil and natural gas recovery wells has attracted traditional oil field drill bit manufacturers to fabricate air hammer

bits. Although the air hammer bit faces are somewhat uniform in design, the shafts are different for each air hammer manufacturer. The air hammer face and shafts are integral to the bit, thus, manufacturing air hammer bits is complicated. Fortunately, the air hammer has proven in the past decade to be very effective in drilling deep boreholes.   This has given rise to competition among traditional drill bit manufacturers to provide improved air hammer bits for deep drilling operations. This competition has in turn resulted in an increase in the quality and durability of air hammer bits (over the traditional air hammer manufacturer-supplied air hammer bits) in the more hostile environments of the deep boreholes. Operational use of the air hammer will be discussed in detail in Chapter 11.
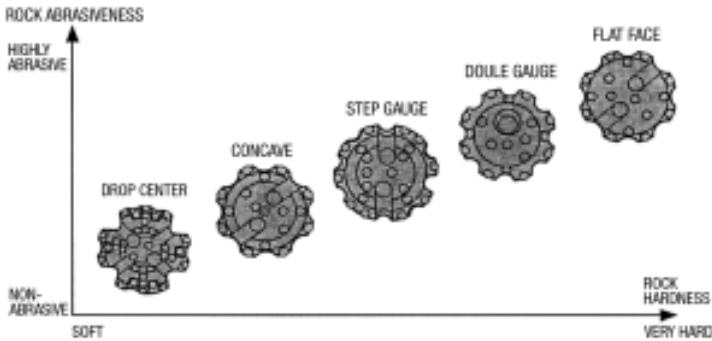
Figure 3-15: Air hammer bit face profile designs and application to rock formation abrasiveness and hardness (courtesy AB Sandvik Rock Tools).

3.2.4 *Classification of Drill Bits*

The International Association of Drilling Contractors (IADC) has approved a standard classification system for identifying similar bit types available from various manufacturers [5]. Table 3-1 gives an example IADC classification chart for insert drill bits (first column). In general, the classification system adopted is a three-digit code. The first digit in the bit classification code is the rock formation series number. The letter "D" precedes the first digit if the bit is diamond or PDC drag type bit. The first digit 1 to 3 are reserved for milled tooth bits in soft, medium, and hard formation categories. The first digit 5 to 8 are for insert bits in soft, medium, hard and extremely hard formation categories.

The second digit is called the type number. Type 0 is reserved for PDC drag bits. Types 1 to 4 designate a formation hardness subclassification from the softest to the hardest formations with each series category.

The third digit is the feature number. These numbers are interpreted differently for drag bits and roller cutter bits. For diamond and PDC drag bits the features numbers are 1 to 8 and refer respectively to: step type, long taper, short taper, non-taper, downhole motor, side-track, oil base, and core ejector.

The third digit feature numbers for roller cutter bits are 1 to 7 and refer respectively to: standard roller bearings, standard roller bearing for air applications, standard roller bearing with gauge protection, sealed roller bearings, sealed roller

bearing with gauge protection, sealed journal bearing, and sealed journal bearing with gauge protection.

Table 3-1: Comparison IADC chart for four manufacturers of insert tri-cone drill bits (courtesy of Reed Rock Bit Company).

Insert Bit Comparison by Type

	IADC CODE	REED	HUGHES	SECURITY	SMITH
SOFT FORMATIONS					
HS-51	435	—	X11	—	—
	437	—	J11	—	—
	515	—	X22	S84	2JS
	517	FP51A	J22	S84F	F2
	525	S52	—	—	—
	527	FP52	—	—	—
SOFT TO MEDIUM FORMATIONS					
HP-SM	532	—	HH33	—	—
	535	S53	X33	—	3JS
	537	FP53/FP53A	J33	S86F	F3
	542	—	—	S8JA	—
	545	—	—	S88	—
	547	—	—	S88F	—
HP-M	612	—	HH44	—	4JA
	615	—	X44	—	4JS
	617	FP62	J44	M84F	F4/F45
	622	Y62 JA/Y62B JA	—	M8JA	5JA
	625	S62	—	—	4JS
	627	FP62B/FP62X	J44C/J55R	M88F/M89TF	F5
MEDIUM TO HARD FORMATIONS					
HP-MH	632	Y63 JA	HH55	—	—
	635	S63	—	—	—
	637	FP63	J55	M89F	F47/F57
HARD FORMATIONS					
HP-H	717	—	—	—	F6
	722	—	—	—	7JA
	725	S72	—	—	—
	727	FP72	—	—	F7
	732	Y73 JA	HH77	—	—
	737	FP73	J77	H84F	—
	739	Y73 RAP	—	—	—
	742	—	—	H8JA	—
	745	S74	—	H88	—
	747	FP74	—	H88F	—
	812	—	HH88	H9JA	—
	815	—	—	H99	—
	817	—	—	H99F	—
	832	Y83 JA	HH99	H10JA	9JA
	835	S83	—	H100	—
	837	FP83	J99	H100F	F9

The above table also shows an insert rock bit comparison chart for four manufacturers (second through fifth columns). Feature 2 on all the bit manufacturers charts shows the insert bits designed for air drilling operations. Although the comparison chart shows insert tri-cone drill bits, the sealed roller bearing and sealed journal bearing bits are also often selected for air and gas drilling operations.

It should be noted that single cone drill bits and air hammer bits are not presently classified in accordance to the IADC code system.

3.3 Bottomhole Assembly

Figure 3-16 shows a typical bottomhole assembly (BHA) for a direct circulation rotary drilling operation. The BHA is the section of the drill string below the drill pipe (see Figure 3-1). This section of the drill string is the most rigid length of the string. It is this section of the drill string that determines how much weight can be placed on the drill bit and how "straight" a vertical borehole will be drilled with the drill string.
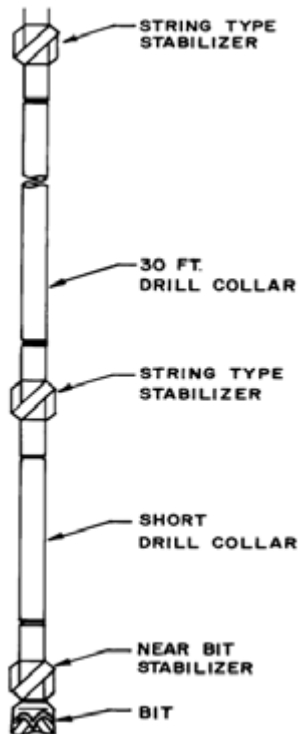
Figure 3-16: Typical bottomhole assembly for direct circulation rotary drilling operations.

The assembly in the above figure is composed of a drill bit at the bottom, drill collar tubulars, a near bit stabilizer directly above the bit, a stabilizer at the middle of the assembly, and a stabilizer at the top of the assembly.   The addition of stabilizers to the drill collar string generally improves the straight drilling capability of the drill string.   Highly stabilized drill strings are necessary when drilling in "crooked hole country". Crooked hole country usually refers to rock formations that tend to deflect the bit and thus the drill string as the drill bit is advanced.

Hard to medium hard rock formations that are tilted to a high angle from horizontal is one of the main causes of severe borehole deviations from vertical.   All deep rotary drilled boreholes will tend to have some deviation and tend to have a cork-screw three dimensional shape (usually to the right).   The deviation from vertical can usually be kept below 3° to 5° with good drilling practices. In general, air drilled boreholes can have more deviation than a mud drilled boreholes (assuming same rock formations). But most of increased deviation from vertical is due to the fact that air drilling penetration rates are significantly higher than a mud drilling operation and drillers tend to take advantage of that increased drilling rate and let the deviation get away from them. To correct this tendency, it is good practice to utilize a more stabilized BHA when drilling an air drilled borehole than would be used in a comparable mud drilled borehole. For more detail regarding the design of stabilized BHA and where and how to apply such assemblies the readers are referred to References 1 and 4 or service company literature.

3.3.1 *Drill Collars*

Drill collars are thick walled tubulars that are used at the bottom of the drill string (see Figure 3-1). Their principal purpose in the drill string is to provide the axial force needed to advance the drill bit (see Figure 1-2).   When drilling a vertical borehole, the axial force is the weight of the drill collars. Drill collars are available in API range lengths given in Table 1-1.   Figure 3-16 shows a BHA with Range 2 (~30 ft long) drill collars. Range 2 lengths are typical for double and triple land rotary drilling rigs. Also shown in Figure 3-16 are short drill collar lengths used to adjust positions of the stabilizers in the BHA.   These shorter drill collar lengths are selected from Range 1 stock of drill collars.

Appendix B gives the dimensions and mechanical properties for API drill collars. These drill collars vary in outside diameter from 2 7/8 inches to 12 inches. Table B-1 shows that a drill collar having an outside diameter of 6 3/4 inches can be obtained with an inside diameter of 1 1/2 inches, 1 3/4 inches, 2 inches, 2 1/4 inches, 2 1/2 inches, 2 13/16 inches, 3 inches, 3 1/4 inches, and 3 1/2 inches.   From this same table a 6 3/4 inch Column (1), by 2 13/16 inch Column (9), drill collar will have a weight per unit length of 100 lb/ft and a standard 30 ft length of this drill collar would weigh 3,000 lb. Table B-2 shows that the 6 3/4 inch Column (3), by 2 13/16 inch Column (11), drill collar is available with either, the 5 inch Double Streamline, or the 4 1/2 inch H-90 connections, Columns (1) and (2).   The recommended make-up torque for each connection type is 22,426 ft-lb, 23,159 ft-lb, respectively, Column (11). These are the recommended make-up torques required to insure that the shoulder connections will not leak circulation fluid and will remain tight when used in a rotary drill operation.

Drill collars are usually fabricated from American Iron and Steel Institute (AISI) 4140 or 4145 heat treated steel. These are chrome-molybdenum steel alloys and have yield stresses in excess of 100,000 psi. In addition to drill collars fabricated of steel are special drill collars fabricated of nonmagnetic nickel alloys (e.g., usually Monel K-500). These nickel alloy drill collars (usually three) are used at the bottom of the drill string to allow magnetic compass like equipment to be used to survey the borehole as the well is drilled. These nickel alloy drill collars have material properties that are almost identical to that of the AISI 4140 heat treated steel of the standard drill collars.

3.3.2 *Stabilizers and Reamers*

Stabilizers and rolling cutter reamers are special thick walled drill collar subs that are placed in the BHA to force the drill collars to rotate at or near the center of the borehole. By keeping the drill collars at or near the center of the borehole the drill bit will drill on a nearly straight course projected by the center axis of the rigid BHA. Stabilizers and rolling cutter reamers have blades or rolling cutters that protrude from the sub wall into the annulus to near the borehole diameter. The space between the blades or rolling cutters allows the air or natural gas flow with entrained rock cuttings to return to the surface nearly unobstructed.

Figure 3-17 shows three rotating blade stabilizers. These three stabilizers are respectively, the integral blade (usually a spiral blade configuration) stabilizer, the big bear stabilizer (a larger type integral blade stabilizer), and the welded blade (spiral blade) stabilizer. The blades on these three stabilizers are machined into (integral) the stabilizer body, or are rigidly attached to the stabilizer body and, therefore, rotate with the body of the stabilizer and, thus, with the drill string itself.

Figure 3-18 shows two sleeve type of blade stabilizers. These stabilizers have replaceable sleeves (with blades). These two stabilizers are respectively, the sleeve type stabilizer, and the rubber sleeve stabilizer. The sleeve type stabilizer has a metal sleeve with the attached metal blades (sleeve rotates) and can be replaced on the stabilizer body when the blades wear. The rubber sleeve stabilizer has a sleeve that has a rubber sheath over a metal substructure (sleeve does not rotate). The rubber sleeve can be replaced on the stabilizer body when the blades wear.

In general, the rotating blade stabilizers are shop repairable. The integral blade stabilizers have gauge protection in the form of tungsten carbide inserts, or replaceable wear pads. Integral blade stabilizers can be used in abrasive, hard rock formations. When the blades are worn, the stabilizers can be returned to the machine shop and the inserts or wear pads replaced. Welded blade stabilizers are not recommended for use in abrasive, hard rock formations. When their blades become worn or damaged they can be returned to the machine shop for repairs.

Non-rotating blade stabilizers can be repaired at the drilling rig location. The worn sleeves can be removed and new ones placed on the stabilizer body. This is an important advantage over the rotating stabilizer. The non-rotating stabilizer is most effective in abrasive, hard rock formations since the sleeve is stationary and acts like a drilling bushing. This action decreases wear on the metal sleeve blades.

Stabilizers are used extensively to improve the straight hole drill capability of a BHA for both mud drilling operations and for air drilling operations. However, care must be exercised in using stabilizers in air drilling operations. The wear rate on

stabilizer blades in air drilling operations will be greater than in a mud drilling operation (assuming similar geologic conditions).
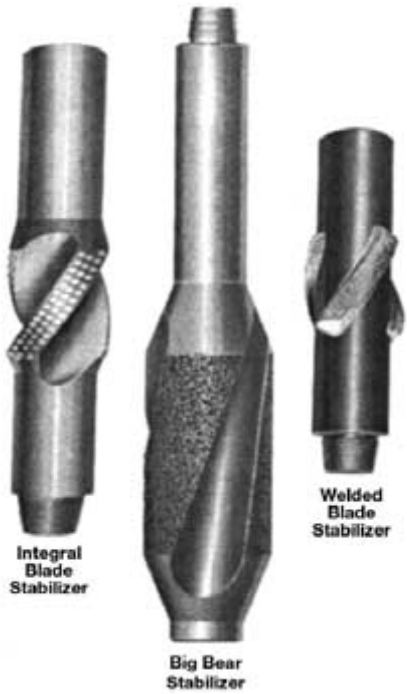
Figure 3-17: Rotating blade stabilizers (courtesy Smith International Incorporated).

Figure 3-19 shows a three point rolling cutter reamer. These reamers have the roller cutters 120˚ apart on the circumference. The rolling cutter reamer is a special type of stabilizer tool that provides "blades" that are cylindrical roller cutter elements that can crush and remove rock from the borehole wall as the drill bit is advanced. Often the reamer is placed just above the drill bit (replacing the near bit stabilizer, see Figure 3-16). Reamers are also available in a four point rolling cutter reamer. These reamers have the rolling cutters 90˚ apart on the circumference.

Such rolling cutter reamers are used when drilling in abrasive, hard rock formations. The gauge of the rolling cutter reamers can be adjusted by replacing the rolling cutter elements on the stabilizer body with different outside diameter elements. Also, damaged rolling cutters can be replaced. These replacements can be accomplished at the drilling rig location. When drilling abrasive, hard rock formations, the gauge of the rolling cutter reamers are usually adjusted to be slightly under the drill bit gauge or at the drill bit gauge. The reamers provide the near-bit stabilization needed for straight drilling in abrasive formations.
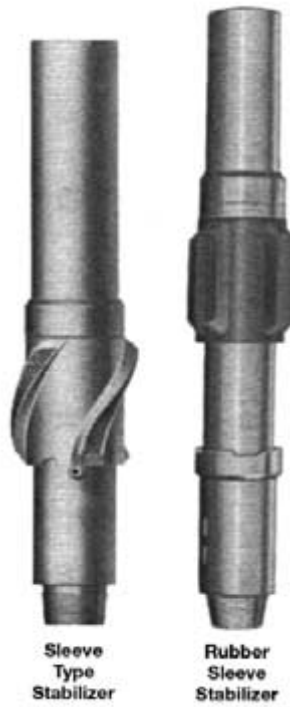
Figure 3-18: Non-rotating blade stabilizers (courtesy of Smith International).

Figure 3-19: Three point rolling cutter reamer (courtesy of Smith International).

3.3.3 *Downhole Surveying Equipment*

BHAs for drill strings used to drill deep vertical wells are usually fitted with several nonmagnetic drill collars. These drill collars are usually near the bottom of the BHA (just above the drill bit). These non-magnetic collars are needed to carry out the downhole surveys required by most natural resource regulatory agencies. Downhole surveys are used to describe the deviation of a drilled borehole from the ideal vertical centerline of the intended well. Knowledge of where an actual well has been drilled is needed to ensure economic and environmentally safe recovery of mineral resources. Also such directional knowledge is used in geotechnical drilling operations where the accuracy of the placement of a well is critical for follow-on construction operations.

The survey is usually accomplished by using a magnetic single-shot instrument. This instrument is usually part of the equipment inventory of a typical double and triple rotary drilling rig. The magnetic single-shot instrument survey is carried out by the drilling rig crew. The single-shot instrument contains a small compass which floats in a liquid and gives borehole compass direction information. The floating compass is also designed with a half sphere top and an extended pendulum bottom. The spherical top of the compass is etched with a traditional compass rose allowing direction determination when viewing the compass from above down the axis of the instrument. Also etched on the spherical top are concentric circles that represent different angles of inclination from the vertical. When viewing the compass from above and down the axis of the instrument, a set of crosshairs shows the concentric circles of angles of inclination. A small single-shot camera is installed in the instrument above the compass. The camera shutter mechanism, exposure light, and timer are battery operated. The instrument timer is set at the surface to give sufficient time for the instrument to be lowered to the bottom of the inside of the drill string. The instrument is lowered on a slick wireline (a simple wire line not having electrical transmission capability). When the instrument is in place at the bottom of the inside of the drill string, the timer actuates the light exposing the small circular film cartridge. Figure 3-20 shows a typical single-shot exposure. This exposed single-shot picture shows a direction of magnetic north (or an azimuth of 0˚) and an inclination of 1.8˚ from vertical. As a well is drilled single-shot survey pictures can be taken every few hundred feet. Calculations can be made using these survey pictures and the measured distance to each survey point to give a three-dimensional plot of the drilling course of the well.

Figure 3-20: Typical single-shot exposure that reads north and 1.8˚ inclination from vertical (courtesy of Sperry-Sun Drilling Services, a Halliburton Company).

Since the magnetic single-shot instrument utilizes a simple compass for directional information, the instrument must be placed in a nonmagnetic portion of the drill string in order for the compass to give accurate azimuth readings. This is why the nonmagnetic drill collars are placed at the bottom of the drill string. When running the single-shot survey care must be taken to make sure that the single-shot instrument is located approximately midway along the nonmagnetic drill collar length section before the camera film is allowed to be exposed.

More details regarding directional drilling operations and surveys will be discussed in Chapter 12.

3.4 Drill Pipe

There are four types of drill pipe that are used in air and gas drilling operations. These are standard API drill pipe, heavy-weight drill pipe, drill rod, and dual wall pipe.

3.4.1 *Standard API Drill Pipe*

Appendix B gives the dimensions and mechanical properties for standard API drill pipe. This is the drill pipe used in most rotary drilling operations (shallow and deep). API drill pipe are fabricated by various API certified manufacturers around the world, principally for use in the drilling of deep wells for the recovery of oil and natural gas. Table B-3 gives the drill pipe dimensions (outside diameter, inside diameter, and weight per unit length) of the pipe body of various drill pipe sizes. API drill pipe size is denoted by the outside diameter of the pipe body and its associated nominal (pipe body) weight per unit length. The nominal weight per unit length defines the wall thickness and the inside diameter. The lengths of drill pipe elements (pipe body and tool joints) are defined in the API range designation of Table 1-1. When tool joints (box and pin) are added to a pipe body the average actual weight per unit length of the drill pipe element is increased above the pipe body nominal weight per unit length. API drill pipe is also classified by API material (steel) grade. Table 3-2 gives the API material grade designations and respective standards for minimum yield, maximum yield, and minimum tensile strength of the steel grade. The actual steel used to produce the various API grades for drill pipe fabrication is one of the AISI grade classifications of steel produced in US steel mills. For an AISI grade of steel to be used to fabricate drill pipe of a particular API grade the AISI grade must satisfy the minimum and maximum specification given in Table 3-2.

Table 3-2: API drill pipe steel grades minimum and maximum mechanical properties [1].

API Grade	E 75	X 95	G 105	S135
Min. Yd. (psi)	75,000	95,000	105,000	135,000
Max. Yd. (psi)	105,000	125,000	135,000	165,000
Min. Ten. (psi)	100,000	105,000	115,000	145,000

Table 3-2 shows that for API E75 grade the minimum yield is 75,000 psi, the maximum yield is 105,000 psi, and the minimum tensile (ultimate) strength is

100,000 psi. Similar data is shown for API X95, API G105, and API S135 steel grades [1, 2].

Table B-4 gives the dimensions and mechanical properties of various drill pipe sizes (and nominal weights) and tool joint combinations for API grade E75 [1, 2]. The approximate (actual) weight per unit length data given in the table is for a 30 ft drill pipe element (Range 2). In general, API grade E75 drill pipe elements are used on single rotary drilling rigs. These drill pipe elements are usually Range 1 lengths (see Table 1-1). Table B-4 also shows the drill pipe body to tool joint type (either external upset or internal upset), the tool joint connection, outside diameter, inside diameter, tensile yield of the pipe body and tool joint (threaded connection), and the torsion yield of the pipe body and tool joint (threaded connection). The data given for tensile yield and torsion yield are based on the minimum yield of the API grade E75 (i.e., 75,000 psi).

An example will be used to demonstrate how to use the API drill pipe tables in Appendix B. Table B-4 gives data for E75 grade steel drill pipe. In Column (1) of Table B-4 is given a 2 3/8 inch nominal size drill pipe (also pipe body size given in Table B-3). In Column (2) is given 6.65 lb/ft nominal unit weight, (also nominal unit weight given in Table B-3). In Column (4) is given the upset type (in this case EU is external upset) and in Column (5) is given the connection type (in this case NC26 (IF)). Column (3) shows that this drill pipe has an actual unit weight of 6.99 lb/ft. Column (6) gives the connection tool joint outside diameter of 3 3/8 inches and Column (7) gives the connection tool joint inside diameter of 1 3/4 inches. Column (8) gives a drift inside diameter of 1.625 inches (the outside diameter of the largest survey or other tool that can pass through the drill pipe element) for this drill pipe. This diameter is governed by the tool joint inside diameter. Column (9) gives an axial tensile force of 138,214 lb to yield the steel of the drill pipe body and Column (10) gives an axial tensile force of 313,681 lb to yield the steel of the tool joint. Thus, the weakest part of the drill pipe element to axial tension is the pipe body. Column (11) gives a torque of 6,250 ft-lb to give torsion yield of the steel of the pipe body and Column (12) gives a torque of 6,875 ft-lb to give torsion yield of the steel of the tool joint box. Thus, the weakest part of the drill pipe element to torque is the pipe body.

Table B-5 gives similar data as in Table B-4 but for the higher strength grades of drill pipe steel (i.e., X95, G105, and S135). In Column (1) of Table B-5 is given a 4 1/2 inch nominal size drill pipe (also pipe body size given in Table B-3). In Column (2) is given 16.60 lb/ft nominal unit weight, (also nominal unit weight given in Table B-3). In Column (4) is given the upset type (in this case EU is external upset) and the steel grade S135. In Column (5) is given the connection type (in this case NC50). Column (3) shows that this drill pipe has an actual unit weight of 18.62 lb/ft. Column (6) gives the connection tool joint outside diameter of 6 5/8 inches and Column (7) gives the connection tool joint inside diameter of 3 1/2 inches. Column (8) gives a drift inside diameter of 3.375 inches (the outside diameter of the largest survey or other tool that can pass through the drill pipe element) for this drill pipe. This diameter is governed by the tool joint inside diameter. Column (9) gives an axial tensile force of 595,004 lb to yield the steel of the drill pipe body and Column (10) gives an axial tensile force of 1,183,908 lb to yield the steel of the tool joint. Thus, the weakest part of the drill pipe element to

axial tension is the pipe body. Column (11) gives a torque of 55,453 ft-lb to give torsion yield of the steel of the pipe body and Column (12) gives a torque of 44,673 ft-lb to give torsion yield of the steel of the tool joint box. Thus, the weakest part of the drill pipe element to torque is the pipe body.

Table B-6 gives a summary of the API connections available for both drill collars and drill pipe. These connections are all API recognized and are used by a variety of fabricators of drill collars and drill pipe. The table gives the outside diameter, inside diameter, and thread data for each connection type and size. Also given are the detailed dimensions of the box and pin of each connection. These dimensions are not used in machining box and pin connections. Readers are referred to Reference 6 to obtain information regarding API connection dimensions and tolerances for machine shop.

3.4.2 *Heavy-Weight Drill Pipe*

Heavy-weight drill pipe is an intermediate weight per unit length drill string element. This type of drill pipe has a heavy wall pipe body with attached extra length tool joints (see Figure 3-21). Heavy-weight drill pipe has the approximate outside dimensions of standard drill pipe to allow easy handling on the drill rig [6].
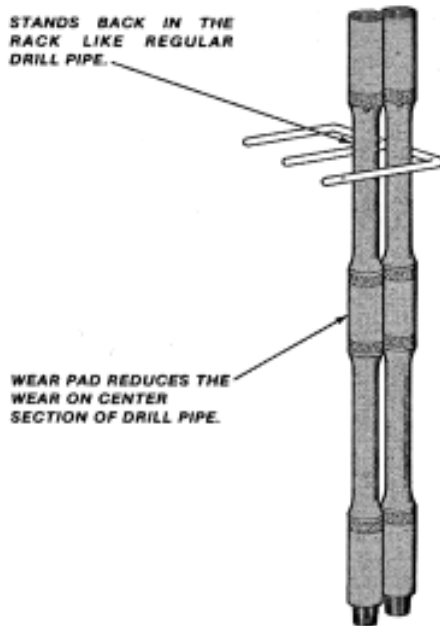
Figure 3-21: Heavy-weight drill pipe standing in rig rack (courtesy of Smith International).

The unique characteristic of this type of drill pipe is that it can be run in compression in the same manner as drill collars. Most heavy-weight drill pipe is fabricated in Range 2 and 3 API lengths. It is also available in custom lengths shorter than Range 2. Heavy-weight drill pipe are available in 3 1/2 inch, 4 inch, 4 1/2 inch, and 5 inch, 5 1/2 inch, and 6 5/8 inch nominal outside diameters. Figure 3-21 shows two typical heavy-weight drill pipe elements standing in a regular drill pipe rack in a drill rig. One unique feature of heavy-weight drill pipe is the wear pad in the center of the element. The wear pad acts as a stabilizer and improves the stiffness of the heavy-weight stand in the drill string and thus reduces the deviation of boreholes.

Table 3-3 gives the dimensional and mechanical properties for Range 2 heavy-weight drill pipe (tube body and tool joints).

Table 3-3: Range 2 heavy-weight drill pipe dimensions and mechanical properties (courtesy of Smith International).

	Tube					Mechanical Properties Tube Section	
	Nominal Tube Dimension						
Nom. Size (in.)	ID (in.)	Wall Thick-ness (in.)	Area (in²)	Center Upset (in.)	Elevator Upset (in.)	Tensile Yield (lb)	Tor-sional Yield (ft-lb)
3½	2¼	.625	5.645	4	3⅝	310,475	18,460
4	2⁹⁄₁₆	.719	7.410	4½	4⅛	407,550	27,635
4½	2¾	.875	9.965	5	4⅝	548,075	40,715
5	3	1.000	12.566	5½	5¼	691,185	56,495
5½	3⅜	1.063	14.812	6	5⅝	814,660	74,140
6⅝	4½	1.063	18.567	7⅛	6¾	1,021,185	118,845

	Tool Joint					Approx. Weight [Including Tube & Joints (lb)]		
				Mechanical Properties				
Nom. Size (in.)	Connection Size (in.)	OD (in.)	ID (in.)	Tensile Yield (lb)	Torsional Yield (ft-lb)	Wt/ ft	Wt/ Jt.	Makeup Torque (ft-lb)
3½	NC 38 (3½ IF)	4¾	2¼	675,045	17,575	23.2	695	9,900
4	NC 40 (4 FH)	5¼	2¹³⁄₁₆	711,475	23,525	27.2	880	13,250
4½	NC 46 (4 IF)	6¼	2⅝	1,024,500	38,800	41.0	1,215	21,800
5	NC 50 (4½ IF)	6⅝	3⅟₁₆	1,266,000	51,375	49.3	1,480	29,400
5½	5½ FH	7	3½	1,349,365	53,080	57.0	1,710	33,200
6⅝	6⅝ FH	8	4½	1,580,485	74,915	70.8	2,290	46,900

Figure 3-22 shows a "tapered" drill string with a drill bit at the bottom, drill collars above the drill bit, heavy-weight drill pipe above the drill collars, and standard drill pipe above the heavy-weight drill pipe.
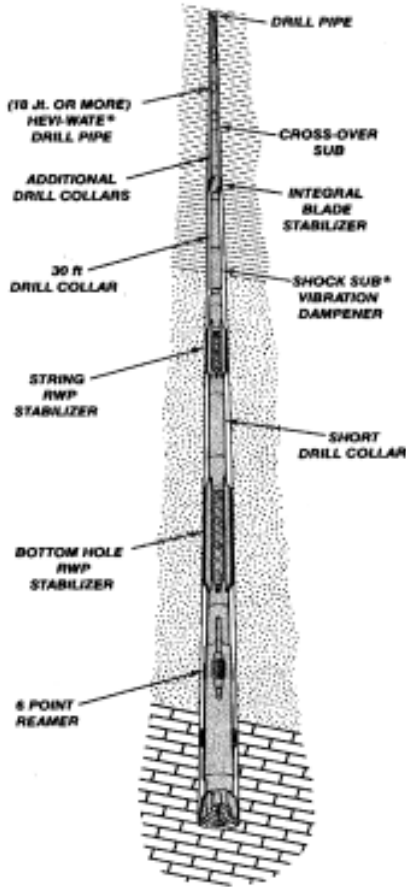
Figure 3-22: Typical tapered drill string using heavy-weight drill pipe (courtesy Smith International).

Heavy-weight drill pipe elements are used in a number of applications in rotary drilling. Since this drill pipe can be used in compression, this drill pipe can be used in place of drill collars in the shallow wells with small single or double rotary drilling rigs. This drill pipe is also used in conventional drill string for vertical drilling operations as transitional stiffness elements between the stiff drill collars and

the very limber drill pipe. Their use as transitional stiffness elements reduces the mechanical failures in the bottom drill pipe elements of the drill string. Heavy-weight drill pipe is also used in directional drilling operations where drill collars can be replaced by the heavy-weight pipe. Using heavy-weight drill pipe in place of drill collars reduces the rotary torque and drag, and increases directional control.

3.4.3 *Drill Rod*

Small rotary drilling rigs often use drill rod as a drill pipe substitute. Drill rod is used in mining, environmental, and geotechnical drilling operations. These rods are available in 2 ft, 5 ft, and 10 ft lengths. They are used in both mud (or water) and air drilling operations. There are two types of drill rods, wireline drill rods, and conventional drill rods.

Wireline Drill Rod

Figure 3-23 shows a schematic profile of wireline drill rod. This type of drill rod has no change in inside diameter at the connections (smooth bore over entire length). This allows wireline coring to proceed through the drill rod. The outside of the rod is also smooth with no increase in outside diameter at the tool joints. The connections are not API but are shouldered connections which give adequate strength in shallow rotary drilling operations.
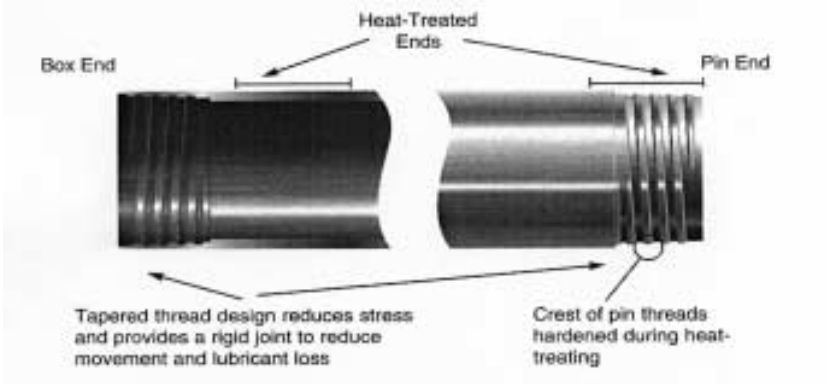
Figure 3-23: Wireline drill rod schematic profile of rod body, and box and pin connections (courtesy Boart Longyear Incorporated).

Table 3-4 gives dimensions and mechanical properties for AQ, BQ, NQ, and HMQ wireline drill rod. Wireline drill rod is available in 5 ft and 10 ft lengths (and custom lengths). This drill rod type is used in the rotary drilling operations where core retrieval is the principal objective. These are usually shallow small diameter boreholes. This drill rod type was originally developed for mining drilling operations but is now used extensively in environmental and geotechnical drilling operations.

Table 3-4: Wireline drill rod dimensions and mechanical properties (courtesy of Boart Longyear Incorporated).

	AQ	BQ	NQ	HMQ
Rod Body OD	1.75 in	2.19 in	2.75 in	3.50 in
ID	1.38 in	1.81 in	2.38 in	3.06 in
Wt/ft	3.14 lb/ft	4.02 lb/ft	5.24 lb/ft	7.69 lb/ft
Max OP Torque	240 ft-lb	340 ft-lb	560 ft-lb	1,100 ft-lb
Max MU Torque	350 ft-lb	470 ft-lb	710 ft-lb	1,200 ft-lb
Wall Profile	Parallel	Parallel	Parallel	Parallel

Standard Conventional Drill Rod

Figure 3-24 shows a schematic profile of standard conventional drill rod. This type of drill rod has a much stronger connection (an abrupt change in inside diameter at the tool joint). The outside of the rod is smooth with no increase in outside diameter at the tool joints.   The connections are API threaded shouldered connections.
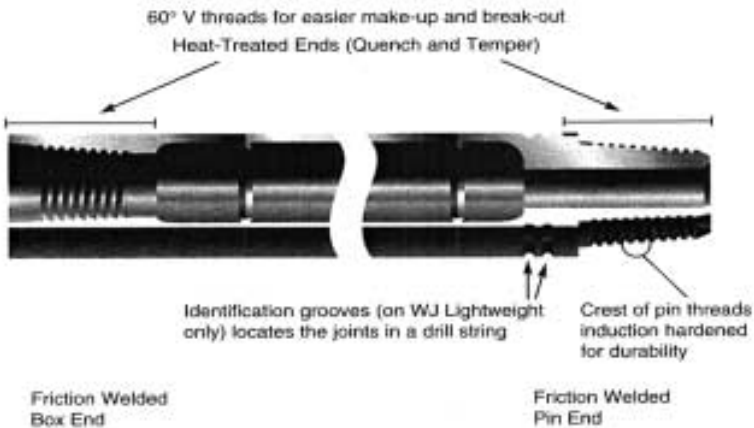
Figure 3-24: Standard conventional drill rod schematic profile of rod body, and box and pin connections (courtesy Boart Longyear Incorporated).

Table 3-5 gives dimensions and mechanical properties for AWJ, AWJ Lightweight, and NWJ standard conventional drill rod. Standard conventional drill rod is available in 2 ft, 5 ft and 10 ft lengths (and custom lengths). The standard conventional rod type is used in shallow small diameter borehole drilling operations. These drilling rods are used exclusively for direct circulation operations. These rods have been traditionally used in mining and geotechnical drilling operations, but there is increased use of this drill rod type for drilling shallow small diameter environmental monitoring wells.

Table 3-5: Standard conventional drill rod dimensions and mechanical properties (courtesy of Boart Longyear Incorporated).

		AWJ	AWJ-LT	NWJ
Rod Body	**OD**	1.75 in	1.75 in	2.63 in
	ID	1.375 in	1.50 in	2.250 in
Tool Joint	**OD**	1.75 in	1.75 in	2.63 in
	ID	0.63 in	0.63 in	1.13 in
Wt/ft (approx.)		3.22 lb/ft	2.35 lb/ft	5.18 lb/ft
Max OP Torque		300 ft-lb	300 ft-lb	650 ft-lb
Max MU Torque		300 ft-lb	300 ft-lb	580 ft-lb
Wall Profile		Internal Upset	Internal Upset	Internal Upset

3.4.4 *Dual Wall Pipe*

Dual wall drill pipe elements are used exclusively in reverse circulation drilling operations. This type of drill pipe is used for drilling shallow (~ 3,000 ft or less) water wells, environmental monitoring wells, geotechnical boreholes, and mining boreholes. These rotary drilling operations can be; a) rotation of the dual wall pipe drill string with a tri-cone or drag type bit, b) rotation of the dual wall pipe drill string with a standard downhole air hammer (with standard air hammer bit), or c) rotation of the dual wall pipe drill string with a reverse circulation downhole air hammer (with reverse circulation air hammer bit). These rotary drilling operations are carried out with hydraulic top drives (for single rotary drilling rigs) and with power swivels (for double and triple rotary drilling rigs).

Figure 3-25 shows the schematic of a typical dual wall drill string set up for five optional bottomhole assemblies. This schematic utilizes the concealed innertube pipe type of dual wall pipe. This type of dual wall pipe has an innertube that is O-ring slip fitted into a similar innertube in the next element of drill pipe when elements are made up to each other. The outer tube of the dual wall pipe are made up with non-API shouldered connections.

At the far right of Figure 3-25 is a tri-cone bit bottom assembly for conventional (reverse circulation) rotary drilling operations. This tri-cone bit threads to a shouldered innertube of the latching bit assembly. The outer tube fits over the top of the drill bit and allows the compressed air to flow from the annulus of the dual wall pipe to the roller cutters of the bit. The bit has a large inner hole that allows the compressed air with entrained cuttings to flow to the surface through the innertube of the dual wall pipe.

Next (moving from right to left) are two alternate conventional rotary drilling bottomhole assemblies. One is an open face bit (drag bit) for coring operations and the other is another tri-cone drill bit configuration. This latter tri-cone bit assembly makes use of a skirted rock bit sub which is often integral to the bit itself. Figure 3-26 shows a skirted tri-cone bit for a dual wall drilling operation.

The next two bottomhole assemblies are for rotary drilling operations using downhole air hammers. The first of these assemblies from the right is a reverse circulation hammer with a large opening in the air hammer bit for the returns (see Chapter 11). The last assembly is a standard direct circulation downhole air hammer with an interchange sub that allows the return air with entrained rock cuttings to flow
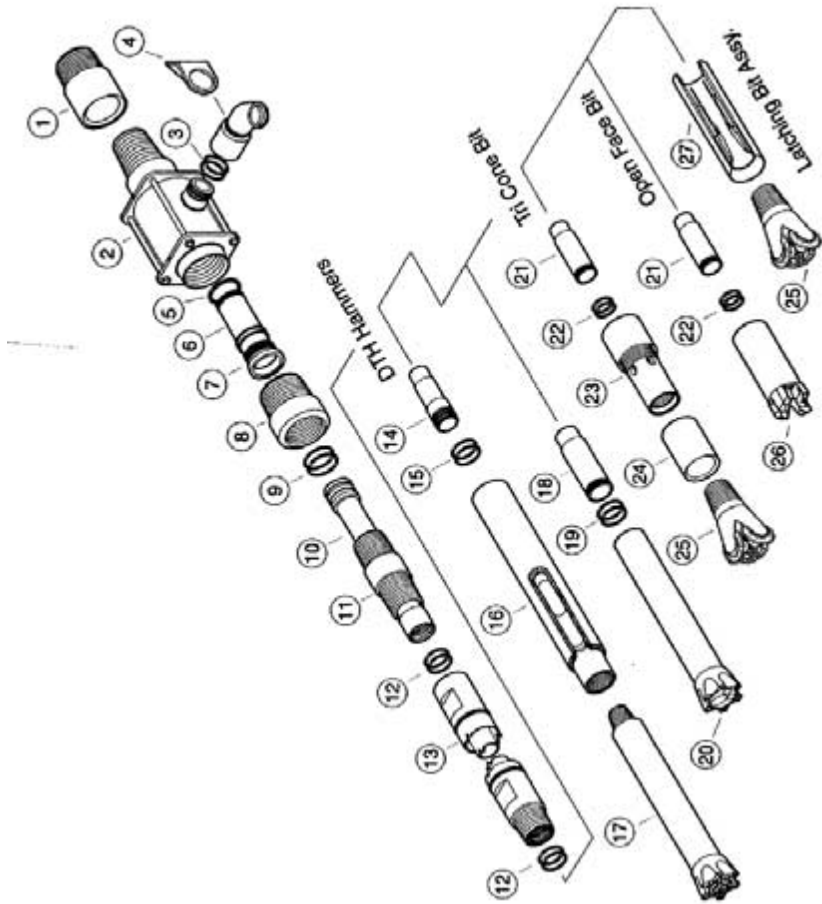
Figure 3-25: Dual wall pipe drill string schematic showing three drill bit string options and two downhole air hammer string options. Nomenclature of above; 1) adapter sub, 2) air swivel, 3) O-ring, 4) air swivel inlet, 5) O-rings, 6) shaft adapter, 7) O-rings, 8) saver sub adapter, 9) O-rings, 10) center tube, 11) saver sub, 12) O-rings, 13) dual wall drill pipe, 14) interchange connector tube, 15) O-rings, 16) interchange sub, 17) standard down-the-hole (DTH) air hammer, 18) connector tube for reverse circulation downhole air hammer, 19) O-rings, 20) reverse circulation downhole air hammer, 21) O-rings, 22) bit connector sleeve, 23) rock bit sub, 24) wear sleeve, 25) tri-cone bit, 26) open face drag bit for coring and, 27) latching bit sub (courtesy of Foremost Industries Incorporated).

from the annulus between the inside of the borehole and the air hammer housing to the inside of the innertube of the dual wall pipe.

Figure 3-26: Skirted tri-cone roller cutter drill bit for dual pipe reverse circulation drilling operations (courtesy of Lang Exploratory Drilling).

Table 3-6 gives the dimensions and mechanical properties of the dual wall pipe designed with O-ring sealed innertubes and threaded outer tubes (i.e., concealed innertube pipe of Drill Systems from Foremost Industries Incorporated).   The working torque values are the maximum recommended torque to be applied to the dual wall drill string during rotary drilling operations. The tension to yield values are the limiting axial tension loads that will initiate the material yield in the top pipe element in the dual pipe drill string. This yield can be in the outer tube of the dual pipe body or in the shouldered threaded connection, whichever is the weakest.

Table 3-6: Concealed innertube pipe (of Drill Systems) dual wall pipe dimensions and mechanical properties (courtesy of Foremost Industries Incorporated).

Dual Wall Pipe OD	3.75 in	4.00 in	4.50 in
Outer Tube ID	3.25 in	3.50 in	4.00 in
Innertube OD	2.125 in	2.25 in	2.750 in
Innertube ID	1.875 in	2.00 in	2.375 in
Pipe Wt/ft	12.6 lb/ft	14.6 lb/ft	21.3 lb/ft
Working Torque	4,800 ft-lb	7,000 ft-lb	8,900 ft-lb
Tension to Yield	200,600 lb	244,200 lb	210,100 lb
Lengths Available	10 ft	10 ft	20 ft

Table 3-6: Continued.

Dual Wall Pipe OD	5.50 in	7.00 in	9.625 in
Outer Tube ID	4.50 in	6.00 in	8.625 in
Innertube OD	3.75 in	5.00 in	6.625 in
Innertube ID	3.25 in	4.50 in	6.063 in
Pipe Wt/ft	27.4 lb/ft	40.2 lb/ft	64.3 lb/ft
Working Torque	15,500 ft-lb	30,500 ft-lb	97,700 ft-lb
Tension to Yield	206,900 lb	466,000 lb	466,000 lb
Lengths Available	20 ft	20 ft	20 ft

Another type of dual wall pipe is fabricated with a threaded shouldered connection (box and pin) across both the outer and innertubes at each end of the pipe element. This dual wall pipe design gives a contiguous single pipe element (no separate innertube). This threaded shouldered connection is a modified 3 1/2 inch API Regular connection (1/2 inch longer and 1/2 inch larger diameter). Each box and pin is fabricated with elliptical "windows" located approximately halfway between the shoulders (see Figures 3-27a and 3-27b).

These windows allow flow communication from the annulus space of one dual wall pipe element to the annulus space of another dual wall pipe element. The central hole in the connection allows unobstructed return flow of air and entrained rock cuttings through the inside of the inside tube of the pipe elements (see Figures 3-27a and 3-27b). This fully threaded dual wall pipe is available in 4.50 inch and 6.625 inch outside diameters. Table 3-6 gives the dimensions and mechanical properties for the these fully threaded dual wall pipe sizes.

An alternate to the above fully threaded shouldered connection is the quick release hex head connection dual wall pipe. This design also gives a contiguous single pipe element (no separate innertube). Figure 3-28 shows these hex head connections. The "box" and "pin" hex heads of ends of two separate pipe elements are fitted together and hardened steel rods inserted in side slots to secure the connections. The hex heads transmit the torque of the rotary drilling action through the drill string. The hardened steel pins transmit the axial tension and compression through the drill string. The four round holes in the faces of the box and pin connections allow for flow communication from annulus space of one dual wall pipe element to the annulus space of another dual wall pipe element. The central hole in the connection allows unobstructed return flow of air and entrained rock cuttings through the inside of the inside tube of the pipe element (see Figure 3-28). In general, the quick release hex head connection is used for the larger diameter dual wall pipe, e.g., 8.625 inch and 10.75 inch outside diameters (or larger).

Table 3-7 gives the dimensions and mechanical properties for these quick release hex head dual wall pipe sizes. The tension to yield values are the limiting axial tension loads that will initiate the material yield in the top pipe element in the dual pipe drill string. This yield can be in the outer tube of the dual pipe body or in the solid rods that are used to make up the connections, which ever is the weakest.

Dual wall pipe are uniquely designed for reverse circulation operations with compressed air (or other gases). The large annulus space in this type of drill string acts as a pressure vessel. The air volumetric flow rates in a reverse circulation operation are low since the rock cuttings are carried to the surface through the inside

tube of the dual wall pipe (see Chapter 8). Therefore, the velocity of the air flow in the annulus is slow.   The flow in the annulus at each connection is somewhat obstructed and therefore not suited for direct circulation.   The inside tube, however, has no obstructions at the connections and allows free flow of the compressed air with entrained rock cuttings.

Figure 3-27a: Pin threaded shouldered connection for dual wall pipe (courtesy of Holte Manufacturing Company).

Figure 3-27b: Box threaded shouldered connection for dual wall pipe (courtesy of Holte Manufacturing Company).

In general dual wall pipe elements are structurally very rigid and stiff.   Thus, this type of pipe can be used in compression.   This eliminates the need for heavy drill collars to place WOB in a reverse circulation, dual wall pipe drilling operation.

Figure 3-28: Box and pin of the quick release hex head connections for dual wall pipe (courtesy of Holte Manufacturing Company).

Table 3-7: Fully threaded connection and quick release hex head connection dual wall pipe dimensions and mechanical properties (courtesy of Holte Manufacturing Company).

Dual Wall Pipe OD	4.50 in	6. 625 in	8.625 in	10.75 in
Outer Tube ID	4.00 in	5.921 in	7.825 in	9.850 in
Innertube OD	2.875 in	4.50 in	5.00 in	7.000 in
Innertube ID	2.259 in	4.00 in	4.408 in	6.276 in
Pipe Wt/ft	23.0 lb/ft	39.0 lb/ft	56.0 lb/ft	90.0 lb/ft
Working Torque	8,000 ft-lb	26,000 ft-lb	42,500 ft-lb	85,000 ft-lb
Tension to Yield	205,000 lb	380,000 lb	410,000 lb	430,000 lb
Lengths Available	10 ft	20 ft	20 ft	20 ft

3.5 Safety Equipment
Drill strings used in direct circulation drilling operations for the recovery of oil, natural gas, or geothermal fluids are usually fitted with several safety valves.

3.5.1 *Float Valves*
Figure 3-29 shows a typical drill string float valve.   This is a safety valve device and is usually placed in the bit sub at the bottom of the drill string.   These valves are used in nearly all deep rotary air and gas drilling operations.   The valve prevents the back flow of compressed air (or other gas) and entrained rock cuttings from entering the annulus space into the inside of the drill string. The valve is fitted with a flapper mechanism.   If circulation is stopped the compressed air and rock cuttings in the annulus will reverse flow and actuate the flapper which in turn stops the back-flow.

Fire float valves and fire stop valves are used only for oil and natural gas recovery drilling operations.

The fire stop valves are placed just above the drill bit and along the drill string at several positions. These valves have a zinc ring that holds back a spring-loaded flapper mechanism (like the float valve above) allowing air circulation from the surface. Wireline equipment can be run through these valves when the fire stop is in the normal open position. Figure 3-30 shows the schematic of the fire stop valve. This valve is basically the reverse of the float valve (compare Figures 3-29 and 3-30).

A single fire float can be installed at the bottom of the drill string. This valve is usually installed in the bit sub just above the drill bit. In normal operation, air flow pressure from circulation forces a spring-loaded piston down allowing the air to circulate. When design temperature is exceeded, a zinc ring melts which in turn allows a sleeve to close over air ports stopping circulation and the supply of air to the bottom of the borehole.

3.5.2 *Kelly Sub Valves*

At the top of the drill string (just above the kelly) is a kelly cock sub which is fitted with a ball valve (see Figure 3-1). In the event of a subsurface blowout, the kelly cock's ball valve can be closed and the sub left made up to the top of the kelly. With the ball valve closed, a pressure gauge can be made up to the top of the sub. Using this pressure gauge, the ball valve can be opened and vital pressure information obtained for the pressure inside the drill string (together with casing head annulus pressure). This information is needed to design the well control procedure.
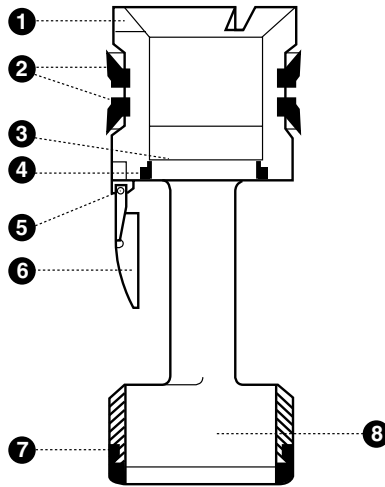
Figure 3-29: Schematic of a typical flapper type float valve for direct circulation operations. 1) Cage, 2) side seal, 3) seal retainer, 4) seal, 5) pin, 6) flapper valve, 7) shock absorber, and 8) location of bevel guide (courtesy of Baker Oil Tools).

FIRE STOP

NORMAL. Flapper in Fire Stop is
open allowing use of wire line
equipment in drill collars.

FIRE. When flapper closes, Fire
Stop halts air flow to stop burnouts
in drill collar assembly.
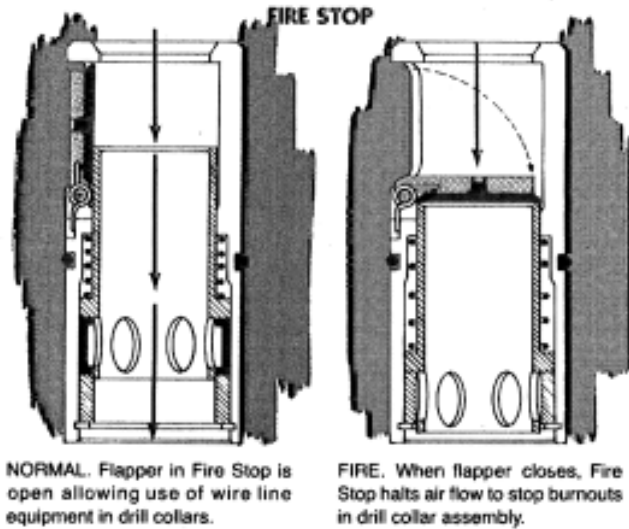
Figure 3-30: Schematic of a typical fire stop valve (courtesy of Wayne M. Sullivan and Associates Incorporated).

3.6 Drill String Design

One of the initial planning steps for a rotary drilling operation is the design of the drill string. The drill string must have the strength to drill to the intended target depth and be light enough so that the hoisting system can extract the string from the well when the target depth has been reached. Described below is the API procedure for drill string design [1].

The axial tension force (or load), F (lb), at the top of the drill string in a vertical well is

$$F = \left[\left(L_p \, w_p \right) + \left(L_c \, w_c \right) \right] K_b \qquad (3\text{-}1)$$

where L_p is the length of the drill pipe (ft),
$\quad w_p$ is the weight per unit length of drill pipe (lb/ft),
$\quad L_c$ is the length of the drill collars (ft),
$\quad w_c$ is the weight per unit length of drill collars (lb/ft),
$\quad K_b$ is the buoyancy factor.

The buoyancy factor is

$$K_b = \left(1 - \frac{\gamma_m}{\gamma_s} \right) \qquad (3\text{-}2)$$

where γ_m is the specific weight of the drill fluid (lb/ft^3),

γ_s is the specific weight of steel (lb/ft^3).

The maximum allowable design axial tension force, F_a (lb), is

$$F_a \ = \ 0.9 \ F_y \tag{3-3}$$

where F_y is the drill pipe tension force to produce material (steel) yield (incipient failure of the drill pipe) (lb). These tension failure values can be obtained from the tables in Appendix B or Tables 3-3, 3-6, and 3-7.

For most drill string designs a factor of safety is used to insure there is a margin-of-overpull (*MOP*) to allow for a stuck drill string. The drill string design factor of safety, *FS*, is given by

$$FS \ = \ \frac{F_a}{F} \tag{3-4}$$

The *MOP* is determined by the rotary drilling rig hoisting capacity. Thus, *MOP* is

$$MOP \ = \ F_c \ - \ F \tag{3-5}$$

where F_c is the hoisting capacity of the rotary drill rig (lb). But the total hoisting axial force cannot exceed F_a.

Illustrative Example 3.1 A section of a vertical well is to be rotary air drilled from 7,000 ft to 10,000 ft with a 7 7/8 inch tri-cone roller cutter drill bit. This is to be a direct circulation drilling operation. Above the drill bit the BHA is made up of 500 ft of 6 3/4 inch by 2 13/16 inch drill collars and similar diameter survey subs and nonmagnetic drill collars. The drill pipe available from the drilling contractor is API 4 1/2 inch, 16.60 lb/ft nominal, EU-S135, NC50(IF). Determine the *FS* and the *MOP* associated with using this drill string to drill this section of the well.

From Appendix B, Table B-1 gives 100 lb/ft for the 6 3/4 inch by 2 13/16 inch drill collar. Table B-5 gives 18.62 lb/ft for the drill pipe actual weight per unit length (includes tool joints). Since the drilling fluid is air, then $\gamma_m = 0$, and $K_b = 1.0$. The maximum axial tension force in the top drill pipe element of the drill string is when the depth is 10,000 ft and when the drill bit is lifted off the bottom of the well (after the target depth has been reached). The maximum axial tension force is determined from Equation 3-1. This is

$$F \ = \ \left[(9,500)(18.62) \ + \ (500)(100) \right] (1.0)$$

$$F \ = \ 226,890 \ lb$$

Table B-5 gives the tension force to produce yield in the drill pipe (in this case the pipe body). This tension force to yield is 595,004 lb. Equation 3-3 can be used to

determine the maximum allowable axial tension force for the drill pipe.   Thus, Equation 3-3 is

$$F_a \; = \; 0.9 \; (595,004)$$

$$F_a \; = \; 535,504 \; \text{lb}$$

The factor of safety is determined from Equation 3-4. Equation 3-4 gives

$$FS \; = \; \frac{535,504}{226,890}$$

$$FS \; = \; 2.36$$

Most land double and triple rotary drilling rigs do not have lifting capacities as high as 535,504 lb. Assuming a rotary drilling rig is selected with a maximum hoisting capacity of 300,000 lb, then Equation 3-5 can be used to determine the *MOP*. Equation 3-5 gives

$$MOP \; = \; 300,000 \; - \; 226,890$$

$$MOP \; = \; 73,110 \; \text{lb}$$

From the calculations above, the additional 73,110 lb (above the weight of the drill string) or, a total axial tension force of 300,000 lb can be safely pulled by the rig hoisting system with the assurance that the drill string will not structurally fail.

Illustrative Example 3.2   The George E. Failing Company Star 30K self-propelled drilling rig (shown in Figure 1-3) is to be used to air drill a shallow well with dual wall pipe (reverse circulation). The well is to be vertical with a depth of 820 ft and will use 5.50 inch concealed inner-tube pipe (see Table 3.6). The drilling operation will drill a borehole having a 6 1/4 inch diameter. The hoisting capacity of this drill rig is 30,000 lb. Determine the factor of safety for this drill string and the *MOP* for this drilling operation.

The 5.50 inch dual wall pipe has a weight per unit length of 27.4 lb/ft (see Table 3-6). Since the drilling fluid is air, then $\gamma_m = 0$, and $K_b = 1.0$. The maximum axial tension force in the top dual wall pipe element of the drill string is when the depth is 820 ft and when the drill bit is lifted off the bottom of the well (after the target depth has been reached). The maximum axial tension force is determined from Equation 3-1. This is

$$F \; = \; (820) \; (27.4) \; (1.0)$$

$$F \; = \; 22,468 \; \text{lb}$$

Table 3-6 gives the axial tension force to produce yield in this dual wall pipe.   This tension force to yield is 206,900 lb.   Equation 3-3 can be used to determine the maximum allowable axial tension force for the drill pipe.   Thus, Equation 3-3 is

$$F_a \;=\; 0.9 \;(206,900)$$

$$F_a \;=\; 186,210 \;\; lb$$

The factor of safety is determined from Equation 3-4.   Equation 3-4 gives

$$FS \;=\; \frac{186,210}{22,468}$$

$$FS \;=\; 8.29$$

The *MOP* for this drilling example is obtained from Equation 3-5.   Equation 3-5 gives

$$MOP \;=\; 30,000 \;-\; 22,468$$

$$MOP \;=\; 7,532 \;\; lb$$

This example demonstrates that the dual wall pipe has very high strength in resisting structural failure.   However, most shallow drilling rigs do not have the hoisting capacity to lift these dual wall drill strings when deep drilling operations are considered. This example shows that the Factor of Safety for the drill string is quite high illustrating this structural strength.   But this low *MOP* value illustrates the inadequate capacity of most single rotary drill rigs that might be used for a typical shallow drilling operation.

References

1. *API Recommended Practices for Drill Stem Design and Operating Limits*, API RP7G, 16th Edition, August 1998.

2. *Drilling Manual*, International Association of Drilling Contractors (IADC), Eleventh Edition, 1992.

3. Roscoe Moss Company, *Handbook of Ground Water Development*, Wiley, 1990.

4. Bourgoyne, A. T., Millheim, K. K., Chenevert, M. E., and Young, F. S., *Applied Drilling Engineering*, SPE, First Printing, 1986.

5. Durrett, E., "Rock Bit Identification Simplified by IADC Action," *Oil and Gas Journal*, Vol. 76, May 22, 1972.

6. *Rotary Shouldered Connections*, Drilco a Division of Smith International Incorporated, 1978.

This page intentionally left blank.

Chapter

Four

Compressors

There are a variety of air and gas compressor designs in use throughout industry. These designs vary greatly in the volume amounts of air or gas moved and the pressures attained. The largest usage of compressors is in the oil and gas production and transportation industries, and in the chemical industry. The information regarding this technology will be used to develop an understanding of how compressors can be used in air and gas drilling operations.

Air or gas compressors are very similar in basic design and operation to liquid pumps. The basic difference is that compressors are movers of compressible fluids; pumps are movers of incompressible fluids (i.e., liquids).

4.1 Compressor Classification

Similar to the classification of pumps, compressors are grouped in one of two general classes: continuous flow (i.e., dynamic) compressors, and intermittent flow (i.e., positive displacement) compressors (see Figure 4-1) [1, 2]. Intermittent flow or positive displacement compressors move the compressible fluid through the compressor in separate volume packages of compressed fluid (these volume packages are separated by moving internal structures in the machine). The most important subclass examples of positive displacement compressors are reciprocating and rotary compressors. Continuous flow or dynamic compressors utilize the kinetic energy of the continuously moving compressible fluid in combination with the internal geometry of the compressor to compress the fluid as it moves through the device. The most important subclass examples of dynamic compressors are centrifugal and axial-flow compressors.
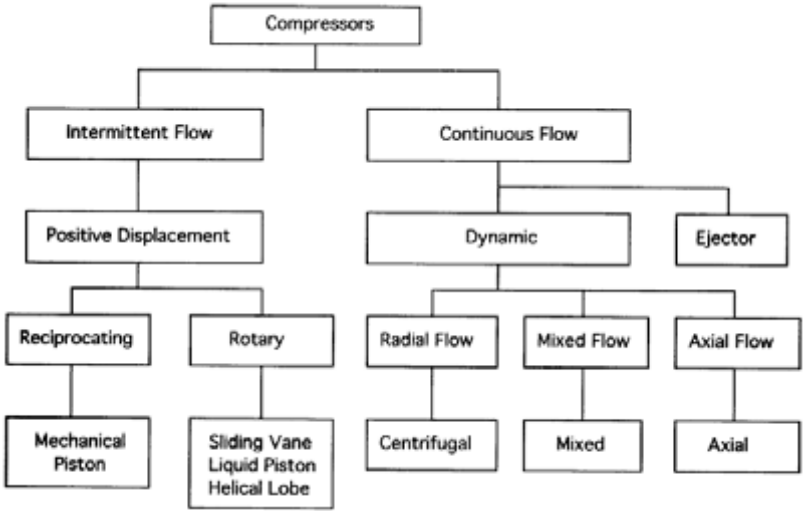
Figure 4-1: Compressor classification [2].

Each of the two general classes of compressors and their subclasses have certain advantages and disadvantages regarding their respective volumetric flow rate capabilities and overall compression pressure ratios. Figure 4-2 shows the typical application range in volumetric flow rates (actual cfm) and compression pressure ratios for most important compressor classes and subclasses [2].

In general, positive displacement compressors are best suited for handling high-pressure ratios (i.e., up to approximately 200), but this can be accomplished with only moderate volumetric flow rate magnitudes (i.e., up to about 10^3 actual cfm). Dynamic compressors are best suited for handling large volumetric flow rates (i.e., up to about 10^6 actual cfm), but with only moderate pressure ratios (i.e., up to approximately 20).

Figure 4-3 gives the general performance curves for various positive displacement and dynamic compressors [2]. The positive displacement compressors, particularly the multistage reciprocating compressors, are very insensitive to downstream back pressure changes. These compressors will produce their rated volumetric flow rate even when the pressure ratio approaches the design limit of the machine. Rotary compressors are fixed pressure ratio machines and are generally insensitive to downstream back pressure ratio changes as long as the output pressures required are below the maximum design pressures of the machines (i.e., problems with slippage). Dynamic compressors are quite sensitive to pressure ratio changes. The volumetric flow rates will change drastically with rather small changes in the downstream back pressure (relative to the pressure ratio around which the machine has been designed). Thus, positive displacement compressors are normally applied to industrial operations where volumetric flow rates are critical and pressure ratios are variable.
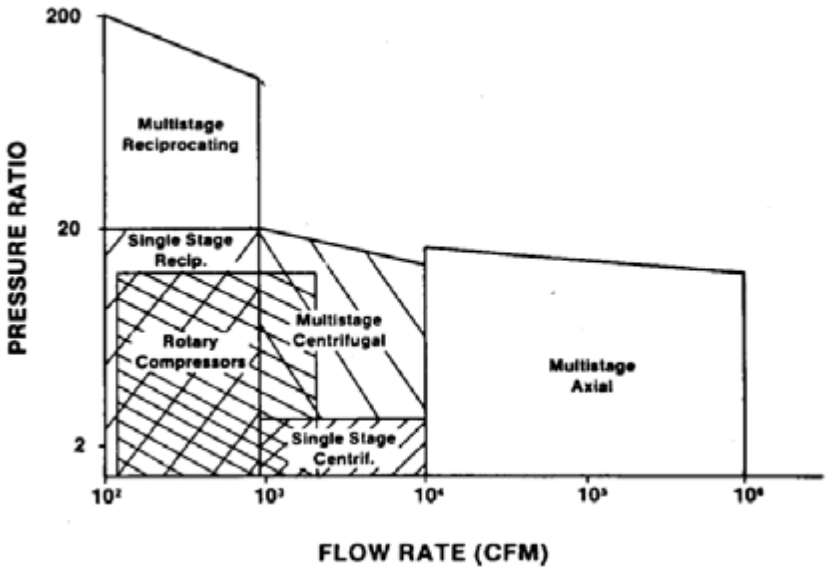
Figure 4-2: Typical application ranges of compressor types [2].
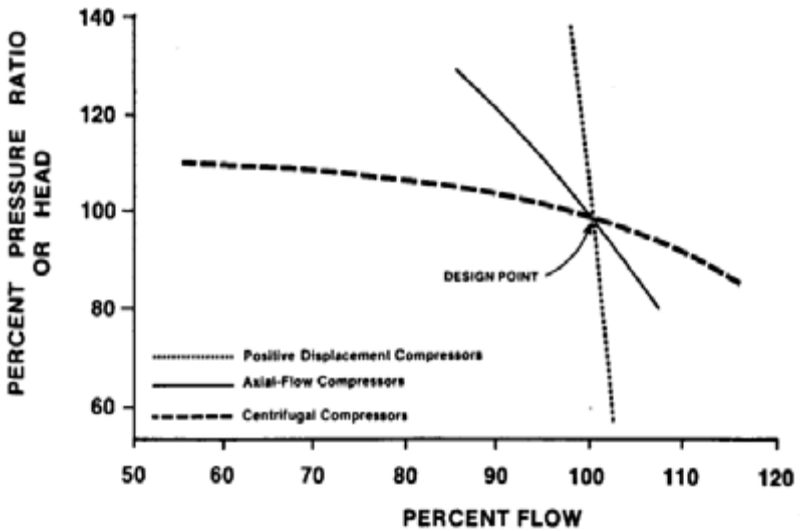
Figure 4-3: General performance curves for various compressor types [2].

Dynamic compressors are generally applied to industrial operations where the volumetric flow rate and pressure ratio requirements are relatively constant.

4.2 Standard Units

In the United States a unit of air or any gas is referenced to the standard cubic foot of dry air. The API Mechanical Equipment Standards standard atmospheric conditions for dry air is a temperature of 60°F (which is $459.67 + 60 = 519.67°R$) and a pressure of 14.696 psia (760 mm, or 29.92 inches Hg). The equation of state for the perfect gas can be written as

$$\frac{P}{\gamma} = \frac{\mathbf{R}_u \, T}{m_w} \tag{4-1}$$

where P is the pressure (lb/ft^2 abs),

γ is the specific weight (lb/ft^3),

$\mathbf{R}_u$ is the universal gas constant (which is 1,545.4 ft-lb/lb-mole-°R),

T is the temperature (°R),

m_w is the mole weight of the gas (lb/lb-mole).

Thus, using Equation 4-1, the specific weight γ, or the weight of 1 ft^3 of dry air is

$$\gamma = \frac{14.696 \, (144) \, (28.96)}{1545.4 \, (519.67)}$$

$$\gamma = 0.0763 \ \text{lb/ft}^3$$

where $m_w = 28.96$ lb/lb-mole (for dry air). Thus, a dry cubic foot of air at the API Mechanical Equipment Standards standard atmospheric condition weighs 0.0763 pounds (or a specific weight of 0.0763 lb/ft^3) [2, 3, 4].

Other organizations within the United States and regions around the world have established slightly different standard atmospheric conditions. For example, ASME standard atmosphere is a temperature of 68°F, a pressure of 14.7 psia, and a relative humidity of 36 percent. The United Kingdom uses a standard atmosphere with a temperature of 60°F and a pressure of 30.00 inches of Hg. Most Continental European countries use a standard atmosphere with a temperature of 15°C (59°F) and pressure of a bar or 750 mm of Hg (14.5 psia) [5].

When selecting and sizing compressors, care should be taken in determining which standard has been used to rate a compressor under consideration, particularly if the compressor has been produced abroad. All further discussions in this section will utilize only the API Mechanical Equipment Standards standard atmospheric conditions.

Compressors are rated by their maximum volumetric flow rate input and their maximum pressure output. The volumetric flow rate input ratings are usually specified in units of *standard cubic feet per minute* (scfm) and the maximum pressure output ratings are specified in units of psig (at a specified standard sea level condition, e.g., API, ASME, etc). The scfm volumetric flow rate refers to the

compressor intake.   The pressure rating refers to the output pressure capability at some standard condition, e.g., API, ASME, etc.

When a compressor is operated at surface location elevations above sea level, the volumetric flow rate intake is referred to as *actual cubic feet per minute* (actual cfm or acfm). Table 4-1 gives the average atmospheric pressure and average atmospheric temperature for the middle northern latitudes (applicable to latitudes 30° N to 60° N) [6].   Appendix D gives additional graphic data for surface elevation atmospheric pressures and temperatures. This data will be used in follow-on examples.

Table 4-1: Atmosphere at elevation (mid latitudes North America) above sea level [6].

Elevation (ft)	Pressure (psia)	Temperature (° F)
0	14.696	59.00
2,000	13.662	51.87
4,000	12.685	44.74
6,000	11.769	37.60
8,000	10.911	30.47
10,000	10.108	23.36

4.3 Continuous Flow (Dynamic) Compressors

The most widely used continuous flow compressors in industry are the centrifugal and axial-flow compressors (or compressors that combine the two designs).

4.3.1 *Centrifugal Compressors*

The centrifugal compressor was the earliest developed dynamic compressor. This type of compressor allows for the continuous flow of the gas through the machine. There is no distinct closed boundary enclosure in which compression takes place. The compression of the gas results from the speed of the flow through a specified geometry within the compressor.   The basic concept of the centrifugal compressor is the use of centrifugal forces on the gas created by high velocity flow of the gas in the cylindrical housing.   Figure 4-4 shows a diagram of a single-stage centrifugal compressor [2]. The gas to be compressed flows into the center of the rotating impeller. The impeller throws the gas out to the periphery by means of its radial blades rotating at high speed. The gas is then guided through the diffuser where the high velocity gas is slowed which results in a higher pressure in the gas. In multistage centrifugal compressors, the gas is passed to the next impeller from the diffuser of the previous impeller (or stage).   In this manner, the compressor may be staged to increase the pressure of the ultimate discharge (see Figure 4-5) [2].   Since the compression pressure ratio at each stage is usually rather low, of the order of 2, there is little need for intercooling between each stage (Figure 4-5 shows an intercooler after first three stages).

The centrifugal compressor must operate at rather high rotation speeds to be efficient. Most commercial centrifugal compressors operate at speeds on the order of 20,000 to 30,000 rpm. With such rotation speeds very large volumes of gas can be compressed with equipment having rather modest external dimensions.   Commercial

centrifugal compressors can operate with volumetric flow rates up to approximately 10^4 actual cfm and with overall multistage compression ratios up to about 20.
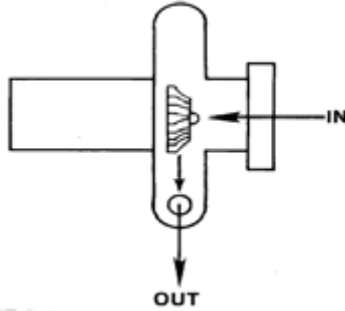
Figure 4-4: Single-stage centrifugal compressor [2].
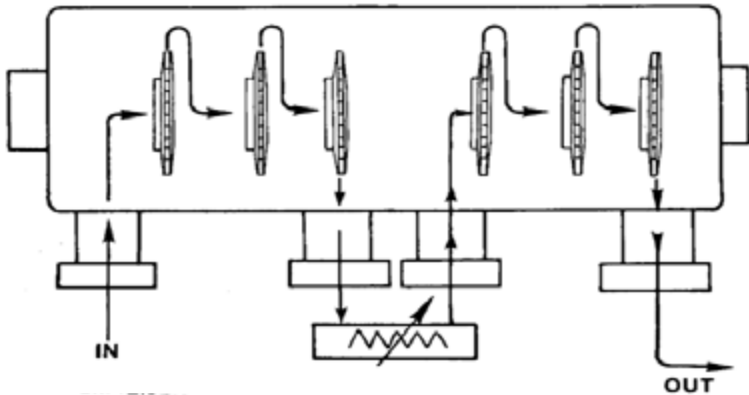
Figure 4-5: Multistage centrifugal compressor with intercooler [2].

Centrifugal compressors are usually used in large processing plants and in some pipeline applications. They can be operated with some small percentage of liquid in the gas flow.

These machines are used principally to compress large volumetric flow rates to rather modest pressures. Thus, their use is more applicable to the petroleum refining and chemical processing industries.

More details regarding the centrifugal compressor can be found in other references [2, 7, 8, 9].

4.3.2 *Axial-Flow Compressors*

Axial-flow compressors are very high-speed, large volumetric flow rate machines. This type of compressor flows gas into the intake ports and propels the

gas axially through the compression space via a series of radial arranged rotating rotor blades and stationary stators (or diffuser) blades (see Figure 4-6) [1]. As in the centrifugal compressor, the kinetic energy of the high-velocity flow exiting each rotor stage is converted to pressure energy in the follow-on stator (diffuser) stage. Axial-flow compressors have a volumetric flow rate range of approximately 3×10^{4} to 10^{6} actual cfm. Their compression ratios are typically around 10 to 20. Because of their small diameter, these machines are the principal compressor design for jet engine applications. There are also applications for axial-flow compressors in large process plant operations where very large constant volumetric flow rates at low compression ratios are needed.

More detail regarding axial-flow compressors can be found in other references [2, 7, 8, 9].

in   out
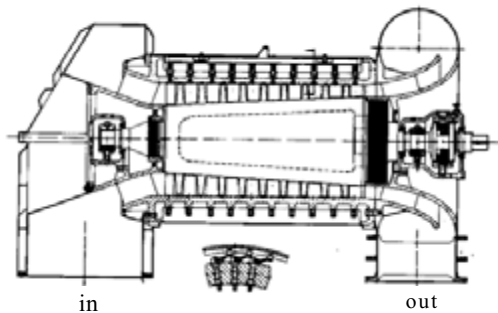
Figure 4-6: Multistage axial-flow compressor [1].

4.4 Positive Displacement Compressors

In general, only the reciprocating compressor allows for rather complete reliable flexibility in applications requiring variable volumetric flow rates and variable pressure ratios. The rotary compressor (which has a fixed pressure ratio built into the compressor design) does not allow for much variation in either.

4.4.1 *Reciprocating Compressors*

The reciprocating compressor is the simplest example of the positive displacement class of compressors. This type of compressor was also the earliest designed. Like reciprocating incompressible fluid pumps, reciprocating compressors can also be either single acting or double acting. Single-acting compressors are usually of the trunk type (see Figure 4-7) [1]. Double-acting compressors are usually of the crosshead type (see Figure 4-8) [1].

Reciprocating compressors are available in both lubricated and non-lubricated versions. The lubricated versions provide lubrication for the moving pistons (in the cylinder) either through an oil lubricated intake gas stream, or via an oil pump and injection of oil to the piston sleeve. There are some applications where oil must be completely omitted from the compressed air or gas exiting the machine. For such applications where a reciprocating piston type of compressor is required, there are

non-liquid lubricated compressors. These compressors have piston rings and wear bands around the periphery of each piston. These wear bands are made of special wear-resistant dry lubricating materials such as polytetrafluorethylene. Trunk type non-lubricated compressors have dry crankcases with permanently lubricated bearings. Crosshead type compressors usually have lengthened piston rods to ensure that no oil wet parts enter the compression space [1, 7].
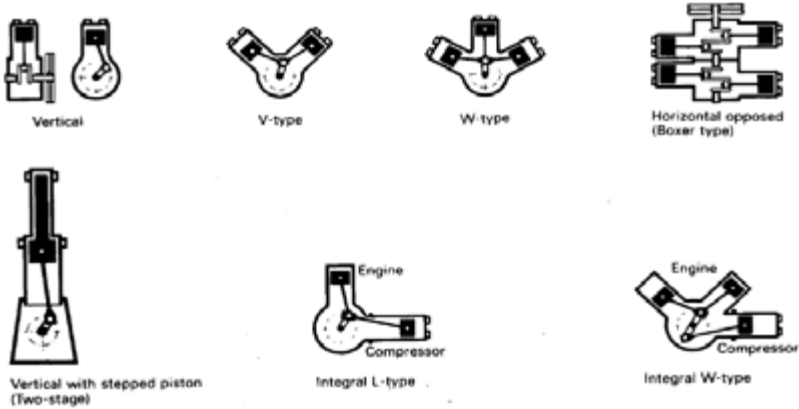
Figure 4-7: Single-acting (trunk type) reciprocating piston compressor [1].
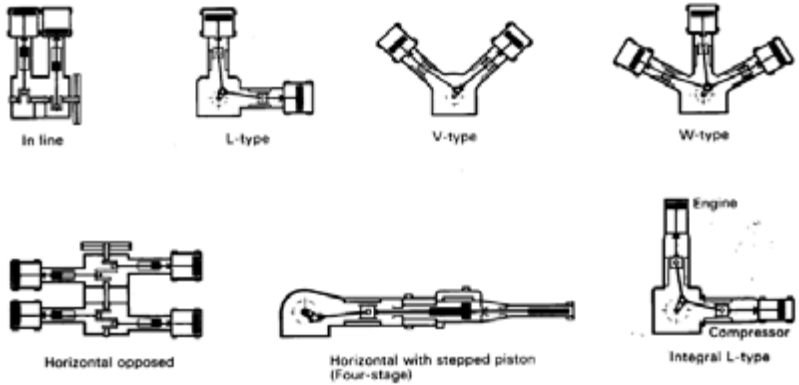
Figure 4-8: Double-acting (crosshead type) reciprocating piston compressor [1].

Most reciprocating compressors have inlet and outlet valves (on the piston heads) that are actuated by a pressure differential. These are called *self-acting valves.* There are some larger multistage reciprocating piston compressors that do have camshaft-controlled valves with rotary slide valves.

The main advantage of the multistage reciprocating piston compressor is the positive control of both the volumetric flow rate, which can be put through the machine, and the pressure of the output.   Many reciprocating piston compressors allow for the rotation to be adjusted, thus, changing the throughput of air or gas.   Also, provided there is adequate input power from the prime mover, reciprocating piston compressors can adjust to any back pressure changes and maintain proper rotation speed (which in turn maintains a given volumetric flow rate).

The main advantage of this subclass of compressor is their extremely high pressure output capability and reliable volumetric flow rates (see Figures 4-2 and 4-3).   The main disadvantage to multistage reciprocating piston compressors is that they can not be practically constructed in machines capable of volumetric flow rates much beyond 1,000 actual cfm.   Also, the higher-capacity compressors are rather large and bulky and generally require more maintenance than similar capacity rotary compressors.   In any positive displacement compressor, like a liquid positive displacement pump, the real volume flow rate is slightly smaller than the mechanical displacement volume.   This is due to the following factors:

• Pressure drop on the suction side
• Heating up of the intake air
• Internal and external leakage
• Expansion of the gas trapped in the clearance volume (reciprocating piston
  compressors only)

Reciprocating compressors can be designed with multiple stages.   Such multistage compressors are designed with nearly equal compression ratios for each stage (it can be shown that equal stages of compression lead to minimum input power requirements).   Thus, since the volumetric flow rate (in actual cfm) is reduced from one stage to the next, the volume displacement of each stage (its geometric size) is progressively smaller.

4.4.2 *Rotary Compressors*

Another important positive displacement compressor is the rotary compressor. This type of compressor is usually of rather simple construction, having no valves and being lightweight.   These compressors are constructed to handle volumetric flow rates up to around 2,000 actual cfm and pressure ratios up to around 15 (see Figure 4-2). Rotary compressors are available in a variety of designs.   The most widely used rotary compressors are the sliding vane, helical lobe (screw), and liquid piston.

The most important characteristic of this type of compressor is that all have a fixed, built-in, compression ratio for each stage of compression (as well as a fixed, built-in volume displacement) [1].   Thus, at a given rotational speed (provided by the prime mover), there will be a predetermined volumetric flow rate through the compressor (the geometry of the compressor inlet is fixed), and the pressure at the outlet will be equal to the built-in design pressure ratio of the machine multiplied by the inlet pressure.

The upper pressure versus volume plot in Figure 4-9 shows the typical situation when the back pressure on the outlet side of the compressor is equal to the built-in design output pressure.   Under these conditions, there is no expansion of the output gas as it exits the compressor and passes through the expansion tank and continues into the initial portion of the pipeline [1].

The middle pressure versus volume plot in Figure 4-9 shows the typical situation when the back pressure on the outlet side of the compressor is above the built-in design output pressure. Under these conditions, the compressor cannot expel the gas volume within it efficiently. Thus, the fixed volumetric flow rate (at a given rotation speed) will be reduced from the volumetric flow rate when the back pressures are equal to, or less than the built-in design output pressure [1].

The lower pressure versus volume plot in Figure 4-9 shows the typical situation when the back-pressure on the outlet side of the compressor is less than the built-in design output pressure. Under these conditions, the gas exiting the compressor expands in the expansion tank and the initial portion of the pipeline until the pressure is equal to the pipeline back pressure [1].

Rotary compressors can also be designed with multiple stages. Such multistage compressors are designed with nearly equal compression ratios for each stage (i.e., minimum input power requirements). Thus, since the volumetric flow rate (in actual cfm) is reduced from one stage to the next, the volume displacement of each stage (its geometric size) is progressively smaller.

Sliding Vane Compressors

The typical sliding vane compressor stage is a rotating cylinder located eccentric to the center-line of a cylindrical housing (see Figure 4-10) [1, 2]. The vanes are in slots in the rotating cylinder, and are allowed to move in and out in these slots to adjust to the changing clearance between the outside surface of the rotating cylinder and the inside bore surface of the housing. The vanes are always in contact with the inside bore due to either pressured gas under the vane (in the slots), or spring forces under the vane. The top of the vanes slide over the inside surface of the bore of the housing as the inside cylinder rotates. Gas is brought into the compression stage through the inlet suction port. The gas is then trapped between the vanes, and as the inside cylinder rotates the gas is compressed to a smaller volume as the clearance is reduced. When the clearance is the smallest, the gas has rotated to the outlet port. At the outlet port, the compressed gas is discharged to a surge tank or pipeline system connected to the outlet side of the compressor. As each set of vanes reaches the outlet port, the gas trapped between the vanes is discharged. The clearance between the rotating cylinder and the stationary cylindrical housing is fixed, and thus the pressure ratio of compression for the stage is fixed. The geometry, e.g., cylinder length, diameter, the inside housing diameter, the inlet area, the outlet area, of each compressor stage determines the stage displacement volume and compression ratio.

The principal seals within the sliding vane compressor are provided by the interface force between the end of the vane and the inside surface of the cylindrical housing. The sliding vanes must be made of a material that will not damage the inside surface of the housing and slide easily on that surface. Therefore, most vane materials are composites such as phenolic resin-impregnated laminated fabrics. Usually vane compressors require oil lubricants to be injected into the gas entering the compression cavity. This lubricant allows smooth action of the sliding vanes against the inside of the housing. There are, however, some sliding vane compressors that may be operated nearly oil-free. These utilize bronze, or carbon/graphite vanes [7].
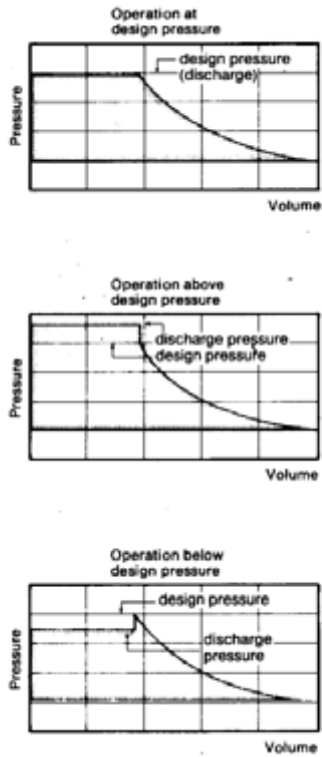
Figure 4-9: Rotary compressors operating with back-pressure at the built-in design pressure (upper), with a back-pressure above the built-in design pressure (middle), and with a back-pressure below the built-in design pressure (lower) [1].

The volumetric flow rate for a sliding vane compression stage, q_s, is approximately

$$q_s = 2.0 \ a \ l \ (d_2 - m \ t) \ N \qquad (4\text{-}2)$$

and

$$a = \frac{d_2 - d_1}{2} \qquad (4\text{-}3)$$

where q_s is volumetric flow rate (cfm),
$\quad a$ is the eccentricity (ft),

l is the length of the cylinder (ft),
d_1 is the outer diameter of the rotary cylinder (ft),
d_2 is the inside diameter of the cylindrical housing (ft),
t is the vane thickness (ft),
m is the number of vanes,
N is the speed of the rotating cylinder (rpm).

Some typical values of a vane compressor stage geometry are $d_1/d_2 = 0.88$, $a = 0.06\ d_2$ and $l/d_2 = 2.00$ to 3.00. Typical vane tip speed usually should not exceed 50 ft/sec.

in

out
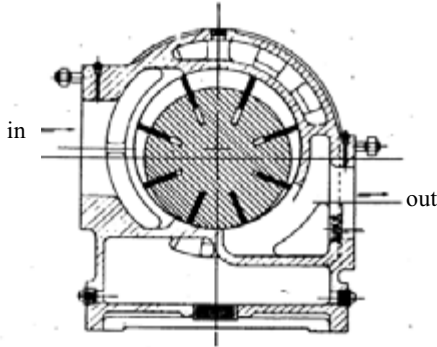
Figure 4-10: Sliding vane rotary compressor.

Helical Lobe Compressors

A typical helical lobe (screw) rotary compressor stage is made up of two rotating helical shaped shafts, or screws. One is a female rotor and the other a male rotor. These two rotating components turn counter to one another (counterrotating) (see Figure 4-11) [1]. As with all rotary compressors, there are no valves. The gas flows (due to negative pressure conditions at the inlet) into the inlet port and is squeezed between the male and female portion of the rotating intermeshing screw elements and the housing. The compression ratio of the stage and its volumetric flow rate are determined by the fixed geometry of the two rotating screw elements and the rotation speed. Thus, the rotary screw compressor is a fixed ratio machine.

Screw compressors operate at rather high speeds. Thus, they are rather high volumetric flow rate compressors with relatively small exterior dimensions.

Most helical lobe rotary compressors use lubricating oil within the compression space. This oil is injected into the compression space and recovered, cooled, and recirculated. The lubricating oil has several functions:
• Seal the internal clearances
• Cool the gas (usually air) during compression
• Lubricate the rotors
• Eliminate the need for timing gears

There are versions of the helical lobe rotary compressor that utilize water injection (rather than oil). The water accomplishes the same purposes as the oil, but the air delivered by these machines can be oil-free.

female rotor

male rotor
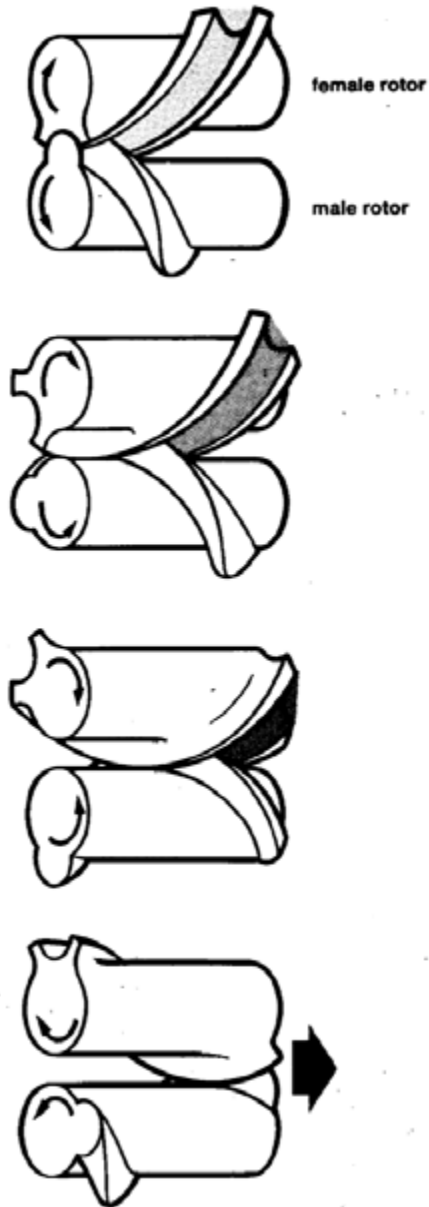
Figure 4-11: Helical lobe (screw) rotary compressor [1].

Some helical lobe rotary compressors have been designed to operate with an entirely liquid-free compression space. Since the rotating elements of the compressor need not touch each other or the housing, lubrication can be eliminated. However, such helical lobe rotary compressor designs require timing gears. These machines can deliver totally oil-free, water-free dry gas.

The helical lobe rotary compressor can be staged very much like the sliding vane compressor. Often helical lobe rotary compressors are utilized in two-stage, three-stage, and four-stage versions.

Detailed calculations regarding the design of the helical lobe rotary compressor are beyond the scope of this book. Additional details can be found in other references [1, 7].

Liquid Piston Compressors

The liquid piston (or liquid ring) rotary compressor utilizes a liquid ring as a piston to perform gas compression within the compression space. The liquid piston compressor stage uses a single rotating element that is located eccentric to the center of the housing (see Figure 4-12) [2]. The rotor has a series of vanes extending radial from it with a slight curvature toward the direction of rotation. A liquid, such as oil, partially fills the compression space between the rotor and the housing walls. As rotation takes place, the liquid forms a ring as centrifugal forces and the vane geometry force the liquid to the outer boundary of the housing. Since the element is located eccentric to the center of the cylindrical housing, the liquid ring (or piston) moves in an oscillatory manner. The compression space in the center of the stage communicates with the gas inlet and outlet parts and allows a gas pocket. The liquid ring alternately uncovers the inlet part and the outlet part. As the system rotates, gas is brought into the pocket, compressed, and released to the outlet port.
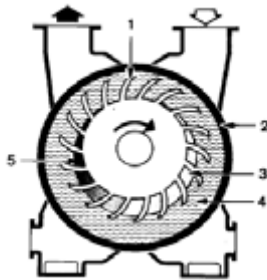
Figure 4-12: Liquid piston rotary compressor, 1) impeller, 2) housing, 3) intake port, 4) working liquid, and 5) discharge port [1].

The liquid piston compressor has rather low overall efficiency, about 50 percent. The main advantage to this type of compressor is that it can be used to compress gases with significant liquid content in the stream.

4.4.3 Summary of Positive Displacement Compressors

The main advantages of the reciprocating piston compressors are: 1) dependable near constant volumetric flow rate and, 2) variable pressure capability (up to the

maximum pressure capability of the compressor). The disadvantages are: 1) bulky, 2) high initial capital costs (relative to the rotary compressor of similar capabilities) and, 3) relatively high maintenance costs due to greater number of moving parts (relative to most rotary compressors).

The main advantages of rotary compressors are: 1) initial low capital cost (relative to reciprocating compressors), 2) less bulky (relative to the reciprocating compressors of similar capabilities) and, 3) general ease of maintenance since these compressors have few moving parts. The main disadvantages are: 1) cannot adjust to flow line back pressures (fixed compression ratios), 2) needs frequent specific maintenance of rotating wear surfaces to prevent slippage and, 3) most rotary compressors operate with oil lubrication in the compression chambers [1, 2, 7].

4.5 Compressor Shaft Power Requirements

The most important single factor affecting the successful outcome of air and gas drilling operations is the availability of constant, reliable volumetric flow rates of air or gas to the well. This must be the case even when there are significant (and frequent) changes in back pressure during these operations. The only two compressor subclasses that can meet these flexibility requirements are the reciprocating compressor and the rotary compressor. In what follows, the important calculation techniques that allow for the proper evaluation and selection of the appropriate compressors for air and gas drilling operations are reviewed [1, 7 and 10]. This section derives the theoretical power required at the compressor shaft to compress the gas in the compressor.

4.5.1 *Basic Single-Stage Shaft Power Requirement*

Figure 4-13 shows a pressure-volume (*P-v*) diagram for a simple compression cycle process (where *P* is pressure and *v* is specific volume in any set of consistent units). In Figure 4-13, point *c* represents the final state, or state 2, of the gas leaving the compressor.

The area *odcm* measures the product $P_2 v_2$ which is the flow-work (ft-lb/lb) required for delivery of the gas from the compressor. Point *b* represents the initial state 1 of the gas and the area *oabn* measures the product $P_1 v_1$ which is the flow-work (ft-lb/lb) supplied in the passage of the fluid to the compressor. The line *bc* represents the state change of the gas during compression. The area *mcbn* measures

$$- \int_1^2 P \, dv \qquad (4\text{-}4)$$

or

$$+ \int_2^1 P \, dv \qquad (4\text{-}5)$$

which is the work ideally required for effecting the actual compression within the compressor. Thus, aside from the work required for increasing the kinetic energy, the net area *abcd* measures the net shaft work required for the induction,

compression, and delivery of the gas under conditions which are assumed to be ideal (absence of fluid or mechanical friction, and mechanically reversible).
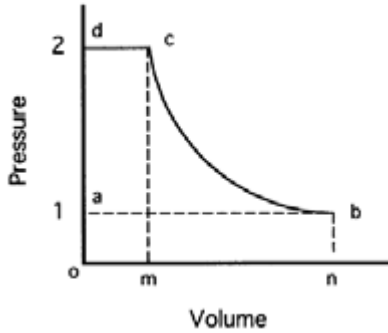
Figure 4-13: Basic pressure-volume diagram.

The total shaft work, W_s (ft-lb/lb), required for compression can be written as

$$W_s = \frac{V_2^2}{2g} - \frac{V_1^2}{2g} + \left(P_2 \, v_2 - \int_1^2 P \, dv - P_1 \, v_1 \right) \qquad (4\text{-}6)$$

or

$$W_s = \frac{V_2^2}{2g} - \frac{V_1^2}{2g} + \left(P_2 \, v_2 + \int_2^1 P \, dv - P_1 \, v_1 \right) \qquad (4\text{-}7)$$

where W_s is the total shaft work (ft-lb/lb),
   V_1 is the velocity of the gas entering the compressor (ft/sec),
   V_2 is the velocity of the gas exiting the compressor (ft/sec),
   g is the acceleration of gravity (32.2 ft/sec^2).
Equation 4-6 can be rewritten as

$$W_s + \frac{V_1^2}{2g} - \frac{V_2^2}{2g} + P_1 \, v_1 - P_2 \, v_2 = - \int_1^2 P \, dv \qquad (4\text{-}8)$$

Assuming a polytropic process, where $P_1 v_1^n = P_2 v_2^n = P v^n = $ constant, and the simplest polytropic process where the exponent term $n \approx k$, where k is the ratio of specific heats for the gas involved in the process (e.g., for air, $k = 1.4$), Equation 4-8 can be written as

$$- \int_1^2 P \, dv \; = \; - \, P_1 \, v_1^k \int_1^2 \frac{dv}{v^k} \tag{4-9}$$

The right-hand side of the above equation can be integrated to yield

$$- \int_1^2 P \, dv \; = \; \frac{P_1 \, v_1}{k-1} \left[\left(\frac{v_1}{v_2} \right)^{k-1} - 1 \right] \tag{4-10}$$

For engineering calculations, Equation 4-1 is often simplified to the form

$$\frac{P}{\gamma} \; = \; \frac{\mathbf{R}_a \, T}{S_g} \tag{4-11}$$

$$\mathbf{R}_a \; = \; \frac{\mathbf{R}_u}{m_w} \tag{4-12}$$

where $\mathbf{R}_a$ is the gas constant for API standard condition air (53.36 ft-lb/lb-°R),
S_g is the specific gravity of the particular gas used (for API standard condition air $S_g = 1.0$).
Equation 4-11 can be further simplified by defining, $\mathbf{R}$ (ft-lb/lb-°R), as the gas constant for any specified gas (e.g., air, natural gas, nitrogen, etc.).   Therefore, the gas constant for any gas is approximately

$$\mathbf{R} \; = \; \frac{\mathbf{R}_a}{S_g} \tag{4-13}$$

Substituting Equation 4-13 into Equation 4-11 yields

$$\frac{P}{\gamma} \; = \; \mathbf{R} \, T \tag{4-14}$$

The specific volume and specific weight of a gas are related by

$$v \; = \; \frac{1}{\gamma} \tag{4-15}$$

Substituting Equation 4-15 into Equation 4-14 yields

$$P \, v \; = \; \mathbf{R} \, T \tag{4-16}$$

or, specifically

$$P_1 \, v_1 \;=\; \mathbf{R} \, T_1 \tag{4-17}$$

Using the definitions for a polytropic process given above, and Equation 4-17, then Equation 4-10 can be reduced to

$$-\int_1^2 P \, dv \;=\; \frac{\mathbf{R} \, T_1}{k-1} \left[\left(\frac{P_2}{P_1} \right)^{\frac{k-1}{k}} - 1 \right] \tag{4-18}$$

Again, using the definitions for a polytropic process and Equation 4-16, then a general relationship between P and T can be obtained. This is

$$\left(\frac{P_2}{P_1} \right)^{\frac{k-1}{k}} = \frac{T_2}{T_1} \tag{4-19}$$

Substituting Equation 4-19 into Equation 4-18 yields

$$-\int_1^2 P \, dv \;=\; \frac{\mathbf{R} \, T_1}{k-1} \left[\frac{T_2}{T_1} - 1 \right] = \frac{\mathbf{R}}{k-1} \left(T_2 - T_1 \right) \tag{4-20}$$

Substituting Equation 4-20 into Equation 4-8 gives

$$W_s + \frac{V_1^2}{2g} - \frac{V_2^2}{2g} + P_1 \, v_1 - P_2 \, v_2 = \frac{\mathbf{R}}{k-1} \left(T_2 - T_1 \right) \tag{4-21}$$

Equation 4-17 was the definition of Pv at state 1. Similarly, the definition of Pv at state 2 is

$$P_2 \, v_2 \;=\; \mathbf{R} \, T_2 \tag{4-22}$$

Substituting Equations 4-17 and 4-22 into Equation 4-21 and rearranging gives

$$W_s = \frac{V_2^2}{2g} - \frac{V_1^2}{2g} + \mathbf{R} \left(T_2 - T_1 \right) + \frac{\mathbf{R}}{k-1} \left(T_2 - T_1 \right) \tag{4-23}$$

The above can be rearranged to give

$$W_s = \frac{k}{k-1} \, \mathbf{R} \, T_1 \left(\frac{T_2}{T_1} - 1 \right) + \frac{V_2^2 - V_1^2}{2g} \tag{4-24}$$

It is more useful to have Equation 4-24 written in terms of pressure instead of temperature. This can be accomplished by substituting Equations 4-17 and 4-19 into Equation 4-24. This gives

$$
W_s = \frac{k}{k-1} P_1 v_1 \left[\left(\frac{P_2}{P_1} \right)^{\frac{k-1}{k}} - 1 \right] + \frac{V_2^2 - V_1^2}{2g}
\tag{4-25}
$$

The last term (the kinetic energy) in Equation 4-25 can be shown in practical applications to be quite small relative to the first term. Thus, this later term is usually neglected. Therefore, the shaft work for compression of gas in a compressor is reduced to

$$
W_s = \frac{k}{k-1} P_1 v_1 \left[\left(\frac{P_2}{P_1} \right)^{\frac{k-1}{k}} - 1 \right]
\tag{4-26}
$$

Compressors can actually be considered steady state flow mechanical devices (even intermittent flow machines). If the weight rate of flow through the compressor is, w (lb/sec), then the time rate of shaft work done, $\dot{W}_s$ (ft-lb/sec), to compress gas in a compressor can be obtained by multiplying Equation 4-26 by w. This gives

$$
\dot{W}_s = \frac{k}{k-1} P_1 \dot{w} v_1 \left[\left(\frac{P_2}{P_1} \right)^{\frac{k-1}{k}} - 1 \right]
\tag{4-27}
$$

The term, $\dot{W}_s$ (ft-lb/sec), is the theoretical power required by the compressor to compress the gas. Using the general relationship between specific volume and specific weight given in Equation 4-15, the volumetric flow rate at state 1 conditions (entering the compressor), Q_1, is

$$
Q_1 = \frac{w}{\gamma_1} = w\, v_1
\tag{4-28}
$$

Therefore, Equation 4-27 can be rewritten as

$$
\dot{W}_s = \frac{k}{k-1} P_1 Q_1 \left[\left(\frac{P_2}{P_1} \right)^{\frac{k-1}{k}} - 1 \right]
\tag{4-29}
$$

The above expression is valid for a single stage compressor and for any set of consistent units. With Equation 4-29, the shaft power to compress a continuous flow rate of gas can be determined knowing properties of the gas (specifically k), the initial pressure and volumetric flow rate of the gas entering the compressor (state 1), and the exit pressure of gas exiting the compressor (state 2).

4.5.2 *Multistage Shaft Power Requirements*

Using the basic expression given in Equation 4-24 (without the kinetic energy terms), the minimum shaft power required for a multistage compressor can be derived [10]. Equation 4-24 can be used for each stage of a multistage compressor and added together for the total shaft work required by the compressor. Such an expression can be minimized to obtain the conditions for minimum shaft work for a multistage compressor. Minimum shaft work is attained when a multistage compressor is designed with equal compression ratios for each stage and with intercoolers that cool the gas entering each stage to a temperature that is nearly the same as the temperature entering the first stage of the compressor [10]. Once these conditions are obtained for the multistage compressor, the expression for the shaft power can be obtained in the same manner as given in Equations 4-25 to 4-29.

Figure 4-14 shows an example schematic of a two stage compressor with an intercooler between the compression stages. The temperature exiting stage 1 (at position 2) will be governed by Equation 4-19. The intercooler cools the gas between positions 2 and 3 under constant volume conditions. Thus, the temperature of the gas entering stage 2 (at position 3) is the same as the temperature entering stage 1 (i.e., position 1). Using these conditions for the minimum shaft power, an expression for the shaft power of a multistage compressor can be derived. This expression is

$$
\dot{W}_s \;=\; \frac{n_s \, k}{k-1} \; P_i \, Q_i \left[\left(\frac{P_o}{P_i} \right)^{\frac{k-1}{n_s \, k}} - 1 \right]
\tag{4-30}
$$

where n_s is the number of compression stages in the multistage compressor,

P_i is the pressure entering the first stage of the compressor (lb/ft^2, abs),

P_o is the pressure exiting the last stage of the compressor (lb/ft^2, abs),

Q_i is the volumetric flow rate entering the first stage of the compressor (ft^3/sec).

The compression ratio for each stage, r_s, is given by

$$
r_s \;=\; \left(\frac{P_o}{P_i} \right)^{\frac{1}{n_s}}
\tag{4-31}
$$

Again, Equations 4-30 and 4-31 are valid for any set of consistent units.

In what follows, two sets for field equations are derived for determining the theoretical power to compress the gas passing through the compressor. One set is

derived for use with the English unit system and the other set for use with the SI unit system.
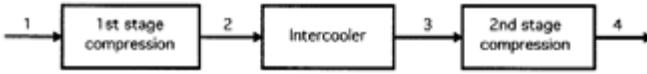
Figure 4-14: Schematic of a two stage compressor [10].

Equation 4-30 is obtained in English units by substituting the following for P_i, P_o, and Q_i (and dividing by 550 ft-lb/hp):

$$P_i = p_i \; 144 \tag{4-32}$$

$$P_o = p_o \; 144 \tag{4-33}$$

$$Q_i = \frac{q_i}{60} \tag{4-34}$$

where p_i is input pressure (psia),
p_o is output pressure (psia),
q_i is the input volumetric flow rate (ft^3/min).
The expression for theoretical shaft power $\dot{W}_s$ in English units (horsepower) is

$$\dot{W}_s = \frac{n_s \, k}{k-1} \frac{p_i \, q_i}{229.17} \left[\left(\frac{p_o}{p_i} \right)^{\frac{k-1}{n_s \, k}} - 1 \right] \tag{4-35a}$$

An alternate expression which is convenient for booster compressor calculations is

$$\dot{W}_s = \frac{n_s \, k}{k-1} \frac{\dot{w}_g}{550} \left(\frac{R \, T_i}{S_g} \right) \left[\left(\frac{p_o}{p_i} \right)^{\frac{k-1}{n_s \, k}} - 1 \right] \tag{4-35b}$$

where T_i is the input gas temperature (°R).
The expression for theoretical shaft power $\dot{W}_s$ in SI units (watts) is

$$\dot{W}_s = \frac{n_s \, k}{k-1} P_i \, Q_i \left[\left(\frac{P_o}{P_i} \right)^{\frac{k-1}{n_s \, k}} - 1 \right] \tag{4-36a}$$

where Q_i is the input volumetric flow rate (m³/sec),

P_i is the input pressure (N/m², abs),

P_o is the output pressure (N/m², abs).

An alternate expression which is convenient for booster compressor calculations is

$$\dot{W}_s = \frac{n_s\,k}{k-1}\,\dot{w}_g\left(\frac{\mathbf{R}\,T_i}{S_g}\right)\left[\left(\frac{P_o}{P_i}\right)^{\frac{k-1}{n_s\,k}} - 1\right] \qquad (4\text{-}36b)$$

where $\dot{w}_g$ is the gas weight rate of flow (N/sec),

T_i is the input gas temperature (K).

The compression ratio for each stage, r_s, is given by

$$r_s = \left(\frac{P_o}{P_i}\right)^{\frac{1}{n_s}} = \left(\frac{p_o}{p_i}\right)^{\frac{1}{n_s}} \qquad (4\text{-}37)$$

Equations 4-35 through 4-37 are valid for both reciprocating and rotary compressors (together with the other pertinent equations in this chapter).

4.6 Prime Mover Input Power Requirements

The above section discusses the theoretical shaft power required to compress the gas in a compressor. In order to obtain the complete picture of compressors, it is necessary to ascertain the prime mover input power requirement to operate the compressor shaft and the actual power available from the prime mover. The application of the above equations will be slightly different depending upon whether reciprocation piston compressors or rotary compressors are being analyzed.

The actual power available from a prime mover is a function of elevation above sea level, and whether the prime mover is naturally aspirated or turbocharged. Figure 4-15 gives the power percentage reduction in power necessary for naturally aspirated and turbocharged prime movers as a function of elevation above sea level [1].

4.6.1 *Compressor System Units*

Compressors used for air and gas drilling operations are driven by stationary prime movers. For small drilling rigs (i.e., drilling depth limits less than 1,000 ft), the compressor is often integrated into the rig design and the compressor is driven by a shared stationary prime mover that also drives the rig drawworks and rotating table (or hydraulic pump and motor rotating system). Larger drilling operations have separate compressor system units that are fabricated with their own dedicated stationary prime movers. These separate compressor system units are usually provided to the operator by a contractor other than the drilling rig contractor.

Primary Compressor System Unit

Primary compressor system units take air directly from the atmosphere. These compressor systems can be rotary or reciprocating compressors. The compressors in

these units can be single stage, or multistage. The prime movers for these units can be fueled by gasoline, propane/butane, diesel, or natural gas.   These units can be fabricated as skid mounted, semi-trailer mounted, or as wheeled trailers.
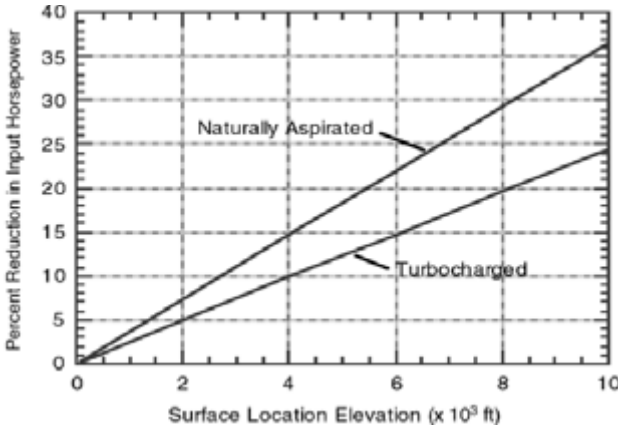
Figure 4-15: Prime mover percentage reduction in power as a function of elevation above sea level [1].

Booster Compressor System Unit

Booster compressor system units are operated downstream from a primary compressor system (sometimes these units are denoted as secondary units).   They accept compressed air from the primary compressor system and compress the air to a higher pressure before sending the air to the drilling rig. Also, a booster compressor system can accept compressed natural gas (or other gases) from a pipeline and compress that gas to a higher pressure before sending the gas to the drilling rig.   The compressors in these units are all reciprocating compressors.   The compressors in these units can be single stage, or multistage. The prime movers for these units can be fueled by gasoline, propane/butane, diesel, or natural gas.   These units can be fabricated as skid mounted, semi-trailer mounted, or as wheeled trailers.

4.6.2 *Reciprocating Compressor Unit*

A reciprocating compressor can adjust its output pressure to match the back-pressure on the machine.   Thus, the reciprocating compressor is somewhat more flexible than the rotary compressor and will tend to use less fuel for a given application than a similarly configured rotary compressor [1, 11].

The intake volumetric flow rate of a real reciprocating compressor is slightly smaller than the theoretical sweep volume (i.e., the calculated intake volumetric flow rate). This is due to the fact that the piston compressor cannot be fabricated without a clearance volume.   This clearance volume at the top of the piston cylinder is necessary in order to have space for the valves and to keep the piston from striking

the top of the cylinder.   This clearance volume results in a volumetric efficiency term, ε_v, that is unique to the reciprocating compressor.   This volumetric efficiency is only applicable to the first stage of the reciprocating compressor.   The expression for the volumetric efficiency, ε_v, of a reciprocating compressor can be approximated as

$$\varepsilon_v = \left\{ 1 - c \left[r_s^{\frac{1}{k}} - 1 \right] \right\}$$

(4-38)

where c is the clearance volume ratio for the compressor model.   The clearance volume ratio is the clearance volume divided by the sweep volume of the first stage piston.   The range of values for the clearance volume term c is from 0.06 to 0.12. Figure 4-16 gives a plot of the term in the brackets for various values of c.   The ordinate of Figure 4-16 is given in terms of $\varepsilon_v/0.96$.   This allows the figure to be readily used for equation constants other than 0.96 [1].
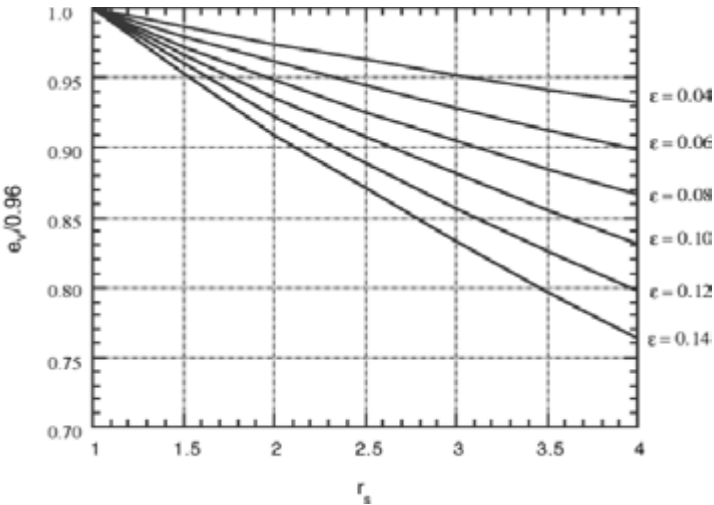
Figure 4-16: Volumetric efficiency term for reciprocating compressor [1].

The mechanical efficiency term, ε_m, is used with the volumetric efficiency term to determine the input power requirement. This mechanical efficiency term is a measure of the friction losses in the mechanical application of the prime mover power to the compressor.   These losses are due to the friction in the bearings and linkages in the compressor system. The values of mechanical efficiency for typical reciprocating compressor systems can vary from about 0.84 to 0.99.

Illustrative Example 4.1   A three-stage reciprocating primary air compressor system unit is rated to have a volumetric flow rate of 900 scfm and a maximum pressure capability of 240 psig at API Mechanical Equipment Standards standard atmospheric conditions.   The compressor has a diesel prime mover that is rated to have a maximum power of 300 horsepower at a compressor shaft speed of 1,000 rpm (at API Standard conditions).   The 1,000 rpm is the shaft speed required for the compressor volumetric flow rate of 900 scfm.   The prime mover is naturally aspirated. This reciprocating compressor system has a clearance ratio of 0.06 and a mechanical efficiency of 0.90.

Determine the horsepower required by the prime mover to operate the compressor against a flow-line back pressure of 150 psig for, a) a surface location at sea level (use API Mechanical Equipment Standards standard atmospheric conditions for sea level) and for, b) a surface location elevation of 6,000 ft (use average mid latitudes data in Table 4-1).

a) Surface location at sea level.

This is a reciprocating piston compressor and, thus, has a volumetric efficiency term.   The volumetric efficiency, ε_v, can be determined using Equation 4-39.

$$n_s = 3$$

$$p_i = 14.696 \text{ psia}$$

$$p_o = 150 + 14.696 = 164.696 \text{ psia}$$

Equation 4-36 becomes

$$r_s = \left(\frac{164.696}{14.696} \right)^{\frac{1}{3}} = 2.238$$

The specific heat ratio for air is

$$k = 1.4$$

The clearance volume ratio for this compressor is

$$c = 0.06$$

With the above values, Equation 4-37 becomes

$$\varepsilon_v = 0.96 \left\{ 1 - 0.06 \left[(2.283)^{\frac{1}{1.4}} - 1 \right] \right\}$$

$$\varepsilon_v = 0.915$$

The rated volumetric flow rate into the compressor is 900 ft³/min.   For this example the compressor is located at sea level, thus,

$$q_i = 900 \text{ scfm}$$

With the above terms the theoretical shaft horsepower required to compress the air moving through the machine is given by Equation 4-35a. Thus, the theoretical shaft horsepower is

$$\dot{W}_s = \frac{(3)\ (1.4)}{(0.4)}\ \frac{(14.696)\ (900)}{229.17} \left[\left(\frac{164.696}{14.696} \right)^{\frac{(0.4)}{(3)\ (1.4)}} - 1 \right]$$

$$\dot{W}_s = 156.8$$

The actual shaft power, $\dot{W}_{as}$, is actual power needed to compress the air to a pressure of 150 psig. Actual shaft power is given by

$$\dot{W}_{as} = \frac{\dot{W}_s}{\varepsilon_m\ \varepsilon_v} \tag{4-39}$$

For this example

$$\varepsilon_m = 0.90$$

and Equation 4-39 becomes

$$\dot{W}_{as} = \frac{156.8}{(0.90)\ (0.915)} = 190.4$$

The above determined 190.4 horsepower is the actual shaft power needed by the compressor to match the back-pressure of 150 psig. This power level is less than the prime mover's rated input power of 300 horsepower, thus, this compressor system is capable of operating at a sea level surface location.

b) Surface location at 6,000 ft above sea level.
The volumetric efficiency, ε_v, can be determined using Equation 4-39.

$$n_s = 3$$

$$p_i = 11.769 \text{ psia}$$

$$p_o = 150 + 11.769 = 161.769 \text{ psia}$$

Equation 4-37 becomes

$$r_s = \left(\frac{161.769}{11.769}\right)^{\frac{1}{3}} = 2.393$$

The specific heat ratio for air is

$$k = 1.4$$

The clearance volume ratio for this compressor is

$$c = 0.06$$

With the above values, Equation 4-38 becomes

$$\varepsilon_v = 0.96 \left\{1 - 0.06 \left[(2.393)^{\frac{1}{1.4}} - 1\right]\right\}$$

$$\varepsilon_v = 0.910$$

The rated volumetric flow rate into the compressor is 900 ft³/min. For this example the compressor is located at 6,000 ft above sea level, thus,

$$q_i = 900 \text{ acfm}$$

With the above terms the theoretical shaft horsepower required to compress the air moving through the machine is given by Equation 4-35a. Thus, the theoretical shaft horsepower is

$$\dot{W}_s = \frac{(3)\,(1.4)}{(0.4)}\,\frac{(11.769)\,(900)}{229.17}\left[\left(\frac{161.769}{11.769}\right)^{\frac{(0.4)}{(3)(1.4)}} - 1\right]$$

$$\dot{W}_s = 137.8$$

For this example

$$\varepsilon_m = 0.90$$

and from Equation 4-39, the actual shaft power is

$$\dot{W}_{as} = \frac{137.8}{(0.90)\,(0.910)} = 168.2$$

The above determined 168.2 horsepower is the actual shaft power needed by the compressor to match the back pressure of 150 psig (at the surface location elevation of 6,000 ft above sea level). At this surface location, the input power available from the prime mover is a derated value (derated from the rated 300 horsepower available at 1,000 rpm). In order for the compressor system to operate at this 6,000 ft surface location elevation, the derated input power available must be greater than the actual shaft power needed. Figure 4-15 shows that for 6,000 ft elevation the power of a naturally aspirated prime mover must be derated by 22 percent. The derated input horsepower available from the prime mover, $\dot{W}_i$, is

$$\dot{W}_i \ = \ 300 \left(1 \ - \ 0.22\right) \ = \ 234$$

For this example, the prime mover derated input power is greater than the actual shaft power needed, thus, the compressor system can be operated at this 6,000 ft surface location elevation.

4.6.3 *Rotary Compressor System Unit*

Rotary compressors have fixed compressor ratios for each stage. These machines have a constant pressure output. These compressors cannot adjust output pressures to match the back pressure in the exit flow-line. The rotary compressors will inject compressed gas into the flow-line at the compressor's rated pressure output. If the back pressure in the exit flow-line is less than the rated pressure output, the gas will expand in the flow-line (or surge tank upstream of the flow-line) to match the back pressure [1, 7].

There is no volumetric efficiency term for the rotary compressor. There is a mechanical efficiency term for these compressors (denoted by the term ε_m). This term is used to determine the input power requirement. The mechanical efficiency term is a measure of the friction losses in the mechanical application of the prime mover power to the compressor. These losses are due to the friction in the bearings and linkages in the overall compressor system. The values of the mechanical efficiency for typical rotary compressor systems can vary from about 0.84 to 0.99.

Illustrative Example 4.2   A three-stage helical lobe (screw) primary air compressor system unit is rated to have a volumetric flow rate of 900 scfm and a maximum pressure capability of 240 psig at API Mechanical Equipment Standards standard atmospheric conditions. The compressor has a diesel prime mover that is rated to have a maximum power of 300 horsepower at a compressor shaft speed of 1,000 rpm (at API Standard conditions). The 1,000 rpm is the shaft speed required for the compressor volumetric flow rate of 900 scfm. The prime mover is naturally aspirated. This rotary compressor system has a mechanical efficiency of 0.90.

Determine the horsepower required by the prime mover to operate the compressor against a flow-line back pressure of 150 psig for, a) a surface location at sea level (use API Mechanical Equipment Standards standard atmospheric conditions for sea level) and for, b) a surface location elevation of 6,000 ft (use average mid latitudes data in Table 4-1).

a) Surface location at sea level.

The total fixed ratio across all three stages that is needed. The atmospheric pressure at sea level (i.e., assuming API Mechanical Equipment Standard atmospheric pressure) is

$$p_i = 14.696 \text{ psia}$$

Thus, the output pressure is

$$p_o = 240 + 14.696 = 254.696 \text{ psia}$$

The total fixed compression ratio across all three stages of the compressor, r_{st}, is

$$r_{st} = \frac{254.696}{14.696} = 17.33$$

This is the fixed mechanical ratio designed into the compressor and must be determined at the standard conditions of the compressor specifications. The above total fixed ratio will be needed to determine the maximum pressure available from the compressor when the compressor system is operated at surface elevations above sea level (part b of this example).

The specific heat ratio for air is

$$k = 1.4$$

The rated volumetric flow rate into the compressor is 900 ft^3/min. For this example the compressor is located at sea level, thus,

$$q_i = 900 \text{ scfm}$$

The number of stages are

$$n_s = 3$$

With the above terms the theoretical shaft horsepower required to compress the air moving through the machine is given by Equation 4-35a. Thus, the theoretical shaft horsepower is

$$\dot{W}_s = \frac{(3)\,(1.4)}{(0.4)} \frac{(14.696)\,(900)}{229.17} \left[\left(\frac{254.696}{14.696} \right)^{\frac{(0.4)}{(3)(1.4)}} - 1 \right]$$

$$\dot{W}_s = 189.1$$

The actual shaft power to give the above theoretical shaft power is obtained from Equation 4-39 (where ε_v is replaced by 1). For this example, Equation 4-39 gives (with $\varepsilon_m = 0.90$)

$$\dot{W}_{as} = \frac{189.1}{0.90} = 210.1$$

The above determined 210.1 horsepower is the actual shaft power needed by the compressor to produce the 240 psig maximum pressure output. This power level is less than the prime mover's rated input power of 300 horsepower, thus, this compressor system is capable of operating at a sea level surface location.

b) Surface location at 6,000 ft above sea level.

This rotary compressor has a total fixed ratio. Therefore, the maximum pressure output this compressor can achieve is reduced from what the compressor can output at sea level conditions. This derated maximum pressure output is determined by multiplying the total fixed ratio across all three stages (obtained in part a above, i.e., $r_{st} = 17.33$) by the new atmospheric pressure condition. Table 4-1 gives the mid latitudes atmospheric pressure at an elevation of 6,000 ft as

$$p_i = 11.769 \text{ psia}$$

The derated maximum pressure output of the compressor is

$$p_o = (17.33)(11.769) = 204.0 \text{ psia}$$

The specific heat ratio for air is

$$k = 1.4$$

The rated volumetric flow rate into the compressor is 900 ft³/min. For this example the compressor is located at 6,000 ft above sea level, thus,

$$q_i = 900 \text{ acfm}$$

With the above terms the theoretical shaft horsepower required to compress the air moving through the machine is given by Equation 4-35a. Thus, the theoretical shaft horsepower is

$$\dot{W}_s = \frac{(3)(1.4)}{(0.4)} \frac{(11.769)(900)}{229.17} \left[\left(\frac{204.0}{11.769} \right)^{\frac{(0.4)}{(3)(1.4)}} - 1 \right]$$

$$\dot{W}_s = 151.4$$

For this example

$$\varepsilon_m \;=\; 0.90$$

and from Equation 4-39, the actual shaft power is

$$\dot{W}_{as} \;=\; \frac{151.4}{0.90} \;=\; 168.3$$

The above determined 168.3 horsepower is the actual shaft power needed by the compressor to produce the 204.0 psig maximum pressure output (at the surface location elevation of 6,000 ft above sea level). At this surface location, the input power available from the prime mover is a derated value (derated from the rated 300 horsepower available at 1,000 rpm). In order for the compressor system to operate at this 6,000 ft surface location elevation, the derated input power available must be greater than the actual shaft power needed. Figure 4-15 shows that for 6,000 ft elevation the input power of a naturally aspirated prime mover must be derated by 22 percent. The derated input horsepower available from the prime mover, $\dot{W}_i$, is

$$\dot{W}_i \;=\; 300 \left(1 \;-\; 0.22\right) \;=\; 234$$

For this example, the prime mover's derated input power is greater than the actual shaft horsepower needed, thus, the compressor system can be operated at this 6,000 ft surface location elevation.

4.6.4 *Fuel Consumption*
In order to effectively plan air or gas drilling operations, it is important to be able to predict the fuel consumption by the prime movers of compressor system units. The consumption of either liquid or gaseous fuels is initially calculated in pounds of fuel used per horsepower-hour (lb/hp-hr). Fuel consumption is very dependent upon the prime mover's power ratio, or percent power utilization of total power available.

Figure 4-17 gives the approximate fuel consumption for prime movers fueled with gasoline, propane/butane, or diesel [3, 12]. Most stationary prime movers can be field converted to operate on propane/butane, or natural gas. Figure 4-18 gives the approximate fuel consumption for prime movers fueled by natural gas [3, 12].

Illustrative Example 4.3   Determine the diesel fuel consumption rate (in gallons per hour) for the primary reciprocating piston compressor system and conditions given in Illustrative Example 4.1 for: a) a surface location at sea level and, b) a surface location elevation of 6,000 ft.
a) Surface location at sea level.
The prime mover has a maximum 300 horsepower available at 1,000 rpm at sea level conditions. The actual shaft power needed by the three-stage reciprocating compressor to match the back pressure of 150 psig is 190.4 horsepower. Thus, the percent load on the prime mover, or power ratio, PR, is

$$PR = \frac{190.4}{300} (100) = 63.5$$

Entering the abscissa of Figure 4-17 with the power ratio percent, the approximate fuel consumption rate can be read on the ordinate using the diesel fuel curve. The approximate fuel consumption rate at this power level is 0.560 lb/hp-hr. The total weight of diesel fuel consumption per hour, $\dot{w}_f$, is

$$\dot{w}_f = 0.560 \ (190.4) = 106.6 \text{ lb/hr}$$

The specific gravity of diesel fuel is 0.8156 at 60°F [5]. The total volume (in United States gallons) of diesel fuel consumption per hour, q_f, is

$$q_f = \frac{106.6}{(0.8156)(8.33)} = 15.7 \text{ gal/hr}$$

where the specific weight of fresh water is 8.33 lb/gal.

b) Surface location at 6,000 ft above sea level.

The prime mover has a derated maximum 234 horsepower available at 1,000 rpm at 6,000 ft elevation. The actual shaft power needed by the three-stage reciprocating compressor to match the back-pressure of 150 psig is 168.2 horsepower. Thus, the percent load on the prime mover, or power ratio is

$$PR = \frac{168.2}{234} (100) = 71.9$$

Entering the abscissa of Figure 4-17 with the power ratio percent, the approximate fuel consumption rate can be read on the ordinate using the diesel fuel curve. The approximate fuel consumption rate at this power level is 0.538 lb/hp-hr. The total weight of diesel fuel consumption per hour is

$$\dot{w}_f = 0.538 \ (168.2) = 90.5 \text{ lb/hr}$$

The specific gravity of diesel fuel is 0.8156, thus, the total volume (in United States gallons) of diesel fuel consumption per hour is

$$q_f = \frac{90.5}{(0.8156)(8.33)} = 13.2 \text{ gal/hr}$$

Illustrative Example 4.4   Determine the diesel fuel consumption rate (in gallons per hour) for the on-board Sullair Model 840 primary rotary screw compressor system. Carry out these calculations for the two surface drilling locations given in Illustrative Example 4.2. These are, a) a surface location at sea level and, b) a surface location elevation of 6,000 ft).

a) Surface location at sea level.

The prime mover has a maximum 300 horsepower available at 1,000 rpm at sea level conditions. The actual shaft power needed by the three-stage rotary compressor to produce the 240 psig maximum pressure output is 210.1 horsepower. Thus, the percent load on the prime mover, or power ratio is

$$PR = \frac{210.1}{300} (100) = 70.1$$
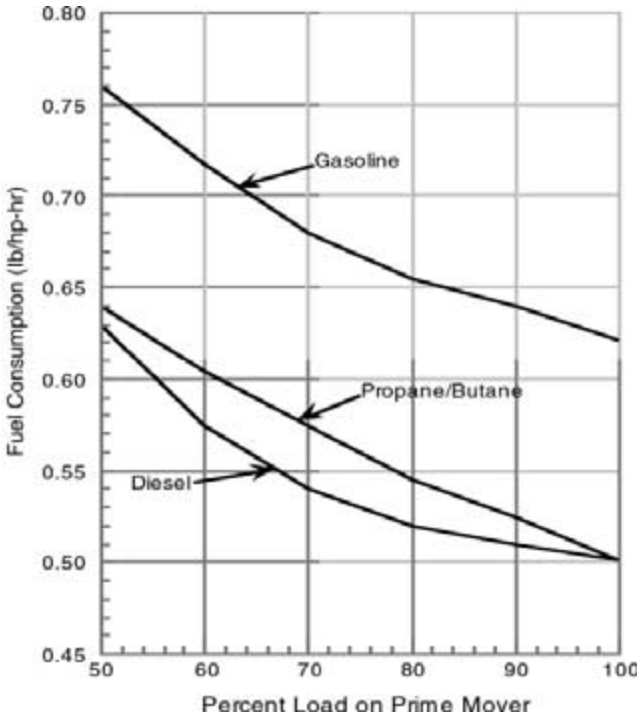
Figure 4-17: Fuel consumption for gasoline, propane/butane, and diesel [3, 12].

Entering the abscissa of Figure 4-17 with the power ratio percent, the approximate fuel consumption rate can be read on the ordinate using the diesel fuel curve. The approximate fuel consumption rate at this power level is 0.540 lb/hp-hr. The total weight of diesel fuel consumption per hour is

$$\dot{w}_f = 0.540 \ (210.1) = 113.5 \ \text{lb/hr}$$

The specific gravity of diesel fuel is 0.8156, thus, the total volume (in United States gallons) of diesel fuel consumption per hour is

$$q_f = \frac{113.5}{(0.8156)(8.33)} = 16.7 \ \text{gal/hr}$$
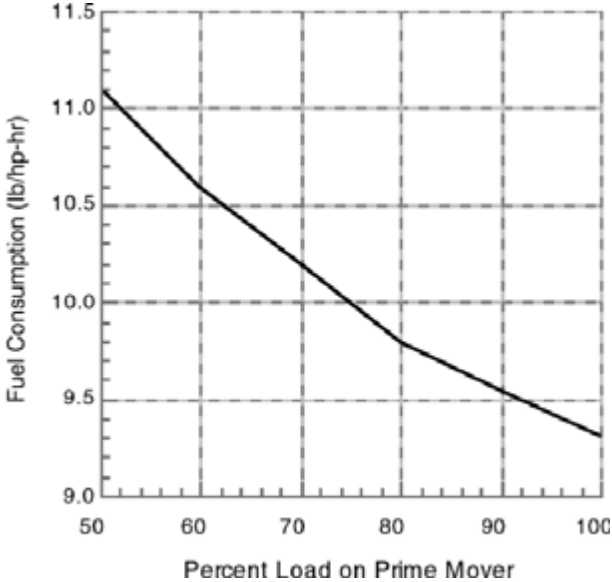
Figure 4-18: Fuel consumption for natural gas [3, 12].

b) Surface location at 6,000 ft above sea level.

The prime mover has a derated maximum 234 horsepower available at 1,000 rpm at 6,000 ft elevation. The actual shaft power needed by the three-stage rotary compressor to produce the 240 psig maximum pressure output is 168.7 horsepower. Thus, the percent load on the prime mover, or power ratio is

$$PR = \frac{168.7}{234} \ (100) = 72.1$$

Entering the abscissa of Figure 4-17 with the power ratio percent, the approximate fuel consumption rate can be read on the ordinate using the diesel fuel curve. The

approximate fuel consumption rate at this power level is 0.537 lb/hp-hr. The total weight of diesel fuel consumption per hour is

$$\dot{w}_f = 0.537\ (168.7) = 90.6\ \text{lb/hr}$$

The specific gravity of diesel fuel is 0.8156, thus, the total volume (in United States gallons) of diesel fuel consumption per hour is

$$q_f = \frac{90.6}{(0.8156)(8.33)} = 13.3\ \text{gal/hr}$$

4.7 Example Compressor System Units

In this section four operational example compressor system units are presented. These units represent the wide variety of units in operation around the US and the world. In follow-on illustrative examples for air and gas drilling operations, stable foam drilling operations, and aerated fluid drilling operations, one of these four compressor system units will be used as the provider of the compressed air or gas. These compressor system units are a mix of reciprocating compressors and rotary compressors.

4.7.1 *Small Drilling Rig with Integrated Rotary Compressor System*

Figure 4-19 shows the portable Tamrock Driltech Model D25K drilling rig. With certain limitations, the rig is capable of drilling to a depth of about 1,000 ft. These small single rigs usually use Range 1 (i.e., 18 ft to 22 ft in length) drill pipe. These small drilling rigs are used for drilling water wells, environmental monitoring wells, and other geotechnical boreholes. Unlike the larger drilling rigs discussed in Chapter 1, these smaller drilling rigs are designed with their mud pumps and/or compressors integrated into the rig deck.

The Tamrock Driltech Model D25K drilling rig is equipped with a Sullair Model 840, two-stage, oil flooded, helical lobe (screw) rotary primary compressor. Figure 4-20 shows this compressor standing alone away from the rig. As can be seen, this rotary compressor is rather small. This emphasizes one of the main advantages of the rotary compressor. For similar volumetric flow rate capacity compressors, the size (footprint) of a rotary compressor will be smaller than that of a reciprocating compressor. The Sullair Model 840 is operated at 1,800 rpm. At this speed, the compressor has a volumetric flow rate of 840 scfm and produces a fixed output pressure of 340 psig (at API Mechanical Equipment Standards standard conditions).

Most small portable single rigs are designed with an integrated on-board air compressor or mud pump. These air compressors (or mud pumps) are placed on the rig deck and can be powered by either the portable rig prime mover (via power-take-off), or by a dedicated stationary prime mover also on the rig deck. The Sullair Model 840 primary compressor of the Tamrock Driltech Model D25K drilling rig is powered by a separate prime mover on the rig deck.

The dedicated deck mounted prime mover for the Tamrock Driltech Model D25K drilling rig is a Caterpillar Model 3406, in-line six cylinder, diesel fueled

prime mover.   The Model 3406 is turbocharged and aftercooled and is rated to produce a peak 400 horsepower at a speed of 1,800 rpm (at API Mechanical Equipment Standards standard conditions).   Figure 4-21 shows a stand alone Caterpillar Model 3406 prime mover.   Unlike skid mounted, compressor system unit which is operated with the larger drilling rigs, the integrated compressor system on a smaller drilling rig usually shares its prime mover with the hydraulic rotary table (rotating head) system and with the hydraulic/chain feed hoist system.   That is the case with this Sullair compressor on this Tamrock Driltech Model D25K.   Thus, when other auxiliary equipment are also being driven by the prime mover, the actual power available to the compressor system will be less than the 400 horsepower.   The prime mover on the Model D25K drives the Sullair compressor (and the other auxiliaries) via a chain drive transmission (often called a "compound").

Small portable drilling rigs can have the drilling rig mounted on a trailer flat bed, on a truck flat bed, or mounted on a tracked vehicle for operations in remote areas.
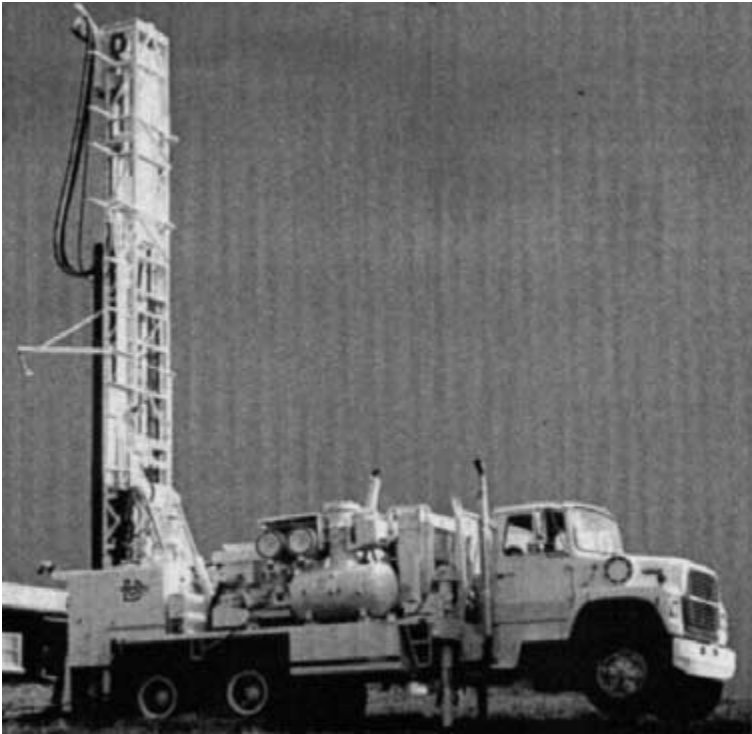
Figure 4-19: Small drilling rig with integrated compressor system (courtesy of Tamrock Driltech).
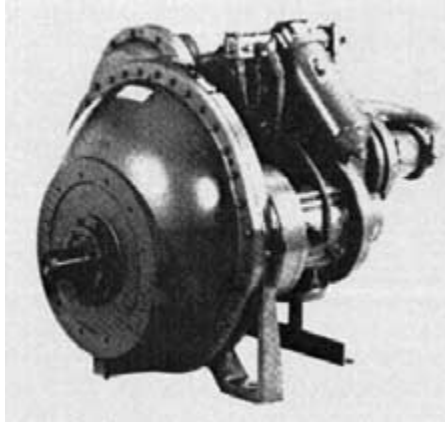
Figure 4-20: Sullair Model 840, two-stage, oil flooded, helical lobe (screw) rotary primary compressor (courtesy of Sullair).
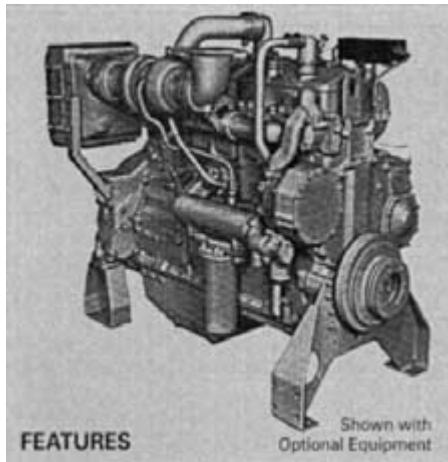
Figure 4-21: Caterpillar Model 3406 diesel prime mover (courtesy of Caterpillar).

4.7.2 *Small Reciprocating Primary and Booster Compressor System*

Most of the compressor systems for air and gas drilling operations are provided as a separate primary compressor system unit (either with a reciprocating compressor or with a rotary compressor) and a separate booster compressor system unit (always a reciprocating compressor). These units are usually skid mounted and each has its own prime mover.

Figure 4-22 shows a skid mounted primary compressor system unit which has a Gardner Denver Model WEN, two-stage, reciprocating piston compressor. The Gardner Denver Model WEN is operated at 1,000 rpm.   At this speed, the compressor has a volumetric flow rate of 700 scfm and a maximum pressure capability of 350 psig (at API Mechanical Equipment Standards standard conditions). The compressor and its cooling subsystem is shown at the right end of the skid in Figure 4-22. On the left end of the skid in Figure 4-22 is the Caterpillar Model D353 prime mover. The Caterpillar Model D353 is an in-line six cylinder, diesel fueled prime mover. This prime mover is turbocharged and aftercooled and is rated to produce a peak of 270 horsepower at a speed of 1,000 rpm (at API Mechanical Equipment Standards standard conditions).

Figure 4-22: Skid mounted reciprocating piston primary compressor system unit (courtesy of Mountain Air Drilling Service)

Figure 4-23 shows a skid mounted booster compressor system unit which has a Gardner Denver Model MDY, two-stage, reciprocating piston compressor.   The compressor is seen at the front end (right end) of the skid in Figure 4-23.   The compressor is driven by a Caterpillar Model D353 prime mover. This is the same prime mover that is used for the primary compressor system unit discussed above. The prime mover is rated to produce a peak 270 horsepower at a speed of 1,000 rpm (at API Mechanical Equipment Standards standard conditions). However, unlike the primary compressor system discussed above, the booster compressor system may be operated at speeds different from the 1,000 rpm. The prime mover would produce an approximate peak of 230 horsepower at 900 rpm, and a peak of 300 horsepower at 1,100 rpm.

This booster compressor system unit is usually operated in series with the primary compressor system.   When the drilling rig requires compressed air at pressures above the 350 psig maximum capability of the primary, the air flow from the primary is conducted to the inlet of the booster. In this series configuration, the booster is engaged and the volumetric flow rate from the primary is further compressed to pressures above 350 psig level.   However, the booster can also be used to compress pipeline natural gas to pressures above typical pipeline pressures for use on a drilling rig.

Figure 4-23: Skid mounted reciprocating piston booster compressor system unit (courtesy of Mountain Air Drilling Service).

4.7.3 *Rotary Primary and Reciprocating Compressor System*

The compressor system unit shown in Figure 4-24 is an unusual design. It is a semi-trailer mounted unit that has both primary compressor and booster compressor driven by one large prime mover. The prime mover drives the primary compressor through a gear box that steps the speed up the primary. The booster compressor is drive directly at the speed of the prime mover.

The primary compressor is a MAN (German manufacture) Model GHH-CF246G, single-stage, oil flooded, rotary helical lobe (screw) compressor.   The helical lobe compressor is driven at 1,969 rpm by the prime mover which is rotating 1,800 rpm. A gearbox with a 1.094 ratio connects the primary to the prime mover. At a rotation speed of 1,969 rpm the helical lobe compressor has a volumetric flow rate of 1,727 scfm and produces a fixed pressure discharge of 190 psig at ASME Standards standard conditions. There is a discharge mechanical adjustment that can be made that will allow a 210 psig fixed pressure discharge but with a slightly lower corresponding volumetric flow rate.

The booster compressor is an Ariel Model JGJ/2, a two-stage, reciprocating piston compressor. Figure 4-24 shows the cooling subsystem at the front end (hitch end) of the trailer mounted unit. This cooling subsystem is the aftercooler for the primary compressor, the innercooler between the first and second stage of the booster, the aftercooler for the booster, and the cooling system for the prime mover. Next is the primary compressor (with the gearbox between it and the prime mover shaft).

The prime mover located next to the cooling subsystem (toward the aft end of the trailer unit). At the aft end of the trailer is the booster compressor. The prime mover for this unit is a Caterpillar Model 3412. This prime mover has a V-12 piston configuration. The prime mover is diesel fueled, turbocharged and aftercooled. The prime mover is operated at a speed of 1,800 rpm and at that speed can produce a peak 740 horsepower (at API Mechanical Equipment Standards standard conditions).

Figure 4-24: Semi-trailer mounted rotary primary and reciprocating booster compressor system unit (courtesy of MI Air Drilling).

4.7.4 *Four-Stage Reciprocating Compressor System*

The compressor system unit shown in Figure 4-25 is another unusual design. This is a semi-trailer mounted unit. The compressor is a large Dresser Clark CFB-4, four-stage reciprocating piston compressor. The compressor is operated at a rotating speed of 900 rpm. At this speed the compressor produces a volumetric flow rate of 1,200 scfm and a continuous maximum pressure of 1,000 psig (at API Mechanical Equipment Standards standard conditions). The compressor can produce a maximum pressure of 1,200 psig in intermittent service. Technically this compressor system is a primary compressor system unit, but in application the unit performs as a combined primary-booster all in one compressor system.

This compressor system is probably one of the most reliable system in the drilling industry. These compressor systems were introduced in the early 1980's to provide compressed air for deep steam production wells in the Geysers geothermal fields of Northern California. This application required the drilling of 11 inch diameter wells to depths in excess of 10,000 ft. During the drilling of these wells, steam inflow to the wells were nearly always encounter which would greatly increases the injection pressure requirements. No similar air drilling requirements have been encountered in the drilling of deep oil and natural gas wells. Not only do these compressor systems produce a very useful volumetric flow rate, but they can produce this volumetric flow rate at a great variety of pressures (i.e., from 100 psig to 1,200 psig). Since these units are reciprocating piston compressors, the volumetric flow rate is not affected by the pressure output. This compressor system is presently the highest quality unit in the market and should be considered for any critical or risky air drilling operation.

The compressor is directly coupled to a Caterpillar Model D398 prime mover. The Caterpillar Model D398 is a V-12 piston configuration. The prime mover is diesel fueled, turbocharged and aftercooled. At the rotation speed of 900 rpm, the prime mover can produce a peak of 760 horsepower.

Figure 4-25: Semi-trailer mounted four-stage reciprocating piston compressor system unit (courtesy of MI Air Drilling).

4.7.5 *Large Reciprocating Primary and Booster Compressor System*

Figure 4-26 shows a semi-trailer mounted primary compressor system unit with an Ingersoll Rand Model HHE, three-stage, reciprocating piston compressor. The compressor is operated at 1,000 rpm. At this speed the compressor has a volumetric flow rate of 1,500 scfm and a maximum pressure capability of 310 psig (at API Mechanical Equipment Standards standard conditions). The aftercooling and innercooling subsystems are at the left end (hitch end) of the trailer in Figure 4-26. The prime mover is in the middle of the trailer and the compressor is mounted at the right end (or aft end) of the trailer. The prime mover is a Caterpillar Model 3508. The prime mover is a diesel fueled, turbocharged Caterpillar Model 3508 with a V-8 cylinder configuration. This prime mover produces a peak of 644 horsepower at a speed of 1,000 rpm (at API Mechanical Equipment Standards standard conditions).

Figure 4-26: Semi-trailer mounted reciprocating piston primary compressor system unit (courtesy of Symbol Incorporated)

Figure 4-27 shows a semi-trailer mounted booster compressor system unit which has an Ariel Model JG-4, two-stage, reciprocating piston compressor. The aftercooler is at the left end of the trailer shown in Figure 4-27. The compressor is at the right end of the trailer and the prime mover is mounted in the middle of the trailer. This booster compressor is driven by a Caterpillar Model D353 prime mover. The Caterpillar Model D353 is an in-line six cylinder, diesel fueled prime mover. This prime mover is turbocharged and aftercooled and is rated to produce a peak of 392 horsepower at a speed of 1,200 rpm (at API Mechanical Equipment Standards standard conditions).

This booster compressor system unit is usually operated in series with the primary compressor system. When the drilling rig requires compressed air at pressures above the 310 psig maximum capability of the primary, the air flow from the primary is conducted to the inlet of the booster. In this series configuration, the booster is engaged and the volumetric flow rate from the primary is further compressed to pressures above 310 psig level (up to a maximum of 1,200 psig). However, the booster can also be used to compress pipeline natural gas to pressures above typical pipeline pressures for use on a drilling rig.

Figure 4-27: Skid mounted reciprocating piston booster compressor system unit (courtesy of Symbol Incorporated).

References

1. *Atlas Copco Manual*, Atlas Copco Company, Fourth Edition, 1982.

2. Brown, R. N., *Compressors: Selection and Sizing*, Gulf Publishing Company, 1986.

3. *API Specification for the Internal-Combustion Reciprocating Engines for Oil-Field Service*, API Std. 7B-11C, Ninth Edition, 1994.

4. *API Recommended Practice for Installation, Maintenance, and Operation of Internal-Combustion Engines*, API RP 7C-11F, Fifth Edition, 1994.

5. Baumeister, T., *Marks' Standard Handbook for Mechanical Engineers*, Seventh Edition, McGraw-Hill Book Company, 1979.

6. *U. S. Standard Atmosphere Supplement, 1966.* U. S. Committee on Extension to the Standard Atmosphere, United States Government Publication, 1966.

7. Loomis, A. W., *Compressed Air and Gas Data*, Ingersoll-Rand Company, Third Edition, 1980.

8. Pichot, P., *Compressor Application Engineering, Vol. 1: Compression Equipment*, Gulf Publishing Company, 1986.

9. Pichot, P., *Compressor Application Engineering, Vol. 2: Drivers for Rotating Equipment*, Gulf Publishing Company, 1986.

10. Burghardt, M. D., *Engineering Thermodynamics with Applications*, Second Edition, Harper and Row Publishers, 1982.

11. Block, H. E. and Hoefner, J. J., *Reciprocating Compressors Operations and Maintenance*, Gulf Publishing Company, 1996.

12. Lyons, W. C., et al, *Standard Handbook of Petroleum and Natural Gas Engineering*, Volume 1, Gulf Publishing Company, 1996.

This page intentionally left blank.

Chapter

Five

Shallow Well Drilling Applications

Shallow drilling operations account for the majority of wells drilled and for the most footage drilled with air and gas drilling technology. Shallow drilling operations use direct and reverse circulation techniques. The calculation tools required to adequately plan shallow drilling operations can be reduced to rather straightforward steps and methods. This chapter outlines these steps and methods and illustrates their application to typical shallow drilling operations. The objective of these steps and methods is to allow engineers and scientists to cost effectively plan their drilling operations and ultimately select their drilling rig, compressor, and other auxiliary air and gas equipment. The additional benefit of this planning process is that the data created by the process can later be used to control the drilling operations as the actual operations progress.

In the examples that follow in this chapter only major friction losses for simple well geometry will be considered. The change of diameters in the drill string due to the use of drill collars (where applicable) will be ignored. This simplification is valid for shallow wells.

5.1 Shallow Well Drilling Planning

Shallow air and gas drilling operations use almost exclusively compressed air as the drilling fluid. Some recent environmental drilling operations have used oxygen stripped atmospheric air (inert air) as the drilling gas. In this chapter atmospheric air will be used as the example drilling gas.

The basic planning steps for a shallow well are as follows:

1. Determine the geometry of the borehole section or sections to be drilled with air or other gases (i.e., openhole diameters, casing inside diameters, and depths).
2. Determine the geometry of the associated drill strings for the sections to be drilled with air or other drilling gas (i.e., drill bit size and type, the drill collar size, drill pipe size and description, and maximum depth).
3. Determine the type of rock formations to be drilled in each section and estimate the anticipated drilling rate of penetration.
4. Determine the elevation of the drilling site above sea level, the temperature of the air during the drilling operation, and the approximate geothermal temperature gradient.
5. Determine whether direct or reverse circulation techniques will be used to drill the well.
6. Determine the required approximate minimum volumetric flow rate of air or other drilling gas needed to carry the rock cuttings from the well when drilling at its maximum depth.
7. Select the contractor compressor(s) that will provide the drilling operation with a volumetric flow rate of air that is greater than the required minimum volumetric flow rate (use a factor of safety of at least 1.2).
8. Using the compressor(s) air volumetric flow rate to be injected into the well, determine the bottomhole and surface injection pressures as a function of drilling depth (over the interval to be drilled).
9. Determine the maximum power required by the compressor(s) and the available maximum derated power from the prime mover(s).
10. Determine the approximate volume of fuel required by the compressor(s) to drill the well.
11. In the event formation water is encountered, determine the approximate flow rate of "mist" injection water and the water carrying capacity of the gas flow.

5.2 Direct Circulation

Direct circulation is extensively used in shallow air drilling operations. In general, direct circulation is used to drill small diameter borehole wells. Reverse circulation is preferred for large diameter borehole wells.

5.2.1 *Minimum Volumetric Flow Rates*

In order to initiate the well planning procedure given above, the geometry of the direct circulation operation must be defined and the anticipated drilling penetration rate estimated. Figures can be prepared for the approximate minimum volumetric flow rates for a variety of shallow well and drill string geometric configurations. The calculations for such figures are carried out using API standard atmospheric conditions (i.e., 14.696 psia and 60˚F, see Chapter 4). Thus, the figures developed will give the minimum volumetric flow rate values for air drilling using air at API standard conditions. Once such figures are developed, the minimum volumetric flow rates can be calculated for any other atmospheric conditions (surface locations) from the minimum volumetric flow rates given for API standard conditions. The minimum volumetric flow rate values are calculated assuming a minimum

bottomhole kinetic energy per unit volume of no less than 3.0 ft-lb/ft^3 (see Chapter 8 for details). The basic equations used to determine the minimum volumetric flow rate are derived in Chapter 6.

The minimum volumetric flow rates are calculated assuming that the boreholes (surface to bottom) are openholes (not cased). The calculations for determining a minimum volumetric flow rate is a trial and error process. The equations needed to determine the minimum volumetric flow rate are outlined below. The critical equation for determining the minimum volumetric flow rate is derived in Chapter 6. This is the equation for the bottomhole pressure, P_{bh}, in the annulus. This equation is

$$P_{bh} = \left[\left(P_{at}^2 + b_a\, T_{av}^2 \right) e^{\frac{2\, a_a\, H}{T_{av}}} - b_a\, T_{av}^2 \right]^{0.5} \tag{5-1}$$

where P_{bh} is the bottomhole pressure in the annulus (lb/ft^2, abs),
  P_{at} is the atmospheric pressure at the exit from the annulus (lb/ft^2, abs),
  H is the depth of the borehole (ft),
  T_{av} is the average temperature of the borehole over the depth interval (°R).
  The constants a_a and b_a are

$$a_a = \left(\frac{S_g}{\mathbf{R}} \right) \left[1 + \frac{\dot{w}_s}{\dot{w}_g} \right] \tag{5-2}$$

and

$$b_a = \frac{f}{2\, g\, (D_h - D_p)} \left(\frac{\mathbf{R}}{S_g} \right)^2 \frac{\dot{w}_g^2}{\left(\frac{\pi}{4} \right)^2 \left(D_h^2 - D_p^2 \right)^2} \tag{5-3}$$

where S_g is the specific gravity of the gas (i.e., $S_g = 1.0$ for air at standard
    conditions),
  $\mathbf{R}$ is the gas constant for API standard dry air (53.36 ft-lb/lb-°R),
  $\dot{w}_s$ is the weight rate of flow of rock cuttings solids (lb/sec),
  $\dot{w}_g$ is the weight rate of flow of the gas (usually air) (lb/sec),
  P_g is the pressure of the gas entering the circulation system (in these
    calculations the API standard atmospheric pressure) (lb/ft^2, abs),
  f is the Fanning friction factor,
  g is the acceleration of gravity (32.2 ft/sec^2),
  D_h is the diameter of the borehole (ft),
  D_p is the outside diameter of the drill pipe (in these calculations the pipe body
    outside diameter) (ft).
It should be noted that the above equations are for any set of consistent units.

Unless field test data are available that give the actual rock specific gravity, the approximate average specific gravity for sedimentary rock is assumed to be 2.7, the average specific gravity for igneous rock is assumed to be 2.8, and the average specific gravity for metamorphic rock is assumed to be 3.0 [1].

Illustrative Examples 5.1, 5.2a, and 5.3a describe the implementation of the basic planning steps Nos. 1 through 6 given in Section 5.1 above.

Illustrative Example 5.1 Using the basic equations above, determine the direct circulation minimum volumetric flow rate for a well with a 4 1/2 inch openhole borehole (4 1/2 inch drill bit diameter) and a uniform drill string composed of a drill pipe outside diameter of 2 3/8 inch. The anticipated drilling rate in a sequence of competent unfractured limestone rock (sedimentary rock) is assumed to be 30 ft/hr. The drilling depth is 1,000 ft.

In order to be able to calculate air drilling conditions at other surface elevations above sea level, all calculations to obtain values like the minimum volumetric flow rate are carried out for a baseline sea level atmosphere. For these calculations and most of those in this treatise the baseline sea level atmosphere is the API Mechanical Equipment Standards standard atmospheric conditions (see Chapter 4). These conditions are a pressure of 14.696 psia and a temperature of 60˚F. Thus, the pressure of the gas (in this case air) that flows into the compressor, P_{at}, is

$$p_{at} = 14.696 \text{ psia}$$

$$P_{at} = p_{at} \; 144$$

$$P_{at} = 2{,}116 \text{ lb/ft}^2 \text{ abs}$$

The atmospheric temperature of the gas (air) that flows into the compressor, T_{at}, that will supply the drilling operation is

$$t_{at} = 60^o \text{F}$$

$$T_{at} = t_{at} + 459.67$$

$$T_{at} = 519.67^o \text{R}$$

Thus, P_g and T_g become

$$P_g = P_{at} = 2{,}116 \text{ lb/ft}^2 \text{ abs}$$

$$T_g = T_{at} = 519.67^o \text{R}$$

Using Equation 4-11, the specific weight of the gas entering the compressor is

$$\gamma_g = \frac{(2,116)\ (1.0)}{(53.36)\ (519.67)}$$

$$\gamma_g = 0.0763\ \text{lb/ft}^3$$

To determine the minimum volumetric flow rate of air at API standard conditions, it is necessary to select (by trial and error) a volumetric flow rate, q_g, that will give a kinetic energy per unit volume of 3.0 ft-lb/ft^3 in the annulus at the bottom of the 1,000 ft borehole. Kinetic energy per unit volume should be a minimum at the bottom of the annulus. The volumetric flow rate selected (trial and error) is (at API standard conditions)

$$q_g = 320.9\ \text{scfm}$$

The value of Q_g is

$$Q_g = \frac{q_g}{60}$$

$$Q_g = 5.35\ \text{ft}^3\text{/sec}$$

The weight rate of flow of the gas, $\dot{w}_g$, is

$$\dot{w}_g = \gamma_g\ Q_g$$

$$\dot{w}_g = 0.0763\ (5.35)$$

$$\dot{w}_g = 0.408\ \text{lb/sec}$$

The borehole diameter, D_h, is

$$d_h = 4.50\ \text{inches}$$

$$D_h = \frac{d_h}{12}$$

$$D_h = 0.375\ \text{ft}$$

The estimated drilling rate of penetrations is 30 ft/hr. The weight rate of flow of the solid rock cuttings, $\dot{w}_s$, in the annulus is

$$\dot{w}_s = \left(\frac{\pi}{4}\right) D_h^2 \ (62.4) \ S_s \left[\frac{K}{(60)\ (60)}\right] \tag{5-4}$$

where K is the drilling rate (ft/hr),
    S_s is the specific gravity of the solid rock cuttings.
Therefore, $\dot{w}_s$ is

$$\dot{w}_s = \left(\frac{\pi}{4}\right) (0.375)^2 \ (62.4) \ (2.7) \left[\frac{30}{(60)\ (60)}\right]$$

$$\dot{w}_s = 0.155 \ \text{lb/sec}$$

The temperature of the rock formations near the surface (geothermal surface temperature) is estimated to be the approximate average year round temperature at that location on the earth's surface. Table 4-1 gives 59°F for the sea level average year round temperature for the mid latitudes of North America (or see Appendix D). Therefore, the absolute temperature of the rock formations at the surface, T_r, is

$$t_r = 59^o\text{F}$$

$$T_r = t_r + 459.67$$

$$T_r = 518.67^o\text{R}$$

The bottomhole temperature is determined from the surface geothermal temperature, the geothermal gradient, and the depth of the borehole. For this example and the figures that follow, the geothermal gradient is approximated to be 0.01°F/ft. Thus, T_{bh}, is

$$T_{bh} = T_r + 0.01 \ (1,000)$$

$$T_{bh} = 528.67^o\text{R}$$

The average temperature of this borehole is

$$T_{av} = \frac{T_r + T_{bh}}{2}$$

$$T_{av} = 523.67^o\text{R}$$

The drill pipe outside diameter, D_p, is

$$d_p = 2.375 \text{ inches}$$

$$D_p = \frac{d_p}{12}$$

$$D_p = 0.198 \text{ ft}$$

The Fanning friction factor, f, for flow in the annulus is determined from the von Karman empirical relationship for turbulent flow conditions [2]. This empirical relationship is

$$f = \left[\frac{1}{2 \log \left(\dfrac{D_h - D_p}{e_{av}} \right) + 1.14} \right]^2 \qquad (5\text{-}5)$$

where e_{av} is the average absolute surface roughness of the annulus (ft).

The openhole outer wall absolute surface roughness, e_{oh}, of the limestone sequence borehole annulus is assumed to be 0.005 ft (see Table 8-1) [2]. The inner surface of the borehole annulus is the outer surface of the drill pipe. The absolute surface roughness of commercial pipe, e_p, is given as 0.00015 ft [2]. The average absolute surface roughness of the annulus is approximated by using a surface area weight average relationship between the openhole surface area and its roughness and the outside surface of the drill string and its roughness. Thus, the value for e_{av} is

$$e_{av} = \frac{e_{oh} \left(\dfrac{\pi}{4} \right) D_h^2 \, H + e_p \left(\dfrac{\pi}{4} \right) D_p^2 \, H}{\left(\dfrac{\pi}{4} \right) D_h^2 \, H + \left(\dfrac{\pi}{4} \right) D_p^2 \, H}$$

The above reduces to

$$e_{av} = \frac{e_{oh} \left(\dfrac{\pi}{4} \right) D_h^2 + e_p \left(\dfrac{\pi}{4} \right) D_p^2}{\left(\dfrac{\pi}{4} \right) D_h^2 + \left(\dfrac{\pi}{4} \right) D_p^2} \qquad (5\text{-}6)$$

Thus, e_{av}, is

$$e_{av} = \frac{(0.005)\left(\frac{\pi}{4}\right)(0.375)^2 + (0.00015)\left(\frac{\pi}{4}\right)(0.198)^2}{\left(\frac{\pi}{4}\right)(0.375)^2 + \left(\frac{\pi}{4}\right)(0.198)^2}$$

$$e_{av} = 0.0039 \text{ ft}$$

Equation 5-5 becomes

$$f = \left[\frac{1}{2\ \log\left(\dfrac{0.375 - 0.198}{0.0039}\right) + 1.14}\right]^2$$

$$f = 0.051$$

With the above values Equation 5-2 becomes

$$a_a = \left(\frac{1.0}{53.36}\right)\left[1 + \left(\frac{0.155}{0.408}\right)\right]$$

$$a_a = 0.026$$

and Equation 5-3 becomes

$$b_a = \frac{0.051}{2\ (32.2)\ (0.375 - 0.198)}\left(\frac{53.36}{1.0}\right)^2 \frac{(0.408)^2}{\left(\dfrac{\pi}{4}\right)^2\left[(0.375)^2 - (0.198)^2\right]^2}$$

$$b_a = 331.6$$

Equation 5-1 becomes

$$P_{bh} = \left\{\left[(2{,}116)^2 + 331.6\ (523.67)^2\right]\ e^{\frac{2\ (0.026)\ (1{,}000)}{523.67}} - 331.6\ (523.67)^2\right\}^{0.5}$$

$$P_{bh} = 3{,}792 \text{ lb/ft}^2 \text{ abs}$$

$$p_{bh} = \frac{P_{bh}}{144}$$

$$p_{bh} = 26.3 \ \text{psia}$$

This is the pressure at the bottom of the borehole in the annulus.

Using Equation 4-11, the specific weight of the air at bottomhole pressure and temperature conditions is

$$\gamma_{bh} = \frac{(3,792) \ (1.0)}{(53.36) \ (528.67)}$$

$$\gamma_{bh} = 0.136 \ \text{lb/ft}^3$$

The volumetric flow rate of the gas at the bottom of the borehole in the annulus, Q_{bh}, is

$$Q_{bh} = \frac{(0.0763) \ (5.35)}{0.136}$$

$$Q_{bh} = 3.007 \ \text{ft}^3/\text{sec}$$

The velocity of the gas at the bottom of the borehole in the annulus, V_{bh}, is

$$V_{bh} = \frac{3.007}{\left(\frac{\pi}{4}\right) \left[(0.375)^2 - (0.198)^2\right]}$$

$$V_{bh} = 37.7 \ \text{ft/sec}$$

The kinetic energy per unit volume at the bottom of the borehole in the annulus, KE_{bh}, is (see Chapter 1 and Equations 1-1 and 1-2)

$$\rho_{bh} = \frac{0.136}{32.2}$$

$$\rho_{bh} = 0.00422 \ \frac{\text{lb} - \text{sec}^2}{\text{ft}^4}$$

$$KE_{bh} = \frac{1}{2} \ (0.00422) \ (37.7)^2$$

$$KE_{bh} = 3.002 \ \frac{ft - lb}{ft^3}$$

The trial and error process for the above example requires an iterative selection process to determine the value of q_g that will give a kinetic energy per unit volume at the bottom of the borehole in the annulus that is equal to 3.0 ft-lb/ft^3. In this example the value of q_g that will give a kinetic energy value equal to 3.0 ft-lb/ft^3 is 320.9 scfm.

Using the calculation procedure as given above, plots can be prepared for the above example geometry for a variety of drilling depths and drilling rates (for API standard conditions and sedimentary rock). Figure 5-1 gives the air minimum volumetric flow rates for a 2 3/8 inch drill pipe in a 4 1/2 inch open borehole. The figure shows the minimum volumetric flow rate of 320.9 scfm for the drilling rate of 30 ft/hr and depth of 1,000 ft.

Figures 5-1 to 5-9 give the air minimum volumetric flow rates at API Mechanical Equipment Standards standard atmospheric conditions and for sedimentary rock for a variety of shallow borehole and drill string geometric configurations. The openhole borehole sizes are 4 1/2 inch, 4 3/4 inch, 5 7/8 inch, 6 inch, 6 1/4 inch, 6 1/2 inch, 6 3/4 inch, 7 5/8 inch, and 7 7/8 inch. The drill pipe sizes are 2 3/8 inch, 2 7/8 inch, and 3 1/2 inch. The figures are developed for various drilling rates (e.g., 30 ft/hr, 60 ft/hr, and 90 ft/hr) and assuming an openhole borehole wall absolute surface roughness of 0.005 ft.

Shallow depth direct circulation operations generally utilize smaller drill bit diameters. Also, the tri-cone drill bits used in these operations have a single large water course (air course) opening in the center of the drill bit body (as opposed to tri-cone drill bits for oil field operations that have three small water course orifices for jetting nozzles). Direct circulation shallow boreholes are usually drilled with small drill pipe and small drill bits like those given in Figures 5-1 to 5-9. Larger diameter shallow boreholes are usually drilled with reverse circulation operations. The exception to this general rule is oil field drilling where blowout safety considerations dictate that direct circulation be used on nearly all intervals.

Direct circulation requires lifting the rock cuttings in the annulus of the borehole as the air flow returns to the surface (flowing vertically upward). The annulus is a large cross-section opening relative to the cross-sectional area of the inside of the drill string. Thus, the resistance to the upward flow in the annulus is dominated by the weight of the rock cuttings being lifted.

Illustrative Example 5.2a Determine the direct circulation approximate minimum volumetric flow rate of air required to drill a 4 3/4 inch openhole borehole (4 3/4 inch drill bit diameter) with a drill string composed of 120 ft of 3 1/2 inch by 1 1/2 inch drill collars (see Table B-1) above the drill bit and API 2 3/8 inch, 4.85 lb/ft nominal, EU, NC 26, Grade E drill pipe above the drill collars to the surface (see Table B-4). The anticipated drilling rate is 30 ft/hr and the maximum depth of the well is 1,200 ft. The formations to be drilled are a sequence of competent unfractured gneisses (metamorphic rock). The drilling location is at 6,000 ft above sea level (in the mid latitudes of North America) and the day time air temperature is approximately 70˚F. This is a typical mining or geotechnical borehole geometry.
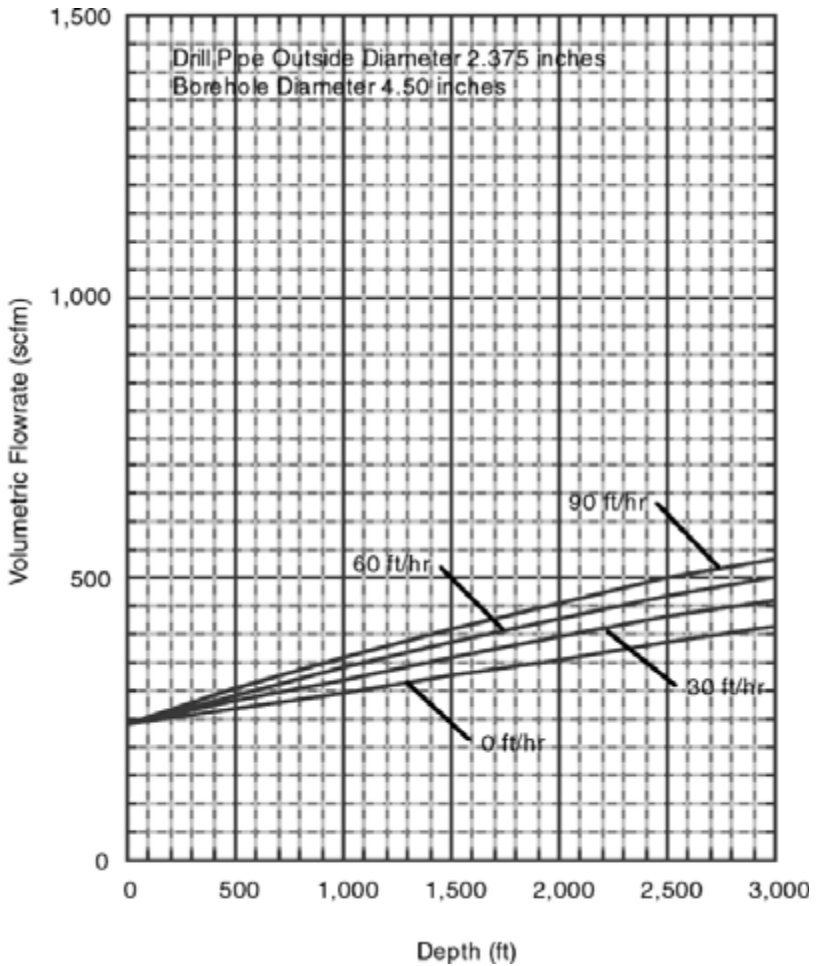
Figure 5-1: Minimum volumetric flow rate of air at API standard conditions for 2 3/8 inch drill pipe and 4 1/2 inch open borehole.
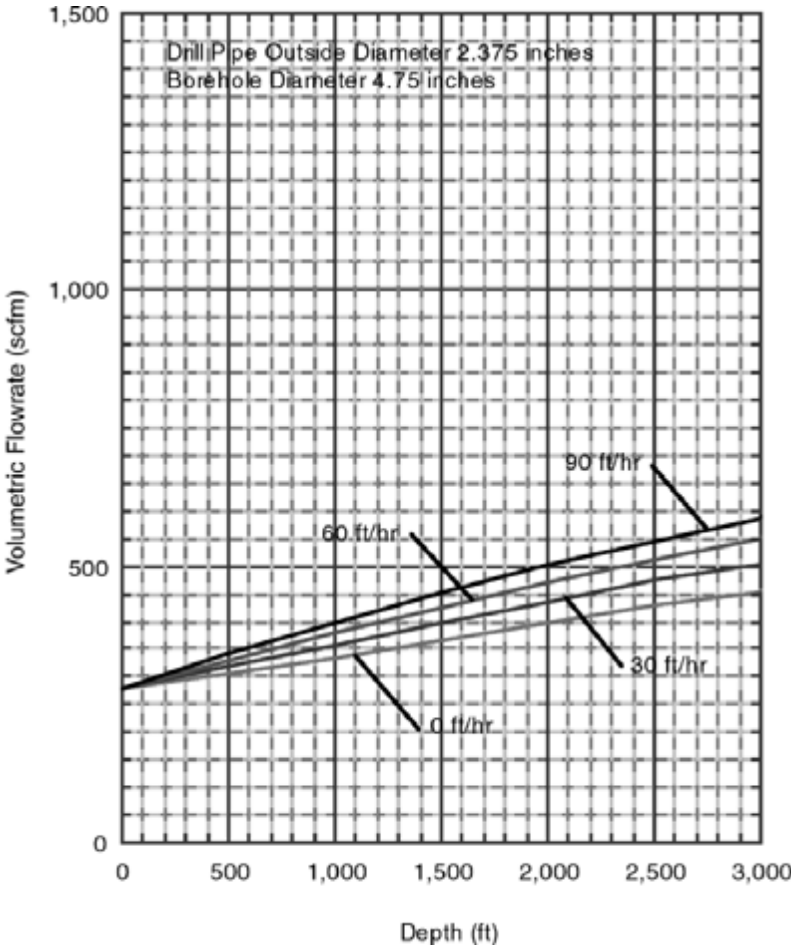
Figure 5-2: Minimum volumetric flow rate of air at API standard conditions for 2 3/8 inch drill pipe and 4 3/4 inch open borehole.
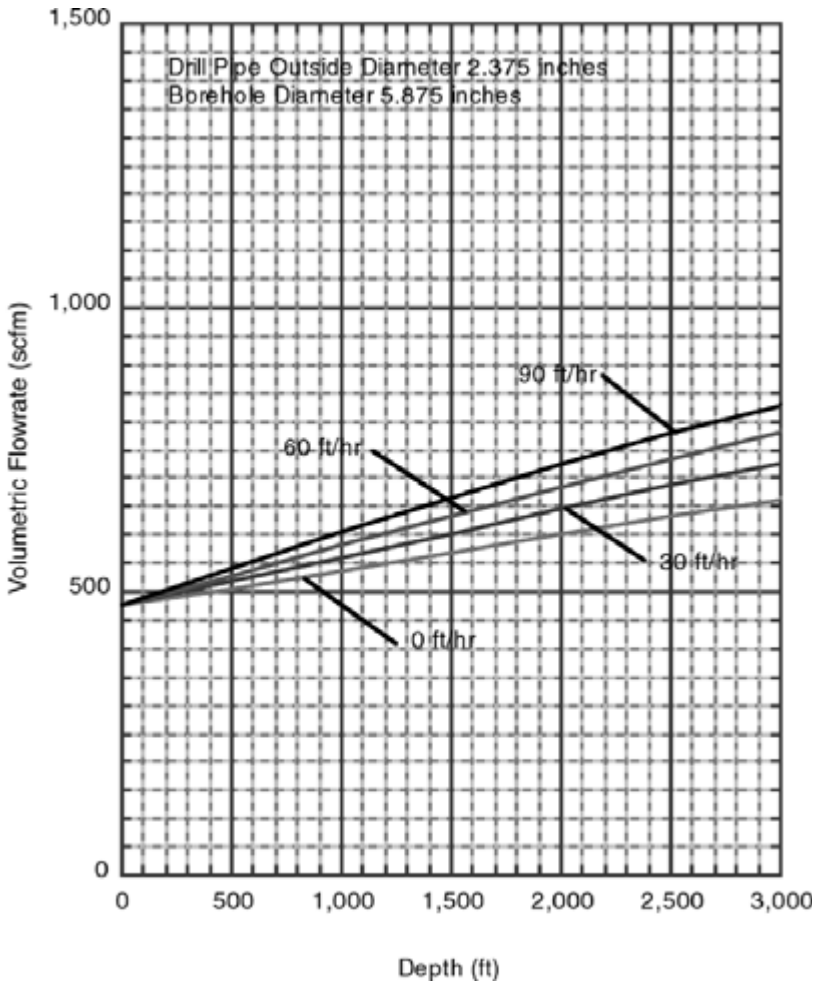
Figure 5-3: Minimum volumetric flow rate of air at API standard conditions for 2 3/8 inch drill pipe and 5 7/8 inch open borehole.
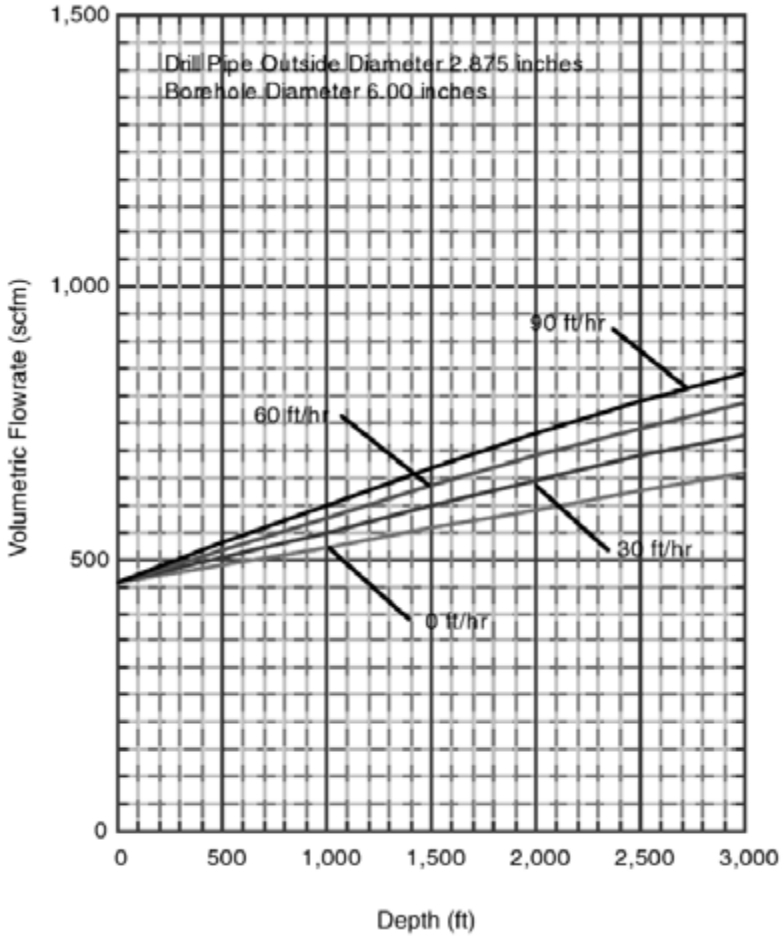
Figure 5-4: Minimum volumetric flow rate of air at API standard conditions for 2 7/8 inch drill pipe and 6 inch open borehole.
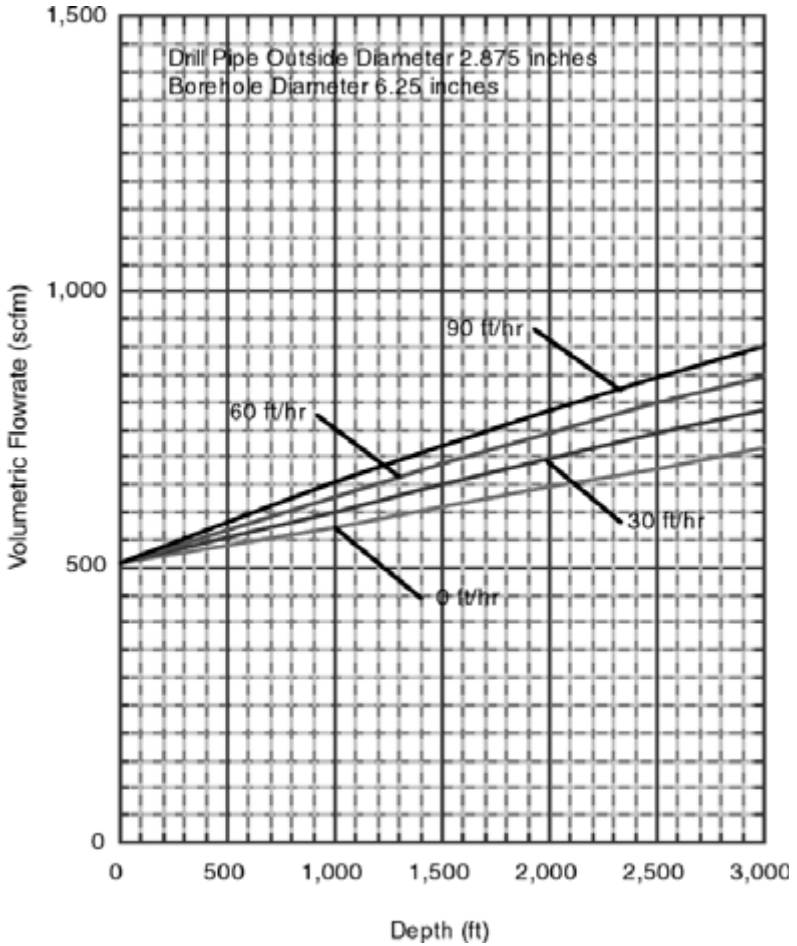
Figure 5-5: Minimum volumetric flow rate of air at API standard conditions for 2 7/8 inch drill pipe and 6 1/4 inch open borehole.
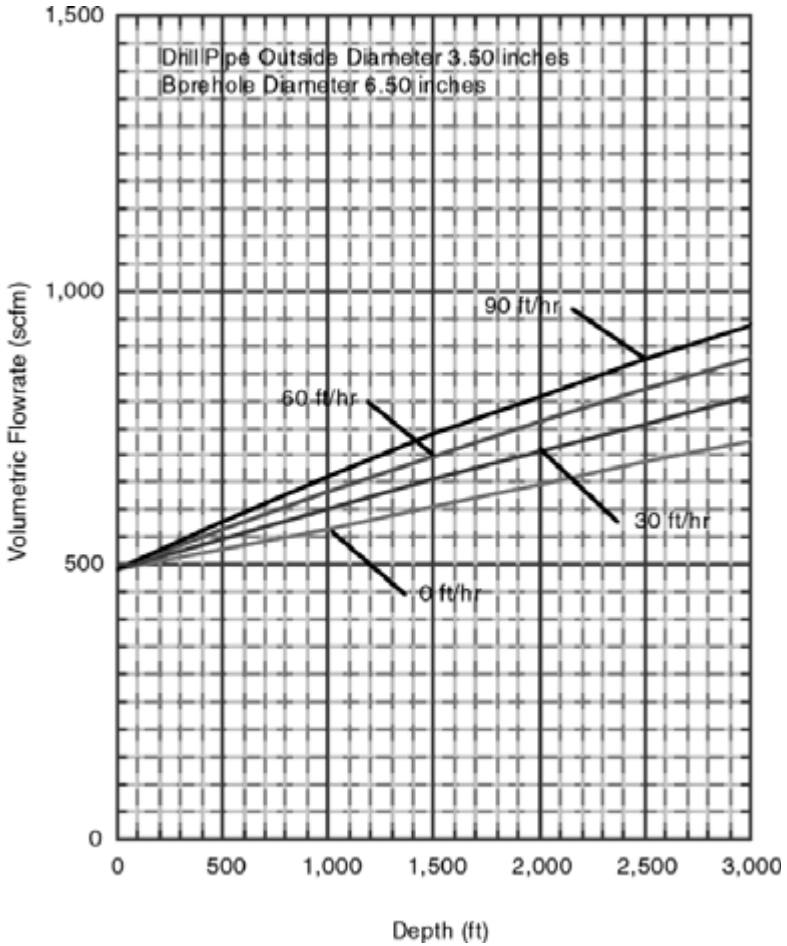
Figure 5-6: Minimum volumetric flow rate of air at API standard conditions for 3 1/2 inch drill pipe and 6 1/2 inch open borehole.
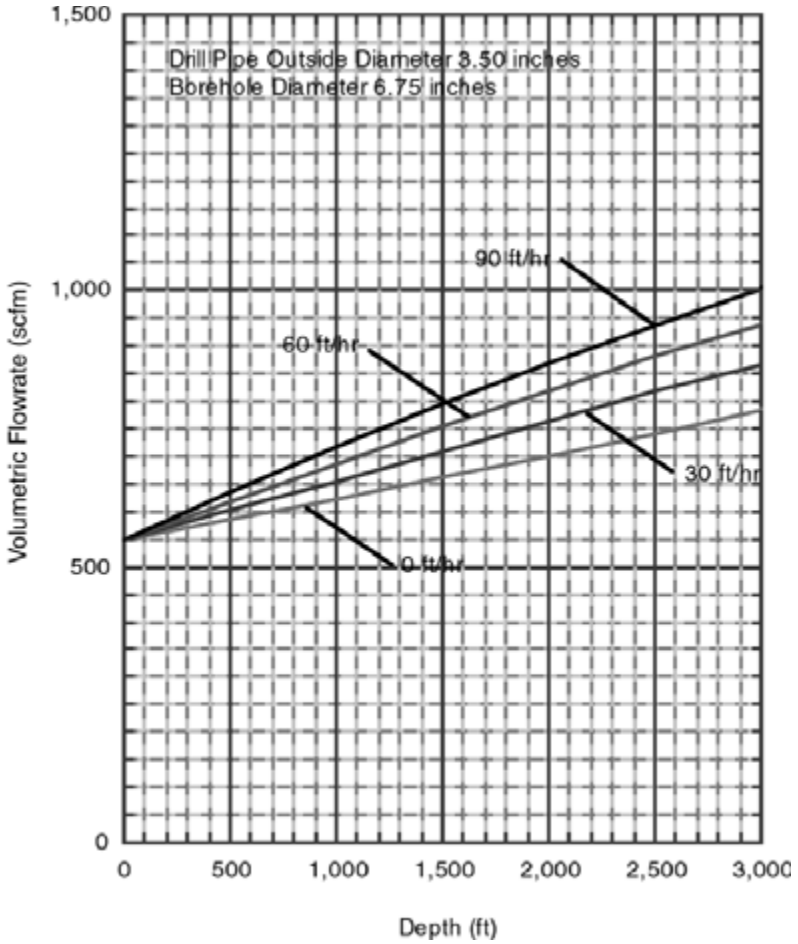
Figure 5-7: Minimum volumetric flow rate of air at API standard conditions for 3 1/2 inch drill pipe and 6 3/4 inch open borehole.
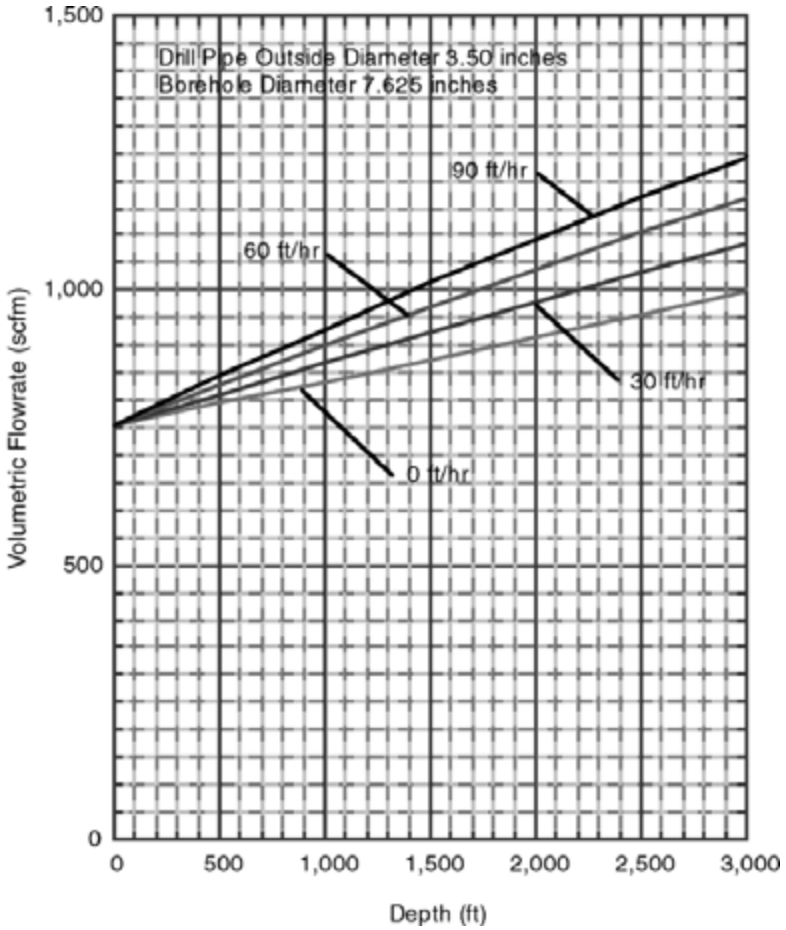
Figure 5-8: Minimum volumetric flow rate of air at API standard conditions for 3 1/2 inch drill pipe and 7 5/8 inch open borehole.
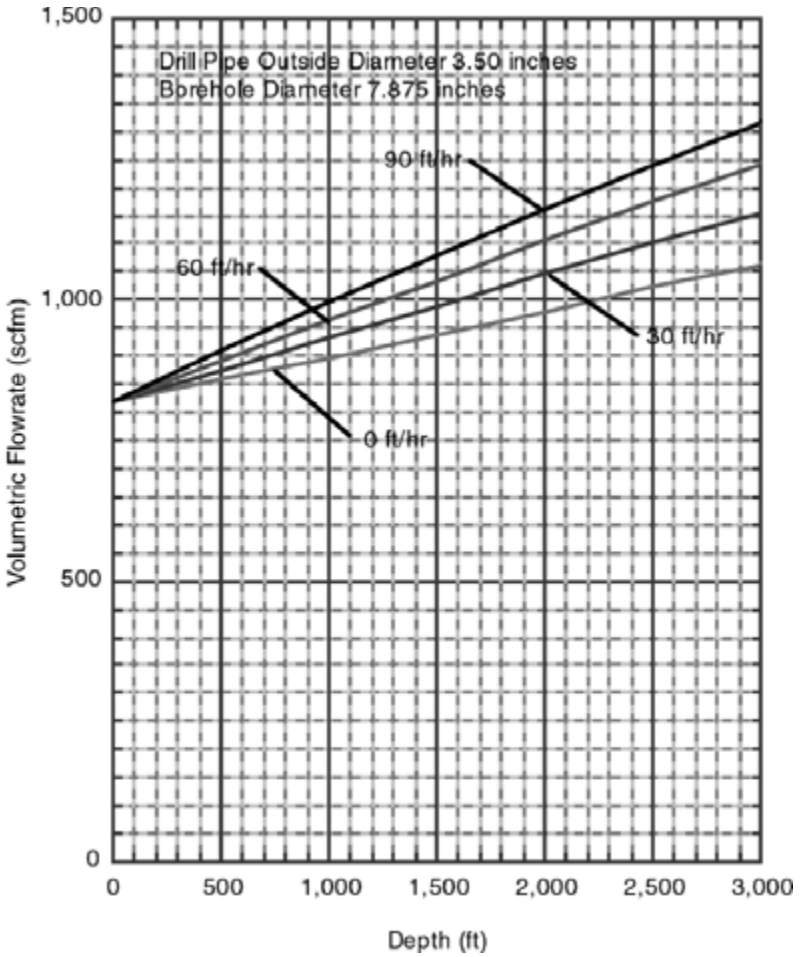
Figure 5-9: Minimum volumetric flow rate of air at API standard conditions for 3 1/2 inch drill pipe and 7 7/8 inch open borehole.

It is only necessary to obtain the approximate minimum volumetric flow rate for a drilling operation.   The borehole is never drilled with only the minimum volumetric flow rate.   Primary compressor units have fixed volumetric flow rate outputs and it is operationally inefficient to vent excess compressed air to the atmosphere.   Erosion of the drill string or the rock formations is usually not a consideration.   Therefore, compressor units are selected to give a total volumetric flow rate that exceeds the required minimum volumetric flow rate.

Figure 5-2 gives the minimum volumetric flow rates of air for a 4 3/4 inch openhole borehole with a 2 3/8 inch drill pipe.   The flow rate is determined for the maximum depth of the well which is 1,200 ft.   The annulus around the drill collars at the bottom of the drill string will have higher air velocities than in the annulus around the drill pipe.   But this is a small effect.   Thus, ignoring the drill collars in the drill string when determining the minimum volumetric flow rate for the well geometry yields a value that is conservative (i.e., a value that is slightly higher than the actual minimum required).   Therefore, Figure 5-2 can be used to determine the approximate minimum volumetric flow rate of air for this example drilling operation.

Since the figures are developed assuming sedimentary rock, the drilling rate must be adjusted for drilling metamorphic rock.   Equation 5-4 shows that the weight rate of flow of solid rock cuttings is linear with the specific gravity of the rock being drilled.   The metamorphic rock formations to be drilled have an average specific gravity of 3.0.   The adjusted drilling rate to compensate for the heavier rock type to be drilled is (see Equation 5-4)

$$K_a = 30 \left(\frac{3.0}{2.7} \right)$$

$$K_a = 33.3 \text{ ft/hr}$$

Using Figure 5-2, the approximate minimum volumetric flow rate for drilling at a depth of 1,200 ft for an adjusted drilling rate of 33.3 ft/hr is approximately 378 scfm.   This is the minimum flow rate for sea level air (API standard conditions).   But the drilling location is at 6,000 ft above sea level and the day time temperature is 70° F.   Thus, the above minimum volumetric flow rate must be adjusted for the atmospheric conditions that exist at the drilling location (i.e., to obtain the actual cubic feet per minute, acfm).   In Illustrative Example 5.1 the specific weight of air at API standard conditions was found to be 0.0763 lb/ft^3.   Table 4-1 gives an average atmospheric pressure of 11.769 psia for a surface location of 6,000 ft above sea level (mid latitudes North America) (also see Appendix D).   The actual atmospheric pressure for the air at the drilling location (that will be utilized by the compressor), P_{at}, is

$$p_{at} = 11.769 \text{ psia}$$

$$P_{at} = p_{at} \, 144$$

$$P_{at} \; = \; 1{,}695 \;\; \text{lb/ft}^2 \;\; \text{abs}$$

The actual atmospheric temperature of the air at the drilling location, T_{at} (that will be used by the compressor), is

$$t_{at} \; = \; 70°\text{F}$$

$$T_{at} \; = \; t_{at} \; + \; 459.67$$

$$T_{at} \; = \; 529.67°\,\text{R}$$

Thus, P_g and T_g become

$$P_g \; = \; P_{at} \; = \; 1{,}695 \;\; \text{lb/ft}^2 \;\; \text{abs}$$

$$T_g \; = \; T_{at} \; = \; 529.67°\,\text{R}$$

Using Equation 4-11, the specific weight of the gas entering the compressor is

$$\gamma_g \; = \; \frac{(1{,}695)\;(1.0)}{(53.36)\;(529.67)}$$

$$\gamma_g \; = \; 0.0600 \;\; \text{lb/ft}^3$$

Note the above specific weight value can also be obtained from Figure D-4 in Appendix D.

The approximate minimum volumetric flow rate for this illustrative example adjusted for the actual atmospheric conditions at the drilling location can be determined by equating the weight rate of flow of the air at the two atmospheric conditions. This reduces to

$$q_g \; = \; 378 \left(\frac{0.0763}{0.0600} \right)$$

$$q_g \; = \; 481 \;\; \text{acfm}$$

The above volumetric flow rate is the adjusted minimum value for the atmospheric conditions at this drilling location (6,000 ft above sea level).

Illustrative Example 5.3a Determine the direct circulation minimum volumetric flow rate of air required to drill a 6 1/4 inch openhole borehole (6 1/4 inch drill bit diameter) and a drill string composed of 240 ft of 4 3/4 inch by 1 1/2 inch drill collars (see Table B-1) above the drill bit and API 2 7/8 inch, 6.85 lb/ft

nominal, EU, NC 31, Grade E drill pipe (see Table B-4). The anticipated drilling rate is assumed to be 90 ft/hr and the maximum drilling depth of the well is 2,400 ft. The formations to be drilled are a sequence of limestone rock. The drilling location (where the drill rig will sit on the surface) is at 4,000 ft above sea level and the day time air temperature during operations is assumed to be approximately 40°F. This is a typical mining or geotechnical borehole geometry.

Figure 5-5 gives the minimum volumetric flow rates of air for a 6 1/4 inch openhole borehole with a 2 7/8 inch drill pipe. The flow rate is determined for the maximum depth of the well which is 2,400 ft. Ignoring the drill collars in the drill string when determining the minimum volumetric flow rate for the well geometry yields a value that is conservative (i.e., a value that is slightly higher than the actual minimum required). Therefore, Figure 5-5 can be used to determine the approximate minimum volumetric flow rate of air for this example drilling operation.

Using Figure 5-5, the approximate minimum volumetric flow rate for drilling at a depth of 2,400 ft and a drilling rate of 90 ft/hr is approximately 835 scfm. This is the minimum flow rate for sea level (API standard conditions) air. But the drilling location is at 4,000 ft above sea level and the day time temperature is 40°F. Thus, the above minimum volumetric flow rate must be adjusted for the atmospheric conditions that exist at the drilling location (i.e., to obtain the actual cubic feet per minute, acfm). In Illustrative Example 5.1 the specific weight of air at API standard conditions was found to be 0.0763 lb/ft^3. Table 4-1 gives an average atmospheric pressure of 12.685 psia for a surface location of 4,000 ft above sea level (mid latitudes North America) (also see Appendix D). The actual atmospheric pressure for the air at the drilling location (that will be used by the compressor), P_{at}, is

$$p_{at} = 12.685 \text{ psia}$$

$$P_{at} = p_{at} \; 144$$

$$P_{at} = 1,827 \text{ lb/ft}^2 \text{ abs}$$

The actual atmospheric temperature of the air at the drilling location, T_{at} (that will be used by the compressor), is

$$t_{at} = 40°F$$

$$T_{at} = t_{at} + 459.67$$

$$T_{at} = 499.67°R$$

Thus, P_g and T_g become

$$P_g = P_{at} = 1,827 \text{ lb/ft}^2 \text{ abs}$$

$$T_g = T_{at} = 499.67^{\circ}\text{R}$$

Using Equation 4-11, the specific weight of the gas entering the compressor is

$$\gamma_g = \frac{(1,827)\,(1.0)}{(53.36)\,(499.67)}$$

$$\gamma_g = 0.0685 \text{ lb/ft}^3$$

Note the above specific weight value can also be obtained from Figure D-4 in Appendix D.

The approximate minimum volumetric flow rate for this illustrative example adjusted for the actual atmospheric conditions at the drilling location can be determined by equating the weight rate of flow of the air at the two atmospheric conditions. This reduces to

$$q_g = 835 \left(\frac{0.0763}{0.0685} \right)$$

$$q_g = 930 \text{ acfm}$$

The above volumetric flow rate is the adjusted minimum value for the atmospheric conditions at this drilling location (4,000 ft above sea level).

5.2.2 *Injection Pressure and the Selection of Compressor Equipment*

The planning process given in Section 5.1 requires that the borehole requirements be compared to the capabilities of the compressor units available. Specifically, these comparisons are made between; a) the required borehole volumetric flow rate and the compressor volumetric flow rate capability, b) the borehole injection pressure (using the compressor volumetric flow rate) and the pressure capability of the compressor and, c) the horsepower required by the compressor and the input capability of the prime mover. For shallow drilling operations the selection of the appropriate compressor equipment often dictates the drilling rig selection. This will be demonstrated in the examples that follow.

Illustrative Examples 5.2b, and 5.3b describe the implementation of the basic planning steps Nos. 7 through 9 given in Section 5.1.

Illustrative Example 5.2b Select the appropriate primary compressor system for the direct circulation drilling operation data given in Illustrative Example 5.2a. This selection will give the actual volumetric flow rate of air to be delivered to the drilling operation. The selection of the appropriate compressor will be made from the example compressor systems listed in Section 4.7 of Chapter 4. In Illustrative Example 5.2a it was found that the drilling location adjusted minimum volumetric flow rate of air for the 4 3/4 inch diameter, 1,200 ft deep borehole was approximately 481 acfm (for a surface drilling location of 6,000 ft above sea level).

Also determine the injection pressure, the input power required by the compressor, and the derated output power available from the prime mover while drilling at 1,200 ft.

a) Sullair Model 840 Rotary Screw Compressor

A candidate compressor is the integrated system on-board the portable Tamrock Driltech Model D25K drilling rig (see Figure 4-19).   The on-board primary compressor is a Sullair Model 840, two-stage, oil flooded, rotary helical lobe (screw) type. This compressor is powered by a Caterpillar Model 3406, diesel fuel, turbocharged prime mover capable of a 400 peak horsepower at the operating speed of 1,800 rpm (see Figure 4-20).   The compressor is capable of producing a volumetric flow rate of 840 scfm and a fixed pressure of 340 psig at API standard conditions. This drilling rig is capable of drilling to about 1,000 ft of vertical depth so it can probably be used for drilling to 1,200 ft with a light weight drill string (check drill string weight against hoisting capability). Even though this drilling rig and its integrated Sullair rotary screw compressor are to be placed at the 6,000 ft surface elevation drilling location, the compressor will still produce the same volumetric flow rate as at sea level conditions. The actual volumetric flow rate of this compressor at the 6,000 ft surface elevation is 840 acfm (see Chapter 4). This volumetric flow rate is greater than the required adjusted minimum volumetric flow rate of 481 acfm (factor of safety of 1.75). Therefore, this compressor unit is capable of producing the volumetric flow rate to drill the borehole.

A comparison must also be made between the injection pressure required to drill this borehole and the pressure capability of the selected compressor system.   The injection pressure is obtained by a sequence of calculation steps that determine the bottomhole pressure in the annulus, the pressure at the bottom of the inside of the drill string, and then the injection pressure (upstream through the circulation system). In these calculations, the actual volumetric flow rate into the compressor is 840 acfm. Also, in these calculations, the actual atmospheric conditions at the drilling location will be used (i.e., 11.769 psia and 70˚F) (see Table 4.1 or Appendix D). The atmospheric pressure of the air, P_{at}, entering the compressor is

$$p_{at} = 11.769 \text{ psia}$$

$$P_{at} = p_{at} \; 144$$

$$P_{at} = 1,695 \text{ lb/ft}^2 \text{ abs}$$

The atmospheric temperature of the air, T_{at}, entering the compressor is

$$t_{at} = 70^o \text{F}$$

$$T_{at} = t_{at} + 459.67$$

$$T_{at} = 529.67^o \text{R}$$

Thus, P_g and T_g become

$$P_g = P_{at} = 1,695 \ \text{lb/ft}^2 \ \text{abs}$$

$$T_g = T_{at} = 529.67^\circ \text{R}$$

Using Equation 4-11, the specific weight of the air entering the compressor is

$$\gamma_g = \frac{(1,695) \ (1.0)}{(53.36) \ (529.67)}$$

$$\gamma_g = 0.0600 \ \text{lb/ft}^3$$

The volumetric flow rate of air entering the top of the compressor, Q_g, is

$$Q_g = \frac{840}{60}$$

$$Q_g = 14.0 \ \text{ft}^3/\text{sec}$$

The weight rate of flow of air in the circulating system in the well is

$$\dot{w}_g = 0.0600 \ (14.0)$$

$$\dot{w}_g = 0.840 \ \text{lb/sec}$$

The borehole diameter, D_h, is

$$d_h = 4.75 \ \text{inches}$$

$$D_h = \frac{d_h}{12}$$

$$D_h = 0.396 \ \text{ft}$$

Using Equation 5-4, the weight rate of flow of the solid rock cuttings in the annulus is

$$\dot{w}_s = \left(\frac{\pi}{4}\right) (0.396)^2 \ (62.4) \ (3.0) \left[\frac{30}{(60) \ (60)}\right]$$

$\dot{w}_s = 0.192$ lb/sec

The drill pipe outside diameter, D_p, is

$d_p = 2.375$ inches

$$D_p = \frac{d_p}{12}$$

$D_p = 0.198$ ft

The metamorphic rock borehole wall absolute surface roughness is assumed to be 0.005 ft (see Table 8-1). Using Equation 5-6, the average surface roughness for the annulus becomes

$$e_{av} = \frac{(0.005)\left(\frac{\pi}{4}\right)(0.396)^2 + (0.00015)\left(\frac{\pi}{4}\right)(0.198)^2}{\left(\frac{\pi}{4}\right)(0.396)^2 + \left(\frac{\pi}{4}\right)(0.198)^2}$$

$e_{av} = 0.0040$ ft

Equation 5-5 becomes

$$f = \left[\frac{1}{2\ \log\left(\dfrac{0.396 - 0.198}{0.0040}\right) + 1.14} \right]^2$$

$f = 0.049$

Equations 5-2 and 5-3 become, respectively,

$$a_a = \left(\frac{1.0}{53.36}\right)\left[1 + \left(\frac{0.192}{0.840}\right)\right]$$

$a_a = 0.023$

$$b_a = \frac{0.049}{2\ (32.2)\ (0.396 - 0.198)}\left(\frac{53.36}{1.0}\right)^2 \frac{(0.840)^2}{\left(\frac{\pi}{4}\right)^2\left[(0.396)^2 - (0.198)^2\right]^2}$$

$$b_a = 903.7$$

The bottomhole temperature is determined from the geothermal temperature of the rock formations at the surface, the regional geothermal gradient, and the depth of the borehole. The geothermal temperature of the rock formations near the surface is assumed to be represented by the temperatures given in Table 4-1 (also see Appendix D). Thus, for a 6,000 ft surface location this temperature is assumed to be 37.6°F. For this example the geothermal gradient is approximated to be 0.01°F/ft. Thus, T_{bh}, is

$$t_r = 37.6^o\,F$$

$$T_r = t_r + 459.67$$

$$T_r = 497.27^o\,R$$

$$T_{bh} = T_r + 0.01\,(1,200)$$

$$T_{bh} = 509.27^o\,R$$

The average temperature of this borehole is

$$T_{av} = \frac{T_r + T_{bh}}{2}$$

$$T_{av} = 503.27^o\,R$$

Using the above values, Equation 5-1 becomes

$$P_{bh} = \left\{ \left[(1,695)^2 + 903.7\,(503.27)^2 \right] e^{\frac{2\,(0.023)\,(1,200)}{503.27}} - 903.7\,(503.27)^2 \right\}^{0.5}$$

$$P_{bh} = 5,456 \ \text{lb/ft}^2 \ \text{abs}$$

$$p_{bh} = \frac{P_{bh}}{144}$$

$$p_{bh} = 37.9 \ \text{psia}$$

This is the pressure at the bottom of the borehole in the annulus.

Most shallow air drilling operations utilize either tri-cone drill bits, or air hammers equipped with air hammer drill bits. Air hammers and their drill bits will be discussed in detail in Chapter 11.

Tri-cone drill bits used in shallow drilling operations have a large single opening in the center of the bit body. These drill bits are less expensive to fabricate than their oil field counterparts which are fabricated with sealed bearings and three water course orifices that can be fitted with nozzles of various inside diameters. Since shallow well tri-cone bits have a large center opening, they can be used for both direct and reverse circulation operations. With the large center opening in the drill bit, the pressure change in the air flow from the bottom of the inside of the drill string (inside the drill bit) to the bottom of the annulus is assumed to be negligible.

Therefore, for this illustrative example the inside of the bottom of the drill string just above the drill bit is assumed to have the same pressure as that at the bottom of the annulus. Thus,

$$p_{bhi} = 37.9 \text{ psia}$$

$$P_{bhi} = p_{bhi} \; 144$$

$$P_{bhi} = 5,456 \text{ lb/ft}^2 \text{ abs}$$

The inside of the drill string is approximated by the inside diameter of the drill pipe. The inside diameter of the API 2 3/8 inch, 4.85 lb/ft nominal, EU, NC 26, Grade E drill pipe is 1.995 inches (see Table B-4).

$$d_i = 1.995 \text{ inches}$$

$$D_i = \frac{d_i}{12}$$

$$D_i = 0.166 \text{ ft}$$

The injection pressure, P_{in}, into the top of the inside of the drill string is determined from

$$P_{in} = \left[\frac{P_{bhi}^2 + b_i \, T_{av}^2 \left(e^{\frac{2 \, a_i \, H}{T_{av}}} - 1 \right)}{e^{\frac{2 \, a_i \, H}{T_{av}}}} \right]^{0.5} \tag{5-7}$$

where

$$a_i = \frac{S_g}{R} \tag{5-8}$$

$$b_i = \frac{f}{2\ g\ D_i} \left(\frac{R}{S_g}\right)^2 \frac{\dot{w}_g^2}{\left(\frac{\pi}{4}\right)^2 D_i^4} \tag{5-9}$$

The Fanning friction factor for the above equation is

$$f = \left[\frac{1}{2\ \log\left(\dfrac{D_i}{e_p}\right) + 1.14}\right]^2 \tag{5-10}$$

Using the above values, Equation 5-10 becomes

$$f = \left[\frac{1}{2\ \log\left(\dfrac{0.166}{0.00015}\right) + 1.14}\right]^2$$

$$f = 0.019$$

Equations 5-8 and 5-9 become, respectively,

$$a_i = \frac{1.0}{53.36}$$

$$a_i = 0.019$$

and

$$b_i = \frac{0.019}{2\ (32.2)\ (0.166)} \left(\frac{53.36}{1.0}\right)^2 \frac{(0.840)^2}{\left(\dfrac{\pi}{4}\right)^2 (0.166)^4}$$

$$b_i = 7,610$$

Equation 5-7 becomes

$$P_{in} = \left[\frac{(5,456)^2 + (7,610)\,(503.27)^2 \left(e^{\frac{2\,(0.019)\,(1,200)}{503.27}} - 1 \right)}{e^{\frac{2\,(0.019)\,(1,200)}{503.27}}} \right]^{0.5}$$

$$P_{in} = 13,860 \ \text{lb/ft}^2 \ \text{abs}$$

$$p_{in} = \frac{P_{in}}{144}$$

$$p_{in} = 96.2 \ \text{psia}$$

The above pressure is the approximate injection pressure into the top of the inside of the drill string. These calculations have been carried out neglecting the drill collar outside and inside diameters. Also, the calculations have ignored the existence of a blooey line type structure (most shallow drilling operations do not have blooey lines). These minor losses are not important in shallow drilling operations (Chapter 8 calculation examples will consider these additional minor losses). The above pressure slightly underestimates the actual pressure that is seen at the pressure gauge just downstream of the compressor. In order for this compressor to be used for this drilling operation, the above injection pressure must be less than the derated fixed pressure of the rotary screw Sullair Model 840 compressor.

The fixed pressure capability of the Sullair Model 840 compressor has a pressure output of 340 psig. However, this output must be derated when the compressor is placed at a surface drilling location above sea level. To determine the derated fixed pressure capability of this compressor for the 6,000 ft surface drilling location, the design fixed ratio of the compressor must be determined. As demonstrated in Chapter 4, the fixed pressure ratio is referenced to sea level conditions (usually API standard conditions). Thus, the assumed design input pressure, p_1 (air flowing into the compressor from the atmosphere), is

$$p_1 = 14.696 \ \text{psia}$$

The output pressure, p_2, is

$$p_2 = 340 + 14.696 = 354.696 \ \text{psia}$$

The total fixed compression ratio across the two stages of this compressor, r_c, is

$$r_c = \frac{p_2}{p_1}$$

$$r_c = \frac{354.696}{14.696}$$

$$r_c = 24.14$$

The approximated derated output pressure, p_{d2}, for this compressor when placed at a 6,000 ft surface drilling location is determined from

$$p_{d2} = r_c \, p_{at}$$

where p_{at} is the actual atmospheric pressure at the 6,000 ft surface drilling location (i.e., 11.679 psia). Thus, the derated output pressure, p_{d2}, is

$$p_{d2} = (24.14) \, (11.769)$$

$$p_{d2} = 284.1 \text{ psia}$$

The above compressor derated pressure of 284.1 psia is greater than the injection pressure of 96.2 psia, therefore, the compressor is capable of producing the injection pressure needed for this example drilling operation.

The last criteria to consider is whether the prime mover has the power to operate at the 6,000 ft surface elevation. The prime mover for this compressor is a diesel fueled, turbocharged, Caterpillar Model 3406 with a peak output of 400 horsepower at 1,800 rpm (at API standard conditions) (see Section 4.7).

The theoretical shaft horsepower, $\dot{W}_s$, required by the compressor is obtained from Equation 4-35a. Equation 4-35a becomes

$$\dot{W}_s = \frac{(2) \, (1.4)}{(0.4)} \frac{(11.769) \, (840)}{229.17} \left[\left(\frac{284.1}{11.769} \right)^{\frac{(0.4)}{(2)(1.4)}} - 1 \right]$$

$$\dot{W}_s = 173.9$$

Assuming a mechanical efficiency, ε_m, is

$$\varepsilon_m = 0.90$$

Then from Equation 4-39, the actual shaft horsepower, $\dot{W}_{as}$, required by the compressor is

$$\dot{W}_{as} = \frac{173.9}{0.9}$$

$$\dot{W}_{as} \ = \ 193.2$$

The above determined 193.2 horsepower is the actual shaft power needed by the compressor to produce the 284.1 psia fixed pressure output at the surface location elevation of 6,000 ft above sea level. At this surface location, the input horsepower available from the prime mover is a derated value (derated from the rated 400 horsepower available at 1,800 rpm). In order for the compressor system to operate at this 6,000 ft surface location elevation, the derated input power available must be greater than the actual shaft power needed. Figure 4-15 shows that for 6,000 ft elevation the input power of a turbocharged prime mover must be derated by approximately 14.8 percent. The derated input horsepower, $\dot{W}_i$, available from the prime mover is

$$\dot{W}_i \ = \ 400 \left(1 \ - \ 0.148\right)$$

$$\dot{W}_i \ = \ 340.8$$

For this example, the prime mover's derated input power is greater than the actual shaft horsepower needed, thus, the compressor system can be operated at this 6,000 ft surface location elevation. This particular example is somewhat complicated since the prime mover for this integrated compressor unit shares its power with other auxiliary equipment on the portable drilling rig. Thus, a portion of the 340.8 horsepower available from the prime mover will be used by the hydraulic rotary head unit. To get a complete assessment of the power available to this compressor these additional power needs should be evaluated.

b) Gardner Denver Model WEN Reciprocating Piston Primary Unit.

If the drilling rig used for this drilling operation does not have an on-board compressor system (see Figure 1-4), then a stand alone compressor unit must be used to provide the compressed air. A candidate stand alone primary compressor system is the skid mounted primary Gardner Denver Model WEN, two-stage, reciprocating piston compressor powered by a Caterpillar Model D353, diesel fueled, turbocharged, prime mover capable of a 270 peak horsepower at the operating speed of 1,000 rpm (see Figure 4-22). This compressor is capable of producing a volumetric flow rate of 700 scfm and a maximum pressure of 350 psig at API standard conditions. When this compressor unit is to be placed at the 6,000 ft surface elevation drilling location, the compressor will still produce the same volumetric flow rate as at sea level conditions. Thus, the actual volumetric flow rate of this compressor at the 6,000 ft surface elevation is 700 acfm (see Chapter 4). This volumetric flow rate is greater than the required adjusted minimum volumetric flow rate of 481 acfm (factor of safety of 1.46). Therefore, this compressor unit is capable of producing the volumetric flow rate to drill the borehole.

A comparison must be made between the injection pressure required to drill this borehole and the pressure capability of the selected compressor system. The injection pressure is obtained by calculating through a sequence of steps that determine the bottomhole pressure in the annulus, the pressure at the bottom of the

inside of the drill string, and then the injection pressure (upstream through the circulation system). In these calculations, the actual volumetric flow rate into the compressor from the atmosphere is 700 acfm. Also, in these calculations, the actual atmospheric conditions at the drilling location will be used (i.e., 11.769 psia and 70˚F) (see Table 4.2 or Appendix D). The atmospheric pressure of the air, P_{at}, entering the compressor is

$$p_{at} = 11.769 \text{ psia}$$

$$P_{at} = p_{at} \; 144$$

$$P_{at} = 1,695 \text{ lb/ft}^2 \text{ abs}$$

The atmospheric temperature of the air, T_{at}, entering the compressor is

$$t_{at} = 70^o \text{F}$$

$$T_{at} = t_{at} + 459.67$$

$$T_{at} = 529.67^o \text{R}$$

Thus, P_g and T_g become

$$P_g = P_{at} = 1,695 \text{ lb/ft}^2 \text{ abs}$$

$$T_g = T_{at} = 529.67^o \text{R}$$

Using Equation 4-11, the specific weight of the gas entering the compressor is

$$\gamma_g = \frac{(1,695)\,(1.0)}{(53.36)\,(529.67)}$$

$$\gamma_g = 0.0600 \text{ lb/ft}^3$$

The volumetric flow rate of air entering the compressor, Q_g, is

$$Q_g = \frac{700}{60}$$

$$Q_g = 11.7 \text{ ft}^3/\text{sec}$$

The weight rate of flow of air in the circulating system in the well is

$$\dot{w}_g = 0.0600 \ (11.7)$$

$$\dot{w}_g = 0.700 \ \text{lb/sec}$$

The borehole diameter, D_h, is

$$d_h = 4.75 \ \text{inches}$$

$$D_h = \frac{d_h}{12}$$

$$D_h = 0.396 \ \text{ft}$$

In this illustrative example the formations to be drilled are metamorphic rock. Therefore, unless actual data are available the average specific gravity of metamorphic rock (i.e., $S_s = 3.0$) is used in Equation 5-4. Using Equation 5-4, the weight rate of flow of the solid rock cuttings in the annulus is

$$\dot{w}_s = \left(\frac{\pi}{4}\right) (0.396)^2 \ (62.4) \ (3.0) \left[\frac{30}{(60) \ (60)}\right]$$

$$\dot{w}_s = 0.192 \ \text{lb/sec}$$

The drill pipe outside diameter, D_p, is

$$d_p = 2.375 \ \text{inches}$$

$$D_p = \frac{d_p}{12}$$

$$D_p = 0.198 \ \text{ft}$$

Using Equation 5-6, the average surface roughness for the annulus becomes

$$e_{av} = \frac{(0.005) \left(\dfrac{\pi}{4}\right) (0.396)^2 \ + \ (0.00015) \left(\dfrac{\pi}{4}\right) (0.198)^2}{\left(\dfrac{\pi}{4}\right) (0.396)^2 \ + \ \left(\dfrac{\pi}{4}\right) (0.198)^2}$$

$$e_{av} = 0.0040 \ \text{ft}$$

Equation 5-5 becomes

$$f = \left[\frac{1}{2 \, \log \left(\dfrac{0.396 - 0.198}{0.0040} \right) + 1.14} \right]^2$$

$$f = 0.049$$

Equations 5-2 and 5-3 become, respectively,

$$a_a = \left(\frac{1.0}{53.36} \right) \left[1 + \left(\frac{0.192}{0.700} \right) \right]$$

$$a_a = 0.024$$

and

$$b_a = \frac{0.049}{2 \, (32.2) \, (0.396 - 0.198)} \left(\frac{53.36}{1.0} \right)^2 \frac{(0.700)^2}{\left(\dfrac{\pi}{4} \right)^2 \left[(0.396)^2 - (0.198)^2 \right]^2}$$

$$b_a = 627.5$$

   The bottomhole temperature is determined from the surface geothermal temperature rock formations at the surface, the geothermal gradient, and the depth of the borehole. The geothermal temperature of the rock formations near the surface is assumed to be represented by the temperatures given in Table 4-1 (also see Appendix D). Thus, for a 6,000 ft surface location this temperature is assumed to be 37.6˚F. For this example the geothermal gradient is approximated to be 0.01˚F/ft.   Thus, T_{bh}, is

$$t_r = 37.6^o \, F$$

$$T_r = t_r + 459.67$$

$$T_r = 497.27^o \, R$$

$$T_{bh} = T_r + 0.01 \, (1,200)$$

$$T_{bh} = 509.27^o \, R$$

The average temperature of this borehole is

$$T_{av} = \frac{T_r + T_{bh}}{2}$$

$$T_{av} = 503.27° R$$

Using the above values, Equation 5-1 becomes

$$P_{bh} = \left\{ \left[(1,695)^2 + 627.5 \ (503.27)^2 \right] e^{\frac{2 \ (0.024) \ (1,200)}{503.27}} - 627.5 \ (503.27)^2 \right\}^{0.5}$$

$$P_{bh} = 4,732 \ \text{lb/ft}^2 \ \text{abs}$$

$$p_{bh} = \frac{P_{bh}}{144}$$

$$p_{bh} = 32.9 \ \text{psia}$$

This is the pressure at the bottom of the borehole in the annulus.

With the large center opening in the drill bit, the pressure change in the air flow from the bottom of the inside of the drill string (inside the drill bit) to the bottom of the annulus is assumed to be negligible. The inside of the bottom of the drill string at the drill bit is assumed to have the same pressure as that at the bottom of the annulus. Thus,

$$p_{bhi} = 32.9 \ \text{psia}$$

$$P_{bhi} = p_{bhi} \ 144$$

$$P_{bhi} = 4,732 \ \text{lb/ft}^2 \ \text{abs}$$

The inside of the drill string is approximated by the inside diameter of the drill pipe. The inside diameter of the API 2 3/8 inch, 4.85 lb/ft nominal, EU, NC 26, Grade E drill pipe is 1.995 inches (see Table B-4).

$$d_i = 1.995 \ \text{inches}$$

$$D_i = \frac{d_i}{12}$$

$$D_i = 0.166 \ \text{ft}$$

The inside surface of the drill pipe is assumed to have the surface roughness of commercial steel which is 0.00015 ft. Equation 5-10 becomes

$$f = \left[\frac{1}{2 \log \left(\dfrac{0.166}{0.00015} \right) + 1.14} \right]^2$$

$$f = 0.019$$

Equations 5-8 and 5-9 become, respectively,

$$a_i = \frac{1.0}{53.36}$$

$$a_i = 0.019$$

and

$$b_i = \frac{0.019}{2 \ (32.2) \ (0.166)} \left(\frac{53.36}{1.0} \right)^2 \frac{(0.700)^2}{\left(\dfrac{\pi}{4} \right)^2 (0.166)^4}$$

$$b_i = 5,285$$

Equation 5-7 becomes

$$P_{in} = \left[\frac{(4,732)^2 + (5,285) \ (503.27)^2 \left(e^{\frac{2 \ (0.019) \ (1,200)}{503.27}} - 1 \right)}{e^{\frac{2 \ (0.019) \ (1,200)}{503.27}}} \right]^{0.5}$$

$$P_{in} = 11,620 \ \text{lb/ft}^2 \ \text{abs}$$

$$p_{in} = \frac{P_{in}}{144}$$

$$p_{in} = 80.7 \ \text{psia}$$

The above pressure is the approximate injection pressure to the top of the inside of the drill string. Again, these calculations have been carried out neglecting the

drill collar outside and inside diameters. Also, the calculations have ignored the existence of a blooey line type structure (most shallow drilling operations do not have blooey lines). These minor losses are not important for shallow drilling operations. The above injection pressure is less than the capability of this reciprocating piston compressor (i.e., 350 psig), therefore, the compressor is capable of producing above injection pressure (the maximum pressure capability of a reciprocating piston compressor is not derated with surface location elevation as long as the prime mover has the power necessary to produce the required pressure).

   The last criteria to check is whether the prime mover of this primary compressor unit has the power to operate at the 6,000 ft surface elevation. The prime mover for this compressor is a diesel fueled, turbocharged, Caterpillar Model D353 with a peak output of 270 horsepower at 1,000 rpm (at API standard conditions).

   The theoretical shaft horsepower, $\dot{W}_s$, required by the compressor is obtained from Equation 4-35a. Equation 4-35a becomes

$$\dot{W}_s = \frac{(2)\,(1.4)}{(0.4)}\,\frac{(11.769)\,(700)}{229.17}\left[\left(\frac{80.7}{11.769}\right)^{\frac{(0.4)}{(2)(1.4)}} - 1\right]$$

$$\dot{W}_s = 79.6$$

The mechanical efficiency, ε_m, is

$$\varepsilon_m = 0.90$$

From Equation 4-37, the first stage compression ratio of this compressor is

$$r_s = \left(\frac{80.7}{11.769}\right)^{0.5}$$

$$r_s = 2.62$$

The volumetric efficiency (only for the reciprocating piston compressor), ε_v, is determined from Equation 4-38. The compressor clearance volume ratio, c, is assumed to be 0.06. Equation 4-38 becomes

$$\varepsilon_v = 0.96\left\{1 - (0.06)\left[(2.62)^{\frac{1}{1.4}} - 1\right]\right\}$$

$$\varepsilon_v = 0.903$$

From Equation 4-39, the actual shaft horsepower, $\dot{W}_{as}$, required by the compressor is

$$\dot{W}_{as} = \frac{79.6}{(0.9)\ (0.903)}$$

$$\dot{W}_{as} = 98.0$$

The above determined 98.0 horsepower is the actual shaft power needed by the compressor to produce the 80.7 psia pressure output at the surface location elevation of 6,000 ft above sea level. At this surface location, the input horsepower available from the prime mover is a derated value (derated from the rated 270 horsepower available at 1,000 rpm). In order for the compressor system to operate at this 6,000 ft surface location elevation, the derated input power available must be greater than the actual shaft power needed. Figure 4-15 shows that for 6,000 ft elevation the input power of a turbocharged prime mover must be derated by approximately 14.8 percent. The derated input horsepower, $\dot{W}_i$, available from the prime mover is

$$W_i = 270\ (1 - 0.148)$$

$$\dot{W}_i = 230.0$$

For this example, the prime mover's derated input power is greater than the actual shaft horsepower needed, thus, the compressor system unit can be operated at this 6,000 ft surface location elevation.

Illustrative Example 5.3b Select the appropriate primary compressor system for the direct circulation drilling operation data given in Illustrative Example 5.3a. This selection will give the actual volumetric flow rate of air to be delivered to the drilling operation. The selection of the appropriate compressor will be made from the example compressor systems listed in Section 4.7 of Chapter 4. In Illustrative Example 5.3a it was found that the drilling location adjusted minimum volumetric flow rate of air for the 6 1/4 inch diameter, 2,400 ft deep borehole was approximately 930 acfm (for a surface drilling location of 4,000 ft above sea level). Also determine the injection pressure, the input power required by the compressor, and the derated output power available from the prime mover while drilling at 2,400 ft.

This depth of borehole will have to be drilled with a drilling rig like that shown in Figure 1-4. A stand alone compressor unit or units must be used to provide the compressed air. The skid mounted primary Gardner Denver Model WEN, two-stage, reciprocating piston compressor is powered by a Caterpillar Model D353, diesel fueled, turbocharged, prime mover capable of a 270 peak horsepower at the operating speed of 1,000 rpm (see Figure 4-22). This compressor is capable of producing a volumetric flow rate of 700 scfm and a maximum pressure of 350 psig at API standard conditions. When this compressor unit is to be placed at the 4,000 ft surface elevation drilling location, the compressor will still produce the same volumetric flow rate as at sea level conditions. Thus, the actual volumetric flow rate of this compressor at the 4,000 ft surface elevation is 700 acfm (see Chapter 4). This volumetric flow rate is not greater than the required adjusted minimum volumetric flow rate of 930 acfm, thus, two of these compressors must be used.

This will give a volumetric flow rate to the drilling operation of 1,400 acfm (factor of safety of 1.51).

A comparison must also be made between the injection pressure required to drill this borehole and the pressure capability of this compressor. The injection pressure is obtained by a sequence of calculation steps that determine the bottomhole pressure in the annulus, the pressure at the bottom of the inside of the drill string, and then the injection pressure (upstream through the circulation system). In these calculations, the actual volumetric flow rate through each of the two compressors is 700 acfm. Also, in these calculations, the actual atmospheric conditions at the drilling location will be used (i.e., 12.685 psia and 40°F) (see Table 4.2 or Appendix D). The atmospheric pressure of the air, P_{at}, entering the compressor is

$$p_{at} = 12.685 \text{ psia}$$

$$P_{at} = p_{at} \, 144$$

$$P_{at} = 1,827 \text{ lb/ft}^2 \text{ abs}$$

The atmospheric temperature of the air, T_{at}, entering the compressor is

$$t_{at} = 40°\text{F}$$

$$T_{at} = t_{at} + 459.67$$

$$T_{at} = 499.67°\text{R}$$

Thus, P_g and T_g become

$$P_g = P_{at} = 1,827 \text{ lb/ft}^2 \text{ abs}$$

$$T_g = T_{at} = 499.67°\text{R}$$

Using Equation 4-11, the specific weight of the atmospheric air entering the compressor is

$$\gamma_g = \frac{(1,827)\,(1.0)}{(53.36)\,(499.67)}$$

$$\gamma_g = 0.0690 \text{ lb/ft}^3$$

The volumetric flow rate of air entering the top of the drill string (and entering the two compressors), Q_g, is

$$Q_g = \frac{1,400}{60}$$

$$Q_g = 23.3 \text{ ft}^3/\text{sec}$$

The weight rate of flow of air through the well is

$$\dot{w}_g = 0.0690 \ (23.3)$$

$$\dot{w}_g = 1.599 \text{ lb/sec}$$

The borehole diameter, D_h, is

$$d_h = 6.25 \text{ inches}$$

$$D_h = \frac{d_h}{12}$$

$$D_h = 0.521 \text{ ft}$$

Using Equation 5-4, the weight rate of flow of the solid rock cuttings in the annulus is

$$\dot{w}_s = \left(\frac{\pi}{4}\right)(0.521)^2 \ (62.4) \ (2.7) \left[\frac{90}{(60)\ (60)}\right]$$

$$\dot{w}_s = 0.897 \text{ lb/sec}$$

The drill pipe outside diameter, D_p, is

$$d_p = 2.875 \text{ inches}$$

$$D_p = \frac{d_p}{12}$$

$$D_p = 0.240 \text{ ft}$$

The sedimentary rock borehole wall absolute surface roughness is assumed to be 0.005 ft (see Table 8-1). Using Equation 5-6, the average surface roughness for the annulus becomes

$$e_{av} = \frac{(0.005)\left(\dfrac{\pi}{4}\right)(0.521)^2 + (0.00015)\left(\dfrac{\pi}{4}\right)(0.240)^2}{\left(\dfrac{\pi}{4}\right)(0.521)^2 + \left(\dfrac{\pi}{4}\right)(0.240)^2}$$

$$e_{av} = 0.0042 \text{ ft}$$

Equation 5-5 becomes

$$f = \left[\frac{1}{2\ \log\left(\dfrac{0.521 - 0.240}{0.0042}\right) + 1.14}\right]^2$$

$$f = 0.043$$

Equations 5-2 and 5-3 become, respectively,

$$a_a = \left(\frac{1.0}{53.36}\right)\left[1 + \left(\frac{0.897}{1.599}\right)\right]$$

$$a_a = 0.029$$

and

$$b_a = \frac{0.043}{2\ (32.2)\ (0.521 - 0.240)}\left(\frac{53.36}{1.0}\right)^2 \frac{(1.599)^2}{\left(\dfrac{\pi}{4}\right)^2\left[(0.521)^2 - (0.240)^2\right]^2}$$

$$b_a = 617.6$$

The bottomhole temperature is determined from the surface geothermal temperature rock formations at the surface, the geothermal gradient, and the depth of the borehole. The geothermal temperature of the rock formations near the surface is assumed to be represented by the temperatures given in Table 4-1 (also see Appendix D). Thus, for a 4,000 ft surface location this temperature is assumed to be 44.7°F. For this example the geothermal gradient is approximated to be 0.01°F/ft. Thus, T_{bh}, is

$$t_r = 44.7^\circ \text{F}$$

$$T_r \;=\; t_r \;+\; 459.67$$

$$T_r \;=\; 504.37^\circ\,\text{R}$$

$$T_{bh} \;=\; T_r \;+\; 0.01\,(2,400)$$

$$T_{bh} \;=\; 528.37^\circ\,\text{R}$$

The average temperature of this borehole is

$$T_{av} \;=\; \frac{T_r \;+\; T_{bh}}{2}$$

$$T_{av} \;=\; 516.37^\circ\,\text{R}$$

Using the above values, Equation 5-1 becomes

$$P_{bh} \;=\; \left\{ \left[(1,827)^2 + 617.6\,(516.37)^2\right] e^{\frac{2\,(0.029)\,(2,400)}{516.37}} \;-\; 617.6\,(516.37)^2 \right\}^{0.5}$$

$$P_{bh} \;=\; 7,474 \ \text{lb/ft}^2 \ \text{abs}$$

$$p_{bh} \;=\; \frac{P_{bh}}{144}$$

$$p_{bh} \;=\; 51.9 \ \text{psia}$$

This is the pressure at the bottom of the borehole in the annulus.
   With the large center opening in the drill bit, the pressure change in the air flow from the bottom of the inside of the drill string (inside the drill bit) to the bottom of the annulus is assumed to be negligible. The inside of the bottom of the drill string at the drill bit is assumed to have the same pressure as that at the bottom of the annulus. Thus,

$$p_{bhi} \;=\; 51.9 \ \text{psia}$$

$$P_{bhi} \;=\; p_{bhi}\,144$$

$$P_{bhi} \;=\; 7,474 \ \text{lb/ft}^2 \ \text{abs}$$

The inside of the drill string is approximated by the inside diameter of the drill pipe. The inside diameter of the API 2 7/8 inch, 6.85 lb/ft nominal, EU, NC 31, Grade E drill pipe is 2.441 inches (see Table B-4).

$$d_i = 2.441 \text{ inches}$$

$$D_i = \frac{d_i}{12}$$

$$D_i = 0.203 \text{ ft}$$

Equation 5-10 becomes

$$f = \left[\frac{1}{2 \ \log \left(\dfrac{0.203}{0.00015} \right) + 1.14} \right]^2$$

$$f = 0.018$$

Equations 5-8 and 5-9 become, respectively,

$$a_i = \frac{1.0}{53.36}$$

$$a_i = 0.019$$

and

$$b_i = \frac{0.018}{2 \ (32.2) \ (0.203)} \left(\frac{53.36}{1.0} \right)^2 \frac{(1.599)^2}{\left(\dfrac{\pi}{4} \right)^2 (0.203)^4}$$

$$b_i = 9,592$$

Equation 5-7 becomes

$$P_{in} = \left[\frac{(7{,}474)^2 + (9{,}592)\,(516.37)^2 \left(e^{\frac{2\,(0.019)\,(2{,}400)}{516.37}} - 1 \right)}{e^{\frac{2\,(0.019)\,(2{,}400)}{516.37}}} \right]^{0.5}$$

$$P_{in} = 21{,}350 \text{ lb/ft}^2 \text{ abs}$$

$$p_{in} = \frac{P_{in}}{144}$$

$$p_{in} = 148.3 \text{ psia}$$

The above pressure is the approximate injection pressure into the top of the inside of the drill string. Again, these calculations have been carried out neglecting the drill collar outside and inside diameters. Also, the calculations have ignored the existence of a blooey line type structure. These minor losses are not important for shallow drilling operations. Therefore, the above pressure slightly underestimates the actual pressure that is seen at the pressure gauge just downstream of the compressor. The above injection pressure is less than the capability of this reciprocating piston compressor (i.e., 350 psig), therefore, the compressor is capable of producing above injection pressure (the maximum pressure capability of a reciprocating piston compressor is not derated with surface location elevation as long as the prime mover has the power necessary to produce the required pressure).

The last criteria to check is whether the prime mover of this primary compressor unit has the power to operate at the 4,000 ft surface elevation. The prime mover for this compressor is a diesel fueled, turbocharged, Caterpillar Model D353 with a peak output of 270 horsepower at 1,000 rpm (at API standard conditions). The theoretical shaft horsepower, $\dot{W}_s$, required by each of the two compressors is obtained from Equation 4-35. Equation 4-35 becomes

$$\dot{W}_s = \frac{(2)\,(1.4)}{(0.4)} \; \frac{(12.685)\left(\frac{1{,}400}{2}\right)}{229.17} \left[\left(\frac{148.3}{12.685} \right)^{\frac{(0.4)}{(2)(1.4)}} - 1 \right]$$

$$\dot{W}_s = 114.1$$

The mechanical efficiency, ε_v, is

$$\varepsilon_m = 0.90$$

From Equation 4-37, the first stage compression ratio of the compressor is

$$r_s = \left(\frac{148.3}{12.685}\right)^{0.5}$$

$$r_s = 3.42$$

The volumetric efficiency (only for the reciprocating piston compressor), ε_v, is determined from Equation 4-38.   The compressor clearance volume ratio, c, is assumed to be 0.06. Equation 4-38 becomes

$$\varepsilon_v = 0.96 \left\{1 - (0.06)\left[(3.42)^{\frac{1}{1.4}} - 1\right]\right\}$$

$$\varepsilon_v = 0.879$$

From Equation 4-39, the actual shaft horsepower, $\dot{W}_{as}$, required by each compressor is

$$\dot{W}_{as} = \frac{114.1}{(0.9)\,(0.879)}$$

$$\dot{W}_{as} = 144.3$$

The above determined 144.3 horsepower is the actual shaft power needed by each of the two compressor to produce the 148.3 psia pressure output at the surface location elevation of 4,000 ft above sea level. At this surface location, the input horsepower available from each of the prime mover of the compressor units is a derated value (derated from the rated 270 horsepower available at 1,000 rpm).   In order for the compressor units to operate at this 4,000 ft surface location elevation, the derated input power available must be greater than the actual shaft power needed. Figure 4-15 shows that for 4,000 ft surface elevation the input power of each of the turbocharged prime movers must be derated by approximately 10 percent.   The derated input horsepower, $\dot{W}_i$, available from each prime mover of each of the compressor units is

$$W_i = 270\,(1 - 0.10)$$

$$\dot{W}_i = 243.0$$

For this example, the prime mover of each of the two compressor units derated input power is greater than the actual shaft horsepower needed. This shows that the compressor units have sufficient power to operate at a surface elevation of 4,000 ft above sea level.

5.2.3 *Prime Mover Fuel Consumption*

In this section the fuel consumption of the prime mover for the compressor system will be discussed. Illustrative examples of the fuel consumption was discussed in detail in Chapter 4. In this section the illustrative examples will be completed with the calculation of the approximate fuel needed on the drilling location for the operation of the compressor system.

Illustrative Examples 5.2c and 5.3c describe the implementation of the basic planning step No. 10 given in Section 5.1 (planning step No. 11 is discussed in Chapter 8 and will not be addressed here).

Illustrative Example 5.2c Determine the approximate total volume of diesel fuel needed at the drilling location to operate the compressor system when using direct circulation to drill the borehole described in Illustrative Examples 5.2a and 5.2b.

a) Sullair Model 840 Rotary Screw Compressor

This primary rotary screw compressor system is integrated into the design of the portable Tamrock Driltech Model D25K drilling rig (see Figure 4-19). For this drilling rig design the prime mover is used to operate both the compressor system and the hydraulic rotary top drive. The prime mover for this compressor is a Caterpillar Model 3406, diesel fueled, turbocharged, motor. To estimate total diesel fuel needed at the drilling location to drill the 1,200 ft deep 4 3/4 inch borehole, it will be necessary to also estimate the power requirements for the operation of the hydraulic rotary top drive system. The anticipated drilling rate of penetration is estimated to be 30 ft/hr. Since the vertical depth to be drilled is 1,200 ft, then the estimated actual drilling time to reach this depth is approximately 40 hours.

In Illustrative Example 5.2b the derated fixed pressure output from the Sullair Model 840 rotary screw compressor with a volumetric flow rate of 840 acfm was found to be 284.1 psia. This will be the pressure output of this rotary compressor regardless of the drilling depth (and, therefore, regardless of the drilling time). Also in Illustrative Example 5.2b for the depth of 1,200 ft the injection pressure (into the top of the inside of the drill string) was found to be 96.2 psia. Using this same injection calculation procedure, the injection pressures for drilling at depths less than 1,200 ft can be obtained.

Figure 5-10 shows the derated fixed pressure output of the compressor and the injection pressure to the drill string as a function of drilling time (or drilling depth). Compressor output pressures that are different from the actual injection pressures is a unique characteristic of rotary compressor systems. The fixed internal design of the rotary compressor dictates a fixed pressure output from the compressor regardless of the back pressure resistance (assuming the back pressure is less than the fixed pressure output). In this case the compressor pressure output is much greater than the injection pressure. Therefore, as air exits the compressor it decompresses when it passes into the surge tank which is usually mounted at the exit of the compressor. This decompression is due to the fact that the back pressure in the flow line to the drill string is less than the fixed pressure output of the rotary screw compressor. This decompression in the surge tank (or surface flow line) must occur in order to allow the pressure in the compressed air flow that exits the compressor to match the injection pressure resistance at the drill string.

In Illustrative Example 5.2b it was found that the actual shaft horsepower required by the compressor to compress air to 284.1 psia was 193.2. The derated horsepower available from the prime mover was 340.4. The prime mover for this rotary compressor is also used to operate the hydraulic pump that operates the top drive system. Thus, to obtain the fuel consumption for this prime mover (using fuel consumption calculations outlined in Chapter 4) the power usage to operate the top drive system must be estimated and added to the compressor horsepower usage. For this example, it is estimated that the torque applied to the top of the drill string is approximately 2,000 ft-lb at a rotary speed of 60 rpm. The horsepower required at the top drive system (at top of drill string), $\dot{W}_{td}$, is [3]
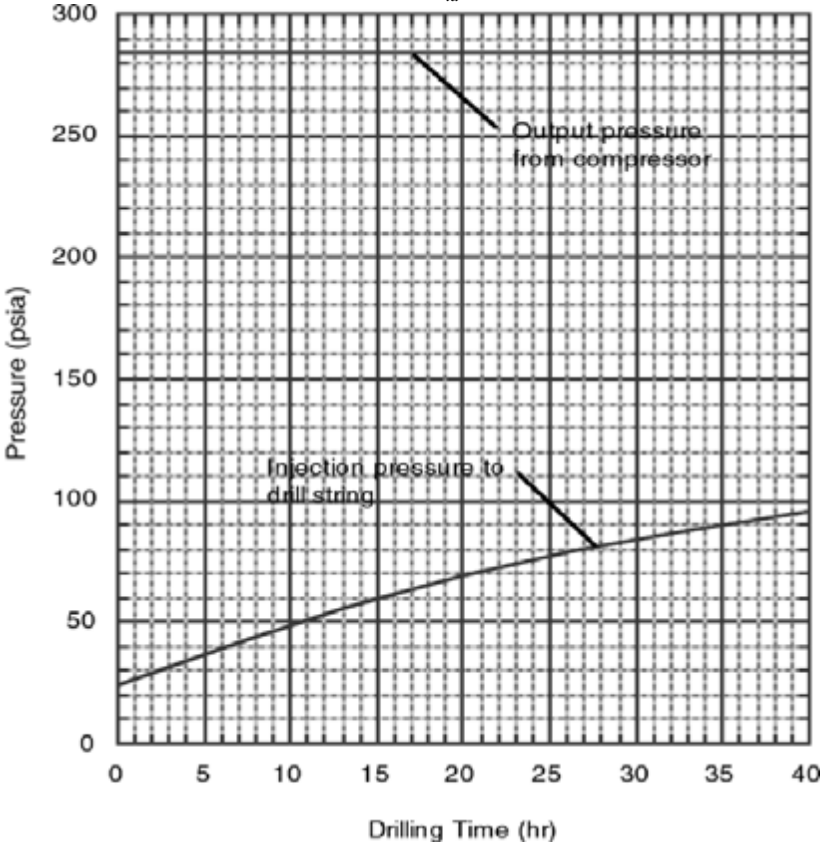
Figure 5-10: Compressor output pressure and drill string injection pressure for Illustrative Example 5.2c.

$$\dot{W}_{td} = \frac{T N}{5,252} \qquad (5\text{-}11)$$

where T is the applied torque to the top of the drill string (ft-lb),
N is the rotary speed (rpm).

For this example, Equation 5-11 becomes

$$\dot{W}_{td} = \frac{(2,000) \ (60)}{5,252}$$

$$\dot{W}_{td} = 22.9$$

Assuming an overall mechanical efficiency for the hydraulic top drive system is, ε_m = 0.8, the actual shaft horsepower needed for the hydraulic pump which operates the top drive system is estimated to be

$$\dot{W}_{td} = \frac{22.9}{0.80}$$

$$\dot{W}_{td} = 28.6$$

Thus, the total actual shaft horsepower required by both the compressor and the hydraulic pump operating the top drive, $\dot{W}_t$, is

$$\dot{W}_t = \dot{W}_{as} + \dot{W}_{td}$$

$$\dot{W}_t = 193.2 + 28.6$$

$$\dot{W}_t = 221.8$$

The prime mover power ratio is

$$PR = \frac{221.8}{340.8} \ (100) = 65.1$$

Figure 4-17 can be used to obtain the approximate diesel fuel consumption rate for the prime mover at this power level. At this power level the approximate diesel fuel consumption rate is 0.558 lb/hp-hr. The total weight rate of flow of diesel fuel to the prime mover is

$$\dot{w}_f = 0.558 \ (221.8) = 123.8 \ \text{lb/hr}$$

The diesel fuel consumption rate (in United States gallons) for drilling at a depth of 1,200 ft is

$$q_f = \frac{123.8}{(0.8156)(8.33)} = 18.2 \text{ gal/hr}$$

Using similar calculations as those given above, the diesel fuel consumption rate for other drilling times (or depths) can be obtained.

Figure 5-11 shows the diesel fuel consumption rate as a function of drilling time (or drilling depth) for this prime mover. The diesel fuel consumption rate for this example is constant through the drilling time of 40 hours. This assumes that the top drive power requirement is also constant over interval drilled.
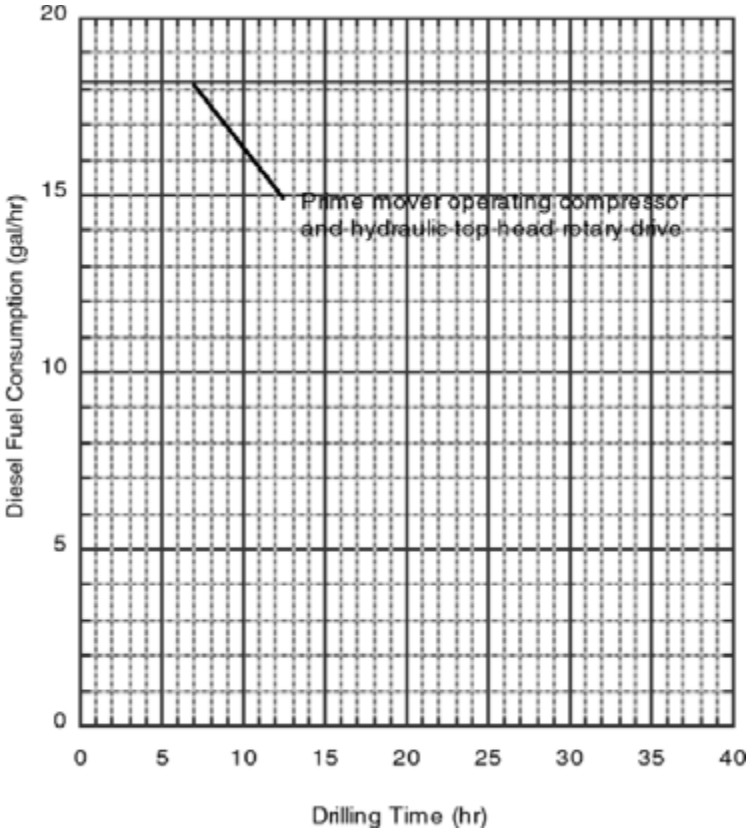
Figure 5-11: Fuel consumption rate as a function of drilling time for rotary compressor of Illustrative Example 5.2c.

The approximate total diesel fuel needed to drill the borehole is given by the integration of the area under the curve in Figure 5-11. This is approximately 728 gallons. It is standard practice to assume a 20 percent additional volume of fuel for blowing the hole between connections and other operations on the drill rig. Therefore, the approximate total diesel fuel needed at the drilling location is 873 gallons. For this example, this diesel fuel amount is for the drilling rig prime mover that operates both the integrated rotary screw compressor and the hydraulic pump that operates the rotary top drive system.

b) Gardner Denver Model WEN Reciprocating Piston Primary Unit

In Illustrative Example 5.2b an alternate combination for drilling this shallow well is the trailer mounted rotary drilling rig (see Figure 1-4) with the stand alone Gardner Denver Model WEN reciprocating piston primary compressor unit (see Figure 4-22). This compressor unit has a volumetric flow rate of 700 acfm. To estimate the total diesel fuel needed by this compressor unit it is necessary to estimate the fuel consumption of the compressor unit's Caterpillar Model D353, diesel fueled, turbocharged, prime mover. The anticipated drilling rate of penetration is estimated to be 30 ft/hr. Since the vertical depth to be drilled is 1,200 ft, then the estimated actual drilling time to reach this depth is approximately 40 hours.

In Illustrative Example 5.2b the injection pressure into the top of the drill string when drilling at 1,200 ft of depth was found to be 80.7 psia. Using similar calculations the injection pressures for lesser depths can be found. Figure 5-12 shows these injection pressures as a function of drilling time (or drilling depth).

The reciprocating piston compressor is not a fixed pressure ratio machine like the rotary screw compressor. As long as there is sufficient power available from the prime mover the reciprocation piston compressor will match the back pressure resistance. Thus, Figure 5-12 shows only one curve indicating the injection pressure is the same as the pressure output of the compressor.

In Illustrative Example 5.2b it was found that the actual shaft horsepower required by this reciprocating piston compressor to compress air to 80.7 psia was 98.0 (at 1,200 ft of depth). Also in Illustrative Example 5.2b the derated horsepower available from the Caterpillar Model D353 was found to be 230.0. At a depth of 1,200 ft, the prime mover power ratio is

$$PR = \frac{98.0}{230.0} \ (100) = 42.6$$

From Figure 4-17 the approximate diesel fuel consumption rate at this power level is approximately 0.690 lb/hp-hr. The total weight rate of diesel fuel consumption per hour is

$$\dot{w}_f = 0.690 \ (98.0) = 67.5 \ \text{lb/hr}$$

The diesel fuel consumption rate (in United States gallons) for the drilling depth of 1,200 ft is

$$q_f = \frac{67.5}{(0.8156)(8.33)} = 9.9 \text{ gal/hr}$$
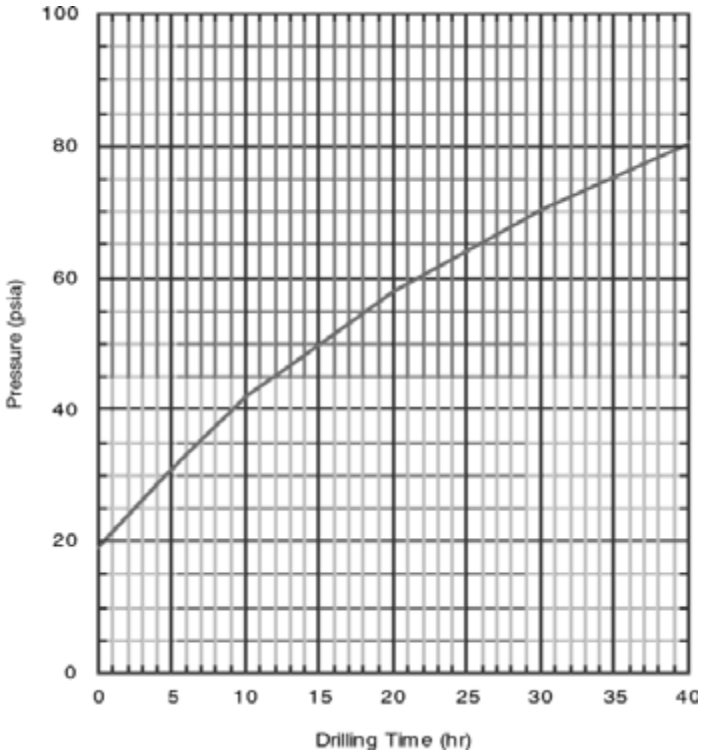
Figure 5-12: Drill string injection pressure (same as compressor output pressure) for Illustrative Example 5.2c.

Using the data in Figure 5-12 and similar calculations as those given above, the diesel fuel consumption rate as a function of drilling time (or drilling depth) can be obtained.   Figure 5-13 shows the diesel fuel consumption rate as a function of drilling time for this reciprocating piston compressor.   The approximate total diesel fuel needed by the compressor to drill the borehole is obtained by the integration of the area under the curve in Figure 5-13.   This is approximately 275 gallons.   It is standard practice to assume a 20 percent additional volume of fuel for blowing the hole between connections and other operations on the drill rig.   Therefore, the approximate total diesel fuel needed for this compressor at the drilling location is 330 gallons.
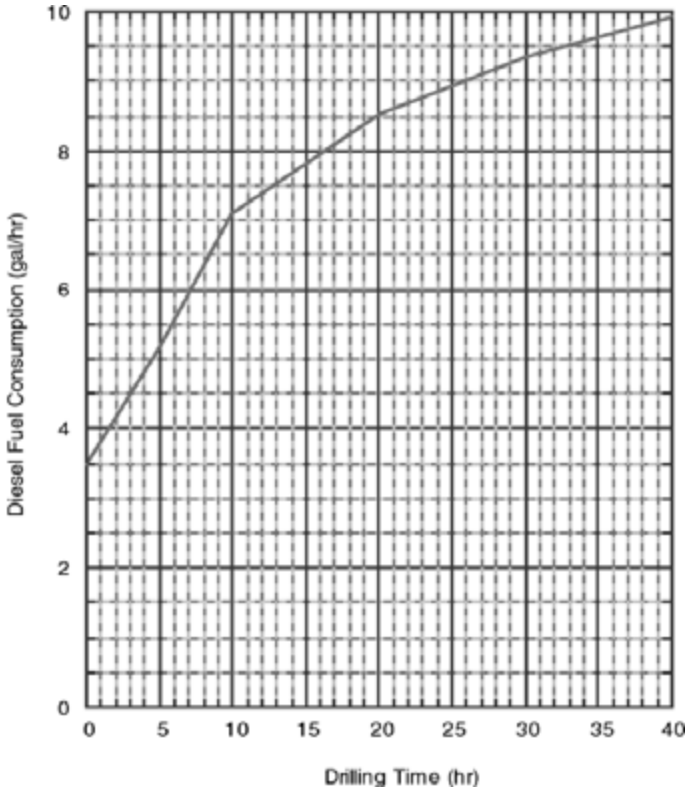
Figure 5-13: Diesel fuel consumption rate as a function of drilling time for reciprocating piston compressor of Illustrative Example 5.2c.

Comparing the diesel fuel consumption results from the rotary screw compressor candidate and from the reciprocating piston compressor candidate it is seen that the stand alone reciprocating piston compressor unit requires less than half the total diesel fuel required by the rotary screw compressor (i.e., 330 gallons as opposed to 873 gallons).   It should be noted that the prime mover for the rotary screw compressor is also being used to provide power for the hydraulic pump for the rotary top drive system. However, the power for this top drive is only about 13 percent of the total power needed from the prime mover. The main reason for this high diesel fuel consumption by the rotary screw compressor is the fact that its pressure output is constant through the drilling time (and depth).

These example calculations illustrate one of the principal advantage of the reciprocating piston compressor over the screw compressor.   Unfortunately most single drilling rigs are usually equipped with on-board rotary compressors. This is due to the fact that rotary compressors are less bulky and have a small surface area

footprint. In general, for a given volumetric flow rate, reciprocating piston compressors are more bulky and have a larger surface area footprint than their rotary compressor counterpart.

Illustrative Example 5.3c Determine the approximate total volume of diesel fuel needed at the drilling location to operate the compressor system when using direct circulation to drill the borehole described in Illustrative Examples 5.3a and 5.3b.

In Illustrative Example 5.3b it was planned that the semi-trailer mounted drilling rig in Figure 1-4 was to be used to drill the 6 1/4 inch diameter, 2,400 ft deep borehole. It was also determined in Illustrative Example 5.3b that two skid mounted primary Gardner Denver Model WEN reciprocating piston compressor primary units (see Figure 4-22) would be needed to air drill the borehole. These two compressor units have a total volumetric flow rate of 1,400 acfm. To estimate the total diesel fuel needed by these stand alone compressor units it is necessary to estimate the fuel consumption of the compressor units' Caterpillar Model D353, diesel fueled, turbocharged, prime movers. The anticipated drilling rate is estimated to be 90 ft/hr. Since the vertical depth to be drilled is 2,400 ft, then the estimated actual drilling time to reach this depth is approximately 26.7 hours.

In Illustrative Example 5.3b the injection pressure into the top of the drill string when drilling at 2,400 ft of depth was found to be 148.3 psia. Using similar calculations the injection pressures for lesser depths can be found. Figure 5-14 shows these injection pressures as a function of drilling time (or drilling depth).

The reciprocating piston compressor is not a fixed pressure ratio machine like the rotary compressor. As long as there is sufficient power available from the prime mover the reciprocation piston compressor will match the back pressure resistance. Thus, Figure 5-14 shows only one curve indicating the injection pressure is the same as the pressure output of the two compressors.

In Illustrative Example 5.3b it was found that the actual shaft horsepower required by each of the two reciprocating piston compressors to compress air to 148.3 psia was 144.3 (at 2,400 ft of depth). Also in Illustrative Example 5.3b the derated horsepower available from the Caterpillar Model D353 was found to be 243.0. At a depth of 2,400 ft, the prime mover power ratio is

$$PR = \frac{144.3}{243.0} (100) = 59.4$$

From Figure 4-17 the diesel fuel consumption rate at this power level is approximately 0.573 lb/hp-hr. The total weight rate of diesel fuel consumption per hour is

$$\dot{w}_f = 0.573 (144.3) = 82.7 \text{ lb/hr}$$

The diesel fuel consumption rate (in United States gallons) for the drilling depth of 2,400 ft is

$$q_f = \frac{82.7}{(0.8156)(8.33)} = 12.2 \text{ gal/hr}$$
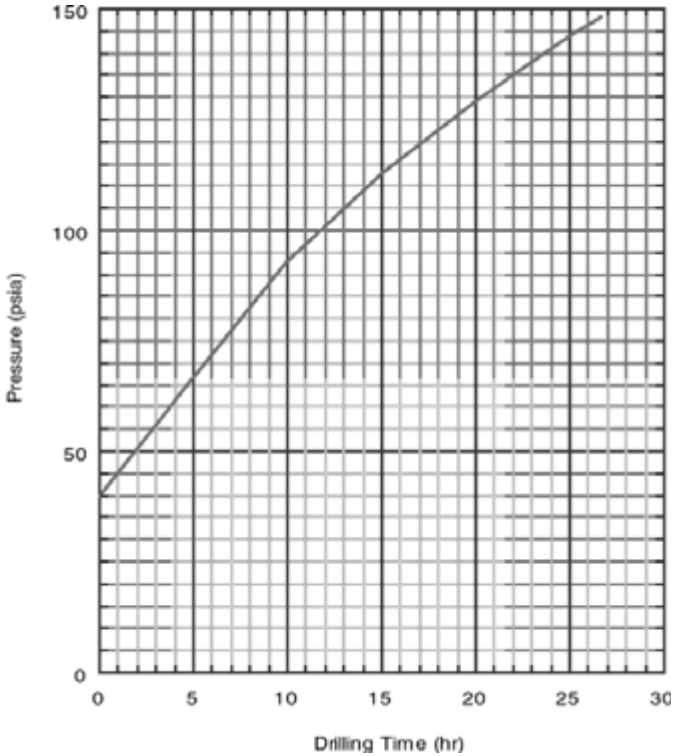
Figure 5-14: Drill string injection pressure (same as compressor output pressure) for Illustrative Example 5.3c.

Using the data in Figure 5-14 and similar calculations as those given above the diesel fuel consumption rate as a function of drilling time (or drilling depth) can be obtained.   Figure 5-15 shows the diesel fuel consumption rate as a function of drilling time (or drill depth) for each of these reciprocating piston compressors.   The approximate total diesel fuel needed (for one compressor unit) to drill the borehole is given by the integration of the area under the curve in Figure 5-15.   This is approximately 281 gallons. It is standard practice to assume a 20 percent additional volume of fuel for blowing the hole between connections and other operations on the drill rig.   Therefore, the approximate diesel fuel needed for a compressor unit is

approximately 337 gallons.   The total diesel fuel required for the two compressor units is, therefore, 674 gallons.

The above Illustrative Examples 5.2a, b and c, and 5.3a, b, and c demonstrate the step by step procedures for carrying out engineering calculations needed to assess the capabilities of air compressor systems used in direct circulation drilling operations.   The   calculations   also   yield   the   approximate   anticipated   fuel consumption for the compressor systems. These fuel consumption amounts will be important information when planning shallow drilling operations in remote areas. Remote area operations are a planning challange to the engineer or earth scientist. Drilling operations generally fail because of insuffcient planning and lack of operator field experience.
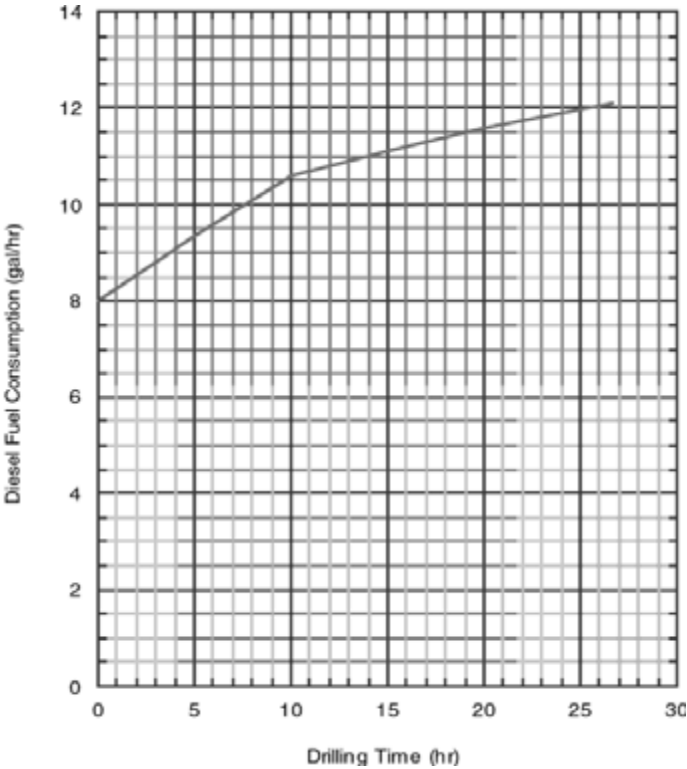
Figure 5-15: Diesel fuel consumption rate as a function of drilling time for reciprocating piston compressor of Illustrative Example 5.3c.

5.3 Reverse Circulation

Reverse circulation is extensively used in shallow air drilling operations. This circulation drilling technique is usually used to drill specialized geotechnical and environmental monitoring boreholes and wells.   Reverse circulation drilling, particularly with dual wall pipe, have important operational advantages for the drilling and development of environmental monitoring wells [4, 5, 6].   This circulation technique is very useful in drilling larger diameter shallow wells.   Tri-cone drill bits fabricated for shallow drilling operations have a single large water course passage through the drill bit body which allows these drill bits to be used for both direct and reverse circulation shallow operations (see Figure 1-9). As will be seen in Chapter 11, air hammers are also a very useful downhole tool for both direct and reverse circulation operations. These tools and their drill bits are designed for direct or reverse circulation drilling operations. In this chapter only tri-cone drill bit operations will be discussed.

5.3.1 *Minimum Volumetric Flow Rates*

In order to initiate the well planning procedure given in Section 5.1, the geometry of the reverse circulation operation must be defined and the anticipated drilling penetration rate estimated. Figures can be prepared to give the approximate minimum volumetric flow rates for a variety of shallow well and drill string geometry. The calculations to prepare the plots for these figures are carried out using API standard atmospheric conditions (i.e., 14.696 psia and 60°F, see Chapter 4). Thus, the figures developed will give the minimum volumetric flow rate values for air drilling using atmospheric air at API standard conditions. Once these figures are developed, the minimum volumetric flow rates can be calculated for any other atmospheric conditions (surface locations) from the minimum volumetric flow rates given for API standard conditions. The approximate minimum volumetric flow rate values are calculated assuming a minimum bottomhole (inside the drill string) kinetic energy per unit volume of no less than 3.0 ft-lb/ft^3 (see Chapter 8 for details). The basic equations used to determine the minimum volumetric flow rate are derived in Chapter 7.

The minimum volumetric flow rates are calculated assuming that the boreholes (surface to bottom) are openholes (not cased). The calculations for determining a minimum volumetric flow rate is a trial and error process. The equations needed to determine the minimum volumetric flow rate are outlined below.   The critical equation for determining the minimum volumetric flow rate is derived in Chapter 7. This is the equation for the pressure above the drill bit inside the drill string, P_{ai}. This equation is

$$P_{ai} \ = \ \left[\left(P_{at}^2 \ + \ b_i \ T_{av}^2 \right) e^{\frac{2 \ a_i \ H}{T_{av}}} \ - \ b_i \ T_{av}^2 \right]^{0.5} \tag{5-12}$$

where P_{at} is the atmospheric pressure at the exit from the annulus (lb/ft^2, abs),

H is the depth of the borehole (ft),

T_{av} is the average temperature of the borehole over the depth interval (°R).

The constants a_i and b_i are

$$a_i = \left(\frac{S_g}{R}\right)\left[1 + \frac{\dot{w}_s}{\dot{w}_g}\right] \qquad (5\text{-}13)$$

and

$$b_i = \frac{f}{2\ g\ D_i}\left(\frac{R}{S_g}\right)^2 \frac{\dot{w}_g^2}{\left(\frac{\pi}{4}\right)^2 D_i^4} \qquad (5\text{-}14)$$

where S_g is the specific gravity of the gas (i.e., $S_g = 1.0$ for air at standard
      conditions),
     R is the gas constant (53.36 ft-lb/lb-° R),
     $\dot{w}_s$ is the weight rate of flow of rock cuttings solids (lb/sec),
     $\dot{w}_g$ is the weight rate of flow of the gas (usually air) (lb/sec),
     f is the Fanning friction factor,
     g is the acceleration of gravity (32.2 ft/sec^2),
     D_i is the inside diameter of the drill pipe (in these calculations the inside
        diameter of the drill pipe or innertube of dual wall pipe) (ft).
It should be noted that the above equations are for any set of consistent units.

Unless field test data are available that give the actual rock specific gravity, the approximate average specific gravity for sedimentary rock is assumed to be 2.7, the average specific gravity for igneous rock is assumed to be 2.8, and the average specific gravity for metamorphic rock is assumed to be 3.0 [1].

Illustrative Examples 5.4, 5.5a, and 5.6a describe the implementation of the basic planning steps Nos. 1 through 6 given in Section 5.1.

Illustrative Example 5.4 Using the basic equations above, determine the reverse circulation minimum volumetric flow rate required to drill a well with a 12 1/4 inch openhole borehole (12 1/4 inch drill bit diameter) and a uniform drill string composed of API 5 1/2 inch, 24.70 lb/ft nominal, IEU, FH, Grade E drill pipe (see Table B-4). The inside diameter of the drill pipe body is 4.670 inches. The anticipated drilling rate in a competent unfractured limestone sequence (sedimentary rock) is assumed to be 78.4 ft/hr and the drilling depth is 1,000 ft.

In order to be able to calculate air drilling conditions at other surface elevations above sea level, all calculations for basic values like the minimum volumetric flow rate are carried out for a baseline reference atmosphere. For these calculations and most of those in this treatise the reference atmosphere is the API Mechanical Equipment Standards standard atmospheric conditions (see Chapter 4). These conditions are a pressure of 14.696 psia and a temperature of 60°F. Thus, the pressure of the gas (in this case air) that will flow into the compressor, P_{at}, is

$$p_{at} = 14.696 \text{ psia}$$

$$P_{at} = p_{at} \, 144$$

$$P_{at} = 2{,}116 \text{ lb/ft}^2 \text{ abs}$$

The atmospheric temperature of the gas (air) that will flow into any compressor, T_{at}, that will supply the drilling operation is

$$t_{at} = 60^\circ \text{F}$$

$$T_{at} = t_{at} + 459.67$$

$$T_{at} = 519.67^\circ \text{R}$$

Thus, P_g and T_g become

$$P_g = P_{at} = 2{,}116 \text{ lb/ft}^2 \text{ abs}$$

$$T_g = T_{at} = 519.67^\circ \text{R}$$

Using Equation 4-11, the specific weight of the gas entering the compressor is

$$\gamma_g = \frac{(2{,}116)\,(1.0)}{(53.36)\,(519.67)}$$

$$\gamma_g = 0.0763 \text{ lb/ft}^3$$

To determine the minimum volumetric flow rate of air at API standard conditions, it is necessary to select (by trial and error) a volumetric flow rate, q_g (scfm), that will give a kinetic energy per unit volume of 3.0 ft-lb/ft^3 in the annulus at the bottom of 1,000 ft depth of the borehole. Kinetic energy per unit volume should be a minimum at the bottom of the annulus. The volumetric flow rate selected (trial and error) is (at API standard conditions)

$$q_g = 472.2 \text{ scfm}$$

The value of Q_g is

$$Q_g = \frac{q_g}{60}$$

$$Q_g = 7.87 \text{ ft}^3/\text{sec}$$

The weight rate of flow of the gas, $\dot{w}_g$, is

$$\dot{w}_g = \gamma_g \, Q_g$$

$$\dot{w}_g = 0.0763 \, (7.87)$$

$$\dot{w}_g = 0.601 \, \text{lb/sec}$$

The borehole diameter D_h is

$$d_h = 12.25 \, \text{inches}$$

$$D_h = \frac{d_h}{12}$$

$$D_h = 1.021 \, \text{ft}$$

The estimated drilling rate of penetration is 78.4 ft/hr. From Equation 5-4, the weight rate of flow of the solid rock cuttings, $\dot{w}_s$, in the annulus is

$$\dot{w}_s = \left(\frac{\pi}{4}\right) (1.021)^2 \, (62.4) \, (2.7) \left[\frac{78.4}{(60) \, (60)}\right]$$

$$\dot{w}_s = 3.00 \, \text{lb/sec}$$

The temperature of the rock formations near the surface (geothermal surface temperature) is estimated to be the approximate average year round temperature at that location on the earth's surface. Table 4-1 gives 59°F for the sea level average year round temperature for the mid latitudes of the North America (also see Appendix D). Therefore, the absolute temperature of the rock formations at the surface, T_r, is

$$t_r = 59°\text{F}$$

$$T_r = t_r + 459.67$$

$$T_r = 518.67°\text{R}$$

The bottomhole temperature is determined from the surface geothermal temperature, the geothermal gradient, and the depth of the borehole. For this example and the figures that follow, the geothermal gradient is approximated to be 0.01° F/ft. Thus, T_{bh} is

$$T_{bh} = T_r + 0.01 (1,000)$$

$$T_{bh} = 528.67 \ R$$

The average temperature of this borehole is

$$T_{av} = \frac{T_r + T_{bh}}{2}$$

$$T_{av} = 523.67 \ R$$

The drill pipe inside diameter, D_i, is

$$d_i = 4.670 \ \text{inches}$$

$$D_i = \frac{d_i}{12}$$

$$D_i = 0.389 \ \text{ft}$$

The Fanning friction factor, f, of the inside of the drill pipe is determined from the von Karman empirical relationship for turbulent flow conditions [1]. This empirical relationship is

$$f = \left[\frac{1}{2 \ \log \left(\dfrac{D_i}{e_p} \right) + 1.14} \right]^2 \tag{5-15}$$

where e_P is the absolute surface roughness for commercial pipe (ft).
   Although this is assumed to be an openhole in the annulus, the cuttings in a reverse circulation operations return to the surface through the inside of the drill string (in this case through the inside of the drill pipe). The absolute surface roughness of commercial pipe, e_p, is given as 0.00015 ft [2]. Equation 5-15 becomes

$$f = \left[\frac{1}{2 \ \log \left(\dfrac{0.389}{0.00015} \right) + 1.14} \right]^2$$

$$f = 0.016$$

With the above values Equation 5-13 becomes

$$a_i = \left(\frac{1.0}{53.36}\right)\left[1 + \left(\frac{3.00}{0.601}\right)\right]$$

$$a_i = 0.112$$

and Equation 5-14 becomes

$$b_i = \frac{0.016}{2\,(32.2)\,(0.389)}\left(\frac{53.36}{1.0}\right)^2 \frac{(0.601)^2}{\left(\frac{\pi}{4}\right)^2 (0.389)^4}$$

$$b_i = 45.6$$

Equation 5-12 becomes

$$P_{ai} = \left\{\left[(2,116)^2 + 45.6\,(523.67)^2\right] e^{\frac{2\,(0.016)\,(1,000)}{523.67}} - 45.6\,(523.67)^2\right\}^{0.5}$$

$$P_{ai} = 3,686 \text{ lb/ft}^2 \text{ abs}$$

$$p_{ai} = \frac{P_{ai}}{144}$$

$$p_{ai} = 25.6 \text{ psia}$$

This is the pressure at the bottom of the inside of the drill string just above the drill bit.

Using Equation 4-11, the specific weight of the air above the drill bit inside the drill pipe can be obtained knowing the pressure and temperature at the bottom of the inside of the drill pipe. The specific weight is

$$\gamma_{ai} = \frac{(3,686)\,(1.0)}{(53.36)\,(528.67)}$$

$$\gamma_{ai} = 0.132 \text{ lb/ft}^3$$

The volumetric flow rate of the gas above the drill bit inside the drill pipe, Q_{ai}, is

$$Q_{ai} = \frac{0.601}{0.132}$$

$$Q_{ai} = 4.552 \text{ ft}^3/\text{sec}$$

The velocity of the gas above the drill bit inside the drill pipe, V_{ai}, is

$$V_{ai} = \frac{4.552}{\left(\frac{\pi}{4}\right)(0.389)^2}$$

$$V_{ai} = 38.3 \text{ ft/sec}$$

The kinetic energy per unit volume of the gas above the drill bit inside the drill pipe, KE_{ai}, is (see Chapter 1 and Equations 1-1 and 1-2)

$$\rho_{ai} = \frac{0.132}{32.2}$$

$$\rho_{ai} = 0.00410 \ \frac{\text{lb} - \text{sec}^2}{\text{ft}^4}$$

$$KE_{ai} = \frac{1}{2}(0.00410)(38.3)^2$$

$$KE_{ai} = 3.007 \ \frac{\text{ft} - \text{lb}}{\text{ft}^3}$$

The trial and error process for the above illustrative example requires an iterative selection of the value of q_g until the kinetic energy above the drill bit inside the drill pipe is equal to 3.0 ft-lb/ft^3. In this illustrative example the value of q_g that will give a kinetic energy value equal to 3.0 ft-lb/ft^3 is 472.2 scfm.

This illustrative example shows the great advantage of reverse circulation techniques over direct circulation techniques in the drilling of shallow large diameter boreholes. The minimum volumetric flow rate of air required to drill this example borehole with the direct circulation technique is 2,232 scfm. This is a factor of five greater volumetric flow rate.

Using the calculation procedure as given above, plots can be prepared for a variety of drilling depths and drilling rates (for API standard conditions). Figures 5-16, 5-17 and 5-18 can be used to obtain the approximate minimum volumetric flow rate for a variety of reverse circulation well geometric configurations and drilling rates (i.e., solids weight rates of flow). Figure 5-16 is limited solids weight rates of flow of 1.0 lb/sec or less. Figure 5-17 is limited solids weight rates of flow between 1.0 lb/sec and 2.0 lb/sec. Figure 5-18 is limited solids weight rates of flow of 2.0 lb/sec to 3.0 lb/sec. All these figures give the air minimum volumetric flow

rates for the depths 500 ft, 1,000 ft, 1,500 ft, 2,000 ft, 2,500 ft, and 3,000 ft.   In Illustrative Example 5.4, the drill bit is assumed to have a rate of penetration (or drilling rate) in the sedimentary rock of 78.4 ft/hr, which gives a solids weight rate of flow in the inside of the drill pipe of 3.00 lb/sec. The example above demonstrates how the curves in Figures 5-16, 5-17, and 5-18 were developed.   The solids weight rate of flow for the example is approximately 3.0 lb/sec.   Entering Figure 5-18 with the above example drill pipe inside diameter of 4.670 inches and moving vertically upward in the figure to the 1,000 ft depth curve, the same approximate minimum volumetric flow rate of 472.2 scfm can be obtained.

All of these curves are created for API standard conditions and sedimentary rock. Figure 5-16 was created using a solids weight rate of flow of 1.0 lb/sec. Figure 5-17 was created using a solids weight rate of flow of 2.0 lb/sec. And Figure 5-18 was created using a solids weight rate of flow of 3.0 lb/sec. It can be seen by comparing these figures that the air minimum volumetric flow rates do not vary significantly from figure to figure. The weight of the solids being carried to the surface do not dominate the resistance to the air flow as in the direct circulation model. Return air flows at high average velocity inside the drill pipe (relative to return flow in the annulus in the direct circulation model). Therefore, reverse circulation return flow resistance is dominated by pipe wall friction.   This reverse circulation flow characteristic allows for the simplification of minimum volumetric flow rate engineering design plots. Thus, the plots in Figures 5-16, 5-17, and 5-18 can be used to determine the approximate minimum volumetric flow rates for a wide variety of well geometry configurations and drilling rates.

For minimum volumetric flow rates for solids weight rates of flow that are greater than 3.0 lb/sec, use the calculation procedure in the above illustrative example.

Illustrative Example 5.5a Determine the approximate reverse circulation minimum volumetric flow rate of air required to drill a 12 1/4 inch openhole borehole (12 1/4 inch drill bit diameter) with a drill string composed of 210 ft of 10 inch by 4 inch drill collars (see Table B-1) above the drill bit and API 5 1/2 inch, 24.70 lb/ft nominal, IEU, FH, Grade E drill pipe above the drill collars to surface (inside diameter of drill pipe body 4.670 inches, see Table B-4). The anticipated drilling rate is assumed to be 30 ft/hr and the maximum depth of the well is 2,400 ft.   The formation to be drilled is a competent unfractured limestone sequence (sedimentary rock). The drilling location (where the drill rig will sit on the surface) is at 2,000 ft above sea level (in the mid latitudes of North America) and the day time air temperature is approximately 80° F.

This well geometry is typical for large diameter deep water wells. Such wells are drilled in the Great Plains of North America and particularly in the many fringe areas around the great deserts of the world. This borehole configuration is also used in mining and geotechnical drilling operations. Using reverse circulation with a conventional drill string (drill collars and drill pipe) is restricted to geologic provinces that are composed of competent rock formations and are not prone to caving.   Such drilling operations, particularly those in remote areas, are more efficiently run with air drilling technology.
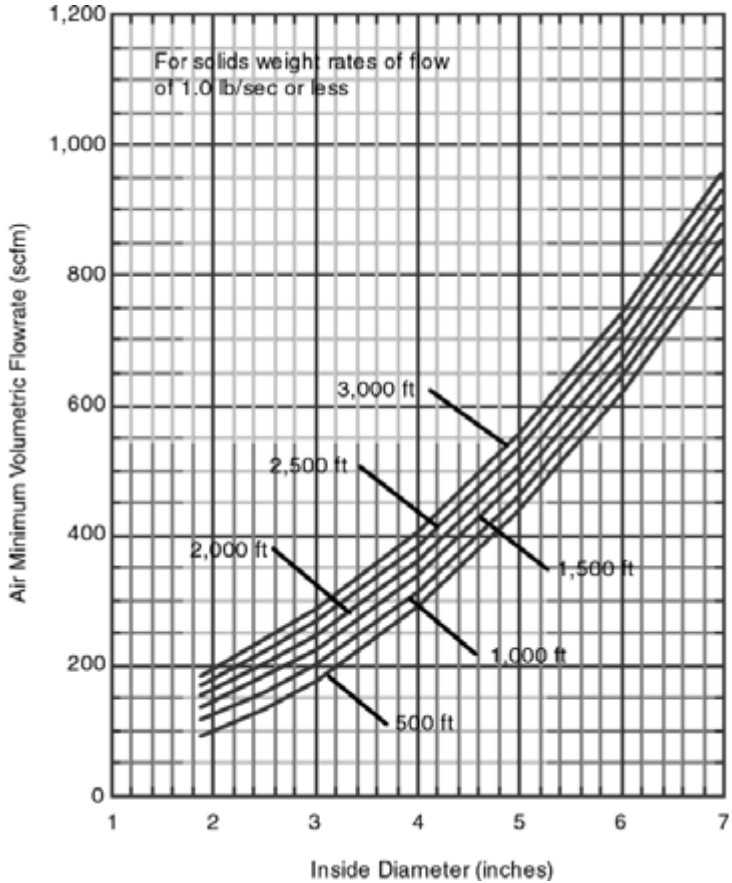
Figure 5-16: Minimum volumetric flow rate of air at API standard conditions for reverse circulation operations. Limited to solids weight rates of flow of 1.0 lb/sec or less.
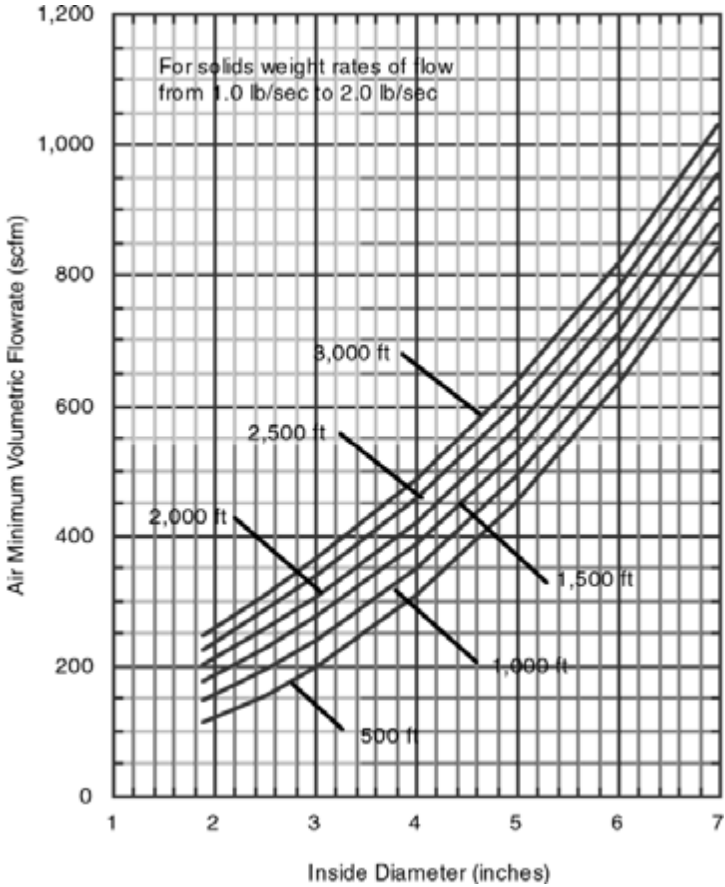
Figure 5-17: Minimum volumetric flow rate of air at API standard conditions for reverse circulation operations. Limited to solids weight rates of flow from 1.0 lb/sec to 2.0 lb/sec.
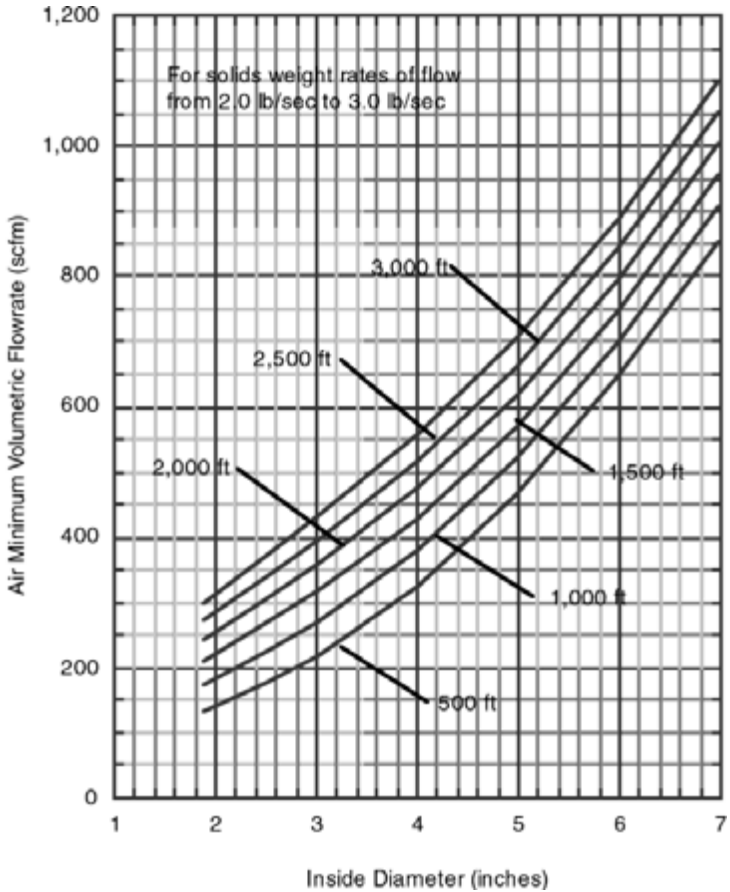
Figure 5-18: Minimum volumetric flow rate of air at API standard conditions for reverse circulation operations. Limited to solids weight rates of flow from 2.0 lb/sec to 3.0 lb/sec.

In remote areas (particularly in the arid regions), water for conventional mud drilling operations is often difficult to find and transport to the drilling location. Air drilling operations utilize atmospheric air. Therefore, the volume of compressor fuel used in drilling operations becomes an important logistical issue.

It is only necessary to obtain the approximate minimum volumetric flow rate for a drilling operation. The borehole is never drilled with only the minimum volumetric flow rate.

The borehole diameter, D_h, is

$$d_h \ = \ 12.25 \text{ inches}$$

$$D_h \ = \ \frac{d_h}{12}$$

$$D_h \ = \ 1.021 \text{ ft}$$

Using Equation 5-4 the approximate solids weight rate of flow for this drilling operation can be obtained. This is

$$\dot{w}_s \ = \ \left(\frac{\pi}{4}\right) (1.021)^2 \ (62.4) \ (2.7) \left[\frac{30}{(60)\ (60)}\right]$$

$$\dot{w}_s \ = \ 1.15 \text{ lb/sec}$$

The above value is greater than the 1.0 lb/sec limit of Figure 5-16, but is between the 1.0 lb/sec to 2.0 lb/sec limit of Figure 5-17. Therefore, using Figure 5-17 the approximate minimum volumetric flow rate can be obtained. The approximate minimum volumetric flow rate is estimated at the maximum depth of the borehole. Entering Figure 5-17 with the drill pipe inside diameter of 4.670 inches, and moving vertically to the approximate depth of 2,400 ft, the approximate minimum volumetric flow rate is found to be 550 scfm.

The specific weight of air at API standard conditions is 0.0763 lb/ft^3 (see Chapter 4 or Appendix D). To obtain the adjusted minimum volumetric flow rate for this example, the specific weight of the air at the actual atmospheric conditions at the drilling location of 2,000 ft above sea level must be obtained. The actual atmospheric pressure for the air at the drilling location (that will be utilized by the compressor), P_{at}, is (see Table 4-1 or Appendix D)

$$p_{at} \ = \ 13.662 \text{ psia}$$

$$P_{at} \ = \ p_{at} \ 144$$

$$P_{at} \ = \ 1,967 \text{ lb/ft}^2 \text{ abs}$$

The actual atmospheric temperature of the air at the drilling location, T_{at} (that will be used by the compressor), is

$$t_{at} = 80°F$$

$$T_{at} = t_{at} + 459.67$$

$$T_{at} = 539.67°R$$

Thus, P_g and T_g become

$$P_g = P_{at} = 1,967 \ \text{lb/ft}^2 \ \text{abs}$$

$$T_g = T_{at} = 539.67°R$$

Using Equation 4-11, the specific weight of the gas entering the compressor is

$$\gamma_g = \frac{(1,967) \ (1.0)}{(53.36) \ (539.67)}$$

$$\gamma_g = 0.0683 \ \text{lb/ft}^3$$

Note the above specific weight value can also be obtained from Figure D-4 in Appendix D.

The approximate minimum volumetric flow rate for this example adjusted for the actual atmospheric conditions at the drilling location can be determined by equating the weight rate of flow of the air at the two atmospheric conditions. This reduces to

$$q_g = 550 \left(\frac{0.0763}{0.0683} \right)$$

$$q_g = 614 \ \text{acfm}$$

The above volumetric flow rate is the adjusted minimum value for the atmospheric conditions at this drilling location (2,000 ft above sea level).

Illustrative Example 5.6a Determine the approximate reverse circulation minimum volumetric flow rate of air for a well with a 5 7/8 inch openhole borehole (5 7/8 inch drill bit diameter) and a drill string composed of 4.50 inch concealed inner-tube dual wall pipe (see Table 3-6). The anticipated drilling rate is assumed to be 40 ft/hr and the maximum depth of the well is 1,200 ft. The formation to be

drilled is a competent unfractured basalt (igneous rock). The drilling location (where the drill rig will sit on the surface) is at 6,000 ft above sea level (in the mid latitudes of North America) and the day time air temperature is approximately 40°F. This is a typical environmental monitoring or geotechnical borehole geometry.

It is only necessary to obtain the approximate minimum volumetric flow rate for a drilling operation.   The borehole is never drilled with only the minimum volumetric flow rate.

The borehole diameter, D_h, is

$$d_h = 5.875 \text{ inches}$$

$$D_h = \frac{d_h}{12}$$

$$D_h = 0.490 \text{ ft}$$

Since Figure 5-16 is independent of rock type, then Equation 5-4 can be used to determine the solids weight rate of flow for igneous rock formation drilling. This is

$$\dot{w}_s = \left(\frac{\pi}{4}\right)(0.490)^2 (62.4)(2.8)\left[\frac{40}{(60)(60)}\right]$$

$$\dot{w}_s = 0.366 \text{ lb/sec}$$

In this example the solids weight rate of flow calculated above is less than 1.0 lb/sec, therefore, Figure 5-16 can be used to determine the approximate minimum volumetric flow rate of air.   The innertube of the dual wall pipe has an inside diameter of 2.375 inches (see Table 3-6).   Entering Figure 5-16 at a diameter of 2.375 inches and moving vertically to the depth of approximately 1,200 ft, the approximate minimum volumetric flow rate is found to be 155 scfm.

The specific weight of air at API standard conditions is 0.0763 lb/ft^3. To obtain the adjusted minimum volumetric flow rate for this example, the specific weight of the air at the actual atmospheric conditions at the drilling location must be obtained. The actual atmospheric pressure for the air at the drilling location (that will be utilized by the compressor), P_{at}, is (see Table 4-1 or Appendix D)

$$p_{at} = 11.769 \text{ psia}$$

$$P_{at} = p_{at}\ 144$$

$$P_{at} = 1,695 \text{ lb/ft}^2 \text{ abs}$$

The actual atmospheric temperature of the air at the drilling location, T_{at} (that will be used by the compressor), is

$$t_{at} = 40°\text{F}$$

$$T_{at} = t_{at} + 459.67$$

$$T_{at} = 499.67°\,\text{R}$$

Thus, P_g and T_g become

$$P_g = P_{at} = 1,695 \text{ lb/ft}^2 \text{ abs}$$

$$T_g = T_{at} = 499.67°\,\text{R}$$

Using Equation 4-11, the specific weight of the gas entering the compressor is

$$\gamma_g = \frac{(1,695)\,(1.0)}{(53.36)\,(499.67)}$$

$$\gamma_g = 0.0636 \text{ lb/ft}^3$$

Note the above specific weight value can also be obtained from Figure D-4 in Appendix D.

The approximate minimum volumetric flow rate for this example adjusted for the actual atmospheric conditions at the drilling location can be determined by equating the weight rate of flow of the air at the two atmospheric conditions. This reduces to

$$q_g = 155 \left(\frac{0.0763}{0.0636} \right)$$

$$q_g = 186 \text{ acfm}$$

The above volumetric flow rate is the adjusted minimum value for the atmospheric conditions at this drilling location (6,000 ft above sea level).

5.3.2 *Injection Pressure and the Selection of Compressor Equipment*

The selection process requires that the borehole requirements be compared to the capabilities of the compressor units available. Specifically, these comparisons are made between; a) the required borehole volumetric flow rate and the compressor volumetric flow rate capability, b) the borehole injection pressure (using the compressor volumetric flow rate) and the pressure capability of the compressor and, c) the horsepower required by the compressor and the input capability of the prime mover. For shallow drilling operations the selection of the appropriate compressor

equipment often dictates the drilling rig selection. This will be demonstrated in the examples that follow.

Illustrative Examples 5.5b, and 5.6b describe the implementation of the basic planning steps Nos. 7 through 9 given in Section 5.1.

Illustrative Example 5.5b Select the appropriate compressor system for the reverse circulation drilling operation data given in Illustrative Example 5.5a. The selection of the appropriate compressor will be made from the example compressor systems listed in Section 4.7 of Chapter 4. In Illustrative Example 5.5a it was found that the drilling location adjusted minimum volumetric flow rate for the 12 1/4 inch diameter, 2,400 ft deep borehole was 614 acfm (for the surface drilling location of 2,000 ft above sea level). Also determine the injection pressure, the input power required by the compressor, and the derated output power available from the primer mover while drilling at 2,400 ft.

The borehole depth and the weight of the drill string in this example requires that a double drilling rig like that shown in Figure 1-4 be used to drill the well. Since this drill rig does not have an on-board compressor, a stand alone compressor unit must be used to provide the compressed air. The semi-trailer mounted Dresser Clark Model CFB-4, four-stage, reciprocating piston primary compressor is selected. This compressor unit is powered by a Caterpillar Model D398, diesel fueled, turbocharged, prime mover capable of a 760 peak horsepower at the operating speed of 900 rpm (see Figure 4-24). This compressor is capable of producing a volumetric flow rate of 1,200 scfm and a maximum pressure of 1,000 psig at API standard conditions. When this compressor unit is placed at the 2,000 ft surface elevation drilling location, it will still produce the same volumetric flow rate as at sea level conditions. Thus, the actual volumetric flow rate of this compressor at the 2,000 ft surface elevation is 1,200 acfm (see Chapter 4). This volumetric flow rate is greater than the required adjusted minimum volumetric flow rate of 614 acfm, thus, the injection flow rate into the annulus of this well will be 1,200 acfm (factor of safety of 1.95).

The reason the small single Tamrock Driltech Model D25K drilling rig with the on-board Sullair Model 840 compressor (rated at 840 scfm) cannot be used in this operation is because this drilling rig has marginal hoisting capability to lift the drill string in this example.

A comparison must also be made between the injection pressure required to drill this borehole and the pressure capability of the selected compressor system. The injection pressure is obtained by a sequence of calculation steps that determine the bottomhole pressure inside the drill string above the drill bit, the bottomhole pressure at the bottom of the annulus, and then the injection pressure (upstream through the circulation system). In these calculations, the actual volumetric flow rate from the compressor is used, the 1,200 acfm. Also, in these calculations, the actual atmospheric conditions at the drilling location will be used (i.e., 13.662 psia and 80°F) (see Table 4.2 or Appendix D). The atmospheric pressure of the air, P_{at}, entering the compressor is

$$p_{at} = 13.662 \text{ psia}$$

$$P_{at} = p_{at} \, 144$$

$$P_{at} = 1,967 \text{ lb/ft}^2 \text{ abs}$$

The atmospheric temperature of the air, T_{at}, entering the compressor is

$$t_{at} = 80^\circ \text{F}$$

$$T_{at} = t_{at} + 459.67$$

$$T_{at} = 539.67^\circ \text{R}$$

Thus, P_g and T_g become

$$P_g = P_{at} = 1,967 \text{ lb/ft}^2 \text{ abs}$$

$$T_g = T_{at} = 539.67^\circ \text{R}$$

Using Equation 4-11, the specific weight of the atmospheric air entering the compressor is

$$\gamma_g = \frac{(1,967)\,(1.0)}{(53.36)\,(539.67)}$$

$$\gamma_g = 0.0683 \text{ lb/ft}^3$$

The volumetric flow rate of air entering the compressor, Q_g, is

$$Q_g = \frac{1,200}{60}$$

$$Q_g = 20.0 \text{ ft}^3/\text{sec}$$

The weight rate of flow of air through the well is

$$\dot{w}_g = 0.0683\,(20.0)$$

$$\dot{w}_g = 1.366 \text{ lb/sec}$$

The borehole diameter, D_h, is

$$d_h = 12.25 \text{ inches}$$

$$D_h = \frac{d_h}{12}$$

$$D_h = 1.021 \text{ ft}$$

Using Equation 5-4, the weight rate of flow of the solid rock cuttings in the annulus is

$$\dot{w}_s = \left(\frac{\pi}{4}\right)(1.021)^2\ (62.4)\ (2.7)\left[\frac{30}{(60)\ (60)}\right]$$

$$\dot{w}_s = 1.149 \text{ lb/sec}$$

The inside diameter of the drill pipe, D_i, is

$$d_i = 4.670 \text{ inches}$$

$$D_i = \frac{d_i}{12}$$

$$D_i = 0.389 \text{ ft}$$

The return flow of the air with the entrained rock cuttings flows to the surface through the inside of the drill string. The surface roughness of commercial pipe is e_p = 0.00015 ft [2]. Equation 5-15 becomes

$$f = \left[\frac{1}{2\ \log\left(\dfrac{0.389}{0.00015}\right)+1.14}\right]^2$$

$$f = 0.016$$

Equations 5-13 and 5-14 become, respectively,

$$a_i = \left(\frac{1.0}{53.36}\right)\left[1 + \left(\frac{1.149}{1.366}\right)\right]$$

$$a_i = 0.035$$

and

$$b_i = \frac{0.016}{2\ (32.2)\ (0.389)} \left(\frac{53.36}{1.0}\right)^2 \frac{(1.366)^2}{\left(\dfrac{\pi}{4}\right)^2 (0.389)^4}$$

$$b_i = 236.1$$

The bottomhole temperature is determined from the surface geothermal temperature rock formations at the surface, the geothermal gradient, and the depth of the borehole. The geothermal temperature of the rock formations near the surface is assumed to be represented by the temperatures given in Table 4-1 (also see Appendix D). Thus, for a 2,000 ft surface location this temperature is assumed to be 51.9°F. For this example the geothermal gradient is approximated to be 0.01°F/ft. Thus, T_{bh} is

$$t_r = 51.9^{\circ}\,F$$

$$T_r = t_r + 459.67$$

$$T_r = 511.57^{\circ}\,R$$

$$T_{bh} = T_r + 0.01\ (2,400)$$

$$T_{bh} = 535.54^{\circ}\,R$$

The average temperature of this borehole is

$$T_{av} = \frac{T_r + T_{bh}}{2}$$

$$T_{av} = 523.54^{\circ}\,R$$

Equation 5-12 becomes

$$P_{ai} = \left\{ \left[(1,967)^2 + 236.1\ (523.54)^2 \right] e^{\frac{2\ (0.035)\ (2,400)}{523.54}} - 236.1\ (523.54)^2 \right\}^{0.5}$$

$$P_{ai} = 5,421\ \text{lb/ft}^2\ \text{abs}$$

$$p_{ai} = \frac{P_{ai}}{144}$$

$$p_{ai} = 37.7 \text{ psia}$$

This is the pressure at the bottom of the inside of the drill string just above the drill bit.

With the large center opening in the drill bit, the pressure change in the air flow from the bottom of the annulus to the bottom of the inside of the drill string (inside the drill bit) is assumed to be negligible. The inside of the bottom of the drill string at the drill bit is assumed to have the same pressure as that at the bottom of the annulus. Thus,

$$p_{bh} = 37.7 \text{ psia}$$

$$P_{bh} = p_{bh} \, 144$$

$$P_{bh} = 5,421 \text{ lb/ft}^2 \text{ abs}$$

The annulus of this borehole is approximated by the diameter of the borehole (drill bit diameter) and the outside diameter of the drill pipe. The 210 ft of drill collars is ignored. The drill pipe is API 5 1/2 inch, 24.70 lb/ft nominal, IEU, FH, Grade E drill pipe (see Table B-4). The outside diameter of the drill pipe, D_p, is

$$d_p = 5.50 \text{ inches}$$

$$D_p = \frac{d_p}{12}$$

$$D_p = 0.458 \text{ ft}$$

The injection pressure, P_{in}, into the top of the annulus space is determined from

$$P_{in} = \left[\frac{P_{bh}^2 + b_a \, T_{av}^2 \left(e^{\frac{2 \, a_a \, H}{T_{av}}} - 1 \right)}{e^{\frac{2 \, a_a H}{T_{av}}}} \right]^{0.5} \tag{5-16}$$

where

$$a_a = \frac{S_g}{R} \tag{5-17}$$

$$b_a = \frac{f}{2\ g\ (D_h - D_p)} \left(\frac{R}{S_g}\right)^2 \frac{\dot{w}_g^2}{\left(\frac{\pi}{4}\right)^2 (D_h^2 - D_p^2)^2} \qquad (5\text{-}18)$$

$$f = \left[\frac{1}{2\ \log\left(\dfrac{D_h - D_p}{e_{av}}\right) + 1.14}\right]^2 \qquad (5\text{-}19)$$

The outer wall absolute surface roughness for the limestone sequence is assumed to be 0.005 ft (see Table 8-1) [2]. The inner surface of the borehole annulus is the outer surface of the drill pipe. The absolute surface roughness of commercial pipe, e_p, is given as 0.00015 ft [2]. The average absolute surface roughness of the annulus is approximated by the calculating the surface area average of these surface roughness. Thus, the value for e_{av} is

$$e_{av} = \frac{e_{oh}\left(\frac{\pi}{4}\right) D_h^2\ H + e_p\left(\frac{\pi}{4}\right) D_p^2\ H}{\left(\frac{\pi}{4}\right) D_h^2\ H + \left(\frac{\pi}{4}\right) D_p^2\ H}$$

The above reduces to

$$e_{av} = \frac{e_{oh}\left(\frac{\pi}{4}\right) D_h^2 + e_p\left(\frac{\pi}{4}\right) D_p^2}{\left(\frac{\pi}{4}\right) D_h^2 + \left(\frac{\pi}{4}\right) D_p^2} \qquad (5\text{-}20)$$

Thus, e_{av}, is

$$e_{av} = \frac{(0.005)\left(\frac{\pi}{4}\right) (1.021)^2 + (0.00015)\left(\frac{\pi}{4}\right) (0.458)^2}{\left(\frac{\pi}{4}\right) (1.021)^2 + \left(\frac{\pi}{4}\right) (0.458)^2}$$

$$e_{av} = 0.0042\ \text{ft}$$

Equation 5-19 becomes

$$f = \left[\frac{1}{2 \ \log \left(\dfrac{1.021 \ - \ 0.458}{0.0042} \right) \ + \ 1.14} \right]^2$$

$$f \ = \ 0.034$$

Equations 5-17 and 5-18 become, respectively,

$$a_i \ = \ \frac{1.0}{53.36}$$

$$a_i \ = \ 0.019$$

and

$$b_a \ = \ \frac{0.034}{2 \ (32.2) \ (1.021 \ - \ 0.458)} \left(\frac{53.36}{1.0} \right)^2 \ \frac{(1.366)^2}{\left(\dfrac{\pi}{4} \right)^2 \left[(1.021)^2 \ - \ (0.458)^2 \right]^2}$$

$$b_a \ = \ 11.8$$

Equation 5-16 becomes

$$P_{in} \ = \ \left[\frac{(5,421)^2 \ + \ (11.8) \ (523.54)^2 \left(e^{\frac{2 \ (0.019) \ (2,400)}{523.54}} \ - \ 1 \right)}{e^{\frac{2 \ (0.019) \ (2,400)}{523.54}}} \right]^{0.5}$$

$$P_{in} \ = \ 5,026 \ \text{lb/ft}^2 \ \text{abs}$$

$$p_{in} \ = \ \frac{P_{in}}{144}$$

$$p_{in} \ = \ 34.9 \ \text{psia}$$

The above pressure is the approximate injection pressure into the top of the borehole annulus. In these calculations the drill collar outside diameter is neglected. Also, the calculations have ignored the friction losses in the surface flow line

leading to the top of the borehole annulus and the vent line leading from the top of the drill string. These losses are not important for shallow drilling operations (Chapter 8 calculation examples will consider these losses which become important for deep boreholes). Therefore, the above pressure slightly underestimates the actual pressure that is seen at the pressure gauge just downstream of the compressor. The above injection pressure is significantly less than the capability of this reciprocating piston compressor (i.e., 1,000 psig), therefore, the compressor is capable of producing the above injection pressure (the maximum pressure capability of a reciprocating piston compressor is not derated with surface location elevation as long as the prime mover has the power necessary to produce the required pressure).

The last criteria to check is whether the prime mover of this primary compressor unit has the power to operate at the 2,000 ft surface elevation. The prime mover for this compressor is a diesel fueled, turbocharged, Caterpillar Model D398 with a peak output of 760 horsepower at 900 rpm (at API standard conditions). The reciprocating piston compressor is not limited by its maximum pressure capability but more by the prime mover capability to produce the power required by the compressor shaft. The theoretical shaft horsepower, $\dot{W}_s$, required by the compressor is obtained from Equation 4-35a. Equation 4-35a becomes

$$\dot{W}_s = \frac{(4)\ (1.4)}{(0.4)}\ \frac{(13.662)\ (1,200)}{229.17}\left[\left(\frac{34.9}{13.662}\right)^{\frac{(0.4)}{(4)(1.4)}} - 1\right]$$

$$\dot{W}_s = 69.4$$

The mechanical efficiency, ε_m, is

$$\varepsilon_m = 0.90$$

The first stage compression ratio of the compressor is

$$r_s = \left(\frac{34.9}{13.662}\right)^{\frac{1}{4}}$$

$$r_s = 1.26$$

The volumetric efficiency (only for the reciprocating piston compressor), ε_v, is determined from Equation 4-38. The compressor clearance volume ratio, c, is assumed to be 0.06. Equation 4-38 becomes

$$\varepsilon_v = 0.96\left\{1 - (0.06)\left[(1.26)^{\frac{1}{1.4}} - 1\right]\right\}$$

$$\varepsilon_v = 0.949$$

From Equation 4-39, the actual shaft horsepower, $\dot{W}_{as}$, required by each compressor is

$$\dot{W}_{as} = \frac{69.4}{(0.9)\ (0.949)}$$

$$\dot{W}_{as} = 81.2$$

The above determined 81.2 horsepower is the actual shaft power needed by the compressor to produce the 34.9 psia pressure output at the surface location elevation of 2,000 ft above sea level. At this surface location, the input horsepower available from the prime mover is a derated value (derated from the rated 760 horsepower available at 900 rpm). In order for the compressor unit to operate at this 2,000 ft surface location elevation, the derated input power available must be greater than the actual shaft power needed. Figure 4-15 shows that for 2,000 ft elevation the input power of a turbocharged prime mover must be derated by approximately 5 percent. The derated input horsepower, $\dot{W}_i$, available from the prime mover is

$$W_i = 760\ (1 - 0.05)$$

$$\dot{W}_i = 722.0$$

For this example, the prime mover of the compressor unit derated input power is greater than the actual shaft horsepower needed, thus, the compressor unit can be operated at this 2,000 ft surface location elevation.

Illustrative Example 5.6b Select the appropriate compressor system for the reverse circulation drilling operation data given in Illustrative Example 5.6a. The selection of the appropriate compressor will be made from the example compressor systems listed in Section 4.7 of Chapter 4. In Illustrative Example 5.6a it was found that the drilling location adjusted minimum volumetric flow rate for the 5 7/8 inch diameter, 1,200 ft deep borehole was 280 acfm (for the surface drilling location of 6,000 ft above sea level). Also determine the injection pressure, the input power required by the compressor, and the derated output power available from the prime mover while drilling at 1,200 ft.

This shallow drilling operation does not require the use of a double drilling rig. Therefore, the most appropriate drill rig for this drilling operation appears to be the portable Tamrock Driltech Model D25K drilling rig (see Figure 4-19). This drill rig has an on-board primary compressor. The compressor is a Sullair Model 840, two-stage, oil flooded, rotary helical lobe (screw). This compressor is powered by a Caterpillar Model 3406, diesel fuel, turbocharged prime mover capable of a 400 peak horsepower at the operating speed of 1,800 rpm (see Figure 4-20). The compressor is capable of producing a volumetric flow rate of 840 scfm and a fixed pressure of 340

psig at API standard conditions. When the drilling rig is moved to the 6,000 ft surface location, the volumetric flow rate from the compressor is 840 acfm. The compressor volumetric flow rate is greater than the required adjusted minimum volumetric flow rate of 280 acfm (factor of safety of 3.00). Therefore, this compressor unit is capable of producing the volumetric flow rate to drill the borehole.

A comparison must also be made between the injection pressure required to drill this borehole and the pressure capability of this compressor system. The injection pressure is obtained by calculating through a sequence of calculation steps that determine the bottomhole pressure in the annulus, the pressure at the bottom of the inside of the drill string, and then the injection pressure (upstream through the circulation system). In these calculations, the actual volumetric flow rate of the compressor is used, the 840 acfm. Also, in these calculations, the actual atmospheric conditions at the drilling location will be used (i.e., 11.769 psia and 40°F). The atmospheric pressure of the air, P_{at}, entering the compressor is

$$p_{at} = 11.769 \text{ psia}$$

$$P_{at} = p_{at} \; 144$$

$$P_{at} = 1,695 \text{ lb/ft}^2 \text{ abs}$$

The atmospheric temperature of the air, T_{at}, entering the compressor is

$$t_{at} = 40°\text{F}$$

$$T_{at} = t_{at} + 459.67$$

$$T_{at} = 499.67°\text{R}$$

Thus, P_g and T_g become

$$P_g = P_{at} = 1,695 \text{ lb/ft}^2 \text{ abs}$$

$$T_g = T_{at} = 499.67°\text{R}$$

Using Equation 4-11, the specific weight of the gas entering the compressor is

$$\gamma_g = \frac{(1,695)\,(1.0)}{(53.36)\,(499.67)}$$

$$\gamma_g = 0.0636 \text{ lb/ft}^3$$

The volumetric flow rate of air entering the compressor, Q_g, is

$$Q_g = \frac{840}{60}$$

$$Q_g = 14.0 \text{ ft}^3/\text{sec}$$

The weight rate of flow of air through the well is

$$\dot{w}_g = 0.0636 \ (14.0)$$

$$\dot{w}_g = 0.890 \text{ lb/sec}$$

The borehole diameter, D_h, is

$$d_h = 5.875 \text{ inches}$$

$$D_h = \frac{d_h}{12}$$

$$D_h = 0.490 \text{ ft}$$

Using Equation 5-4, the weight rate of flow of the solid rock cuttings in the annulus is

$$\dot{w}_s = \left(\frac{\pi}{4}\right)(0.490)^2 \ (62.4) \ (2.8) \left[\frac{40}{(60) \ (60)}\right]$$

$$\dot{w}_s = 0.365 \text{ lb/sec}$$

The inside surface of the innertube of the dual wall pipe has a surface roughness of commercial pipe which is $e_p = 0.00015$ ft [1]. Equation 5-15 becomes

$$f = \left[\frac{1}{2 \ \log\left(\dfrac{0.198}{0.00015}\right) + 1.14}\right]^2$$

$$f = 0.018$$

Equations 5-13 and 5-14 become, respectively,

$$a_i = \left(\frac{1.0}{53.36}\right)\left[1 + \left(\frac{0.890}{0.365}\right)\right]$$

$$a_i = 0.026$$

and

$$b_i = \frac{0.018}{2\,(32.2)\,(0.198)}\left(\frac{53.36}{1.0}\right)^2 \frac{(0.890)^2}{\left(\dfrac{\pi}{4}\right)^2 (0.198)^4}$$

$$b_i = 3,431$$

The bottomhole temperature is determined from the surface geothermal temperature rock formations at the surface, the geothermal gradient, and the depth of the borehole. The geothermal temperature of the rock formations near the surface is assumed to be represented by the temperatures given in Table 4-1 (also see Appendix D). Thus, for a 6,000 ft surface location this temperature is assumed to be 37.6˚F. For this example the geothermal gradient is approximated to be 0.01˚F/ft. Thus, T_{bh}, is

$$t_r = 37.6^{\circ}\,\text{F}$$

$$T_r = t_r + 459.67$$

$$T_r = 497.27^{\circ}\,\text{R}$$

$$T_{bh} = T_r + 0.01\,(1,200)$$

$$T_{bh} = 509.27^{\circ}\,\text{R}$$

The average temperature of this borehole is

$$T_{av} = \frac{T_r + T_{bh}}{2}$$

$$T_{av} = 503.27^{\circ}\,\text{R}$$

Equation 5-12 becomes

$$P_{ai} = \left\{ \left[(1,695)^2 + 3,431 \ (503.27)^2 \right] e^{\frac{2 \ (0.026) \ (1,200)}{503.27}} - 3,431 \ (503.27)^2 \right\}^{0.5}$$

$$P_{ai} = 10,960 \ \text{lb/ft}^2 \ \text{abs}$$

$$p_{ai} = \frac{P_{ai}}{144}$$

$$p_{ai} = 76.1 \ \text{psia}$$

This is the pressure at the bottom of the inside of the innertube in the dual wall pipe just above the drill bit.

   With the large center opening in the drill bit, the pressure change in the air flow from the bottom of the annulus to the bottom of the inside of the drill string (inside the drill bit) is assumed to be negligible.   The inside of the bottom of the drill string at the drill bit is assumed to have the same pressure as that at the bottom of the annulus.   Thus,

$$p_{bh} = 76.1 \ \text{psia}$$

$$P_{bh} = p_{bh} \ 144$$

$$P_{bh} = 10,960 \ \text{lb/ft}^2 \ \text{abs}$$

   The outside diameter of the innertube of the dual wall pipe is 2.750 inches and the inside diameter of the outer tube of the dual wall pipe is 4.000 inches (see Table 3-6).   These pipe surfaces form the annulus of the dual wall pipe.   Thus,

$$d_{oi} = 2.750 \ \text{inches}$$

$$D_{oi} = \frac{d_{oi}}{12}$$

$$D_{oi} = 0.229 \ \text{ft}$$

and

$$d_{io} = 4.000 \ \text{inches}$$

$$D_{io} = \frac{d_{io}}{12}$$

$$D_{io} = 0.333 \text{ ft}$$

Equation 5-19 becomes

$$f = \left[\frac{1}{2 \, \log \left(\dfrac{0.333 - 0.229}{0.00015} \right) + 1.14} \right]^2$$

$$f = 0.021$$

Equations 5-17 and 5-18 become, respectively,

$$a_a = \frac{1.0}{53.36}$$

$$a_a = 0.019$$

and

$$b_a = \frac{0.021}{2 \, (32.2) \, (0.333 - 0.229)} \left(\frac{53.36}{1.0} \right)^2 \frac{(0.890)^2}{\left(\dfrac{\pi}{4} \right)^2 \left[(0.333)^2 - (0.229)^2 \right]^2}$$

$$b_a = 3,409$$

Equation 5-16 becomes

$$P_{in} = \left[\frac{(10,960)^2 + (3,409) \, (503.27)^2 \left(e^{\frac{2 \, (0.019) \, (1,200)}{503.27}} - 1 \right)}{e^{\frac{2 \, (0.019) \, (1,200)}{503.27}}} \right]^{0.5}$$

$$P_{in} = 13,550 \text{ lb/ft}^2 \text{ abs}$$

$$p_{in} = \frac{P_{in}}{144}$$

$$p_{in} = 94.1 \text{ psia}$$

   The above pressure is the approximate injection pressure into the top of the borehole annulus. The calculations have ignored the tool joint obstruction losses (inside the dual wall pipe annulus) and of a blooey line type structure (most shallow drilling operations do not have blooey lines). These losses are usually not important in shallow drilling operations (Chapter 8 calculation examples will consider these additional minor losses). Therefore, the above calculated pressure will only slightly underestimate the actual pressure that is seen at the pressure gauge just downstream of the compressor. In order for this compressor to be used for this drilling operation, the above injection pressure must be less than the derated fixed pressure of the rotary screw Sullair Model 840.

   The fixed pressure capability of the Sullair Model 840 compressor is an output of 340 psig (at API standard conditions). However, this output must be derated when the compressor is placed at a surface drilling location above sea level. To determine the derated fixed pressure capability of this compressor for the 6,000 ft surface drilling location, the design fixed ratio of the compressor must be determined. As demonstrated in Chapter 4, the fixed pressure ratio is referenced to sea level conditions (usually API standard conditions). Thus, the assumed design input pressure, p_1 (air flowing into the compressor from the atmosphere), is

$$p_1 = 14.696 \text{ psia}$$

The output pressure at API standard conditions, p_2, is

$$p_2 = 340 + 14.696 = 354.696 \text{ psia}$$

The total fixed compression ratio across the two stages of this compressor, r_c, is

$$r_c = \frac{p_2}{p_1}$$

$$r_c = \frac{354.696}{14.696}$$

$$r_c = 24.14$$

The approximated derated output pressure, p_{d2}, for this compressor when placed at a 6,000 ft surface drilling location is determined from

$$p_{d2} = r_c \, p_{at}$$

where p_{at} is the actual atmospheric pressure at the 6,000 ft surface drilling location (i.e., 11.679 psia) (see Table 4-1 or Appendix D). Thus, the derated output pressure, p_{d2}, is

$$p_{d2} = (24.14)\,(11.769)$$

$$p_{d2} = 284.1 \text{ psia}$$

The above compressor derated pressure of 284.1 psia is greater than the injection pressure of 94.1 psia, therefore, the compressor is capable of producing the injection pressure needed for this example drilling operation.

The last criteria to check is whether the prime mover has the power to operate at the 6,000 ft surface elevation. The prime mover for this compressor is a diesel fueled, turbocharged, Caterpillar Model 3406 with a peak output of 400 horsepower at 1,800 rpm (at API standard conditions). The theoretical shaft horsepower, $\dot{W}_s$, required by the compressor is obtained from Equation 4-35a. Equation 4-35a becomes

$$\dot{W}_s = \frac{(2)\ (1.4)}{(0.4)}\ \frac{(11.769)\ (840)}{229.17}\ \left[\left(\frac{284.1}{11.769} \right)^{\frac{(0.4)}{(2)(1.4)}} - 1 \right]$$

$$\dot{W}_s = 173.9$$

Assuming a mechanical efficiency, ε_m, is

$$\varepsilon_m = 0.90$$

From Equation 4-39, the actual shaft horsepower, $\dot{W}_{as}$, required by the compressor is

$$\dot{W}_{as} = \frac{173.9}{0.9}$$

$$\dot{W}_{as} = 193.2$$

The above determined 193.2 horsepower is the actual shaft power needed by the compressor to produce the 284.1 psia fixed pressure output at the surface location elevation of 6,000 ft above sea level. At this surface location, the input horsepower available from the prime mover is a derated value (derated from the rated 400 horsepower available at 1,800 rpm). In order for the compressor system to operate at this 6,000 ft surface location elevation, the derated input power available must be greater than the actual shaft power needed. Figure 4-15 shows that for 6,000 ft elevation the input power of a turbocharged prime mover must be derated by approximately 14.8 percent. The derated input horsepower, $\dot{W}_i$, available from the prime mover is

$$\dot{W}_i = 400 \left(1 - 0.148 \right)$$

$$\dot{W}_i \;=\; 340.8$$

For this example, the prime mover's derated input power is greater than the actual shaft horsepower needed, thus, the compressor system can be operated at this 6,000 ft surface location elevation. This particular example is somewhat complicated since the prime mover for this integrated compressor unit shares its power with other auxiliary equipment on the portable drilling rig. Thus, a portion of the 340.8 horsepower available from the prime mover will be used by the hydraulic rotary head unit. To get a complete assessment of the power available to this compressor these additional power needs should be taken into account.

5.3.3 *Prime Mover Fuel Consumption*

In this section the fuel consumption of the prime mover for the compressor system will be discussed. Illustrative examples of the fuel consumption were discussed in detail in Chapter 4. In this section the illustrative examples will be completed with the calculation of the approximate fuel needed on the drilling location for the operation of the compressor system.

Illustrative Examples 5.5c, and 5.6c describe the implementation of the basic planning step No. 10 given in Section 5.1 (planning step No. 11 is discussed in Chapter 8).

Illustrative Example 5.5c Determine the total diesel fuel needed by the semi-trailer mounted stand alone Dresser Clark Model CFB-4, four-stage reciprocating piston primary compressor unit (see Figure 4-25) used in Illustrative Example 5.5b. This compressor unit has a volumetric flow rate of 1,200 acfm. To estimate the total diesel fuel needed by this compressor unit it is necessary to estimate the fuel consumption of the compressor units' Caterpillar Model D398, diesel fueled, turbocharged, prime mover. The anticipated drilling rate of penetration is estimated to be 30 ft/hr. Since the vertical depth to be drilled is 2,400 ft, then the estimated actual drilling time to reach this depth is approximately 80 hours.

In Illustrative Example 5.5b the injection pressure into the top the annulus when drilling at 2,400 ft of depth was found to be 34.9 psia. Using similar calculations the injection pressures for lesser depths can be found. Figure 5-19 shows these injection pressures as a function of drilling time (or drilling depth).

The reciprocating piston compressor is not a fixed pressure ratio machine like the rotary screw compressor. As long as there is sufficient power available from the prime mover the reciprocation piston compressor will match the back pressure resistance. Thus, Figure 5-19 shows only one curve indicating the injection pressure is the same as the pressure output of the compressor.

In Illustrative Example 5.5b it was found that the actual shaft horsepower required by this reciprocating piston compressor to compress air to 34.9 psia was 81.2 (at 2,400 ft of depth). Also in Illustrative Example 5.5b the derated horsepower available from the Caterpillar Model D398 was found to be 722.0. Drilling at a depth of 2,400 ft, the prime mover power ratio is

$$PR = \frac{81.2}{722.0} \ (100) \ = \ 11.3$$

Figure 4-17 does not give data for power ratios less than 50 percent so a diesel fuel consumption rate 0.700 lb/hp-hr will be assumed for power levels below 40 percent. The total weight rate of diesel fuel consumption per hour is

$$\dot{w}_f \ = \ 0.700 \ (81.2) \ = \ 56.9 \ \text{lb/hr}$$
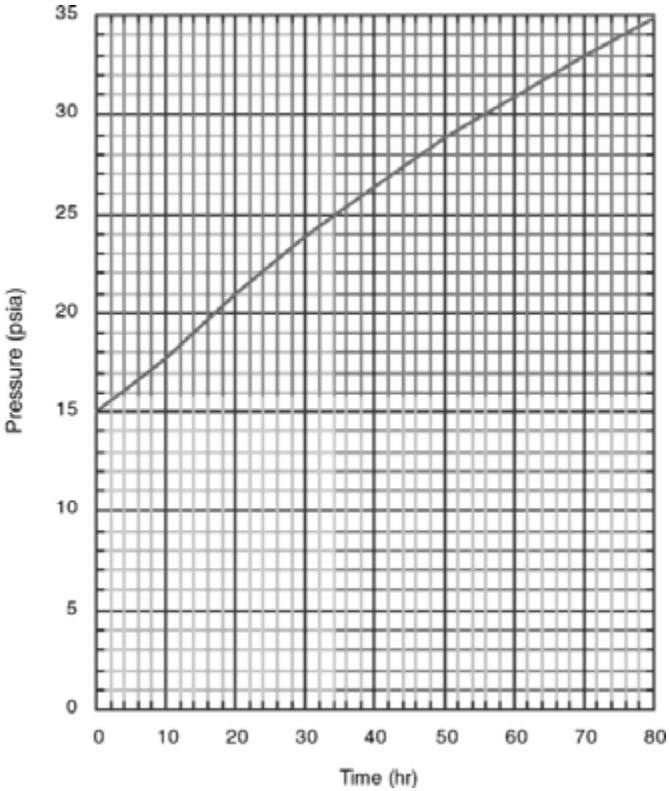
Figure 5-19: Drill string injection pressure (same as compressor output pressure) for Illustrative Example 5.5c.

The diesel fuel consumption rate (in United States gallons) for the drilling depth of 2,400 ft is

$$q_f = \frac{56.9}{(0.8156)(8.33)} = 8.4 \text{ gal/hr}$$

Using the data in Figure 5-19 and similar calculations as those given above, the diesel fuel consumption rate as a function of drilling time (or drilling depth) can be obtained.   Figure 5-20 shows the diesel fuel consumption rate as a function of drilling time (or drill depth) for this reciprocating piston compressor.
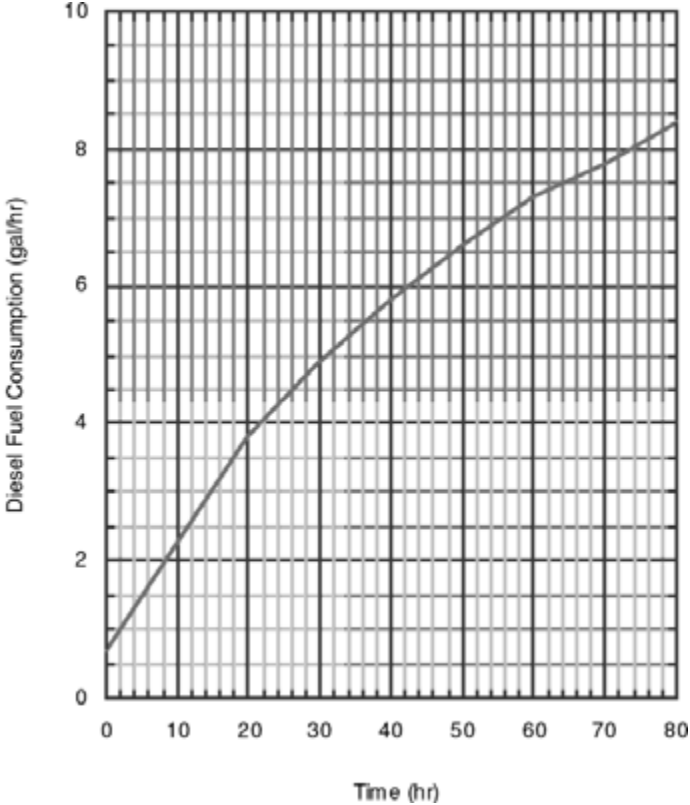
Figure 5-20: Fuel consumption rate as a function of drilling time for reciprocation piston compressor of Illustrative Example 5.5c.

The approximate total diesel fuel needed to drill the borehole is given by the integration of the area under the curve in Figure 5-20. This is approximately 360

gallons. It is standard practice to assume a 20 percent additional volume of fuel for blowing the hole between connections and other operations on the drill rig. Therefore, the approximate total diesel fuel needed for this compressor at the drilling location is 432 gallons.

This example shows the advantages of the combination of reverse circulation drilling operations and the reciprocating piston compressor. The low injection pressure is the result of low velocity of the air as it moves down the large annulus space between the inside of the openhole borehole and the outside of the drill string (drill pipe and drill collars). When the air velocity is low, pipe friction losses are low. Therefore, the weight of the air column in the annulus dominates the pressure change from the top of the annulus to the bottom of the annulus. This is illustrated by the fact that the injection pressure at the top of the annulus is slightly less than the pressure at the bottom of the annulus.

On the other hand, the resistance to the return air flow which flows up the inside of the drill string (with the entrained rock cuttings) is dominated by pipe friction loss. The weight of the air (with the cuttings) column contributes to pressure changes in the inside of the drill string, but pipe friction loss is the main component of losses.

This illustrative example demonstrates the calculation procedure used to plan a typical "deep" water well drilling operation. This particular drilling operation uses standard API drill string components (drill collars and drill pipe) and a tri-cone drill bit that can be used for reverse circulation operations. This is an openhole reverse circulation operation. The injected air (at low volumetric flow rate) moves very slowly down the openhole annulus and has very little cleaning power to counter caving problems. Therefore, openhole reverse circulation drilling operations should be restricted to locations that have highly competent rock formations.

Illustrative Example 5.6c Determine the total diesel fuel needed by the portable single Tamrock Driltech Model D25K drilling rig with the on-board, Sullair Model 840 two-stage rotary screw primary compressor unit (see Figure 4-19) used in Illustrative Example 5.6b. This compressor system has a volumetric flow rate of 840 acfm. The prime mover for this compressor is a Caterpillar Model 3406, diesel fueled, turbocharged motor. This prime mover is also used to operate the hydraulic pump that in turn operates the rotary top drive system. To estimate total diesel fuel needed at the drilling location to drill the 1,200 ft deep, 5 7/8 inch borehole, it will be necessary to also estimate the power requirements for the operation of the hydraulic rotary top drive system. The anticipated drilling rate of penetration is estimated to be 40 ft/hr. Since the vertical depth to be drilled is 1,200 ft, then the estimated actual drilling time to reach this depth is approximately 30 hours.

In Illustrative Example 5.6b the derated fixed pressure output from the fixed ratio Sullair Model 840 rotary screw compressor with a volumetric flow rate of 840 acfm was found to be 284.1 psia. This will be the pressure output of this rotary compressor regardless of the drilling depth (and, therefore, regardless of the drilling time). Also in Illustrative Example 5.6b for the depth of 1,200 ft the injection pressure (into the top of the dual wall pipe annulus) was found to be 94.1 psia.

Using this same injection calculation procedure, the injection pressures for drilling at depths less than 1,200 ft can be obtained.

Figure 5-21 shows the derated fixed pressure output of the compressor and the injection pressure to the drill string as a function of drilling time (or drilling depth). Compressor output pressures that are different from the actual injection pressures is a unique characteristic of rotary compressor systems. The fixed internal design of the rotary compressor dictates a fixed pressure output from the compressor regardless of the back pressure resistance (assuming the back pressure is less than the fixed pressure output). In this case the back pressure resistance is the injection pressure. Therefore, as air exits the compressor it decompresses when it passes into the surge tank at the exit of the compressor to match the injection pressure resistance in the flow line to the dual wall pipe annulus.
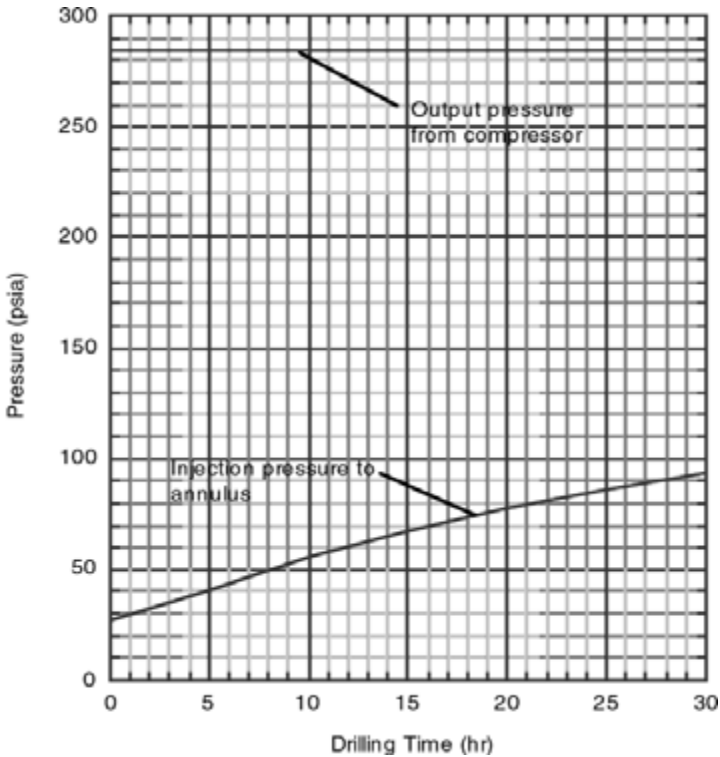
Figure 5-21: Compressor output pressure and dual wall pipe annulus injection pressure for Illustrative Example 5.6c.

In Illustrative Example 5.6b it was found that the actual shaft horsepower required by the compressor to compress air to 284.1 psia was 193.2. The derated horsepower available from the prime mover was 340.4. The prime mover for this rotary compressor is also used to operate the hydraulic pump that operates the top drive system. Thus, to obtain the fuel consumption for this prime mover (using fuel consumption calculations outlined in Chapter 4) the power usage to operate the top drive system must be estimated and added to the above compressor usage. For this example, it is estimated that the torque applied to the top of the drill string is 2,000 ft-lb at a rotary speed of 60 rpm. For this example, Equation 5-11 becomes

$$\dot{W}_{td} = \frac{(2,000)\,(60)}{5252}$$

$$\dot{W}_{td} = 22.9$$

Assuming an overall mechanical efficiency for the hydraulic top drive system to be, $\varepsilon_m = 0.8$, the actual shaft horsepower needed for the hydraulic pump which operated the top drive system is estimated to be

$$\dot{W}_{td} = \frac{22.9}{0.80}$$

$$\dot{W}_{td} = 28.6$$

Thus, the total actual shaft horsepower required by both the compressor and the hydraulic pump operating the top drive, $\dot{W}_t$, is

$$\dot{W}_t = \dot{W}_{as} + \dot{W}_{td}$$

$$\dot{W}_t = 193.2 + 28.6$$

$$\dot{W}_t = 221.8$$

The prime mover power ratio is

$$PR = \frac{221.8}{340.8}\,(100) = 65.1$$

From Figure 4-17 the approximate diesel fuel consumption rate at this power level is 0.558 lb/hp-hr. The total weight rate of diesel fuel consumption per hour is

$$\dot{w}_f = 0.558\,(221.8) = 123.8 \text{ lb/hr}$$

The diesel fuel consumption rate (in United States gallons) for a drilling depth of 1,200 ft is

$$q_f = \frac{123.8}{(0.8156)(8.33)} = 18.2 \text{ gal/hr}$$

Using similar calculations as those given above, the diesel fuel consumption rate for other drilling times (or drilling depth) can be obtained. Figure 5-22 shows the diesel fuel consumption rate as a function of drilling time for the drill rig prime mover.
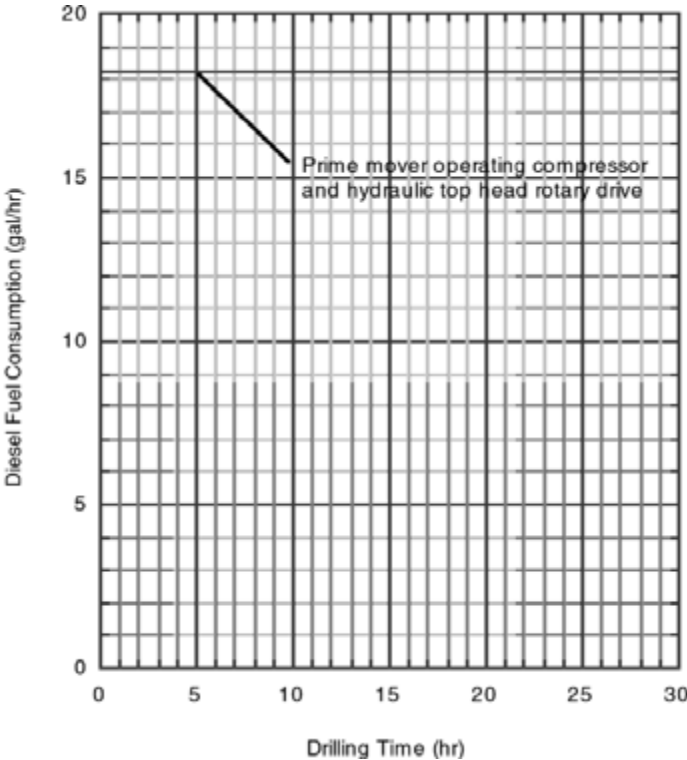
Figure 5-22: Fuel consumption rate as a function of drilling time for rotary compressor of Illustrative Example 5.6c.

The diesel fuel consumption rate for this example is constant through the drilling time of 30 hours. The approximate total diesel fuel needed to drill the borehole is given by the integration of the area under the curve in Figure 5-22. This is approximately 728 gallons. It is standard practice to assume a 20 percent additional volume of fuel for blowing the hole between connections and other operations on the drill rig. Therefore, the approximate total diesel fuel needed at the drilling location is 873 gallons. For this example, this diesel fuel amount is for the drilling rig prime mover that operates both the integrated rotary screw compressor and the hydraulic pump that operates the rotary top drive system.

This illustrative example demonstrates the calculation procedure used to plan a typical dual wall pipe reverse circulation drilling operation. This particular drilling operation uses the concealed inner-tube pipe and the special skirted tri-cone drill bit fabricated for this type of operations (see Figure 3-36). The injected air (at low volumetric flow rate) moves slowly down the annulus inside the dual pipe. No air moves down the annulus between the outside of the dual pipe and the openhole.

5.4 Conclusions

These illustrative examples given in this chapter the relative fuel efficiencies of the reciprocating piston compressor and the rotary type compressor. In general, the reciprocating piston compressor is the more fuel efficient machine for most shallow drilling operations, but its bulk limits its applicability in small rig operations.

Reverse circulation techniques are uniquely applicable to shallow drilling operations. The principal advantage to using reverse circulation techniques (vis-à-vis direct circulation technique) is that the minimum volumetric flow rates are significantly less than the corresponding minimum volumetric flow rates for direct circulation drilling (for the same well geometry and drilling rates, etc). The principal disadvantage to the reverse circulation technique is the high resistance to the air flow up the inside of the drill string (due to pipe friction). This pipe friction resistance ultimately restricts the reverse circulation technique to shallow drilling operations since return flow pipe friction losses become excessive for the long pipe lengths that accompany deep drilling operations (i.e., usually at depths greater than approximately 3,000 ft).

The illustrative examples given in this shallow drilling chapter were developed considering only the major friction flow losses in simple openhole drill pipe geometry. Consideration of only these major losses is deemed appropriate for shallow well analysis due to the length of the drill strings considered and the simplicity of the surface flow equipment used in most shallow drilling operations. Deep drilling operations require consideration of major and minor flow losses and more complicated well geometry. Chapter 8 will consider these in detail.

References

1. Lapedes, D. H., *McGraw-Hill Encyclopedia of the Geological Sciences*, McGraw-Hill, 1978.

2. Daugherty, R. L., Franzini, J. B., and Finnemore, E. J., *Fluid Mechanics with Engineering Applications*, Eighth Edition, McGraw-Hill, 1985.

3. Baumeister, T., *Marks' Standard Handbook for Mechanical Engineers*, Seventh Edition, McGraw-Hill Book Company, 1979.

4. Roscoe Moss Company, *Handbook of Ground Water Development*, Wiley, 1990.

5. *Handbook of Suggested Practices for the Design and Installation of Ground-Water Monitoring Wells*, EPA 600/4-89/034, National Water Well Association, 1989.

6. *RCRA Ground-Water Monitoring: Draft Technical Guidance*, EPA/530-R-93-001, USEPA, November 1992.

This page intentionally left blank.

Chapter

Six

Direct Circulation Models

In order to make reasonable predictions of the flow characteristics for direct circulation air and gas drilling operations, aerated fluids drilling operations, and stable foam drilling operations it is necessary to derive a consistent theory that can be used, with certain simplifying limitations, to develop specific equations to model each of the above operations.

6.1 Basic Assumptions

Direct circulation is defined as the injection of the drilling fluid into the inside of the top of the drill string, the flow of the fluid down the inside of the drill string, through the bit orifices or nozzles, the entraining of the rock cuttings into the drilling fluid at the bottom of the borehole, and then the flow of the drilling fluid with the entrained cuttings up the annulus between the outside of the drill string and the inside of the borehole.

Figure 6-1 shows a simplified U-tube schematic representation of direct circulation flow. In general, in air and gas drilling operations two phase flow occurs in the inside of the drill string and through the orifices or nozzles in the drill bit. Three phase flow occurs when the fluids with entrained rock cuttings move up the annulus from the bottom of the well to the surface. The three phases are a compressible gas, an incompressible fluid, and the solid rock cuttings from the advance of the drill bit. The compressible gases that are used most in drilling are air, natural gas, nitrogen (or air stripped of oxygen). The incompressible fluids

used are treated fresh water, treated salt water (formation water), water based drilling muds, diesel oil, oil based drilling muds, and crude oil (formation oil).

It is assumed that compressible gases can be approximated by the perfect gas law. Further, it is assumed that the mixture of compressed gas and incompressible fluid will be uniform and homogeneous. When the solid rock cuttings are added to the mixture of compressible gas and incompressible fluid, the solid rock particles are assumed to be uniform in size and density and will be distributed uniformly in the mixture of gas and fluid. Also, it is assumed that the rock particles move with the same velocity as circulating gas and fluid and that the resulting uniform mixtures can be approximated by known basic fluid mechanics relationships [1].

The assumption of uniformity of the two or three phases in the mixtures is an important issue in light of the technology developed for gas lift assisted oil production [2, 3]. The aeration of oil (or other formation produced fluids) from the bottom of a well with the flow of gas from the surface (down the annulus between the casing and the production tubing) is somewhat similar to the aeration of fluid and rock cuttings from the bottom of a well with a flow of gas and fluid from the surface (down the inside of the drill string). However, in most oil production situations the two phase flow takes place inside of the tubing. In the drilling situation, the gas and fluid are injected together into the top of the drill string and move together down the inside of the drill string, through the bit orifices or nozzles, and then the resulting three phase flow (gas, fluid, and rock cuttings) moves up the annulus to the surface. Thus, the geometry of flow for the two operations is quite different and probably not comparable [4].

6.2 General Derivation

The term, P_{in}, represents the pressure of the injected drilling fluids into the top of drill string. The U-tube representation in Figure 6-1 shows the larger inside diameter of the drill pipe at the top of the drill string where the drilling fluids are injected. Below the drill pipe is shown the smaller inside diameter of the drill collars and below the drill collars is shown a schematic of the drill bit orifices (or nozzles). The schematic shows the smaller annulus space between the outside of the drill collars and inside of the open borehole. Above is the annulus space between the outside of the drill pipe and the inside of the open borehole. Then at the top (in the annulus space) is the largest annulus space between the outside of the drill pipe and the inside of the casing. At the top of the annulus the drilling fluids with the entrained cuttings exit the circulation system at a pressure, P_e.

As in all compressible flow problems, the process of solution must commence with a known pressure and temperature and in this case the pressure and temperature at the exit from the circulation system. Therefore, the derivation will begin with the analysis of the flow of the gas in the annulus and will continue through the circulation system in the upstream direction. Thus, this derivation will start with the annulus, continues through the drill bit orifices, and then continue up the inside of the drill string to the surface. Figure 6-1 shows the pressure, P, at any position in the annulus which is referenced from the surface to a depth by the term h. The total depth of the well is H. The differential pressure, dP, in the upward flowing three phase flow occurs over an incremental distance of dh. This differential pressure can be approximated as [1]

$$dP = \gamma_{mix} \left[1 + \frac{f V^2}{2g \left(D_h - D_p \right)} \right] dh \qquad (6\text{-}1)$$

where P is fluid pressure (lb/ft^2, abs),

      h is the reference depth (ft),

      H is the total depth (ft)

      γ_{mix} is the specific weight of the mixture of air (or other gas) , incompressible fluid, and the rock cuttings (lb/ft^3),

      f is the Fanning friction factor,

      V is the average velocity in the annulus (ft/sec),

      D_h is the inside diameter of the borehole (ft),

      D_p is the outside diameter of the drill pipe (ft),

      g is the acceleration of gravity (32.2 ft/sec^2).
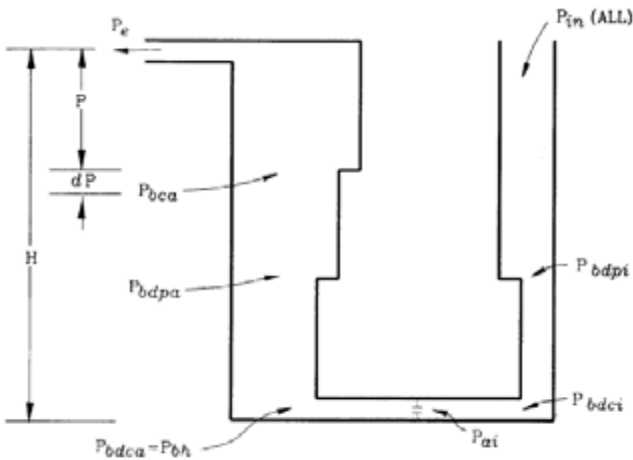
Figure 6-1: Schematic of direct circulation. P_{in} is the injection pressure into the top of the drill string, P_{bdpi} is pressure at bottom of drill pipe inside the drill string, P_{bdci} is pressure at bottom of drill collars inside the drill string, P_{ai} is pressure above drill bit inside the drill string, P_{bdca} is pressure at bottom of drill collars in the annulus, P_{bh} is bottomhole pressure in the annulus, P_{bdpa} is pressure at bottom of drill pipe in the annulus, P_{bca} is pressure at the bottom of casing in the annulus, and P_e is pressure at the top of the annulus.

The first term on the right side of Equation 6-1 represents the incremental pressure change due to the hydrostatic weight of the column of fluid (with entrained rock cuttings) in the annulus. The second term on the right side of Equation 6-1 represents the incremental increase pressure change due to the friction loss of the flowing fluid mixture.

6.2.1 *Weight Rate of Flow of the Gas*

In order to carry out the derivation of the governing equations for direct circulation, the weight rate of flow of air (or gas) to the well must be determined. Assuming the compressed air is provided by compressor(s), the weight rate of flow through the circulating system is determined from the atmospheric pressure and temperature of the air at the compressor location on the surface of the earth, and the characteristics of the compressor(s). For air, the atmospheric pressure for sea level and various elevations above sea level can be approximated for most of North America by the mid latitudes data given in Table 4-1. These reference pressures are denoted as p_r. Thus, the atmospheric pressure of the air entering the primary compressor(s) is, p_{at}, and this pressure can be approximated as

$$p_{at} \approx p_r \qquad\qquad (6\text{-}2)$$

where p_{at} is atmospheric pressure (psia),
   p_r is the reference atmospheric pressure (psia).
Similar data as that given in Table 4-1 for North America mid latitudes can be obtained for the other continents and latitudes around the world.

The above approximation is used when the actual atmospheric pressure at the drilling site has not been measured and recorded. The gas pressure, P_g, is

$$P_g = P_{at} = p_{at}\ 144 \qquad\qquad (6\text{-}3)$$

where P_{at} is the atmospheric pressure (lb/ft^2, abs),
   P_g is the gas pressure (lb/ft^2, abs).
To determine the weight rate of flow through the primary compressor(s) the actual temperature of the atmosphere, t_{at}, must be used. The absolute gas temperature, T_g, of the air entering the compressor(s) is

$$T_g = T_{at} = t_{at} + 459.67 \qquad\qquad (6\text{-}4)$$

where t_{at} is the atmospheric temperature (°F),
   T_{at} is absolute atmospheric temperature (°R),
   T_g is absolute gas temperature (°R).
Equation 4-11 in Chapter 4 gives the perfect gas law. This equation relates absolute pressure, specific weight, and absolute temperature [1]. The equation is

$$\frac{P}{\gamma} = \frac{\mathbf{R}\ T}{S_g} \qquad\qquad (6\text{-}5)$$

where P is pressure (lb/ft^2, abs),
   T is absolute temperature (°R),
   γ is specific weight (lb/ft^3),
   $\mathbf{R}$ is the gas constant (53.3 ft-lb/lb-°R),
   S_g is the specific gravity of the gas ($S_g = 1.0$ for air at standard conditions).

Substituting Equations 6-3 and 6-4 into Equation 6-5 and solving for the specific weight of the gas (in this case air) entering the compressor(s), γ_g, gives

$$\gamma_g = \frac{P_g\, S_g}{\mathbf{R}\, T_g} \qquad\qquad (6\text{-}6)$$

The weight rate of flow of the gas, $\dot{w}_g$, through the circulation system is

$$\dot{w}_g = \gamma_g\, Q_g \qquad\qquad (6\text{-}7)$$

where $\dot{w}_g$ is the weight rate of flow of gas (lb/sec),

Q_g is the volumetric flow rate of air into the circulation system (actual ft^3/sec). This volumetric flow rate is usually the flow rate entering the primary compressor(s) (see Chapter 4).

If the circulation system is natural gas from a pipeline and p_{pl} and t_{pl} are the pressure and temperature of the gas entering directly into the circulation system from the pipeline (or exiting the booster compressor from a pipeline), then, the absolute pressure of the gas, P_g, is

$$P_g = P_{pl} = p_{pl}\, 144 \qquad\qquad (6\text{-}8)$$

The absolute temperature of the gas, T_g, is

$$T_g = T_{pl} = t_{pl} + 459.67 \qquad\qquad (6\text{-}9)$$

where p_{pl} is the pipeline pressure (psia),

P_{pl} is the pipeline pressure (lb/ft^2, abs),

t_{pl} is the pipeline temperature (°F),

T_{pl} is the absolute pipeline temperature (°R).

Substituting Equations 6-8 and 6-9 into Equation 6-6 the specific weight of the gas from a pipeline can be obtained. This is

$$\gamma_g = \frac{P_g\, S}{\mathbf{R}\, T_g} = \frac{P_{pl}\, S}{\mathbf{R}\, T_{pl}} \qquad\qquad (6\text{-}10)$$

Substituting the result from Equation 6-10 into Equation 6-7 gives the weight rate of flow of gas from a pipeline, where Q_g is the volumetric flow rate of natural gas from the pipeline at the pressure p_{pl} and temperature t_{pl}. Note that the volumetric flow rate in a pipeline is usually given in either scfm, or in acfm at the surface location temperature and must be converted to obtain the actual volumetric flow rate at p_{pl} and t_{pl}. In order to use natural gas from a pipeline it is necessary to place a meter run in the flow line leading from the pipeline. This meter run allows an

accurate determination of the volumetric flow rate of natural gas being supplied to the drilling operation.

6.2.2 *Three-Phase Flow in the Annulus*

The weight rate of flow of incompressible drilling fluid (usually drilling mud), $\dot{w}_m$, into the well is

$$\dot{w}_m = \gamma_m \, Q_m \qquad\qquad (6\text{-}11)$$

where $\dot{w}_m$ is the weight rate of flow of drilling mud (lb/sec),

   γ_m is the specific weight of the drilling mud (lb/ft^3),
   Q_m is the volumetric flow rate of drilling mud (ft^3/sec).

The weight rates of flow $\dot{w}_g$ and $\dot{w}_m$ enter the well through the top of the drill string and flow to the bottom of the string and exit into the annulus through the openings in the drill bit (open orifices or the bit nozzles). After passing through the drill bit, the fluids entrain the rock cuttings generated by the drill bit as the bit is advanced. The entrained weight rate of flow of the solids, $\dot{w}_s$, is

$$\dot{w}_s = \frac{\pi}{4} \, D_h^2 \, (62.4) \, (2.7) \, \kappa \qquad\qquad (6\text{-}12)$$

where $\dot{w}_s$ is the weight rate of flow of solid rock cuttings (lb/sec),

   D_h is the diameter of the drilled hole (i.e., the bit diameter) (ft),
   κ is the penetration rate (ft/sec).

In the above equation the specific weight of fresh water is 62.4 lb/ft^3. The average specific gravity of sedimentary rocks is 2.7. If igneous or metamorphic rocks are to be drilled, an average value of 2.80 and 3.00, respectively, can be used if the actual specific gravity of the rocks to be drilled are not known [5].

The total weight rate of flow, $\dot{w}_t$, in the annulus from the bottom of the well to the surface is

$$\dot{w}_t = \dot{w}_g + \dot{w}_m + \dot{w}_s \qquad\qquad (6\text{-}13)$$

The drilling mud and the rock cutting solids do not change volume when the pressure is changed. However, the air (or gas) does change volume as a function of pressure change and, therefore, as a function of depth. Thus, the specific weight of the gas at any position in the annulus is

$$\gamma = \frac{P \, S}{R \, T_{av}} \qquad\qquad (6\text{-}14)$$

where T_{av} is the average temperature of the gas over a depth interval (°R). This average temperature term is determined by taking the average of the sum of the

geothermal temperatures at the top and bottom of the depth interval. The geothermal temperature at depth, t_h, is determined from the approximate expression

$$t_h \;=\; t_r \;+\; \beta\,H \tag{6-15}$$

where t_r is the reference temperature (°F),

   t_h is the geothermal temperature at depth (°F),

   β is the geothermal gradient constant (°F/ft).

The reference surface geothermal temperature, t_r, is assumed to be the temperatures given in Table 4-1 for sea level and various elevations above sea level. These temperatures represent North American mid latitudes year round averages. It is assumed that these temperatures also represent an average constant deep soil or rock temperatures near the surface of the earth at the elevations given in the table. The value of the geothermal gradient constant is determined from temperature logs of offset wells and other geophysical data. An average value of the geothermal gradient that can be used when the actual gradient has not been determined is 0.01°F/ft. The absolute reference surface geothermal temperature is

$$T_r \;=\; t_r \;+\; 459.67 \tag{6-16}$$

where T_r is the absolute reference temperature (°R). The absolute geothermal temperature at the bottom of the depth interval is

$$T_h \;=\; t_h \;+\; 459.67 \tag{6-17}$$

where T_h is the absolute bottomhole temperature (°R). The absolute average temperature, T_{av}, over the depth interval is given by

$$T_{av} \;=\; \frac{T_r \;+\; T_h}{2} \tag{6-18}$$

The relationship between the weight rate of flow of the gas and the specific weight and volumetric flow rate of gas at any position in the annulus is given by

$$\dot{w}_g \;=\; \gamma_g\,Q_g \;=\; \gamma\,Q \tag{6-19}$$

Substituting Equations 6-6 and 6-14 into the two terms on the right side of Equation 6-19 gives a relationship between the specific weight and volumetric flow rate at the surface and the specific weight of volumetric flow rate at any position in the annulus. This is

$$\frac{P_g\,S}{\mathbf{R}\,T_g}\,Q_g \;=\; \frac{P\,S}{\mathbf{R}\,T_{av}}\,Q \tag{6-20}$$

Solving Equation 6-20 for Q yields

$$Q = \left(\frac{P_g}{P}\right)\left(\frac{T_{av}}{T_g}\right) Q_g \qquad (6\text{-}21)$$

The three phase flow of gas, incompressible fluid, and rock cuttings up the annulus can be described by a mixed specific weight term which is a function of its position in the annulus. This mixed specific weight, γ_{mix}, is

$$\gamma_{mix} = \frac{\dot{w}_t}{\left(\dfrac{P_g}{P}\right)\left(\dfrac{T_{av}}{T_g}\right) Q_g + Q_m} \qquad (6\text{-}22)$$

In the derivation of Equation 6-22 the volume contribution of the solids (the rock cuttings) is assumed to be small and negligible relative to the volumes of the gas and the incompressible fluid in the mixture.

The velocity of this mixture changes as a function of its position in the annulus. The velocity, V, of the three phase flow in the annulus is

$$V = \frac{Q + Q_m}{\dfrac{\pi}{4}\left(D_h^2 - D_p^2\right)} \qquad (6\text{-}23)$$

where D_h is the inside diameter of the outer surface of the annulus (the borehole) (ft),
D_p is the outside diameter of the drill string (drill pipe and collars) (ft).
Substituting Equation 6-21 into Equation 6-23 yields

$$V = \frac{\left(\dfrac{P_g}{P}\right)\left(\dfrac{T_{av}}{T_g}\right) Q_g + Q_m}{\dfrac{\pi}{4}\left(D_h^2 - D_p^2\right)} \qquad (6\text{-}24)$$

Substituting Equations 6-22 and 6-24 into Equation 6-1 yields

$$dP = \left[\frac{\dot{w}_t}{\left(\dfrac{P_g}{P}\right)\left(\dfrac{T_{av}}{T_g}\right) Q_g + Q_m}\right]$$

$$\times \left\{ 1 + \frac{f}{2g\left(D_h - D_p\right)} \left[\frac{\left(\dfrac{P_g}{P}\right)\left(\dfrac{T_{av}}{T_g}\right) Q_g + Q_m}{\dfrac{\pi}{4}\left(D_h^2 - D_p^2\right)} \right]^2 \right\} dh \qquad (6\text{-}25)$$

Equation 6-25 contains only two independent variables, P and h. All of the other terms in the equation are known constants. Separating variables in Equation 6-25 and integrating from the surface to the bottom of the well yields

$$\int_{P_e}^{P_{bh}} \frac{dP}{B_a(P)} = \int_0^H dh \qquad (6\text{-}26)$$

where P_e is the exit pressure at the top annulus (lb/ft^2, abs),

P_{bh} is the bottomhole pressure at the bottom of the annulus (lb/ft^2, abs), and

$$B_a(P) = \left[\frac{\dot{w}_t}{\left(\dfrac{P_g}{P}\right)\left(\dfrac{T_{av}}{T_g}\right) Q_g + Q_m} \right]$$

$$\times \left\{ 1 + \frac{f}{2g\left(D_h - D_p\right)} \left[\frac{\left(\dfrac{P_g}{P}\right)\left(\dfrac{T_{av}}{T_g}\right) Q_g + Q_m}{\dfrac{\pi}{4}\left(D_h^2 - D_p^2\right)} \right]^2 \right\}$$

For this general derivation, the exit pressure, P_e, is the pressure at the entrance to the blooey line (in the case of air or gas drilling), or the pressure at the entrance to the return flow line (in the case of aerated fluid drilling), or the back pressure upstream of the control valve in the exit flow line (in the case of stable foam drilling).

The Fanning friction factor f given in the above equation is determined by the standard fluid mechanics empirical expressions relating the friction factor to the Reynolds number, diameter (or hydraulic diameter), and absolute pipe roughness. In general, the values for Reynolds number, diameter, and absolute pipe roughness are known. The classic expression for the Reynolds number is

$$N_R = \frac{\left(D_h - D_p\right) V}{v}$$

$$(6\text{-}27)$$

where $D_h - D_p$ is the hydraulic diameter for the annulus (ft),

V is the velocity (ft/sec),

v is the kinematic viscosity of the drilling fluid (ft^2/sec).

There are three flow conditions that can exist in the annulus. These are laminar, transitional, and turbulent flow conditions [1].

The empirical expression for the Fanning friction factor for laminar flow conditions is

$$f = \frac{64}{N_R}$$

$$(6\text{-}28)$$

This equation can be solved directly once the Reynolds number is known. In general, Equation 6-28 is valid for values for Reynolds numbers from 0 to 2,000.

The empirical expression for the Fanning friction factor for transitional flow conditions is known as the Colebrook equation. The Fanning friction factor cannot be determined directly and must be solved by trial and error. This empirical expression is

$$\frac{1}{\sqrt{f}} = -2 \log \left[\frac{\left(\dfrac{e}{D_h - D_p}\right)}{3.7} + \frac{2.51}{N_R \sqrt{f}} \right]$$

$$(6\text{-}29)$$

where e is the absolute roughness of the annulus surface (ft). Note the logarithm in the above equation is to the base ten. In general, Equation 6-29 is valid for values of Reynolds numbers from 2,000 to 4,000.

The empirical expression for the Fanning friction factor for turbulent flow conditions is known as the von Karman equation. This empirical expression is

$$f = \left[\frac{1}{2 \log \left(\dfrac{D_h - D_p}{e}\right) + 1.14} \right]^2$$

$$(6\text{-}30)$$

Note the logarithm in the above equation is to the base ten. In general, Equation 6-30 is valid for values of Reynolds numbers greater than 4,000.

For follow-on calculations for the flow in the annulus the absolute roughness for commercial pipe, $e_p = 0.00015$ ft, will be used for the outside surfaces of the drill

pipe and drill collars, and inside surface of the casing. The openhole surfaces of boreholes can be approximated with an absolute roughness, $e_{oh} = 0.01$ ft (i.e., this example value is the same as concrete pipe which approximates borehole surfaces in limestone and dolomite sedimentary rocks, or in similar competent igneous and metamorphic rocks, see Table 8-1).

Equation 6-26 together with Equations 6-27 through 6-30 can be used in sequential integration steps starting at the top of the annulus (with the known exit pressure) and continuing for each subsequent change in annulus cross-sectional area until the bottomhole pressure is determined. These sequential calculation steps require trial and error solutions. The trial and error process requires the selection of the upper limit of the pressure in each integral on the right side of Equation 6-26. This upper limit pressure selection must give a right side integral solution that is equal to the left side integral solution.

6.2.3 *Two-Phase Flow Through the Bit*

There are three basic calculation techniques for determining the pressure change through the constrictions of the drill bit orifices or nozzles.

The first technique assumes that the mixture of incompressible fluid and the gas passing through the orifices has a high incompressible fluid volume fraction. Under these conditions the mixture is assumed to act as an incompressible fluid. Thus, borrowing from mud drilling technology, the pressure change through the drill bit, ΔP_b, can be approximated by [6, 7]

$$\Delta P_b = \frac{\left(\dot{w}_g + \dot{w}_m \right)^2}{2g \, \gamma_{mixbh} \, C^2 \left(\frac{\pi}{4} \right)^2 D_e^4} \tag{6-31}$$

where ΔP_b is pressure change (lb/ft^2),

γ_{mixbh} is the mixture specific weight at the bottom of the annulus (lb/ft^3),
C is the fluid flow loss coefficient for drill bit orifices or nozzles (the
value of this constant is dependent on the type of gas or aerated flow),
D_e is the equivalent single orifice inside diameter (ft).
For drill bits with n equal diameter orifices (or nozzles), D_e becomes

$$D_e = \sqrt{n \, D_n^2} \tag{6-32}$$

where n is the number of equal diameter orifices (or nozzles),
D_n is the orifice (or nozzle) inside diameter (ft).
The pressure change obtained from Equation 6-31 is added to the bottomhole pressure P_{bh} obtained from Equation 6-26. The pressure above the drill bit inside the drill string, P_{ai}, is

$$P_{ai} = P_{bh} + \Delta P_b \tag{6-33}$$

where P_{bh} is bottomhole pressure (lb/ft^2, abs),

P_{ai} is pressure above the drill bit inside the drill string (lb/ft^2, abs).

For fluid mixtures that have a high gas volume fraction, the pressure above the drill bit inside the drill string can be approximated by [8]

$$P_{ai} = P_{bh} + \left[\frac{\left(\dot{w}_g + \dot{w}_m \right)^2}{g \, A_n^2} \right] \left[\frac{1}{\gamma_{mixbh}} - \frac{1}{\gamma_{mixai}} \right] \qquad (6\text{-}34)$$

where A_n is the total cross-sectional area of the drill bit orifices (or nozzles) (ft^2),

γ_{mixai} is the mixture specific weight above the drill bit (lb/ft^3).

Equation 6-34 must be solved by trial and error techniques since γ_{mixai} depends on the pressure P_{ai}. Note that this equation does not account for friction flow loss through the orifices and nozzles.

For fluid mixtures that are nearly all gas (with little incompressible fluid), the pressure above the drill bit inside the drill string will depend upon whether the critical flow conditions exist in the orifices or nozzle throats. The critical pressure through the bit orifices or nozzles is [1]

$$\left(\frac{P_{bh}}{P_{ai}} \right)_c = \left(\frac{2}{k + 1} \right)^{\frac{k}{k-1}} \qquad (6\text{-}35)$$

where k is the ratio of specific heats for the gas.

The right-hand side of Equation 6-35 is determined only by the value of the specific heat ratio constant of a gas (e.g., for air $k = 1.4$ and for natural gas $k = 1.28$). Thus, for air the critical pressure ratio is 0.528 and for natural gas the critical ratio is 0.549. Therefore, if P_{ai} is determined to be

for air $$P_{ai} \geq \frac{P_{bh}}{0.528} \qquad (6\text{-}36)$$

for natural gas $$P_{ai} \geq \frac{P_{bh}}{0.549} \qquad (6\text{-}37)$$

the flow through the orifice or nozzle throat is sonic. Under these sonic flow conditions, the upstream pressure, P_{ai}, does not depend on downstream pressure, P_{bh}. For these sonic flow conditions the upstream pressure P_{ai} is

$$P_{ai} = \frac{\dot{w}_g \, T_{bh}^{0.5}}{A_n \left[\left(\dfrac{g \, k \, S}{R} \right) \left(\dfrac{2}{k+1} \right)^{\left(\frac{k+1}{k-1} \right)} \right]^{0.5}} \tag{6-38}$$

where T_{bh} is the temperature of the gas at the bottom of the well (°R),
      A_n is the total cross-sectional area of the drill bit orifices (or nozzles) (ft^2).
If the upstream pressure is less than the right hand side of either Equations 6-36 (or 6-37), the flow through the orifices or nozzles is subsonic and the upstream pressure will be dependent on the pressure and temperature at the bottom of the borehole annulus. The subsonic flow condition is a more complicated calculation situation than the sonic flow condition.   In this calculation situation and knowing the bottomhole pressure and bottomhole temperature, the bottomhole specific weight must be determined using Equation 4-11.   Knowing the bottomhole pressure, temperature, and specific weight, the upstream pressure can be obtained for the subsonic condition. This equation is

$$P_{ai} = P_{bh} \left[\frac{\left(\dfrac{\dot{w}_g}{A_n} \right)^2}{2g \left(\dfrac{k}{k-1} \right) P_{bh} \, \gamma_{bh}} + 1 \right]^{\frac{k}{k-1}} \tag{6-39}$$

where γ_{bh} is the specific weight of the gas at the bottom of the annulus (lb/ft^3). Note that Equations 6-38 and 6-39 do not account for friction flow loss through the orifices and nozzles.

6.2.4 *Two-Phase Flow in the Drill String*
      The combined gas and incompressible fluid are injected into the top of the inside drill string. Therefore, the flow of the fluids inside of the drill string must be assumed to be two phase. The differential pressure, dP, in the downward flowing two phase flow occurs over the incremental distance of dh at the depth h for a total depth of well of H.
      The differential pressure at a depth h can be approximated as

$$dP = \gamma_{mix} \left[1 - \frac{f \, V^2}{2g \, D_i} \right] dh \tag{6-40}$$

where D_i is the inside diameter of the drill pipe, or drill collars (ft).

The two-phase flow of gas and incompressible fluid down the inside of the drill string can be described by a mixed specific weight term which is a function of position in the drill string. This mixed specific weight term is

$$\gamma_{mix} = \frac{\dot{w}_g + \dot{w}_m}{\left(\dfrac{P_g}{P}\right)\left(\dfrac{T_{av}}{T_g}\right)Q_g + Q_m}$$

(6-41)

The velocity of this mixture changes as a function of its position in the drill string. The velocity of the two-phase flow in the drill string is

$$V = \frac{\left(\dfrac{P_g}{P}\right)\left(\dfrac{T_{av}}{T_g}\right)Q_g + Q_m}{\dfrac{\pi}{4}D_i^2}$$

(6-42)

Equations 6-41 and 6-42 are functions of the pressure P at a depth of h. Substituting Equations 6-41 and 6-42 into Equation 6-40 yields

$$dP = \left[\frac{\dot{w}_g + \dot{w}_m}{\left[\left(\dfrac{P_g}{P}\right)\left(\dfrac{T_{av}}{T_g}\right)Q_g + Q_m\right]}\right]$$

$$\times \left\{1 - \frac{f}{2g\,D_i}\left[\frac{\left(\dfrac{P_g}{P}\right)\left(\dfrac{T_{av}}{T_g}\right)Q_g + Q_m}{\dfrac{\pi}{4}D_i^2}\right]^2\right\}dh$$

(6-43)

Equation 6-43 contains only two independent variables, P and h. Separating variables in Equation 6-43 and integrating from the bottom of the inside of the drill string to the surface of the well yields

$$\int_{P_{in}}^{P_{ai}}\frac{dP}{B_i\,(P)} = \int_0^H dh$$

(6-44)

where

$$B_i\,(P)\;=\;\left[\dfrac{\dot{w}_g\;+\;\dot{w}_m}{\left(\dfrac{P_g}{P}\right)\left(\dfrac{T_{av}}{T_g}\right)Q_g\;+\;Q_m}\right]$$

$$\times\left\{1\;-\;\dfrac{f}{2g\,D_i}\left[\dfrac{\left(\dfrac{P_g}{P}\right)\left(\dfrac{T_{av}}{T_g}\right)Q_g\;+\;Q_m}{\dfrac{\pi}{4}\,D_i^2}\right]^2\right\}$$

and P_{in} is the injection pressure into the inside of the drill string (lb/ft^2, abs).

The Fanning friction factor f given in the above equation is determined by the standard fluid mechanics empirical expressions relating the friction factor to the Reynolds number, diameter, and absolute pipe roughness. In general, the values for Reynolds number, diameter, and absolute pipe roughness are known.   The classic expression for the Reynolds number is

$$N_R\;=\;\dfrac{D_i\,V}{v} \tag{6-45}$$

where D_i is the inside diameter for the drill string (ft),

There are three flow conditions that can exist in the inside of the drill string. These are laminar, transitional, and turbulent flow conditions.

The empirical expression for the Fanning friction factor for laminar flow conditions is

$$f\;=\;\dfrac{64}{N_R} \tag{6-46}$$

This equation can be solved directly once the Reynolds number is known.   In general, Equation 6-46 is valid for values for Reynolds numbers from 0 to 2,000.

The empirical expression for the Fanning friction factor for transitional flow conditions is known as the Colebrook equation. the Fanning friction factor cannot be determined directly and must be solved by trial and error.   This empirical expression is

$$\frac{1}{\sqrt{f}} = -2 \log \left[\frac{\left(\frac{e}{D_i} \right)}{3.7} + \frac{2.51}{N_R \sqrt{f}} \right] \tag{6-47}$$

where e is the absolute roughness of the inside surface of the drill string (ft). In general, Equation 6-47 is valid for values of Reynolds numbers from 2,000 to 4,000.

The empirical expression for the Fanning friction factor for turbulent flow conditions is known as the von Karman equation. This empirical expression is

$$f = \left[\frac{1}{2 \log \left(\frac{D_i}{e} \right) + 1.14} \right]^2 \tag{6-48}$$

In general, Equation 6-48 is valid for values of Reynolds numbers greater than 4,000.

For follow-on calculations for flow in the drill string the absolute roughness for commercial pipe, $e_p = 0.00015$ ft, will be used for the inside surfaces of the drill pipe and drill collars.

Equation 6-45 together with Equations 6-46 through 6-48 can be used in sequential integration steps starting at the bottom of the inside of the drill string (with the known pressure above the drill bit inside the drill string) and continuing for each subsequent change in cross-sectional area inside the drill string until the injection pressure is determined. These sequential calculation steps require trial and error solutions. The trial and error process requires the selection of the upper limit of the pressure in each integral on the right side of Equation 6-44. This upper limit pressure selection must give a right side integral solution that is equal to the left side integral solution.

6.3 Air and Gas Drilling Model

Air (or gas) drilling is a special case of the theory derived in Section 6.2 above. The governing equations for air (or gas) drilling operations can be obtained by setting $Q_m = 0$ in the equations derived in Section 6.2.

There is two phase flow in the annulus (gas and rock cuttings). Setting $Q_m = 0$ in Equation 6-25 yields

$$dP = \left[\frac{\dot{w}_t}{\left(\frac{P_g}{P} \right) \left(\frac{T_{av}}{T_g} \right) Q_g} \right]$$

$$\times \left\{ 1 \; + \; \frac{f}{2g \left(D_h \; - \; D_p\right)} \left[\frac{\left(\dfrac{P_g}{P}\right)\left(\dfrac{T_{av}}{T_g}\right) Q_g}{\dfrac{\pi}{4}\left(D_h^2 \; - \; D_p^2\right)} \right]^2 \right\} \; dh \qquad (6\text{-}49)$$

where (see Equation 6-13)

$$\dot{w}_t \; = \; \dot{w}_g \; + \; \dot{w}_s$$

The exit pressure in direct circulation air (or gas) drilling operations is atmospheric pressure, P_{at}, at the top of the annulus. Separating variables in Equation 6-49 yields

$$\int_{P_{at}}^{P_{bh}} \frac{dP}{B_a \; (P)} \; = \; \int_0^H dh \qquad (6\text{-}50)$$

where

$$B_a \; (P) \; = \; \left[\frac{\dot{w}_t}{\left(\dfrac{P_g}{P}\right)\left(\dfrac{T_{av}}{T_g}\right) Q_g} \right] \left\{ 1 \; + \; \frac{f}{2g \left(D_h \; - \; D_p\right)} \left[\frac{\left(\dfrac{P_g}{P}\right)\left(\dfrac{T_{av}}{T_g}\right) Q_g}{\dfrac{\pi}{4}\left(D_h^2 \; - \; D_p^2\right)} \right]^2 \right\}$$

Using Equations 6-5, 6-6 or 6-10, 6-7 and 6-12, Equation 6-50 can be rearranged to give

$$\int_{P_{at}}^{P_{bh}} \frac{P \; dP}{\left(P^2 \; + \; b_a \; T_{av}^2\right)} \; = \; \frac{a_a}{T_{av}} \int_0^H dh \qquad (6\text{-}51)$$

where

$$a_a \; = \; \left(\frac{S}{R}\right)\left[1 \; + \left(\frac{\dot{w}_s}{\dot{w}_g}\right) \right] \qquad (6\text{-}52)$$

$$b_a = \frac{f}{2g\left(D_h - D_p\right)} \left(\frac{\mathbf{R}}{\mathbf{S}}\right)^2 \frac{\dot{w}_g^2}{\left(\frac{\pi}{4}\right)^2 \left(D_h^2 - D_p^2\right)^2} \tag{6-53}$$

In the above form, both sides of Equation 6-51 can be integrated. Using the constants in Equations 6-52 and 6-53 the solution to Equation 6-51 is

$$\left| \frac{1}{2} \ln \left(P^2 + b_a T_{av}^2\right) \right|_{P_{at}}^{P_{bh}} = \frac{a_a}{T_{av}} \left| h \right|_0^H \tag{6-54}$$

Evaluating Equation 6-54 at the limits and rearranging the results gives

$$\ln\left[\frac{P_{bh}^2 + b_a T_{av}^2}{P_{at}^2 + b_a T_{av}^2}\right] = \frac{2\,a_a}{T_{av}} H \tag{6-55}$$

Raising both sides of Equation 6-55 to the natural exponent, e, gives

$$\frac{P_{bh}^2 + b_a T_{av}^2}{P_{at}^2 + b_a T_{av}^2} = e^{\frac{2\,a_a\,H}{T_{av}}} \tag{6-56}$$

Equation 6-59 can be rearranged and a solution obtained for P_{bh}. This yields

$$P_{bh} = \left[\left(P_{at}^2 + b_a T_{av}^2\right) e^{\frac{2\,a_a\,H}{T_{av}}} - b_a T_{av}^2\right]^{0.5} \tag{6-57}$$

The flow of gas to the well must be sufficient to carry solid rock cuttings from the bottom of the annulus to the surface. Therefore, it is assumed that the flow condition in both the annulus and the inside of the drill string is turbulent. The empirical von Karman relationship for determining the Fanning friction factor for the annulus is

$$f = \left[\frac{1}{2\,\log\left(\dfrac{D_h - D_p}{e}\right) + 1.14}\right]^2 \tag{6-58}$$

For follow-on calculations for flow in the annulus the absolute roughness for commercial pipe, $e_p = 0.00015$ ft, will be used for the outside surfaces of the drill

pipe and drill collars, and inside surface of the casing. The openhole surfaces of boreholes can be approximated with an absolute roughness, $e_{oh} = 0.01$ ft (i.e., this example value is the same as concrete pipe which approximates borehole surfaces in limestone and dolomite sedimentary rocks, or in similar competent igneous and metamorphic rocks, see Table 8-1).

Equation 6-57 together with Equations 6-52, 6-53 and 6-58 can be used in sequential calculation steps starting at the top of the annulus and continuing for each subsequent change in cross-sectional area in the annulus until the bottomhole pressure is determined.

The flow condition through the drill bit orifices or nozzles is single phase (air or gas) flow. The character (sonic or subsonic) of the gas flow through the drill bit orifices or nozzles is determined by the critical pressure ratio equation. The critical pressure ratio equation for bottomhole conditions is

$$\left(\frac{P_{bh}}{P_{ai}} \right)_c = \left(\frac{2}{k + 1} \right)^{\frac{k}{k-1}} \tag{6-59}$$

Using $k = 1.4$ for air and $k = 1.28$ for natural gas, then from Equation 6-59 if P_{ai} is determined to be

for air $$P_{ai} \geq \frac{P_{bh}}{0.528} \tag{6-60}$$

for natural gas $$P_{ai} \geq \frac{P_{bh}}{0.549} \tag{6-61}$$

the flow through the orifice or nozzle throat is sonic.   Under these sonic flow conditions, the upstream pressure, P_{ai}, does not depend on downstream pressure, P_{bh}. For sonic flow conditions the upstream pressure is

$$P_{ai} = \frac{\dot{w}_g \, T_{bh}^{0.5}}{A_n \left[\left(\frac{g \, k \, S}{R} \right) \left(\frac{2}{k + 1} \right)^{\left(\frac{k+1}{k-1} \right)} \right]^{0.5}} \tag{6-62}$$

If the upstream pressure is less than the right hand side of either Equation 6-60 (or 6-61), the flow through the orifices or nozzles is subsonic and the upstream pressure will be dependent upon the pressure and temperature at the bottom of the well (downstream). For these subsonic conditions the upstream pressure is

$$P_{ai} = P_{bh} \left[\frac{\left(\dfrac{\dot{w}_g}{A_n}\right)^2}{2g \left(\dfrac{k}{k-1}\right) P_{bh} \, \gamma_{bh}} + 1 \right]^{\frac{k}{k-1}}$$
(6-63)

The flow in the inside of the drill string is single phase flow (air or other gases). Setting $Q_m = 0$ in Equation (6-43) yields

$$dP = \left[\frac{\dot{w}_g}{\left(\dfrac{P_g}{P}\right)\left(\dfrac{T_{av}}{T_g}\right) Q_g} \right]$$

$$\times \left\{ 1 - \frac{f}{2g \, D_i} \left[\frac{\left(\dfrac{P_g}{P}\right)\left(\dfrac{T_{av}}{T_g}\right) Q_g}{\dfrac{\pi}{4} D_i^2} \right]^2 \right\} dh$$
(6-64)

Separating variables in Equation 6-64 yields

$$\int_{P_{in}}^{P_{ai}} \frac{dP}{B_i(P)} = \int_0^H dh$$
(6-65)

where

$$B_i(P) = \left[\frac{\dot{w}_g}{\left(\dfrac{P_g}{P}\right)\left(\dfrac{T_{av}}{T_g}\right) Q_g} \right] \left\{ 1 - \frac{f}{2g \, D_i} \left[\frac{\left(\dfrac{P_g}{P}\right)\left(\dfrac{T_{av}}{T_g}\right) Q_g}{\dfrac{\pi}{4} D_i^2} \right]^2 \right\}$$

Using Equations 6-5, 6-6 or 6-10, and 6-7, Equation 6-65 can be rearranged to give

$$\int_{P_{in}}^{P_{ai}} \frac{P \, dP}{\left(P^2 - b_i \, T_{av}^2\right)} = \frac{a_i}{T_{av}} \int_0^H dh \qquad (6\text{-}66)$$

where

$$a_i = \frac{S}{R} \qquad (6\text{-}67)$$

$$b_i = \frac{f}{2g \, D_i} \left(\frac{R}{S}\right)^2 \frac{\dot{w}_g^2}{\left(\frac{\pi}{4}\right)^2 D_i^4} \qquad (6\text{-}68)$$

In the above form, both sides of Equation 6-66 can be integrated. Using the constants in Equations 6-67 and 6-68 the solution to Equation 6-66 is

$$\left| \frac{1}{2} \ln \left(P^2 - b_i \, T_{av}^2\right) \right|_{P_{in}}^{P_{ai}} = \frac{a_i}{T_{av}} \left| h \right|_0^H \qquad (6\text{-}69)$$

Evaluating Equation 6-69 at the limits and rearranging the results gives

$$\ln \left[\frac{P_{ai}^2 - b_i \, T_{av}^2}{P_{in}^2 - b_i \, T_{av}^2} \right] = \frac{2 \, a_i}{T_{av}} H \qquad (6\text{-}70)$$

Raising both sides of Equation 6-70 to the natural exponent gives

$$\frac{P_{ai}^2 - b_i \, T_{av}^2}{P_{in}^2 - b_i \, T_{av}^2} = e^{\frac{2 \, a_i \, H}{T_{av}}} \qquad (6\text{-}71)$$

Equation 6-71 can be rearranged and a solution obtained for P_{in}. This yields

$$P_{in} = \left[\frac{P_{ai}^2 + b_i \, T_{av}^2 \left(e^{\frac{2 \, a_i \, H}{T_{av}}} - 1 \right)}{e^{\frac{2 \, a_i \, H}{T_{av}}}} \right]^{0.5} \qquad (6\text{-}72)$$

The empirical von Karman relationship for determining the approximate Fanning friction factor for the inside of the drill string is

$$f = \left[\frac{1}{2 \, \log \left(\frac{D_i}{e} \right) \, + \, 1.14} \right]^2 \tag{6-73}$$

For follow-on calculations for flow in the drill string the absolute roughness for commercial pipe, $e_p = 0.00015$ ft, will be used for the inside surfaces of the drill pipe and drill collars.

Equation 6-72 together with Equations 6-67, 6-68 and 6-73 can be used in sequential calculation steps starting at the bottom of the inside of the drill string and continuing for each subsequent change in cross-sectional area in the drill string until the surface injection pressure is determined.

6.4 Aerated Fluid Drilling Model

Aerated fluid drilling governing equations are very little changed from the direct circulation general derivation given in Section 6.2. The gases used in aerated fluid drilling are usually either air, or natural gas, or nitrogen (air stripped of oxygen). The fluids used are usually drilling mud, or diesel oil, or formation oil.

The flow condition in the annulus is three phase flow (gas, fluid, and solids). The exit pressure in aerated fluid drilling operations is the atmospheric pressure, P_{at}, at the exit at the top of the annulus. Equation 6-26 becomes

$$\int_{P_{at}}^{P_{bh}} \frac{dP}{B_a\,(P)} = \int_0^H dh \tag{6-74}$$

where

$$B_a\,(P) = \left[\frac{\dot{w}_t}{\left(\frac{P_g}{P} \right) \left(\frac{T_{av}}{T_g} \right) Q_g \, + \, Q_m} \right.$$

$$\times \left\{ 1 \, + \, \frac{f}{2g \left(D_h \, - \, D_p \right)} \left[\frac{\left(\frac{P_g}{P} \right) \left(\frac{T_{av}}{T_g} \right) Q_g \, + \, Q_m}{\frac{\pi}{4} \left(D_h^2 \, - \, D_p^2 \right)} \right]^2 \right\}$$

The Fanning friction factor f given in the above equation is determined by the standard fluid mechanics empirical expressions relating the friction factor to the Reynolds number, diameter (or hydraulic diameter), and absolute pipe roughness. In general, the values for Reynolds number, diameter, and absolute pipe roughness are known. The classic expression for the Reynolds number is

$$\mathbf{N_R} = \frac{\left(D_h - D_p\right) V}{v} \tag{6-75}$$

Three flow conditions that can exist in the annulus. These are laminar, transitional, and turbulent flow conditions.

The empirical expression for the Fanning friction factor for laminar flow conditions is

$$f = \frac{64}{\mathbf{N_R}} \tag{6-76}$$

This equation can be solved directly once the Reynolds number is known. In general, Equation 6-76 is valid for values for Reynolds numbers from 0 to 2,000.

The empirical expression for the Fanning friction factor for transitional flow conditions is known as the Colebrook equation. This equation cannot be solved directly and must be solved by trial and error. This empirical expression is

$$\frac{1}{\sqrt{f}} = -2 \log \left[\frac{\left(\dfrac{e}{D_h - D_p} \right)}{3.7} + \frac{2.51}{\mathbf{N_R} \sqrt{f}} \right] \tag{6-77}$$

In general, Equation 6-77 is valid for values of Reynolds numbers from 2,000 to 4,000.

The empirical expression for the Fanning friction factor for turbulent flow conditions is known as the von Karman equation. This empirical expression is

$$f = \left[\frac{1}{2 \log \left(\dfrac{D_h - D_p}{e} \right) + 1.14} \right]^2 \tag{6-78}$$

In general, Equation 6-78 is valid for values of Reynolds numbers greater than 4,000.

For follow-on calculations for flow in the annulus the absolute roughness for commercial pipe, $e_p = 0.00015$ ft, will be used for the outside surfaces of the drill

pipe and drill collars, and inside surface of the casing. The openhole surfaces of boreholes will be approximated with an absolute roughness, $e_{oh} = 0.01$ ft (i.e., this example value is the same as concrete pipe which approximates borehole surfaces in limestone and dolomite sedimentary rocks, or in similar competent igneous and metamorphic rocks, see Table 8-1).

Equation 6-74 together with Equations 6-75 through 6-78 can be used in sequential trial and error integration steps starting at the top of the annulus (with the known exit pressure) and continuing for each subsequent change in annulus cross-sectional area until the bottomhole pressure is determined.

The mixture of incompressible fluid and the gas passing through the orifices has a high incompressible fluid volume fraction and can, therefore, be assumed to act physically as an incompressible mixture. Thus, borrowing from mud drilling technology, the pressure change through the drill bit, ΔP_b, can be approximated by

$$\Delta P_b = \frac{\left(\dot{w}_g + \dot{w}_m\right)^2}{2g\,\gamma_{mixbh}\,C^2\left(\dfrac{\pi}{4}\right)^2 D_e^4} \tag{6-79}$$

The value of C represents the aerated fluid flow loss coefficient of the drill bit orifices (or nozzles). Experiments have shown that aerated fluid flow is very complex. The gas and incompressible fluid components in the aerated mixture appear to alternate their passage through the nozzles. This means the aerated flow through the nozzles is inefficient. The value of C for aerated fluid flow should be taken as 0.70 to 0.85. For drill bits with n equal diameter orifices (or nozzles), D_e becomes

$$D_e = \sqrt{n\,D_n^2} \tag{6-80}$$

The pressure change obtained from Equation 6-79 is added to the bottomhole pressure P_{bh} obtained from Equation 6-74. The pressure above the drill bit inside the drill string, P_{ai}, is

$$P_{ai} = P_{bh} + \Delta P_b \tag{6-81}$$

The flow condition in the inside of the drill string is two phase (gas and incompressible fluid) flow. Equation 6-44 becomes

$$\int_{P_{in}}^{P_{ai}} \frac{dP}{B_i\,(P)} = \int_0^H dh \tag{6-82}$$

where

$$B_i \ (P) \ = \ \left[\frac{\dot{w}_g \ + \ \dot{w}_m}{\left(\dfrac{P_g}{P} \right) \left(\dfrac{T_{av}}{T_g} \right) Q_g \ + \ Q_m} \right]$$

$$\times \left\{ 1 \ - \ \frac{f}{2g \ D_i} \left[\frac{\left(\dfrac{P_g}{P} \right) \left(\dfrac{T_{av}}{T_g} \right) Q_g \ + \ Q_m}{\dfrac{\pi}{4} \ D_i^2} \right]^2 \right\}$$

The Fanning friction factor f given in the above equation is determined by the standard fluid mechanics empirical expressions relating the friction factor to the Reynolds number, diameter, and absolute pipe roughness. In general, the values for Reynolds number, diameter, and absolute pipe roughness are known.   The classic expression for the Reynolds number is

$$\mathbf{N_R} \ = \ \frac{D_i \ V}{\nu} \tag{6-83}$$

Three flow conditions that can exist in the annulus.   These are laminar, transitional, and turbulent flow conditions.
The empirical expression for the Fanning friction factor for laminar flow conditions is

$$f \ = \ \frac{64}{\mathbf{N_R}} \tag{6-84}$$

This equation can be solved directly once the Reynolds number is known.   In general, Equation 6-84 is valid for values for Reynolds numbers from 0 to 2,000.
The empirical expression for the Fanning friction factor for transitional flow conditions is known as the Colebrook equation.   This equation cannot be solved directly and must be solved by trial and error. This empirical expression is

$$\frac{1}{\sqrt{f}} \ = \ - \ 2 \ \log \left[\frac{\left(\dfrac{e}{D_i} \right)}{3.7} \ + \ \frac{2.51}{\mathbf{N_R} \ \sqrt{f}} \right] \tag{6-85}$$

In general, Equation 6-87 is valid for values of Reynolds numbers from 2,000 to 4,000.

The empirical expression for the Fanning friction factor for turbulent flow conditions is known as the von Karman equation. This empirical expression is

$$ f = \left[\frac{1}{2 \, \log \left(\dfrac{D_i}{e} \right) + 1.14} \right]^2 \tag{6-86}$$

In general, Equation 6-86 is valid for values of Reynolds numbers greater than 4,000.

For follow-on calculations for flow in the drill string the absolute roughness for commercial pipe, $e_p = 0.00015$ ft, will be used for the inside surfaces of the drill pipe and drill collars.

Equation 6-82 together with Equations 6-83 through 6-86 can be used in sequential trial and error integration steps starting at the bottom of the inside of the drill string (with the known pressure above the drill bit inside the drill string) and continuing for each subsequent change in drill string cross-sectional area until the injection pressure is determined.

6.5 Stable Foam Drilling Model

Stable foam drilling is a special case of the general derivation given in Subsection 6.2.1. In stable foam drilling operations, the mixture of gas (usually air or nitrogen) and water (with a surfactant) are specified (foam quality) at the top and, therefore, throughout the annulus. Foam quality, Γ, is defined as

$$ \Gamma = \frac{Q_g}{Q_g + Q_f} \tag{6-87}$$

where Q_g is the volumetric flow rate of gas (ft^3/sec),

Q_f is the volumetric flow rate of the incompressible fluid (ft^3/sec).

The control of the foam quality at the top allows the foam quality at the bottom of the annulus to be calculated. This control is accomplished by placing a valve on the flow line from the annulus. Upstream of the valve is a pressure gauge and by maintaining a specified back pressure upstream of the valve the foam quality at this position can be determined. Knowing the foam quality at this position (and the other flow characteristics of the circulating system), the foam quality at any position in the annulus (particularly at the bottom of the annulus) can be determined. The foam quality at the bottom of the annulus must be maintained at approximately 0.60 or greater [9]. If the foam quality at this position drops much below this level, the foam will collapse and the flow will be in three separate phases. To maintain the bottomhole foam quality in the annulus at a value of approximately 0.60 or greater, the foam quality upstream of the back pressure valve is usually in the range 0.90 to 0.98.

The flow down the annulus is three phase flow (gas, fluid, and solids). The exit pressure for stable foam drilling operations is the back pressure, P_{bp}, upstream of the valve in the flow line from the annulus. Equation 6-26 becomes

$$\int_{P_{bp}}^{P_{bh}} \frac{dP}{B_a\,(P)} \;=\; \int_{0}^{H} dh \tag{6-88}$$

where P_{bp} is the back pressure on the annulus (lb/ft^2, abs), and

$$B_a\,(P) \;=\; \left[\frac{\dot{w}_t}{\left(\dfrac{P_g}{P}\right)\left(\dfrac{T_{av}}{T_g}\right)Q_g \;+\; Q_f}\right]$$

$$\times \left\{1 \;+\; \frac{f}{2g\left(D_h - D_p\right)}\left[\frac{\left(\dfrac{P_g}{P}\right)\left(\dfrac{T_{av}}{T_g}\right)Q_g \;+\; Q_f}{\dfrac{\pi}{4}\left(D_h^2 - D_p^2\right)}\right]^2\right\}$$

where the total weight rate of flow, $\dot{w}_t$, in the annulus from the bottom of the well to the surface is (see Equation 6-13)

$$\dot{w}_t \;=\; \dot{w}_g \;+\; \dot{w}_f \;+\; \dot{w}_s$$

The Fanning friction factor f given in the above equation is determined by the standard fluid mechanics empirical expressions relating the friction factor to the Reynolds number, diameter (or hydraulic diameter), and absolute pipe roughness. In general, the values for Reynolds number, diameter, and absolute pipe roughness are known. The classic expression for the Reynolds number is

$$\mathbf{N_R} \;=\; \frac{\left(D_h - D_p\right)V}{v} \tag{6-89}$$

There are three flow conditions that can exist in the annulus. These are laminar, transitional, and turbulent flow conditions.

The empirical expression for the Fanning friction factor for laminar flow conditions is

$$f = \frac{64}{N_R} \tag{6-90}$$

This equation can be solved directly once the Reynolds number is known. In general, Equation 6-90 is valid for values for Reynolds numbers from 0 to 2,000.

The empirical expression for the Fanning friction factor for transitional flow conditions is known as the Colebrook equation. The Fanning friction factor cannot be determined directly and must be solved by trial and error. This empirical expression is

$$\frac{1}{\sqrt{f}} = -2 \log \left[\frac{\left(\dfrac{e}{D_h - D_p} \right)}{3.7} + \frac{2.51}{N_R \sqrt{f}} \right] \tag{6-91}$$

where e is the absolute roughness of the annulus surface (ft). In general, Equation 6-94 is valid for values of Reynolds numbers from 2,000 to 4,000.

The empirical expression for the Fanning friction factor for turbulent flow conditions is known as the von Karman equation. This empirical expression is

$$f = \left[\frac{1}{2 \log \left(\dfrac{D_h - D_p}{e} \right) + 1.14} \right]^2 \tag{6-92}$$

In general, Equation 6-92 is valid for values of Reynolds numbers greater than 4,000.

For follow-on calculations for flow in the annulus the absolute roughness for commercial pipe, $e_p = 0.00015$ ft, will be used for the outside surfaces of the drill pipe and drill collars, and inside surface of the casing. The openhole surfaces of boreholes will be approximated with an absolute roughness, $e_{oh} = 0.01$ ft (i.e., this example value is the same as concrete pipe which approximates borehole surfaces in limestone and dolomite sedimentary rocks, or in similar competent igneous and metamorphic rocks, see Table 8-1).

Equation 6-88 together with Equations 6-89 through 6-92 can be used in sequential trial and error integration steps starting at the top of the annulus (with the known exit pressure) and continuing for each subsequent change in annulus cross-sectional area until the bottomhole pressure is determined.

If the stable foam is not preformed at injection, the flow down the inside of the drill string is that of an aerated fluid mixture. Such an aerated mixture can be assumed to pass through the nozzles in much the same manner as an incompressible fluid. Thus, borrowing from mud drilling technology, the pressure change through the drill bit, ΔP_b, can be approximated by

$$\Delta P_b = \frac{\left(\dot{w}_g + \dot{w}_f\right)^2}{2g \, \gamma_{mixbh} \, C^2 \left(\dfrac{\pi}{4}\right)^2 D_e^4} \tag{6-93}$$

The magnitude of C represents the loss coefficient of the drill bit nozzles for the aerated fluid mixture of the stable foam components. The value of C for this aerated fluid mixture is assumed to be 0.70 to 0.85. For drill bits with n equal diameter orifices (or nozzles), D_e becomes

$$D_e = \sqrt{n \, D_n^2} \tag{6-94}$$

The pressure change obtained from Equation 6-93 is added to the bottomhole pressure P_{bh} obtained from Equation 6-88. The pressure above the drill bit inside the drill string, P_{ai}, is

$$P_{ai} = P_{bh} + \Delta P_b \tag{6-95}$$

For performed stable foam flowing through the orifices (or nozzles), the pressure above the drill bit inside the drill string can be approximated by

$$P_{ai} = P_{bh} + \left[\frac{\left(\dot{w}_g + \dot{w}_f\right)^2}{g \, A_n^2}\right]\left[\frac{1}{\gamma_{mixbh}} - \frac{1}{\gamma_{mixai}}\right] \tag{6-96}$$

Equation 6-96 must be solved by trial and error techniques since γ_{mixai} depends on the pressure P_{ai}. Note that this equation does not account for friction flow loss through the orifices and nozzles.

For fluid mixtures that are nearly all gas (with little incompressible fluid), the pressure above the drill bit inside the drill string will depend upon whether the critical flow conditions exist in the orifices or nozzle throats. The critical pressure through the bit orifices or nozzles is

$$\left(\frac{P_{bh}}{P_{ai}}\right)_c = \left(\frac{2}{k + 1}\right)^{\frac{k}{k-1}} \tag{6-97}$$

The right hand side of Equation 6-97 is determined only by the value of the specific heat ratio constant of a gas (e.g., for air $k = 1.4$ and for natural gas $k = 1.28$). Thus, for air the critical pressure ratio is 0.528 and for natural gas the critical ratio is 0.549. Therefore, if P_{ai} is determined to be

for air
$$P_{ai} \geq \frac{P_{bh}}{0.528}$$
(6-98)

for natural gas
$$P_{ai} \geq \frac{P_{bh}}{0.549}$$
(6-99)

the flow through the orifice or nozzle throat is sonic.   Under these sonic flow conditions, the upstream pressure, P_{ai}, does not depend on downstream pressure, P_{bh}.
    For these sonic flow conditions the upstream pressure P_{ai} is

$$P_{ai} = \frac{\dot{w}_g \, T_{bh}^{0.5}}{A_n \left[\left(\frac{g \, k \, S}{R} \right) \left(\frac{2}{k \, + \, 1} \right)^{\left(\frac{k+1}{k-1} \right)} \right]^{0.5}}$$
(6-100)

    If the upstream pressure is less than the right hand side of either Equations 6-98 or 6-99, the flow through the orifices or nozzles is subsonic and the upstream pressure will be dependent on the pressure and temperature at the bottom of the borehole annulus. Under these subsonic conditions the upstream pressure is

$$P_{ai} = P_{bh} \left[\frac{\left(\frac{\dot{w}_g}{A_n} \right)^2}{2g \left(\frac{k}{k \, - \, 1} \right) P_{bh} \, \gamma_{bh}} + 1 \right]^{\frac{k}{k-1}}$$
(6-101)

Note that Equations 6-100 and 6-101 do not account for friction flow loss through the orifices and nozzles.
    The flow condition in the inside of the drill string is two phase (gas and fluid) flow. Equation 6-44 becomes

$$\int_{P_{in}}^{P_{ai}} \frac{dP}{B_i \, (P)} = \int_0^H dh$$
(6-102)

where

$$B_i \ (P) \ = \ \left[\frac{\dot{w}_g \ + \ \dot{w}_m}{\left(\dfrac{P_g}{P} \right) \left(\dfrac{T_{av}}{T_g} \right) Q_g \ + \ Q_m} \right]$$

$$\times \left\{ 1 \ - \ \frac{f}{2g \ D_i} \left[\frac{\left(\dfrac{P_g}{P} \right) \left(\dfrac{T_{av}}{T_g} \right) Q_g \ + \ Q_m}{\dfrac{\pi}{4} \ D_i^2} \right]^2 \right\}$$

The Fanning friction factor f given in the above equation is determined by the standard fluid mechanics empirical expressions relating the friction factor to the Reynolds number, diameter, and absolute pipe roughness. In general, the values for Reynolds number, diameter, and absolute pipe roughness are known. The classic expression for the Reynolds number is

$$\mathbf{N_R} \ = \ \frac{D_i \ V}{v} \tag{6-103}$$

There are three flow conditions that can exist in the annulus. These are laminar, transitional, and turbulent flow conditions.

The empirical expression for the Fanning friction factor for laminar flow conditions is

$$f \ = \ \frac{64}{\mathbf{N_R}} \tag{6-104}$$

This equation can be solved directly once the Reynolds number is known. In general, Equation 6-104 is valid for values for Reynolds numbers from 0 to 2,000.

The empirical expression for the Fanning friction factor for transitional flow conditions is known as the Colebrook equation. This equation cannot be solved directly and must be solved by trial and error. This empirical expression is

$$\frac{1}{\sqrt{f}} \ = \ - \ 2 \ \log \left[\frac{\left(\dfrac{e}{D_i} \right)}{3.7} \ + \ \frac{2.51}{\mathbf{N_R} \ \sqrt{f}} \right] \tag{6-105}$$

where e is the absolute roughness of the annulus surface (ft). In general, Equation 6-105 is valid for values of Reynolds numbers from 2,000 to 4,000.

The empirical expression for the Fanning friction factor for turbulent flow conditions is known as the von Karman equation. This empirical expression is

$$ f = \left[\frac{1}{2 \, \log\left(\dfrac{D_i}{e}\right) + 1.14} \right]^2 \qquad (6\text{-}106) $$

In general, Equation 6-106 is valid for values of Reynolds numbers greater than 4,000.

For follow-on calculations for flow in the drill string the absolute roughness for commercial pipe, $e_p = 0.00015$ ft, will be used for the inside surfaces of the drill pipe and drill collars.

Equation 6-102 together with Equations 6-103 through 6-106 can be used in sequential trial and error integration steps starting at the bottom of the inside of the drill string (with the known pressure above the drill bit inside the drill string) and continuing for each subsequent change in drill string cross-sectional area until the injection pressure is determined.

References

1. Daugherty, R. L., Franzini, J. B., and Finnemore, E. J., *Fluid Mechanics with Engineering Applications*, Eighth Edition, McGraw-Hill, 1985.

2. Brown, K. E., and Beggs, H. D., *The Technology of Artificial Lift Methods*, Vol. 1, PennWell Books, 1977.

3. Brown, K. E., et al, *The Technology of Artificial Lift Methods*, Vol. 2a, PennWell Books, 1980.

4. Personal communications with Stefan Miska, Department of Petroleum Engineering, University of Tulsa, January 1999.

5. Lapedes, D. H., *McGraw-Hill Encyclopedia of the Geological Sciences*, McGraw-Hill, 1978.

6. Gatlin, C., *Petroleum Engineering: Drilling and Well Completions*, Prentice-Hall, 1960.

7. Bourgoyne, A. T., Millheim, K. K., Chenevert, M. E., and Young, F. S., *Applied Drilling Engineering*, SPE, First Printing, 1986.

8. Guo, B., Hareland, G., and Rajtar, J., "Computer Simulation Predicts

Unfavorable Mud Rate and Optimum Air Injection Rate for Aerated Mud Drilling," SPE Paper 26892, Presented at the SPE Eastern Regional Conference and Exhibition, Pittsburgh, Pennsylvania, November 2-4,1993.

9. Beyer, A. H., Millhone, R. S., and Foote, R. W., "Flow Behavior of Foam as a Well Circulating Fluid", SPE Paper 3986, Presented at the SPE 47th Annual Fall Meeting, San Antonio, Texas, October 8-11, 1972.

This page intentionally left blank.

Part 2: Air and Gas Drilling Fundamentals

This page intentionally left blank.

Seven

Reverse Circulation Models

In order to make reasonable predictions of the flow characteristics for reverse circulation air and gas drilling operations and aerated fluids drilling operations, it is necessary to derive consistent theory that can be used, with certain simplifying limitations, to develop specific equations to model each of the above operations. It should be noted that stable foam cannot be applied to reverse circulation operations.

7.1 Basic Assumptions

Reverse circulation is defined as the injection of the drilling fluid into the top of the annulus, the flow of the fluid down the annulus to the bottom of the borehole, the entraining of the rock cuttings into the drilling fluid at the bottom of the borehole as the fluid sweeps past the bit cutting face, and then the flow of the drilling fluid with the entrained cuttings up the inside of the drill string.

Figure 7-1 shows a simplified U-tube schematic representation of reverse circulation flow. In general, in air and gas drilling operations two phase flow occurs in the flow of fluids down the annulus to the bottom of the borehole. Three phase flow occurs when the flow of the fluids at the bottom of the borehole entrains the rock cuttings that are generated by the advance of the drill bit. This three phase flow continues through the single large opening in the drill bit and then up the inside of the drill string to the surface. The three phases are the circulating fluids, a compressible gas and an incompressible fluid, and the solid rock cuttings. The compressible gases that are used in reverse circulation drilling are air, natural gas, and nitrogen (and air stripped of oxygen). The incompressible fluids that are used

are usually treated and untreated fresh water, treated and untreated salt water (formation water), and water-based drilling muds.

It is assumed that the compressible gases can be approximated by the perfect gas law. Further, it is assumed that the mix of compressed gas and incompressible fluid will be uniform and homogeneous. When the solid rock cuttings are added to the mixture of compressible gas and incompressible fluid, then the solid rock cutting particles will be uniform in size and density and will be distributed uniformly in the mixture of gas and fluid. Also, it is assumed that the rock particles move with the same velocity as circulating gas and fluid and that the resulting uniform mixtures can be approximated by known basic fluid mechanics relationships [1].

The assumption of uniformity of the two or three phases in the mixtures is an important issue in light of the technology developed for gas lift assistance of oil production [2, 3]. The aeration of oil (or other formation fluids) at the bottom of a well with the flow of gas from the surface (down the annulus between the casing and the production tubing) is similar to the aeration of circulating fluid and entraining of rock cuttings at the bottom of a well with a flow of gas and fluid from the surface (down the annulus). However, the gas lift published pressure gradient plots have been extrapolated from empirical data derived from experiments carried out on small inside diameter production tubing. New experiments with aerated drilling fluids have shown that the present production pressure gradient plots do not correlate with new experiments carried out on larger diameter tubulars [4].

Reverse circulation operations do not have the variety of air and gas techniques available. In general, reverse circulation operations use compressed air or other gases as drilling fluids, and aerated fluids as drilling fluids.

7.2 General Derivation

The term, P_{in}, represents the pressure of the injected drilling fluid into the top of the annulus. The U-tube representation in Figure 7-1 shows the largest annulus space between the outside of the drill pipe and the inside of the casing. Next is the annulus space between the outside of the drill pipe and the inside of the openhole. Then at the bottom of the annulus is the space between the outside of the drill collars and the inside of the openhole. At the bottom of the drill string is the single large opening in the drill bit which allows the drilling fluids with entrained rock cuttings to pass into the inside of the drill string. The schematic shows the smaller inside diameter of the drill collars. Above the drill collars is the larger inside diameter of the drill pipe. At the top of the drill pipe the drilling fluid with the entrained cuttings exits the circulation system at a pressure, P_e.

As in all compressible flow problems, the process of solution must commence with a known pressure and temperature and in this case the pressure and temperature at the exit. Therefore, the derivation will begin with the analysis of the inside of the drill string. Figure 7-1 shows the pressure, P, at any position in the inside of the drill string which is referenced from the surface to a depth h. The total depth of the well is H. The differential pressure, dP, in the upward flowing three phase flow occurs over an incremental distance of dh. This differential pressure can be approximated as [1]

$$dP = \gamma_{mix} \left[1 + \frac{f\, v^2}{2g\, D_i} \right] dh \qquad\qquad (7\text{-}1)$$

where P is fluid pressure (lb/ft^2, abs),

h is the reference depth (ft),

H is the total depth (ft)

γ_{mix} is the specific weight of the mixture of air (or other gas) , incompressible fluid, and the rock cuttings (lb/ft^3),

f is the Fanning friction factor,

V is the average velocity in the annulus (ft/sec),

D_i is the inside diameter of the drill string (ft),

g is the acceleration of gravity (32.2 ft/sec^2).
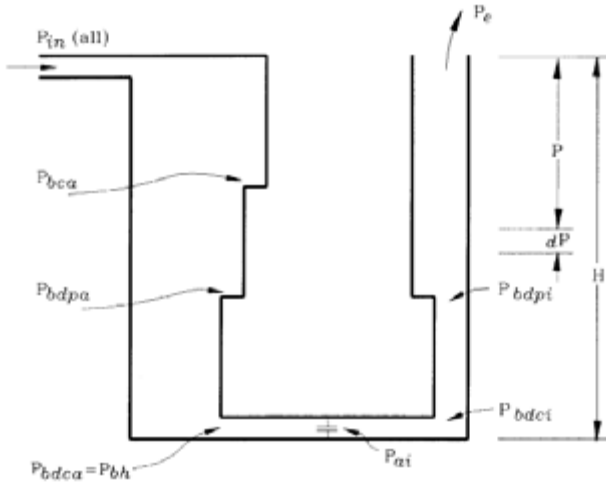
Figure 7-1: Schematic of reverse circulation. P_{in} is injection pressure into the top of the annulus, P_{bca} is pressure at bottom of casing in the annulus, P_{bdpa} is pressure at bottom of drill pipe in the annulus, P_{bdca} is pressure at bottom of drill collars in the annulus, P_{bh} is bottomhole pressure in the annulus, P_{ai} is pressure above drill bit inside the drill string, P_{bdci} is pressure at bottom of drill collars inside the drill string, P_{bdpi} is pressure at bottom of drill pipe inside the drill string, and P_e is pressure at the exit at the top of the inside of the drill string.

The first term on the right side of Equation 7-1 represents the incremental pressure change due to the hydrostatic weight of the column of fluids (with entrained rock cuttings) inside the drill string. The second term on the right side of Equation 7-1 represents the incremental pressure change due to the friction resistance to the flowing fluids in the drill string.

7.2.1 *Weight Rate of Flow of the Gas*

In order to carry out the derivation of the governing equations for reverse circulation, the weight rate of flow of air (or gas) to the well must be determined. Assuming the compressed air is provided by compressor(s), the weight rate of flow through the circulating system is determined from the atmospheric pressure and temperature of the air at the compressor location on the surface of the earth, and the characteristics of the compressor(s). For air, the atmospheric pressure for sea level and various elevations above sea level can be approximated for most of North America using the mid latitudes data given in Table 4-1.   These reference pressures are denoted as p_r. Thus, the atmospheric pressure of the air entering the primary compressor(s) is, p_{at}, and this pressure can be approximated as

$$p_{at} \approx p_r \tag{7-2}$$

where p_{at} is atmospheric pressure (psia),
  p_r is the reference atmospheric pressure (psia).
Similar data as that given in Table 4-1 for North America mid latitudes can be obtained for the other continents and latitudes around the world.

The above approximation is used when the actual atmospheric pressure at the drilling site has not been measured and recorded. The gas pressure, P_g, is

$$P_g = P_{at} = p_{at} \ 144 \tag{7-3}$$

where P_{at} is the atmospheric pressure (lb/ft^2, abs),
  P_g is the gas pressure (lb/ft^2, abs).
To determine the weight rate of flow through the primary compressor(s) the actual temperature of the atmosphere, t_{at}, must be used.   The absolute gas temperature, T_g, of the air entering the compressor(s) is

$$T_g = T_{at} = t_{at} + 459.67 \tag{7-4}$$

where t_{at} is the atmospheric temperature (˚F),
  T_{at} is absolute atmospheric temperature (˚R),
  T_g is absolute gas temperature (˚R).
Equation 4-11 in Chapter 4 gives the perfect gas law.   This equation relates absolute pressure, specific weight, and absolute temperature [1]. The equation is

$$\frac{P}{\gamma} = \frac{\mathbf{R} \ T}{S_g} \tag{7-5}$$

where P is pressure (lb/ft^2, abs),
  T is absolute temperature at any position in the annulus (˚R).
  γ is specific weight (lb/ft^3),
  $\mathbf{R}$ is the gas constant (53.3 ft-lb/lb-˚R),
  S_g is the specific gravity of the gas (S_g = 1.0 for air at standard conditions).

Substituting Equations 7-3 and 7-4 into Equation 7-5 and solving for the specific weight of the gas (in this case air) entering the compressor(s), γ_g, gives

$$\gamma_g = \frac{P_g\ S}{\mathbf{R}\ T_g} = \frac{P_{at}}{\mathbf{R}\ T_{at}} \qquad\qquad (7\text{-}6)$$

The weight rate of flow of the gas, $\dot{w}_g$, through the circulation system is

$$\dot{w}_g = \gamma_g\ Q_g \qquad\qquad (7\text{-}7)$$

where $\dot{w}_g$ is the weight rate of flow of gas (lb/sec),

Q_g is the volumetric flow rate of air into the circulation system (actual ft^3/sec). This volumetric flow rate is usually the flow rate entering the primary compressor(s) (see Chapter 4).

If the circulation system is natural gas from a pipeline and p_{pl} and t_{pl} are the pressure and temperature of the gas entering directly into the circulation system from the pipeline (or exiting the booster compressor from a pipeline), then, the absolute pressure of the gas, P_g, is

$$P_g = P_{pl} = p_{pl}\ 144 \qquad\qquad (7\text{-}8)$$

and the absolute temperature of the gas, T_g, is

$$T_g = T_{pl} = t_{pl} + 459.67 \qquad\qquad (7\text{-}9)$$

where p_{pl} is the pipeline pressure (psia),

P_{pl} is the pipeline pressure (lb/ft^2, abs),
t_{pl} is the pipeline temperature (°F),
T_{pl} is the absolute pipeline temperature (°R).

Substituting Equations 7-8 and 7-9 into Equation 7-6 the specific weight of the gas from a pipeline can be obtained. This is

$$\gamma_g = \frac{P_g\ S}{\mathbf{R}\ T_g} = \frac{P_{pl}\ S}{\mathbf{R}\ T_{pl}} \qquad\qquad (7\text{-}10)$$

Substituting the result from Equation 7-10 into Equation 7-7 gives the weight rate of flow of gas from a pipeline, where Q_g is the volumetric flow rate of natural gas from the pipeline at the pressure p_{pl} and temperate t_{pl}. Note that the volumetric flow rate in a pipeline is usually given in either scfm, or in acfm at the surface location temperature and must be converted to obtain the actual volumetric flow rate at p_{pl} and t_{pl}. In order to use natural gas from a pipeline it is necessary to place a meter run in the flow line leading from the pipeline. The meter run allows an accurate

determination of the volumetric flow of natural gas being supplied to the drilling operation.

7.2.2 Three-Phase Flow in the Drill String

The weight rate of flow of incompressible drilling fluid (usually drilling mud), $\dot{w}_m$, into the well is

$$\dot{w}_m = \gamma_m \, Q_m \qquad\qquad (7\text{-}11)$$

where $\dot{w}_m$ is the weight rate of flow of drilling mud (lb/sec),

γ_m is the specific weight of the drilling mud (lb/ft^3),
Q_m is the volumetric flow rate of drilling mud (ft^3/sec).

The weight rates of flow $\dot{w}_g$ and $\dot{w}_m$ enter the well through the top of the annulus space and flow to the bottom of the annulus where the two-phase flow entrains the rock cuttings. The weight rate of flow of solids, $\dot{w}_s$, entrained by the two-phase flow is

$$\dot{w}_s = \frac{\pi}{4} \, D_h^2 \, (62.4) \, (2.7) \, \kappa \qquad\qquad (7\text{-}12)$$

where $\dot{w}_s$ is the weight rate of flow of solids rock cuttings (lb/sec),

D_h is the diameter of the drilled hole (i.e., the bit diameter) (ft),
κ is the penetration rate (ft/sec).

In the above equation, the specific weight of fresh water is 62.4 lb/ft^3 and the average specific gravity of sedimentary rocks is 2.7. If igneous or metamorphic rocks are to be drilled, then an average value of 2.80 and 3.00, respectively, can be used if the actual specific gravity of the rocks to be drilled is not known [5].

The total weight rate of flow, $\dot{w}_t$, inside the drill string from the bottom of the string to the surface is

$$\dot{w}_t = \dot{w}_g + \dot{w}_m + \dot{w}_s \qquad\qquad (7\text{-}13)$$

The drilling muds and the rock cutting solids do not change volume when the pressure is changed. However, the air (or gas) does change volume when the pressure is changed and, therefore, the gas volume is a function of depth. Thus, the specific weight of the gas at any position inside the drill string is

$$\gamma = \frac{P \, S}{R \, T_{av}} \qquad\qquad (7\text{-}14)$$

where T_{av} is the average temperature of the gas over the depth interval (°R). This average temperature term is determined by taking the average of the sum of the geothermal temperature at the top and bottom of the depth interval. The geothermal temperature at depth, t_h, is determined from the approximate expression

$$t_h = t_r + \beta H \tag{7-15}$$

where t_r is the reference temperature (°F),

   t_h is the geothermal temperature at depth (°F),

   β is the geothermal gradient constant (°F/ft).

The reference surface geothermal temperature is assumed to be the temperatures given in Table 4-1 for sea level and various elevations above sea level. These temperatures represent North American mid latitudes year round averages. It is assumed that these temperatures also represent an average constant deep soil or rock temperatures near the surface of the earth at the elevations given in the table. The value of the geothermal gradient constant is determined from temperature logs of offset wells and other geophysical data. An average value of the geothermal gradient that can be used when the actual gradient has not been determined is 0.01°F/ft. The absolute reference surface geothermal temperature is

$$T_r = t_r + 459.67 \tag{7-16}$$

where T_r is the absolute reference temperature (°R). The absolute geothermal temperature at the bottom of the depth interval is

$$T_h = t_h + 459.67 \tag{7-17}$$

where T_h is the absolute bottomhole temperature (°R). The absolute average temperature, T_{av}, over the depth interval is given by

$$T_{av} = \frac{T_o + T_h}{2} \tag{7-18}$$

The relationship between the weight rate of flow of the gas and the specific weight and volumetric flow rate of gas at any position inside the drill string is given by

$$\dot{w}_g = \gamma_g Q_g = \gamma Q \tag{7-19}$$

Substituting Equations 7-6 and 7-14 into the two terms on the right side of Equation 7-19 gives a relationship between the known specific weight and volumetric flow rate at the surface and the specific weight of volumetric flow rate at any position inside the drill string. This is

$$\frac{P_g S}{R\, T_g} Q_g = \frac{P S}{R\, T_{av}} Q \tag{7-20}$$

Solving Equation 7-20 for Q yields

$$Q = \left(\frac{P_g}{P}\right)\left(\frac{T_{av}}{T_g}\right) Q_g \tag{7-21}$$

The three-phase flow of gas, incompressible fluid, and rock cuttings up the inside of the drill string can be described by a mixed specific weight term which is a function of its position inside the drill string. This mixed specific weight, γ_{mix}, is

$$\gamma_{mix} = \frac{\dot{w}_t}{\left(\dfrac{P_g}{P}\right)\left(\dfrac{T_{av}}{T_g}\right) Q_g + Q_m} \tag{7-22}$$

In the derivation of Equation 7-22 the volume of the solids (the rock cuttings) is assumed to be small and negligible relative to the volumes of the gas and the incompressible fluid in the mixture.

The velocity of this mixture changes as a function of its position inside the drill string. The velocity, V, of the three-phase flow inside the drill string is

$$V = \frac{Q + Q_m}{\dfrac{\pi}{4} D_i^2} \tag{7-23}$$

where D_i is the inside diameter of the drill string (ft),

Substituting Equation 7-21 into Equation 7-23 yields

$$V = \frac{\left(\dfrac{P_g}{P}\right)\left(\dfrac{T_{av}}{T_g}\right) Q_g + Q_m}{\dfrac{\pi}{4} D_i^2} \tag{7-24}$$

Substituting Equations 7-22 and 7-24 into Equation 7-1 yields

$$dP = \left[\frac{\dot{w}_t}{\left(\dfrac{P_g}{P}\right)\left(\dfrac{T_{av}}{T_g}\right) Q_g + Q_m}\right]$$

$$\times \left\{ 1 + \frac{f}{2g\, D_i} \left[\frac{\left(\dfrac{P_g}{P}\right)\left(\dfrac{T_{av}}{T_g}\right) Q_g + Q_m}{\dfrac{\pi}{4}\, D_i^2} \right]^2 \right\} \, dh \qquad (7\text{-}25)$$

Equation 7-25 contains only two independent variables, P and h.   All of the other terms in the equation are known constants. Separating variables in Equation 7-25 and integrating from the exit (at the surface) to the bottom of the inside of the drill string yields

$$\int_{P_e}^{P_{ai}} \frac{dP}{B_i\,(P)} = \int_0^H dh \qquad (7\text{-}26)$$

where P_e is the exit pressure at the top of the inside of the drill string (lb/ft^2, abs),

P_{ai} is the pressure above the bit inside the drill string (lb/ft^2, abs),

and

$$B_i\,(P) = \left[\frac{\dot{w}_t}{\left(\dfrac{P_g}{P}\right)\left(\dfrac{T_{av}}{T_g}\right) Q_g + Q_m} \right]$$

$$\times \left\{ 1 + \frac{f}{2g\, D_i} \left[\frac{\left(\dfrac{P_g}{P}\right)\left(\dfrac{T_{av}}{T_g}\right) Q_g + Q_m}{\dfrac{\pi}{4}\, D_i^2} \right]^2 \right\}$$

For this general derivation, the exit pressure, P_e, is atmospheric pressure at the end of the blooey line from the annulus (in the case of air or gas drilling) and at the end of the flow line from the annulus (in the case of aerated fluid drilling).

The Fanning friction factor f given in the above equation is determined by the standard fluid mechanics empirical expressions relating the friction factor to the Reynolds number, diameter, and absolute pipe roughness. In general, the values for Reynolds number, diameter, and absolute pipe roughness are known.   The classic expression for the Reynolds number is

$$N_R = \frac{D_i \, V}{v} \tag{7-27}$$

where D_i is the inside diameter for the drill string (ft),
     V is the velocity (ft/sec),
      v is the kinematic viscosity of the drilling fluid (ft²/sec).
    There are three flow conditions that can exist inside the drill string.   These are laminar, transitional, and turbulent flow conditions [1].
    The empirical expression for the Fanning friction factor for laminar flow conditions is

$$f = \frac{64}{N_R} \tag{7-28}$$

This equation can be solved directly once the Reynolds number is known.   In general, Equation 7-28 is valid for values for Reynolds numbers from 0 to 2,000.
    The empirical expression for the Fanning friction factor for transitional flow conditions is known as the Colebrook equation. the Fanning friction factor cannot be determined directly and must be solved by trial and error.   This empirical expression is

$$\frac{1}{\sqrt{f}} = -2 \, \log \left[\frac{\left(\dfrac{e}{D_i}\right)}{3.7} + \frac{2.51}{N_R \, \sqrt{f}} \right] \tag{7-29}$$

where e is the absolute roughness of the inside surface of the drill string (ft). Note the logarithm in the above equation is to the base ten. Equation 7-29 is valid for values of Reynolds numbers from 2,000 to 4,000.
    The empirical expression for the Fanning friction factor for turbulent flow conditions is known as the von Karman equation. This empirical expression is

$$f = \left[\frac{1}{2 \, \log \left(\dfrac{D_i}{e}\right) + 1.14} \right]^2 \tag{7-30}$$

Note the logarithm in the above equation is to the base ten. Equation 7-30 is valid for values of Reynolds numbers greater than 4,000.
    For follow-on calculations in the drill string the absolute roughness for commercial pipe, $e_p = 0.00015$ ft, will be used for the inside surfaces of the drill pipe and drill collars.

Equation 7-26 together with Equations 7-27 through 7-30 can be used in sequential integration steps starting at the top of the inside of the drill string (with the known exit pressure) and continuing for each subsequent change in cross-sectional area inside the drill string until the pressure above the drill bit inside the drill string is determined. These sequential calculation steps require trial and error solutions. The trial and error process requires the selection of the upper limit of the pressure in each integral on the right side of Equation 7-26. This upper limit pressure selection must give a right side integral solution that is equal to the left side integral solution.

7.2.3 *Three-Phase Flow Through the Bit*

There are three basic calculation techniques for determining the pressure change through the constriction of the single drill bit (or water course) orifice.

The first technique assumes that the mixture of incompressible fluid, gas, and rock cuttings passing through the single orifice has a high incompressible fluid volume fraction. Under these conditions the mixture is assumed to act as an incompressible fluid. Thus, borrowing from mud drilling technology, the pressure change through the drill bit, ΔP_b, can be approximated by [6, 7]

$$\Delta P_b \;=\; \frac{\dot{w}_t^2}{2g\,\gamma_{mixai}\,C^2\left(\dfrac{\pi}{4}\right)^2 D_{bi}^4} \tag{7-31}$$

where ΔP_b is pressure change (lb/ft^2),

γ_{mixai} is the mixture specific weight above the drill bit inside the drill string (lb/ft^3),

C is the fluid flow loss coefficient for drill bit orifices or nozzles (the value of this constant is dependent on the type of gas or aerated flow),

D_{bi} is the drill bit single orifice inside diameter (ft).

The pressure change obtained from Equation 7-31 is subtracted from the pressure above the drill bit inside the drill string P_{ai} obtained from Equation 7-26. The annulus bottomhole pressure, P_{bh}, is

$$P_{bh} \;=\; P_{ai} \;-\; \Delta P_b \tag{7-32}$$

where P_{bh} is bottomhole pressure (lb/ft^2, abs),

P_{ai} is pressure above the drill bit inside the drill string (lb/ft^2, abs).

For fluid mixtures that have a high gas volume fraction, the pressure above the drill bit inside the drill string can be approximated by [8]

$$P_{bh} \;=\; P_{ai} \;-\; \left[\frac{\dot{w}_t^2}{g\,A_{bi}^2}\right]\left[\frac{1}{\gamma_{mixbh}} \;-\; \frac{1}{\gamma_{mixai}}\right] \tag{7-33}$$

where A_{bi} is the cross-sectional area of the single drill bit orifice (ft^2),

γ_{mixbh} is the mixture specific weight at the bottom of the annulus (lb/ft^3).

Equation 7-33 must be solved by trial and error techniques since γ_{mixai} depends on the pressure P_{bh}. Note that this equation does not account for friction flow loss through the orifices and nozzles.

For fluid mixtures that are nearly all gas (with little incompressible fluid and rock cuttings) and subsonic flow conditions, the pressure above the drill bit inside the drill string is determined from [1]

$$2g \left(\frac{k}{k-1} \right) P_{bh} \, \gamma_{bh} \left[\left(\frac{P_{ai}}{P_{bh}} \right)^{\frac{2}{k}} - \left(\frac{P_{ai}}{P_{bh}} \right)^{\frac{k+1}{k}} \right] = \left(\frac{\dot{w}_g}{A_{bi}} \right)^2 \qquad (7\text{-}34)$$

where k is the ratio of specific heats for the gas (e.g., for air $k = 1.4$ and for natural gas $k = 1.28$).

γ_{bh} is the specific weight of the gas at the bottom of the annulus (lb/ft^3).

Equation 7-34 must be solved by trial and error for P_{bh}. Note that Equation 7-34 does not account for friction flow loss through the single drill bit orifice.

The above equations will generally yield results that show that for most practical parameters the annulus bottomhole pressure, P_{bh}, differs very little from the pressure above the drill bit inside the drill string, P_{ai}. Therefore, it can usually be assumed that

$$P_{bh} \approx P_{ai} \qquad (7\text{-}35)$$

7.2.4 *Two-Phase Flow in the Annulus*

The downward flow condition in the annulus is two phase. The differential pressure, dP, occurs over the incremental distance of dh. This differential pressure can be approximated as

$$dP = \gamma_{mix} \left[1 - \frac{f \, v^2}{2g \left(D_h - D_p \right)} \right] dh \qquad (7\text{-}36)$$

where D_h is the inside diameter of the annulus (ft) (the borehole),

D_p is the outside diameter of the drill string (pipe and collars) (ft).

The two phase flow of gas and incompressible fluid down the annulus space to the bottom of the well can be described by a mixed specific weight term which is a function of position in the annulus. This mixed specific weight term is

$$\gamma_{mix} = \frac{\dot{w}_g + \dot{w}_m}{\left(\dfrac{P_g}{P} \right) \left(\dfrac{T_{av}}{T_g} \right) Q_g + Q_m} \qquad (7\text{-}37)$$

The velocity of this mixture changes as a function of its position in the annulus. The velocity of the two phase flow in the annulus is

$$V = \frac{\left(\dfrac{P_g}{P}\right)\left(\dfrac{T_{av}}{T_g}\right) Q_g + Q_m}{\dfrac{\pi}{4}\left(D_h^2 - D_p^2\right)} \tag{7-38}$$

Substituting Equations 7-37 and 7-38 into Equation 7-36 yields

$$dP = \left[\frac{\dot{w}_g + \dot{w}_m}{\left(\dfrac{P_g}{P}\right)\left(\dfrac{T_{av}}{T_g}\right) Q_g + Q_m}\right]$$

$$\times \left\{1 - \frac{f}{2g\left(D_h - D_p\right)}\left[\frac{\left(\dfrac{P_g}{P}\right)\left(\dfrac{T_{av}}{T_g}\right) Q_g + Q_m}{\dfrac{\pi}{4}\left(D_h^2 - D_p^2\right)}\right]^2\right\} dh \tag{7-39}$$

Equation 7-39 contains only two independent variables, P and h. Separating variables in Equation 7-39 and integrating from the injection (at the surface) to bottom of the annulus yields

$$\int_{P_{in}}^{P_{bh}} \frac{dP}{B_a\,(P)} = \int_0^H dh \tag{7-40}$$

where

$$B_a\,(P) = \left[\frac{\dot{w}_g + \dot{w}_m}{\left(\dfrac{P_g}{P}\right)\left(\dfrac{T_{av}}{T_g}\right) Q_g + Q_m}\right]$$

$$\times \left\{ 1 - \frac{f}{2g \left(D_h - D_p \right)} \left[\frac{\left(\dfrac{P_g}{P} \right) \left(\dfrac{T_{av}}{T_g} \right) Q_g + Q_m}{\dfrac{\pi}{4} \left(D_h^2 - D_p^2 \right)} \right]^2 \right\}$$

where P_{in} is the injection pressure into the top of the annulus space (lb/ft², abs).

The Fanning friction factor f given in the above equation is determined by the standard fluid mechanics empirical expressions relating the friction factor to the Reynolds number, diameter (or hydraulic diameter), and absolute pipe roughness. In general, the values for Reynolds number, diameter, and absolute pipe roughness are known. The classic expression for the Reynolds number is

$$N_R = \frac{\left(D_h - D_p \right) V}{v} \tag{7-41}$$

where $D_h - D_p$ is the hydraulic diameter for the annulus (ft).

There are three flow conditions that can exist in the annulus. These are laminar, transitional, and turbulent flow conditions.

The empirical expression for the Fanning friction factor for laminar flow conditions is

$$f = \frac{64}{N_R} \tag{7-42}$$

This equation can be solved directly once the Reynolds number is known. Equation 7-42 is valid for values for Reynolds numbers from 0 to 2,000.

The empirical expression for the Fanning friction factor for transitional flow conditions is known as the Colebrook equation. The Fanning friction factor cannot be determined directly and must be solved by trial and error. This empirical expression is

$$\frac{1}{\sqrt{f}} = -2 \log \left[\frac{\left(\dfrac{e}{D_h - D_p} \right)}{3.7} + \frac{2.51}{N_R \sqrt{f}} \right] \tag{7-43}$$

where e is the absolute roughness of the annulus surface (ft). Equation 7-43 is valid for values of Reynolds numbers from 2,000 to 4,000.

The empirical expression for the Fanning friction factor for turbulent flow conditions is known as the von Karman equation. This empirical expression is

$$f = \left[\cfrac{1}{2\,\log\left(\cfrac{D_h - D_p}{e}\right) + 1.14} \right]^2 \qquad (7\text{-}44)$$

In general, Equation 7-44 is valid for values of Reynolds numbers greater than 4,000.

For follow-on calculations for flow in the annulus the absolute roughness for commercial pipe, $e_p = 0.00015$ ft, will be used for the outside surfaces of the drill pipe and drill collars, and inside surface of the casing. For a dual pipe drill string, the inside surfaces of the annulus in the drill string will also have the absolute roughness of commercial pipe. For conventional drill strings, the openhole surfaces of boreholes can be approximated with an absolute roughness, $e_{oh} = 0.01$ ft (i.e., this example value is the same as concrete pipe which approximates borehole surfaces in limestone and dolomite sedimentary rocks, or in similar competent igneous and metamorphic rocks, see Table 8-1).

Equation 7-40 together with Equations 7-41 through 7-44 can be used in sequential integration steps starting at the top of the annulus (with the known exit pressure) and continuing for each subsequent change in annulus cross-sectional area until the bottomhole pressure is determined. These sequential calculation steps usually require trial and error solutions. The trial and error process requires the selection of the upper limit of the pressure in each integral on the right side of Equation 7-40. This upper limit pressure selection must give a right side integral solution that is equal to the left side integral solution.

7.3 Air and Gas Drilling Model

Air drilling techniques are used extensively in reverse circulation drilling operations. This is particularly the case for reverse circulation drilling operations that utilize dual wall pipe. Dual wall pipe reverse circulation operations use either special skirted tri-cone drill bits (see Chapter 3) or air hammers with air hammer bits (see Chapter 11). In general, reverse circulation air drilling operations utilize either compressed air or compressed inert atmospheric air (stripped of most of its oxygen) as drilling gases.

Air (or gas) drilling is a special case of the theory derived in Section 7.2 above. The governing equations for air (or gas) drilling operations can be obtained by setting $Q_m = 0$ in the equations derived in Section 7.2.

Two phase flow conditions occur inside of the drill string (gas and solids). Setting $Q_m = 0$ in Equation 7-25 yields

$$dP = \left[\cfrac{\dot{w}_t}{\left(\cfrac{P_g}{P}\right)\left(\cfrac{T_{av}}{T_g}\right) Q_g} \right]$$

$$\times \left\{ 1 + \frac{f}{2g\,D_i} \left[\frac{\left(\dfrac{P_g}{P}\right)\left(\dfrac{T_{av}}{T_g}\right) Q_g}{\dfrac{\pi}{4}\,D_i^2} \right]^2 \right\} dh \qquad\qquad (7\text{-}45)$$

where

$$\dot{w}_t = \dot{w}_g + \dot{w}_s$$

The exit pressure in reverse circulation air (or gas) drilling operations is atmospheric pressure, P_{at}, at the top of the inside of the drill string.   Separating variables in Equation 7-45 yields

$$\int_{P_{at}}^{P_{ai}} \frac{dP}{B_i\,(P)} = \int_0^H dh \qquad\qquad (7\text{-}46)$$

where

$$B_i\,(P) = \left[\frac{\dot{w}_t}{\left(\dfrac{P_g}{P}\right)\left(\dfrac{T_{av}}{T_g}\right) Q_g} \right] \left\{ 1 + \frac{f}{2g\,D_i} \left[\frac{\left(\dfrac{P_g}{P}\right)\left(\dfrac{T_{av}}{T_g}\right) Q_g}{\dfrac{\pi}{4}\,D_i^2} \right]^2 \right\}$$

Using Equations 7-5, 7-6 or 7-10, 7-7 and 7-12, Equation 7-46 can be rearranged to give

$$\int_{P_{at}}^{P_{ai}} \frac{P\,dP}{\left(P^2 + b_i\,T_{av}^2\right)} = \frac{a_i}{T_{av}} \int_0^H dh \qquad\qquad (7\text{-}47)$$

where

$$a_i = \left(\frac{S}{R}\right)\left[1 + \left(\frac{\dot{w}_s}{\dot{w}_g}\right) \right] \qquad\qquad (7\text{-}48)$$

$$b_i = \frac{f}{2g\, D_i} \left(\frac{\mathbf{R}}{S}\right)^2 \frac{\dot{w}_g^2}{\left(\frac{\pi}{4}\right)^2 D_i^4} \tag{7-49}$$

In the above form, both sides of Equation 7-47 can be integrated. Using Equations 7-48 and 7-49 the solution to Equation 7-47 is

$$\left| \frac{1}{2} \ln \left(P^2 + b_i\, T_{av}^2\right) \right|_{P_{at}}^{P_{ai}} = \frac{a_i}{T_{av}} \left| h \right|_{0}^{H} \tag{7-50}$$

Evaluating Equation 7-50 at the limits and rearranging the results gives

$$\ln \left[\frac{P_{ai}^2 + b_i\, T_{av}^2}{P_{at}^2 + b_i\, T_{av}^2} \right] = \frac{2\, a_i}{T_{av}} H \tag{7-51}$$

Raising both sides of Equation 7-51 to the natural exponential exponent gives

$$\frac{P_{ai}^2 + b_i\, T_{av}^2}{P_{at}^2 + b_i\, T_{av}^2} = e^{\frac{2\, a_i\, H}{T_{av}}} \tag{7-52}$$

Equation 7-52 can be rearranged and a solution obtained for P_{ai}. This yields

$$P_{ai} = \left[\left(P_{at}^2 + b_i\, T_{av}^2\right) e^{\frac{2\, a_i\, H}{T_{av}}} - b_i\, T_{av}^2 \right]^{0.5} \tag{7-53}$$

    The flow of gas to the well must be sufficient to carry solid rock cuttings from the bottom of the annulus to the surface. Therefore, it is assumed that the flow condition in both the inside of drill string and the annulus is turbulent. The empirical von Karman relationship for determining the approximate Fanning friction factor for the inside of the drill string is

$$f = \left[\frac{1}{2\, \log \left(\dfrac{D_i}{e}\right) + 1.14} \right]^2 \tag{7-54}$$

For follow-on calculations for flow in the drill string the absolute roughness for commercial pipe, e_p = 0.00015 ft, will be used for the inside surfaces of the drill pipe and drill collars.

Equation 7-53 together with Equations 7-48, 7-49 and 7-54 can be used in sequential calculation steps starting at the top of the inside of the drill string and continuing for each subsequent change in cross-sectional area in the inside of the drill string until the pressure above the drill bit inside of the drill string is determined.

There is a single water course in reverse circulation drill bits. Using Equation 7-53 the pressure at the bottom of the inside of the drill string, P_{ai}, is obtained. The pressure at the bottom of the annulus, P_{bh}, can be obtained by trial and error using the expression

$$2g \left(\frac{k}{k-1} \right) P_{bh} \, \gamma_{bh} \left[\left(\frac{P_{ai}}{P_{bh}} \right)^{\frac{2}{k}} - \left(\frac{P_{ai}}{P_{bh}} \right)^{\frac{k+1}{k}} \right] = \left(\frac{\dot{w}_g}{A_{bi}} \right)^2 \qquad (7\text{-}55)$$

Note that Equation 7-55 does not account for friction flow loss through the single drill bit orifice.

The above equations will generally yield results that show that for most practical parameters the annulus bottomhole pressure, P_{bh}, differs very little from the pressure above the drill bit inside the drill string, P_{ai}. Therefore, it can usually be assumed that

$$P_{bh} \approx P_{ai} \qquad (7\text{-}56)$$

The flow in the annulus is single phase flow (air or gas). Setting $Q_m = 0$ in Equations 7-39 yields

$$dP = \left[\frac{\dot{w}_g}{\left(\dfrac{P_g}{P} \right) \left(\dfrac{T_{av}}{T_g} \right) Q_g} \right]$$

$$\times \left\{ 1 - \frac{f}{2g \, (D_h - D_p)} \left[\frac{\left(\dfrac{P_g}{P} \right) \left(\dfrac{T_{av}}{T_g} \right) Q_g}{\dfrac{\pi}{4} \, (D_h^2 - D_p^2)} \right]^2 \right\} dh \qquad (7\text{-}57)$$

Separating variables in Equation 7-57 yields

$$\int_{P_{in}}^{P_{bh}} \frac{dP}{B_a\,(P)} = \int_0^H dh \tag{7-58}$$

where

$$B_a\,(P) = \left[\frac{\dot{w}_g}{\left(\frac{P_g}{P}\right)\left(\frac{T_{av}}{T_g}\right)Q_g}\right]\left\{1 - \frac{f}{2g\,(D_h - D_p)}\left[\frac{\left(\frac{P_g}{P}\right)\left(\frac{T_{av}}{T_g}\right)Q_g}{\frac{\pi}{4}\,(D_h^2 - D_p^2)}\right]^2\right\}$$

Using Equations 7-5, 7-6 or 7-10, and 7-7, Equation 7-58 can be rearranged to give

$$\int_{P_{in}}^{P_{bh}} \frac{P\,dP}{\left(P^2 - b_a\,T_{av}^2\right)} = \frac{a_a}{T_{av}} \int_0^H dh \tag{7-59}$$

where

$$a_a = \frac{S}{R} \tag{7-60}$$

$$b_a = \frac{f}{2g\,(D_h - D_p)}\left(\frac{R}{S}\right)^2 \frac{\dot{w}_g^2}{\left(\frac{\pi}{4}\right)^2 (D_h^2 - D_p^2)^2} \tag{7-61}$$

In the above form, both sides of Equation 7-59 can be integrated. Using Equations 7-60 and 7-61 the solution to Equation 7-59 is

$$\left|\, \frac{1}{2}\, \ln\left(P^2 - b_a\,T_{av}^2\right)\,\right|_{P_{in}}^{P_{bh}} = \frac{a_a}{T_{av}}\, \left|\, h \,\right|_0^H \tag{7-62}$$

Evaluating Equation 7-62 at the limits and rearranging the results gives

$$\ln\left[\frac{P_{bh}^2 - b_a\,T_{av}^2}{P_{in}^2 - b_a\,T_{av}^2}\right] = \frac{2\,a_a}{T_{av}}\,H \tag{7-63}$$

Raising both sides of Equation 7-63 to the natural exponential exponent gives

$$\frac{P_{bh}^2 - b_a T_{av}^2}{P_{in}^2 - b_a T_{av}^2} = e^{\frac{2 \, a_a \, H}{T_{av}}}$$

(7-64)

Equation 7-64 can be rearranged and a solution obtained for P_{in}. This yields

$$P_{in} = \left[\frac{P_{bh}^2 + b_a T_{av}^2 \left(e^{\frac{2 \, a_a \, H}{T_{av}}} - 1 \right)}{e^{\frac{2 \, a_a \, H}{T_{av}}}} \right]^{0.5}$$

(7-65)

The empirical von Karman relationship for determining the approximate Fanning friction factor for the annulus is

$$f = \left[\frac{1}{2 \, \log \left(\dfrac{D_h - D_p}{e} \right) + 1.14} \right]^2$$

(7-66)

For follow-on calculations for flow in the annulus the absolute roughness for commercial pipe, $e_p = 0.00015$ ft, will be used for the outside surfaces of the drill pipe and drill collars, and inside surface of the casing. For a dual pipe drill string, the inside surfaces of the annulus in the drill string will also have the absolute roughness of commercial pipe. For conventional drill strings, the openhole surfaces of boreholes can be approximated with an absolute roughness, $e_{oh} = 0.01$ ft (i.e., this example value is the same as concrete pipe which approximates borehole surfaces in limestone and dolomite sedimentary rocks, or in similar competent igneous and metamorphic rocks, see Table 8-1).

Equation 7-65 together with Equations 7-60, 7-61 and 7-66 can be used in sequential calculation steps starting at the bottom of the annulus and continuing for each subsequent change in cross-sectional area in the annulus until the surface injection pressure is determined.

7.4 Aerated Fluid Drilling Model

The aerated fluid drilling governing equations are very little changed from the reverse circulation general derivation given in Section 7.2. The flow condition inside of the drill string is three phase flow (gas, fluid, and solids). The exit pressure in aerated fluid drilling operations is the atmospheric pressure, P_{at}. Therefore, Equation 7-26 becomes

$$\int_{P_{at}}^{P_{ai}} \frac{dP}{B_i\ (P)} = \int_0^H dh \tag{7-67}$$

where

$$B_i\ (P) = \left[\frac{\dot{w}_t}{\left(\dfrac{P_g}{P}\right)\left(\dfrac{T_{av}}{T_g}\right) Q_g + Q_m} \right]$$

$$\times \left\{ 1 + \frac{f}{2g\ D_i} \left[\frac{\left(\dfrac{P_g}{P}\right)\left(\dfrac{T_{av}}{T_g}\right) Q_g + Q_m}{\dfrac{\pi}{4}\ D_i^2} \right]^2 \right\}$$

The Fanning friction factor f given in the above equation is determined by the standard fluid mechanics empirical expressions relating the friction factor to the Reynolds number, diameter, and absolute pipe roughness. In general, the values for Reynolds number, diameter, and absolute pipe roughness are known. The classic expression for the Reynolds number is

$$N_R = \frac{D_i\ V}{v} \tag{7-68}$$

There are three flow conditions that can exist inside the drill string. These are laminar, transitional, and turbulent flow conditions.

The empirical expression for the Fanning friction factor for laminar flow conditions is

$$f = \frac{64}{N_R} \tag{7-69}$$

This equation can be solved directly once the Reynolds number is known. In general, Equation 7-69 is valid for values for Reynolds numbers from 0 to 2,000.

The empirical expression for the Fanning friction factor for transitional flow conditions is known as the Colebrook equation. the Fanning friction factor cannot be determined directly and must be solved by trial and error. This empirical expression is

$$\frac{1}{\sqrt{f}} = -2 \log \left[\frac{\left(\dfrac{e}{D_i}\right)}{3.7} + \frac{2.51}{\mathbf{N_R} \sqrt{f}} \right] \tag{7-70}$$

Equation 7-70 is valid for values of Reynolds numbers from 2,000 to 4,000.

The empirical expression for the Fanning friction factor for turbulent flow conditions is known as the von Karman equation. This empirical expression is

$$f = \left[\frac{1}{2 \log \left(\dfrac{D_i}{e}\right) + 1.14} \right]^2 \tag{7-71}$$

Equation 7-71 is valid for values of Reynolds numbers greater than 4,000.

For follow-on calculations for flow in the drill string the absolute roughness for commercial pipe, $e_p = 0.00015$ ft, will be used for the inside surfaces of the drill pipe and drill collars.

Equation 7-67 together with Equations 7-68 through 7-71 can be used in sequential trial and error integration steps starting at the top of the inside of the drill string (with the known exit pressure) and continuing for each subsequent change in cross-sectional area inside the drill string until the pressure above the drill bit inside the drill string is determined. These sequential change in drill string cross-sectional area until the pressure at the bottom of the inside drill string is determined.

The mixture of incompressible fluid and the gas passing through the single orifice has a high incompressible volume fraction and can, therefore, be assumed to act physically as an incompressible mixture. Thus, borrowing from mud drilling technology, the pressure change through the drill bit, ΔP_b, can be approximated by

$$\Delta P_b = \frac{\dot{w}_t^2}{2g \, \gamma_{mixai} \, C^2 \left(\dfrac{\pi}{4}\right)^2 D_{bi}^4} \tag{7-72}$$

The value of C represents the aerated fluid flow loss coefficient of the drill bit orifice. Experiments have shown that aerated fluid flow is ver complex. The gas and incompressible fluid components in the aerated mixture appear to alternate their passage through the orifice. This means the aerated flow through the orifice is inefficient. The value of C for aerated fluid flow should be taken as 0.70 to 0.85. The pressure change obtained from Equation 7-72 is subtracted from the pressure above the drill bit inside the drill string P_{ai} obtained from Equation 7-67. The annulus bottomhole pressure, P_{bh}, is

$$P_{bh} \;=\; P_{ai} \;-\; \Delta P_b \tag{7-73}$$

For fluid mixtures that have a high gas volume fraction, the pressure above the drill bit inside the drill string can be approximated by

$$P_{bh} \;=\; P_{ai} \;-\; \left[\frac{\dot{w}_t^2}{g\,A_{bi}^2}\right]\left[\frac{1}{\gamma_{\mathrm{mixbh}}} \;-\; \frac{1}{\gamma_{\mathrm{mixai}}}\right] \tag{7-74}$$

Equation 7-74 must be solved by trial and error techniques since γ_{mixai} depends on the pressure P_{bh}. Note that this equation does not account for friction flow loss through the orifices and nozzles.

The above equation will yield calculations that show that for most practical parameters the bottomhole pressure, P_{bh}, will differ very little from the pressure above the drill bit opening inside the drill string, P_{ai}. Therefore, it can usually be assumed that

$$P_{bh} \;\approx\; P_{ai} \tag{7-75}$$

The flow condition in the annulus is two phase (gas and fluid) flow. Equation 7-75 becomes

$$\int_{P_{in}}^{P_{bh}} \frac{dP}{B_a\,(P)} \;=\; \int_0^H dh \tag{7-76}$$

where

$$B_a\,(P) \;=\; \left[\frac{\dot{w}_g \;+\; \dot{w}_m}{\left(\dfrac{P_g}{P}\right)\left(\dfrac{T_{av}}{T_g}\right) Q_g \;+\; Q_m}\right]$$

$$\times\left\{1 \;-\; \frac{f}{2g\,(D_h \;-\; D_p)} \left[\frac{\left(\dfrac{P_g}{P}\right)\left(\dfrac{T_{av}}{T_g}\right) Q_g \;+\; Q_m}{\dfrac{\pi}{4}\,(D_h^2 \;-\; D_p^2)}\right]^2\right\}$$

The Fanning friction factor f given in the above equation is determined by the standard fluid mechanics empirical expressions relating the friction factor to the

Reynolds number, diameter (or hydraulic diameter), and absolute pipe roughness.   In general, the values for Reynolds number, diameter, and absolute pipe roughness are known. The classic expression for the Reynolds number is

$$N_R = \frac{\left(D_h - D_p\right) V}{v}$$

(7-77)

There are three flow conditions that can exist in the annulus. These are laminar, transitional, and turbulent flow conditions.

The empirical expression for the Fanning friction factor for laminar flow conditions is

$$f = \frac{64}{N_R}$$

(7-78)

This equation can be solved directly once the Reynolds number is known.   In general, Equation 7-78 is valid for values for Reynolds numbers from 0 to 2,000.

The empirical expression for the Fanning friction factor for transitional flow conditions is known as the Colebrook equation. The Fanning friction factor cannot be determined directly and must be solved by trial and error.   This empirical expression is

$$\frac{1}{\sqrt{f}} = -2 \log \left[\frac{\left(\dfrac{e}{D_h - D_p}\right)}{3.7} + \frac{2.51}{N_R \sqrt{f}} \right]$$

(7-79)

Equation 7-79 is valid for values of Reynolds numbers from 2,000 to 4,000.

The empirical expression for the Fanning friction factor for turbulent flow conditions is known as the von Karman equation. This empirical expression is

$$f = \left[\frac{1}{2 \log \left(\dfrac{D_h - D_p}{e}\right) + 1.14} \right]^2$$

(7-80)

Equation 7-80 is valid for values of Reynolds numbers greater than 4,000.

For follow-on calculations for flow in the annulus the absolute roughness for commercial pipe, $e_p = 0.00015$ ft, will be used for the outside surfaces of the drill pipe and drill collars, and inside surface of the casing. For a dual pipe drill string, the inside surfaces of the annulus in the drill string will also have the absolute

roughness of commercial pipe. For conventional drill strings, the openhole surfaces of boreholes can be approximated with an absolute roughness, $e_{oh} = 0.01$ ft (i.e., this example value is the same as concrete pipe which approximates borehole surfaces in limestone and dolomite sedimentary rocks, or in similar competent igneous and metamorphic rocks, see Table 8-1).

Equation 7-76 together with Equations 7-77 through 7-80 can be used in sequential trial and error integration steps starting at the bottom of the annulus (with the known pressure at the bottom of the annulus) and continuing for each subsequent change in annulus cross-sectional area until the injection pressure is determined.

References

1. Daugherty, R. L., Franzini, J. B., and Finnemore, E. J., *Fluid Mechanics with Engineering Applications*, Eighth Edition, McGraw-Hill, 1985.

2. Brown, K. E., and Beggs, H. D., *The Technology of Artificial Lift Methods*, Vol. 1, PennWell Books, 1977.

3. Brown, K. E., et al, *The Technology of Artificial Lift Methods*, Vol. 2a, PennWell Books, 1980.

4. Personal communications with Stefan Miska, Department of Petroleum Engineering, University of Tulsa, January 1999.

5. Lapedes, D. H., *McGraw-Hill Encyclopedia of the Geological Sciences*, McGraw-Hill, 1978.

6. Gatlin, C., *Petroleum Engineering: Drilling and Well Completions*, Prentice-Hall, 1960.

7. Bourgoyne, A. T., Millheim, K. K., Chenevert, M. E., and Young, F. S., *Applied Drilling Engineering*, SPE, First Printing, 1986.

8. Guo, B., Hareland, G., and Rajtar, J., "Computer Simulation Predicts Unfavorable Mud Rate and Optimum Air Injection Rate for Aerated Mud Drilling," SPE Paper 26892, Presented at the SPE Eastern Regional Conference and Exhibition, Pittsburgh, Pennsylvania, November 2-4, 1993.

This page intentionally left blank.

Chapter

Eight

Air, Gas, and Unstable Foam Drilling

Deep drilling operations with air and gas drilling technology are used in the recovery of oil and natural gas, recovery of geothermal steam and hot water, and for some mining and geotechnical projects. In the late 1970's, it was estimated that air and gas drilling technology was being used on only about 10 percent of the deep wells drilled and completed [1, 2]. Today, most of North America's oil and natural gas producing fields are mature and are sensitive to formation damage caused by traditional mud drilling operations. The existence of formation damage has lead to the development of underbalanced drilling completion operations. Even though underbalanced drilling and completion operations have applications in mud drilling operations, the vast majority of these operations are air and gas drilling technology based. Currently, it is estimated that about 30 percent of the oil and natural gas recovery drilling and completion operations utilize air and gas drilling technology. As more oil and natural gas producing fields mature this percentage will increase.

This chapter outlines the steps and methods used to plan a successful deep air and gas drilling operation. This chapter also illustrates the application of these steps and methods to the planning of a typical deep drilling operations. The objective of these steps and methods is to allow engineers and scientists to cost effectively plan their drilling operations and ultimately select their drilling rig, compressor, and other auxiliary air and gas equipment. The additional benefit of this planning process, is that the data created by the process can later be used to control the drilling operations as the actual operations progress. Air and gas drilling operations are different from traditional mud drilling operations and require more intensive attention on the part of the on-site drilling operation supervisors.

8.1 Deep Well Drilling Planning

Deep air and gas drilling operations use a variety of compressed gases as the drilling fluid. The majority of the operations use compressed air. In some oil and natural gas recovery operations it is necessary to drill with a gas that will not support downhole combustion. This objective has been realized by using natural gas and using oxygen stripped atmospheric air (inert air) as drilling gases. The use of natural gas from a pipeline as a drilling gas has been in use since the 1930's. The use of inert air is a new technology and has become commercially viable in the last five years. In this chapter atmospheric air, natural gas, and oxygen stripped atmospheric air will be used as the example drilling gases.

The basic planning steps for a deep well are as follows:

1. Determine the geometry of the borehole section or sections to be drilled with air or other gases (i.e., openhole diameters, the casing inside diameters, and depths).
2, Determine the geometry of the associated drill strings for the sections to be drilled with air or other gases (i.e., drill bit size and type, the drill collar size, drill pipe size, and maximum depth).
3. Determine the type of rock formations to be drilled and estimate the anticipated drilling rate of penetration. Also, estimate the quantity and depth location of any formation water that might be encountered.
4. Determine the elevation of the drilling site above sea level, the temperature of the air during the drilling operation, and the approximate geothermal temperature.
5. Establish the objective of the air (or other gases) drilling operation:
   • To decrease or eliminate formation damage,
   • To allow underbalanced drilling operations.
6. Determine whether direct or reverse circulation techniques will be used to drill the well.
7. Determine the required approximate minimum volumetric flow rate of air (or other gases) to carry the rock cuttings from the well when drilling at its maximum depth.
8. Select the contractor compressor(s) that will provide the drilling operation with a volumetric flow rate of air that is greater than the required minimum volumetric flow rate (use a factor of safety of at least 1.2).
9. Using the compressor(s) air volumetric flow rate to be injected into the well, determine the bottomhole and surface injection pressures as a function of drilling depth (over the interval to be drilled). Also, determine the maximum power required by the compressor(s) and the available maximum derated power from the prime mover(s).
10. Determine the approximate volume of fuel required by the compressor(s) to drill the well.
11. In the event formation water is encountered, determine the approximate volumetric flow rate of "mist" injection water needed to allow formation water or formation oil to be carried from the well during the drill operation.
12. Determine the approximate volumetric flow rate of formation water or formation oil that can be carried from the well during the drilling operation (assuming the injected air is saturated for bottomhole conditions).

In Chapter 6 the basic direct circulation drilling planning governing equations have been derived and summarized. In Chapter 7 the basic reverse circulation drilling planning governing equations have been derived and summarized. In this chapter only direct circulation illustrative examples are discussed. Reverse circulation examples are discussed in Chapter 5.

8.2 Minimum Volumetric Flow Rate

There are various research groups that over the past three decades have developed several mathematical and empirical models for use in attempting to describe the gas flow mechanics of air and gas drilling operations. Each of the models developed over the decades have made a variety of assumptions concerning the specific weight of the gas and rock cuttings mixture created at the bottom of the hole as the drill bit advances.

8.2.1 *Discussion of Theories*

In 1957, R. R. Angel developed the first field useful mathematical and empirical model for air and gas drilling operations [3, 4]. This initial work by Angel was supported by industry (i.e., Phillips Petroleum Company) and continues to be useful to drilling supervisors and drilling engineers even today. This modeling effort drew heavily from the large body of engineering knowledge related to industrial pneumatic conveying (the transport of solids by flowing air). Thus, this model was developed from the outset to be an engineering tool. The major air and rock cuttings mixture assumption made in this model was that the rock cutting particles move together from the bottom of the borehole to the surface with the velocity of the local air flow. Through the decades other researchers have improved on this model [5].

In 1981, interest in air and gas drilling technology found its way into academic research [6, 7]. This research was carried out at University of Tulsa and Pennsylvania State University and was supported by U. S. Department of Energy. In this effort experimental work was carried out to ascertain the relationship between the motion of the air and the rock cuttings particles. This experimental work found that the vertical drilling annulus geometry with an upward flow of air and rock cuttings chokes in much the same way as industrial pneumatic conveying. This experimental work also showed that under simulated practical drilling conditions small rock particles flow with a velocity that was near that of the air. This research effort resulted in a model that was a variation on the original Angel work. The slip of the rock cutting particles relative to the air flow was ignored. The model resulted in a air and rock mixture value that was nearly the same as that given by the original Angel model.

In 1983, the first model was proposed that took into account a rock cutting particle velocity that was different from that of the air flow [8]. This model can yield an improved air and rock mixture value which can improve the accuracy of the predictions from the model. The problem with this model is that the individual average velocities of the particles are difficult to determine analytically for inclusion in this model.

In 1992, additional theoretical work was carried out to further refine the inclusion of the effect of rock cuttings particle velocities [9]. This model also suffered from the difficulty involved in determining average particle velocities.

8.2.2 *Engineering Practice*

Figures 8-1 and 8-2 illustrate typical slug and non-slug (cluster) flow of particles in industrial pneumatic conveying [10].   From the theoretical and experimental studies in the pneumatic conveying literature it is clear that the higher the velocity of the gas in the vertical flow line, the more the particle velocities approach the average velocity of the gas flow.

Figure 8-1: Schematic of dense solids phase flow known as "slugging" [10].

Figure 8-2: Schematic of dense solids phase flow known as "non-slugging" or "clusters" [10].

For an air or gas drilling operation, this is also the desirable transport situation. However, the larger the particles being transported the greater the slip velocity of the particle relative to the gas flow velocity. Further, as the gas volumetric flow rate decreases, the cutting particles begin to slip in the gas flow transporting them. This causes the rock cuttings particles to transition from the dilute phase solids flow condition (where the particles are spread out in the gas) to that of a dense phase solids flow condition (where the particles are clumped together) (see Figures 8-1 and 8-2). When this occurs, the rock cuttings slow (relative to the gas flow) and the pressure forcing the gas to flow in the flow line increases. This condition is known as choking.

Figure 8-3 can be used to further understand the choking condition. The figure is a schematic representation of empirical data. The line AB in the figure refers to zero solids flow in the pipe (in our case the annulus). The family of curves of increasing solids flow rates are also presented in the figure. A fixed solids weight rate flow, $\dot{G}_1$, at a high gas velocity (at point C), the solids volumetric concentration is low (well below one percent) and the particles are generally uniformly dispersed. This is dilute phase solids flow.
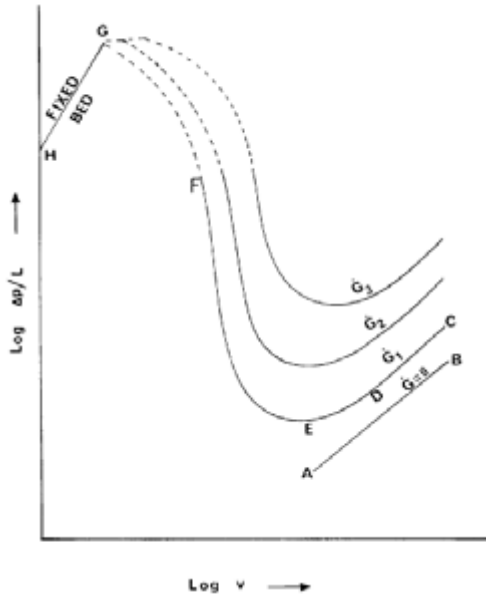
Figure 8-3: Solids flow characteristics in vertical pneumatic conveying. Note that the units of $\dot{G}$ is lb/sec [10].

As has been seen in Chapter 6 and 7, the pressure gradient in fully developed vertical conveying is made up of two components, a wall frictional loss component and a hydrostatic weight component. As the velocity of the gas is decreased for this

fixed solids flow rate, the solids volumetric concentration in the pipe increases and the wall frictional loss decreases. Thus, the line CD shows an overall pressure gradient decrease with the decrease in gas velocity. This line indicates that the decrease in frictional loss component is significantly higher than the increase in the hydrostatic component. As the gas velocity is further decreased beyond point D, the hydrostatic component becomes more significant and the resulting curve defines a minimum at point E. A further decrease in gas flow rate (and velocity) leads to an increase in the pressure gradient. This is shown as the curve EF and indicates the dominance of the hydrostatic component. The solids concentration along curve EF is high and is dense phase solids flow.

In general, for air and gas drilling systems the choking point can be defined as the inflection point along the curve EF. Fortunately, the choking condition is rarely observed in actual vertical air or gas drilling operations. This is due to two important air and gas drilling operational facts. 1) As the drill bit advances, the rotating drill string breaks up larger rock particles into smaller more easily transported particles when the larger particles collide with the drill string surface. This breaking action occurs all along the drill string length, but is likely very pronounced around and just above the drill collars. This mechanism has been observed in vertical drilling operations where downhole pneumatic motors have been tested (drilling with no drill string rotation and with rotation) [11]. 2) As will be seen in the illustrative examples to follow, the actual volumetric flow rate used in an air drilling operation is determined by the primary compressor output(s) to be used at the drilling location. If the approximate minimum volumetric flow rate to the borehole is determined to be 1,000 scfm, and the compressors to be used to supply the compressed air are rated at 700 scfm each, then two compressors will be used to supply the air. Thus, the actual volumetric flow rate to the well is 1,400 scfm. This gives a factor of safety (above the minimum required) of 1.4. It is standard engineering practice to use a volumetric flow rate factor of safety of at least 1.2. This approximate minimum factor of safety (i.e., 1.2) is also used in determining the actual volumetric flow rate to be taken from a natural gas pipeline for a gas drilling operation. The use of primary compressor flow rates that are above the minimum volumetric flow rate would result in an operational point for the air and gas system somewhere along the curve CD.

8.2.3 *Engineering Planning Graphs*

In order to initiate the well planning process given above, the geometry of the well must be defined and the anticipated drilling penetration rate estimated. Figures with graphs can be prepared for the approximate minimum volumetric flow rates for a variety of deep well and drill string geometric configurations. These figures are presented in Appendix E. The calculations for such figures are carried out using API Mechanical Equipment Standards standard atmospheric conditions (i.e., 14.696 psia and 60˚F, see Chapter 4). Thus, the figures developed will give the minimum volumetric flow rate values for air drilling using air at these API standard atmospheric conditions (see Chapter 4). Once such figures are developed, the minimum volumetric flow rates can be determined for any other atmospheric conditions (surface locations) from the minimum volumetric flow rates given for API standard conditions. The minimum volumetric flow rate values are calculated

assuming a minimum bottomhole kinetic energy per unit volume of no less than 3.0 ft-lb/ft^3. Also, it is assumed that the drilling is in sedimentary rock formations with an average specific gravity of 2.7. These deep boreholes figures are developed for a uniform borehole diameter with the top two thirds of the depth assumed to be cased and the bottom one third assumed to be openhole. The basic equations used to determine the minimum volumetric flow rate are derived in Chapter 6.

Illustrative Examples 8.1 and 8.2 describe the implementation of the basic planning steps Nos. 1 through 7 given in Section 8.1.

Illustrative Example 8.1 The borehole to be used in this illustrative example will be used as a basic example in this chapter and in Chapters 9 and 10. The 7 7/8 inch diameter borehole is to be drilled out of the bottom of API 8 5/8 inch diameter, 28.00 lb/ft nominal, Grade H-40, casing set to 7,000 ft (see Figure 8-4 for well casing and openhole geometric configuration). The inside diameter of this casing is 8.017 inches. The openhole interval below the casing shoe is to be drilled from 7,000 ft to 10,000 ft. The drill string is made up of 500 ft of 6 3/4 inch by 2 13/16 inch drill collars above the drill bit and API 4 1/2 inch, 16.60 lb/ft nominal, EU-S135, NC50 (IF) to the surface. The drilling is to be carried out at a surface location at sea level (assume API Mechanical Standards standard atmospheric conditions, see Chapter 4). The regional geothermal gradient is approximately 0.01°F/ft. The anticipated drilling rate of penetrations in a sandstone and limestone sequence (sedimentary rock) is approximately 60 ft/hr. The blooey line for this drilling operation is a single horizontal section of casing that runs 200 ft from just above the BOP stack to the burn pit. The casing used for the blooey line is API 8 5/8 inch, 24.00 lb/ft nominal, Grade J-55, casing. The inside diameter of this casing is 8.097 inches, Two gate valves are in the blooey line at the end of the line that is attached to the BOP stack. These valves have an inside diameter of 7 9/16 inch. This is a typical borehole geometric configuration for an oil or natural gas recovery well. This illustrative example will demonstrate how the approximate minimum volumetric flow rate is determined.

The approximate minimum volumetric flow rate will be determined for the deepest depth in the interval to be drilled. This is 10,000 ft. This will give the largest minimum volumetric flow rate for the well. Although the details of the borehole and drill string geometric configuration are important for determining accurate pressures in the annulus and inside the drill string (particularly, bottomhole and injection pressures), these details are not as important in obtaining the approximate minimum volumetric flow rate.

For this example, this slightly larger inside diameter will be ignored relative to the openhole 7.875 inch borehole. Thus, the entire length of the borehole will be assumed to have a uniform inside diameter of 7.875 inch. Instead of the actual depth to the bottom of the casing for this particular example, a depth of two thirds of the total depth will be used for the cased section of the well (~6,667 ft). Further, for this calculation the major and minor friction losses in the blooey line will be ignored (ignoring the Tee at the top of the annulus and the blooey line length). The drill pipe outside diameter changes at the tool joints will be ignored and the 500 ft of drill collar outside diameter change will ignored. Therefore, the outside of the

drill string will be assumed to have a uniform dimension of a 4 1/2 inch outside diameter from top to bottom.
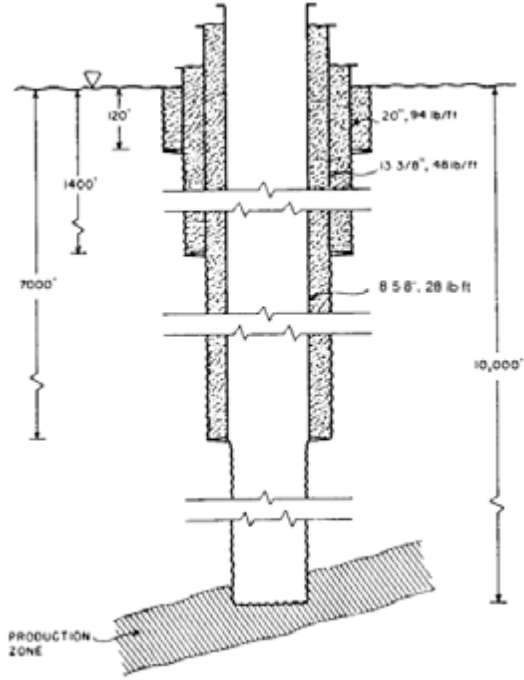
Figure 8-4: Illustrative Example 8.1 casing and openhole well geometric configuration.

In order to be able to calculate air drilling conditions at other surface elevations above sea level, all calculations to obtain values like the minimum volumetric flow rate are carried out for a baseline sea level atmosphere. For these calculations and most of those in this treatise the baseline sea level atmosphere is the API standard conditions (see Chapter 4). These conditions are a pressure of 14.696 psia and a temperature of 60°F. Thus, the pressure of the gas (in this case air) that flows into the compressor, P_{at}, is

$$p_{at} = 14.696 \text{ psia}$$

$$P_{at} = p_{at} \; 144$$

$$P_{at} = 2,116 \text{ lb/ft}^2 \text{ abs}$$

where p_{at} is atmospheric pressure (psia),
  P_{at} is atmospheric pressure (lb/ft^2, abs).

The atmospheric temperature of the air that flows into the compressor, T_{at}, that will supply the drilling operation is

$$t_{at} = 60°\,F$$

$$T_{at} = t_{at} + 459.67$$

$$T_{at} = 519.67°\,R$$

where t_{at} is atmospheric temperature (°F),
   T_{at} is absolute atmospheric temperature (°R).
Thus, P_g and T_g become

$$P_g = P_{at} = 2{,}116 \text{ lb/ft}^2 \text{ abs}$$

$$T_g = T_{at} = 519.67°\,R$$

where P_g is the gas pressure (lb/ft^2, abs),
   T_g is the absolute gas temperature (°R).
Using Equation 4-11, the specific weight of the gas entering the compressor is

$$\gamma_g = \frac{(2{,}116)\,(1.0)}{(53.36)\,(519.67)}$$

$$\gamma_g = 0.0763 \text{ lb/ft}^3$$

where γ_g is the specific weight of the gas (lb/ft^3),
   R is the gas constant for API standard conditions air (53.36 ft-lb/lb-°R),
   S_g is the specific gravity of the particular gas used (for API standard conditions
      air $S_g = 1.0$).
   To determine the minimum volumetric flow rate of air at API standard conditions, it is necessary to select (by trial and error) a volumetric flow rate, q_g (scfm), that will give a kinetic energy per unit volume of 3.0 ft-lb/ft^3 in the annulus at the bottom of the 10,000 ft depth borehole. Kinetic energy per unit volume should be a minimum at the bottom of the annulus. The volumetric flow rate selected (trial and error) is (at API standard conditions)

$$q_g = 1{,}588.8 \text{ scfm}$$

where q_g is the gas volumetric flow rate in the circulation system (scfm or acfm).
The value of Q_g is

$$Q_g = \frac{q_g}{60}$$

$$Q_g = 26.48 \text{ ft}^3/\text{sec}$$

where Q_g is the gas volumetric flow rate (ft³/sec). The weight rate of flow of the gas, $\dot{w}_g$, is

$$\dot{w}_g = \gamma_g Q_g$$

$$\dot{w}_g = 0.0763 \ (26.48)$$

$$\dot{w}_g = 2.019 \text{ lb/sec}$$

where $\dot{w}_g$ is the weight rate of flow of the gas in the circulation system (lb/sec).
    The borehole diameter is

$$d_h = 7.875 \text{ inches}$$

$$D_h = \frac{d_h}{12}$$

$$D_h = 0.656 \text{ ft}$$

where d_h is the inside diameter of the borehole (inches),
        D_h is the inside diameter of the borehole (ft).
    The estimated drilling rate of penetration is 60 ft/hr. The weight rate of flow of the solid rock cuttings, $\dot{w}_s$, in the annulus is

$$\dot{w}_s = \left(\frac{\pi}{4}\right) D_h^2 \ (62.4) \ S_s \left[\frac{\kappa}{(60) \ (60)}\right] \tag{8-1}$$

where κ is the drilling rate (ft/hr),
        S_s is the specific gravity of the solid rock cuttings.
Therefore, $\dot{w}_s$ is

$$\dot{w}_s = \left(\frac{\pi}{4}\right) (0.656)^2 \ (62.4) \ (2.7) \left[\frac{60}{(60) \ (60)}\right]$$

$$\dot{w}_s = 0.950 \text{ lb/sec}$$

The temperature of the rock formations near the surface (geothermal surface temperature) is estimated to be the approximate average year round temperature at that location on the earth's surface. Table 4-1 gives 59°F for the sea level average year round reference temperatures for the mid latitudes   of North America (or see Appendix D). Therefore, the absolute reference temperature of the rock formations at the surface, T_r, is

$$t_r = 59° F$$

$$T_r = t_r + 459.67$$

$$T_r = 518.67° R$$

where t_r is the reference temperature (°F),
    T_r is the absolute reference temperature (°R).
    It is assumed that two thirds of the borehole depth is cased. Thus, the temperature at a depth of 6,667 ft must be determined. This temperature is determined from the surface geothermal temperature, the geothermal gradient, and the depth to the bottom of the cased section of the borehole. For this example, and for the figures in Appendix E, the geothermal gradient is approximated to be 0.01°F/ft. Thus, the temperature at the bottom of the cased section of the borehole, T_c, is

$$T_c = T_r + 0.01 \, (6,667)$$

$$T_c = 585.34° R$$

where T_c is the absolute temperature at the bottom of the casing (°R).
    The average temperature of this cased section of the borehole is

$$T_{avc} = \frac{T_r + T_c}{2}$$

$$T_{avc} = 552.00° R$$

where T_{avc} is the average absolute temperature over the depth to the bottom of the cased section of the borehole (°R).
    The drill pipe outside diameter of the drill pipe in the cased section of the borehole is

$$d_p = 4.50 \text{ inches}$$

$$D_p = \frac{d_p}{12}$$

$$D_p = 0.375 \text{ ft}$$

where d_p is the outside diameter of the drill pipe (inches),
     D_p is the outside diameter of the drill pipe (ft).
     In what follows, Equations 6-52, 6-53, 6-57, and 6-58 from Chapter 6 will be used to complete this illustrative example.   These equations will be used in sequential calculations through the annulus.   The values of the constants and the pressures obtained will be denoted by the subscripts ac or ao for the annulus cased section and the annulus openhole section, respectively.
     The Fanning friction factor, f_{ac}, for flow in the cased section of the annulus is determined from the von Karman empirical relationship for turbulent flow conditions [12]. This empirical relationship is given by Equation 6-58. This is

$$f_{ac} = \left[\frac{1}{2 \log\left(\dfrac{D_h - D_p}{e_p}\right) + 1.14} \right]^2$$

where e_p is the absolute surface roughness of the cased section of the annulus (ft). Both surfaces of the annulus in the cased section of the borehole is commercial pipe surfaces (i.e., the inside surface of the casing and the outside surface of the drill pipe). Thus, the absolute surface roughness of the annulus is the commercial pipe roughness. Therefore, e_p, is given as 0.00015 ft [12]. Equation 6-58 becomes

$$f_{ac} = \left[\frac{1}{2 \log\left(\dfrac{0.656 - 0.375}{0.00015}\right) + 1.14} \right]^2$$

$$f_{ac} = 0.017$$

With the above values Equations 6-52 and 6-53 become, respectively,

$$a_{ac} = \left(\frac{1.0}{53.36}\right)\left[1 + \left(\frac{0.950}{2.019}\right)\right]$$

$$a_{ac} = 0.028$$

and

$$b_{ac} = \frac{0.017}{2\,(32.2)\,(0.656\,-\,0.375)}\left(\frac{53.36}{1.0}\right)^2 \frac{(2.019)^2}{\left(\frac{\pi}{4}\right)^2\left[(0.656)^2\,-\,(0.375)^2\right]^2}$$

$$b_{ac} = 209.1$$

Equation 6-57 is used to obtain the pressure at the bottom of sequential sections of a borehole that has a different geometric configuration and/or friction loss characteristics. Thus, for this illustrative example, Equation 6-57 can be used to find the pressure in the annulus at the bottom of the cased section of this borehole. This pressure is

$$P_{ac} = \left\{\left[(2,116)^2 + 209.1\,(552.00)^2\right]e^{\frac{2\,(0.028)\,(10,000)}{552.00}} - 209.1\,(552.00)^2\right\}^{0.5}$$

$$P_{ac} = 8,309 \ \text{lb/ft}^2 \ \text{abs}$$

$$p_{ac} = \frac{P_{ac}}{144}$$

$$p_{ac} = 57.7 \ \text{psia}$$

The bottom one-third of the borehole depth is an openhole.   Thus, the temperature at a depth of 10,000 ft must be determined. This temperature is

$$T_{bh} = T_r + 0.01\,(10,000)$$

$$T_{bh} = 618.67^\circ\text{R}$$

The average temperature of this openhole section of the borehole is

$$T_{avo} = \frac{T_c + T_{bh}}{2}$$

$$T_{avo} = 602.01^\circ\text{R}$$

The bottom one third of this example borehole is an openhole section.   The openhole annulus wall absolute surface roughness for the sandstone and limestone sequence, e_{oh}, can be assumed to be similar to the inside surface of a commercial concrete pipe. Similar correlations can be made for openhole borehole walls in a variety of rock types and rock physical characteristics. Rock types can be igneous, sedimentary, and metamorphic.   The rock physical characteristics vary between

competent low fractures to non-competent highly fractured. Table 8-1 correlates borehole wall inside absolute surface roughness values for these rock formations categories with the absolute surface roughness values of known engineering pressure conduits [12].

Using Table 8-1, the borehole wall absolute surface roughness for this example borehole is assumed to be approximately

$$e_{oh} = 0.01 \text{ ft}$$

Table 8-1: Openhole wall absolute surface roughness for a rock formation types.

Rock Formation Types	Surface Roughness (ft)

Competent, low fracture
   - Igneous (e.g., granite, basalt)
   - Sedimentary (e.g., limestone, sandstone)
   - Metamorphic (e.g., gneiss)
	0.001 to 0.02

Competent, medium fracture
   - Igneous (e.g., granite, basalt)
   - Sedimentary (e.g., limestone, sandstone)
   - Metamorphic (e.g., gneiss)
	0.02 to 0.03

Poor competence, highly fracture
   - Igneous (e.g, breccia)
   - Sedimentary (e.g., sandstone, shale)
   - Metamorphic (e.g., schist)
	0.03 to 0.04

The inner surface of this annulus section is the outer surface of the drill pipe body which has the absolute surface roughness of commercial steel pipe, e_p. The absolute surface roughness of commercial steel pipe is

$$e_p = 0.00015 \text{ ft}$$

The average absolute surface roughness of the annulus is approximated by using a surface area weight average relationship between the openhole surface area and its roughness and the outside surface of the drill string and its roughness. Thus, the value for e_{avo} is

$$e_{avo} = \frac{e_{oh} \left(\dfrac{\pi}{4}\right) D_h^2 H_o + e_p \left(\dfrac{\pi}{4}\right) D_p^2 H_o}{\left(\dfrac{\pi}{4}\right) D_h^2 H_o + \left(\dfrac{\pi}{4}\right) D_p^2 H_o}$$

The term H_o cancels and the above reduces to

$$e_{avo} = \frac{e_{oh} \left(\dfrac{\pi}{4}\right) D_h^2 + e_p \left(\dfrac{\pi}{4}\right) D_p^2}{\left(\dfrac{\pi}{4}\right) D_h^2 + \left(\dfrac{\pi}{4}\right) D_p^2} \tag{8-2}$$

Thus, e_{avo}, is

$$e_{avo} = \frac{(0.01) \left(\dfrac{\pi}{4}\right) (0.656)^2 + (0.00015) \left(\dfrac{\pi}{4}\right) (0.375)^2}{\left(\dfrac{\pi}{4}\right) (0.656)^2 + \left(\dfrac{\pi}{4}\right) (0.375)^2}$$

$$e_{avo} = 0.0076 \text{ ft}$$

Equation 6-58 becomes

$$f_{ao} = \left[\frac{1}{2 \ \log \left(\dfrac{0.656 - 0.375}{0.0076} \right) + 1.14} \right]^2$$

$$f_{ao} = 0.055$$

With the above values Equations 6-52 and 6-53 become, respectively,

$$a_{ao} = \left(\frac{1.0}{53.36}\right) \left[1 + \left(\frac{0.950}{2.019}\right) \right]$$

$$a_{ao} = 0.028$$

and

$$b_{ac} = \frac{0.055}{2\,(32.2)\,(0.656 - 0.375)} \left(\frac{53.36}{1.0}\right)^2 \frac{(2.019)^2}{\left(\frac{\pi}{4}\right)^2 \left[(0.656)^2 - (0.375)^2\right]^2}$$

$$b_{ac} = 674.6$$

Equation 6-57 becomes

$$P_{bh} = \left\{ \left[(8,309)^2 + 674.6\,(602.01)^2\right] e^{\frac{2\,(0.028)\,(10,000)}{602.01}} - 674.6\,(602.01)^2 \right\}^{0.5}$$

$$P_{bh} = 13,450 \ \text{lb/ft}^2 \ \text{abs}$$

$$p_{bh} = \frac{P_{bh}}{144}$$

$$p_{bh} = 93.4 \ \text{psia}$$

Using Equation 4-11, the specific weight of the air at bottomhole pressure and temperature conditions is

$$\gamma_{bh} = \frac{(13,450)\,(1.0)}{(53.36)\,(618.67)}$$

$$\gamma_{bh} = 0.407 \ \text{lb/ft}^3$$

The volumetric flow rate of the gas at the bottom of the borehole in the annulus, Q_{bh}, is

$$Q_{bh} = \frac{(0.0763)\,(26.48)}{0.407}$$

$$Q_{bh} = 4.964 \ \text{ft}^3/\text{sec}$$

The velocity of the gas at the bottom of the borehole in the annulus, V_{bh}, is

$$V_{bh} = \frac{4.964}{\left(\frac{\pi}{4}\right)\left[(0.656)^2 - (0.375)^2\right]}$$

$$V_{bh} = 21.8 \text{ ft/sec}$$

In Chapter 1 an analytic comparison was made between an air drilling example and a mud drilling example. Using Equations 1-1 and 1-2 from that discussion, the kinetic energy per unit volume at the bottom of the borehole in the annulus, KE_{bh}, is

$$\rho_{bh} = \frac{0.407}{32.2}$$

$$\rho_{bh} = 0.0126 \ \frac{lb - sec^2}{ft^4}$$

$$KE_{bh} = \frac{1}{2} \ (0.0126) \ (21.8)^2$$

$$KE_{bh} = 3.003 \ \frac{ft - lb}{ft^3}$$

The trial and error process for the above requires an iterative selection of the value of q_g until the kinetic energy at the bottom of the borehole in the annulus is equal to 3.0 ft-lb/ft³. In this example the value of q_g that will give a kinetic energy value equal to 3.0 ft-lb/ft³ is 1,588.8 scfm. Figure E-13 in Appendix E gives the air minimum volumetric flow rates for a 4 1/2 inch drill pipe in a 7 7/8 inch borehole. Figure E-13 shows the approximate minimum volumetric flow rate of 1,588.8 scfm for the drilling rate of 30 ft/hr and depth of 10,000 ft. This example demonstrates how these figures Appendix E were developed.

Illustrative Example 8.2 As in Illustrative Example 8.1, a 7 7/8 inch diameter borehole (drill bit diameter) is to be drilled out of the bottom of API 8 5/8 inch diameter, 28.00 lb/ft nominal, Grade H-40, casing set to 7,000 ft (see Figure 8-4 for well casing and openhole geometric configuration). The openhole interval below the casing shoe is to be drilled from 7,000 ft to 10,000 ft. The drill string is made up of 500 ft of 6 3/4 inch by 2 13/16 inch drill collars above the drill bit and API 4 1/2 inch, 16.60 lb/ft nominal, EU-S135, NC50 (IF) to the surface. The drilling is to be carried out at a surface elevation location of 4,000 ft above sea level where the actual atmospheric temperature is 60°F. The regional geothermal gradient is approximately 0.01°F/ft. The anticipated drilling rate of penetrations in the sedimentary rock formations is 60 ft/hr. The blooey line for this drilling operation is a single horizontal section of casing that runs 200 ft from just above the BOP stack to the burn pit. The casing used for the blooey line is API 8 5/8 inch, 24.00 lb/ft nominal, Grade J-55, casing. Two gate valves are in the blooey line at the end of the line that is attached to the BOP stack. These valves have an inside diameter of 7 9/16 inch. Determine the direct circulation approximate minimum volumetric flow rate for this drilling operation.

It is only necessary to obtain the approximate minimum volumetric flow rate for a drilling operation. The borehole is never drilled with only the minimum

volumetric flow rate. Compressor units are selected to give a total volumetric flow rate that exceeds the determined minimum volumetric flow rate.

Figure E-13 gives the minimum volumetric flow rates of air for a 7 7/8 inch borehole with a 4 1/2 inch drill pipe. The flow rate is determined for the maximum depth of the well which is 10,000 ft. The annulus around the drill collars at the bottom of the drill string will have higher air velocities than in the annulus around the drill pipe. This means the lowest velocity in the annulus is at the bottom of the drill pipe. Therefore, by making the assumption that the borehole has no drill collars, a conservative estimate is made of the approximate minimum volumetric flow rate for the borehole. Therefore, Figure E-13 can be used to determine the approximate minimum volumetric flow rate of air for this example drilling operation.

Using Figure E-13, the approximate minimum volumetric flow rate for drilling at a depth of 10,000 ft is approximately 1,588.8 scfm (also found in Illustrative Example 5.1).   This is the minimum flow rate for sea level (API standard conditions) air. But the drilling location is at 4,000 ft above sea level and the drilling operation actual atmospheric temperature is 60° F.   Thus, the above minimum volumetric flow rate must be adjusted for the atmospheric conditions that exist at the drilling location (i.e., to obtain the actual cubic feet per minute, acfm). In Illustrative Example 8.1 the specific weight of air at API standard conditions was found to be 0.0763 lb/ft³. Table 4-1 gives an average atmospheric pressure of 12.685 psia for a surface location of 4,000 ft above sea level (mid latitudes North America) (also see Appendix D). The actual atmospheric pressure for the air at the drilling location (that will be utilized by the compressor), P_{at}, is

$$p_{at} \;=\; 12.685 \;\; \text{psia}$$

$$P_{at} \;=\; p_{at} \; 144$$

$$P_{at} \;=\; 1{,}827 \;\; \text{lb/ft}^2 \;\; \text{abs}$$

The actual atmospheric temperature of the air at the drilling location, T_{at}, (that will be used by the compressor) is

$$t_{at} \;=\; 60^{\circ}\,\text{F}$$

$$T_{at} \;=\; t_{at} \;+\; 459.67$$

$$T_{at} \;=\; 519.67^{\circ}\,\text{R}$$

Thus, P_g and T_g become

$$P_g \;=\; P_{at} \;=\; 1{,}827 \;\; \text{lb/ft}^2 \;\; \text{abs}$$

$$T_g \;=\; T_{at} \;=\; 519.67^{\circ}\,\text{R}$$

Using Equation 4-11, the specific weight of the gas entering the compressor is

$$\gamma_g \;=\; \frac{(1,827)\;(1.0)}{(53.36)\;(519.67)}$$

$$\gamma_g \;=\; 0.0659 \;\; \text{lb/ft}^3$$

Note the above specific weight value can also be obtained from Figure D-4 in Appendix D.

The approximate minimum volumetric flow rate for this illustrative example adjusted for the actual atmospheric conditions at the drilling location can be determined by equating the weight rate of flow of the air at the two atmospheric conditions. This reduces to

$$q_g \;=\; 1,588.8 \left(\frac{0.0763}{0.0659} \right)$$

$$q_g \;=\; 1,840 \;\; \text{acfm}$$

The above volumetric flow rate is the adjusted minimum value for the atmospheric conditions at this drilling location (4,000 ft above sea level).

8.3 Injection Pressure and Selection of Compressor Equipment

The planning process given in Section 8.1 requires that the borehole requirements be compared to the capabilities of the compressor units available. Specifically, these comparisons are made between: a) the borehole volumetric flow rate and the compressor volumetric flow rate capability, b) the borehole injection pressure (using the compressor volumetric flow rate) and the pressure capability of the compressor, and c) the horsepower required by the compressor and the input capability of the prime mover. This will be demonstrated in the examples that follow.

8.3.1 *Selection of Compressor Equipment*

The volumetric flow rate capabilities of the available compressor units must be compared with the approximate minimum volumetric flow rate required by the geometric configuration of the well and the anticipated parameters of the drilling operation.

Illustrative Example 8.3a describes the implementation of the basic planning step No. 8 given in Section 8.1.

Illustrative Example 8.3a Select the appropriate compressor system for the direct circulation drilling operations data given in Illustrative Example 8.2a. The selection of the appropriate compressor will be made from the example compressor systems listed in Section 4.7 of Chapter 4. In Illustrative Example 8.2a it was found that the drilling location adjusted minimum volumetric flow rate of air for the

7 7/8 inch diameter, 10,000 ft deep borehole was approximately 1,840 acfm (for a surface drilling location of 4,000 ft above sea level).

There are several possible candidate compressor units that could be used to provide the compressed air supply for this example drilling operation. Two of these candidates are discussed below.

Figures 4-22 and 4-23 show skid mounted Gardner Denver Model WEN, two-stage, reciprocating piston primary unit and the Gardner Denver Model MDY, two-stage, reciprocating piston booster compressor unit. The primary compressor has a volumetric flow rate capability of 700 acfm at the 4,000 ft surface elevation location. Thus, four primary compressor units would be needed for this operation (or 2,800 acfm) and would give a volumetric flow rate factor of safety of 1.52.

Figure 4-24 shows a semi-trailer mounted unit which has a MAN Model GHH-CF2466, two-stage, rotary screw primary compressor and an Ariel Model JGJ/2, two stage, reciprocating piston booster compressor integrated so that both compressors can be driven by one large prime mover. The primary compressor has an approximate volumetric flow rate capability of 1,727 acfm at the 4,000 ft of surface elevation location. This compressor system is rated at ASME standard atmospheric conditions. The specific weight of air at ASME standard conditions (i.e., 14.7 psia, 68°F, and 36 percent relative humidity) is 0.0750 lb/ft^3 (see Chapter 4). Therefore, the volumetric flow rate output of this compressor unit adjusted to the reference API standard conditions is

$$q = \left(\frac{0.0750}{0.0763}\right)(1,727)$$

$$q = 1,698 \text{ scfm}$$

or the above can be read as

$$q = 1,698 \text{ acfm}$$

Thus, two of these compressor units would be required for the drilling operation (or 3,396 acfm) and would give a volumetric flow rate factor of safety of 1.85.

Figure 4-25 shows a semi-trailer mounted unit that has a Dresser Clark Model CFB-4, four stage, reciprocating piston primary compressor. This four stage compressor system is operated as a combined primary-booster system with a continuous maximum output pressure of 1,000 psig. This compressor has a volumetric flow rate capability of 1,200 acfm at the 4,000 ft of surface elevation location. Thus, two compressor units would be required for the drilling operation (or 2,400 acfm) and would give a volumetric flow rate factor of safety of 1.30.

Of these three candidate compressor systems, the semi-trailer mounted unit with the Dresser Clark Model CFB-4, four stage, reciprocating piston compressor system is selected for follow-on example calculations. This system should be more economic than the other candidates since it is a single unit four stage reciprocating piston compressor and two of these units have an overall factor of safety nearest to the required 1.2. Also, this compressor system is capable of continuous operation at

pressures up to 1,000 psig and intermittent operation at pressures up to 1,200 psig. These high pressures are usually not encountered in air and gas drilling operations. But sometimes unforeseen high back pressures are encountered while drilling (e.g., high influx of formation water or producing fluids) and such pressures have to be managed in order not to lose the well. Also, if more volumetric flow rate is required (to lift formation fluids) during the drilling operation, a third compressor unit can placed in service (all deep drilling operations have a standby compressor available). The addition of this third compressor will also result in higher injection pressures.

8.3.2 *Major and Minor Losses and Injection Pressure*

Once the compressor system units have been selected for a given drilling operation, the actual volumetric flow rate capability of the compressor system will be known. Knowing the actual volumetric flow rate to be injected into the top of the drill string, calculations can be made to determine the injection pressure required by the individual compressors in the system. It is important to accurately determine the injection pressure. Once the injection pressure has been determined, this value is compared to the maximum output capability of the compressor. If the obtained injection pressure value is less than the maximum pressure capability of the compressors, then the compressor system is tentatively capable of providing compressed air to the drilling operation. To complete the assessment of the compressor system, the prime mover of the compressor must be checked to ascertain if it is capable of producing the power needed to produce the required pressure. The power output of a prime mover is sensitive to its surface elevation location. The power output of a prime mover will decrease as the surface elevation location above sea level is increased. Therefore, it is necessary to compare the horsepower needed by the compressor to the horsepower available by the prime mover at its surface elevation location.

The calculation procedure for determining the injection pressure requires working from the exit to the blooey line (i.e., the known atmospheric pressure) upstream through the circulation system to injection pressure. During this calculation procedure, all the pressure positions in the annulus and inside the drill string where there are changes in annulus and drilling string geometry will be determined. Of particular interest to the oil and natural gas recovery industry and the geothermal fluids recovery industry is the determination of the bottomhole pressure. In underbalanced drilling operations it is very important to design the drill string used to drill the well. A properly designed drill string will yield the bottomhole pressure lower than the pore pressure in the fluids producing formation. Thus, accurate pressure prediction in the circulation system is needed to assure that the drilling operation will not cause formation damage.

In order to calculate accurate circulation pressures (i.e., bottomhole and injection pressures) it is necessary to utilize all possible standard fluid mechanics major and minor friction loss terms in carrying out these calculations. Descriptions of these major and minor losses are detailed in the fluid mechanics literature [12]. These losses will be explained and utilized in the calculations used in the illustrative examples that follow.

Illustrative Example 8.3b describes the implementation of the basic planning step No. 9 given in Section 8.1.

    Illustrative Example 8.3b Determine the bottomhole and injection pressures while drilling at 10,000 ft of depth for the drilling operations described in Illustrative Examples 8.2 and 8.3a. Compare the injection pressure to the maximum pressure capability of the selected semi-trailer mounted Dresser Clark Model CFB-4, four-stage, reciprocating piston compressor.　Also, determine the horsepower required by the compressor and the maximum derated horsepower of the Caterpillar Model D398 prime mover. Compare the compressor required horsepower and the maximum derated horsepower from the prime mover.

   General Data

    Table 4-1 gives an average atmospheric pressure of 12.685 psia for a surface location of 4,000 ft above sea level (mid latitudes North America) (also see Appendix D). The actual atmospheric pressure for the air at the drilling location (that will be utilized by the compressor), P_{at}, is

$$p_{at} \ = \ 12.685 \ \text{psia}$$

$$P_{at} \ = \ p_{at} \ 144$$

$$P_{at} \ = \ 1{,}827 \ \text{lb/ft}^2 \ \text{abs}$$

The actual atmospheric temperature of the air at the drilling location (that will be used by the compressor), T_{at}, is

$$t_{at} \ = \ 60^\circ \text{F}$$

$$T_{at} \ = \ t_{at} \ + \ 459.67$$

$$T_{at} \ = \ 519.67^\circ \text{R}$$

Thus, P_g and T_g become

$$P_g \ = \ P_{at} \ = \ 1{,}827 \ \text{lb/ft}^2 \ \text{abs}$$

$$T_g \ = \ T_{at} \ = \ 519.67^\circ \text{R}$$

Using Equation 4-11, the specific weight of the gas entering the compressor is

$$\gamma_g \ = \ \frac{(1{,}827) \ (1.0)}{(53.36) \ (519.67)}$$

$$\gamma_g \ = \ 0.0659 \ \text{lb/ft}^3$$

Note the above specific weight value can also be obtained from Figure D-4 in Appendix D.

The selected reciprocating piston compressor has an actual volumetric flow rate of 1,200 acfm. Two of these compressor are required to adequately drill this well. Therefore, the actual volumetric flow rate to the well while drilling the openhole interval from 7,000 ft to 10,000 ft will be 2,400 acfm. Thus,

$$q_g = 2,400 \text{ acfm}$$

The value of Q_g is

$$Q_g = \frac{q_g}{60}$$

$$Q_g = 40.00 \text{ ft}^3/\text{sec}$$

The weight rate of flow of the gas, $\dot{w}_g$, is

$$\dot{w}_g = \gamma_g Q_g$$

$$\dot{w}_g = 0.0659 \ (40.00)$$

$$\dot{w}_g = 2.635 \text{ lb/sec}$$

The openhole interval of this well has an inside diameter of the drill bit. The drill bit diameter, D_h, is

$$d_h = 7.875 \text{ inches}$$

$$D_h = \frac{d_h}{12}$$

$$D_h = 0.656 \text{ ft}$$

The estimated drilling rate of penetration is 60 ft/hr. From Equation 8-1, $\dot{w}_s$, in the annulus is

$$\dot{w}_s = \left(\frac{\pi}{4}\right) (0.656)^2 \ (62.4) \ (2.7) \left[\frac{60}{(60)\ (60)}\right]$$

$$\dot{w}_s = 0.950 \text{ lb/sec}$$

The temperature of the rock formations near the surface (geothermal surface temperature) is estimated to be the approximate average year-round temperature at that location on the earth's surface. Table 4-1 gives 44.74° F for average year round temperature for a surface elevation location of 4,000 ft above sea level (for mid latitudes of North America, or see Appendix D). Therefore, the absolute reference temperature of the rock formations at the surface, T_r, is

$$t_r = 44.74^{\circ}\,F$$

$$T_r = t_r + 459.67$$

$$T_r = 504.41^{\circ}\,R$$

Blooey Line

The calculation procedure must be initiated with the known atmospheric pressure at the exit to the blooey line. It is assumed that the air will exit the well annulus and enter the blooey line with the surface geothermal temperature of 44.74° F (or 504.41°R). It is further assumed that the temperature of the air flow in the blooey line does not change until it exits the blooey line (i.e., the steel blooey line will be at nearly the surface geothermal temperature at steady state flow conditions). The standard isothermal gas pipeline flow equation can be used to determine the major loss due to pipe wall friction [12]. This equation can be adjusted to also include the minor loss for the T turn at the top of the annulus into the blooey line and to include the losses due to the two valves at the entrance end of the blooey line. Therefore, the equation for the pressure in the air (or gas) flow at the entrance end of the blooey line, P_b, can be approximated as

$$P_b = \left[\left(f_b\,\frac{L_b}{D_b} + K_t + \Sigma\,K_v \right) \left(\frac{w_g^2\,\mathbf{R}\,T_r}{g\,A_b^2\,S_g} \right) + P_{at}^2 \right]^{0.5} \qquad (8\text{-}3)$$

where f_b is the Fanning friction factor for the blooey line,
  L_b is the length of the blooey line (ft),
  D_b is the inside diameter of the blooey line (ft),
  A_b is the cross-sectional area of the inside of the blooey line (ft^2),
  K_t is the minor loss factor for the T turn at the top of the annulus,
  K_v is the minor loss factor for the valves in the blooey line.
  The loss factor for K_t for the single blind Tee at the top of the annulus is approximately 25 (see Figures 8-5 and 8-6, direct circulation only).   These approximate minor loss values for Tee's have been obtained from air and gas drilling operations in the San Juan Basin and in the Permian Basin. The gate valves (with the gate in the full open position) in a blooey line have a open inside diameter that is nearly the same as the inside diameter of the blooey line. The loss factor for K_v for gate valves that have an inside diameter slightly less than the inside diameter of the blooey line is approximately 0.2 [12].
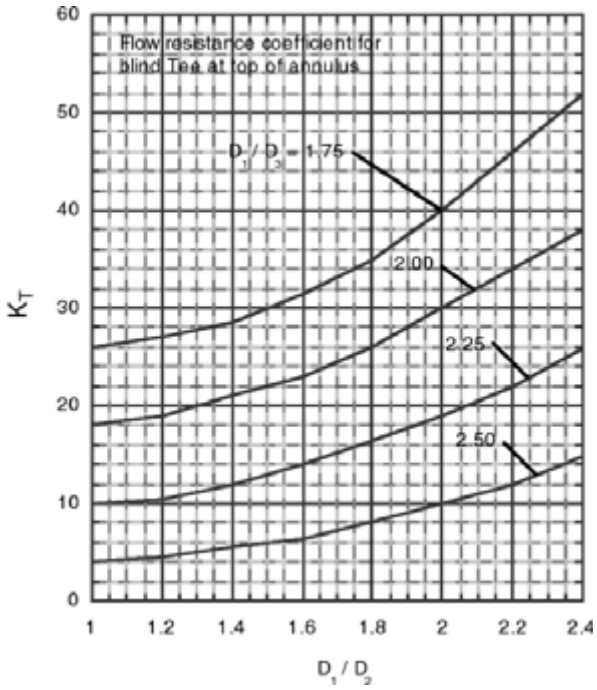
Figure 8-5: Flow resistance coefficient for the blind Tee at top of annulus.
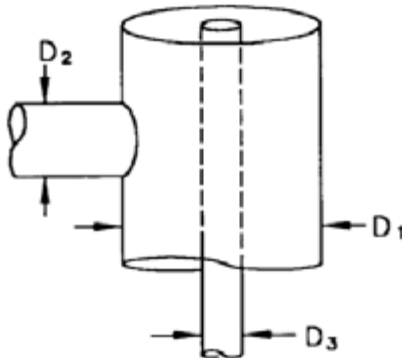
Figure 8-6: Dimensions of the blind Tee at top of annulus (for Figure 8-5).

For this example, the length of the blooey line, L_b, is

$$L_b = 200 \text{ ft}$$

The inside diameter of the blooey line, D_b, is

$$d_b = 8.097 \text{ inches}$$

$$D_b = \frac{d_b}{12}$$

$$D_b = 0.668 \text{ ft}$$

The blooey line is fabricated of commercial steel pipe, therefore, the inside surface roughness is

$$e_p = 0.00015 \text{ ft}$$

The Fanning friction factor for flow in the blooey line is determined from

$$f_b = \left[\frac{1}{2 \, \log\left(\dfrac{D_b}{e_p}\right) + 1.14} \right]^2 \tag{8-4}$$

Equation 8-4 becomes

$$f_b = \left[\frac{1}{2 \, \log\left(\dfrac{0.668}{0.00015}\right) + 1.14} \right]^2$$

$$f_b = 0.014$$

The inside cross-sectional area, A_b, of the blooey line is

$$A_b = \left(\frac{\pi}{4}\right) D_b^2$$

$$A_b = 0.358 \ \text{ft}^2$$

Equation 8-3 becomes

$$P_b = \left\{ \left[(0.014) \left(\frac{200}{0.668} \right) + 25 + 2 \ (0.2) \right] \left[\frac{(2.635)^2 \ (53.36) \ (504.41)}{(32.2) \ (0.358)^2 (1.0)} \right] + (1,827)^2 \right\}^{0.5}$$

$$P_b = 2,163 \ \text{lb/ft}^2 \ \text{abs}$$

$$p_b = \frac{P_b}{144}$$

$$p_b = 15.02 \ \text{psia}$$

Geometry in the Annulus

Major and minor friction losses must be included in order to obtain accurate bottomhole and injection pressures.   Therefore, it is necessary to include the geometric dimensions of the drill pipe tool joints. When drilling at 10,000 ft, the drill string is composed of 9,500 ft of API 4 1/2 inch, 16.60 lb/ft nominal, EU-S135, NC50 (IF) from the surface to the top of the drill collars.   The 4 1/2 inch outside diameter body of the drill pipe has an inside diameter of 3.826 inches (see Table B-3). Approximately every 30 ft there are tool joints which are about 1 1/2 ft in length. The outside diameter of these tool joints is 6 5/8 inches with an inside diameter of 3 3/4 inches. For the calculations that follow, the drill pipe tool joint lengths will be "lumped" together as a continuous length to approximate their contribution to the overall major (wall friction) loss in the flow system. Thus, the drill pipe tool joints of the drill pipe in the 7,000 ft cased section of the borehole are calculated as a "lump" at the bottom of this cased section. The drill pipe tool joints of the drill pipe in the 2,500 ft openhole section of the borehole are calculated as a "lump" at the bottom of this openhole section.

These lumped approximations for the drill pipe tool joints are somewhat rough approximations, but will give quite accurate bottomhole and injection pressures. Using this lumped approximation, the pressure terms along the annulus around the drill pipe and inside the drill pipe are in error by a few percent. However, this short-coming can obviously be relieved by calculating a short 1 1/2 ft long tool joint every 30 ft along the entire drill pipe length of the drill string. This can easily be accomplished with a sophisticated computer program.   But these lumped approximations are very useful in demonstrating the calculation technique steps. These lumped approximations are very easy to incorporate in an engineering calculation program and it has been found that these approximations are quite adequate for most engineering practice applications.   The lumped length approximations will be denoted by the numbers 1 through 5.   These numbered lengths will start at the top of the borehole (1) and continue to the bottom (5).

The total length of the lumped drill pipe body increment (first), H_1, in this cased section of the annulus is

$$H_1 = 7,000 - 1.5 \left(\frac{7,000}{30} \right)$$

$$H_1 = 6,650 \text{ ft}$$

The inside diameter of the casing along this length in this cased section of the annulus is

$$d_1 = 8.017 \text{ inches}$$

$$D_1 = \frac{d_1}{12}$$

$$D_1 = 0.668 \text{ ft}$$

and the outside diameter of the drill pipe body along this length is

$$d_2 = 4.50 \text{ inches}$$

$$D_2 = \frac{d_2}{12}$$

$$D_2 = 0.375 \text{ ft}$$

The individual tool joint length along the drill string is assumed to be approximately 1.5 ft (30 ft drill pipe lengths). The total length of the lumped drill pipe tool joint increment (second), H_2, in this cased section of the annulus is

$$H_2 = 1.5 \left(\frac{7,000}{30} \right)$$

$$H_2 = 350 \text{ ft}$$

The inside diameter of the casing along this length of the cased section of the annulus is

$$D_1 = 0.668 \text{ ft}$$

and the outside diameter of the drill pipe tool joints along this length is

$$d_3 = 6.625 \text{ inches}$$

$$D_3 = \frac{d_3}{12}$$

$$D_3 = 0.552 \text{ ft}$$

The total length of the lumped drill pipe body increment (third), H_3, in the openhole section of the annulus is

$$H_3 = 2,500 - 1.5 \left(\frac{2,500}{30} \right)$$

$$H_3 = 2,375 \text{ ft}$$

The inside diameter of the openhole along this length of the openhole section of the annulus is

$$d_h = 7.875 \text{ inches}$$

$$D_h = \frac{d_h}{12}$$

$$D_h = 0.656 \text{ ft}$$

and the outside diameter of the drill pipe body along this length is

$$D_2 = 0.375 \text{ ft}$$

The total length of the lumped drill pipe tool joints increment (fourth), H_4, in the openhole section of the annulus is

$$H_4 = 1.5 \left(\frac{2,500}{30} \right)$$

$$H_4 = 125 \text{ ft}$$

The inside diameter of the openhole along this length of the openhole section of the annulus is

$$D_h = 0.656 \text{ ft}$$

and the outside diameter of the drill pipe tool joints along this length is

$$D_3 = 0.552 \text{ ft}$$

The total length of the drill collars increment (fifth), H_5, in the openhole section of the annulus is

$$H_5 = 500 \text{ ft}$$

The inside diameter of the openhole along this length of the openhole section of the annulus is

$$D_h = 0.656 \text{ ft}$$

and the outside diameter of the drill collars along this length is

$$d_4 = 6.75 \text{ inches}$$

$$D_4 = \frac{d_4}{12}$$

$$D_4 = 0.563 \text{ ft}$$

Using the description of the annulus geometry given above each of the five increment changes in cross-sectional arean can be analyzed starting with the gas flow exiting at the top of the annulus.

Cased Section of the Annulus (Surface to 7,000 ft)

The first annulus seciton increment is denoted by the length H_1.   The temperature at the bottom of the length H_1 in the cased annulus section (bottom of the drill pipe body lumped geometry), T_1, is

$$T_1 = T_r + 0.01 \ H_1$$

$$T_1 = T_r + 0.01 \ (6,650)$$

$$T_1 = 570.91^{\circ} \text{R}$$

The average temperature of this cased section length H_1 is

$$T_{av1} = \frac{T_r + T_1}{2}$$

$$T_{av1} = 537.66^{\circ} \text{R}$$

Since both surfaces in this annulus section are commercial steel, then the surface roughness is

$$e_p = 0.00015 \text{ ft}$$

Therefore, Equation 6-58 becomes

$$f_{a1} = \left[\frac{1}{2 \ \log \left(\dfrac{0.668 \ - \ 0.375}{0.00015} \right) \ + 1.14} \right]^2$$

$$f_{a1} = 0.017$$

With the above values Equations 6-52 and 6-53 become, respectively,

$$a_{a1} = \left(\frac{1.0}{53.36} \right) \left[1 \ + \ \left(\frac{0.950}{2.635} \right) \right]$$

$$a_{a1} = 0.025$$

and

$$b_{a1} = \frac{0.017}{2 \ (32.2) \ (0.668 \ - \ 0.375)} \left(\frac{53.36}{1.0} \right)^2 \frac{(2.635)^2}{\left(\dfrac{\pi}{4} \right)^2 \left[(0.668)^2 \ - \ (0.375)^2 \right]^2}$$

$$b_{a1} = 304.7$$

Equation 6-57 becomes

$$P_{a1} = \left\{ \left[(2,164)^2 + \ 304.7 \ (537.66)^2 \right] e^{\dfrac{2 \ (0.025) \ (6,650)}{537.66}} \ - \ 304.7 \ (537.66)^2 \right\}^{0.5}$$

$$P_{a1} = 9,285 \ \text{lb/ft}^2 \ \text{abs}$$

$$p_{a1} = \frac{P_{a1}}{144}$$

$$p_{a1} = 64.5 \ \text{psia}$$

The second annulus seciton increment is denoted by the length H_2.   The temperature at the bottom of the length H_2 in the cased annulus section (bottom of the drill pipe tool joints lumped geometry), T_2, is

$$T_2 = T_r + 0.01 (H_1 + H_2)$$

$$T_2 = T_r + 0.01 (7,000)$$

$$T_2 = 574.41^\circ R$$

The average temperature of this cased section length H_2 is

$$T_{av2} = \frac{T_1 + T_2}{2}$$

$$T_{av2} = 572.66^\circ R$$

Since both surfaces in this annulus section are commercial steel, then the surface roughness is

$$e_p = 0.00015 \text{ ft}$$

Therefore, Equation 6-58 becomes

$$f_{a2} = \left[\frac{1}{2 \, \log \left(\dfrac{0.668 - 0.552}{0.00015} \right) + 1.14} \right]^2$$

$$f_{a2} = 0.021$$

With the above values Equations 6-52 and 6-53 become, respectively

$$a_{a2} = \left(\frac{1.0}{53.36} \right) \left[1 + \left(\frac{0.950}{2.635} \right) \right]$$

$$a_{a2} = 0.025$$

and

$$b_{a2} = \frac{0.021}{2 \, (32.2) \, (0.668 - 0.552)} \left(\frac{53.36}{1.0} \right)^2 \frac{(2.635)^2}{\left(\dfrac{\pi}{4} \right)^2 \left[(0.668)^2 - (0.552)^2 \right]^2}$$

$$b_{a2} = 4,476$$

Equation 6-57 becomes

$$P_{a2} = \left\{ \left[(9,285)^2 + 4,476 \ (572.66)^2 \right] e^{\frac{2 \ (0.025) \ (350)}{572.66}} - 4,476 \ (572.66)^2 \right\}^{0.5}$$

$$P_{a2} = 11,640 \ \text{lb/ft}^2 \ \text{abs}$$

$$p_{a2} = \frac{P_{a2}}{144}$$

$$p_{a2} = 80.8 \ \text{psia}$$

Openhole Section of the Annulus (7,000 ft to 10,000 ft)

The third annulus seciton increment is denoted by the length H_3.   The temperature at the bottom of the length H_3 in the openhole annulus section (bottom of the drill pipe body lumped geometry), T_3, is

$$T_3 = T_r + 0.01 \ (H_1 + H_2 + H_3)$$

$$T_3 = T_r + 0.01 \ (9,375)$$

$$T_3 = 598.16^\circ R$$

The average temperature of this openhole annulus section H_3 is

$$T_{av3} = \frac{T_2 + T_3}{2}$$

$$T_{av3} = 586.29^\circ R$$

It is assumed that the inside surface of the openhole annulus section has a surface roughness of 0.01 ft (see Table 8-1). The inner surface of this annulus section is the outer surface of the drill pipe body which has an absolute surface roughness of 0.00015 ft.   Using Equation 8-2, the average absolute surface roughness of this annulus section, e_{av3}, is

$$e_{av3} = \frac{(0.01)\left(\dfrac{\pi}{4}\right)(0.656)^2 + (0.00015)\left(\dfrac{\pi}{4}\right)(0.375)^2}{\left(\dfrac{\pi}{4}\right)(0.656)^2 + \left(\dfrac{\pi}{4}\right)(0.375)^2}$$

$$e_{av3} = 0.0076 \text{ ft}$$

Equation 6-58 becomes

$$f_{a3} = \left[\frac{1}{2 \ \log\left(\dfrac{0.656 - 0.375}{0.0076}\right) + 1.14}\right]^2$$

$$f_{a3} = 0.055$$

With the above values Equations 6-52 and 6-53 become, respectively,

$$a_{a3} = \left(\frac{1.0}{53.36}\right)\left[1 + \left(\frac{0.950}{2.635}\right)\right]$$

$$a_{a3} = 0.025$$

and

$$b_{a3} = \frac{0.055}{2\,(32.2)\,(0.656 - 0.375)}\left(\frac{53.36}{1.0}\right)^2 \frac{(2.635)^2}{\left(\dfrac{\pi}{4}\right)^2\left[(0.656)^2 - (0.375)^2\right]^2}$$

$$b_{a3} = 11,490$$

Equation 6-58 becomes

$$P_{a3} = \left\{\left[(11,640)^2 + 11,149\,(586.29)^2\right]\,e^{\frac{2\,(0.025)\,(2,375)}{586.29}} - 11,149\,(586.29)^2\right\}^{0.5}$$

$$P_{a3} = 16,030 \text{ lb/ft}^2 \text{ abs}$$

$$p_{a3} = \frac{P_{a3}}{144}$$

$$p_{a3} = 111.3 \text{ psia}$$

The fourth annulus seciton increment is denoted by the length H_4.   The temperature at the bottom of the length H_4 in the openhole annulus section (bottom of the drill pipe tool joints lumped geometry), T_4, is

$$T_4 = T_r + 0.01 \, (H_1 + H_2 + H_3 + H_4)$$

$$T_4 = T_r + 0.01 \, (9,500)$$

$$T_4 = 599.41^\circ \text{R}$$

The average temperature of this openhole annulus section H_4 is

$$T_{av4} = \frac{T_3 + T_4}{2}$$

$$T_{av4} = 598.79^\circ \text{R}$$

Using Equation 8-2, the average absolute surface roughness of this annulus section, e_{av4}, is

$$e_{av4} = \frac{(0.01) \left(\dfrac{\pi}{4}\right) (0.656)^2 + (0.00015) \left(\dfrac{\pi}{4}\right) (0.552)^2}{\left(\dfrac{\pi}{4}\right) (0.656)^2 + \left(\dfrac{\pi}{4}\right) (0.552)^2}$$

$$e_{av4} = 0.0059 \text{ ft}$$

Equation 6-58 becomes

$$f_{a4} = \left[\frac{1}{2 \, \log \left(\dfrac{0.656 - 0.552}{0.0059}\right) + 1.14}\right]^2$$

$$f_{a4} = 0.076$$

With the above values Equations 6-52 and 6-53 become, respectively,

$$a_{a4} = \left(\frac{1.0}{53.36}\right)\left[1 + \left(\frac{0.950}{2.635}\right)\right]$$

$$a_{a4} = 0.025$$

and

$$b_{a4} = \frac{0.076}{2\,(32.2)\,(0.656 - 0.552)}\left(\frac{53.36}{1.0}\right)^2 \frac{(2.635)^2}{\left(\frac{\pi}{4}\right)^2\left[(0.656)^2 - (0.552)^2\right]^2}$$

$$b_{a4} = 22,870$$

Equation 6-57 becomes

$$P_{a4} = \left\{\left[(16,030)^2 + 22,870\,(598.79)^2\right]e^{\frac{2\,(0.025)\,(125)}{598.79}} - 22,870\,(598.79)^2\right\}^{0.5}$$

$$P_{a4} = 18,643 \text{ lb/ft}^2 \text{ abs}$$

$$p_{a4} = \frac{P_{a4}}{144}$$

$$p_{a4} = 129.5 \text{ psia}$$

The fifth annulus seciton increment is denoted by the length H_5. The temperature at the bottom of the length H_5 in the openhole annulus section (bottom of the drill collar geometry), T_5, is

$$T_5 = T_r + 0.01\,(H_1 + H_2 + H_3 + H_4 + H_5)$$

$$T_5 = T_r + 0.01\,(10,000)$$

$$T_5 = 604.41^\circ\text{R}$$

The average temperature of drill collar length H_5 is

$$T_{av5} = \frac{T_4 + T_5}{2}$$

$$T_{av5} = 601.91^\circ\text{R}$$

Using Equation 8-2, the average absolute surface roughness of this annulus section, e_{av5}, is

$$e_{av5} = \frac{(0.01)\left(\dfrac{\pi}{4}\right)(0.656)^2 + (0.00015)\left(\dfrac{\pi}{4}\right)(0.563)^2}{\left(\dfrac{\pi}{4}\right)(0.656)^2 + \left(\dfrac{\pi}{4}\right)(0.563)^2}$$

$$e_{av5} = 0.0058 \text{ ft}$$

Equation 6-58 becomes

$$f_{a5} = \left[\frac{1}{2 \, \log\left(\dfrac{0.656 \; - \; 0.563}{0.0058}\right) + 1.14}\right]^2$$

$$f_{a5} = 0.079$$

With the above values Equations 6-52 and 6-53 become, respectively,

$$a_{a5} = \left(\frac{1.0}{53.36}\right)\left[1 + \left(\frac{0.950}{2.635}\right)\right]$$

$$a_{a5} = 0.025$$

and

$$b_{a5} = \frac{0.079}{2 \, (32.2) \, (0.656 \; - \; 0.563)}\left(\frac{53.36}{1.0}\right)^2 \frac{(2.635)^2}{\left(\dfrac{\pi}{4}\right)^2 \left[(0.656)^2 \; - \; (0.563)^2\right]^2}$$

$$b_{a5} = 32,210$$

Equation 6-57 becomes

$$P_{a5} = \left\{\left[(22,870)^2 + 32,210 \, (601.91)^2\right] e^{\frac{2 \, (0.025) \, (500)}{601.91}} - 32,210 \, (601.91)^2\right\}^{0.5}$$

$$P_{a5} = 29,454 \ \text{lb/ft}^2 \ \text{abs}$$

$$p_{a5} = \frac{P_{a5}}{144}$$

$$p_{a5} = 204.5 \ \text{psia}$$

The above value is the bottomhole pressure in the annulus.

Drill Bit Open Orifices

The drill bit used in this example operation has three open orifices, each with an inside diameter of 0.70 inches. Thus, the inside diameter of the open orifice, D_o, is

$$d_o = 0.70 \ \text{inches}$$

$$D_o = \frac{d_o}{12}$$

$$D_o = 0.0583 \ \text{ft}$$

The total cross-sectional area of flow through the drill bit orifices, A_o, is

$$A_o = 3 \left(\frac{\pi}{4} \right) (0.0583)^2$$

$$A_o = 0.00802 \ \text{ft}^2$$

Using Equation 4-11 the specific weight of the air flow at the bottom of the annulus, γ_{a5}, is

$$\gamma_{a5} = \frac{(29,454)(1.0)}{(53.36)(604.41)}$$

$$\gamma_{a5} = 0.913 \ \text{lb/ft}^3$$

Equation 6-63 is used to determine the pressure inside the drill bit just above the open orifices. The flow through open orifices is generally subsonic. Therefore, Equation 6-63 must be used to determine the pressure upstream of bottomhole annulus pressure. Thus, Equation 6-63 becomes

$$P_{i5} = (29,454) \left[\frac{\left(\dfrac{2.635}{0.00802}\right)^2}{2\,(32.2)\left(\dfrac{1.4}{0.4}\right)(29,454)\,(0.913)} + 1 \right]^{\frac{1.4}{0.4}}$$

$$P_{i5} = 31,330 \ \text{lb/ft}^2 \ \text{abs}$$

$$p_{i5} = \frac{P_{i5}}{144}$$

$$p_{i5} = 217.6 \ \text{psia}$$

where for air k = 1.4 [12].

The open orifice diameters considered in this example yield only a slight increase in the pressure (from approximately 205 psia at the bottom of the annulus to a pressure of approximately 218 psia inside the drill bit above the orifices).

If jetting nozzles are inserted in the drill bit orifice openings they will create sonic flow at the nozzle throats. This will result in higher pressures inside the drill bit above the nozzles. Higher pressures above the nozzles will affect the pressures inside the drill string. When nozzles are used, the pressure inside the drill string will be higher and the injection pressure will be higher than where open orifices are used. In general, jetting nozzles are only used in air and gas drill operations when downhole motors or downhole air hammers are used. This will be demonstrated in Chapter 11 where a downhole motor and an air hammer will be employed in the drill string.

Geometry Inside the Drill String

Starting at the bottom of the drill string, the total length of the drill collars length increment, H_5, in the openhole section is

$$H_5 = 500 \ \text{ft}$$

The inside diameter of the drill collars length in this openhole section is

$$d_5 = 2.8125 \ \text{inches}$$

$$D_5 = \frac{d_5}{12}$$

$$D_5 = 0.234 \ \text{ft}$$

The total length of the drill pipe tool joints lumped geometry increment, H_4, in the openhole section is

$$H_4 = 125 \text{ ft}$$

The inside diameter of the drill pipe tool joints lumped geometry in this openhole section is

$$d_6 = 3.50 \text{ inches}$$

$$D_6 = \frac{d_6}{12}$$

$$D_6 = 0.292 \text{ ft}$$

The total length of the lumped drill pipe body geometry increment, H_3, in the openhole section is

$$H_3 = 2,375 \text{ ft}$$

The inside diameter of the drill pipe body lumped geometry in this openhole section is

$$d_7 = 3.826 \text{ inches}$$

$$D_7 = \frac{d_7}{12}$$

$$D_7 = 0.319 \text{ ft}$$

The total length of the lumped drill pipe tool joints geometry increment, H_2, in the cased section is

$$H_2 = 350 \text{ ft}$$

The inside diameter of the drill pipe tool joints lumped geometry in this cased section is

$$D_6 = 0.292 \text{ ft}$$

The total length of the lumped drill pipe body geometry increment, H_1, in the cased section is

$$H_1 = 6,650 \text{ ft}$$

The inside diameter of the drill pipe body lumped geometry in this cased section is

$$D_7 = 0.319 \text{ ft}$$

Inside the Drill String (10,000 ft to 7,000 ft)

The fifth drill string section increment is denoted by the length H_5.   The temperature at the bottom of the drill collars (bottomhole tempreature) in the openhole section is

$$T_5 = 604.41^\circ \text{R}$$

The average temperature of the drill collar length H_5 and, thus, the temperature of the gas flow inside the drill collars is

$$T_{av5} = 601.91^\circ \text{R}$$

The inside surface of the drill collars has the surface roughness of commercial steel. Therefore, over this drill collar length the surface roughness is

$$e_p = 0.00015 \text{ ft}$$

With the above, Equation 6-73 becomes

$$f_{i5} = \left[\frac{1}{2 \, \log \left(\dfrac{0.234}{0.00015} \right) + 1.14} \right]^2$$

$$f_{i5} = 0.018$$

Equations 6-67 and 6-68 become, respectively,

$$a_{i5} = \frac{1.0}{53.36}$$

$$a_{i5} = 0.019$$

and

$$b_{i5} = \frac{0.018}{2 \, (32.2)} \left(\frac{53.36}{1.0} \right)^2 \frac{(2.635)^2}{\left(\dfrac{\pi}{4} \right)^2 (0.234)^5}$$

$$b_{i5} = 12,420$$

Equation 6-72 becomes

$$P_{i4} = \left[\frac{(31,330)^2 + (12,420) \, (601.91)^2 \left(e^{\frac{2 \, (0.019) \, (500)}{601.91}} - 1 \right)}{e^{\frac{2 \, (0.019) \, (500)}{601.91}}} \right]^{0.5}$$

$$P_{i4} = 33,010 \text{ lb/ft}^2 \text{ abs}$$

$$p_{i4} = \frac{P_{i4}}{144}$$

$$p_{i4} = 229.2 \text{ psia}$$

The pressure given above is the flowing air pressure at the top of the drill collar length inside the drill string in the openhole section of the borehole.

The fourth drill string section increment is denoted by the length H_4. The temperature at the bottom of the drill pipe tool joints lumped geometry length in the openhole section is

$$T_4 = 599.41^\circ \text{R}$$

The average temperature of the drill pipe tool joints lumped length along H_4 and, thus, the temperature of the gas flow inside this drill string length is

$$T_{av4} = 598.79^\circ \text{R}$$

The inside surface of the drill pipe tool joint has the surface roughness of commercial steel. Therefore, over this lumped drill pipe tool joint length the surface roughness is

$$e_p = 0.00015 \text{ ft}$$

With the above, Equation 6-73 becomes

$$f_{i4} = \left[\frac{1}{2 \, \log \left(\dfrac{0.292}{0.00015} \right) + 1.14} \right]^2$$

$$f_{i4} = 0.017$$

Equations 6-67 and 6-68 become, respectively,

$$a_{i4} = \frac{1.0}{53.36}$$

$$a_{i4} = 0.019$$

and

$$b_{i4} = \frac{0.017}{2\,(32.2)} \left(\frac{53.36}{1.0}\right)^2 \frac{(2.635)^2}{\left(\dfrac{\pi}{4}\right)^2 (0.292)^5}$$

$$b_{i4} = 3,958$$

Equation 6-72 becomes

$$P_{i3} = \left[\frac{(33,010)^2 + (3,958)\,(598.79)^2 \left(e^{\frac{2\,(0.019)\,(125)}{598.79}} - 1\right)}{e^{\frac{2\,(0.019)\,(125)}{598.79}}}\right]^{0.5}$$

$$P_{i3} = 33,050 \ \text{lb/ft}^2 \ \text{abs}$$

$$p_{i3} = \frac{P_{i3}}{144}$$

$$p_{i3} = 229.5 \ \text{psia}$$

The pressure given above is the flowing air pressure at the top of the lumped drill pipe tool joint length inside the drill string in the openhole section of the borehole.

The third drill string section increment is denoted by the length H_3. The temperature at the bottom of the drill pipe body lumped geometry length in the openhole section is

$$T_3 = 598.16\,^{\circ}\text{R}$$

The average temperature of the drill pipe body lumped geometry length along H_3 and, thus, the temperature of the gas flow inside this drill string length is

$$T_{av3} = 586.29^\circ\,\text{R}$$

The inside surface of the drill pipe body has the surface roughness of commercial steel. Therefore, over this lumped drill pipe body length the surface roughness is

$$e_p = 0.00015 \text{ ft}$$

With the above, Equation 6-73 becomes

$$f_{i3} = \left[\dfrac{1}{2\;\log\left(\dfrac{0.319}{0.00015}\right) + 1.14} \right]^2$$

$$f_{i3} = 0.016$$

Equations 6-67 and 6-68 become, respectively,

$$a_{i3} = \dfrac{1.0}{53.36}$$

$$a_{i3} = 0.019$$

and

$$b_{i3} = \dfrac{0.016}{2\;(32.2)} \left(\dfrac{53.36}{1.0}\right)^2 \dfrac{(2.635)^2}{\left(\dfrac{\pi}{4}\right)^2 (0.319)^5}$$

$$b_{i3} = 2,486$$

Equation 6-72 becomes

$$P_{i2} = \left[\dfrac{(33,050)^2 + (2,486)\,(586.29)^2 \left(e^{\frac{2\;(0.019)\;(2,375)}{586.29}} - 1 \right)}{e^{\frac{2\;(0.019)\;(2,375)}{586.29}}} \right]^{0.5}$$

$$P_{i2} = 32,540 \text{ lb/ft}^2 \text{ abs}$$

$$p_{i2} = \frac{P_{i2}}{144}$$

$$p_{i2} = 225.9 \text{ psia}$$

The pressure given above is the flowing air pressure at the top of the lumped drill pipe body length inside the drill string in the openhole section of the borehole.

Inside the Drill String (7,000 ft to Surface)

The second drill string section increment is denoted by the length H_2. The temperature at the bottom drill pipe tool joints lumped geometry length in the cased section is

$$T_2 = 574.41^{\circ} \text{R}$$

The average temperature of the drill pipe tool joints lumped geometry along H_2 and, thus, the temperature of the gas flow inside this drill string length is

$$T_{av2} = 572.66^{\circ} \text{R}$$

The inside surface of the drill pipe body has the surface roughness of commercial steel. Therefore, over this lumped drill pipe body length the surface roughness is

$$e_p = 0.00015 \text{ ft}$$

With the above, Equation 6-73 becomes

$$f_{i2} = \left[\frac{1}{2 \ \log \left(\dfrac{0.292}{0.00015} \right) + 1.14} \right]^2$$

$$f_{i2} = 0.017$$

Equations 6-67 and 6-68 become, respectively,

$$a_{i2} = \frac{1.0}{53.36}$$

$$a_{i2} = 0.019$$

and

$$b_{i2} = \frac{0.017}{2\,(32.2)} \left(\frac{53.36}{1.0}\right)^2 \frac{(2.635)^2}{\left(\dfrac{\pi}{4}\right)^2 (0.292)^5}$$

$$b_{i2} = 3{,}958$$

Equation 6-72 becomes

$$P_{i1} = \left[\frac{(32{,}540)^2 + (3{,}958)\,(572.66)^2 \left(e^{\frac{2\,(0.019)\,(350)}{572.66}} - 1\right)}{e^{\frac{2\,(0.019)\,(350)}{572.66}}}\right]^{0.5}$$

$$P_{i1} = 32{,}620 \ \text{lb/ft}^2 \ \text{abs}$$

$$p_{i1} = \frac{P_{i1}}{144}$$

$$p_{i1} = 226.5 \ \text{psia}$$

The pressure given above is the flowing air pressure at the top of the lumped drill pipe tool joints length inside the drill string in the cased section of the borehole.

The first drill string section increment is denoted by the length H_1. The temperature at the bottom drill pipe body lumped geometry length in the cased section is

$$T_1 = 570.91^\circ\text{R}$$

The average temperature of the drill pipe body lumped geometry along H_1 and, thus, the temperature of the gas flow inside this drill string length is

$$T_{av1} = 537.66^\circ\text{R}$$

The inside surface of the drill pipe body has the surface roughness of commercial steel. Therefore, over this lumped drill pipe body length the surface roughness is

$$e_p = 0.00015 \ \text{ft}$$

With the above, Equation 6-73 becomes

$$f_{i1} = \left[\frac{1}{2 \, \log \left(\dfrac{0.319}{0.00015} \right) + 1.14} \right]^2$$

$$f_{i1} = 0.016$$

Equations 6-67 and 6-68 become, respectively,

$$a_{i1} = \frac{1.0}{53.36}$$

$$a_{i1} = 0.019$$

and

$$b_{i1} = \frac{0.016}{2 \, (32.2)} \left(\frac{53.36}{1.0} \right)^2 \frac{(2.635)^2}{\left(\dfrac{\pi}{4} \right)^2 (0.319)^5}$$

$$b_{i1} = 2,486$$

Equation 6-72 becomes

$$P_{in} = \left[\frac{(32,540)^2 + (2,486) \, (537.66)^2 \left(e^{\frac{2 \, (0.019) \, (6,650)}{537.66}} - 1 \right)}{e^{\frac{2 \, (0.019) \, (6,650)}{537.66}}} \right]^{0.5}$$

$$P_{in} = 30,590 \ \text{lb/ft}^2 \ \text{abs}$$

$$p_{in} = \frac{P_{in}}{144}$$

$$p_{in} = 212.4 \ \text{psia}$$

The injection pressure given above is the flowing air pressure at the top of the lumped drill pipe body length inside the drill string in the cased section of the borehole. This is the approximate injection at the top of the drill string required to

force a volumetric flow rate of 2,400 acfm through the circulation system.   This injection pressure is the pressure the compressor output must match.

Figure 8-7 shows the air flow pressures in the annulus and inside the drill string as a function of depth for this illustrative example. The figure shows the pressure at the bottom of the annulus is approximately 205 psia (p_{a5} above). If a target oil or natural gas rock formation pore pressure at the bottom of the borehole is above this value, the oil or natural gas will flow into the borehole as the drill bit is advanced into the producing rock formation. This would be underbalanced drilling.   If the pore pressure is less than this value, rock cuttings from the advance of the drill bit will be forced into the exposed pores around the bottom of the borehole resulting in formation damage.

Figure 8-7: Pressure profile in the inside of the drill string and in the annulus for Illustrative Example 8.3b (q_g = 2,400 acfm and a drilling depth of 10,000 ft).

The injection pressure of approximately 212 psia is less than the capability of the selected four stage reciprocating piston compressor (i.e., 1,000 psig), therefore, the compressor is capable of producing the above injection pressure (the maximum pressure capability of a reciprocating piston compressor is not derated with surface location elevation as long as the prime mover has the power necessary to produce the required pressure).

The last criteria to check is whether the prime mover of this primary compressor unit has the power to operate at the 4,000 ft surface elevation. The prime mover for this compressor is a diesel fueled, turbocharged, Caterpillar Model D398 with a peak output of 760 horsepower at 900 rpm (at API standard conditions) (see Section 4.7 in Chapter 4). The theoretical shaft horsepower, $\dot{W}_s$, required by each of the two compressors is obtained from Equation 4-35a. Equation 4-35a becomes

$$\dot{W}_s = \frac{(4)\,(1.4)}{(0.4)} \frac{(12.685)\left(\dfrac{2,400}{2}\right)}{229.17} \left[\left(\frac{212.4}{12.685}\right)^{\frac{(0.4)}{(4)(1.4)}} - 1\right]$$

$$\dot{W}_s = 207.4$$

The mechanical efficiency, ε_m, is

$$\varepsilon_m = 0.90$$

This is a four-stage reciprocating piston compressor. Therefore,

$$n_s = 4$$

The first stage compressor ratio is

$$r_s = \left(\frac{212.4}{12.685}\right)^{\frac{1}{4}}$$

$$r_s = 2.02$$

The volumetric efficiency (only for the reciprocating piston compressor), ε_v, is determined from Equation 4-38. The compressor clearance volume ratio, c, is assumed to be 0.06. Equation 4-38 becomes

$$\varepsilon_v = 0.96 \left\{1 - (0.06)\left[(2.02)^{\frac{1}{1.4}} - 1\right]\right\}$$

$$\varepsilon_v = 0.922$$

From Equation 4-39, the actual shaft horsepower, $\dot{W}_{as}$, required by each compressor is

$$\dot{W}_{as} = \frac{207.4}{(0.90)\ (0.922)}$$

$$\dot{W}_{as} = 249.9$$

The above determined 249.9 horsepower is the actual shaft power needed by each of the two compressors to produce the 212.4 psia pressure output at the surface location elevation of 4,000 ft above sea level (while drilling at a depth of 10,000 ft). At this surface location, the input horsepower available from the Caterpillar Model D398 prime mover is a derated value (derated from the rated 760 horsepower available at 900 rpm). In order for the compressor units to operate at this 4,000 ft surface location elevation, the derated input power available must be greater than the actual shaft power needed. Figure 4-15 shows that for 4,000 ft elevation the input power of a turbocharged prime mover must be derated by approximately 10 percent. The derated input horsepower, $\dot{W}_i$, available from the prime mover is

$$W_i = 760\ (1 - 0.10)$$

$$\dot{W}_i = 684.0$$

For this illustrative example, the prime mover of each of the two compressor units derated input power is greater than the actual shaft horsepower needed, thus, the selected compressor units can be operated at this 4,000 ft surface location elevation (while drilling at a depth of 10,000 ft).

8.4 Prime Mover Fuel Consumption

In this section the fuel consumption of the prime mover for the compressor system will be discussed. Illustrative examples of the fuel consumption were discussed in detail in Chapter 4. In this section the illustrative examples in this chapter will be completed with the calculation of the approximate fuel needed on the drilling location for the compressor system.

Illustrative Example 8.3c describes the implementation of the basic planning step No. 10 given in Section 8.1.

Illustrative Example 8.3c In Illustrative Example 8.3a the semi-trailer mounted unit with the Dresser Clark CFB-4, four-stage, reciprocating piston compressor system was selected for the drilling operation. In Illustrative Examples 8.3a and 8.3b two of these compressor units were utilized to drill the interval from 7,000 ft to 10,000 ft. Each compressor unit has a volumetric flow rate of 1,200 acfm. To estimate the total diesel fuel needed by each compressor unit it is necessary to estimate the fuel consumption of the compressor units' Caterpillar Model D398, diesel fueled, turbocharged, prime mover. The anticipated drilling rate of penetration

is estimated to be 60 ft/hr. The vertical interval section to be drilled is from a depth of 7,000 ft to a depth of 10,000 ft, or a 3,000 ft length of borehole. Therefore, the estimated actual drilling time to drill this interval is approximately 50 hours.

In Illustrative Example 8.3b the injection pressure into the top of the drill string when drilling at 10,000 ft of depth was found to be approximately 212.4 psia. Using similar calculations, the injection pressures for depths from 7,000 ft to 10,000 ft can be obtained.   Figure 8-8 shows these injection pressures as a function of drilling time (or drilling depth).
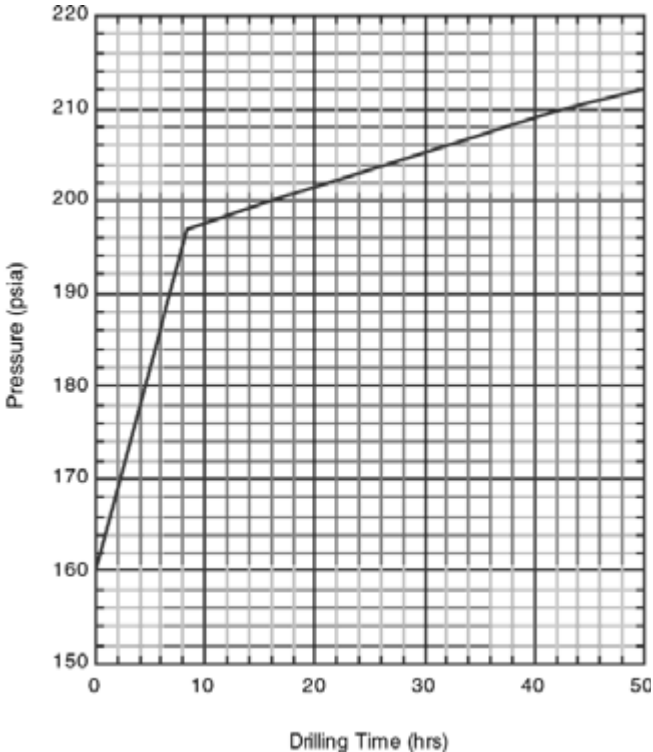
Figure 8-8: Drill string injection pressure (same as compressor output pressure) for Illustrative Example 8.3c.

The reciprocating piston compressor is not a fixed pressure ratio machine like the rotary compressor. As long as there is sufficient power available from the prime mover the reciprocating piston compressor will match the back pressure resistance.

Thus, Figure 8-8 shows only one curve indicating the injection pressure is the same as the pressure output of the compressor units.

In Illustrative Example 8.3b it was found that the actual shaft horsepower required by each of the two reciprocating piston compressor units to compress air to 212.4 psia was approximately 249.9 (at 10,000 ft of depth).   Also in Illustrative Example 8.8c the derated horsepower available from the Caterpillar Model D398 prime mover at the surface elevation of 4,000 ft was found to be 684.   Drilling at a depth of 10,000 ft, the prime mover power ratio is

$$PR = \frac{249.9}{684.0} (100) = 36.5$$

Figure 4-17 does not give data for power ratios less than 50 percent so a diesel fuel consumption rate 0.700 lb/hp-hr will be assumed for power levels below 40 percent. The total weight rate of diesel fuel consumption per hour is

$$\dot{w}_f = 0.700 (249.9) = 174.9 \text{ lb/hr}$$

The diesel fuel consumption rate (in United States gallons) for the drilling depth of 10,000 ft is

$$q_f = \frac{174.9}{(0.8156)(8.33)} = 25.7 \text{ gal/hr}$$

Using the data in Figure 8-8 and similar calculations as those given above, the diesel fuel consumption rate as a function of drilling time (or drilling depth) can be obtained. Figure 8-9 shows the diesel fuel consumption rate as a function of drilling time (or drilling depth) for each of the two reciprocating piston compressor units. The approximate total diesel fuel needed for each compressor unit is obtained by the integration of the area under the curve in Figure 8-9. This is approximately 1,257 gallons. It is standard practice to assume a 20 percent additional volume of fuel for blowing the hole between connections and other compressor operations on the drill rig. Therefore, the approximate diesel fuel needed for each compressor unit is 1,509 gallons.   Therefore, the total diesel fuel needed at the drilling location for compressor operations is approximately 3,018 gallons.

Illustrative Examples 8.2, 8.3a, 8.3b, and 8.3c demonstrate the calculation procedures (step Nos. 1 to 10 given in Section 8.1) used to plan a typical deep oil or natural gas well drilling operation.

Illustrative Example 8.4 In Illustrative Examples 8.3a, 8.3b, and 8.3c the semi-trailer mounted unit with the Dresser Clark CFB-4, four-stage, reciprocating piston compressor system was selected for the example drilling operation described in that series of examples. In this illustrative example the drilling problem in the Illustrative Example 8.3 series is to be solved using another candidate compressor system unit. This compressor system unit is the semi-trailer mounted unit with both the rotary primary and the reciprocating booster compressors driven by one

large prime mover (see Figure 4-24).   This compressor unit has a MAN Model GHH-CF246G, single-stage, rotary screw primary compressor and an Ariel Model JGJ/2, two-stage, reciprocating piston booster compressor (see Figure 4-24 in Chapter 4).   These two compressors are driven by a single Caterpillar Model 3412 prime mover. The rotary primary compressor has an API rated volumetric flow rate of 1,698 scfm (adjusted from ASME standard atmospheric conditions, see Illustrative Example 3.3a, and Chapter 4). The rotary primary compressor also has a fixed pressure output of 190 psig (at ASME standard atmospheric conditions, see Chapter 4).   The Caterpillar Model 3412 prime mover is API rated at 740 horsepower at 1,800 rpm (the operating speed for the system).
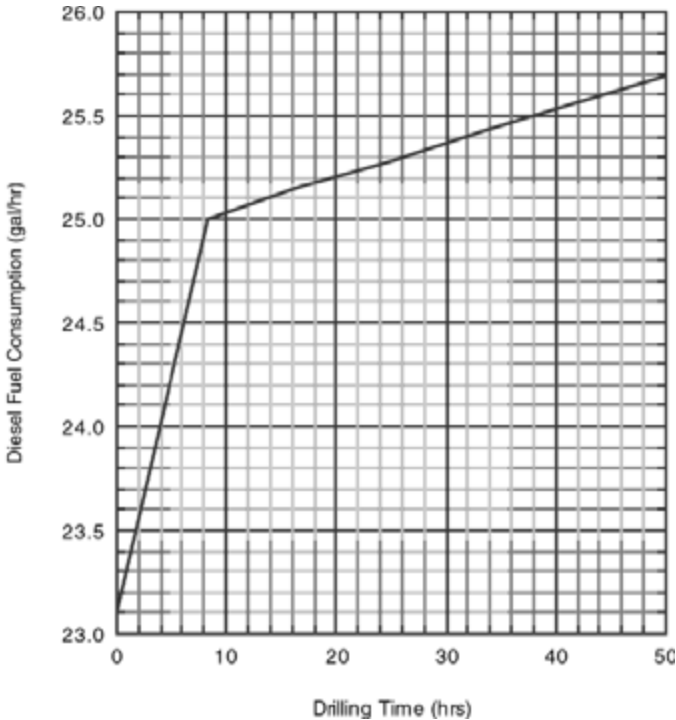
Figure 8-9: Fuel consumption rate as a function of drilling time for the reciprocating piston compressor of Illustrative Example 8.3c.

In the compressor selection process of Illustrative Example 8.3a it was found that this candidate compressor system would require the volumetric flow rate output of two units (or 3,396 acfm) to drill the example borehole.   Using this new

volumetric flow rate, detailed calculations to determine the pressures in the annulus and inside the drill string can be carried out in the same manner as those in Illustrative Example 8.3b (for a drilling depth of 10,000 ft). Figure 8-10 shows the air flow pressures in the annulus and inside the drill string as a function of depth for this illustrative example. The figure shows an injection pressure of 294 psia and a pressure at the bottom of the annulus of approximately 269 psia. Comparing these pressures to those shown in Figure 8.7 (for $q_g = 2,400$ acfm) it is clear that the general pressure increases through the circulation system for this example are due to the higher volumetric flow rate used for this illustrative example (i.e., $q_g = 2,400$ acfm).
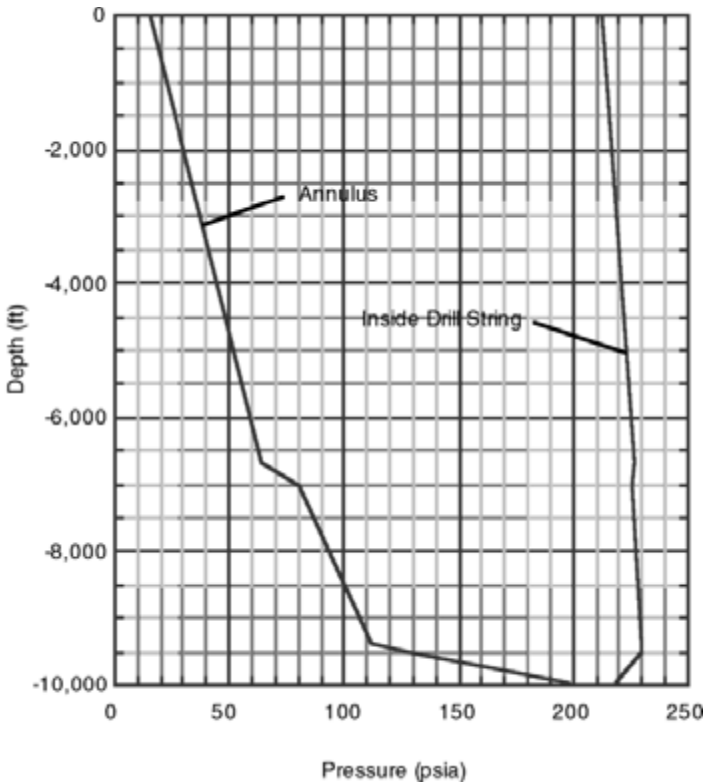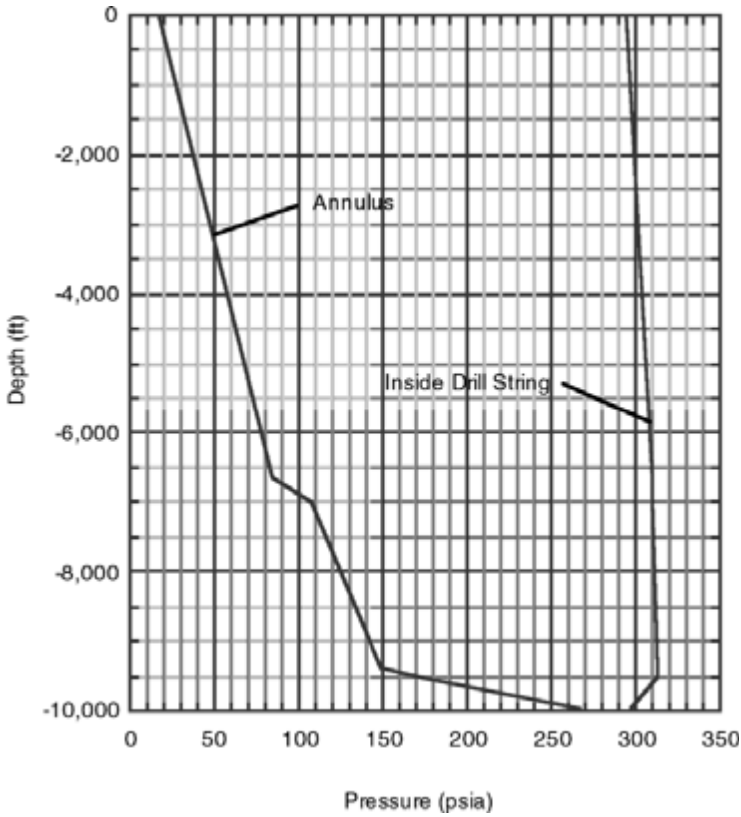

Figure 8-10: Pressure profile in the inside the drill string and the annulus for Illustrative Example 8.4 ($q_g = 3,396$ acfm and a drilling depth of 10,000 ft).

    Drilling at 10,000 ft of depth, the injection pressure is approximately 294 psia. For this combined primary and booster compressor system, the maximum pressure the booster can attain is limited by the prime mover power capability. Therefore, it is necessary to assess whether the prime mover of this unique combined compressor system has the power to operate at the 4,000 ft surface elevation and produce the 294 psia injection pressure output required to drill at 10,000 ft of depth. The prime mover for this combined primary and booster compressor system is a diesel fueled, turbocharged, Caterpillar Model 3412 with a peak output of 740 horsepower at 1,800 rpm (at API standard conditions) (see Section 4.7 in Chapter 4). The theoretical shaft horsepower, $\dot{W}_s$, required by each of the two compressor units is obtained from Equation 4-35a.

Primary Compressor

The primary compressor is a single-stage rotary screw compressor which has a fixed pressure output rated at ASME standard atmospheric conditions of 190 psig. ASME standard atmospheric pressure is 14.7 psia. Thus, the input pressure, p_{1s}, is

$$p_{1s} = 14.7 \text{ psia}$$

The output pressure, p_{2s}, of the primary compressor at the ASME standard conditions is

$$p_{2s} = 190 + p_{1s}$$

$$p_{2s} = 204.7 \text{ psia}$$

The fixed compression ratio for this single-stage primary, r_{sp}, is

$$r_{sp} = \frac{p_{2s}}{p_{1s}}$$

$$r_{sp} = \frac{204.7}{14.7}$$

$$r_{sp} = 13.9$$

The derated pressure output, p_{2d}, of this primary compressor when operated at 4,000 ft of surface location elevation will be

$$p_{2d} = r_{sp} \, p_{at}$$

where p_a, is the actual atmospheric pressure at the surface location elevation. The above becomes

$$p_{2d} = (13.9) \, (12.685)$$

$$p_{2d} = 176.6 \text{ psia}$$

The theoretical shaft horsepower, $\dot{W}_{sp}$, required by the primary compressor in each unit is determined from Equation 4-35a. Equation 4-35a becomes

$$\dot{W}_{sp} = \frac{(1)\ (1.4)}{(0.4)} \ \frac{(12.685) \left(\dfrac{3,398}{2}\right)}{229.17} \left[\left(\frac{204.7}{12.685}\right)^{\frac{(0.4)}{(1)(1.4)}} - 1\right]$$

$$\dot{W}_{sp} = 368.8$$

The assumed mechanical efficiency, ε_m, is

$$\varepsilon_m = 0.90$$

Rotary compressors have no volumetric efficiency term, therefore, the actual shaft horsepower, $\dot{W}_{as\ p}$, required by each compressor can be obtained from Equation 4-39. This is

$$\dot{W}_{asp} = \frac{368.8}{(0.90)}$$

$$\dot{W}_{asp} = 409.8$$

The above determined 409.8 horsepower is the actual shaft power needed by the rotary screw primary compressor to produce the 176.6 psia pressure output at the surface location elevation of 4,000 ft above sea level (while drilling at a depth of 10,000 ft).

Booster Compressor

This is a two-stage reciprocating piston booster compressor. Therefore,

$$n_s = 2$$

The theoretical shaft horsepower, $\dot{W}_{sb}$, required by this booster compressor in each unit is determined from Equation 4-35a. Equation 4-35a becomes

$$\dot{W}_{sb} = \frac{(2)\ (1.4)}{(0.4)} \ \frac{(12.685) \left(\dfrac{3,398}{2}\right)}{229.17} \left[\left(\frac{293.9}{176.6}\right)^{\frac{(0.4)}{(2)(1.4)}} - 1\right]$$

$$\dot{W}_{sb} = 49.6$$

The first stage compressor ratio is

$$r_{sb} = \left(\frac{293.9}{176.6}\right)^{\frac{1}{2}}$$

$$r_{sb} = 1.29$$

The volumetric efficiency (only for the reciprocating piston compressor), ε_v, is determined from Equation 4-38. The compressor clearance volume ratio, c, is assumed to be 0.06. Equation 4-38 becomes

$$\varepsilon_v = 0.96 \left\{ 1 - (0.06) \left[(1.29)^{\frac{1}{1.4}} - 1 \right] \right\}$$

$$\varepsilon_v = 0.949$$

From Equation 4-39, the actual shaft horsepower, $\dot{W}_{asb}$, required by each compressor is

$$\dot{W}_{asb} = \frac{49.6}{(0.90)\,(0.949)}$$

$$\dot{W}_{asb} = 58.1$$

The above determined 58.1 horsepower is the actual shaft power needed by the reciprocating piston booster compressor to produce the 293.9 psia pressure output (with an input of 176.6 psia from the primary) at the surface location elevation of 4,000 ft above sea level (while drilling at a depth of 10,000 ft).

Total Horsepower of Compressor System

The total actual shaft horsepower, $\dot{W}_{ast}$, needed by the combined primary and booster compressor system in each unit is

$$\dot{W}_{ast} = \dot{W}_{asp} + \dot{W}_{asb}$$

$$\dot{W}_{ast} = 409.8 + 58.1$$

$$\dot{W}_{ast} = 467.9$$

At this surface location, the input horsepower available from the Caterpillar Model 3412 prime mover is a derated value (derated from the rated 740 horsepower available at 1,800 rpm). In order for the compressor units to operate at this 4,000 ft

surface location elevation, the derated input power available must be greater than the total actual shaft power needed. Figure 4-15 shows that for 4,000 ft elevation the input power of a turbocharged prime mover must be derated by approximately 10 percent. The derated input horsepower, $\dot{W}_i$, available from the prime mover is

$$W_i = 740 \ (1 - 0.10)$$

$$\dot{W}_i = 666.0$$

For this illustrative example, the prime mover of each of the two compressor units derated input power is greater than the total actual shaft horsepower needed, thus, these compressor units can be operated at this 4,000 ft surface location elevation (while drilling at a depth of 10,000 ft).

Fuel Consumption

The anticipated drilling rate of penetration is estimated to be 60 ft/hr. The vertical interval section to be drilled is from a depth of 7,000 ft to depth of 10,000 ft, or a 3,000 ft length of borehole. Therefore, the estimated actual drilling time to drill this interval is approximately 50 hours.

The injection pressure into the top the drill string while drilling at 10,000 ft of depth was found to be approximately 293.9 psia. Using similar calculations, the injection pressures for depths from 7,000 ft to 10,000 ft can be obtained. Figure 8-11 shows these injection pressures as a function of drilling time (or drilling depth).

These compressor system units are a unique combination of a rotary screw primary compressor (with a fixed pressure ratio) and a reciprocating piston booster compressor driven by a single Caterpillar Model 3412 prime mover.   Since the injection pressure required (293.9 psia) is greater than the fixed ratio derated output pressure of the rotary screw primary compressor (176.6 psia), then the reciprocating piston booster will match its output with the required injection pressure. Thus, for this operational situation Figure 8-11 shows only one curve indicating the injection pressure is the same as the pressure output of the compressor units. (Note that if the injection pressure is less than the derated output pressure of the rotary screw primary compressor, there would be two curves on Figure 8-11. One flat horizontal line for at 176.6 psia for the primary compressor pressure output and another curve representing the actual back pressure   which is the injection pressure.   The compressor system fuel consumption is determined from the primary compressor output pressure.)

Above it was found that the total actual shaft horsepower required by the combined primary and booster compressor system in each of the two units to compress air to 293.9 psia was approximately 467.9 (at 10,000 ft of depth). Also in the above the derated horsepower available from the Caterpillar Model 3412 prime mover at the surface elevation of 4,000 ft was found to be approximately 666. Drilling at a depth of 10,000 ft, the prime mover power ratio is

$$PR = \frac{467.9}{666.0} \ (100) = 70.3$$

Figure 4-17 gives a diesel fuel consumption rate of 0.538 lb/hp-hr for a prime mover power ratio of 70.3 percent. The total weight rate of diesel fuel consumption per hour is

$$\dot{w}_f \ = \ 0.583 \ (467.9) \ = \ 251.7 \ \text{lb/hr}$$

The diesel fuel consumption rate (in United States gallons) for the drilling depth of 10,000 ft is

$$q_f \ = \ \frac{251.7}{(0.8156)(8.33)} \ = \ 37.1 \ \text{gal/hr}$$
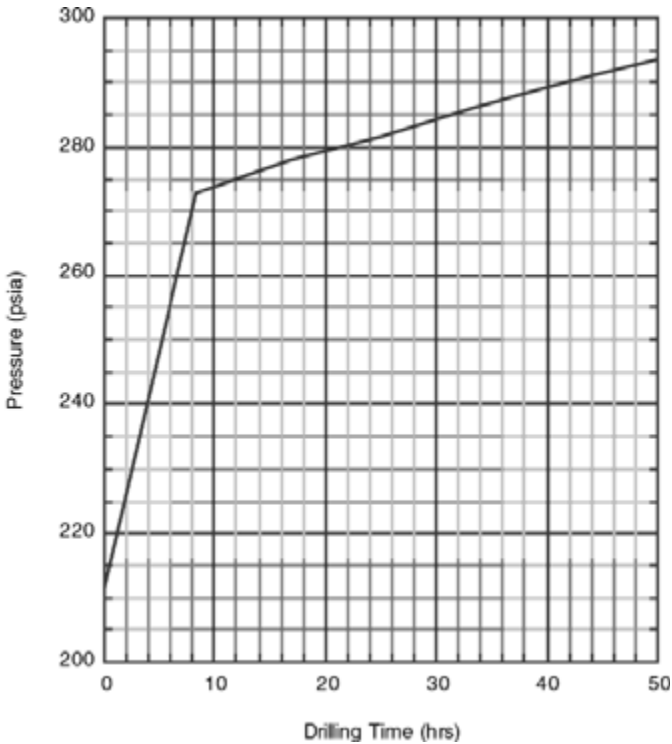
Figure 8-11: Drill string injection pressure (same as booster compressor output pressure) for Illustrative Example 8.4 ($q_g = 3{,}396$ acfm).

   Using the data in Figure 8-11 and similar calculations as those given above, the diesel fuel consumption rate as a function of drilling time (or drilling depth) can be obtained.   Figure 8-12 shows the diesel fuel consumption rate as a function of drilling time (or drilling depth) for each of the compressor units required for this drilling operation. The approximate total diesel fuel needed for each compressor unit is obtained by the integration of the area under the curve in Figure 8-12.   This is approximately 1,793 gallons.   It is standard practice to assume a 20 percent additional volume of fuel for blowing the hole between connections and other compressor operations on the drill rig. Therefore, the approximate diesel fuel needed for each compressor unit is 2,152 gallons.   Therefore, the total diesel fuel needed at the drilling location for compressor operations is approximately 4,304 gallons.
   Illustrative Examples 8.4 demonstrates the calculation procedures (step Nos. 1 to 10 given in Section 8.1) used to plan a typical deep oil or natural gas well drilling operation.
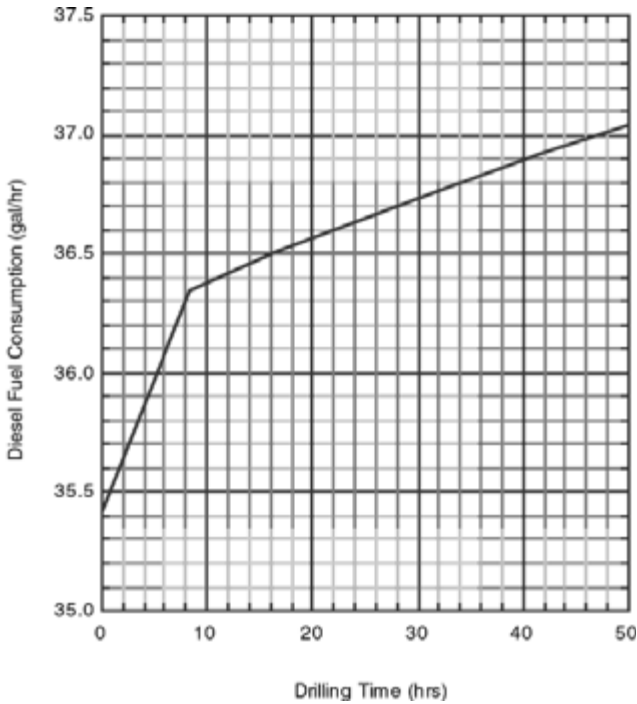
Figure 8-12: Fuel consumption rate as a function of drilling time for the combined primary and booster compressor unit used in Illustrative Example 8.4 ($q_g = 3,396$ acfm).

8.5 Water Injection

Water is injected into the volumetric flow rate of air (or other gases) flowing from the compressors to the top of the inside of the drill string for three important reasons. These reasons are

- Saturate the air or other gas with water vapor at bottomhole annulus pressure and temperature conditions.
- Eliminate the stickiness of the small rock cuttings flour generated by the advance of the drill bit,
- Assist in suppressing the combustion of the mixture of produced hydrocarbons and oxygen rich air.

Figure 8-13 shows the typical "mist" pump. The figure shows a typical stand-alone skid mounted positive displacement duplex liquid pump driven with a Caterpillar Model 3304, diesel fueled, naturally aspirated, prime mover. This pump forces liquid into the pressurized air flow line from the compressors to the standpipe on the drill rig (see Figure 2-1).

Figure 8-13: Liquid "mist" pump for air (or natural gas) drilling operations.

The liquid pump draws its water from a liquid tank (located at the left back end to the skid mounted unit shown in Figure 8-13). Often other additives are mixed in the suction tank. These are typically corrosion inhibitors, polymer, and a foamer [13]. Table 8-2 gives the approximate volume mix of these additives.

Table 8-2: Typical approximate additives volumes per 20 bbls of water for unstable foam drilling (actual commercial product volumes may vary).

Additives	Volume per 20 bbls of Water
Foamer	4.2 to 8.4 gals
Polymer	1 to 2 quarts
Corrosion Inhibitor	0.5 gals

"Mist" injection is the old term which was the injection of water with basically no additives. Modern air drilling defines injection of water with additives as unstable foam drilling operations.

8.5.1 *Saturation of Gas at Bottomhole Conditions*

Water is injected into the air or other circulation gases at the surface in order to saturate the gas with water vapor at bottomhole conditions. The reason this is done is to assure that the circulation gas as it flows out of the drill bit orifices into the annulus will be able to carry formation water coming into the annulus as whole droplets.

If water is not injected into the gas at the surface and the gas is dry when it comes out of the drill bit orifices, a portion of the formation water will be absorbed by the gas as water vapor. Thus, the dry gas will be saturated by the formation water. This saturation process decreases the internal energy (i.e., enthalpy) in the gas as the gas enters the annulus. This reduction in internal energy at the bottom of the annulus dramatically reduces the kinetic energy per unit volume of the gas as it flows from the bottom of the annulus to the surface (this reduction in kinetic energy per unit volume is mainly due to a reduction in velocity). The reduction in kinetic energy per unit volume in the annulus reduces the carrying capacity of the gas throughout the annulus. This reduction in carrying capacity of the circulation gas occurs when the circulation system needs all of its carrying capacity to carry to the surface the additional load (beyond the rock cuttings load) of the formation water flowing into the annulus.

By injecting water at the surface into the gas, the gas becomes saturated with water vapor inside the drill string as it flows down the string. Therefore, the gas is saturated with water vapor when it reaches the bottom of the inside of the drill string and flows into the annulus. As this saturation process occurs inside of the drill string the compressor systems at the surface continue to maintain compression in the gas column and, thus, maintain the internal energy of the column. Therefore, when this gas enters the annulus it is already saturated with water vapor and cannot absorb the formation water as water vapor. Further, the gas has the internal energy to carry the new load of formation water as droplets. This is the most efficient method of carrying an influx of formation water from the annulus of a well. In general, it is not efficient to try to use dry gas to absorb formation water as a water vapor and, in essence, "dry-out" a well.

The empirical formula for determining the saturation of various gases including air can be found in a variety of chemistry handbooks and other literature. The empirical formula for the saturation pressure of air, p_{sat}, can be written as [14]

$$p_{\text{sat}} = 10^{\left[6.39416 - \left(\frac{1,750.286}{217.23 + 0.555 \, t_{bh}} \right) \right]} \qquad (8\text{-}5)$$

where p_{sat} is saturation pressure of the air at annulus bottomhole conditions (psia). The approximate volumetric flow rate of injected water to an air drilling operation is determined by the relationship between the above saturation pressure and the

bottomhole pressure in the annulus, and the weight rate of flow of air being injected into the top of the drill string. Thus, the flow rate of injected water, q_{iw}, is determined from [15]

$$q_{iw} = \left(\frac{p_{sat}}{p_{bh} - p_{sat}} \right) \left(\frac{3,600}{8.33} \right) \dot{w}_g \qquad (8\text{-}6)$$

where q_{iw} is the volumetric flow rate of injected water (gal/hr or bbl/hr).

Illustrative Examples 8.5 describes the implementation of the basic planning step No. 11 given in Section 8.1.

Illustrative Example 8.5 Determine the volumetric flow rate of injected water needed to saturate the volumetric flow rate of air at bottomhole conditions in the Illustrative Example 8.3 series (drilling at a depth of 10,000 ft). Assume the injected water has a specific gravity of 1.0.

In Illustrative Example 8.3a compressors were selected for drilling the 10,000 ft deep borehole. The total volumetric flow rate of air delivered by these compressors was 2,400 acfm. In Illustrative Example 8.3b it was found that while drilling at 10,000 ft the bottomhole annulus pressure was 204.5 psia and the bottomhole annulus temperature was 604.41 R (or 144.74˚F). In Illustrative Example 8.3b the weight rate of flow of air through the circulation system for the example was 2.635 lb/sec.

Using the bottomhole temperature given above, Equation 8-5 becomes

$$p_{sat} = 10^{\left[6.39416 - \left(\frac{1,750.286}{217.23 + 0.555 \ (144.74)} \right) \right]}$$

$$p_{sat} = 3.251 \ \text{psia}$$

Using the bottomhole pressure, the weight rate of flow and the above saturation pressure, Equation 8-6 becomes

$$q_{iw} = \left(\frac{3.251}{204.5 - 3.251} \right) \left(\frac{3,600}{8.33} \right) (2.635)$$

$$q_{iw} = 18.5 \ \text{gal/hr}$$

The above water injection volumetric rate is slightly less than half a barrel per hour.

The illustrative example above demonstrates that very little injected water is needed to saturate an air flow at bottomhole conditions. This is also the case for the other two important gases used for drilling operations, natural gas and inert air. In essence, it requires a small volumetric flow rate of injected water to create a more

effective formation water carrying circulation gas.   Nearly all injected water is injected with additives (see Table 8-2).

After water has been injected into the circulation gas, it is necessary to determine how much formation water can be carried from the openhole section of a borehole. Since the injected water saturates the circulation gas, it can be assumed that the formation water will be carried from the well as droplets. Since the gas volumetric flow rate to the well is known and is greater than the minimum volumetric flow rate needed to clean the well (carry the anticipated drilling rate of rock cuttings), then the extra volumetric flow rate of gas (beyond the minimum) will allow a much greater drilling rate. This additional drilling rate that the gas volumetric flow rate can support can also be droplets of formation water. Thus, the additional drilling rate can be converted to a weight rate of flow or a volumetric flow rate of formation water that can be carried from the well.

Illustrative Examples 8.6 describes the implementation of the basic planning step No. 12 given in Section 8.1.

Illustrative Example 8.6 Determine the influx of formation water into the annulus that can be carried from the example well in the Illustrative Example 8.3 series (drilling at a depth of 10,000 ft). Assume a formation water specific gravity of 1.07.

The Illustrative Example 8.3b the 10,000 ft deep well was drilled with an air circulation volumetric flow rate of 2,400 acfm. In Illustrative Example 8.2 the minimum volumetric flow rate required to clean the example well was found to be 1,840 acfm.   Using a actual volumetric flow rate of 2,400 acfm (from the compressors) with either the problem setups in Illustrative Examples 8.1 and 8.2, or the more detailed problem set-up in Illustrative Example 8.3b, trial and error calculations can be made to determine the drilling rate value κ that can be supported by this volumetric flow rate. Using the more detailed problem setup in Illustrative Example 8.3b the minimum kinetic energy position in the annulus of the well is found to be at the bottom of the drill pipe body inside the cased section of the well (i.e., at the bottom of H_1). Using the minimum kinetic energy criteria of 3.0 ft-lb/ft^3 at the bottom of H_1, the calculated maximum drilling rate that can be supported by the volumetric flow rate of 2,400 acfm is found to be approximately 400 ft/hr. Using a 20 percent factor of safety reduction of calculated maximum drilling rate, the actual sustainable maximum drilling rate is

$$\kappa_{max} = 400 \ (1 - 0.20)$$

$$\kappa_{max} = 320 \ \text{ft/hr}$$

The approximate volumetric flow rate of formation water, q_{fw}, that can be carried is

$$q_{fw} = \frac{\pi}{4} \ D_h^2 \left(\kappa_{max} - \kappa \right) \frac{(62.4) \ S_s}{(8.33) \ S_{fw}} \qquad (8\text{-}7)$$

where q_{fw} is the volumetric flow rate of formation water (gal/hr or bbl/hr),

κ is the actual drilling rate used in the well,

S_{fw} is the specific gravity of the formation water.

For this illustrative example Equation 8-7 becomes

$$q_{fw} = \frac{\pi}{4} (0.656)^2 (320 - 60) \frac{(62.4)(2.7)}{(8.33)(1.07)}$$

$$q_{fw} = 1,663 \text{ gal/hr}$$

or

$$q_{fw} = \frac{1,663}{42} = 40 \text{ bbl/hr}$$

The influx of formation water into the annulus can increase the bottomhole pressure in the annulus and injection pressure into the top of the drill string. If water is injected into the injected gas flow to the well, the gas entering the annulus will be saturated and the injected water and the formation water in the annulus can be assumed to be carried as droplets (or as a particle mass). Also, the injected water can be assumed to be carried as droplets in the inside of the drill string. Therefore, in order to assess the effects of injected water and lifted formation water in the annulus, Equation 6-52 is altered to include the weight rates of flow of injected water, $\dot{w}_{iw}$, and the lifted formation water, $\dot{w}_{fw}$. Equation 6-52 becomes

$$a_a = \left(\frac{S_g}{R}\right)\left[1 + \left(\frac{\dot{w}_s + \dot{w}_{iw} + \dot{w}_{fw}}{\dot{w}_g}\right)\right] \tag{8-8}$$

where $\dot{w}_{iw}$ is the weight rate of flow of injected water (lb/sec),

$\dot{w}_{fw}$ is the weight rate of flow of formation water (lb/sec).

For flow in the inside the drill string, Equation 6-69 becomes

$$a_i = \left(\frac{S_g}{R}\right)\left[1 + \left(\frac{\dot{w}_{iw}}{\dot{w}_g}\right)\right] \tag{8-9}$$

The values of $\dot{w}_{iw}$ and $\dot{w}_{fw}$ are, respectively,

$$\dot{w}_{iw} = \frac{q_{iw}(42)(8.33)}{(3,600)} \tag{8-10}$$

$$\dot{w}_{fw} = \frac{q_{fw}\ (42)\ (8.33)}{(3,600)} \tag{8-11}$$

Illustrative Example 8.7 Determine the bottomhole and injection pressures for the example well given in the Illustrative Example 8.3 series. If the volumetric flow rate of injected water is a constant 2 bbl/hr, determine the bottomhole and injection pressures for the volumetric flow rates of formation water of 0 bbl/hr to 35 bbl/hr. Assume a formation water specific gravity 1.07.

Using Equations 8-8 to 8-10 in the problem setup in Illustrative Example 8.3b the bottomhole and injection pressures can be calculated for a constant volumetric flow rate of injected water of 2 bbl/hr and the volumetric flow rate of formation water of 0 bbl/hr to 35 bbl/hr. Figure 8-14 shows the increases in bottomhole and injection pressures as a function of the volumetric flow rate of formation water being carried from the well (while drilling a depth of 10,000 ft).
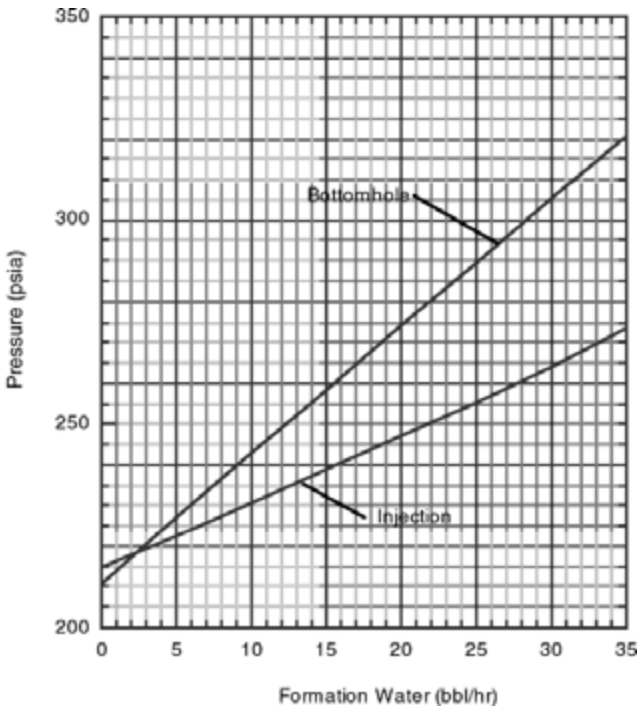
Figure 8-14: Illustrative Example 8.7 bottomhole and injection pressures as a function of formation water being carried from the well (drilling at a depth of 10,000 ft).

The figure shows that the bottomhole pressure increases nearly linearly with the increase in formation water volume being carried out of the well. At a formation water volumetric flow rate influx of 0 bbl/hr the bottomhole pressure is approximately 210 psia. At a formation water volumetric flow rate influx of 35 bbl/hr the bottomhole pressure is approximately 320 psia. This increase in bottomhole pressure due to formation water influx is an important formation damage consideration.

The figure also shows a less steep linear increase in injection pressure as a function of formation water influx. At a formation water volumetric flow rate influx of 0 bbl/hr the injection pressure is approximately 215 psia (2 bbl/hr of fresh water is still being injected at the surface). At a formation water volumetric flow rate influx of 35 bbl/hr the injection pressure is approximately 273 psia. Therefore, an influx of formation water to a well annulus will increase the power requirements of the prime movers of the two compressor units and, thus, the diesel fuel required to drill the openhole interval.

8.5.2 *Eliminate Stickiness*

The Illustrative Example 8.5 demonstrated that the water injected volumetric flow rate to the well in order to saturate the circulation air flow at bottomhole conditions is quite small. But there are other reasons for injecting water into the injected air flow. The next level of injected water volumetric flow rate (with additives) is that needed to eliminate stickiness.

As the drill bit advances in some types of rock formations, the cutting action of the bit creates rock particles and a small amount of "rock flour". Rock flour is very small cuttings particles that act mechanically very much like the flour one cooks with in the kitchen. If a borehole is originally dry, the circulation air will efficiently carry the rock cutting particles and the rock flour up the annulus to the surface as the drill bit is advanced. If a water bearing formation is drilled, formation water will begin to flow into the annulus. When the water combines with the rock flour, the flour particles being to stick to each other. This is very much like placing cooking flour in a bowl and putting a small amount of water in with it and mixing it. The cooking flour will become sticky and nearly impossible to work with a spoon. In the open borehole, the slightly wetted rock flour sticks to the nonmoving inside surface of the borehole. Because the gas flow eddy currents form just above the top of the drill collars, "mud rings" of this sticky rock flour form at this location on the borehole wall (see Figure 8-15). These mud rings can build up and create a constriction to the annulus gas flow. This flow constriction will in turn cause the injection pressure to increase slightly (by 5 to 10 psi) in a matter of a minute or so. This rather sharp increase in pressure should alert the driller that mud rings are forming due to an influx of formation water (or perhaps even crude oil). If mud rings are allowed to continue to form they will begin to resist the rotation of the drill string. This in turn will increase the applied torque at the top of the drill string and increase the danger of a drill string torque failure. Also, the existence of mud rings creates a confined chamber of high pressure air. If hydrocarbon rock formations are being drilled, the potential for ignition increases. The solution to this operational problem is to begin to inject water into the circulation gas. As seen in Illustrative Example 8.5, the initial one-fourth to a half barrel per hour of injected

water will be used to saturate the drilling gas with water vapor. Additional injected water is needed to reduce the stickiness (in much the same way the cooking flour stickiness is reduced by adding more water). The amount of water added to eliminate the mud ring stickiness must be determined experimentally and will be somewhat unique for each drilling operation. As seen in Figure 8-14, additional injected water will increase the bottomhole and injection pressures.

The procedure for eliminating mud rings is as follows:

1. Begin injecting sufficient water to saturate the gas flow with water vapor.
2. Curtail drilling ahead but continue gas circulation.
3. Bring the rotations of the drill string up to about 100 rpm and lift the drill string up to the top of the drilling mast and lower it several times. This will allow the drill collars to smash into the mud ring structures and break them off the borehole wall.
4. Return to drilling ahead.
5. If the mud rings begin to form again (the injection pressure increases again), increase the water injection flow rate and repeat the above sequence.
6. Continue the above five steps until the volumetric flow rate of injected water reduces the stickiness of the rock flour so that the mud rings no longer form on the open borehole wall.

For the example borehole given in Illustrative Example 8.5, the typical injected water volumetric flow rate to eliminate rock flour stickiness would be of the order of approximately 2 to 10 bbl/hr.
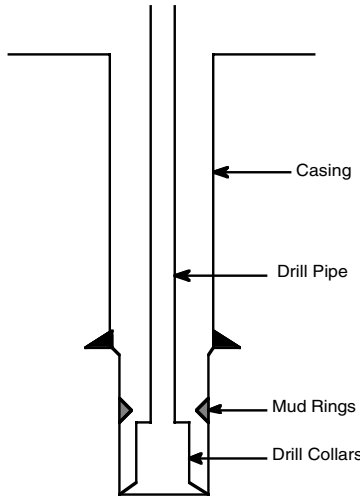
Figure 8-15: Mud ring on the openhole section borehole wall.

8.5.3 *Suppression of Hydrocarbon Ignition*

The next higher level of water injection volumetric flow rate is the volume needed to suppress the ignition of downhole explosions and fires due to the mixture of circulation air with produced oil, natural gas, or coal dust and fragments as the drill bit is advanced. When drilling into rock formations that are coal seams, or reservoir rock containing oil or natural gas, the steel drill bit action on the rock cutting face can easily cause a spark. If the circulation gas is air then the three ingredients for downhole ignition are present (i.e., hydrocarbons, a spark, and an oxygen source). Increasing the water injection volumetric flow rate (with additives) to the borehole and creating unstable foam at the bottom of the well will suppress most fire and explosion hazards for a vertical well [16, 17]. This tends to be successful in vertical wells but not successful in horizontal boreholes [18]. This is because vertical wells tend to penetrate the vertical thickness of the hydrocarbon producing reservoir (usually a horizontal sedimentary rock formation). The vertical thickness of these reservoirs tend to be of the order of a few hundred feet. Thus, at a drilling rate of 60 ft/hr, the exposure time in the hazardous production zone is only a few hours. On the other hand, horizontal boreholes require the drilling of several thousands of feet of openhole in the hydrocarbon bearing reservoir. The drilling rates in horizontal boreholes are usually about half the drilling rates in vertical wells. Thus, the exposure time in a horizontal borehole is of the order of ten to near one hundred hours. The unsuccessful record of ignition suppression with unstable foam in horizontal boreholes is generally considered the consequence of the long exposure (drilling time) in hydrocarbon producing rock formations. There are of course other drilling methods that can be used to suppress or eliminate hydrocarbon ignition. These methods require the use of circulation gases that will not support ignition. These other circulation gases are natural gas for a gas pipeline, industrial liquid nitrogen based gas, and inert atmospheric air (created by placing stripper/filter equipment downstream from the compressors to remove oxygen). The use of these other drilling gases can significantly increase drilling operation costs.

Figure 8-16 gives the ignition (ignition zone) parameters of pressure versus the percent mixture of natural gas with atmospheric air [19, 20]. In general, natural gas presents the somewhat greater hazard relative to exposure to oil and coal. This is because the mixture of air and natural gas creates an explosive hazard whereas the mixture of oil and coal creates more of a downhole fire hazard. Figure 8-16 shows that the hazard of ignition increases with higher pressures (the wider the region of ignition at the top of Figure 8-16). Thus, the deeper the drilling operation, the higher the bottomhole pressures and in turn the ignition probability in the presence of hydrocarbons.

Using the data in Figure 8-16 and applicable field case histories, Figure 8-17 has been prepared as a water injection guideline for suppressing the ignition of downhole hydrocarbon mixtures with air. The guidelines in this figure are only applicable for vertical boreholes in which the exposed oil and natural gas producing reservoirs, and solid coal seam thicknesses are of the order of 200 ft or less.

There may be no absolute way to prevent downhole explosions and fires when drilling with air in hydrocarbon bearing rock formations, but measures can be taken to decrease the chance of ignition. As in any air drilling operation, constant supervision is necessary. But air and gas drilling operations are unique in that the warning signs of downhole problems are usually in the form of rapid increases of

injection pressures of as little as 5 to 10 psi. This type of warning requires intense attention of drilling operations supervisors. Pressure recorders with rapid pressure rate increase alarms can be installed for use by drilling supervisors. Such pressure alarms will only be useful for operations using drill bits with open orifices (subsonic flow in the throat of the orifices).
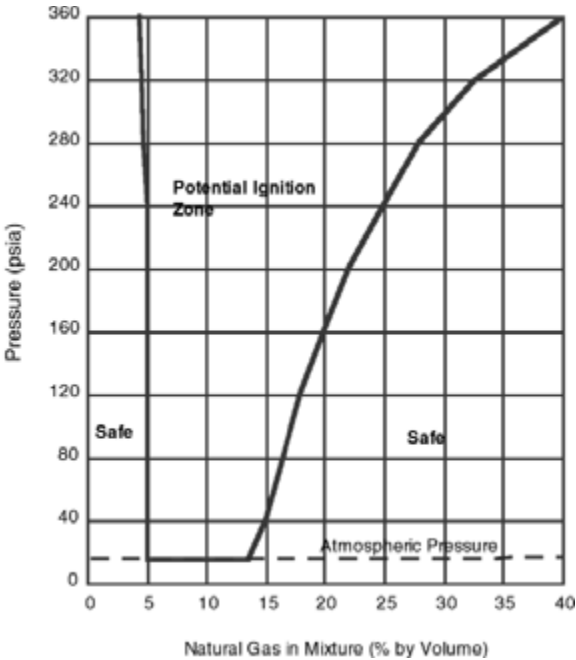
Figure 8-16: Ignition mixture by volume of natural gas and atmospheric air [19].

As the drill bit of a vertical dry air drilling operation approaches a hydrocarbon bearing rock formation, the following steps should be taken to prevent hydrocarbon downhole ignition [19, 20]:

1. Drilling should be immediately stopped.
2. Air injection should be shut off and the gas flare monitored. If the flare is sustained, the operator should note the wetness of the cuttings at the sample catcher (indicating whether the gas is wet; black smoke and/or yellow color of burning gas (indicating distillate in gas); sparks at the end of the blooey line (indicating drill cuttings are damp from distillate). If the gas flare will not sustain or burn when the air is turned off, air should be turned back on.

3. With the air turned on and flowing to the well, and it has been determined that the gas is wet, no drilling should be carried out since rock flour and cuttings will likely form mud rings. With air on, raise

   and lower the drilling string with the drill string rotating at approximately 100 rpm to smash up existing mud rings and prevent formation of new mud rings.

4. If the gas is wet (with water or distillate), begin the injection of water and additives (given in Table 8-1) into the injected air flow. Use Figure 8-16 as a guideline to determine the amount of water to be injected into a vertical well. Begin to drill with unstable foam circulation fluid. (Note an alternative is to switch to natural gas, industrial nitrogen, or inert atmospheric as the circulation gas.)
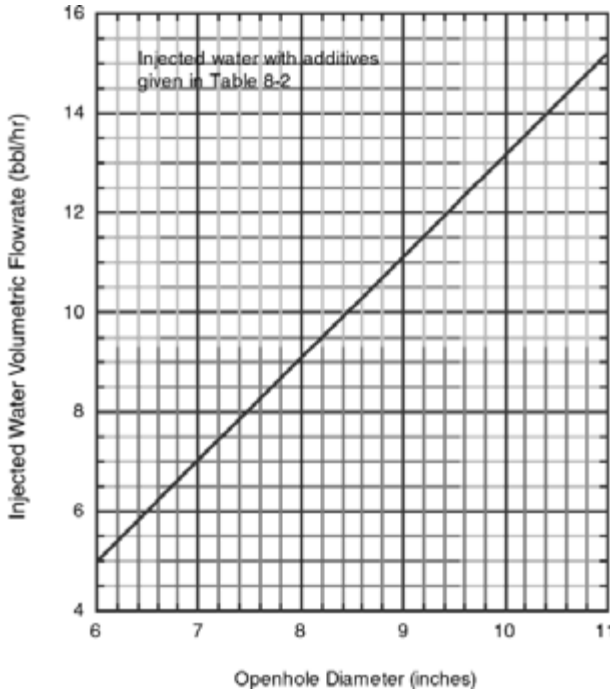
Figure 8-17: Guideline for water injection (with foam drilling additives) to suppress ignition of downhole hydrocarbons (for vertical boreholes with hydrocarbon bearing formations of approximately 200 ft or less).

5. If the gas is dry and there are no sparks and no black smoke nor wet samples at the surface, drill 5 to 10 ft and then raise and lower the drill string to avoid a pressure increase due to mud rings. Continue drilling at 5 to 10 ft increments until the wet gas condition does not exist.

There is a new technology that allows underbalanced drilling operations to be carried out using inert atmosphere. This new technology has allowed for the development of an industrial sized filter system that strips most of the oxygen from the compressed air output of the primary compressor [21]. The compressed inert atmosphere gas either flows directly to the top of the drill string or via a booster compressor to the drill string.

8.6 Drilling and Completion Problems

There are important drilling completion problems that are unique to air and gas drilling operations. These require unique solutions.

8.6.1 *Sloughing Shales*

Since the drilling circulation fluid is not heavy, there is a constant threat of caving and sloughing of the openhole borehole wall. Air and gas drilling operations will have drilling penetration rates that can be twice that of mud drilling operations. This faster drilling penetration rate is an important feature since openhole integrity is very dependent upon the length of time the hole remains open and unsupported by cement and casing.

When drilling with air and gas the shale sequences of rock formations are usually the most susceptible to caving or sloughing. This is due mainly to bedding layered texture of shale and the generally weak bonding between these layers. Thus, when these shales are penetrated with a drill bit, the openhole wall surfaces of the exposed shale formations tend to break off and the large fragments fall into the annulus space between the openhole wall and the drill collar and drill pipe outside surfaces. This sloughing of shale formations can be temporarily controlled by injecting additional additives into water being injected into the circulation air or gas (in addition to those given in Table 8.2). Table 8.3 gives the formula for these additional additives. This formula has been successfully used in the San Juan Basin.

Table 8-3: Typical approximate additive weights or volumes per 20 bbls of water for controlling sloughing shales (actual commercial product may vary).

Additives	Weights or Volumes per 20 bbls of Water
Foamer	8.5 gallons
Bentonite	40 lbs
CMC	2 lbs
Corn Starch	5 lbs
Soda Ash	1 quart

8.7.2 *Casing and Cementing*

When drilling with air or gas, the borehole will be basically dry when the borehole is cased and cemented. The well is not filled with treated water and the

casing is floated into the well (making use of buoyancy) as is done in mud drilling operations. This presents some special problems for air and gas drilling operations.

When an openhole section of a gas drilling well is to be cased, the casing with a casing shoe on the bottom is lowered into the dry well. A pre-flush of about 20 bbls of CMC (carboxymethyl-cellulose) treated water must be pumped inside the casing just prior to pumping the cement. A diaphragm (bottom) plug is run ahead of the CMC treated water pre-flush, another diaphragm (bottom) plug run behind the CMC treated water pre-flush and ahead of the cement, and a final top plug run behind the cement. Fresh water is pumped directly behind the top plug and fills the inside of the casing to the surface. The CMC treated water pre-flush seals the surface of the dry borehole walls prior to the cement and precludes the cement from hydrating as it flows from the inside of the casing to the annulus between the openhole and the outside of the casing. This CMC treated water pre-flush is essential. If the pre-flush is not used the initial cement flowing through the casing shoe to the untreated openhole of the borehole will immediately set-up and disallow the remaining cement to flow to the annulus.

Once the casing and cementing operations are properly carried out and the cement successfully sets up in the annulus, it is necessary to remove the water from inside the casing in order to return to gas drilling operations (drill out the cement at the casing shoe and continue drilling ahead). There are several safe operational procedures that can be used to removing water from the inside of the casing after a successful cementing operation.

Aerated Fluid Procedure

The aerated fluid procedure is as follows [22]:

1. Run the drill string made up with the appropriate bottomhole assembly and drill bit to a depth a few tens of feet above the last cement plug.
2. Start the mud pump running as slowly as possible, to pump water at a rate of 1.5 to 2.0 bbl/min. This reduces fluid friction resistance to the moving fluids in the circulation system.
3. Bring one compressor and booster on line to aerate the water being pumped to the top of the drill string. The air rate to the well should be about 100 to 150 acfm per barrel of water. If the air volumetric flow rate is too high, the standpipe pressure will exceed the pressure rating of the compressor and the compressor will shut down. Therefore, the compressor must be slowed down until air is mixed with the water going into the drill string.
4. As the fluid column in the annulus (between the inside of the casing and the outside of the drill string) is aerated, the standpipe pressure will drop. Additional compressors can be added (i.e., increasing air volumetric flow rate) to further lighten the fluid column and unload the water from the casing.
5. After the hole has been unloaded, the water injection pumps should be kept in operation to clean the borehole.
6. At this point, begin air or mist drilling. Drill out the cement at the bottom of the casing and drill an additional 20 ft to 100 ft to allow any sloughing walls of the borehole to clean up.
7. Once the hole has been stabilized, stop drilling and blow the hole with

air and injected water to eliminate rock cuttings. Continue this drilling and cleaning procedure for 15 to 30 minutes or until the air flow (with injected water) returning to the surface is clean (i.e., shows a fine spray and white color).

8. With the drill bit directly on bottom, continue flowing air with no injected water into the drill string. Air should flow to the well at normal drilling volumetric flow rates until the water and surfactant remaining in the well are swept to the surface.

9. Continuously blow the hole with air for about 30 minutes to an hour.

10. Begin normal air drilling. After 5 ft to 10 ft have been drilled, the hole should go to dry dust drilling (although it is sometimes necessary to drill as much as 60 ft to 90 ft before dry dust appears at the surface). If the hole does not dust after these steps have been carried out, inject another surfactant slug into the air flow to the well. If dry dusting cannot be achieved, unstable foam drilling may be required to complete the air drilling operation.

Air Lift Procedure

The air lift procedure is as follows:

1. Calculate the lifting capability of the primary and booster compressors on the drilling location. Run the drill string made up with the appropriate bottomhole assembly and drill bit to a depth a few hundred feet above this calculated compressor pressure limit.

2. Start the compressors and force compressed air to the bottom of the drill string and begin aerating the water column in the annulus and flow this aerated water column to the surface (removing this portion of the column from the well).

3. Once this column of water has been removed, shut down the compressors and lower the drill string a similar distance as defined by the lifting capability limit determined in No. 1 above. Start up the compressors and remove this next column of water from the well.

4. Continue lowering the drill string in increments and air lifting the entire water column from the well.

5. With the drill bit directly on bottom, continue flowing air into the drill string. Air should flow to the well at normal drilling volumetric flow rates until the water and surfactant remaining in the well are swept to the surface.

6. Continuously blow the hole with air for about 30 minutes to an hour.

7. Begin normal air drilling. After 5 ft to 10 ft have been drilled, the hole should go to dry dust drilling (although it is sometimes necessary to drill as much as 60 ft to 90 ft before dry dust appears at the surface). If the hole does not dust after these steps have been carried out, inject another surfactant slug into the air flow to the well. If dry dusting cannot be achieved, unstable foam drilling may be required to complete the air drilling operation.

Slug Procedure

The slug procedure (also known as "rocking the well") is similar to that given in the aerated fluid procedure given above. However, in the slug procedure the mud

pump and the air compressors are alternately allowed to force packages of water slugs or compressed air into the top of the drill string. After a series of slugs have been injected into the top of the drill string and these slugs have passed into the annulus, the well water column in the annulus will begin to be lifted (or unloaded) to the surface. To create these slugs, it is necessary for operational personnel at the drilling location to rapidly turn on and off the mud pump and compressors in a sequence that will produce slugs of water and air inside the drill string. Thus, this procedure creates high transient pressures in the mud pump, compressors, and surface line piping to the drill rig. These transient pressures are not generally predictable and, therefore, pose a safety hazard to personnel and equipment. Therefore, this procedure is not recommended for use.

8.7 Field Comparisons

The following case histories of vertical drilling operations demonstrate the accuracy of the planning calculation procedures discussed earlier that utilize complete major and minor friction loss terms [23].

Case History No. 1 This was a sidetrack re-drill of an existing 17,000 ft deep gas well in West Texas (Ellenberger formation). The casing and openhole profile for this well was 9 5/8 inch casing from surface to 8,900 ft, 7 5/8 inch liner from 8,900 ft to 12,000 ft, 5 1/2 inch liner from 12,000 ft to 15,900 ft, and a 4 1/2 inch openhole from 15,900 ft to 17,000 ft TD. The drill string profile (while drilling at 17,000 ft) for this well was 4 1/2 inch drill pipe from surface to 7,900 ft, 3 1/2 inch drill pipe from 7,900 ft to 10,500 ft, and 2 7/8 inch drill pipe from 10,500 ft to 17,000 ft. The drilling gas was inert atmospheric air (specific gravity of approximately 0.95) with a volumetric flow rate to the well of approximately 2,300 scfm (surface elevation location of approximately 3,300 ft). No water and additives were being injected. The predicted surface injection pressure was 1,245 psig and the actual injected pressure was approximately 1,000 to 1,300 psig. The predicted bottomhole pressure was 576 psig.

Case History No. 2 This was another sidetrack re-drill of an existing West Texas gas well (Ellenberger formation). The well was drilled to 14,900 ft. The casing and openhole profile for this well was 5 1/2 inch casing set from surface to 13,200 ft, and a 4 1/2 inch openhole from 13,200 ft to 14,900 ft TD. The drill string profile (while drilling at 14,900 ft) for this well was 2 3/8 inch drilling tubing from surface to 14,480 ft, 2 3/8 inch drill pipe from 14,480 ft to 14,600 ft, and 3 1/8 inch drill collars from 14,600 ft to 14,900 ft. The circulation fluid was natural gas with a specific gravity of 0.86. The natural gas volumetric flow rate to the well was approximately 1,400 acfm (at a surface elevation location of approximately 3,300 ft atmospheric temperature approximately 60˚F). No water and additives were being injected. The predicted surface injection pressure was 659 psig and the actual injected pressure was approximately 700 psig. The predicted bottomhole pressure was 218 psig.

The above two case histories show clearly the reduction in bottomhole pressures that can be attained when a slim drill sting is used to drill deep boreholes with small casing and openhole profiles. This reduction in bottomhole pressure is a very important issue when drilling into low pore pressure mature gas or oil fields. Air or

natural gas drilling can cause formation damage in low pore pressure reservoirs, but good drilling string design can usually avoid such damage.

8.8 Conclusions

The discussion in this chapter has concentrated on direct circulation operations. It has been tacitly assumed that there are few reverse circulation operations deeper than the 3,000 ft depth criteria set by this book (see Chapter 5). But it should be noted that for those rare drilling situations where reverse circulation is used to drill beyond 3,000 ft, the discussions given above for major and minor losses, water injection, and drilling and completions problems are, in general, applicable to reverse circulation operations.

The demonstration calcuations in this chapter have utilized lumped geometry approximations for the drill pipe body and drill pipe tool joints.   Such approximations appear to adequately model the overall friction resistance in the circulation system and give accurate results for bottomhole and injection pressures. An improvement to this drill string geometry approximation technique can be made by programming each tool joint indivdually at its proper location in the drill string. This type of program would be best carried out using a higher level computer language such as C++ or FORTRAN. Such a programmed solution would improve the detail pressure versus depth accuracy of the model. However, a comparison of this type of program gives very little change in bottomhole and injection pressures, and in the required volumetric flow rate of gas.

References

1. Lyons, W. C., *Air and Gas Drilling Manual,* First Edition, Gulf Publishing Company, 1984.

2. *Underbalanced Drilling Manual*, Gas Research Institute Publication, GRI Reference No. GRI-97/0236, 1997.

3. Angel, R. R., "Volumetric Requirements for Air or Gas Drilling," *Petroleum Transactions, AIME*, 1957.

4. Angel, R. R., *Volume Requirements for Air and Gas Drilling*, Gulf Publishing Company, 1958.

5. Wolcott, D. S., and Sharma, M. P., "Analysis of Air Drilling Circulating Systems with Application to Volume Requirement Estimations," SPE Paper No. 15950, *Proceedings of SPE Eastern Regional Meeting,* Columbus, Ohio, November 12-14, 1986.

6. Ikoku, C. U., and Williams, C. R., "Drill Cuttings Transport in Vertical Annuli by Air, Mist and Foam in Aerated Drilling Operations," Contracts for Field Projects and Supporting research on Enhanced Oil Recovery and Improved Drilling Technology: Progress Review No. 24, February 1981.

7. Machado, C. J, and Ikoku, C. U., "Experimental Determination of Solids Fraction and Minimum Volumetric Requirements in Air and Gas Drilling," *Journal of Petroleum Technology*, November 1982.

8. Mitchell, R. F., "Simulation of Air and Mist Drilling for Geothermal Wells." *Journal of Petroleum Technology*, November 1983.

9. Tian, S. and Adewumi, M. A., "Development of Hydrodynamic-Model-Based Air-Drilling Design Procedures", *SPE Drilling Engineering*, December 1992.

10. Marcus, R. D., Leung, L. S., Klinzing, G. E., and Rizk, F., *Pneumatic Conveying of Solids*, Chapman and Hall, 1990.

11. Lyons, W. C., Miska, S., and Johnson, P. W., "Downhole Pneumatic Turbine Motor: Testing and Simulation Results," *SPE Drilling Engineering*, September 1990.

12. Daugherty, R. L., Franzini, J. B., and Finnemore, E. J., *Fluid Mechanics with Engineering Applications*, Eighth Edition, McGraw-Hill, 1985.

13. *API Recommended Practice for Testing Foam Agents for Mist Drilling*, API RP-46, First Edition, November 1966.

14. *Handbook of Chemistry*, McGraw-Hill, 1956.

15. Miska, S., "Should We Consider Air Humidity in Air Drilling Operations," *Drill Bit*, July 1984.

16. Scott, S. L., Wu, Y., and Bridges, T. J., "Air Foam Improves Efficiency of Completion and Workover Operations in Low-Pressure Gas Wells," *SPEDC*, December 1995.

17. Hutchinson, S. O., "Stable Foam Lowers Production, Drilling and Remedial Costs," *17th Annual Southwestern Petroleum Short Course*, April 1970.

18. Kitsios, E., Kamphuis, H., Quaresma, V., Rovig, J. W., and Reynolds, E., "Underbalanced Drilling Through Oil Production Zones with Stable Foam in Oman," IADC/SPE 27525, Presented at the 1994 IADC/SPE Drilling Conference, Dallas, Texas, February 15-18, 1994.

19. U.S. Bureau of Mines Report Investigations No. 3798.

20. Coward, H. F., and Jones, G. W., "Limits of Flammability of Gases and Vapors," Bureau of Mines Bullitin 503, Washington 1952.

21. Allan, P. D., "Nitrogen Drilling System for Gas Drilling Applications," SPE 28320, Presented at the SPE 69th Annual Technical Conference and Exhibition, New Orleans, Louisiana, 25-28 September 1994.

22. Hook, R. A., Cooper, L. W., and Payne, B. R., "Air, Mist and Foam Drilling: A Look at Latest Techniques: Parts I and II," *World Oil*, April and May 1977.

23. Giffin, D. R., and Lyons, W. C., "Case Histories of Design and Implementation of Underbalanced Wells," SPE 55606, Presented at the 1999 Rocky Mountain Regional Meeting, Gillette, Wyoming, May 15-18, 1999.

This page intentionally left blank.

Nine

Aerated Fluids Drilling

The term aerated fluids describes the broad category of drilling fluids that are basically incompressible fluids injected with compressed air or other gases. Aerated drilling fluids have been used to drill both shallow and deep boreholes since the advent of air and gas drilling technology in the mid-1930's. The first engineering discussion of an aerated drilling mud project was given in 1953 [1]. Aerated drilling fluids were initially used to drill through rock formations that had fracture and/or pore systems that could drain the incompressible drilling fluids (e.g., fresh water, water and oil based drilling muds, formation water, and formation crude oil) from the annulus. These borehole drilling fluid theft rock formations are called lost circulation sections. The injection of air into drilling muds has been considered an important technological tool in countering the detrimental effects of lost circulation sections. The injection of air into drilling mud creates bubbles in the mud and because of the surface tension properties of the bubbles relative to the properties of rock and drilling mud, the bubbles tend to fill in the fracture or pore openings in the borehole wall as the aerated mud attempts to flow to the thief fractures and pores [2]. This bubble blockage restricts the flow of the drilling mud into these lost circulation sections and thereby allows the drilling operations to safely progress. Aerated fluids have been used to avoid lost circulation in shallow water well drilling, geotechnical drilling, mining drilling, and in deep oil and natural gas recovery drilling operations. Aerated fluids drilling operations are nearly always direct circulation operations.

Since the late 1980s another important application for aerated fluids drilling operations has emerged. This is underbalanced drilling applied to oil and natural gas

recovery operations.   Over the past two decades practical field research has demonstrated that most oil and natural gas bearing rock formations can be more efficiently produced if they are drilled with a drilling fluids that have hydrostatic flowing bottomhole pressures that are slightly less than the pore pressures of the potential producing rock formations being drilled. Underbalanced drilling operations allow the oil or natural gas to be produced into the annulus as the drilling operation progresses. The underbalanced drilling operation allows the natural fracture and pore systems to be keep clear of rock cutting fines and drilling mud filter cake, thereby, avoiding formation damage.   Formation damage has been a problem in oil and natural gas recovery operations nearly since the discovery of oil and natural gas mineral deposits. Underbalanced drilling operations are often carried out using a variety of incompressible fluids (e.g., crude oil, formation water, or clear water) and a variety compressible gases (e.g., air, inert atmosphere, or natural gas).   Inert atmosphere is created by a filter system (placed downstream of the primary compressor) that strips most of the oxygen from the intake air [3].   This filter process results in a nearly inert atmospheric gas.   The success of aerated drilling fluid drilling in underbalanced drilling operations in the oil and natural gas recovery industry has prompted other industrial drilling uses of this technology.   In particular, aerated fluids drilling technology is being experimented with for drilling deep water wells and for drilling environmental monitoring wells.

This chapter outlines the steps and methods used to plan a successful aerated fluids drilling operation. This chapter also illustrates the application of these steps and methods to typical deep drilling operations. The objective of these steps and methods is to allow engineers and scientists to cost effectively plan their drilling operations and ultimately select their drilling rig, compressor, and other auxiliary air and gas equipment. The additional benefit of this planning process is that the data created by the process can be later used to control the drilling operations as the actual operations progress.

9.1 Deep Well Drilling Planning

Aerated drilling operations use a variety of incompressible fluids and compressed gases to develop a gasified drilling fluid. The majority of the operations use a standard fresh water based drilling mud with injected compressed air.   More recently inert atmosphere has been used as the injected gas to reduce the corrosion of the drill string and the borehole casing. In this chapter a standard drilling mud and atmospheric air will be used as the example aerated drilling fluid.

The basic planning steps for a deep well are as follows:
1. Determine the geometry of the borehole section or sections to be drilled with the aerated drilling fluids (i.e., openhole diameters, the casing inside diameters, and maximum depths).
2. Determine the geometry of the associated drill string for the sections to be drilled with aerated drilling fluids (i.e., drill bit size and type, the drill collar size, drill pipe size and description, and maximum depth).
3. Determine the type of rock formations to be drilled in each section and estimate the anticipated drilling rate of penetration.
4. Determine the elevation of the drilling site above sea level, the temperature of the air during the drilling operation, and the approximate geothermal

temperature gradient.
5. Establish the objective of the aerated drilling fluids operation:
    • To drill through loss of circulation formations,
    • To counter formation water entering the annulus,
    • To maintain low bottom hole pressures to either preclude fracturing of the rock formations, or to allow underbalanced drilling operations.
6. Determine whether direct or reverse circulation techniques will be used to drill well.
7. If underbalanced drilling is the objective, determine the bottomhole pressure limit that must be maintained in order to avoid formation damage.
8. For either of the above objectives, determine the required approximate volumetric flow rate of incompressible fluid to be used in the aerated fluid drilling operation. This is usually the minimum volumetric flow rate required to clean the rock cuttings from the bottom of the well and transport the cuttings to the surface. In most aerated drilling operations, the incompressible fluid volumetric flow rate is held constant as drilling progresses through the openhole interval.
9. Determine the approximate volumetric flow rate of air (or other gas) to be injected with the flow of incompressible fluid into the top of the drill string (or into the annulus) as a function of drilling depth in the openhole interval.
10. Using the incompressible fluid and air volumetric flow rates to be injected into the well, determine the bottomhole pressure and the surface injection pressure as a function of drilling depth (over the openhole interval to be drilled).
11. Select the contractor compressor(s) that will provide the drilling operation with the appropriate air or gas volumetric flow rate needed to properly aerate the drilling fluid. Also, determine the maximum power required by the compressor(s) and the available maximum derated power from the prime mover(s).
12. Determine the approximate volume of fuel required by the compressor(s) to drill the well.

In Chapter 6 the basic direct circulation drilling planning governing equations have been derived and summarized. The equations in this chapter will be utilized in the discussions and illustrative examples that follow. Also, in Chapter 7 reverse circulation drilling planning governing equations have been derived and summarized.

9.2 Aerated Fluids Drilling Operations

There are several drill string and well configurations used for aerated fluid drilling operations. These are divided into two general technique classes of air (or gas) injection operations; drill pipe injection and annulus injection [4].

9.2.1 *Drill Pipe Injection*

Figure 9-1 shows a schematic of the drill pipe injection aerated drilling configuration. In this configuration both incompressible fluid and compressible air (or other gas) are injected together into the top of the drill string (at P_{in}). These two fluid streams mix as they go down the inside of the drill string and pass through the drill bit nozzles. When the mixture of these fluids flows into the bottom of the

annulus, the rock cuttings (from the advance of the drill bit) are entrained and the resulting mixture flows to the surface in the annulus. The mixture exits the annulus (at P_e) into a horizontal flow line.   This horizontal flow line flows to either, conventional open mud tanks, or to sealed returns tanks. Conventional open mud tanks are used when the returning air is not mixed with contaminated fluids or gases, or mixed with produced hydrocarbons.   Sealed returns tanks are used to contain contaminated fluids and gases, or hydrocarbons.
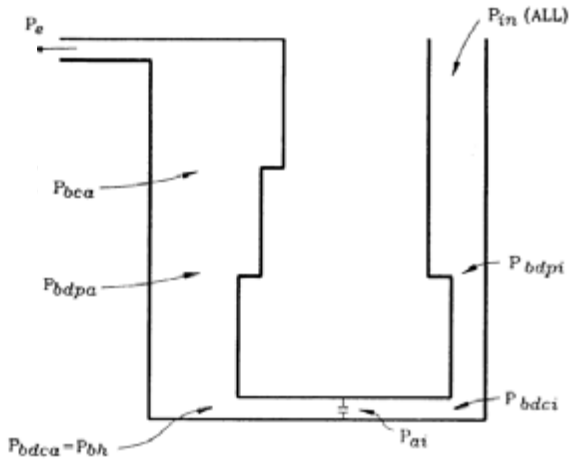
Figure 9-1: Schematic of direct circulation. P_{in} is the injection pressure into the top of the drill string. P_{bdpi} is the pressure at the bottom of the drill pipe inside the drill string. P_{bdci} is pressure at bottom of drill collars inside the drill string, P_{ai} is pressure above drill bit inside the drill string, P_{bdca} is pressure at bottom of drill collars in the annulus, P_{bh} is bottomhole pressure in annulus, P_{bdpa} is pressure at bottom of drill pipe in the annulus, P_{bca} is pressure at bottom of casing in the annulus, and P_e is pressure at the top of the annulus.

An alternative to flowing the mixture inside the drill string to the drill bit is to place a jet sub above the drill collars to allow most of the compressed air (or other gas) to pass from the inside of the drill string into the annulus before the two-phase mixture flows through the inside of the drill collars. Figure 9-2 shows a schematic of the jet sub drill string injection drilling configuration.   Jet sub drill string injection technique is usually used for deep aerated drilling operations where the bottom section of the well is usually drilled with a small diameter drill bit and corresponding small diameter drill collars.   In much the same way as bubbles provide a resistance mechanism to counter loss of circulation zones, the surface tension of the bubbles in the aerated fluid creates high pipe friction resistance when flowing through small inside diameter drill collar opens. This increased resistance to flow is not modeled by conventional friction factors derived from homogeneous fluids experiments [5 to 9]. Thus, in order to reduce circulation pumping pressures

the jet sub is placed in the drill string in the drill pipe section above the drill collars. Usually the jet sub is placed several drill pipe joints above the drill pipe to drill collar transition. There are usually two to three jet nozzles in the jet sub.   The jet sub orifices can be sized to allow the compressed gas to be vented to the annulus before the gas aerated fluid can flow to the drill collars.   The orifices in the jet subs can be sized using Equations 6-35 to 6-39.

When the aerated drill string injection technique is used to drill through loss of circulation zones, a constant volumetric flow rate of incompressible drilling fluid is circulated through the top of the drill string.   The actual volumetric flow rate of the incompressible drilling fluid is the flow rate that will adequately clean and carry the rock cuttings from the bottom of the annulus.   The volumetric flow rate of injected compressible gas is determined by trial and error in the field. The flow rate of gas is increased until the desired reduction or elimination of drilling fluid loss is obtained. Underbalanced drilling operations require that a constant bottomhole pressure be maintained as the drill bit is advanced and the well is deepened. To accomplish this a constant volumetric flow rate of incompressible drilling fluid is injected into the inside of the drill string. The actual volumetric flow rate of the incompressible drilling fluid is the flow rate that will adequately clean and carry the rock cuttings from the bottom of the annulus.   In order to maintain a nearly constant bottomhole annulus pressure, the volumetric flow rate of injected compressed gas must be increased as the well is deepened.
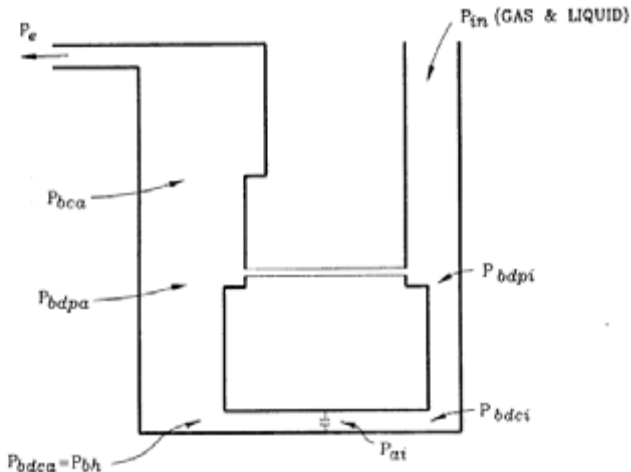
Figure 9-2: Schematic of jet sub drill pipe injection aerated flow.

9.2.2 *Annulus Injection*

Figure 9-3 shows a schematic of the annulus injection aerated drilling configuration (can be accomplished as parasite tubing string drilling, parasite casing drilling,   or   through   completion   drilling) [4].   In   this   configuration   the

incompressible drilling fluid is injected into the drill string and the compressed gas injected into the annulus. This aerated drilling technique is also used to reduce the drilling fluid pressures in the openhole of the annulus. In the early years of aerated drilling, the technique was used to eliminate the threat of formation fracture (and the eventual loss of drilling fluid). More recently, this technique has been used for limited underbalanced drilling operations (usually in the geometry of parasite casing drilling, or through completion drilling).

Figure 9-3 shows the schematic of parasite tubing string aerated drilling. This configuration is carried out by attaching a small diameter tubing string to the outside of the casing string that is installed just above the openhole. The casing string with the parasite tubing string is placed and cemented into the well in the normal fashion. Care must be taken to keep the tubing flow line open and clear while the cement is placed around the casing. After the cement has set, the incompressible drilling fluid can be direct circulated down the inside of the drill string to the drill bit, through the drill bit, and up the annulus to the surface. As the incompressible drilling fluid is circulating, the compressed gas is injected into the top of the tubing string. The compressed gas exits the bottom of the tubing string into the annulus. In this manner, the incompressible drilling fluid is aerated in the annulus from the depth where the tubing string exits into the annulus to the surface.
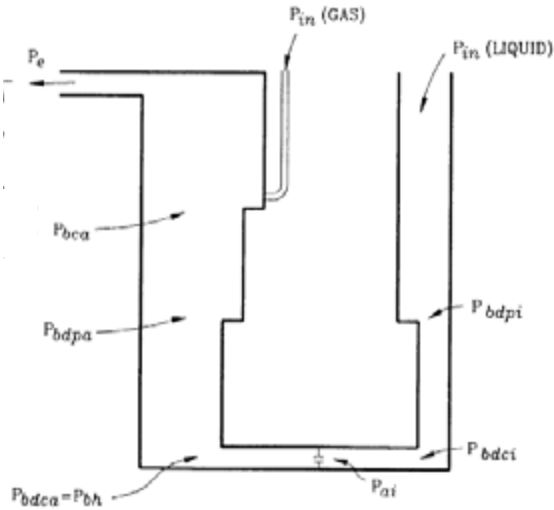
Figure 9-3: Schematic of annulus injection aerated flow (parasite tubing string example).

An alternative annulus injection technique to that of using the parasite tubing string is to utilize an annulus created by hanging a temporary casing string off the inside of the last cemented casing string. This alternative technique would be carried out in much the same manner as the parasite tubing string technique described above.

9.2.3 *Advantages and Disadvantages*

Given below are the advantages and disadvantages of the drill pipe injection technique.

The advantages to the drill pipe injection technique are as follows:

- The technique does not require any additional downhole equipment, therefore, drill pipe injection is less costly than annulus injection.
- Nearly the entire annulus is filled with aerated fluid, thus, lower bottomhole pressures can be relative to annulus injection.
- Since the gas is injected into the annulus at or near the bottom of the annulus, less gas volumetric flow rate is needed to achieve a given bottomhole pressure than via annulus injection.

The disadvantages to the drill pipe injection technique are as follows:

- Aeration of the incompressible drilling fluid cannot be continued when circulation is discontinued for connections and tripping. Therefore, it is difficult to maintain underbalanced drilling operations.
- Since the injected gas is trapped under pressure inside the drill string by the various string floats, time must be allowed for the pressure bleed-down when making connections and trips. Here again the bleed-down makes it difficulty to maintain a constant bottomhole pressure.
- The flow down the inside of the drill string is two phase flow and, therefore, high pipe friction losses are present. The high friction losses results in high pump and compressor pressures during injection.
- The gas phase in the aerated flow attenuates the pulses of conventional (measure-while-drilling) MWD systems. Therefore, conventional mud pulse telemetry MWD cannot be used.

Given below are the advantages and disadvantages of the annulus injection technique.

The advantages to the annulus injection technique are as follows:

- Aeration of the incompressible drilling fluid in the annulus above the gas annulus entrance position can continue during connections and trips.
- Flow down the inside of the drill string is single phase, therefore, conventional mud pulse MWD can be used in aerated directional drilling operations.
- The compressor pressure to maintain injection flow will usually be low when compared to the pressure required for direct circulation (to the drill bit) aerated drilling operations.

The disadvantages to the annulus injection technique are as follows:

- Because the parasite tubing string or the temporary casing are placed at a particular fixed location in the well, the aeration technique is more inflexible than the drill pipe injection technique.
- Initiating (kickoff) gas flow to the annulus requires very high compressor pressures.
- Since the gas is injected into the annulus at fixed depths that are well above the bottom of the annulus, higher gas volumetric flow rates are required to maintain constant bottomhole pressures than in the drill pipe injection technique.

9.3 Minimum Volumetric Flow Rates

Most aerated drilling operations are planned with a constant volumetric flow rate of incompressible drilling fluid and only the volumetric flow rate of the compressed gas is allowed to vary. The volumetric flow rate of gas is usually increased as the depth is increased in order to maintain the same aerated fluid properties in the annulus column. The drill pipe injection technique requires that both the incompressible drilling fluid injection and the compressed gas injection be suspended when connections and trips are made. Similarly, the annulus injection technique requires that the incompressible drilling fluid injection be suspended when connections and trips are made. Further, the cleaning, lifting, and suspension capabilities of the incompressible drilling mud is in general independent of the depth of drilling. Conversely, the cleaning and lifting capabilities of compressed gas are dependent of the depth of drilling. Also, it must be noted that compressed gas drilling fluids have little or no suspension capabilities. Therefore, when designing an aerated drilling fluid, the injected compressed gas should not be assumed to contribute to bottomhole cleaning, lifting, and suspension of rock cuttings in the annulus. The additional cleaning and lifting properties of the compressed gas to the aerated drilling fluid should be considered as a bonus. This argument requires that the incompressible drilling fluid properties and circulation characteristics be designed to provide the aerated drilling operations with stand-alone cleaning, lifting, and suspension capabilities of the rock cuttings in the annulus.

9.3.1 *Discussion of Theories*

There are a variety of minimum volumetric flow rate theories which can be used to design incompressible drilling fluid properties and circulation characteristics for direct circulation drilling operations [10 to 12]. In order to formulate a workable procedure for determining the minimum volumetric flow rates of incompressible drilling fluid and compressed gas to a borehole, the primary operational reasons for using aerated fluid drilling should be reviewed. These reasons are; 1) to control loss of circulation drilling situations, and 2) to facilitate underbalanced drilling operations. Although aerated fluid drilling will generally improve some important drilling parameters, for example penetration rate and openhole wall stability, it is usually not possible to optimize all these parameters and still successfully accomplish the primary mission of either loss of circulation control, or underbalanced drilling.

For aerated drilling applications the minimum volumetric flow rate will be determined using a rather simple, straight-forward procedure which requires that the circulating incompressible fluid be capable, on its own, of maintaining a minimum concentration of rock cuttings in the largest annulus section of the well [13]. This requires that the average velocity of the fluid, V_f, in the largest annulus section be the sum of the critical concentration velocity, V_c, and the terminal velocity, V_t, of the average size rock cutting particle in the incompressible drilling fluid.

Thus, the average fluid velocity in the annulus, V_f, is

$$V_f \qquad V_c \qquad V_t \tag{9-1}$$

where V_f is the incompressible drilling fluid (ft/sec),

V_c is the critical concentration velocity (ft/sec),
V_t is the terminal velocity of the rock cuttings particle (ft/sec).
It is tacitly assumed that if the incompressible drilling fluid can carry the rock cuttings on its own, then the injection of gas into the fluid will enhance the overall carrying capacity of the aerated fluid.

The critical concentration velocity is the additional velocity needed to distribute the rock cuttings through the incompressible drilling fluid at a predetermined concentration factor. The usual concentration factor is 0.04. Therefore, the critical concentration velocity, V_c, is

$$V_c = \frac{\overline{}}{3,600 \ C} \tag{9-2}$$

where   is the instantaneous drilling rate (ft/hr or m/hr),
        C is the concentration factor (usually assumed to be 0.04).
Equations 9-1 and 9-2 equation can be used with any consistent set of units.

Terminal Velocities (English Units)
For direct circulation operations the terminal velocity of the rock cutting particle is assessed in the annulus section of the borehole where the cross-sectional area is the largest. The terminal velocity will depend on the actual flow conditions in the annulus section (i.e., whether the flow is laminar, transitional, or turbulent).

Empirical data indicates that laminar flow conditions exist when the non-dimensional Reynolds number for the flow is between 0 and 2,000. The empirical relationship for the terminal velocity of a rock cutting particle in an annulus with laminar flow, V_{t1}, is

$$V_{t1} = 0.0333 \ D_c^2 \ \frac{s \quad f}{e} \tag{9-3a}$$

where V_{t1} is the terminal velocity of the particle in laminar flow (ft/sec),
        D_c is the approximate diameter of the rock cutting particle (ft),
        s is the specific weight of the solid rock cutting (lb/ft^3),
        f is the specific weight of the incompressible drilling fluid (lb/ft^3),
        e is the effective absolute viscosity (lb-sec/ft^2).
Empirical data indicates that transition flow conditions exist when the non-dimensional Reynolds number for the flow is between 2,000 and 4,000. The empirical relationship for the terminal velocity of a rock cutting particle in an annulus with transition flow, V_{t2}, is

$$V_{t2} = 0.492 \ D_c \ \frac{s \quad f}{f^{\frac{1}{3}} \ e} ^{\frac{2}{3}} \tag{9-4a}$$

where V_{t2} is the terminal velocity of the particle in transition flow (ft/sec).

Empirical data indicates that turbulent flow conditions exist when the non-dimensional Reynolds number for the flow is greater than 4,000. The empirical relationship for the terminal velocity of a rock cutting particle in an annulus with turbulent flow, V_{t3}, is

$$V_{t3} = 5.35 \left[D_c \frac{\gamma_s - \gamma_f}{\gamma_f} \right]^{\frac{1}{2}} \tag{9-5a}$$

where V_{t3} is the terminal velocity of the particle in turbulent flow (ft/sec).

Terminal Velocities (SI Units)

Empirical data indicates that laminar flow conditions exist when the non-dimensional Reynolds number for the flow is between 0 and 2,000. The empirical relationship for the terminal velocity of a rock cutting particle in an annulus with laminar flow, V_{t1}, is

$$V_{t1} = 0.0333 \, D_c^2 \frac{\gamma_s - \gamma_f}{\mu_e} \tag{9-3b}$$

where V_{t1} is the terminal velocity of the particle in laminar flow (m/sec),

D_c is the approximate diameter of the rock cutting particle (m),

γ_s is the specific weight of the solid rock cutting (N/m^3),

γ_f is the specific weight of the incompressible drilling fluid (N/m^3),

μ_e is the effective absolute viscosity (N-sec/m^2).

Empirical data indicates that transition flow conditions exist when the non-dimensional Reynolds number for the flow is between 2,000 and 4,000. The empirical relationship for the terminal velocity of a rock cutting particle in an annulus with transition flow, V_{t2}, is

$$V_{t2} = 0.331 \, D_c \frac{\left(\gamma_s - \gamma_f \right)^{\frac{2}{3}}}{\gamma_f^{\frac{1}{3}} \mu_e^{\frac{1}{3}}} \tag{9-4b}$$

where V_{t2} is the terminal velocity of the particle in transition flow (m/sec).

Empirical data indicates that turbulent flow conditions exist when the non-dimensional Reynolds number for the flow is greater than 4,000. The empirical relationship for the terminal velocity of a rock cutting particle in an annulus with turbulent flow, V_{t3}, is

$$V_{t3} = 2.95 \left[D_c \frac{\gamma_s - \gamma_f}{\gamma_f} \right]^{\frac{1}{2}} \tag{9-5b}$$

where V_{t3} is the terminal velocity of the particle in turbulent flow (m/sec).

Note that Equations 9-3a to 9-5a and 9-3b and 9-5b were originally developed in field units [11, 12]. To be consistent with most of the other equations in this treatise, these equations have been re-stated in consistent English system units (Equations 9-3a to 9-5a) and consistent SI units (Equations 9-3b to 9-5b).

The non-dimensional Reynolds number, N_R, is defined as

$$N_R \quad \frac{D\,V}{} \tag{9-6}$$

where D is the inside diameter (or hydraulic diameter) of the pressure conduit (ft),

   V is average velocity of the fluid in the pressure conduit (ft/sec),

   is the kinematic viscosity of the flowing fluid (ft^2/sec).

The above non-dimensional Reynolds number equation above can be used with any consistent of units.

9.3.2 *Engineering Practice*

Engineering practice is to design the incompressible drilling fluid to have minimum, but adequate, cleaning, lifting, and suspension capabilities to drill a planned openhole interval. Modern aerated drilling operations utilize a variety of incompressible drilling fluids. These can be fresh and salt water drilling muds, oil based drilling muds, fresh waters, formation waters, and formation crude oils. In the initial design of the aerated drilling fluid, the compressed gas contributions are neglected.

The minimum volumetric flow rate of the incompressible drilling fluid will be determined using Equations 9-1, 9-2, 9-3a,. 9-4a, 9-5a, and 9-6 above. When assessing the cleaning, lifting, and suspension capabilities of Newtonian incompressible drilling fluids (e.g., waters and oils), analysis should include the possibility of laminar, transition, and turbulent flow conditions. Traditionally, non-Newtonian incompressible drilling fluids (e.g., drilling muds) have been analyzed assuming that no transition flow conditions exist and that turbulent flow conditions begin at the Reynolds number of approximately 2,000.

Once the incompressible drilling fluid minimum volumetric flow rate has been determined, an optimum volumetric flow rate of injected compressed gas can be determined using the basic equations derived in Chapter 6.

It should be noted that for follow-on aerated drilling fluids analyses, even those that have a non-Newtonian incompressible fluid component like a water based drilling mud, transition flow conditions will be considered along with laminar and turbulent flow conditions.

Illustrative Examples 9.1 describes the implementation of the basic planning steps Nos. 1 through 8 in Section 9.1.

Illustrative Example 9.1 The borehole to be used in this illustrative example is the basic example used in Chapter 8. The 7 7/8 inch diameter borehole is to be drilled out of the bottom of API 8 5/8 inch diameter, 28.00 lb/ft nominal, Grade H-40, casing set to 7,000 ft (see Figure 9-4 for well casing and openhole geometric configuration). The drill bit to be used to drill the interval is a 7 7/8 inch diameter

tri-cone roller cutter insert type (nozzles 11/32 inches). The anticipated drilling rate in a sandstone and limestone sequence in the interval is approximate 60 ft/hr. The average rounded diameter of the rock cutting particles generated by this drill bit is estimated to be 0.198 inch. The openhole interval below the casing shoe is to be from 7,000 ft to 10,000 ft.
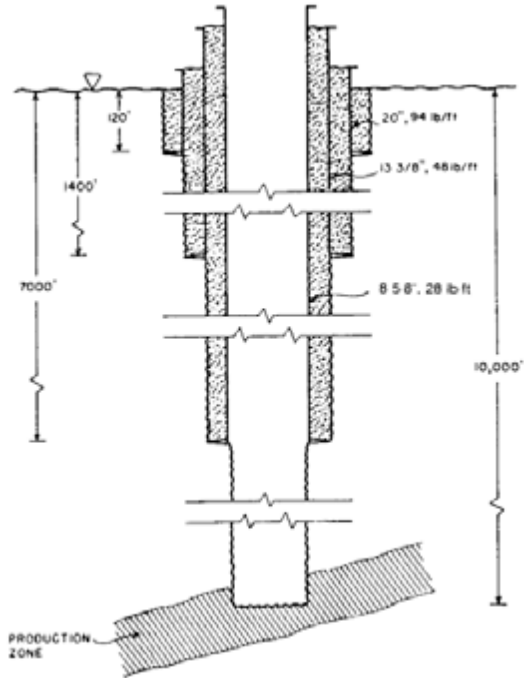
Figure 9-4: Illustrative Example 9.1 casing and openhole well geometric configuration.

The drill string for this illustrative example is made up of 500 ft of 6 3/4 inch by 2 13/16 inch drill collars above the drill bit and API 4 1/2 inch, 16.60 lb/ft nominal, EU-S135, NC50 (IF) to the surface. The drilling is to be carried out at a surface location of 4,000 ft above sea level where the actual atmospheric temperature is 60°F. The regional geothermal gradient is approximately 0.01°F/ft. The borehole is to be drilled with an aerated fluid composed of a fresh water base drilling mud and compressed air. The drilling mud is to have a specific weight of 10 lb/gal drilling mud with a plastic viscosity of 30 cps and a plastic yield stress of 5 lb/100 ft². Drill pipe injection technique will be used and the drilling operation will be carried out to maintain a bottomhole pressure of 3,500 psig while drilling the interval from the 7,000 ft to 10,000 ft. A horizontal section of API line pipe that runs 100 ft from just above the BOP stack to the mud tank is to be used as the return flow line. The surface return flow line is API 6 5/8 inch line pipe, 32.71 lb/ft nominal, Grade B. The inside diameter of this line pipe is 5.625 inches. Two gate valves are

installed in the return flow line at the end of the line that is attached to the BOP stack.   These valves have an inside diameter of 5 9/16 inch.   Determine the approximate minimum volumetric flow rate of the drilling mud that will be needed for this aerated drilling operation.

The incompressible drilling fluid to be used for this aerated drilling operation is to be a standard fresh water drilling mud with plastic fluid properties. As has been argued above, the drilling mud properties and flow characteristics will be designed to clean, lift, and suspend the rock cuttings. The plastic viscosity (30 cps) and the plastic yield stress (5 lb/100 ft^2) are typical drilling mud properties that enhance bottomhole cleaning, lifting, and suspension of rock cuttings. With the above data. determine the drilling mud minimum volumetric flow rate required to clean the well.

The incompressible fluid to be used in this illustrative example is a water base drilling mud with plastic properties. Therefore, the minimum volumetric flow rate of the incompressible drilling fluid is determined using Equations 9-1, 9-2, 9-3a, 9-5a, and 9-6 above (transition flow is assumed not to exist).   The anticipated drilling rate is 60 ft/hr. Using Equation 9-2, the critical concentration velocity is

$$V_c \quad \frac{60}{3,600 \ (0.04)}$$

$$V_c \quad 0.417 \ \text{ft/sec}$$

The specific weight of the sedimentary rock to be drilled is approximately

$$_s \quad (2.7) \ (62.4)$$

$$_s \quad 168.5 \ \text{lb/ft}^3$$

where the specific gravity of sedimentary rock is assumed to be approximately 2.7 (see Chapter 6). The specific weight of the 10 lb/gal drilling mud in consistent units is (subscript f is replaced by m)

$$_m \quad \frac{10 \ (12)^3}{231}$$

$$_m \quad 75.0 \ \text{lb/ft}^3$$

The absolute plastic viscosity of the drilling mud in consistent units is

$$_{mp} \quad 30 \ (0.001) \ (0.02089)$$

$$_{mp} \quad 0.0006267 \ \frac{\text{lb} \quad \text{sec}}{\text{ft}^2}$$

Assuming laminar flow conditions, the effective absolute viscosity of the drilling mud is equal to the plastic viscosity. Therefore, the effective absolute viscosity is

$$\mu_{e1} \quad \mu_{mp} \quad 0.0006267 \ \frac{lb \ sec}{ft^2}$$

The approximate average diameter of the rock cuttings particle in consistent units is

$$D_c \quad \frac{0.198}{12}$$

$$D_c \quad 0.0165 \ ft$$

Substituting the above values for, γ_s, γ_m, μ_{e1}, and D_c into Equation 9-3a yields the terminal velocity for laminar flow conditions. Equation 9-3a gives

$$V_{t1} \quad 0.0333 \ (0.0165)^2 \ \frac{168.5 \quad 75.0}{0.0006267}$$

$$V_{t1} \quad 1.353 \ ft/sec$$

Using Equation 9-1, the total velocity of the fluid is

$$V_{m1} \quad 0.417 \quad 1.353$$

$$V_{m1} \quad 1.770 \ ft/sec$$

The above total velocity of the fluid must be the minimum average velocity of the incompressible fluid in the borehole annulus section where the cross-sectional area is the largest. In this illustrative example, the largest cross-sectional area of the annulus is in the cased section of the well where the inside diameter of the casing is 8.017 inch and the outside of the diameter of the drill pipe is 4.50 inch. Thus, this annulus cross-sectional area, A_a, is

$$A_a \quad \frac{\pi}{4} \quad \frac{8.017}{12}^2 \quad \frac{4.50}{12}^2$$

$$A_a \quad 0.240 \ ft^2$$

The volumetric flow rate in the above annulus section is

$$Q_{a1} \quad (0.240) \ (1.770)$$

Q_{a1} $0.425 \ \text{ft}^3/\text{sec}$

In field units, the above is

$$q_{a1} \quad \frac{0.425 \ (60) \ 12^{\ 3}}{231}$$

q_{a1} $190.8 \ \text{gal/min}$

It is necessary to check and see if the above volumetric flow rate did indeed give laminar flow conditions in the largest annulus cross-sectional area.   This is accomplished by calculating the non-dimensional Reynolds number for this annulus cross-section and the above volumetric flow rate (with the annulus average fluid velocity of 1.770 ft/sec). The hydraulic diameter for this annulus cross-section, D_{hy}, is

$$D_{hy} \quad \frac{8.017}{12} \quad \frac{4.50}{12}$$

D_{hy} $0.293 \ \text{ft}$

Using Equation 1-2. the drilling mud density, $_m$, is

$$_m \quad \frac{75.0}{32.2}$$

$$_m \quad 2.329 \ \frac{\text{lb} \ \ \text{sec}^2}{\text{ft}^4}$$

The general equation for kinematic viscosity, , is

$$— \tag{9-7}$$

where   is kinematic viscosity (ft^2/sec).   The drilling mud effective kinematic viscosity for laminar conditions is

$$_{e1} \quad \frac{0.0006267}{2.329}$$

$_{e1}$ $0.0002691 \ \text{ft}^2/\text{sec}$

Substituting the above values for, D_{hy}, V_{m1}, $_{e1}$ into Equation 9-6 yields the Reynolds number for the volumetric flow rate derived from the laminar flow terminal velocity equation. Equation 9-6 gives

$$N_{R1} \quad \frac{(0.293)\ (1.770)}{0.0002691}$$

$$N_{R1} \quad 1,928$$

The Reynolds number calculated above is below 2,000 and, thus, the volumetric flow rate of 190.8 gal/min produces laminar flow conditions in largest cross-section of the annulus. Therefore, the use of Equation 9-3a and the actual flow conditions it yielded are consistent.

Since the incompressible drilling fluid in this illustrative example is a drilling mud with plastic fluid properties, turbulent flow conditions are assumed to exist at Reynolds numbers greater than 2,000 (i.e., the transition flow condition Equation 9-4a is not needed for this example). In order to complete the analysis to determine the minimum volumetric flow rate for the incompressible fluid, turbulent flow conditions must also be assessed.

Substituting the above values for, $_s$, $_m$, and D_c into Equation 9-5a yields the terminal velocity for turbulent flow conditions. Equation 9-5a gives

$$V_{t3} \quad 5.35 \quad 0.0165 \quad \frac{168.5 \quad 75.0}{75.0}^{\frac{1}{2}}$$

$$V_{t3} \quad 0.767 \ \text{ft/sec}$$

Using Equation 9-1, the total velocity of the fluid is

$$V_{m3} \quad 0.417 \quad 0.767$$

$$V_{m3} \quad 1.184 \ \text{ft/sec}$$

The volumetric flow rate in the annulus section is

$$Q_{a3} \quad (0.240)\ (1.184)$$

$$Q_{a3} \quad 0.284 \ \text{ft}^3\text{/sec}$$

In field units, the above is

$$q_{a3} \quad \frac{0.284 \quad (60)\ \ 12^{\ 3}}{231}$$

q_{a3} 127.5 gal/min

It is again necessary to check and see if the above volumetric flow rate did indeed give turbulent flow conditions in the largest annulus cross-sectional area. This is accomplished by calculating the non-dimensional Reynolds number for this annulus cross-section and the above volumetric flow rate (with the average annulus velocity of 1.184 ft/sec).

For turbulent flow conditions, the effective absolute viscosity of a drilling mud with a plastic viscosity must to be modified before it is used in the Reynolds number equation [10]. Therefore, assuming turbulent flow conditions, the effective absolute viscosity is

$$\mu_{e3} \qquad \frac{p}{3.2}$$

$$\mu_{e3} \qquad \frac{0.0006267}{3.2}$$

$$\mu_{e3} \qquad 0.000196 \ \frac{lb \quad sec}{ft^2}$$

The effective kinematic viscosity for the drilling mud with plastic properties is

$$\nu_{e3} \qquad \frac{0.000196}{2.369}$$

$$\nu_{e3} \qquad 0.000083 \ ft^2/sec$$

Substituting the values for, D_h, V_{m3}, ν_{e3} into Equation 9-6 yields the Reynolds number for the volumetric flow rate derived from the laminar flow terminal velocity equation. Equation 9-6 gives

$$N_{R3} \qquad \frac{(0.293) \ (1.184)}{0.000083}$$

$$N_{R3} \qquad 4,196$$

The Reynolds number above is greater than 2,000.   This indicates that the volumetric flow rate of 127.5 gal/min produces turbulent flow conditions in the largest cross-section of the annulus.

The turbulent flow analysis result is inconsistent with the result of the laminar flow analysis. Also, since the turbulent flow analysis indicates turbulent flow conditions exist at a lower volumetric flow rate than the laminar flow analysis, then the laminar flow analysis is considered valid and the turbulent flow analysis invalid.

Therefore, the minimum volumetric flow rate of the incompressible drilling fluid (the drilling mud) is assumed to be approximately 191 gal/min.

The results obtained for the illustrative example above require that additional explanation be given for the utility and applicability of Equations 9-1, 9-2, 9-3a (and 9-3b), 9-4a (and 9-4b), and 9-5a (and 9-5b).

Equation 9-1 and the 0.04 concentration factor allows an estimate of the rock particle cuttings concentration velocity, V_c, in the incompressible fluid (usually drilling mud). In Equation 9-2 this concentration velocity is added to the particle terminal velocity (in the fluid), V_t, to obtain the minimum fluid velocity, V_f, in the largest annulus cross-section of the borehole. This minimum fluid velocity gives an allowable distribution of particles in the fluid flow that has been shown by field operations to yield trouble free drilling operations. The concentration factor of 0.04 can be adjusted to a smaller value if drilling conditions require a more conservative engineering planning approach.

Equations 9-3a to 9-5a (and 9-3b to 9-5b) give the terminal velocities for the three well known flow conditions, laminar, transition, and turbulent. The terminal velocity for laminar flow is V_{t1}, for transition flow , V_{t2}, and for turbulent, V_{t3}. These terminal velocity equations were obtained from laboratory experiments. Thus, these are empirically derived separate equations and do not represent a single continuous theory (of equations). Therefore, one expression will not match up with the next expression as the Reynolds number is increased through the three flow conditions. Thus, these expressions should be applied with prudence and engineering judgment.

The rock cutting particle average diameter term, D_c, used in all of the three terminal velocity equations can be estimated via several methods. Two of these methods are described below.

In vertical rotary air drilling operations where the drill string is rotated, it is known that the mechanical interactions of the particles with the rotating drill string will reduce the size of the particles as they are transported to the surface in the annulus [13]. Thus, the higher the rotary speed of the drill string, the smaller the particle diameter. The particle average diameter can be estimated as

$$D_c \qquad \overline{\quad 60 \quad N \quad} \qquad\qquad (9\text{-}8)$$

where N is the drill string (drill bit) speed (rpm).

An alternate method can be used to approximate average diameter of particles generated by a downhole motor using a tri-cone drill bit (no drill string rotation). This method assumes that the average diameter of the particles is approximately half the base diameter of the mill or insert tooth root diameter on a cone face. This is a reasonable estimate considering that these drill bits destroy rock with a crushing action and there is no rotation of the drill string. Figure 3.5 shows a schematic of this crushing action and illustrates the cutting sizes generated.

9.4 Injection Pressure and Selection of Compressor Equipment

Over the past two decades, the analyses of aerated fluid vertical drilling problems have been carried out by two distinct analytic methodologies.

The first methodology ignores the major and minor friction losses due to fluid flow inside the drill string and in the annulus. This methodology includes only the fluid column weight [14, 15]. This methodology was originally derived and adapted for aerated drilling from the large body of literature pertaining to multiphase flow of oil and natural gas in production tubing [16, 17].

The second methodology can include all the complexity of the fluid flow friction losses. The initial application of this methodology also came from adapting multi-phase oil and gas flow tubing production theory to aerated drilling annulus problems. This production theory application includes only major friction losses and was not applicable to complicated borehole geometry. New additions to this methodology, which do not come from production literature, have included major and minor losses and can be applied to complicated borehole geometry.

In Chapter 6 the basic aerated fluid drilling governing equations have been derived and their auxiliary friction factor, and nozzle flow equations presented. These equations form the foundation for both methodologies as they are discussed in this treatise.

9.4.1 *Non-Friction Approximation*

The simple non-friction methodology allows straight forward deterministic approximate solutions of aerated drilling problems. However, the practical applicability of these non-friction solutions is limited to shallow (generally less than 3,000 ft of depth) wells with simple geometric profiles. The non-friction solution will be applied to a deep well example only as a demonstration and ultimate comparison of the results to those obtained from the friction solution.

In what follows, the basic equations in Chapter 6 for aerated drilling are used to derive the non-friction governing equation. Letting f 0 in Equation 6-74 yields

$$\int_{P_e}^{P_{bh}} \frac{dP}{\dfrac{\dot{w}_t}{\dfrac{P_g}{P}\dfrac{T_{av}}{T_g}Q_g \quad Q_m}} \quad \int_0^H dh$$

where P_{bh} is the pressure at the bottom of the annulus (lb/ft^2, abs),
P_e is the pressure at the exit from the annulus (lb/ft^2, abs).
The above equation can be rearranged and integrated to yield

$$\left| P_g \frac{T_{av}}{T_g}\frac{Q_g}{\dot{w}_t} \ln P \quad \frac{Q_m}{\dot{w}_t} P \right|_{P_e}^{P_{bh}} \quad \left| h \right|_0^H$$

Evaluating above equation at the limits, rearranging the result and solving for gas volumetric flow rate, Q_g, yields

$$Q_g \quad \cfrac{\dot{w}_m \quad \dot{w}_s \quad H \quad P_{bh} \quad P_e \quad Q_m}{P_g \quad \cfrac{T_{av}}{T_g} \quad \ln \quad \cfrac{P_{bh}}{P_e} \quad {}_g \quad H} \tag{9-9}$$

Illustrative Example 9.2 below describes the implementation of the basic planning step No. 9 in Section 9.1. The non-friction solution is applied to a deep well example. This is only done as a demonstration. It is instructive to compare the non-friction solution results to the full friction solutions results that will be obtained later in this chapter. The approximate values for the volumetric flow rates of the incompressible fluid (drilling mud) and the compressible gas (air) can be used as a initial values for the complicated trial and error solution required for the full friction solution.

Illustrative Example 9.2   Using the non-friction method and the given data and the results obtained in Illustrative Example 9.1, determine the approximate volumetric flow rate of air required for the incompressible drilling fluid (drilling mud) volumetric flow rate of approximately 191 gal/min while drilling at 10,000 ft.
Table 4-1 gives an average atmospheric pressure of 12.685 psia for a surface location of 4,000 ft above sea level (mid latitudes North America) (also see Appendix D). The actual atmospheric pressure for the air at the drilling location (that will be used by the compressor), P_{at}, is

p_{at} 12.685 psia

P_{at} p_{at} 144

P_{at} 1,826.6 lb/ft^2 abs

The actual atmospheric temperature of the air at the drilling location (that will be used by the compressor), T_{at}, is

t_{at} 60°F

T_{at} t_{at} 459.67

T_{at} 519.67°R

Thus, P_g and T_g become

P_g P_{at} 1,826.6 lb/ft^2 abs

T_g T_{at} 519.67°R

Using Equation 4-11, the specific weight of the gas entering the compressor is

$$\gamma_g \quad \frac{(1,827)\ (1.0)}{(53.36)\ (519.67)}$$

$$\gamma_g \quad 0.0659 \ \text{lb/ft}^3$$

Note the above specific weight value can also be obtained from Figure D-4 in Appendix D.

The bottomhole pressure, P_{bh}, in absolute pressure is

$$p_{bh} \quad 3,500 \quad 12.685$$

$$p_{bh} \quad 3,512.685 \ \text{psia}$$

$$P_{bh} \quad p_{bh}\ 144$$

$$P_{bh} \quad 505,826 \ \text{lb/ft}^2 \ \text{abs}$$

The temperature of the rock formations near the surface (geothermal surface temperature) is estimated to be the approximate average year round temperature at that location on the earth's surface. Table 4-1 gives 44.74°F for average year round temperature for a surface elevation location of 4,000 ft above sea level (for mid latitudes of North America, or see Appendix D). Therefore, the absolute temperature of the rock formations at the surface, T_r, is

$$t_r \quad 44.74°\text{F}$$

$$T_r \quad t_r \quad 459.67$$

$$T_r \quad 504.41°\text{R}$$

The depth of the well, H, is

$$H \quad 10,000 \ \text{ft}$$

The bottomhole temperature, T_{bh}, is

$$T_{bh} \quad T_r \quad 0.01\ H$$

$$T_{bh} \quad 604.41°R$$

The borehole average temperature, T_{av}, is

$$T_{av} \quad \frac{T_{sr} \quad T_{bh}}{2}$$

$$T_{av} \quad \frac{504.41 \quad 604.41}{2}$$

$$T_{av} \quad 554.41°R$$

The openhole diameter, D_h, is

$$d_h \quad 7.875 \text{ inches}$$

$$D_h \quad \frac{d_h}{12}$$

$$D_h \quad 0.656 \text{ ft}$$

The estimated drilling rate of penetration is 60 ft/hr.   The weight rate of flow of solids, $\dot{w}_s$, from the advance of the drill bit is

$$\dot{w}_s \quad \frac{}{4} \quad D_h^2 \quad 62.4 \quad S_s \quad \frac{}{(60)\ (60)} \tag{9-10}$$

$$\dot{w}_s \quad \frac{}{4} \quad 0.656^2 \quad 62.4 \quad 2.7 \quad \frac{60}{60 \quad 60}$$

$$\dot{w}_s \quad 0.949 \text{ lb/sec}$$

The volumetric flow rate of drilling mud, Q_m, in consistent units is

$$Q_m \quad \frac{191 \quad 231}{12^3 \quad 60}$$

$$Q_m \quad 0.426 \text{ ft}^3/\text{sec}$$

The weight rate of flow of the drilling mud, $\dot{w}_m$, is

$$\dot{w}_m \quad 75.0 \quad 0.426$$

$$\dot{w}_m \quad 31.92 \text{ lb/sec}$$

Substituting the values of H, $\dot{w}_m$, $\dot{w}_s$, Q_m, P_g, P_{bh}, T_g, and T_{av} into Equation 9-9 yields

$$Q_g \quad \frac{(0.949 \quad 31.92) \; 10,000 \quad 505,826 \quad 1,827 \quad 0.426}{1,827 \quad \dfrac{554.41}{519.67} \quad \ln \quad \dfrac{505,826}{1,827} \quad 0.0659 \quad 10,000}$$

$$Q_g \quad 11.05 \ \text{ft}^3/\text{sec}$$

The air volumetric flow rate in field units is

$$q_g \quad (11.05) \; (60)$$

$$q_g \quad 663 \ \text{acfm}$$

The volumetric flow rate of compressed air determined above is the flow rate to be injected into the incompressible fluid volumetric flow rate of 191 gal/min. This gas flow rate has been determined with the non-friction method. Similar solutions (in magnitude) will be obtained when using the oil and gas production based non-friction methods [14, 15]. Although this non-friction method is invalid for a deep boreholes with complicated geometric profiles, the solution does give a lower bound value for the full friction solution. The full friction solution will be demonstrated in the next section.

9.4.2 *Major and Minor Losses and Injection Pressure*

The governing equations for the second methodology, presented in Chapter 6, requires trial and error solutions and is applicable to deep wells with complicated borehole geometry. As major and minor friction losses are added to allow the analytic solution to simulate more closely the actual drilling situation (for a given incompressible volumetric flow rate), the volumetric flow rate of compressed gas must be increased to compensate for the added friction in the system.

Illustrative Examples 9.3 describes the full implementation of the basic planning steps Nos. 9 to 11 in Section 9.1.

Illustrative Example 9.3   In this illustrative example the given data in Illustrative Example 9.1 is used for a solution using the friction solution method given in Chapter 6 (Equations 6-74 to 6-86). Using the general data and results obtained in Illustrative Examples 9.1 and 9.2, determine the approximate volumetric flow rate of the compressed air required for the incompressible drilling fluid (drilling mud) volumetric flow rate of 191 gal/min while drilling at 10,000 ft. Also determine the compressed air injection pressure while drilling at 10,000 ft. Select an appropriate compressor system from those given in Chapter 4. Determine the highest compressor power required from the prime mover to drill the interval from

7,000 ft to 10,000 ft and determine the derated power available from the prime mover.

General Data

The solution to a full friction aerated drilling problem must be carried out by trial and error. The trial and error technique requires the selection of the magnitude of the volumetric flow rate of the compressed air, q_g, that will result in a bottomhole pressure in the annulus of 3,500 psig. This trial and error technique further requires that the upper limit pressures in each depth interval be selected so that the overall interval integrals are satisfied. The trial and error q_g that will satisfy these limitations is

$$q_g \quad 1,168 \text{ acfm}$$

The volumetric flow rate of the compressed air, Q_g, in consistent units is

$$Q_g \quad \frac{1,168}{60}$$

$$Q_g \quad 19.47 \text{ ft}^3/\text{sec}$$

Table 4-1 gives an average atmospheric pressure of 12.685 psia for a surface location of 4,000 ft above sea level (mid latitudes North America) (also see Appendix D). The actual atmospheric pressure for the air at the drilling location (that will be used by the compressor), P_{at}, is

$$p_{at} \quad 12.685 \text{ psia}$$

$$P_{at} \quad p_{at} \, 144$$

$$P_{at} \quad 1,826.6 \text{ lb/ft}^2 \text{ abs}$$

The actual atmospheric temperature of the air at the drilling location (that will be used by the compressor), T_{at}, is

$$t_{at} \quad 60°\text{F}$$

$$T_{at} \quad t_{at} \quad 459.67$$

$$T_{at} \quad 519.67°\text{R}$$

Thus, P_g and T_g become

$$P_g \quad P_{at} \quad 1,826.6 \text{ lb/ft}^2 \text{ abs}$$

$$T_g \quad T_{at} \quad 519.67°R$$

Using Equation 4-11, the specific weight of the gas entering the compressor is

$$\gamma_g \quad \frac{(1,826.6)\ (1.0)}{(53.36)\ (519.67)}$$

$$\gamma_g \quad 0.0659\ \text{lb/ft}^3$$

The weight rate of flow of the air, $\dot{w}_g$, is

$$\dot{w}_g \quad (0.0659)\ (19.47)$$

$$\dot{w}_g \quad 1.283\ \text{lb/sec}$$

The volumetric flow rate of drilling mud, Q_m, in consistent units is

$$Q_m \quad \frac{191 \quad 231}{12^{\ 3} \quad 60}$$

$$Q_m \quad 0.426\ \text{ft}^3/\text{sec}$$

The weight rate of flow of the drilling mud, $\dot{w}_m$, is

$$\dot{w}_m \quad 75.0 \quad 0.426$$

$$\dot{w}_m \quad 31.92\ \text{lb/sec}$$

The openhole diameter, D_h, is

$$d_h \quad 7.875\ \text{inches}$$

$$D_h \quad \frac{d_h}{12}$$

$$D_h \quad 0.656\ \text{ft}$$

The estimated drilling rate of penetration is 60 ft/hr. Using Equation 9-10, the weight rate of flow of solids, $\dot{w}_s$, from the advance of the drill bit is

$$\dot{w}_s \quad \frac{\pi}{4} \quad 0.656^2 \quad 62.4 \quad 2.7 \quad \frac{60}{60 \quad 60}$$

$$\dot{w}_s \quad 0.949 \text{ lb/sec}$$

The total weight rate of flow, $\dot{w}_t$, in the annulus is

$$\dot{w}_t \quad 1.282 \quad 31.92 \quad 0.949$$

$$\dot{w}_t \quad 34.15 \text{ lb/sec}$$

The absolute viscosity of the drilling mud, μ_m, is

$$\mu_m \quad 30 \text{ cps}$$

$$\mu_m \quad (30)\,(0.001)\,(0.2089)$$

$$\mu_m \quad 0.0006267 \quad \frac{\text{lb} \quad \text{sec}}{\text{ft}^2}$$

Using Equation 1-2, the density of the drilling mud, ρ_m, is

$$\rho_m \quad \frac{75.0}{32.2}$$

$$\rho_m \quad 2.329 \quad \frac{\text{lb} \quad \text{sec}^2}{\text{ft}^4}$$

From Equation 9-7, the kinematic viscosity of the drilling mud, ν_m, is

$$\nu_m \quad \frac{0.0006267}{2.329}$$

$$\nu_m \quad 0.0002691 \quad \frac{\text{ft}^2}{\text{sec}}$$

Surface Return Flow Line

The calculation procedure must be initiated with the known atmospheric pressure at the exit to the surface return flow line. It is assumed that the drilling mud and air mixture will exit the well annulus and enter the surface return flow line at the surface geothermal temperature of 44.74°F (or 504.41°R). It is further assumed that the temperature of the drilling mud and air flow in the surface return flow line does not change as it flows through the return flow line (i.e., the steel

surface return flow line will be at nearly the surface geothermal temperature at steady state flow conditions). Equation 6-74 can be altered to allow its application to horizontal flow in the surface return flow line. This altered equation is

$$\int_{P_g}^{P_s} \frac{dP}{B_s(P)} = \int_0^{L_s} dl \tag{9-11}$$

where

$$B_s(P) = \frac{\dot{w}_t}{\dfrac{P_g}{P}\dfrac{T_r}{T_g}Q_g + Q_m} + \frac{f_{sr}}{2g\,D_{sr}}\frac{\left(\dfrac{P_g}{P}\dfrac{T_r}{T_g}Q_g + Q_m\right)^2}{\dfrac{\pi}{4}D_{sr}^2}$$

and P_{sr} is the pressure at the entrance of the surface return flow line (lb/ft^2, abs),
f_{sr} is the Fanning friction factor for flow in the surface return flow line,
D_{sr} is the inside diameter of the surface return flow line (ft),
L_{sr} is the length of the surface return flow line (ft).

In order to obtain the approximate value of the Fanning friction factor for Equation 9-11, it is necessary to estimate the Reynolds number and, thus, the flow conditions inside the surface return flow line. This is accomplished by determining the Reynolds number at the exit end of the surface return flow line and assuming this Reynolds number approximates the flow conditions throughout the flow line.

The inside diameter of the surface return flow line, D_{sr}, is

$$d_{sr} = 5.625 \text{ inches}$$

$$D_{sr} = \frac{5.625}{12}$$

$$D_{sr} = 0.469 \text{ ft}$$

The length of the surface return flow line, L_{sr}, is

$$L_{sr} = 100.0 \text{ ft}$$

The absolute viscosity of the gas (air) at atmospheric conditions, μ_g, is

$$\mu_g = 0.012 \text{ cps}$$

$$\mu_g = (0.012)(0.001)(0.02089)$$

$$\mu_g \quad 0.000000251 \ \frac{lb \ sec}{ft^2}$$

Using Equation 1-2, the density of the gas, γ_g, is

$$\gamma_g \quad \frac{0.0659}{32.2}$$

$$\gamma_g \quad 0.002046 \ \frac{lb \ sec^2}{ft^4}$$

From Equation 9-7, the kinematic viscosity of the gas, ν_g, is

$$\nu_g \quad \frac{0.000000251}{0.002046}$$

$$\nu_g \quad 0.000123 \ \frac{ft^2}{sec}$$

The kinematic viscosity of the aerated drilling fluid (the mixture of the drilling mud and the compressed air) can be approximated with an average kinematic viscosity term. This average kinematic viscosity term can be approximated by weight averaging the separate viscosities with the weight rates of flow of the separate fluids. Therefore, the average kinematic viscosity at the exit end of the surface return flow line, ν_{sr}, is

$$\nu_{sr} \quad \frac{\dot{w}_g \nu_g \quad \dot{w}_m \nu_m}{\dot{w}_g \quad \dot{w}_m} \qquad\qquad (9\text{-}12)$$

The average kinematic viscosity at the exit end of the surface return flow line, ν_{sr}, is

$$\nu_{sr} \quad \frac{(1.282) \ (0.000123) \quad (31.92) \ (0.0002691)}{1.282 \quad 31.92}$$

$$\nu_{sr} \quad 0.000263 \ ft^2/sec$$

The average velocity of the aerated drilling fluid (the mixture of the drilling mud and the compressed air) as the mixture exits the end of the surface return flow line into the atmosphere, V_{sr}, is

$$V_{sr} = \frac{(19.47 + 0.4256)}{\frac{\pi}{4} (0.469)^2}$$

$$V_{sr} = 115.3 \ \text{ft/sec}$$

Equation 6-74 can be altered to allow its application to the horizontal flow in the surface flow line. Thus, the Reynolds number of the aerated drilling fluid as it exits the surface return flow line, N_{Rsr}, is

$$N_{Rsr} = \frac{V_{sr} \ D_{sr}}{\nu_{sr}}$$

$$N_{Rsr} = \frac{(115.3) \ (0.469)}{0.000263}$$

$$N_{Rsr} = 205,100$$

The Reynolds number calculation above is greater than 4,000. This indicates that the flow condition is turbulent. Therefore, the empirical von Karman equation (i.e., Equation 6-48) must be used to determine the Fanning friction factor for the aerated fluid flow inside the return flow line. Equation 6-48 can be modified for application to the surface return flow line situation.

The surface roughness of the inside of the steel surface return flow line is the absolute surface roughness of commercial steel pipe, e_p. This is

$$e_p = 0.00015 \ \text{ft}$$

The Fanning friction factor, f_{sr}, for flow inside the return flow line is

$$f_{sr} = \frac{1}{\left[2 \ \log \left(\frac{0.469}{0.00015} \right) + 1.14 \right]^2}$$

$$f_{sr} = 0.015$$

Equation 9-11 for the surface return flow line increment can be solved for the pressure at the entrance end of the line, P_{sr}. This involves selecting this upper limit of the left side intergal by a trial and error procedure. The magnitude of the upper limit pressure on the left side of the equation is selected to allow the left side integral to equal the right side integral. The integration can be carried out on the

computer using one of the commercial analytic software programs (e.g., MathCad). The trial and error magnitude of the upper limit pressure is

$$p_{sr} \quad 18.91 \ \text{psia}$$

$$P_{sr} \quad p_{sr} \ 144$$

$$P_{sr} \quad 2,723.3 \ \text{lb/ft}^2 \ \text{abs}$$

Substituting the values of L_{sr}, $\dot{w}_t$, Q_g, Q_m, P_g, P_{at}, P_{sr}, T_g, T_r, D_{sr}, f_{sr}, and g into the left side of Equation 9-11 gives

$$\int_{1,826.6}^{2,723.3} \frac{dP}{\dfrac{34.15}{\dfrac{34,519.6}{P} \ 0.426} \quad \dfrac{0.015}{30.20} \quad \dfrac{\left(\dfrac{34,519.6}{P}\right)^2 \ 0.426}{\dfrac{}{4}(0.469)^2}} \quad 100$$

Substituting the value of L_{sr} into the right side of Equation 9-11 gives

$$\int_0^{100} 1 \ dh \quad 100$$

The aerated drilling fluid flows from the top of the annulus into the entrance of the surface return flow line. The friction flow loss of the turn and of the two valves at the entrance of the surface return flow line must be included. The approximate specific weight of the aerated drilling fluid just after it passes through the Tee and the valves at the top of the annulus is determined using the above determined P_{sr}. The approximate specific weight at the Tee, $_{Tee}$, is

$$_{Tee} \quad \frac{\dot{w}_t}{\dfrac{P_g}{P_{sr}} \quad \dfrac{T_r}{T_g} \quad Q_g \quad Q_m}$$

Substituting the values of $\dot{w}_t$, P_g, P_{sr}, T_g, T_r, Q_g, and Q_m into the above equation gives the specific weight just downstream of the Tee and valves. This is

$$\gamma_{Tee} \quad \frac{34.15}{\dfrac{1,826.6}{2,723.3} \quad \dfrac{504.41}{519.67} \quad (19.47) \quad 0.426}$$

$$\gamma_{Tee} \quad 2.607 \ \text{lb/ft}^3$$

The approximate velocity of the aerated fluid flow just downstream of the Tee and valves is

$$V_{Tee} \quad \frac{\dfrac{P_g}{P_{sr}} \ \dfrac{T_r}{T_g} \ Q_g \quad Q_m}{\dfrac{}{4} \ D_{sr}^2}$$

Substituting the values of Q_g, Q_m, P_g, P_{sr}, T_g, T_r, and D_{sr} into the above equation gives

$$V_{Tee} \quad \frac{\dfrac{1,826.6}{2,723.3} \ \dfrac{504.41}{519.67} \ (19.47) \quad 0.426}{\dfrac{}{4} \ (0.469)^2}$$

$$V_{Tee} \quad 75.91 \ \text{ft/sec}$$

The approximate pressure change, $\exists P_{Tee}$, through the two valves and Tee is

$$\exists P_{Tee} \quad \gamma_{Tee} \ K_{Tee} \quad 2 \ K_v \quad \frac{V_{Tee}^2}{2g}$$

where K_{Tee} is the minor loss flow resistance coefficient for the Tee,
K_v is the minor loss flow resistance coefficient for a valve.
Using the dimensions of the Tee, Figure 8-5 can be used to obtain the approximate minor loss resistance coefficient of the Tee. This is

$$K_{Tee} \quad 27$$

The approximate minor loss resistance coefficient for the valve is [18]

$$K_v \quad 0.2$$

Substituting the values of γ_{Tee}, K_{Tee}, K_v, V_{Tee}, and g into the above equation gives

$$\exists P_{Tee} \quad 2.607 \ \%_7 \quad 2 \quad 0.2 \ \&\frac{75.91}{2 \ 32.2}^2$$

$$\exists P_{Tee} \quad 6,391.0 \ \text{lb/ft}^2$$

The pressure upstream of the Tee at the top of the annulus, P_{Tee}, is

$$P_{Tee} \quad P_{sr} \quad \exists P_{Tee}$$

$$P_{Tee} \quad 2,723.3 \quad 6,391.0$$

$$P_{Tee} \quad 9,114.3 \ \text{lb/ft}^2 \ \text{abs}$$

$$p_{Tee} \quad P_{Tee} \ 144$$

$$p_{Tee} \quad 63.3 \ \text{psia}$$

Geometry in the Annulus

Major and minor friction losses must be included in order to obtain accurate bottomhole and injection pressures. Therefore, it is necessary to include the geometric dimensions of the drill pipe tool joints. When drilling at 10,000 ft, the drill string is composed of 9,500 ft of API 4 1/2 inch, 16.60 lb/ft nominal, EU-S135, NC50 (IF) from the surface to the top of the drill collars. The 4 1/2 inch outside diameter body of the drill pipe has an inside diameter of 3.826 inches (see Table B-3). Approximately every 30 ft there are tool joints which are about 1 1/2 ft in length. The outside diameter of these tool joints is 6 5/8 inches with an inside diameter of 3 1/2 inches. For the calculations that follow, the drill pipe tool joint lengths will be "lumped" together as a continuous length to approximate their contribution to the overall major (wall friction) loss in the flow system. Thus, the drill pipe tool joints of the drill pipe in the 7,000 ft cased section of the borehole are calculated as a "lump" at the bottom of this cased section. The drill pipe tool joints of the drill pipe in the 2,500 ft openhole section of the borehole are calculated as a "lump" at the bottom of this openhole section.

These lumped approximations for the drill pipe tool joints are somewhat rough approximations, but will give quite accurate bottomhole and injection pressures. Using this lumped approximation, the pressure terms along the annulus around the drill pipe and inside the drill pipe are in error by a few percent. However, this short-coming can obviously be relieved by calculating a short 1 1/2 ft long tool joint every 30 ft along the entire drill pipe length of the drill string. This can easily be accomplished with a sophisticated computer program. But these lumped approximations are very useful in demonstrating the calculation technique steps. These lumped approximations are very easy to incorporate in an engineering calculation program and it has been found that these approximations are quite adequate for most engineering practice applications.

The calculation sequence for this illustrative example is divided into five depth increments. The increments start at the top of the borehole with the first increment at the top and the fifth increment at the bottom.

The total length of the lumped drill pipe body increment (first), H_1, in the cased section of the borehole is

$$H_1 \quad 7,000 \quad 1.5 \quad \frac{7,000}{30}$$

$$H_1 \quad 6,650 \text{ ft}$$

The inside diameter of the casing along this length of the cased section of the borehole is

$$d_1 \quad 8.017 \text{ inches}$$

$$D_1 \quad \frac{d_1}{12}$$

$$D_1 \quad 0.668 \text{ ft}$$

and the outside diameter of the drill pipe body along this length is

$$d_2 \quad 4.50 \text{ inches}$$

$$D_2 \quad \frac{d_2}{12}$$

$$D_2 \quad 0.375 \text{ ft}$$

The total length of the lumped drill pipe tool joints increment (second), H_2, in the cased section of the borehole is

$$H_2 \quad 1.5 \quad \frac{7,000}{30}$$

$$H_2 \quad 350 \text{ ft}$$

The inside diameter of the casing along this length of the cased section of the borehole is

$$D_1 \quad 0.668 \text{ ft}$$

and the outside diameter of the drill pipe tool joints along this length is

d_3 6.625 inches

D_3 $\dfrac{d_3}{12}$

D_3 0.552 ft

The total length of the lumped drill pipe body increment (third), H_3, in the openhole section of the borehole is

H_3 2,500   1.5 $\dfrac{2,500}{30}$

H_3 2,375 ft

The inside diameter of the openhole along this length of the openhole section of the borehole is

d_h 7.875 inches

D_h $\dfrac{d_h}{12}$

D_h 0.656 ft

and the outside diameter of the drill pipe body along this length is

D_2 0.375 ft

The total length of the lumped drill pipe tool joints increment (fourth), H_4, in the openhole section of the borehole is

H_4 1.5 $\dfrac{2,500}{30}$

H_4 125 ft

The inside diameter of the openhole along this length of the openhole section of the borehole is

D_h 0.656 ft

and the outside diameter of the drill pipe tool joints along this length is

$$D_3 \quad 0.552 \text{ ft}$$

The total length of the drill collar increment (fifth), H_5, in the openhole section of the borehole is

$$H_5 \quad 500 \text{ ft}$$

The inside diameter of the openhole along this length of the openhole section of the borehole is

$$D_h \quad 0.656 \text{ ft}$$

and the outside diameter of the drill collars along this length is

$$d_4 \quad 6.75 \text{ inches}$$

$$D_4 \quad \frac{d_4}{12}$$

$$D_4 \quad 0.563 \text{ ft}$$

Using the description of the annulus geometry given above each of the five increment changes in cross-sectional area can be analyzed starting with the gas flow exiting at the top of the annulus.

Cased Section of the Annulus (Surface to 7,000 ft)

The first annulus section increment is denoted by the length H_1.   The temperature at the bottom of the length H_1 in the cased annulus section of the borehole (bottom of the drill pipe body lumped geometry), T_1, is

$$T_1 \quad T_r \quad 0.01 \; H_1$$

$$T_1 \quad T_r \quad 0.01 \; (6,650)$$

$$T_1 \quad 570.91°R$$

The average temperature of this cased annulus section H_1 is

$$T_{av1} \quad \frac{T_r \quad T_1}{2}$$

$$T_{av1} \quad 537.66°R$$

In order to obtain the approximate value of the Fanning friction factor for Equation 6-74, it is necessary to estimate the Reynolds number and, thus, the flow

conditions in the cased annulus section along H_1.   This is accomplished by determining the Reynolds number at the exit end of this annulus section and assuming this Reynolds number approximates the flow conditions throughout the annulus section.

Using Equation 4-11, the approximate specific weight of the gas as it exits this cased annulus section and starts into the Tee is determined from P_{Tee}. This is

$$\gamma_{ga1} = \frac{(9,114.3)\ (1.0)}{(53.36)\ (504.41)}$$

$$\gamma_{ga1} = 0.339\ \text{lb/ft}^3$$

Using Equation 1-2, the density of the gas as it exits this annulus section, ρ_{ga1}, is

$$\rho_{ga1} = \frac{0.339}{32.2}$$

$$\rho_{ga1} = 0.0110\ \frac{\text{lb}\ \ \text{sec}^2}{\text{ft}^4}$$

From Equation 9-7, the kinematic viscosity of the gas at this location, ν_{ga1}, is

$$\nu_{ga1} = \frac{0.000000251}{0.0110}$$

$$\nu_{ga1} = 0.0000238\ \frac{\text{ft}^2}{\text{sec}}$$

The kinematic viscosity of the aerated drilling fluid mixture can be approximated with an average kinematic viscosity term. This average kinematic viscosity term can be defined by weight averaging the separate viscosities with the weight rates of flow of the separate fluids. Therefore, the kinematic viscosity term can be modified to determine the average kinematic viscosity, ν_{ava1}, of the mixture as it exits this annulus section. This is

$$\nu_{ava1} = \frac{\dot{w}_g\ \nu_{ga1} \quad \dot{w}_m\ \nu_m}{\dot{w}_g \quad \dot{w}_m}$$

The average kinematic viscosity of the mixture as it exits this annulus section, ν_{ava1}, is

$$\mu_{ava1} \quad \frac{(1.282)\,(0.0000238)}{1.282} \quad \frac{(31.92)\,(0.0002691)}{31.92}$$

$$\mu_{ava1} \quad 0.000260 \ \text{ft}^2/\text{sec}$$

The approximate average velocity of the aerated drilling fluid as it exits this annulus section, V_{a1}, is

$$V_{a1} \quad \frac{\dfrac{1,826.6}{9,114.3} \quad \dfrac{537.66}{519.67} \quad (19.47) \quad 0.426}{\dfrac{}{4} \, \%0.668 \,^2 \quad 0.375 \,^2 \, \&}$$

$$V_{a1} \quad 18.59 \ \text{ft/sec}$$

Using Equation 6-75, the Reynolds number of the aerated drilling fluid as it exits this annulus section, $\mathbf{N_{Ra1}}$, is

$$\mathbf{N_{Ra1}} \quad \frac{(18.59)\,(0.668 \quad 0.375)}{0.000260}$$

$$\mathbf{N_{Ra1}} \quad 20,980$$

The Reynolds number calculation above is greater than 4,000. This indicates that the flow condition is turbulent. Therefore, the empirical von Karman equation (i.e., Equation 6-78) is used to determine the approximate Fanning friction factor for the aerated flow in this annulus section.

Both annulus section surfaces are commercial steel with the surface roughness

$$e_p \quad 0.00015 \ \text{ft}$$

Therefore, Equation 6-78 becomes

$$f_{a1} \quad \frac{1}{2 \ \log \ \dfrac{0.668 \quad 0.375}{0.00015} \quad 1.14}^{2}$$

$$f_{a1} \quad 0.017$$

Equation 6-74 for the first increment in the annulus can be solved for the pressure at bottom of the increment, P_{a1}. This involves selecting this upper limit by a trial and error procedure. The magnitude of the upper limit pressure on the left side of the equation is selected to allow the left side integral to equal the right side integral. The integration can be carried out on the computer using one of the commercial analytic software programs. The trial and error magnitude of the upper limit pressure that satisfies Equation 6-74 for this annulus section is

p_{a1} $1,865.5$ psia

P_{a1} p_{a1} 144

P_{a1} $268,632$ lb/ft^2 abs

Substituting the values of $\dot{w}_t$, Q_g, Q_m, P_g, P_{Tee}, P_{a1}, T_g, T_{av1}, D_1, D_2, f_{a1}, and g into the left side of Equation 6-74 gives

$$\int_{9114.3}^{268,623} \frac{dP}{\frac{34.15}{\frac{36,795.1}{P}\,0.426} \, 1 \, \frac{0.017}{18.87} \, \frac{\left(\frac{36,795.1}{P}\,0.426\right)^2}{-\frac{\pi}{4}\left(0.668^2 \quad 0.375^2\right)}} \quad 6,650 &$$

Substituting the value of H_1 into the right side of Equation 6-74 gives

$$\int_{0}^{6,650} 1 \, dh \quad 6,650$$

As can be seen in the above, the right and left hands sides of Equation 6-74 yield the same answer. This shows that the upper limit pressure is correct.

The second annulus section increment is denoted by length H_2. The temperature at the bottom of the length H_2 in the cased annulus section of the borehole (bottom of the drill pipe tool joints lumped geometry), T_2, is

T_2 T_r $0.01\,(H_1 \quad H_2)$

T_2 T_r $0.01\,(6,650 \quad 350)$

T_2 $574.41°R$

The average temperature of this cased annulus section H_2 is

$$T_{av2} \quad \frac{T_1 \quad T_2}{2}$$

$$T_{av2} \quad 572.66°R$$

In order to obtain the approximate value of the Fanning friction factor for Equation 6-74, it is necessary to estimate the Reynolds number and, thus, the flow conditions in the cased annulus section along H_2.   This is accomplished by determining the Reynolds number at the exit end of this annulus section and assuming this Reynolds number approximates the flow conditions throughout the annulus section.

Using Equation 4-11, the approximate specific weight of the gas as it exits this cased annulus section and starts into the annulus section above is determined from P_{a1}.   This is

$$_{ga2} \quad \frac{(268,632) \ (1.0)}{(53.36) \ (572.66)}$$

$$_{ga2} \quad 8.79 \ \text{lb/ft}^3$$

Using Equation 1-2, the density of the gas as it exits this annulus section, $_{ga2}$, is

$$_{ga2} \quad \frac{8.79}{32.2}$$

$$_{ga2} \quad 0.273 \ \frac{\text{lb} \quad \text{sec}^2}{\text{ft}^4}$$

From Equation 9-7, the kinematic viscosity of the gas at this location, $_{ga2}$, is

$$_{ga2} \quad \frac{0.000000251}{0.273}$$

$$_{ga2} \quad 0.000000918 \ \frac{\text{ft}^2}{\text{sec}}$$

The average kinematic viscosity of the mixture at this position, $_{ava1}$, is

$$_{ava2} \quad \frac{(1.282) \ (0.000000918) \quad (31.92) \ (0.0002691)}{1.282 \quad 31.92}$$

$$_{ava2} \quad 0.000259 \ \text{ft}^2/\text{sec}$$

The approximate average velocity of the aerated drilling fluid as it exits this annulus section, V_{a2}, is

$$V_{a2} = \frac{\dfrac{1,826.6}{268,632}\dfrac{572.66}{519.67}(19.47)\ 0.426}{\dfrac{\pi}{4}\left(0.668^2 - 0.552^2\right)}$$

$$V_{a2} = 5.14 \text{ ft/sec}$$

Using Equation 6-75, the Reynolds number of the aerated drilling fluid as it exits this annulus section, N_{Ra2}, is

$$N_{Ra2} = \frac{(5.14)\,(0.668 - 0.552)}{0.000259}$$

$$N_{Ra2} = 8,333$$

The Reynolds number calculation above is greater than 4,000. This indicates that the flow condition is turbulent. Therefore, the empirical von Karman equation (i.e., Equation 6-78) is used to determine the approximate Fanning friction factor for the aerated flow in this annulus section.

Both annulus section surfaces are commercial steel with the surface roughness

$$e_p = 0.00015 \text{ ft}$$

Therefore, Equation 6-78 becomes

$$f_{a2} = \frac{1}{\left[2\,\log\dfrac{0.668 - 0.552}{0.00015} + 1.14\right]^2}$$

$$f_{a2} = 0.021$$

Equation 6-74 for the second increment in the annulus can be solved for the pressure at the bottom of the increment, P_{a2}. This involves selecting this upper limit by a trial and error procedure. The magnitude of the upper limit pressure on the left side of the equation is selected to allow the left side integral to equal the right side integral. The integration can be carried out on the computer using one of the commercial analytic software programs. The trial and error magnitude of the upper limit pressure that satisfies Equation 6-74 for this annulus section is

P_{a2} 2,022.9 psia

P_{a2} p_{a2} 144

P_{a2} 291,298 lb/ft^2 abs

Substituting the values of $\dot{w}_t$, Q_g, Q_m, P_g, P_{a1}, P_{a2}, T_g, T_{av2}, D_2, D_3, f_{a2}, and g into the left side of Equation 6-74 gives

$$\int_{268,632}^{291,298} \frac{dP}{\frac{34.15}{\left(\frac{39,190.3}{P}\right)^{0.426}} \left(1 + \frac{0.021}{7.47} \frac{\left(\frac{39,190.3}{P}\right)^{0.426}}{\frac{1}{4}\left(0.668\right)^2} \left(0.552\right)^2\right)} = 350$$

Substituting the values of H_1 and H_2 into the right side of Equation 6-74 gives

$$\int_{6,650}^{6,650+350} 1 \, dh = 350$$

As can be seen in the above, the right and left hand sides of Equation 6-74 yield the same answer. This shows that the upper limit pressure is correct.

Openhole Section of the Annulus (7,000 ft to 10,000 ft)

The third annulus section increment is denoted by the length H_3.   The temperature at the bottom of the length H_3 in the openhole annulus section of the borehole (bottom of the drill pipe body lumped geometry), T_3, is

T_3 T_r $0.01 (H_1 + H_2 + H_3)$

T_3 T_r $0.01 (6,650 + 350 + 2,375)$

T_3 598.16°R

The average temperature of this openhole annulus section H_3 is

$$T_{av3} = \frac{T_2 + T_3}{2}$$

T_{av3} 586.29°R

In order to obtain the approximate value of the Fanning friction factor for Equation 6-74, it is necessary to estimate the Reynolds number and, thus, the flow conditions in the openhole annulus section along H_3.   This is accomplished by determining the Reynolds number at the exit end of this annulus section and assuming this Reynolds number approximates the flow conditions throughout the annulus section.

Using Equation 4-11, the approximate specific weight of the gas as it exits this openhole annulus section is determined from P_{a2}.   This is

$$\gamma_{ga3} \quad \frac{(291,298)\,(1.0)}{(53.36)\,(586.29)}$$

$$\gamma_{ga3} \quad 9.31 \ \text{lb/ft}^3$$

Using Equation 1-2, the density of the gas as it exits this annulus section, ρ_{ga3}, is

$$\rho_{ga3} \quad \frac{9.31}{32.2}$$

$$\rho_{ga3} \quad 0.289 \ \frac{\text{lb} \quad \text{sec}^2}{\text{ft}^4}$$

From Equation 9-7, the kinematic viscosity of the gas at this location, ν_{ga3}, is

$$\nu_{ga3} \quad \frac{0.000000251}{0.289}$$

$$\nu_{ga3} \quad 0.000000867 \ \frac{\text{ft}^2}{\text{sec}}$$

The average kinematic viscosity of the mixture at this position, ν_{ava3}, is

$$\nu_{ava3} \quad \frac{(1.282)\,(0.000000867) \quad (31.92)\,(0.0002691)}{1.282 \quad 31.92}$$

$$\nu_{ava3} \quad 0.000259 \ \text{ft}^2/\text{sec}$$

The approximate average velocity of the aerated drilling fluid as it exits this annulus section, V_{a3}, is

$$V_{a3} \quad \frac{\dfrac{1,826.6}{291,298} \quad \dfrac{586.29}{519.67} \quad (19.47) \quad 0.426}{\dfrac{}{4} \; \%0.656^{\,2} \quad 0.375^{\,2} \; \&}$$

$V_{a3} \quad 2.47 \ \text{ft/sec}$

Using Equation 6-75, the Reynolds number of the aerated drilling fluid as it exits this annulus section, N_{Ra3}, is

$$N_{Ra3} \quad \frac{(2.47) \ (0.656 \quad 0.375)}{0.000259}$$

$N_{Ra3} \quad 2,680$

The Reynolds number calculation above is greater than 2,000 and less than 4,000. This indicates that the flow condition is transition.   Therefore, the empirical Colebrook equation (i.e., Equation 6-77) is used to determine the approximate Fanning friction factor in this annulus section.

The surfaces of this example openhole annulus section have two different surface roughnesses. The inside surface of this openhole borehole is a wall drilled in a sandstone and limestone rock sequence. Unless such a rock sequence is highly fractured, the inside surface of the borehole approximates the inside surface of a concrete water pipe used in community water systems.   Table 8-1 correlates the inside surface of borehole roughness for a variety of rock formation types with those of known engineering pressure conduits.   From this table the surface roughness for the inside wall of a borehole in the example sandstone and limestone rock sequence, e_{oh}, is

$e_{oh} \quad 0.01 \ \text{ft}$

The inner surface of this annulus section is the outer surface of the drill pipe body lumped geometry has the surface roughness of commercial steel pipe, e_p. The surface roughness of commercial steel pipe is

$e_p \quad 0.00015 \ \text{ft}$

Thus, using Equation 8-2, the average absolute surface roughness of this annulus section, e_{av3}, is

$$e_{av3} \quad \frac{(0.01) \; \overline{}_4 \; (0.656)^2 \quad (0.00015) \; \overline{}_4 \; (0.375)^2}{\overline{}_4 \; (0.656)^2 \quad \overline{}_4 \; (0.375)^2}$$

$$e_{av3} \quad 0.0076 \text{ ft}$$

Equation 6-77 must be solved by trial and error. A value for f_{a3} must be selected that will satisfy the Colebrook equation. This value is

$$f_{a3} \quad 0.065$$

The Colebrook equation is

$$\frac{1}{\sqrt{0.065}} \quad 2 \; \log \quad \frac{\dfrac{0.0076}{0.656 \quad 0.375}}{3.7} \quad \frac{2.51}{2,688 \; \sqrt{0.065}}$$

The right and left sides of the above yield

$$3.92 \quad 3.92$$

Equation 6-74 for the third increment in the annulus can be solved for the pressure at the bottom of the increment, P_{a3}. This involves selecting this upper limit by a trial and error procedure. The magnitude of the upper limit pressure on the left side of the equation is selected to allow the left side integral to equal the right side integral. The integration can be carried out on the computer using one of the commercial analytic software programs. The trial and error magnitude of the upper limit pressure is

$$p_{a3} \quad 3,094.3 \text{ psia}$$

$$P_{a3} \quad p_{a3} \; 144$$

$$P_{a3} \quad 445,579 \text{ lb/ft}^2 \text{ abs}$$

Substituting the values of $\dot{w}_t$, Q_g, Q_m, P_g, P_{a2}, P_{a3}, T_g, T_{av3}, D_h, D_1, f_{a3}, and g into the left side of Equation 6-74 gives

$$\int_{291,298}^{445,579} \cfrac{dP}{\cfrac{34.15}{\cfrac{40,123.1}{P}\,0.426} + 1\left[\cfrac{0.065}{18.10}\cfrac{\cfrac{40,123.1}{P}\,0.426}{\cfrac{\pi}{4}\,0.656^2 \quad 0.375^2}\right]^2} = 2,375$$

Substituting the values of H_1, H_2 and H_3 into the right side of Equation 6-74 gives

$$\frac{6,650 \quad 350 \quad 2.375}{6,650 \quad 350}\; 1\; dh = 2,375$$

As can be seen in the above, the right and left hand sides of Equation 6-74 yield the same answer. This shows that the upper limit pressure is correct.

The fourth annulus section increment is denoted by length H_4. The temperature at the bottom of the length H_4 in the openhole annulus section of the borehole (bottom of the drill pipe tool joints lumped geometry), T_4, is

$$T_4 = T_r + 0.01\,(H_1 + H_2 + H_3 + H_4)$$

$$T_4 = T_r + 0.01\,(6,650 + 350 + 2,375 + 125)$$

$$T_4 = 599.41°R$$

The average temperature of this openhole annulus section H_4 is

$$T_{av4} = \frac{T_3 + T_4}{2}$$

$$T_{av4} = 598.79°R$$

In order to obtain the approximate value of the Fanning friction factor for Equation 6-74, it is necessary to estimate the Reynolds number and, thus, the flow conditions in the openhole annulus section along H_4. This is accomplished by determining the Reynolds number at the exit end of this annulus section and assuming this Reynolds number approximates the flow conditions throughout the annulus section.

Using Equation 4-11, the approximate specific weight of the gas as it exits this openhole annulus section is determined from P_{a3}. This is

$$\gamma_{ga4} = \frac{(445,579)\,(1.0)}{(53.36)\,(598.78)}$$

$$\rho_{ga4} \quad 13.95 \ \text{lb/ft}^3$$

Using Equation 1-2, the density of the gas as it exits this annulus section, ρ_{ga4}, is

$$\rho_{ga4} \quad \frac{13.95}{32.2}$$

$$\rho_{ga4} \quad 0.433 \ \frac{\text{lb} \ \text{sec}^2}{\text{ft}^4}$$

From Equation 9-7, the kinematic viscosity of the gas at this location, γ_{ga4}, is

$$\gamma_{ga4} \quad \frac{0.000000251}{0.433}$$

$$\gamma_{ga4} \quad 0.000000579 \ \frac{\text{ft}^2}{\text{sec}}$$

The average kinematic viscosity of the mixture as it exits this annulus section, γ_{ava4}, is

$$\gamma_{ava4} \quad \frac{(1.282) \ (0.000000579) \quad (31.92) \ (0.0002691)}{1.282 \quad 31.92}$$

$$\gamma_{ava4} \quad 0.000259 \ \text{ft}^2/\text{sec}$$

The approximate average velocity of the aerated drilling fluid as it exits this annulus section, V_{a4}, is

$$V_{a4} \quad \frac{\dfrac{1,826.6}{445,579} \ \dfrac{598.79}{519.67} \ (19.47) \quad 0.426}{-\dfrac{\%}{4} \, (0.656)^2 \quad 0.552^{\ 2} \ \&}$$

$$V_{a4} \quad 5.24 \ \text{ft/sec}$$

Using Equation 6-75, the Reynolds number of the aerated drilling fluid as it exits this annulus section, N_{Ra4}, is

$$N_{Ra4} \quad \frac{(5.24) \ (0.656 \quad 0.552)}{0.000259}$$

N_{Ra4} 2,108

The Reynolds number calculation above is greater than 2,000 and less than 4,000. This indicates that the flow condition is transitional. Therefore, the empirical Colebrook equation (i.e., Equation 6-77) is used to determine the approximate Fanning friction factor in this annulus section.

Using Equation 8-2, the average absolute surface roughness of this annulus section, e_{av4}, is

$$e_{av4} \quad \dfrac{(0.01) \quad \overline{}_4 \quad (0.656)^2 \quad (0.00015) \quad \overline{}_4 \quad (0.552)^2}{\overline{}_4 \quad (0.656)^2 \quad \overline{}_4 \quad (0.552)^2}$$

e_{av4} 0.0059 ft

Equation 6-77 must be solved by trial and error. A value for f_{a4} must be selected that will satisfy the Colebrook equation. This value is

f_{a4} 0.085

The Colebrook equation is

$$\dfrac{1}{\sqrt{0.085}} \quad 2 \ \log \quad \dfrac{\dfrac{0.0059}{0.656 \quad 0.552}}{3.7} \quad \dfrac{2.51}{2,108 \ \sqrt{0.085}}$$

The right and left sides of the above yield

3.42   3.42

Equation 6-74 for the fourth increment in the annulus can be solved for the pressure at the bottom of the increment, P_{a4}. This involves selecting this upper limit by a trial and error procedure. The magnitude of the upper limit pressure on the left side of the equation is selected to allow the left side integral to equal the right side integral. The integration can be carried out on the computer using one of the commercial analytic software programs. The trial and error magnitude of the upper limit pressure is

p_{a4} 3,171.6 psia

$$P_{a4} \quad p_{a4} \; 144$$

$$P_{a4} \quad 456,707 \; \text{lb/ft}^2 \; \text{abs}$$

Substituting the values of $\dot{w}_t$, Q_g, Q_m, P_g, P_{a3}, P_{a4}, T_g, T_{av4}, D_h, D_3, f_{a4}, and g into the left side of Equation 6-74 gives

$$\int_{445,579}^{456,707} \frac{dP}{\dfrac{34.15}{\dfrac{40,978.2}{P}\;0.426} \quad 1 \quad \dfrac{0.085}{6.70} \quad \dfrac{\left(\dfrac{40,978.2}{P}\;0.426\right)^2}{\dfrac{1}{4}\;0.656^2 \quad 0.552^2}} \; \& \quad 125$$

Substituting the values of H_1, H_2, H_3, and H_4 into the right side of Equation 6-74 gives

$$\int_{6,650 \;\; 350 \;\; 2,375}^{6,650 \;\; 350 \;\; 2.375 \;\; 125} 1 \; dh \quad 125$$

As can be seen in the above, the right and left hand sides of Equation 6-74 yield the same answer. This shows that the upper limit pressure is correct.

The fifth annulus section increment is denoted by the length H_5. The temperature at the bottom of the length H_4 in the openhole annulus section of the borehole (bottom of the drill collars lumped geometry), T_5, is

$$T_5 \quad T_r \quad 0.01 \; (H_1 \quad H_2 \quad H_3 \quad H_4 \quad H_5)$$

$$T_5 \quad T_r \quad 0.01 \; (6,650 \quad 350 \quad 2,375 \quad 125 \quad 350)$$

$$T_5 \quad 604.41°\text{R}$$

The average temperature of this openhole annulus section H_5 is

$$T_{av5} \quad \frac{T_4 \quad T_5}{2}$$

$$T_{av5} \quad 601.91°\text{R}$$

In order to obtain the approximate value of the Fanning friction factor for Equation 6-74, it is necessary to estimate the Reynolds number and, thus, the flow conditions in the openhole annulus section along H_5. This is accomplished by

determining the Reynolds number at the exit end of this annulus section and assuming this Reynolds number approximates the flow conditions throughout the annulus section.

Using Equation 4-11, the approximate specific weight of the gas as it exits this openhole annulus section is determined from P_{a4}. This is

$$\gamma_{ga5} \quad \frac{(456,707)\ (1.0)}{(53.36)\ (601.91)}$$

$$\gamma_{ga5} \quad 14.22 \ \text{lb/ft}^3$$

Using Equation 1-2, the density of the gas as it exits this annulus section, ρ_{ga5}, is

$$\rho_{ga5} \quad \frac{14.22}{32.2}$$

$$\rho_{ga5} \quad 0.442 \ \frac{\text{lb} \ \ \text{sec}^2}{\text{ft}^4}$$

From Equation 9-7, the kinematic viscosity of the gas at this location, ν_{ga5}, is

$$\nu_{ga5} \quad \frac{0.000000251}{0.442}$$

$$\nu_{ga5} \quad 0.000000568 \ \frac{\text{ft}^2}{\text{sec}}$$

The average kinematic viscosity of the mixture as it exits this annulus section, ν_{ava5}, is

$$\nu_{ava5} \quad \frac{(1.282)\ (0.000000568) \quad (31.92)\ (0.0002691)}{1.282 \quad 31.92}$$

$$\nu_{ava5} \quad 0.000259 \ \text{ft}^2/\text{sec}$$

The approximate average velocity of the aerated drilling fluid as it exits this annulus section, V_{a5}, is

$$V_{a5} \quad \frac{\dfrac{1,826.6}{456,707} \quad \dfrac{601.91}{519.67} \ (19.47) \quad 0.426}{\dfrac{}{4} \ \%0.656)^2 \quad 0.563^{\ 2} \ \&}$$

$$V_{a5} \quad 5.78 \text{ ft/sec}$$

Using Equation 6-75, the Reynolds number of the aerated drilling fluid as it exits this annulus section, N_{Ra5}, is

$$N_{Ra5} \quad \frac{(5.78)\,(0.656 \quad 0.563)}{0.000259}$$

$$N_{Ra5} \quad 2,083$$

The Reynolds number calculation above is greater than 2,000 and less than 4,000. This indicates that the flow condition is transitional. Therefore, the empirical Colebrook equation (i.e., Equation 6-77) is used to determine the approximate Fanning friction factor for this annulus section.

Using Equation 8-2, the average absolute surface roughness of this annulus section, e_{av5}, is

$$e_{av5} \quad \frac{(0.01) \quad \dfrac{-}{4} \quad (0.656)^2 \quad (0.00015) \quad \dfrac{-}{4} \quad (0.563)^2}{\dfrac{-}{4}\,(0.656)^2 \quad \dfrac{-}{4}\,(0.563)^2}$$

$$e_{av5} \quad 0.0058 \text{ ft}$$

Equation 6-77 must be solved by trial and error. A value for f_{a5} must be selected that will satisfy the Colebrook equation. This value is

$$f_{a5} \quad 0.088$$

The Colebrook equation is

$$\frac{1}{\sqrt{0.088}} \quad 2 \ \log \quad \frac{\dfrac{0.0058}{0.656 \quad 0.563}}{3.7} \quad \frac{2.51}{2,083 \ \sqrt{0.088}}$$

The right and left sides of the above yield

$$3.36 \quad 3.36$$

Equation 6-74 for the fifth increment in the annulus can be solved for the pressure at the bottom of the increment, P_{a5}. This involves selecting this upper

limit by a trial and error procedure. The magnitude of the upper limit pressure on the left side of the equation is selected to allow the left side integral to equal the right side integral. The integration can be carried out on the computer using one of the commercial analytic software programs. The trial and error magnitude of the upper limit pressure is

$$p_{a5} \quad 3,512.9 \ \text{psia}$$

$$P_{a5} \quad p_{a5} \ 144$$

$$P_{a5} \quad 505,858 \ \text{lb/ft}^2 \ \text{abs}$$

Substituting the values of $\dot{w}_t$, Q_g, Q_m, P_g, P_{a4}, P_{a5}, T_g, T_{av5}, D_h, D_4, f_{a5}, and g into the left side of Equation 6-74 gives

$$\int_{456,707}^{505,858} \frac{dP}{\dfrac{34.15}{\dfrac{41,192.0}{P} \ 0.426} \quad 1 \quad \dfrac{0.088}{5.99} \quad \dfrac{\dfrac{41,192.0}{P} \ 0.426}{-\dfrac{4}{0.656 \ ^2} \quad 0.563 \ ^2}} \quad 500$$

Substituting the values of H_1, H_2, H_3, H_4, and H_5 into the right side of Equation 6-74 gives

$$\int_{6,650 \ \ 350 \ \ 2,375 \ \ 125}^{6,650 \ \ 350 \ \ 2.375 \ \ 125 \ \ 500} 1 \ dh \quad 500$$

As can be seen in the above, the right and left hand sides of Equation 6-74 yield the same answer. This shows that the upper limit pressure is correct.

Drill Bit Nozzles

It is assumed that the 7 7/8 inch tri-cone roller cone drill bit is equipped with three 11/32 inch diameter jet nozzles. Therefore, the inside diameter of each nozzle D_n, is

$$d_n \quad 0.3437 \ \text{inches}$$

$$D_n \quad \frac{d_n}{12}$$

$$D_n \quad 0.02865 \ \text{ft}$$

From Equation 6-80, the equivalent single diameter for this drill bit, D_e, is

$$D_e \quad \sqrt{3 \quad 0.02865 \;^2}$$

$$D_e \quad 0.0496 \text{ ft}$$

The approximate specific weight of the aerated fluid at the bottom of the annulus, $_{mixbh}$, is

$$_{mixbh} \quad \frac{\dot{w}_g \quad \dot{w}_m}{\dfrac{P_g}{P_{a5}} \quad \dfrac{T_5}{T_g} \quad Q_g \quad Q_m}$$

Substituting the values of $\dot{w}_g$, $\dot{w}_m$, P_g, P_{a5}, T_g, T_6, Q_g, and Q_m into the above equation gives, the specific weight of the aerated fluid mixture at the bottom of the annulus is

$$_{mixbh} \quad \frac{1.282 \quad 31.92}{\dfrac{1,826.6}{505,858} \quad \dfrac{604.41}{519.67} \quad (19.47) \quad 0.426}$$

$$_{mixbh} \quad 65.4 \text{ lb/ft}^3$$

Using Equation 6-79, the pressure change in the aerated fluid through the drill bit, $\exists P_b$, can be approximated by

$$\exists P_b \quad \frac{1.282 \quad 31.92 \;^2}{2 \; (32.2) \; (65.4) \; (0.81)^2 \quad \dfrac{2}{4} \quad 0.0496 \;^4}$$

$$\exists P_b \quad 106,782 \text{ lb/ft}^2$$

where the nozzle loss coefficient is taken to be 0.81 (see Chapter 6, Section 6.4).

Using Equation 6-81, the pressure in the aerated fluid just above the drill bit inside the drill string, P_{i5}, is

$$P_{i5} \quad P_{a5} \quad \exists P_b$$

Using the above equation, the pressure in the aerated fluid just above the drill bit inside the drill string is

P_{i5} $505,858$ $106,782$

P_{i5} $612,640$ lb/ft^2 abs

p_{i5} $\dfrac{P_{i5}}{144}$

p_{i5} $4,254$ psia

Geometry Inside the Drill String

Starting at the bottom of the drill string, the total length of the drill collars increment, H_5, in the openhole section of the borehole is

H_5 500 ft

The inside diameter of the drill collars in this openhole section is

d_5 2.8125 inches

D_5 $\dfrac{d_5}{12}$

D_5 0.234 ft

The total length of the drill pipe tool joints lumped geometry increment, H_4, in the openhole section is

H_4 125 ft

The inside diameter of the drill pipe tool joints lumped geometry in this openhole section is

d_6 3.50 inches

D_6 $\dfrac{d_6}{12}$

D_6 0.292 ft

The total length of the drill pipe body lumped geometry increment, H_3, in the openhole section is

H_3 $2,375$ ft

The inside diameter of the drill pipe body lumped geometry in this openhole section is

d_7 3.826 inches

D_7 $\dfrac{d_7}{12}$

D_7 0.319 ft

The total length of the lumped drill pipe tool joints geometry increment, H_2, in the cased section is

H_2 350 ft

The inside diameter of the drill pipe tool joints lumped geometry in this cased section is

D_6 0.292 ft

The total length of the lumped drill pipe body geometry increment, H_1, in the cased section is

H_1 6,650 ft

The inside diameter of the drill pipe body lumped geometry in this cased section is

D_7 0.319 ft

Inside the Drill String (10,000 ft to 7,000 ft)

The fifth drill string section increment is denoted by the length H_5.   The temperature at the bottom of the drill collars (bottomhole temperature) in the openhole section is

T_5 604.41°R

The average temperature of the drill collar length H_5 and, thus, the temperature of the aerated fluid flow inside the drill collars is

T_{av5} 601.91°R

In order to obtain the approximate value of the Fanning friction factor for Equation 6-82, it is necessary to estimate the Reynolds number and, thus, the flow conditions inside the drill collars along H_5.   This is accomplished by determining the Reynolds number at the entrance end of the inside of the drill collar section and

assuming this Reynolds number approximates the flow conditions throughout the inside of the drill collar section.

Using Equation 4-11, the approximate specific weight of the gas as it enters this drill collar section is determined from P_{i5}. This is

$$\gamma_{gi5} \quad \frac{(612,640) \ (1.0)}{(53.36) \ (601.91)}$$

$$\gamma_{gi5} \quad 19.07 \ \text{lb/ft}^3$$

Using Equation 1-2, the density of the gas as it enters this drill collar section, ρ_{gi5}, is

$$\rho_{gi5} \quad \frac{19.07}{32.2}$$

$$\rho_{gi5} \quad 0.592 \ \frac{\text{lb} \ \ \text{sec}^2}{\text{ft}^4}$$

From Equation 9-7, the kinematic viscosity of the gas at this location, ν_{gi5}, is

$$\nu_{gi5} \quad \frac{0.000000251}{0.592}$$

$$\nu_{gi5} \quad 0.000000423 \ \frac{\text{ft}^2}{\text{sec}}$$

The average kinematic viscosity of the mixture as it enters this drill collar section, ν_{avi5}, is

$$\nu_{avi5} \quad \frac{(1.282) \ (0.000000423) \quad (31.92) \ (0.0002691)}{1.282 \quad 31.92}$$

$$\nu_{avi5} \quad 0.000259 \ \text{ft}^2/\text{sec}$$

Using the inside diameter of the drill collars, D_5, the approximate average velocity of the aerated drilling fluid as it enters this drill collar section, V_{i5}, is

$$V_{i5} \quad \frac{\dfrac{1,826.6}{612,640} \quad \dfrac{601.91}{519.67} \quad (19.47) \quad 0.426}{\dfrac{}{4} \quad 0.234^{\ 2}}$$

V_{i5} 11.42 ft/sec

Using Equation 6-83, the Reynolds number of the aerated drilling fluid as it enters this drill collar section, N_{Ri5}, is

$$\mathbf{N_{Ri5}} \qquad \frac{(11.42)\ (0.234)}{0.000259}$$

$$\mathbf{N_{Ri5}} \qquad 10,350$$

The Reynolds number calculation above is greater than 4,000. This indicates that the flow condition is turbulent. Therefore, the empirical von Karman equation (i.e., Equation 6-86) is used to determine the approximate Fanning friction factor for the aerated fluid flow inside drill collars.

The inside surface of the drill collars is commercial steel with the surface roughness

e_p 0.00015 ft

With the above, Equation 6-86 becomes

$$f_{i5} \qquad \frac{1}{\left(2\ \log\ \dfrac{0.234}{0.00015}\ 1.14 \right)^{2}}$$

$$f_{i5} \qquad 0.018$$

Equation 6-82 for the fifth increment inside the drill string can be solved for the pressure at the top of the increment, P_{i4}. This involves selecting this lower limit by a trial and error procedure. The magnitude of the lower limit pressure on the left side of the equation is selected to allow the left side integral to equal the right side integral. The integration can be carried out on the computer using one of the commercial analytic software programs. The trial and error magnitude of the lower limit pressure is

p_{i4} 3,985.5 psia

P_{i4} p_{i4} 144

P_{i4} 573,888 lb/ft^2 abs

Substituting the values of $\dot{w}_g$, $\dot{w}_m$, Q_g, Q_m, P_g, P_{i4}, P_{i5}, T_g, T_{av5}, D_5, f_{i5}, and g into the left side of Equation 6-82 gives

$$\int_{573,888}^{612,640} \frac{dP}{\dfrac{33.20}{\dfrac{41,192.0}{P}\,0.426}\left[1+\dfrac{0.018}{15.07}\,\dfrac{\dfrac{41,192.0}{P}\,0.426}{-\,0.234^2}{4}\right]^2} = 500$$

Substituting the values of H_1, H_2, H_3, H_4, and H_5 into the right side of Equation 6-82 gives

$$\int_{6,650\ 350\ 2,375\ 125}^{6,650\ 350\ 2.375\ 125\ 500} 1\ dh = 500$$

As can be seen in the above, the right and left hand sides of Equation 6-82 yield the same answer. This shows that the lower limit pressure is correct.

The fourth drill string section increment is denoted by the length H_4. The temperature at the bottom of the drill pipe tool joints lumped geometry in the openhole section is

$$T_4 \quad 599.41°\text{R}$$

The average temperature of the drill pipe tool joints lumped geometry along H_4 and, thus, the temperature of the aerated fluid flow inside the this drill string length is

$$T_{av4} \quad 598.79°\text{R}$$

In order to obtain the approximate value of the Fanning friction factor for Equation 6-82, it is necessary to estimate the Reynolds number and, thus, the flow conditions inside the drill pipe tool joints lumped geometry along H_4. This is accomplished by determining the Reynolds number at the entrance end of the inside of this drill string section and assuming this Reynolds number approximates the flow conditions throughout the inside this drill string section.

Using Equation 4-11, the approximate specific weight of the gas as it enters this drill string section is determined from P_{i4}. This is

$$g_{i4} \quad \frac{(573,888)\ (1.0)}{(53.36)\ (598.79)}$$

$$g_{i4} \quad 17.96 \ \text{lb/ft}^3$$

Using Equation 1-2, the density of the gas as it enters this drill string section, γ_{gi4}, is

$$\gamma_{gi4} \quad \frac{17.96}{32.2}$$

$$\gamma_{gi4} \quad 0.558 \ \frac{\text{lb} \ \ \text{sec}^2}{\text{ft}^4}$$

From Equation 9-7, the kinematic viscosity of the gas at this location, ν_{gi4}, is

$$\nu_{gi4} \quad \frac{0.000000251}{0.558}$$

$$\nu_{gi4} \quad 0.000000449 \ \frac{\text{ft}^2}{\text{sec}}$$

The average kinematic viscosity of the mixture as it enters this drill string section, ν_{avi4}, is

$$\nu_{avi4} \quad \frac{(1.282) \ (0.000000449) \quad (31.92) \ (0.0002691)}{1.282 \quad 31.92}$$

$$\nu_{avi4} \quad 0.000259 \ \text{ft}^2/\text{sec}$$

Using the inside diameter of the drill pipe tool joints, D_6, the approximate average velocity of the aerated drilling fluid as it enters this drill string section, V_{i4}, is

$$V_{i4} \quad \frac{\dfrac{1,826.6}{573,888} \quad \dfrac{598.79}{519.67} \ (19.47) \quad 0.426}{\dfrac{-}{4} \ 0.292 \ ^2}$$

$$V_{i4} \quad 7.44 \ \text{ft/sec}$$

Using Equation 6-83, the Reynolds number of the aerated drilling fluid as it enters this drill string section, N_{Ri4}, is

$$N_{Ri4} \quad \frac{(7.44) \ (0.292)}{0.000259}$$

$$N_{Ri4} \quad 8,386$$

The Reynolds number calculation above is greater than 4,000. This indicates that the flow condition is turbulent. Therefore, the empirical von Karman equation (i.e., Equation 6-86) is used to determine the approximate Fanning friction factor for the aerated fluid flow inside this drill string section.

The inside surface of the drill pipe tool joints is commercial steel with the surface roughness

$$e_p \quad 0.00015 \ \text{ft}$$

With the above, Equation 6-86 becomes

$$f_{i4} \quad \frac{1}{\left[2 \ \log \left(\dfrac{0.292}{0.00015} \right) \quad 1.14 \right]^2}$$

$$f_{i4} \quad 0.017$$

Equation 6-82 for the fourth increment inside the drill string can be solved for the pressure at the top of the increment, P_{i3}. This involves selecting this lower limit by a trial and error procedure. The magnitude of the lower limit pressure on the left side of the equation is selected to allow the left side integral to equal the right side integral. The integration can be carried out on the computer using one of the commercial analytic software programs. The trial and error magnitude of the lower limit pressure is

$$p_{i3} \quad 3{,}924.7 \ \text{psia}$$

$$P_{i3} \quad p_{i3} \ 144$$

$$P_{i3} \quad 565{,}157 \ \text{lb/ft}^2 \ \text{abs}$$

Substituting the values of $\dot{w}_g$, $\dot{w}_m$, Q_g, Q_m, P_g, P_{i3}, P_{i4}, T_g, T_{av4}, D_6, f_{i4}, and g into the left side of Equation 6-82 gives

$$\int_{565,157}^{573,888} \frac{dP}{\left[\dfrac{33.20}{\dfrac{40,978.5}{P} \ 0.426} \ 1 \right] \left[\dfrac{0.017}{18.80} \ \dfrac{\left(\dfrac{40,978.5}{P} \ 0.426 \right)^2}{\overline{4} \ 0.292 ^2} \right]} \quad 125$$

Substituting the values of H_1, H_2, H_3, and H_4 into the right side of Equation 6-82 gives

$$\frac{6{,}650 \;\; 350 \;\; 2.375 \;\; 125}{6{,}650 \;\; 350 \;\; 2{,}375} \quad 1 \; dh \quad 125$$

As can be seen in the above, the right and left hand sides of Equation 6-82 yield the same answer. This shows that the lower limit pressure is correct.

The third drill string section increment is denoted by the length H_3. The temperature at the bottom of the drill pipe body lumped geometry in the openhole section is

$$T_3 \quad 598.16°\text{R}$$

The average temperature of the drill pipe body lumped geometry along H_3 and, thus, the temperature of the aerated fluid flow inside the this drill string length is

$$T_{av3} \quad 586.29°\text{R}$$

In order to obtain the approximate value of the Fanning friction factor for Equation 6-82, it is necessary to estimate the Reynolds number and, thus, the flow conditions inside the drill pipe body lumped geometry along H_3. This is accomplished by determining the Reynolds number at the entrance end of the inside of this drill string section and assuming this Reynolds number approximates the flow conditions throughout the inside this drill string section.

Using Equation 4-11, the approximate specific weight of the gas as it enters this drill string section is determined from P_{i3}. This is

$$\gamma_{gi3} \quad \frac{(565{,}157) \; (1.0)}{(53.36) \; (586.29)}$$

$$\gamma_{gi3} \quad 18.07 \; \text{lb/ft}^3$$

Using Equation 1-2, the density of the gas as it enters this drill string section, ρ_{gi3}, is

$$\rho_{gi3} \quad \frac{18.07}{32.2}$$

$$\rho_{gi3} \quad 0.561 \; \frac{\text{lb} \;\; \text{sec}^2}{\text{ft}^4}$$

From Equation 9-7, the kinematic viscosity of the gas at this location, ν_{gi3}, is

$$\nu_{gi3} \quad \frac{0.000000251}{0.561}$$

$$\nu_{gi3} \quad 0.000000447 \quad \frac{\text{ft}^2}{\text{sec}}$$

The average kinematic viscosity of the mixture as it enters this drill string section, ν_{avi3}, is

$$\nu_{avi3} \quad \frac{(1.282)\,(0.000000447)}{1.282} \quad \frac{(31.92)\,(0.0002691)}{31.92}$$

$$\nu_{avi3} \quad 0.000259 \ \text{ft}^2/\text{sec}$$

Using the inside diameter of the drill pipe tool body, D_7, the approximate average velocity of the aerated drilling fluid as it enters this drill string section, V_{i3}, is

$$V_{i3} \quad \frac{\dfrac{1{,}826.6}{565{,}157} \quad \dfrac{586.29}{519.67} \quad (19.47) \quad 0.426}{\dfrac{}{4} \quad 0.319^{\ 2}}$$

$$V_{i3} \quad 6.22 \ \text{ft/sec}$$

Using Equation 6-83, the Reynolds number of the aerated drilling fluid as it enters this drill string section, $\mathbf{N_{Ri3}}$, is

$$\mathbf{N_{Ri3}} \quad \frac{(6.22)\,(0.319)}{0.000259}$$

$$\mathbf{N_{Ri3}} \quad 7{,}665$$

The Reynolds number calculation above is greater than 4,000. This indicates that the flow condition is turbulent. Therefore, the empirical von Karman equation (i.e., Equation 6-86) is used to determine the approximate Fanning friction factor for the aerated fluid flow inside this drill string section.

The inside surface of the drill pipe body is commercial steel with the surface roughness

$$e_p \quad 0.00015 \ \text{ft}$$

With the above, Equation 6-86 becomes

$$f_{i3} \qquad \left[\frac{1}{2 \ \log \ \dfrac{0.319}{0.00015} \ \ 1.14} \right]^{2}$$

$$f_{i3} \qquad 0.016$$

Equation 6-82 for the third increment inside the drill string can be solved for the pressure at the top of the increment, P_{i2}. This involves selecting this lower limit by a trial and error procedure. The magnitude of the lower limit pressure on the left side of the equation is selected to allow the left side integral to equal the right side integral. The integration can be carried out on the computer using one of the commercial analytic software programs. The trial and error magnitude of the lower limit pressure is

$$p_{i2} \qquad 2,814.0 \ \text{psia}$$

$$P_{i2} \qquad p_{i2} \ 144$$

$$P_{i2} \qquad 405,216 \ \text{lb/ft}^{2} \ \text{abs}$$

Substituting the values of $\dot{w}_{g}$, $\dot{w}_{m}$, Q_{g}, Q_{m}, P_{g}, P_{i2}, P_{i3}, T_{g}, T_{av3}, D_{7}, f_{i3}, and g into the left side of Equation 6-82 gives

$$\int_{405,216}^{565,157} \frac{dP}{33.20 \ \left[\dfrac{40,123.1}{P} \ 0.426 \right] \ \ 1 \ \dfrac{0.016 \ \left[\dfrac{40,123.1}{P} \ 0.426 \right]^{2}}{20.54 \ \ \dfrac{}{4} \ 0.319^{2}}} \qquad 2,375$$

Substituting the values of H_1, H_2, and H_3 into the right side of Equation 6-82 gives

$$\int_{6,650 \ 350}^{6,650 \ 350 \ 2,375} 1 \ dh \qquad 2,375$$

As can be seen in the above, the right and left hand sides of Equation 6-82 yield the same answer. This shows that the lower limit pressure is correct.

Inside the Drill String (7,000 ft to Surface)
    The second drill string section increment is denoted by the length H_2.   The temperature at the bottom of the drill pipe tool joints lumped geometry in the cased section is

$$T_2 \quad 574.41°R$$

The average temperature of the drill pipe tool joints lumped geometry along H_2 and, thus, the temperature of the aerated fluid flow inside the this drill string length is

$$T_{av2} \quad 572.66°R$$

    In order to obtain the approximate value of the Fanning friction factor for Equation 6-82, it is necessary to estimate the Reynolds number and, thus, the flow conditions inside the drill pipe tool joints lumped geometry along H_2.   This is accomplished by determining the Reynolds number at the entrance end of the inside of this drill string section and assuming this Reynolds number approximates the flow conditions throughout the inside this drill string section.
    Using Equation 4-11, the approximate specific weight of the gas as it enters this drill string section is determined from P_{i1}.   This is

$$\gamma_{gi2} \quad \frac{(405,216)\ (1.0)}{(53.36)\ (572.66)}$$

$$\gamma_{gi2} \quad 13.26\ \text{lb/ft}^3$$

Using Equation 1-2, the density of the gas as it enters this drill string section, γ_{gi2}, is

$$\gamma_{gi2} \quad \frac{13.26}{32.2}$$

$$\gamma_{gi2} \quad 0.412\ \frac{\text{lb}\ \text{sec}^2}{\text{ft}^4}$$

From Equation 9-7, the kinematic viscosity of the gas at this location, γ_{gi2}, is

$$\gamma_{gi2} \quad \frac{0.000000251}{0.412}$$

$$\gamma_{gi2} \quad 0.000000609\ \frac{\text{ft}^2}{\text{sec}}$$

The average kinematic viscosity of the mixture as it enters this drill string section, ν_{avi2}, is

$$\nu_{avi2} \quad \frac{(1.282)\ (0.000000609)}{1.282} \quad \frac{(31.92)\ (0.0002691)}{31.92}$$

$$\nu_{avi2} \quad 0.000259 \ \text{ft}^2/\text{sec}$$

Using the inside diameter of the drill pipe tool joints, D_6, the approximate average velocity of the aerated drilling fluid as it enters this drill string section, V_{i2}, is

$$V_{i2} \quad \frac{\dfrac{1,826.6}{405,216} \quad \dfrac{572.66}{519.67} \quad (19.47) \quad 0.426}{\dfrac{-}{4} \quad 0.292 \ ^2}$$

$$V_{i2} \quad 7.82 \ \text{ft/sec}$$

Using Equation 6-83, the Reynolds number of the aerated drilling fluid as it enters this drill string section, N_{Ri2}, is

$$N_{Ri2} \quad \frac{(7.82)\ (0.292)}{0.000259}$$

$$N_{Ri2} \quad 8,813$$

The Reynolds number calculation above is greater than 4,000. This indicates that the flow condition is turbulent. Therefore, the empirical von Karman equation (i.e., Equation 6-86) is used to determine the approximate Fanning friction factor for the aerated fluid flow inside this drill string section.

The inside surface of the drill pipe tool joints is commercial steel with the surface roughness

$$e_p \quad 0.00015 \ \text{ft}$$

With the above, Equation 6-86 becomes

$$f_{i2} \quad \frac{1}{2 \ \log \dfrac{0.292}{0.00015} \quad 1.14}^{\,2}$$

f_{i2} 0.017

Equation 6-82 for the second increment inside the drill string can be solved for the pressure at the top of the increment, P_{i1}. This involves selecting this lower limit by a trial and error procedure. The magnitude of the lower limit pressure on the left side of the equation is selected to allow the left side integral to equal the right side integral. The integration can be carried out on the computer using one of the commercial analytic software programs. The trial and error magnitude of the lower limit pressure is

p_{i1} 2,651.9 psia

P_{i1} p_{i1} 144

P_{i1} 381,868 lb/ft^2 abs

Substituting the values of $\dot{w}_g$, $\dot{w}_m$, Q_g, Q_m, P_g, P_{i1}, P_{i2}, T_g, T_{av2}, D_6, f_{i2}, and g into the left side of Equation 6-82 gives

$$\left.\int_{381,868}^{405,216} \frac{dP}{\cfrac{33.20}{\cfrac{39,190.3}{P}\,0.426}\left(1 + \cfrac{0.017}{18.80}\cfrac{\left(\cfrac{39,190.3}{P}\,0.426\right)^2}{\cfrac{}{4}\,0.292^2}\right)}\right. = 350$$

Substituting the values of H_1, and H_2 into the right side of Equation 6-82 gives

$$\int_{6,650}^{6,650\ 350} 1\ dh = 350$$

As can be seen in the above, the right and left hand sides of Equation 6-82 yield the same answer. This shows that the lower limit pressure is correct.

The first drill string section increment is denoted by the length H_1. The temperature at the bottom of the drill pipe body lumped geometry in the cased section is

T_1 570.91°R

The average temperature of the drill pipe body lumped geometry along H_1 and, thus, the temperature of the aerated fluid flow inside the this drill string length is

$$T_{av1} \quad 537.66°R$$

In order to obtain the approximate value of the Fanning friction factor for Equation 6-82, it is necessary to estimate the Reynolds number and, thus, the flow conditions inside the drill pipe body lumped geometry along H_1.   This is accomplished by determining the Reynolds number at the entrance end of the inside of this drill string section and assuming this Reynolds number approximates the flow conditions throughout the inside this drill string section.

Using Equation 4-11, the approximate specific weight of the gas as it enters this drill string section is determined from P_{in}.   This is

$$\gamma_{gi1} \quad \frac{(381,868) \ (1.0)}{(53.36) \ (537.66)}$$

$$\gamma_{gi1} \quad 13.31 \ \text{lb/ft}^3$$

Using Equation 1-2, the density of the gas as it enters this drill string section, γ_{gi1}, is

$$\gamma_{gi1} \quad \frac{13.31}{32.2}$$

$$\gamma_{gi1} \quad 0.413 \ \frac{\text{lb} \ \text{sec}^2}{\text{ft}^4}$$

From Equation 9-7, the kinematic viscosity of the gas at this location, γ_{gi1}, is

$$\gamma_{gi1} \quad \frac{0.000000251}{0.413}$$

$$\gamma_{gi1} \quad 0.000000606 \ \frac{\text{ft}^2}{\text{sec}}$$

The average kinematic viscosity of the mixture as it enters this drill string section, γ_{avi1}, is

$$\gamma_{avi1} \quad \frac{(1.282) \ (0.000000606) \quad (31.92) \ (0.0002691)}{1.282 \quad 31.92}$$

$$\gamma_{avi1} \quad 0.000259 \ \text{ft}^2/\text{sec}$$

Using the inside diameter of the drill pipe tool joints, D_7, the approximate average velocity of the aerated drilling fluid as it enters the drill string section, V_{i1}, is

$$V_{i1} \quad \frac{\dfrac{1,826.6}{381,868} \quad \dfrac{537.66}{519.67} \quad (19.47) \quad 0.426}{\dfrac{}{4} \quad 0.319^{\,2}}$$

$$V_{i1} \quad 6.54 \ \text{ft/sec}$$

Using Equation 6-83, the Reynolds number of the aerated drilling fluid as it enters this drill string section, N_{Ri2}, is

$$\mathbf{N_{Ri1}} \quad \frac{(6.54)\ (0.319)}{0.000259}$$

$$\mathbf{N_{Ri1}} \quad 8,056$$

The Reynolds number calculation above is greater than 4,000. This indicates that the flow condition is turbulent. Therefore, the empirical von Karman equation (i.e., Equation 6-86) is used to determine the approximate Fanning friction factor for the aerated fluid flow inside this drill string section.

The inside surface of the drill pipe tool joints is commercial steel with the surface roughness

$$e_p \quad 0.00015 \ \text{ft}$$

With the above, Equation 6-86 becomes

$$f_{i1} \quad \frac{1}{\left(2\ \log \ \dfrac{0.319}{0.00015} \quad 1.14 \right)^{2}}$$

$$f_{i1} \quad 0.016$$

Equation 6-82 for the first increment inside the drill string can be solved for the pressure at the top of the increment, P_{in}. This involves selecting this lower limit by a trial and error procedure. The magnitude of the lower limit pressure on the left side of the equation is selected to allow the left side integral to equal the right side integral. The integration can be carried out on the computer using one of the commercial analytic software programs. The trial and error magnitude of the lower limit pressure is

$$p_{in} \quad 236.6 \ \text{psia}$$

$$P_{in} \quad p_{in} \; 144$$

$$P_{in} \quad 34,070 \; \text{lb/ft}^2 \; \text{abs}$$

Substituting the values of $\dot{w}_g$, $\dot{w}_m$, Q_g, Q_m, P_g, P_{in}, P_{i1}, T_g, T_{av1}, D_7, f_{i1}, and g into the left side of Equation 6-82 gives

$$\int_{34,070}^{381,868} \frac{dP}{\dfrac{33.20}{\dfrac{36,795.1}{P} \; 0.426} \quad 1 \quad \dfrac{0.016}{20.54} \; \dfrac{\left(\dfrac{36,795.1}{P} \; 0.426\right)^2}{- \; 0.319 \;^2}} \quad 6,650$$

Substituting the values of H_1 into the right side of Equation 6-82 gives

$$\int_0^{6,650} 1 \; dh \quad 6,650$$

As can be seen in the above, the right and left hand sides of Equation 6-82 yield the same answer. This shows that the lower limit pressure is correct.

The injection pressure while drilling at 10,000 ft of depth is approximately 237 psia. This is the approximate injection pressure for both the compressed air and the drilling mud as they enter the surface flow lines that lead to the top of the drill string. When drilling at a depth of 10,000 ft, the corresponding injection pressure above is a air volumetric flow rate of 1,168 acfm (with a drilling mud volumetric flow rate of 191 gal/hr). This compressed air injection pressure is the pressure the compressor output must match.

Figure 9-5 shows the aerated drilling fluid (both air and mud) pressures in the annulus and inside the drill string as a function of depth for this illustrative example (while drilling at the depth of 10,000 ft). The figure shows the pressure at the bottom of the annulus is approximately 3,512 psia (p_{a5} above). If a target oil or natural gas rock formation pore pressure at the bottom of the borehole is above this value, the oil or natural gas will flow into the borehole as the drill bit is advanced into the producing rock formation. This would be underbalanced drilling. If the pore pressure is less than this value, rock cuttings from the advance of the drill bit will be forced into the exposed pores around the bottom of the borehole resulting in formation damage.

To drill this borehole with an aerated drilling fluid from 7,000 ft to 10,000 ft and maintain a constant bottomhole pressure in the annulus of 3,500 psig will require that volumetric flow rate of the compressed air be varied as the drilling progresses. Therefore, while drilling at 10,000 ft of depth, the highest air volumetric flow rate will be required. However, this will also require the lowest

injection pressure. And while drilling at 7,000 ft of depth, the lowest air volumetric flow rate and highest injection pressure will be required.

The anticipated drilling rate of penetration is estimated to be 60 ft/hr. The vertical interval section to be drilled is from a depth of 7,000 ft to a depth of 10,000 ft, or a 3,000 ft length of borehole. Therefore, the estimated actual drilling time to drill this interval is approximately 50 hours. Using similar calculations as those given above, the injection pressures as a function of drilling depth and, thus, drilling time can be obtained. Figure 9-6 shows the injection pressure as a function of drilling time for the interval from 7,000 ft to 10,000 ft. Figure 9-7 shows the injection air volumetric flow rate as a function of drilling time for the interval from 7,000 ft to 10,000 ft.
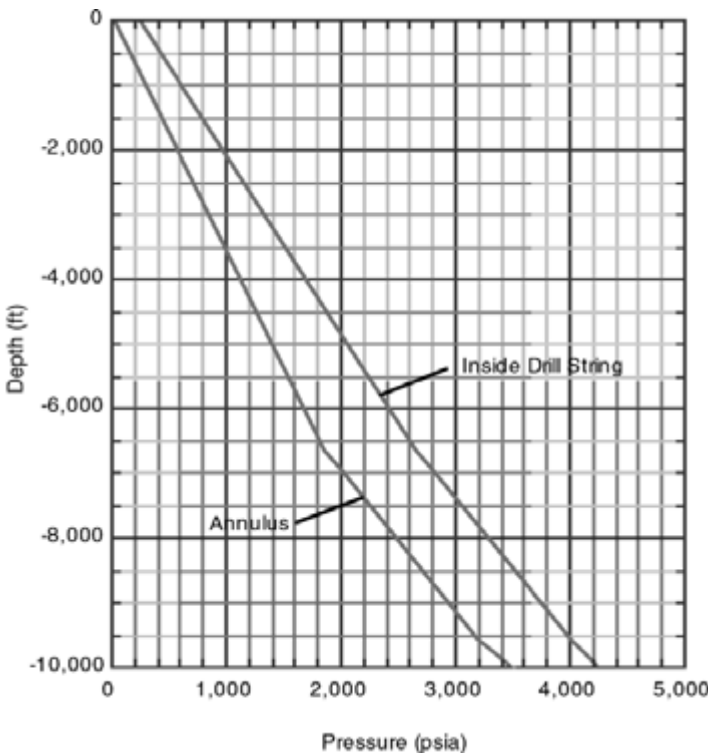
Figure 9-5: Pressure profile in the inside of the drill string and in the annulus for Illustrative Example 9.3 (q_g = 1,168 acfm and a drilling depth of 10,000 ft).

Figure 9-7 shows that the maximum air volumetric flow rate injected into the drill string is 1,168 acfm (at a drilling depth of 10,000 ft) and from Figure 9-6 the maximum air injection pressure into the drill string is 420 psia (at a drilling depth of 7,000 ft). This data allows for the selection of the primary compressor unit to be used in the drilling operation. The primary compressor unit for an aerated drilling operation must be used in a different manner than its use in an air drilling operation. As can be seen in Figures 9-6 and 9-7, the aerated drilling operation requires varying the air volumetric flow rate as the drilling progresses. Since primary compressors output a constant volumetric flow rate, it is necessary to measure with a flow meter the volumetric flow rate flowing to the top of the drill string and vent the remainder of the compressor output to the atmosphere.
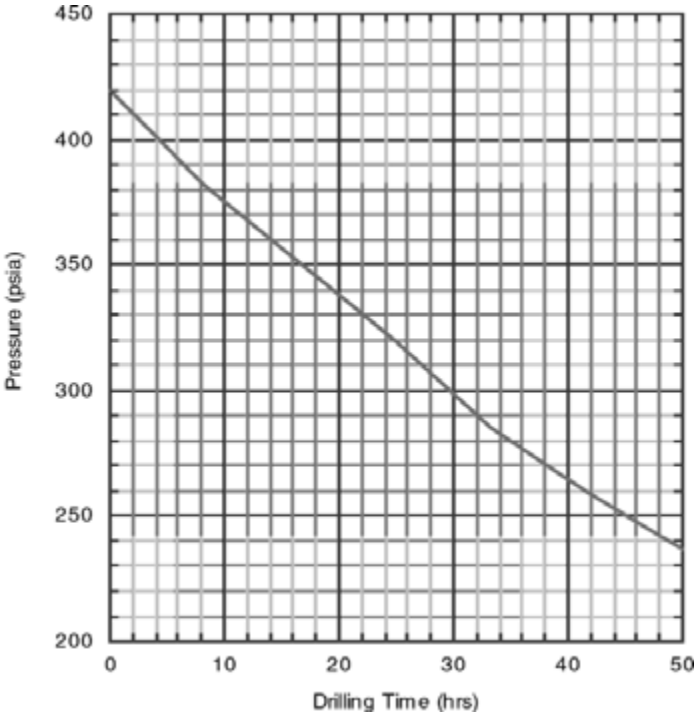
Figure 9-6: Drill string injection pressure as a function of drilling time (drilling depth) for Illustrative Example 9.3.

There are several possible candidate compressor units given in Section 4.7 of Chapter 4 that could be used to provide the compressed air for this example drilling

operation. The most appropriate is the semi-trailer mounted unit with a Dresser Clark Model CFB-4, four stage, reciprocating piston primary compressor with a rated volumetric flow rate of 1,200 scfm (see Figure 4-25).   This four-stage compressor system is operated as a combined primary-booster system with a continuous maximum pressure output of 1,000 psig.   The prime mover for this compressor unit is a diesel fueled, turbocharged, Caterpillar Model D398 with a peak output of 760 horsepower at 900 rpm (at API standard conditions). This compressor system has sufficient air volumetric flow rate to meet the maximum requirement of 1,168 acfm and the maximum injection pressure of 420 psia.

The last criteria is to check whether the prime mover of this primary compressor unit has the power to operate at the 4,000 ft surface elevation. The highest injection pressure occurs while drilling out of the casing shoe at a depth of 7,000 ft. This injection pressure is approximately 420 psia.   Even though the required air volumetric flow rate at this depth is approximately 120 acfm, the compressor must output the full 1,200 acfm (the remainder is vented). The compressor is a four-stage reciprocating piston compressor. Therefore,

$$n_s \quad 4$$

The theoretical shaft horsepower, $\dot{W}_s$, required by the compressors is obtained from Equation 4-35a. Equation 4-35a becomes

$$\dot{W}_s \quad \frac{(4)\ (1.4)}{(0.4)} \quad \frac{(12.685)\ 1{,}200}{229.17} \quad \frac{420.0}{12.685}^{\frac{(0.4)}{(4)(1.4)}} \quad 1$$

$$\dot{W}_s \quad 264.1$$

The mechanical efficiency, $\ni_m$, is

$$\ni_m \quad 0.90$$

The first stage compressor ratio is

$$r_s \quad \frac{420.0}{12.685}^{\frac{1}{4}}$$

$$r_s \quad 2.40$$

The volumetric efficiency (only for the reciprocating piston compressor), $\ni_v$, is determined from Equation 4-37.   The compressor clearance volume ratio, c, is assumed to be 0.06. Equation 4-37 becomes

$$\mathfrak{I}_v \qquad 0.96 \quad 1 \qquad 0.06 \qquad 2.40 \ ^{\frac{1}{1.4}} \qquad 1$$

$$\mathfrak{I}_v \qquad 0.910$$

From Equation 4-38, the actual shaft horsepower, $\dot{W}_{as}$, required by each compressor is

$$\dot{W}_{as} \qquad \frac{264.1}{(0.90) \ (0.910)}$$

$$\dot{W}_{as} \qquad 322.5$$
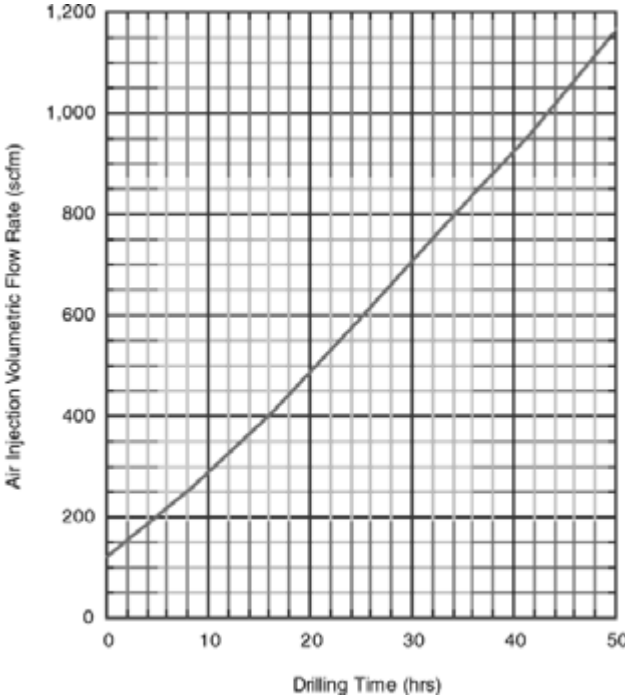
Figure 9-7: Drill string air injection volumetric flow rate as a function of drilling time (drilling depth) for Illustrative Example 9.3.

The above determined 322.5 horsepower is the actual shaft power needed by each of the two compressors to produce the 420 psia pressure output at the surface location elevation of 4,000 ft above sea level (while drilling at a depth of 7,000 ft). At this surface location, the input horsepower available from the Caterpillar Model D398 prime mover is a derated value (derated from the rated 760 horsepower available at 900 rpm). In order for the compressor units to operate at this 4,000 ft surface location elevation, the derated input power available must be greater than the actual shaft power needed. Figure 4-15 shows that for 4,000 ft elevation the input power of a turbocharged prime mover must be derated by approximately 10 percent. The derated input horsepower, $\dot{W}_i$, available from the prime mover is

$$\dot{W}_i \quad 760 \, (1 \quad 0.10)$$

$$\dot{W}_i \quad 684.0$$

For this illustrative example, the prime mover of the compressor unit derated input power is greater than the actual shaft horsepower needed, thus, the selected compressor unit can be operated at this 4,000 ft surface location elevation (while drilling at a depth of 10,000 ft).

The volumetric flow rate of gas to create an aerated drilling fluid is very dependent upon the flow resistance in the circulation system. This resistance is the sum of the major and minor flow friction losses in the flow system. This friction resistance creates choking of the system and, therefore, generally increases the average pressure and in turn increases the average specific weight of the aerated drilling fluid in the annulus and elsewhere in the circulation system. Therefore, if it is required to maintain a constant bottomhole pressure limit, more gas volumetric flow rate will be required to reduce the average pressure and the specific weight in the annulus.

A major contributor to this choking effect is the inside diameter of the surface return flow line (relative to the annulus inside of diameter). In Illustrative Example 9.3 the surface return flow line inside diameter was 5.625 inches. For this example, the required maximum volumetric flow rate when drilling at 10,000 ft was determined to be 1,168 acfm. If the surface return flow line inside diameter is changed to 4.00 inches the required maximum volumetric flow rate becomes 1,575 acfm. This is a 35 percent increase in gas volumetric flow rate required. Thus, the design of the surface return flow line and the drill string to reduce choking can dramatically reduce the gas volumetric flow rate needed to provide the required aerated drilling fluid.

9.5 Prime Mover Fuel Consumption

In this section the fuel consumption of the prime mover for the compressor system will be discussed. Illustrative examples of the fuel consumption were discussed in detail in Chapter 4. In this section the illustrative example in this chapter will be completed with the calculation of the approximate fuel needed on the drilling location for the compressor system.

Illustrative Examples 9.3 describe the implementation of the basic planning step No. 12 given in Section 9.1.

    Illustrative Example 9.4 In Illustrative Example 9.3 the semi-trailer mounted unit with the Dresser Clark CFB-4, four-stage, reciprocating piston compressor system was selected for the drilling operation. In Illustrative Examples 9.3 the compressor unit was utilized to drill the interval from 7,000 ft to 10,000 ft. The compressor unit has a volumetric flow rate of 1,200 acfm. The compressed air flowing to the drilling operation varies over the drilled interval from 120 acfm to 1,168 acfm. But the compressor must output 1,200 acfm. The volumetric flow rate to the borehole must be varied and the excess is vented to the atmosphere. Therefore, to estimate the total diesel fuel needed by the compressor unit it is necessary to estimate the fuel consumption of the compressor units' Caterpillar Model D398, diesel fueled, turbocharged, prime mover. The anticipated drilling rate of penetration is estimated to be 60 ft/hr. The vertical interval section to be drilled is from a depth of 7,000 ft to a depth of 10,000 ft, or a 3,000 ft length of borehole. Therefore, the estimated actual drilling time to drill this interval is approximately 50 hours.

    The reciprocating piston compressor is not a fixed pressure ratio machine like the rotary compressor. As long as there is sufficient power available from the prime mover the reciprocating piston compressor will match the back pressure resistance. Thus, Figure 9-6 shows only one curve indicating the injection pressure is the same as the pressure output of the compressor unit.

    In Illustrative Example 9.3 it was found that the actual shaft horsepower required by the reciprocating piston compressor unit to compress air to 420 psia was approximately 322.1 (at 7,000 ft of depth). Also in Illustrative Example 9.3 the derated horsepower available from the Caterpillar Model D398 prime mover at the surface elevation of 4,000 ft was found to be 684. Drilling at a depth of 7,000 ft, the prime mover power ratio is

$$PR \quad \frac{322.1}{684.0} \ (100) \quad 47.1$$

Entering the abscissa of Figure 4-17 with the power ration percent, the approximate fuel consumption rate can be read on the ordinate using the diesel fuel curve. The approximate fuel consumption rate at this power level is 0.650 lb/hp-hr. The total weight of diesel fuel consumption per hour is

$$\dot{w}_f \quad 0.650 \ (322.1) \quad 209.4 \ \text{lb/hr}$$

The diesel fuel consumption rate (in United States gallons) for the drilling depth of 7,000 ft is

$$q_f \quad \frac{209.4}{(0.8156)(8.33)} \quad 30.8 \ \text{gal/hr}$$

    Using the data in Figure 9-6 and similar calculations as those given above, the diesel fuel consumption rate as a function of drilling time (or drilling depth) can be obtained. Figure 9-8 shows the diesel fuel consumption rate as a function of drilling

time (or drilling depth) for the reciprocating piston compressor unit.   The approximate total diesel fuel needed for the compressor unit is obtained by the integration of the area under the curve in Figure 9-8. This is approximately 1,500 gallons. It is standard practice to assume a 20 percent additional volume of fuel for circulating the well and other compressor operations on the drill rig. Therefore, the approximate diesel fuel needed for the compressor unit is approximately 1,800 gallons.

Illustrative Examples 9-3 and 9-4 demonstrate the calculation procedures (step Nos. 1 to 12 given in Section 9.1) used to plan a typical deep oil or natural gas well drilling operation.
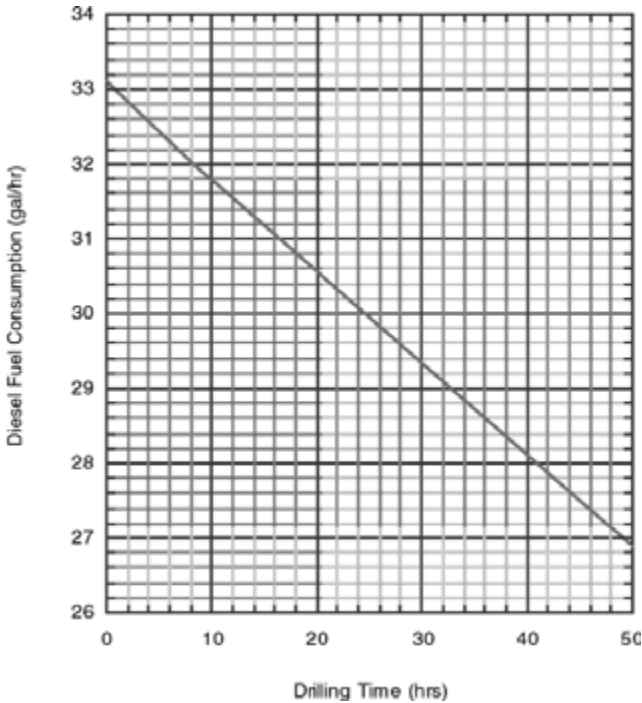
Figure 9-8: Fuel consumption rate as a function of drilling time for compressor used in Illustrative Example 9.3 ($q_g = 1,200$ acfm from the compressor).

9.6 Field Comparison

The following case history of vertical drilling operation demonstrates the accuracy of the planning calculation procedures discussed earlier that utilize complete major and minor friction loss terms.

Case History This was a vertical well drilled to 8,130 ft in the San Juan Basin of New Mexico (Dakota formation target). This was an unusual well in that nearly all of the borehole was openhole drilling. A 9 5/8 inch surface casing was run from surface to 380 ft. The openhole was drilled with aerated drilling fluid over most of the interval from the bottom of the casing to the depth of 8,130 ft. The aerated drilling fluid was used to reduce drilling fluid loss as the borehole advanced. The openhole was drilled with an 8 3/4 inch drill bit to a depth of 3,592 ft. At that depth the drill bit size was changed to a 7 7/8 inch drill bit and drilling continued to the bottom of the well with this drill bit size. Most of the formations that were drilled in this long openhole interval were shale sections. The drill string profile (while drilling at 7,968 ft with the 7 7/8 inch tri-cone roller cutter drill bit) for this well was 4 1/2 inch drill pipe from surface to 7,356 ft and 6 inch drill collars to 7,968 ft. The incompressible drilling fluid (drilling mud) was approximately 9 lb/gal and was injected into the well at a volumetric flow rate of 250 gal/min. The drilling gas was inert atmospheric air (specific gravity of approximately 0.97) with an injection volumetric flow rate to the well of approximately 400 acfm (surface elevation location of approximately 5,700 ft). Using the major and minor fluid flow lose calculations as described in this chapter, the surface injection pressure for the aerated drilling fluid was calculated to be 513 psig. The actual field injection pressure was approximately 650 psig. The predicted bottomhole pressure was 3,421 psig. No field data were recorded for bottomhole pressures. Although the injection pressure correlation between predicted and actual is not extremely accurate, the accuracy is acceptable considering the long openhole section in this well. The longer the openhole section, the more uncertain the diameter and surface roughness.

The above case history clearly demonstrate the accuracy of the aerated drilling calculation process. This comparison calculation was carried out using the same drill pipe body and drill pipe tool joints lumped geometry approximations as those in Illustrative Example 9.3 above. The success of these calculations depends upon the careful inclusion of all major and minor fluid flow friction losses.

9.7 Conclusions

The discussion in this chapter has concentrated on direct circulation operations. It has been tacitly assumed that there are few reverse circulation operations deeper than the 3,000 ft depth criteria set in this book (see Chapter 5). But it should be noted that for those rare drilling situations where reverse circulation is used to drill beyond 3,000 ft, the discussions given above for major and minor fluid flow friction losses are, in general, applicable to reverse circulation operations.

The demonstration calcuations in this chapter have utilized lumped geometry approximations for the drill pipe body and drill pipe tool joints. Such approximations appear to adequately model the overall friction resistance in the circulation system and give accurate results for bottomhole and injection pressures. An improvement to this drill string geometry approximation technique can be made by programming each tool joint indivdually at its proper location in the drill string. This type of program would be best carried out using a higher level computer language such as C++ or FORTRAN. Such a programmed solution would improve the detail pressure versus depth accuracy of the model. However, a comparison of

this type of program gives very little change in bottomhole and injection pressures, and in the required volumetric flow rate of gas.

References

1. Bobo, R. A., and Barrett, H. M., "Aeration of Drilling Fluids," *World Oil*, Vol 145, No. 4, 1953.

2. Graves, S. L., Niederhofer, J. D., and Beavers, W. M., "A Combination Air and Fluid Drilling Technique for Zones of Lost Circulation in the Black Warrior Basin," *SPE Drilling Engineering*, February 1986.

3. Allan, P. D., "Nitrogen Drilling System for Gas Drilling Applications," SPE 28320, Presented at the SPE 69th Annual Technical Conference and Exhibition, New Orleans, Louisiana, September 25-28, 1994.

4. *Underbalanced Drilling Manual*, Gas Research Institute Publication, GRI Reference No. GRI-97/0236, 1997.

5. Hegedorn, A. R., and Brown, K. E., "Experimental Study of Pressure Gradients Occurring During Continuous Two-Phase Flow in Small Diameter Vertical Conduits," *Journal of Petroleum Technology*, April 1965.

6. Langlinais, J. P., Bourgoyne, A. T., and Holden, W. R., "Frictional Pressure Losses for the Flow of Drilling Mud and Mud/Gas Mixtures," SPE 11993, Presented at the 58th Annual Technical Conference and Exhibition, San Francisco, California, October 5-8, 1983.

7. Mitchell, B. J., "Test Data Fill Theory Gap on Using Foam as a Drilling Fluid," *Oil and Gas Journal*, September 1971.

8. Krug, J. A., and Mitchell, B. J., "Charts Help Find Volume, Pressure Needed for Foam Drilling," *Oil and Gas Journal*, February 7, 1972.

9. Blauer, R. E., Mitchell, B. J., and Kohlhaas, C. A., "Determination of Laminar, Turbulent and Transitional Foam Flow Friction Losses in Pipes," SPE 4885, Presented at the 1974 Annual SPE California Regional Meeting, San Francisco, California, November 2-4, 1974.

10. Gatlin, C., *Petroleum Engineering: Drilling and Well Completions*, Prentice-Hall, 1960.

11. Bourgoyne, A. T., Millheim, K. K., Chenevert, M. E., and Young, F. S., *Applied Drilling Engineering*, *SPE*, First Printing, 1986.

12. Moore, P. L., *Drilling Practices Manual*, The Petroleum Publishing Company, 1974.

13. Guo, B., Hareland, G., and Rajtar, J., "Computer Simulation Predicts Unfavorable Mud Rate and Optimum Air Injection Rate for Aerated Mud Drilling," SPE 26892, Presented at the 1993 Eastern Regional Conference and Exhibition held in Pittsburgh, Pennsylvania, Novermber 2-4, 1993.

14. Poettman, F. H., and Carpenter, P. G., *Drilling and Production Practice*, API, 1952.

15. Poettman, F. H., and Bergman, W. E., "Density of Drilling Muds Reduced by Air Injection," *World Oil*, August 1955.

16. Brown, K. E., and Beggs, H. D., *The Technology of Artificial Lift Methods*, Vol. 1, PennWellBooks, 1977.

17. Brown, K. E., et al, *The Technology of Artificial Lift Methods*, Vol. 2a, PennWell Books, 1980.

18. Daugherty R. L., Franzini, J. B., and Finnemore, E. J., *Fluid Mechanics with Engineering Applications*, Eight Edition, McGraw-Hill, 1985.

This page intentionally left blank.

Chapter

Ten

Stable Foam Drilling

The term stable foam describes a special class of aerated drilling fluids. This class of drilling fluid is made up of a special mixture incompressible fluids injected with compressed air or other gases. To create a stable foam drilling fluid, the incompressible component is usually made up of treated fresh water with a surfactant foaming agent. The term stiff foam refers to the use of viscosified water instead of fresh non-viscosified water in the incompressible fluid component (typical viscosity additives are polyanionic cellulose, xanthan gum polymers, and carboxymethyl cellulose). The surfactant foaming agent usually comprises about two to five percent by volume of the treated water being injected (depending on the surfactant product). The mixture of the incompressible fluid (with surfactant) and compressed air (or other gase) flows as an aerated fluid as the mixture flows down the inside of the drill string. Nozzles in the drill bit are required in order to allow the foam to be generated at the bottom of the annulus as the aerated fluid mixture passes through the drill bit. There are some shallow drilling situations where the foam can be preformed at the surface and injected into the inside of the drill string. But in deep drilling operations, it is not possible to maintain the mixture as a foam as it flows inside the drill string. The pressures inside the drill string are too high to allow foam properties to be maintained. Thus, for this discussion of stable foam drilling fluids, it will be assumed that the mixture flows as an aerated drilling fluid down the inside of the drill string, is transformed into a foam as the mixture passes through the drill bit nozzles, and then flows up the annulus as a stable foam.

A new term foam quality, , must be introduced to the discussion so that the physical characteristics and the operational parameters of stable foam drilling

operations can be adequately described and examined.   In Chapter 6 the basic equations have been derived and their auxiliary friction factor, and nozzle flow equations presented. These equations form the foundation for both methodologies as they are discussed in this treatise. Foam quality is given by Equation 6-87. This is

$$\frac{Q_g}{Q_g \quad Q_f}$$

where Q_g is the volumetric flow rate of the compressible gas (ft^3/sec),
  Q_f is the volumetric flow rate of the incompressible fluid (ft^3/sec).
The foam quality value is a function of the pressure in the annulus since the volumetric flow rate of the compressed gas in affected by the pressure magnitude. Laboratory and field experiments have been conducted that show that stable foam will exist within certain limits of the foam quality value. These are approximately the foam qualities of 0.60 and 0.98 [1 to 3]. If the foam quality value falls below approximately 0.60, the foam will separate into its two phases. If the foam quality value is above 0.98, the foam also separates into two phases (and is denoted as a "mist"). For a stable foam drilling operation the lower foam quality value is usually found at the bottom of the annulus and the higher foam quality value at the top of the annulus.

Stable foam drilling fluids are used primarily to counter formation water or loss of circulation problems (above the target depth) in boreholes that have formation damage sensitive production formations.   The effectiveness of this type of drilling fluid in countering these downhole problems resides somewhere between the effectiveness of air drilling and traditional aerated drilling. The actual selection of stable foam drilling fluids over either air drilling or aerated drilling fluids is not a distinct analytic process. Such a selection is usually made after investigating the drilling problem experiences in number of offset wells in a given drilling province. Further, stable foam drilling fluids can be preferable to other low bottomhole pressure producing circulation systems in areas where surface water is difficult to acquire. Stable foam circulation systems were first used in production workover operations [1 to 3].   The first engineering discussion of stable foam drilling operations for oil and gas recovery applications was given in 1971 [4].

Although stable foam drilling fluids are a special class of aerated drilling fluid, the physical properties of drilling foam is unlike nearly all other drilling fluid classes. The actual injection weight rates of flow of both the incompressible fluids and compressible gases are low relative to flow rates in air and gas drilling and aerated drilling operations. The stable foam is generated as the mixture flows through drill bit nozzles to the annulus. The stable foam creates an intricate bubble structure that flows through the annulus space some what like saving foam from a can. Although the bubble structure has a low specific weight, the structure has been found to have plastic viscosities and a yield point similar to the plastic property of drilling muds [4, 5].

Stable foam drilling fluids were initially used to drill through rock formations that had fracture and/or pore systems that would drain traditional incompressible drilling fluids (e.g., fresh water, water and oil based drilling muds, formation water,

and formation crude oil) from the annulus. These borehole drilling fluid theft rock formations are called lost circulation sections. The use of foam creating mixtures has been considered an important technological tool in countering the detrimental effects of lost circulation sections.   The stable foam creates bubbles with surface tension properties that tend to fill in the fracture or pore openings in the borehole wall as the foam attempts to flow to the thief fractures and pores. Foam bubble blockage restricts or stops the flow of foam into these lost circulation sections and thereby allows the drilling operations to safely progress. Stable foam drilling fluids can also be effective in countering the flow of formation water into the annulus. Sufficient surfactant can be added to the injected fluid stream at the top of the drill string that will allow the formation water to be foamed as the water enters the annulus.   Stable foams have been used to avoid lost circulation in shallow water well drilling, geotechnical drilling, mining drilling, and in deep oil and natural gas recovery drilling operations. Stable foam drilling operations are nearly always direct circulation operations.

Since the late 1980s another important application for stable foam drilling operations has emerged. This is underbalanced drilling applied to oil and natural gas recovery operations.   Over the past two decades practical field research has demonstrated that most oil and natural gas bearing rock formations can be more efficiently produced if they are drilled with drilling fluids that have hydrostatic flowing bottomhole pressures that are slightly less than the pore pressures of the potential producing rock formations being drilled. Underbalanced drilling operations allow the oil or natural gas to be produced into the annulus as the drilling operation progresses. The underbalanced drilling operation allows the natural fracture and pore systems to be kept clear of rock cutting fines and drilling mud filter cake, thereby, avoiding formation damage. Formation damage has been a problem in oil and natural gas recovery operations nearly since the discovery of oil and natural gas mineral deposits. Underbalanced drilling operations are often carried out using a variety of incompressible fluids (e.g., crude oil, formation water, or clear water) and a variety compressible gases (e.g., air, inert atmosphere, or natural gas).   Inert atmosphere is created by a filter system (placed downstream of the primary compressor) that strips most of the oxygen from the intake air [6].   This filter process results in a nearly inert atmospheric gas. The filter process can be designed to yield an atmospheric gas with an oxygen content that will not support combustion. Field units typically produce and inert atmospheric gas with about 5 percent oxygen content.   The success of stable foam drilling fluid based underbalanced drilling operations in the oil and natural gas recovery industry have prompted other industrial uses of this technology.   In particular, stable foam underbalanced drilling technology is being experimented with in deep water well and environmental monitoring well drilling operations.

This chapter outlines the steps and methods used to plan a successful stable foam drilling operation. This chapter also illustrates the application of these steps and methods to typical deep drilling operations. The objective of these steps and methods is to allow engineers and scientists to cost effectively plan their drilling operations and ultimately select their drilling rig, compressor, and other auxiliary air and gas equipment. The additional benefit of this planning process, is that the data

created by the process can be later used to control the drilling operations as the actual operations progress.

10.1 Deep Well Drilling Planning

Stable foam drilling operations can use a variety of incompressible fluids and compressed gases to develop a stable foam. The majority of the operations use fresh water and a commercial surfactant with injected compressed air.   Commercial surfactants for drilling operations can be obtained for drilling service companies [7]. Recently developed inert atmosphere filter machines have been used to generate injected gas to reduce the corrosion of the drill string and the borehole casing.   In this chapter fresh water, surfactant and atmospheric air will be used as the example of a stable foam drilling fluid.

The basic planning steps for a deep well are as follows:

1. Determine the geometry of the borehole section or sections to be drilled with the stable foam drilling fluids (i.e., openhole diameters, the casing inside diameters, and maximum depths).
2. Determine the geometry of the associated drill string for the sections to be drilled with stable foam drilling fluids (i.e., drill bit size and type, the drill collar size, drill pipe size and description, and maximum depth).
3. Determine the type of rock formations to be drilled in each section and estimate the anticipated drilling rate of penetration.
4. Determine the elevation of the drilling site above sea level, the temperature of the air during the drilling operation, and the approximate geothermal temperature gradient.
5. Establish the objective of the stable foam drilling fluids operation:
    • To drill through loss of circulation formations,
    • To counter formation water entering the annulus (by injecting additional surfactant to foam the formation water in the annulus),
    • To maintain low bottom hole pressures to either preclude fracturing of the rock formations, or to allow underbalanced drilling operations.
6. If underbalanced drilling is the objective, it should be understood that stable foam drilling operations cannot maintain near constant bottomhole annulus pressures.
7. For either of the above objectives, determine the required approximate volumetric flow rate of the mixture of incompressible fluid (with surfactant) and the compressed air (or other gas) to be used to create the stable foam drilling fluid. This required mixture volumetric flow rate is governed by, a) the foam quality at the top of annulus (i.e., return flow line back pressure) and, b) the rock cuttings carrying capacity of the flowing mixture in the critical annulus cross-sectional area (usually the largest cross-sectional area of the annulus). The rock cuttings carrying capability of the stable foam can be estimated using a minimum kinetic energy per unit volume value in the critical annulus cross-sectional.
8. Using the incompressible fluid and air volumetric flow rates to be injected into the well, determine the bottomhole pressure and the surface injection pressure as a function of drilling depth (over the openhole interval to be drilled).

9. Select the contractor compressor(s) that will provide the drilling operation with the appropriate air or gas volumetric flow rate needed to create the stable foam drilling fluid. Also, determine the maximum power required by the compressor(s) and the available maximum derated power from the prime mover(s).

10. Determine the approximate volume of fuel required by the compressor(s) to drill the well.

In Chapter 6 the basic direct circulation drilling planning governing equations have been derived and summarized. The equations in this chapter will be utilized in the discussions and illustrative examples that follow.

10.2 Stable Foam Drilling Operations

Stable foam drilling operations are carried out using only drill string injection configurations. Figure 10-1 shows a schematic of the drill pipe injection stable foam drilling configuration.   Both incompressible fluid (with surfactant) and compressible air (or other gas) are injected together into the top of the drill string (at P_{in}). These fluid streams mix as they go down the inside of the drill string and pass through the drill bit nozzles. The stable foam is created when the fluids pass through the drill bit nozzles. As the stable foam is generated in the bottom of the annulus, the rock cuttings (from the advance of the drill bit) are entrained in the foam and the resultingmixtureflows to the surface in the annulus. The mixture exits the annulus (at P_e) into a surface horizontal flow line.   This horizontal flow line flows to either, a burn pit, or to sealed returns tanks. The burn pit is used when the returning air is mixed with hydrocarbons that can be burned off as they enter the pit. Sealed returns tanksareused to contain contaminated fluids and gases, or hydrocarbons. Sealed returns tanks are particularly useful in underbalanced drillingoperations.

Given below are the advantages and disadvantages of the stable foam drill pipe injection technique.

The advantages are as follows:
- The technique does not require any additional downhole equipment.
- Nearly the entire annulus is filled with the stable foam drilling fluid, thus, low bottomhole pressures can be achieved.
- Since the bubble structures of stable foam drilling fluids have a high fluid yield point, these structures can support rock cuttings in suspension when drilling operations are discontinued to make connections. Stable foams have seven to eight times the rock cutting carrying capacity of water.
- Rock cuttings retrieved from the foam at the surface are easy to analyze for rock properties information.

The disadvantages are as follows:
- Stable foam fluids injection cannot be continued when circulation is discontinued during connections and tripping. Therefore, it can be difficult to maintain underbalanced conditions during connections and trips.
- Since the injected gas is trapped under pressure inside the drill string by the various string floats, time must be allowed for the pressure bleed-down when making connections and trips. Here again the bleed-down

makes it difficult to maintain a underbalanced condtions.
- The flow down the inside of the drill string is two phase flow and, therefore, high pipe friction losses are present. The high friction losses result in high pump and compressor pressures during injection.
- The gas phase in the stable foam attenuates the pulses of conventional (measure-while-drilling) MWD systems. Therefore, conventional mud pulse telemetry MWD cannot be used.
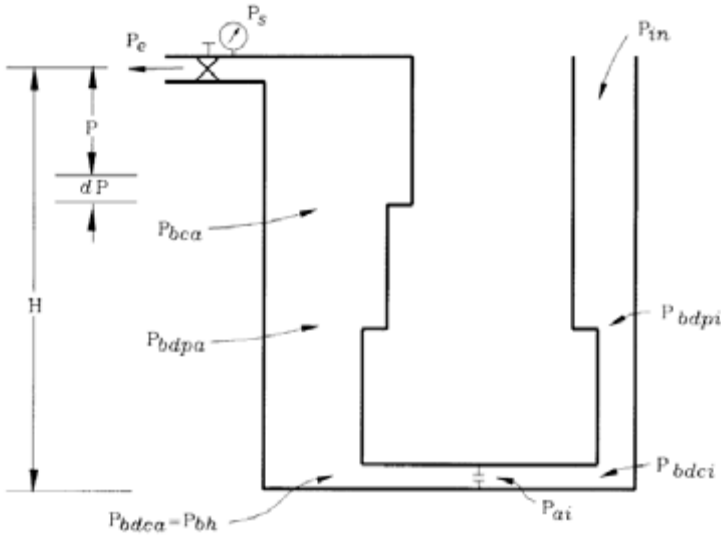
Figure 10-1: Schematic of direct circulation. P_{in} is the injection pressure into the top of the drill string. P_{bdpi} is the pressure at the bottom of the drill pipe inside the drill string. P_{bdci} is pressure at bottom of drill collars inside the drill string, P_{ai} is pressure above drill bit inside the drill string, P_{bdca} is pressure at bottom of drill collars in the annulus, P_{bh} is bottomhole pressure in annulus, P_{bdpa} is pressure at bottom of drill pipe in the annulus, P_{bca} is pressure at bottom of casing in the annulus, P_s is surface pressure at the top of the annulus (usually back pressure created by an adjustable valve), P_e is the exit pressure at the end of the surface return flow line.

10.3 Minimum Volumetric Flow Rates

Most stable foam vertical drilling operations are drilled over a depth interval with variable incompressible fluid volumetric flow rates and variable compressible gas volumetric flow rates. These variable volumetric flow rates are necessary in order to keep the annulus surface exit foam quality and the annulus bottomhole quality at predetermined values. The requirement of varible volumetric flow rates versus depth make the control of stable foam drilling operations complicated. In addition of keeping the foam qualities at the top and bottom of the annulus at predetermined values, the control of the flow rates must also assure that the foam

flow in the annulus has sufficient rock cuttings carrying capacity to clean borehole as the drill bit is advanced.

10.3.1 *Discussion of Theories*

There are few minimum volumetric flow rate theories available for planning stable foam drilling operations. Stable foam drilling fluids have high effective viscosities and yield points. Experiments at Colorado School of Mines have found that spherical rock particles will fall at terminal velocities of the order of 10 to 20 ft/min [8]. These terminal velocities are quite low when compared to terminal velocities in water. These experiments also showed that terminal velocities tend to increase with increasing foam quality.

Based on the above experiments, basic graphs were developed to be used to obtain approximate volumetric flow rates of incompressible fluids (and surfactants) and compressible gases that would provide sufficient bottomhole cleaning [9]. These graphs were developed assuming a uniform well geometry (no changes in annulus cross-sectional area) and a minimum bottomhole stable foam velocity of about 90 ft/min. These graphs were an attempt to provide drilling operations planners with a method to determine injection flow rates for foam drilling operations (similar to those used in Chapter 8 from Appendix E for air and gas drilling). However, from what has been found from comparing analyzes and field experiments for aerated drilling operations, the details of the major and minor friction flow losses in the circulation system have significant influence on the volumetric flow rate magnitudes of incompressible fluid and compressible gases required for a well geometry. What the above experimental and theoretical work contributed was the realization that stable foam drilling minimum volumetric flow rates (of incompressible fluid and compressible gases) can be determined in much the same way as the air and gas drilling minimum volumetric flow rates (i.e., making use of the kinetic energy per unit volume expression Equation 1-1).

10.3.2 *Engineering Practice*

It is clear from the stable foam terminal velocity experiments and stable foam properties experiments at Colorado School of Mines that the rock cuttings particles can be assumed to move at approximately the same velocity of the foam fluid. Assuming that the bottomhole foam quality cannot be less than approximately 0.60 (to prevent foam collapse), it can be determined that for most deep boreholes a bottomhole foam velocity of approximately 90 ft/min will be equivalent to a bottomhole kinetic energy per unit volume of the order 2.0 to 3.0 ft-lb/ft^3. Thus, for stable foam drilling calculations, a similar bottomhole cleaning kinetic energy per unit volume value (or criteria) may be used to determine the minimum volumetric flow rates for stable foam (i.e., incompressible fluid and compressible gas). This kinetic energy per unit volume value was also found in Chapter 1 to be relevent to bottomhole cleaning in conventional mud drilling operations. Therefore, similar to the calculations for air and gas drilling analyzes, a kinetic energy per unit volume criteria of approximately 2.0 to 3.0 ft-lb/ft^3 will be used to determine the minimum volumetric flow rates of incompressible fluid and compressible gas to be injected into the top of the drill string for stable foam drilling operations.

10.4 Injection Pressure and Selection of Compressor Equipment

Over the past two decades, the analyses of stable foam fluid vertical drilling problems have been carried out by two distinct analytic methodologies.

The first methodology ignores the major and minor friction losses due to fluid flow inside the drill string and in the annulus. This methodology includes only the fluid column weight [10, 11].

The second methodology can include all the complexity of the fluid flow friction losses [11]. The initial application of this methodology came from adapting multi-phase oil and gas flow tubing production theory to stable foam drilling annulus problems. This production theory application includes only major friction losses and was not applicable to complicated borehole geometry. New additions to this methodology, which do not come from production literature, have included major and minor losses and can be applied to complicated borehole geometry.

10.4.1 *Non-Friction Approximation*

The simple non-friction methodology allows straight forward deterministic approximate solutions of stable foam drilling problems. However, the practical applicability of these non-friction solutions is limited to shallow (generally less than 3,000 ft of depth) wells with simple geometric profiles.

In what follows, the basic equations in Chapter 6 for stable foam drilling are used to derive the non-friction governing equation. Letting f　0 in Equation 6-88 yields

$$\int_{P_s}^{P_{bh}} \frac{dP}{\dfrac{\dot{w}_t}{\dfrac{P_g}{P}\dfrac{T_{av}}{T_g}Q_g \quad Q_f}} \quad \int_0^H dh$$

where P_s is the surface pressure at the top of the annulus (lb/ft^2, abs). This surface pressure is usually a back pressure at the top of the annulus created by an adjustable valvue. The above equation can be rearranged and integrated to yield

$$\left| P_g \frac{T_{av}}{T_g} \quad \frac{Q_g}{\dot{w}_t} \quad \ln P \quad \frac{Q_f}{\dot{w}_t} \quad P \right|_{P_s}^{P_{bh}} \quad \left| h \right|_0^H$$

Evaluating above equation at the limits, rearranging the result and solving for gas volumetric flow rate, Q_g, yields

$$Q_g = \frac{\dot{w}_f + \dot{w}_s + H + P_{bh} + P_s + Q_f}{P_g \dfrac{T_{av}}{T_g} \ln \dfrac{P_{bh}}{P_s} + \gamma_g H} \tag{10-1}$$

Illustrative Example 10.1 below describes the implementation of the basic planning steps Nos. 1 through 7 in Section 10.1. The non-friction solution is applied to a deep well example. This is only done as a demonstration. It is instructive to compare the non-friction solution results to the full friction solution results that will be obtained later in this chapter. The approximate values for the volumetric flow rates of the incompressible fluid (water and surfactant) and the compressible gas (air) can be used as initial values for the complicated trial and error solution required for the full friction solution.

Illustrative Example 10.1   The borehole to be used in this illustrative example is the basic example used in Chapters 8 and 9. The 7 7/8 inch diameter borehole is to be drilled out of the bottom of API 8 5/8 inch diameter, 28.00 lb/ft nominal, Grade H-40, casing set to 7,000 ft (see Figure 10-2 for well casing and openhole geometric configuration). The drill bit to be used to drill the interval is a 7 7/8 inch diameter tri-cone roller cutter insert type (nozzles 9/32 inches). The anticipated drilling rate in a sandstone and limestone sequence (sedimentary rock) is approximate 60 ft/hr. The openhole interval below the casing shoe is to be drilled from 7,000 ft to 10,000 ft.

The drill string for this illustrative example is made up of 500 ft of 6 3/4 inch by 2 13/16 inch drill collars above the drill bit and API 4 1/2 inch, 16.60 lb/ft nominal, EU-S135, NC50 (IF) to the surface. The drilling is to be carried out at a surface location of 4,000 ft above sea level where the actual atmospheric temperature is 60°F. The regional geothermal gradient is approximately 0.01°F/ft. The borehole is to be drilled with a stable foam drilling fluid composed of fresh water (with a surfactant) and compressed air.

A horizontal section of API line pipe that runs 100 ft from just above the BOP stack to the burn pit is to be used as the return flow line. The surface return flow line is API 6 5/8 inch line pipe, 32.71 lb/ft nominal, Grade B. The inside diameter of this line pipe is 5.625 inches. Two gate valves are installed in the return flow line at the end of the line that is attached to the BOP stack. These valves have an inside diameter of 5 9/16 inch. Just downstream of the two gate valves is an adjustable ball valve that can be used to place a back pressure on the flow of stable foam from the annulus. The back pressure is assumed to be 17.0 psig.

The stable foam is to be composed of treated fresh water (with a commercial surfactant) and compressed air. The foam quality at the top of the annulus is to be maintained at 0.98 and the foam quality at the bottom of the annulus is to be 0.60 or greater.

Using the non-friction method, determine the approximate volumetric flow rates of incompressible fluid (fresh water and surfactant) and of compressible gas (air) required to give adequate bottomhole cleaning while drilling at 10,000 ft (i.e., an annulus minimum kinetic energy per unit volume of approximately 3.0 ft-lb/ft^3).

Also, determine the bottomhole annulus pressure and annulus foam quality while drilling at 10,000 ft (i.e., an annulus minimum foam quality of approximately 0.60).
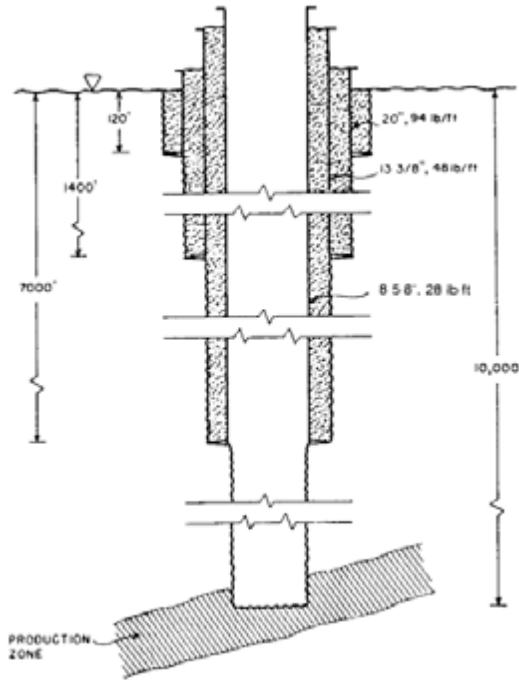
Figure 10-2: Illustrative Example 10.1 casing and openhole well geometric configuration.

Table 4-1 gives an average atmospheric pressure of 12.685 psia for a surface location of 4,000 ft above sea level (mid latitudes North America) (also see Appendix D). The actual atmospheric pressure for the air at the drilling location (that will be used by the compressor), P_{at}, is

$$p_{at} \quad 12.685 \text{ psia}$$

$$P_{at} \quad p_{at} \ 144$$

$$P_{at} \quad 1,826.6 \text{ lb/ft}^2 \text{ abs}$$

The actual atmospheric temperature of the air at the drilling location (that will be used by the compressor), T_{at}, is

$$t_{at} \quad 60°F$$

$$T_{at} \quad t_{at} \quad 459.67$$

$$T_{at} \quad 519.67°R$$

Thus, P_g and T_g become

$$P_g \quad P_{at} \quad 1{,}826.6 \text{ lb/ft}^2 \text{ abs}$$

$$T_g \quad T_{at} \quad 519.67°R$$

Using Equation 4-11, the specific weight of the gas entering the compressor is

$$g \quad \frac{(1{,}827)\ (1.0)}{(53.36)\ (519.67)}$$

$$g \quad 0.0659 \text{ lb/ft}^3$$

Note the above specific weight value can also be obtained from Figure D-4 in Appendix D.

The back pressure at the top of the annulus is 17 psig. The back pressure, P_{bp}, in absolute pressure is

$$p_{bp} \quad 17.0 \quad 12.685$$

$$p_{bp} \quad 29.685 \text{ psia}$$

$$P_{bp} \quad p_{bp}\ 144$$

$$P_{bp} \quad 4{,}275 \text{ lb/ft}^2 \text{ abs}$$

Note that the back pressure can be adjusted to improve annulus bottomhole foam quality and kinetic energy per unit volume values.

The temperature of the rock formations near the surface (geothermal surface temperature) is estimated to be the approximate average year round temperature at that location on the earth's surface. Table 4-1 gives 44.74°F for average year round temperature for a surface elevation location of 4,000 ft above sea level (for mid latitudes of North America, or see Appendix D). Therefore, the absolute temperature of the rock formations at the surface, T_r, is

$$t_r \quad 44.74°F$$

$$T_r \quad t_r \quad 459.67$$

$$T_r \quad 504.41°R$$

The depth of the well, H, is

$$H \quad 10,000 \text{ ft}$$

The bottomhole temperature, T_{bh}, is

$$T_{bh} \quad T_r \quad 0.01 \ H$$

$$T_{bh} \quad 604.41°R$$

The borehole average temperature, T_{av}, is

$$T_{av} \quad \frac{T_{sr} \quad T_{bh}}{2}$$

$$T_{av} \quad \frac{504.41 \quad 604.41}{2}$$

$$T_{av} \quad 554.41°R$$

A simplified borehole geometry is assumed for the non-friction solution. The borehole is assumed to be a uniform diameter represented by the openhole diameter (the drill bit diameter). The openhole diameter, D_h, is

$$d_h \quad 7.875 \text{ inches}$$

$$D_h \quad \frac{d_h}{12}$$

$$D_h \quad 0.656 \text{ ft}$$

The drill string outside diameter is assumed to be a uniform diameter represented by the outside diameter of the drill pipe. The drill pipe outside diameter, D_p, is

$$d_p \quad 4.50 \text{ inches}$$

$$D_p \quad \frac{d_p}{12}$$

D_p 0.375 ft

The estimated drilling rate of penetration is 60 ft/hr. The weight rate of flow of solids, $\dot{w}_s$, from the advance of the drill bit is

$$\dot{w}_s \quad \frac{}{4} \ D_h^2 \ 62.4 \ S_s \ \overline{(60)\ (60)} \qquad\qquad (10\text{-}2)$$

$$\dot{w}_s \quad \frac{}{4} \ 0.656^{\,2} \ 62.4 \ 2.7 \ \frac{60}{60 \quad 60}$$

$$\dot{w}_s \quad 0.949 \ \text{lb/sec}$$

Although the non-friction solution is less complex than the friction solution, it is still necessary to use trial and error to obtain the value of the incompressible fluid (in this example fresh water with surfactant) volumetric flow rate required to yield an annulus bottomhole kinetic energy per unit volume of approximately 3.0 ft-lb/ft^3. Also, the bottomhole foam quality must be greater than 0.60. Note that since the surface foam quality is defined as 0.98, the volumetic fow rate of the compressible gas (air) is defined when the incompressible fluid is defined.

It is assumed that the volumetric flow rate of water (with surfactant), q_w, into the top of the inside of the drill string is

$$q_w \quad 84.0 \ \text{gal/min}$$

The volumetric flow rate of water, Q_w, in consistent units is

$$Q_w \quad \frac{84.0 \quad 231}{12^{\,3} \quad 60}$$

$$Q_w \quad 0.187 \ \text{ft}^3/\text{sec}$$

The specific weight of the incompressible fluid is

$$_w \quad 62.4 \ \text{lb/ft}^3$$

The weight rate of flow of the incompressible fluid is

$$\dot{w}_w \qquad _w \ Q_w$$

$$\dot{w}_w \quad (62.4)\ (0.187)$$

$$\dot{w}_w \quad 11.68 \text{ lb/sec}$$

The definition of foam quality given by Equation 6-87, can be evaluated at the top of the annulus upstream from the back pressure valve. Equation 6-87 defined at the top of the annulus (upstream from the back pressure valve) is

$$bp \quad \frac{Q_{gbp}}{Q_{gbp} \quad Q_w} \tag{10-3}$$

Solving Equation 10-3 for Q_{gbp} gives

$$Q_{gbp} \quad Q_w \quad \frac{bp}{1 \quad bp}$$

Substituting the values for bp and Q_w gives

$$Q_{gbp} \quad (0.187) \quad \frac{0.98}{1 \quad 0.98}$$

$$Q_{gbp} \quad 9.17 \text{ ft}^3/\text{sec}$$

Using Equation 4-11 the specific weight of the gas (air) upstream of the back pressure valve can be obtained. This is

$$bp \quad \frac{(4,275)\,(1.0)}{(53.36)\,(504.41)}$$

$$bp \quad 0.159 \text{ lb/ft}^3$$

The weight rate of flow of gas, $\dot{w}_g$, is

$$\dot{w}_g \quad bp \; Q_{gbp}$$

$$\dot{w}_g \quad (0.159)\,(9.17)$$

$$\dot{w}_g \quad 1.456 \text{ lb/sec}$$

The volumetric flow rate of the gas at the surface location atmospheric conditions is

$$Q_g = \frac{\dot{w}_g}{g}$$

$$Q_g = \frac{1.456}{0.0659}$$

$$Q_g = 22.11 \ \text{ft}^3/\text{sec}$$

$$q_g = Q_g \times 60$$

$$q_g = 1,327 \ \text{acfm}$$

With the above values, Equation 10-1 can be used to obtain by trial and error the bottomhole pressure. Equation 10-1 is rearranged in the form

$$Q_g \, P_g \, \frac{T_{av}}{T_g} \ \ln \frac{P_{bh}}{P_{bp}} = g \, H = \dot{w}_w = \dot{w}_s \, H = P_{bh} = P_{bp} \, Q_w$$

In the above, P_s has been replaced by P_{bp}, $\dot{w}_f$ replaced by $\dot{w}_w$, and Q_f replaced by Q_w.

All values in the above equation are known except for bottomhole pressure P_{bh}. The value of P_{bh} must be obtained by a trial and error process. The bottomhole pressure is assumed to be

$$p_{bh} = 547 \ psig$$

or

$$p_{bh} = 547 + 12.685$$

$$p_{bh} = 559.685 \ psia$$

$$P_{bh} = p_{bh} \times 144$$

$$P_{bh} = (559.685) \, 144$$

$$P_{bh} = 80,595 \ \text{lb/ft}^2 \ \text{abs}$$

Substituting the values of H, $\dot{w}_w$, $\dot{w}_s$, g, Q_g, Q_w, P_g, P_{bp}, P_{bh}, T_g, and T_{av} into the above equation yields

$$(22.11) \quad (1,827) \quad \frac{554.41}{519.67} \quad \ln \quad \frac{80,595}{4,275} \quad (0.0659) \ (10,000)$$

$$11.68 \quad 0.949 \ (10,000) \quad 80,595 \quad 4,275 \ (0.187)$$

The left and right sides of the above give, respectively,

$$1.12 \qquad 1.12$$

Using Equation 4-11, the specific weight of the gas at bottomhole pressure and temperature conditions is

$$_{bh} \quad \frac{(80,595) \ (1.0)}{(53.36) \ (604.41)}$$

$$_{bh} \quad 2.50 \ \text{lb/ft}^3$$

The volumetric flow rate of the gas at bottomhole pressure and temperature conditions, Q_{gbh}, is

$$Q_{gbh} \quad \frac{\dot{w}_g}{_{bh}}$$

$$Q_{gbh} \quad \frac{1.456}{2.50}$$

$$Q_{gbh} \quad 0.583 \ \text{ft}^3/\text{sec}$$

The foam quality at the bottom of the annulus is

$$_{bh} \quad \frac{Q_{gbh}}{Q_{gbh} \quad Q_w}$$

$$_{bh} \quad \frac{0.583}{0.583 \quad 0.187}$$

$$_{bh} \quad 0.76$$

The above foam quality value is greater than 0.60.   Therefore, the mixture of water, surfactant, and gas (air) is a stable foam.

The specific weight of the stable foam (mixture of water, surfactant, and air), γ_{mibhx}, at the bottomhole pressure and temperature conditions is

$$\gamma_{mixbh} = \frac{\dot{w}_g}{Q_{gbh}} + \frac{\dot{w}_w}{Q_w}$$

$$\gamma_{mixbh} = \frac{1.456}{0.583} + \frac{11.68}{0.187}$$

$$\gamma_{mixbh} = 17.06 \ \text{lb/ft}^3$$

The density of the stable foam, ρ_{mixbh}, at the bottomhole pressure and temperature is

$$\rho_{mixbh} = \frac{\gamma_{mixbh}}{g}$$

$$\rho_{mixbh} = \frac{17.06}{32.2}$$

$$\rho_{mixbh} = 0.530 \ \frac{\text{lb} \ \text{sec}^2}{\text{ft}^4}$$

where g is the acceleration of gravity (32.2 ft/sec^2).
The velocity of the foam in the annulus at bottomhole pressure and temperature conditions, V_{bh}, is

$$V_{bh} = \frac{Q_{gbh} + Q_w}{\frac{\pi}{4}\left(D_h^2 - D_p^2\right)}$$

$$V_{bh} = \frac{0.583 + 0.187}{\frac{\pi}{4}\left(0.656^2 - 0.375^2\right)}$$

$$V_{bh} = 3.38 \ \text{ft/sec}$$

Using Equation 1-1, the kinetic energy per unit volume at bottomhole pressure and temperature conditions, KE_{bh}, is

$$KE_{bh} \quad \frac{1}{2} \quad _{mixbh} \; V_{bh}^2$$

$$KE_{bh} \quad \frac{1}{2} \quad 0.530 \quad 3.38^{\,2}$$

$$KE_{bh} \quad 3.03 \; \frac{ft \quad lb}{ft^3}$$

The volumetric flow rates of incompressible fluid (water and surfactant) and compressible gas (air) were determined by trial and error to give a bottomhole kinetic energy per unit volume of approximately 3.0 ft-lb/ft³. These volumetic flow rates have been determined with the non-friction method. Although this method is invalid for deep boreholes with complicated geometric profiles, the solution does give a lower bound value for the full friction solution. The full friction solution will be demonstrated in the next section.

10.4.2 *Major and Minor Losses and Injection Pressure*
The governing equations for the second methodology, presented in Chapter 6, requires trial and error solutions and can be applicable to deep wells with complicated borehole geometry. As major and minor friction losses are added to allow the analytic solutions to simulate more closely the actual drilling situation, the volumetric flow rates of incompressible fluid and compressed gas must be increased to compensate for the added friction in the system.

Illustrative Examples 10.2 describes the full implementation of the basic planning steps Nos. 1 to 8 in Section 10.1.

Illustrative Example 10.2   In this illustrative example the given data in Illustrative Example 10.1 is used for a solution using the friction solution method given in Chapter 6 (Equations 6-87 to 6-106). Using the general data and results obtained in Illustrative Examples 10.1, determine the approximate volumetric flow rates of the incompressible fluid and the compressed air required while drilling at 10,000 ft. Determine the foam bottomhole annulus pressure and the incompressible fluid and compressed gas injection pressure while drilling at 10,000 ft. Select an appropriate compressor system from those given in Chapter 4. Determine the highest compressor power required from the prime mover to drill the interval from 7,000 ft to 10,000 ft and determine the derated power available from the prime mover.

General Data
It is required that the foam quality at the top of the annulus (upstream of the back pressure valve) be approximately 0.98. This foam quality requirement defines the relationship of the volumetric flow rate of the incompressible fluid to the volumetric flow rate of the compressible gas. Thus, the defined foam quality dictates that only one of the components (either, the flow rate of the incompressible fluid or the flow rate of the compressible gas) be sought by trial and error technique. The other component is automatically known via the defined foam quality value. In this

example, the volumetric flow rate of the incompressible fluid will be sought. Therefore, the trial and error process requires the selection of the magnitude of the volumetric flow rate of the incompressible fluid (water and surfactant), q_w, required to yield a minimum kinetic energy per unit volume in the annulus of approximately 3.0 ft-lb/ft^3. Also, the minimum annulus foam quality must be greater than 0.60. This trial and error technique further requires that the upper limit pressures in each depth interval of the annulus be selected so that the overall interval integrals are satisfied.

Table 4-1 gives an average atmospheric pressure of 12.685 psia for a surface location of 4,000 ft above sea level (mid latitudes North America) (also see Appendix D). The actual atmospheric pressure for the air at the drilling location (that will be used by the compressor), P_{at}, is

$$p_{at} \quad 12.685 \text{ psia}$$

$$P_{at} \quad p_{at} \; 144$$

$$P_{at} \quad 1{,}826.6 \text{ lb/ft}^2 \text{ abs}$$

The actual atmospheric temperature of the air at the drilling location (that will be used by the compressor), T_{at}, is

$$t_{at} \quad 60°F$$

$$T_{at} \quad t_{at} \quad 459.67$$

$$T_{at} \quad 519.67°R$$

Thus, P_g and T_g become

$$P_g \quad P_{at} \quad 1{,}826.6 \text{ lb/ft}^2 \text{ abs}$$

$$T_g \quad T_{at} \quad 519.67°R$$

Using Equation 4-11, the specific weight of the gas entering the compressor is

$$_g \quad \frac{(1{,}827)\;(1.0)}{(53.36)\;(519.67)}$$

$$_g \quad 0.0659 \text{ lb/ft}^3$$

Note the above specific weight value can also be obtained from Figure D-4 in Appendix D.

The back pressure at the top of the annulus is 17 psig.   The back pressure, P_{bp}, in absolute pressure is

$$p_{bp} \quad 17.0 \quad 12.685$$

$$p_{bp} \quad 29.685 \ \text{psia}$$

$$P_{bp} \quad p_{bp} \ 144$$

$$P_{bp} \quad 4,275 \ \text{lb/ft}^2 \ \text{abs}$$

Note that the back pressure can be adjusted to improve the annulus foam quality and kinetic energy per unit volume values.

The trial and error q_w that will satisfy these limitations is

$$q_w \quad 105.0 \ \text{gal/min}$$

The volumetric flow rate of water, Q_w, in consistent units is

$$Q_w \quad \frac{105.0 \quad 231}{12^3 \quad 60}$$

$$Q_w \quad 0.234 \ \text{ft}^3/\text{sec}$$

The specific weight of the incompressible fluid is

$$_w \quad 62.4 \ \text{lb/ft}^3$$

The weight rate of flow of the incompressible fluid, $\dot{w}_w$ is

$$\dot{w}_w \quad _w \ Q_w$$

$$\dot{w}_w \quad (62.4) \ (0.234)$$

$$\dot{w}_w \quad 14.60 \ \text{lb/sec}$$

Solving Equation 10-3 for Q_{gbp} gives

$$Q_{gbp} \quad Q_w \quad \frac{bp}{1 \quad bp}$$

Substituting the values for $_{bp}$ and Q_w gives

$$Q_{gbp} \quad (0.234) \quad \frac{0.98}{1 \quad 0.98}$$

$$Q_{gbp} \quad 11.46 \ \text{ft}^3/\text{sec}$$

Using Equation 4-11 the specific weight of the gas (air) upstream of the back pressure valve can be obtained. This is

$$_{bp} \quad \frac{(4,275) \ (1.0)}{(53.36) \ (504.41)}$$

$$_{bp} \quad 0.159 \ \text{lb/ft}^3$$

The weight rate of flow of gas, $\dot{w}_g$, is

$$\dot{w}_g \quad _{bp} \ Q_{gbp}$$

$$\dot{w}_g \quad (0.159) \ (11.46)$$

$$\dot{w}_g \quad 1.821 \ \text{lb/sec}$$

The volumetric flow rate of the gas at the surface location atmospheric conditions is

$$Q_g \quad \frac{\dot{w}_g}{g}$$

$$Q_g \quad \frac{1.821}{0.0659}$$

$$Q_g \quad 27.64 \ \text{ft}^3/\text{sec}$$

$$q_g \quad Q_g \ 60$$

$$q_g \quad 1,658 \ \text{acfm}$$

The openhole diameter, D_h, is

$$d_h \quad 7.875 \ \text{inches}$$

$$D_h \quad \frac{d_h}{12}$$

$$D_h \quad 0.656 \text{ ft}$$

The estimated drilling rate of penetration is 60 ft/hr. Using Equation 10-2, the weight rate of flow of solids, $\dot{w}_s$, from the advance of the drill bit is

$$\dot{w}_s \quad \frac{-}{4} \quad 0.656^2 \quad 62.4 \quad 2.7 \quad \frac{60}{60 \quad 60}$$

$$\dot{w}_s \quad 0.949 \text{ lb/sec}$$

The total weight rate of flow, $\dot{w}_t$, in the annulus is

$$\dot{w}_t \quad 1.821 \quad 14.60 \quad 0.949$$

$$\dot{w}_t \quad 17.37 \text{ lb/sec}$$

The absolute viscosity of the water (and surfactant), $_w$, is assumed to be approximately

$$_w \quad 1 \text{ cps}$$

$$_w \quad (1.0)\ (0.001)\ (0.2089)$$

$$_w \quad 0.00002089 \quad \frac{\text{lb} \quad \text{sec}}{\text{ft}^2}$$

Using Equation 1-2, the density of the incompressible fluid, $_w$, is

$$_w \quad \frac{62.4}{32.2}$$

$$_w \quad 1.938 \quad \frac{\text{lb} \quad \text{sec}^2}{\text{ft}^4}$$

From Equation 9-7, the kinematic viscosity of the incompressible, $_w$, is

$$_w \quad \frac{0.00002089}{1.938}$$

$$\nu_w = 0.00001078 \ \frac{ft^2}{sec}$$

Surface Return Flow Line

The calculation procedure must be initiated with the known back pressure in the surface return flow line. It is assumed that the foam will exit the well annulus and enter the surface return flow line at the surface geothermal temperature of 44.74°F (or 504.41 R). It is further assumed that the temperature of the foam in the surface return flow line does not change as it flows through the return flow line (i.e., the steel surface return flow line will be at nearly the surface geothermal temperature at steady state flow conditions). Equation 6-102 can be altered to allow its application to horizontal flow in the surface return flow line. This altered equation is

$$\int_{P_g}^{P_s} \frac{dP}{B_s\,(P)} = \int_0^{L_s} dl \tag{10-4}$$

where

$$B_s\,(P) = \frac{\dot{w}_t}{\left(\dfrac{P_g}{P}\dfrac{T_r}{T_g}Q_g + Q_m\right)} + \frac{f_{sr}}{2g\,D_{sr}}\frac{\left(\dfrac{P_g}{P}\dfrac{T_r}{T_g}Q_g + Q_m\right)^2}{\left(\dfrac{\forall}{4}D_{sr}^2\right)}$$

and P_{sr} is the pressure at the entrance of the surface return flow line (lb/ft², abs),
   f_{sr} is the Fanning friction factor for flow in the surface return flow line,
   D_{sr} is the inside diameter of the surface return flow line (ft),
   L_{sr} is the length of the surface return flow line (ft).

In order to obtain the approximate value of the Fanning friction factor for Equation 10-4, it is necessary to estimate the Reynolds number and, thus, the flow conditions inside the surface return flow line. This is accomplished by determining the Reynolds number near the exit end just upstream of the back pressure valve. It is assumed this Reynolds number approximates the flow conditions throughout the flow line.

The inside diameter of the surface return flow line, D_{sr}, is

$$d_{sr} = 5.625 \ inches$$

$$D_{sr} = \frac{5.625}{12}$$

$$D_{sr} = 0.469 \ ft$$

The length of the surface return flow line (between the Tee and the back pressure valve), L_{sr}, is

$$L_{sr} = 100.0 \ \text{ft}$$

The absolute viscosity of the stable foam, μ_{sf}, can be approximated by [4]

$$\mu_{sf} = \mu_w \left(1 + 3.6 \Gamma \right) \tag{10-5}$$

where Γ is the foam quality at any position in the annulus.

Using Equation 10-5, the absolute viscosity of the foam just upstream of the back pressure valve, μ_{sfbp}, is

$$\mu_{sfbp} = 0.00002089 \left[1 + 3.6 \ (0.98) \right]$$

$$\mu_{sfbp} = 0.00009459 \ \frac{\text{lb} \cdot \text{sec}}{\text{ft}^2}$$

The specific weight of the foam just upstream of the back pressure valve, γ_{sfbp}, is approximated by

$$\gamma_{sfbp} = \cfrac{\dot{w}_t}{\cfrac{P_{at}}{P_{bp}} \ \cfrac{T_r}{T_{at}} \ Q_g + Q_w}$$

$$\gamma_{sfbp} = \cfrac{17.37}{\cfrac{1,826.6}{4,274.6} \ \cfrac{504.41}{519.67} \ (27.64) + 0.234}$$

$$\gamma_{sfbp} = 1.485 \ \text{lb/ft}^3$$

From Equation 1-2, the density of the foam just upstream of the back pressure valve, ρ_{sfbp}, is

$$\rho_{sfbp} = \frac{1.485}{32.2}$$

$$\rho_{sfbp} = 0.0461 \ \frac{\text{lb} \cdot \text{sec}^2}{\text{ft}^4}$$

From Equation 9-7, the kinematic viscosity of the foam just upstream of the back pressure valve, $_{sfbp}$, is

$$_{sfbp} \quad \frac{0.00009459}{0.0461}$$

$$_{sfbp} \quad 0.00205 \ \frac{ft^2}{sec}$$

The average velocity of the foam just upstream of the back pressure valve, V_{sfbp}, is

$$V_{sfbp} \quad \frac{Q_{gbp} \quad Q_w}{\overline{} \quad D_{sr}^2}$$
$$\frac{}{4}$$

$$V_{sfbp} \quad \frac{(11.46 \quad 0.234)}{\dfrac{}{4} \quad 0.469^{\ 2}}$$

$$V_{sfbp} \quad 67.8 \ ft/sec$$

Equation 6-103 can be altered to allow its application to the horizontal flow in the surface flow line. Thus, the Reynolds number of the foam flow just upsteam of the back pressure valve, $\mathbf{N_{Rsfbp}}$, is

$$\mathbf{N_{Rsfbp}} \quad \frac{V_{sfbp} \ D_{sr}}{_{sfbp}}$$

$$\mathbf{N_{Rsfbp}} \quad \frac{(67.8) \ (0.469)}{0.00205}$$

$$\mathbf{N_{Rsfbp}} \quad 15,489$$

The Reynolds number calculation above is greater than 4,000. This indicates that the flow condition is turbulent. Therefore, the empirical von Karman equation (i.e., Equation 6-106) must be used to determine the Fanning friction factor for the aerated fluid flow inside the return flow line. Equation 6-106 can be modified for application to the surface return flow line situation.

The surface roughness of the inside of the steel surface return flow line is the absolute surface roughness of commercial steel pipe, e_p. This is

$$e_p \qquad 0.00015 \ \text{ft}$$

Using Equation 106, the Fanning friction factor, f_{sr}, for flow inside the return flow line is

$$f_{sr} \qquad \cfrac{1}{\left(2 \ \log \cfrac{0.469}{0.00015} \ 1.14 \right)^2}$$

$$f_{sr} \qquad 0.015$$

Equation 10-4 for the surface return flow line increment can be solved for the pressure at the entrance end of the line, P_{sr}. This involves selecting this upper limit of the left side integral by a trial and error procedure. The magnitude of the upper limit pressure on the left side of the equation is selected to allow the left side integral to equal the right side integral. The integration can be carried out on the computer using one of the commercial analytic software programs (e.g., MathCad). The trial and error magnitude of the upper limit pressure is

$$p_{sr} \qquad 31.98 \ \text{psia}$$

$$P_{sr} \qquad p_{sr} \ 144$$

$$P_{sr} \qquad 4,604.4 \ \text{lb/ft}^2 \ \text{abs}$$

Substituting the values of L_{sr}, $\dot{w}_t$, Q_g, Q_m, P_g, P_{bp}, P_{sr}, T_g, T_r, D_{sr}, f_{sr}, and g into the left side of Equation 10-4 gives

$$\int_{4,274.6}^{4,604.4} \cfrac{dP}{\left(\cfrac{17.37}{\left(\cfrac{49,004.7}{P}\right)0.234}\right)\left(\cfrac{0.015}{30.20}\cfrac{\left(\cfrac{49,004.7}{P}\right)0.234}{-\cfrac{(0.469)^2}{4}}\right)} \qquad 100$$

Substituting the value of L_{sr} into the right side of Equation 10-4 gives

$$\int_0^{100} 1 \ dh \qquad 100$$

The stable foam flows from the top of the annulus into the entrance of the surface return flow line. The friction flow loss of the turn and of the two valves at the entrance of the surface return flow line must be included.   The approximate specific weight of the foam just after it passes through the Tee and the valves at the top of the annulus is determined using the above value for P_{sr}.   The approximate specific weight at the Tee, γ_{Tee}, is

$$\gamma_{Tee} \quad \frac{\dot{w}_t}{\dfrac{P_g}{P_{sr}} \quad \dfrac{T_r}{T_g} \quad Q_g \quad Q_w}$$

Substituting the values of $\dot{w}_t$, P_g, P_{sr}, T_g, T_r, Q_g, and Q_w into the above equation gives the specific weight just downstream of the Tee and valves. This is

$$\gamma_{Tee} \quad \frac{17.37}{\dfrac{1,826.6}{4,604.4} \quad \dfrac{504.41}{519.67} \quad (27.64) \quad 0.234}$$

$$\gamma_{Tee} \quad 1.597 \ \text{lb/ft}^3$$

The approximate velocity of the foam flow just downstream of the Tee and valves is

$$V_{Tee} \quad \frac{\dfrac{P_g}{P_{sr}} \quad \dfrac{T_r}{T_g} \quad Q_g \quad Q_m}{\dfrac{}{4} \ D_{sr}^2}$$

Substituting the values of Q_g, Q_m, P_g, P_{sr}, T_g, T_r, and D_{sr} into the above equation gives

$$V_{Tee} \quad \frac{\dfrac{1,826.6}{4,604.4} \quad \dfrac{504.41}{519.67} \quad (27.64) \quad 0.234}{\dfrac{}{4} \ (0.469)^2}$$

$$V_{Tee} \quad 63.02 \ \text{ft/sec}$$

The approximate pressure change, $\ni P_{Tee}$, through the two valves and Tee is

$$\partial P_{Tee} \quad \quad _{Tee} \; K_{Tee} \quad \quad 2 \; K_v \quad \frac{V_{Tee}^2}{2g}$$

where K_{Tee} is the minor loss flow resistance coefficient for the Tee,
    K_v is the minor loss flow resistance coefficient for a valve.
Using the dimensions of the Tee, Figure 8-5 can be used to obtain the approximate minor loss resistance coefficient of the Tee. This is

$$K_{Tee} \quad \quad 27$$

The approximate minor loss resistance coefficient for the valve is [12]

$$K_v \quad \quad 0.2$$

Substituting the values of $_{Tee}$, K_{Tee}, K_v, V_{Tee}, and g into the above equation gives

$$\partial P_{Tee} \quad \quad 1.597 \quad 27 \quad \quad 2 \quad 0.2 \quad \frac{63.02^{\,2}}{2 \quad 32.2}$$

$$\partial P_{Tee} \quad \quad 2,698.7 \; \text{lb/ft}^2$$

The pressure upstream of the Tee at the top of the annulus, P_{Tee}, is

$$P_{Tee} \quad \quad P_{sr} \quad \quad \partial P_{Tee}$$

$$P_{Tee} \quad \quad 4,604.4 \quad \quad 2,698.7$$

$$P_{Tee} \quad \quad 7,303.1 \; \text{lb/ft}^2 \; \text{abs}$$

$$p_{Tee} \quad \quad P_{Tee} \; 144$$

$$p_{Tee} \quad \quad 50.7 \; \text{psia}$$

Geometry in the Annulus

Major and minor friction losses must be included in order to obtain accurate bottomhole and injection pressures. Therefore, it is necessary to include the geometric dimensions of the drill pipe tool joints. When drilling at 10,000 ft, the drill string is composed of 9,500 ft of API 4 1/2 inch, 16.60 lb/ft nominal, EU-S135, NC50 (IF) from the surface to the top of the drill collars. The 4 1/2 inch outside diameter body of the drill pipe has an inside diameter of 3.826 inches (see Table B-3). Approximately every 30 ft there are tool joints which are about 1 1/2 ft in length. The outside diameter of these tool joints is 6 5/8 inches with an inside diameter of 3 1/2 inches. For the calculations that follow, the drill pipe tool joint

lengths will be "lumped" together as a continuous length to approximate their contribution to the overall major (wall friction) loss in the flow system. Thus, the drill pipe tool joints of the drill pipe in the 7,000 ft cased section of the borehole are calculated as a "lump" at the bottom of this cased section. The drill pipe tool joints of the drill pipe in the 2,500 ft openhole section of the borehole are calculated as a "lump" at the bottom of this openhole section.

These lumped approximations for the drill pipe tool joints are somewhat rough approximations, but will give accurate bottomhole and injection pressures. Using this lumped approximation, the pressure terms along the annulus around the drill pipe and inside the drill pipe are in error by a few percent. However, this short-coming can obviously be relieved by calculating a short 1 1/2 ft long tool joint every 30 ft along the entire drill pipe length of the drill string. This can easily be accomplished with a sophisticated computer program. But these lumped approximations are very useful in demonstrating the calculation technique steps. These lumped approximations are very easy to incorporate in an engineering calculation program and it has been found that these approximations are adequate for most engineering practice applications.

The calculation sequence for this illustrative example is divided into five depth increments. The increments start at the top of the borehole with the first increment at the top and the fifth increment at the bottom.

The total length of the lumped drill pipe body increment (first), H_1, in this cased section of the annulus is

$$H_1 \quad 7,000 \quad 1.5 \quad \frac{7,000}{30}$$

$$H_1 \quad 6,650 \text{ ft}$$

The inside diameter of the casing along this length in this cased section of the annulus is

$$d_1 \quad 8.017 \text{ inches}$$

$$D_1 \quad \frac{d_1}{12}$$

$$D_1 \quad 0.668 \text{ ft}$$

and the outside diameter of the drill pipe body along this length is

$$d_2 \quad 4.50 \text{ inches}$$

$$D_2 \quad \frac{d_2}{12}$$

D_2 0.375 ft

   The individual tool joint length along the drill string is assumed to be approximately 1.5 ft (30 ft drill pipe lengths). The total length of the lumped drill pipe tool joints increment (second), H_2, in this cased section of the annulus is

$$H_2 \quad 1.5 \quad \frac{7,000}{30}$$

H_2 350 ft

The inside diameter of the casing along this length of this cased section of the annulus is

D_1 0.668 ft

and the outside diameter of the drill pipe tool joints along this length is

d_3 6.625 inches

$$D_3 \quad \frac{d_3}{12}$$

D_3 0.552 ft

   The total length of the lumped drill pipe body increment (third), H_3, in the openhole section of the annulus is

$$H_3 \quad 2,500 \quad 1.5 \quad \frac{2,500}{30}$$

H_3 2,375 ft

The inside diameter of the openhole along this length of the openhole section of the annulus is

d_h 7.875 inches

$$D_h \quad \frac{d_h}{12}$$

D_h 0.656 ft

and the outside diameter of the drill pipe body along this length is

D_2 0.375 ft

The total length of the lumped drill pipe tool joints increment (fourth), H_4, in the openhole section of the annulus is

$$H_4 \quad 1.5 \ \frac{2,500}{30}$$

H_4 125 ft

The inside diameter of the openhole along this length of this openhole section of the annulus is

D_h 0.656 ft

and the outside diameter of the drill pipe tool joints along this length is

D_3 0.552 ft

The total length of the drill collar increment (fifth), H_5, in the openhole section of the annulus is

H_5 500 ft

The inside diameter of the openhole along this length of the openhole section of the annulus is

D_h 0.656 ft

and the outside diameter of the drill collars along this length is

d_4 6.75 inches

$$D_4 \quad \frac{d_4}{12}$$

D_4 0.563 ft

Using the description of the annulus geometry given above each of the five increment changes in cross-sectional area can be analyzed starting with the stable foam flow exiting at the top of the annulus.

Cased Section of the Annulus (Surface to 7,000 ft)
The first annulus section increment is denoted by the length H_1. The temperature at the bottom of the length H_1 in the cased annulus section (bottom of the drill pipe body lumped geometry), T_1, is

$$T_1 = T_r + 0.01 \, H_1$$

$$T_1 = T_r + 0.01 \,(6,650)$$

$$T_1 = 570.91°R$$

The average temperature of this cased annulus section H_1 is

$$T_{av1} = \frac{T_r + T_1}{2}$$

$$T_{av1} = 537.66°R$$

In order to obtain the approximate value of the Fanning friction factor for Equation 6-88, it is necessary to estimate the Reynolds number and, thus, the flow conditions in the cased annulus section along H_1. This is accomplished by determining the Reynolds number at the exit end of this annulus section and assuming this Reynolds number approximates the flow conditions throughout the annulus section.
Using Equation 4-11, the approximate specific weight of the gas as it exits this cased annulus section and starts into the Tee is determined from P_{Tee}. This is

$$\gamma_{ga1} = \frac{(7,303.1)\,(1.0)}{(53.36)\,(537.66)}$$

$$\gamma_{ga1} = 0.271 \text{ lb/ft}^3$$

The volumetric flowrate of the gas as it exits this cased annulus section and starts into the Tee is

$$Q_{ga1} = \frac{\dot{w}_g}{\gamma_{ga1}}$$

$$Q_{ga1} = \frac{1.821}{0.271}$$

$$Q_{ga1} = 6.71 \text{ ft}^3/\text{sec}$$

The foam quality as it exits this cased annulus section and starts into the Tee is

$$\Gamma_{sfa1} = \frac{Q_{ga1}}{Q_{ga1} + Q_w}$$

$$\Gamma_{sfa1} = \frac{6.71}{6.71 + 0.234}$$

$$\Gamma_{sfa1} = 0.966$$

Using Equation 10-5, the absolute viscosity of the foam as it exits this cased annulus section and starts into the Tee is

$$\mu_{sfa1} = 0.00002089 \left[1 + 3.6 \, (0.966) \right]$$

$$\mu_{sfa1} = 0.00009356 \; \frac{lb \; sec}{ft^2}$$

The specific weight of the foam as it exits this cased annulus section and starts into the Tee is approximated by

$$\gamma_{sfa1} = \frac{\dot{w}_g + \dot{w}_w}{\left(\dfrac{P_{at}}{P_{Tee}} \right) \left(\dfrac{T_{av1}}{T_{at}} \right) Q_g + Q_w}$$

$$\gamma_{sfa1} = \frac{1.821 + 14.60}{\left(\dfrac{1,826.6}{4,604.4} \right) \left(\dfrac{537.66}{519.67} \right) (27.64) + 0.234}$$

$$\gamma_{sfa1} = 2.223 \; lb/ft^3$$

From Equation 1-2, the density of the foam as it exits this cased annulus section and starts into the Tee is

$$\rho_{sfa1} = \frac{2.223}{32.2}$$

$$\rho_{sfa1} = 0.0690 \; \frac{lb \; sec^2}{ft^4}$$

From Equation 9-7, the kinematic viscosity of the foam as it exits this cased annulus section and starts into the Tee is

$$\nu_{sfa1} \quad \frac{0.00009635}{0.0690}$$

$$\nu_{sfa1} \quad 0.00136 \; \frac{ft^2}{sec}$$

The average velocity of the foam as it exits this cased annulus section and starts into the Tee is

$$V_{sfa1} \quad \frac{\dfrac{P_{at}}{P_{Tee}} \; \dfrac{T_{av1}}{T_{at}} \; Q_g \quad Q_w}{\dfrac{}{4} \; D_1^2 \quad D_2^2}$$

$$V_{sfa1} \quad \frac{\dfrac{1,826.6}{4,604.4} \; \dfrac{537.66}{519.67} \; (27.64) \quad 0.234}{\dfrac{}{4} \; 0.668^{\,2} \quad 0.375^{\,2}}$$

$$V_{sfa1} \quad 30.8 \; ft/sec$$

Using Equation 6-89 the Reynolds number of the foam as it exits this cased annulus section and starts into the Tee is

$$N_{Rsfa1} \quad \frac{V_{sfa1} \; D_1 \quad D_2}{\nu_{sfa1}}$$

$$N_{Rsfa1} \quad \frac{(30.8)\;(0.668 \quad 0.375)}{0.00136}$$

$$N_{Rsfa1} \quad 6,652$$

The Reynolds number calculation above is greater than 4,000. This indicates that the flow condition is turbulent. Therefore, the empirical von Karman equation (i.e., Equation 6-92) must be used to determine the Fanning friction factor for the foam flow in this annulus section.

Both annulus section surfaces are commercial steel with the surface roughness

$$e_p \quad 0.00015 \text{ ft}$$

Therefore, Equation 6-92 becomes

$$f_{a1} \quad \cfrac{1}{\left[2 \ \log \ \cfrac{0.668 \quad 0.375}{0.00015} \quad 1.14 \right]^2}$$

$$f_{a1} \quad 0.017$$

Equation 6-88 for the first increment in the annulus can be solved for the pressure at bottom of the increment, P_{a1}. This involves selecting this upper limit of the intergral by a trial and error procedure.   The magnitude of the upper limit pressure on the left side of the equation is selected to allow the left side integral to equal the right side integral. The integration can be carried out on the computer using one of the commercial analytic software programs.   The trial and error magnitude of the upper limit pressure that satisfies Equation 6-88 for this annulus section is

$$p_{a1} \quad 489.6 \text{ psia}$$

$$P_{a1} \quad p_{a1} \ 144$$

$$P_{a1} \quad 70{,}502 \text{ lb/ft}^2 \text{ abs}$$

Substituting the values of $\dot{w}_t$, Q_g, Q_w, P_g, P_{Tee}, P_{a1}, T_g, T_{av1}, D_1, D_2, f_{a1}, and g into the left side of Equation 6-88 gives

$$\int_{4{,}604.4}^{70{,}502} \cfrac{dP}{\left[\cfrac{17.37}{\cfrac{52{,}235.0}{P} \quad 0.234} \quad 1 \quad \cfrac{0.017}{18.87} \quad \cfrac{\cfrac{52{,}235.0}{P} \quad 0.234}{\cfrac{-}{4} \quad 0.668^2 \quad 0.375^2} \right]} \quad 6{,}650$$

Substituting the value of H_1 into the right side of Equation 6-88 gives

$$\int_{0}^{6{,}650} 1 \ dh \quad 6{,}650$$

As can be seen in the above, the right and left hand sides of Equation 6-88 yield the same answer. This shows that the upper limit pressure is correct.

The second annulus section increment is denoted by the length H_2. The temperature at the bottom of the length H_2 in the cased annulus section (bottom of the drill pipe tool joints lumped geometry), T_2, is

$$T_2 = T_r + 0.01 \, (H_1 + H_2)$$

$$T_2 = T_r + 0.01 \, (6,650 + 350)$$

$$T_2 = 574.41°R$$

The average temperature of this cased annulus section H_2 is

$$T_{av2} = \frac{T_1 + T_2}{2}$$

$$T_{av2} = 572.66°R$$

In order to obtain the approximate value of the Fanning friction factor for Equation 6-91, it is necessary to estimate the Reynolds number and, thus, the flow conditions in the cased annulus section along H_2. This is accomplished by determining the Reynolds number at the exit end of this annulus section and assuming this Reynolds number approximates the flow conditions throughout the annulus section.

Using Equation 4-11, the approximate specific weight of the gas as it exits this cased annulus section is determined from P_{a1}. This is

$$\gamma_{a2} = \frac{(70,504) \, (1.0)}{(53.36) \, (572.66)}$$

$$\gamma_{a2} = 2.307 \ \text{lb/ft}^3$$

The volumetric flowrate of the gas as it exits this cased annulus section is

$$Q_{ga2} = \frac{\dot{w}_g}{\gamma_{ga2}}$$

$$Q_{ga2} = \frac{1.821}{2.307}$$

$$Q_{ga2} = 0.789 \ \text{ft}^3/\text{sec}$$

The foam quality as it exits this cased annulus section is

$$\Gamma_{sfa2} \quad \frac{Q_{ga2}}{Q_{ga2} \quad Q_w}$$

$$\Gamma_{sfa2} \quad \frac{0.789}{0.789 \quad 0.234}$$

$$\Gamma_{sfa2} \quad 0.771$$

Using Equation 10-5, the absolute viscosity of the foam as it exits this cased annulus section is

$$\mu_{sfa2} \quad 0.00002089 \quad 1 \quad 3.6 \ (0.771)$$

$$\mu_{sfa2} \quad 0.00007890 \quad \frac{lb \quad sec}{ft^2}$$

The specific weight of the foam as it exits this cased annulus section is approximated by

$$\gamma_{sfa2} \quad \frac{\dot{w}_g \quad \dot{w}_w}{\dfrac{P_{at}}{P_{a1}} \quad \dfrac{T_{av2}}{T_{at}} \quad Q_g \quad Q_w}$$

$$\gamma_{sfa2} \quad \frac{1.821 \quad 14.60}{\dfrac{1,826.6}{70,502} \quad \dfrac{572.66}{519.67} \ (27.64) \quad 0.234}$$

$$\gamma_{sfa2} \quad 16.049 \ \ lb/ft^3$$

Using Equation 1-2, the density of the foam as it exits this cased annulus is

$$\rho_{sfa2} \quad \frac{16.049}{32.2}$$

$$\rho_{sfa2} \quad 0.498 \quad \frac{lb \quad sec^2}{ft^4}$$

From Equation 9-7, the kinematic viscosity of the foam as it exits this cased annulus section is

$$\nu_{sfa2} \quad \frac{0.00007890}{0.498}$$

$$\nu_{sfa2} \quad 0.0001584 \ \frac{ft^2}{sec}$$

The average velocity of the foam as it exits this cased annulus section is

$$V_{sfa2} \quad \frac{\dfrac{P_{at}}{P_{a1}} \quad \dfrac{T_{av2}}{T_{at}} \quad Q_g \quad Q_w}{\dfrac{\pi}{4} \quad D_1^2 \quad D_3^2}$$

$$V_{sfa2} \quad \frac{\dfrac{1,826.6}{70.502} \quad \dfrac{572.66}{519.67} \quad (27.64) \quad 0.234}{\dfrac{\pi}{4} \quad 0.668^{\,2} \quad 0.552^{\,2}}$$

$$V_{sfa2} \quad 9.20 \ ft/sec$$

Using Equation 6-89 the Reynolds number of the foam as it exits this cased annulus section is

$$N_{Rsfa2} \quad \frac{V_{sfa2} \quad D_1 \quad D_3}{\nu_{sfa2}}$$

$$N_{Rsfa2} \quad \frac{(9.20) \ (0.668 \quad 0.552)}{0.0001584}$$

$$N_{Rsfa2} \quad 22,542$$

The Reynolds number calculation above is greater than 4,000. This indicates that the flow condition is turbulent. Therefore, the empirical von Karman equation (i.e., Equation 6-92) must be used to determine the Fanning friction factor for the foam flow in this annulus section.

Both annulus section surfaces are commercial steel with the surface roughness

$$e_p \quad 0.00015 \ ft$$

Therefore, Equation 6-92 becomes

$$f_{a2} = \frac{1}{\left[2 \ \log\left(\dfrac{0.668}{0.00015}\right) + 0.552\right]^2 + 1.14}$$

$$f_{a2} = 0.021$$

Equation 6-88 for the second increment in the annulus can be solved for the pressure at bottom of the increment, P_{a2}. This involves selecting this upper limit of the intergral by a trial and error procedure. The magnitude of the upper limit pressure on the left side of the equation is selected to allow the left side integral to equal the right side integral. The integration can be carried out on the computer using one of the commercial analytic software programs. The trial and error magnitude of the upper limit pressure that satisfies Equation 6-88 for this annulus section is

$$p_{a2} = 541.9 \ \text{psia}$$

$$P_{a2} = p_{a2} \ 144$$

$$P_{a2} = 78,039 \ \text{lb/ft}^2 \ \text{abs}$$

Substituting the values of $\dot{w}_t$, Q_g, Q_w, P_g, P_{a1}, P_{a2}, T_g, T_{av2}, D_1, D_3, f_{a2}, and g into the left side of Equation 6-88 gives

$$\int_{70,502}^{78,039} \frac{dP}{\left[\dfrac{17.37}{\dfrac{55,635.3}{P} + 0.234} + \dfrac{0.021}{7.47}\left(\dfrac{1}{-\dfrac{4}{0.668^2} \cdot \dfrac{\dfrac{55,635.3}{P} + 0.234}{0.552^2}}\right)\right]} = 350$$

Substituting the value of H_1 and H_2 into the right side of Equation 6-88 gives

$$\int_{6,650}^{6,650 + 350} 1 \ dh = 350$$

As can be seen in the above, the right and left hand sides of Equation 6-88 yield the same answer. This shows that the upper limit pressure is correct.

Openhole Section of the Annulus (7,000 ft to 10,000 ft)
   The third annulus section increment is denoted by the length H_3.   The temperature at the bottom of the length H_3 in the openhole annulus section (bottom of the drill pipe body lumped geometry), T_3, is

$$T_3 \quad T_r \quad 0.01 \ (H_1 \quad H_2 \quad H_3)$$

$$T_3 \quad T_r \quad 0.01 \ (6,650 \quad 350 \quad 2,375)$$

$$T_3 \quad 598.16°R$$

The average temperature of this openhole annulus section H_3 is

$$T_{av3} \quad \frac{T_2 \quad T_3}{2}$$

$$T_{av3} \quad 586.29°R$$

   In order to obtain the approximate value of the Fanning friction factor for Equation 6-88, it is necessary to estimate the Reynolds number and, thus, the flow conditions in the openhole annulus section along H_3.   This is accomplished by determining the Reynolds number at the exit end of this annulus section and assuming this Reynolds number approximates the flow conditions throughout the annulus section.
   Using Equation 4-11, the approximate specific weight of the gas as it exits this openhole annulus section is determined from P_{a2}.   This is

$$_{a3} \quad \frac{(78,039) \ (1.0)}{(53.36) \ (586.29)}$$

$$_{a3} \quad 2.495 \ \text{lb/ft}^3$$

The volumetric flowrate of the gas as it exits this openhole annulus section is

$$Q_{ga3} \quad \frac{\dot{w}_g}{_{ga3}}$$

$$Q_{ga3} \quad \frac{1.821}{2.495}$$

$$Q_{ga3} \quad 0.730 \ \text{ft}^3/\text{sec}$$

The foam quality as it exits this openhole annulus section is

$$sfa3 \quad \frac{Q_{ga3}}{Q_{ga3} \quad Q_w}$$

$$sfa3 \quad \frac{0.730}{0.730 \quad 0.234}$$

$$sfa3 \quad 0.757$$

Using Equation 10-5, the absolute viscosity of the foam as it exits this openhole annulus section is

$$sfa3 \quad 0.00002089 \quad 1 \quad 3.6\,(0.757)$$

$$sfa3 \quad 0.00007784 \quad \frac{\text{lb} \quad \text{sec}}{\text{ft}^2}$$

The specific weight of the foam as it exits this openhole annulus section is approximated by

$$sfa3 \quad \frac{\dot{w}_g \quad \dot{w}_w}{\dfrac{P_{at}}{P_{a2}} \quad \dfrac{T_{av3}}{T_{at}} \quad Q_g \quad Q_w}$$

$$sfa3 \quad \frac{1.821 \quad 14.60}{\dfrac{1,826.6}{78,039} \quad \dfrac{586.29}{519.67} \quad (27.64) \quad 0.234}$$

$$sfa3 \quad 17.036 \ \text{lb/ft}^3$$

Using Equation 1-2, the density of the foam as it exits this openhole annulus is

$$sfa3 \quad \frac{17.036}{32.2}$$

$$sfa3 \quad 0.529 \quad \frac{\text{lb} \quad \text{sec}^2}{\text{ft}^4}$$

From Equation 9-7, the kinematic viscosity of the foam as it exits this openhole annulus section is

$$sfa3 \quad \frac{0.00007784}{0.529}$$

$$sfa3 \quad 0.0001475 \ \frac{\text{ft}^2}{\text{sec}}$$

The average velocity of the foam as it exits this openhole annulus section is

$$V_{sfa3} \quad \frac{\dfrac{P_{at}}{P_{a2}} \quad \dfrac{T_{av3}}{T_{at}} \quad Q_g \quad Q_w}{\overline{} \quad D_h^2 \quad D_2^2}$$

$$V_{sfa3} \quad \frac{\dfrac{1,826.6}{78.039.4} \quad \dfrac{586.29}{519.67} \quad (27.64) \quad 0.234}{\overline{} \quad 0.656^{\ 2} \quad 0.375^{\ 2}}$$

$$V_{sfa3} \quad 4.23 \ \text{ft/sec}$$

Using Equation 6-89 the Reynolds number of the foam as it exits this openhole annulus section is

$$\mathbf{N_{Rsfa3}} \quad \frac{V_{sfa3} \quad D_h \quad D_2}{sfa3}$$

$$\mathbf{N_{Rsfa3}} \quad \frac{(4.23) \ (0.656 \quad 0.375)}{0.0001475}$$

$$\mathbf{N_{Rsfa3}} \quad 8,088$$

The Reynolds number calculation above is greater than 4,000. This indicates that the flow condition is turbulent. Therefore, the empirical von Karman equation (i.e., Equation 6-92) must be used to determine the Fanning friction factor for the foam flow in this annulus section.

The surfaces of this example openhole annulus section has two different surface roughness. The inside surface of this openhole borehole is a wall drilled in a sandstone and limestone rock sequence. Unless such a rock sequence is highly fractured, the inside surface of the openhole borehole approximates the inside surface of a concrete water pipe used in community water systems. Table 8-1 correlates the borehole inside surface roughness for a variety of rock formation types with the

absolute surface roughness values with those of known engineering pressure conduits. From this table the absolute surface roughness for the inside wall of a borehole in the example sandstone and limestone sequence, e_{oh}, is

$$e_{oh} \quad 0.01 \text{ ft}$$

The inner surface of this annulus section is the outer surface of the drill pipe body lumped geometry has the absolute surface roughness of commercial steel pipe, e_p. The surface roughness of commercial steel pipe is

$$e_p \quad 0.00015 \text{ ft}$$

Thus, using Equation 8-2, the average absolute surface roughness of this annulus section, e_{av3}, is

$$e_{av3} \quad \frac{(0.01) \quad \dfrac{-}{4} \quad (0.656)^2 \quad (0.00015) \quad \dfrac{-}{4} \quad (0.375)^2}{\dfrac{-}{4} \quad (0.656)^2 \quad \dfrac{-}{4} \quad (0.375)^2}$$

$$e_{av3} \quad 0.0076 \text{ ft}$$

Therefore, Equation 6-92 becomes

$$f_{a3} \quad \frac{1}{\left[2 \ \log \ \dfrac{0.656 \quad 0.375}{0.0076} \quad 1.14 \right]^2}$$

$$f_{a3} \quad 0.055$$

Equation 6-88 for the third increment in the annulus can be solved for the pressure at bottom of the increment, P_{a3}. This involves selecting this upper limit of the intergral by a trial and error procedure. The magnitude of the upper limit pressure on the left side of the equation is selected to allow the left side integral to equal the right side integral. The integration can be carried out on the computer using one of the commercial analytic software programs. The trial and error magnitude of the upper limit pressure that satisfies Equation 6-88 for this annulus section is

$$p_{a3} \quad 919.1 \text{ psia}$$

$$P_{a3} = p_{a3} \, 144$$

$$P_{a3} = 132,346 \text{ lb/ft}^2 \text{ abs}$$

Substituting the values of $\dot{w}_t$, Q_g, Q_w, P_g, P_{a2}, P_{a3}, T_g, T_{av3}, D_h, D_2, f_{a3}, and g into the left side of Equation 6-88 gives

$$\int_{78,039}^{132,346} \frac{dP}{\dfrac{17.37}{\dfrac{56,959.5}{P} \, 0.234} + 1 \dfrac{0.055}{18.10} \dfrac{\dfrac{56,959.5}{P} \, 0.234}{\dfrac{-}{4} \, 0.656^{\,2} \quad 0.375^{\,2}}^{2}} = 2,375$$

Substituting the value of H_1, H_2 and H_3 into the right side of Equation 6-88 gives

$$\int_{6,650 \quad 350}^{6,650 \quad 350 \quad 2,375} 1 \, dh = 2,375$$

As can be seen in the above, the right and left hand sides of Equation 6-88 yield the same answer. This shows that the upper limit pressure is correct.

The fourth annulus section increment is denoted by the length H_4. The temperature at the bottom of the length H_4 in the openhole annulus section (bottom of the drill pipe tool joints lumped geometry), T_4, is

$$T_4 = T_r + 0.01 \, (H_1 + H_2 + H_3 + H_4)$$

$$T_4 = T_r + 0.01 \, (6,650 + 350 + 2,375 + 125)$$

$$T_4 = 599.41°R$$

The average temperature of this openhole annulus section H_4 is

$$T_{av4} = \frac{T_3 + T_4}{2}$$

$$T_{av4} = 598.79°R$$

In order to obtain the approximate value of the Fanning friction factor for Equation 6-88, it is necessary to estimate the Reynolds number and, thus, the flow conditions in the openhole annulus section along H_4. This is accomplished by determining the Reynolds number at the exit end of this annulus section and

assuming this Reynolds number approximates the flow conditions throughout the annulus section.

Using Equation 4-11, the approximate specific weight of the gas as it exits this cased annulus section is determined from P_{a3}. This is

$$\gamma_{a4} \quad \frac{(132,346)\ (1.0)}{(53.36)\ (598.79)}$$

$$\gamma_{a4} \quad 4.142\ \text{lb/ft}^3$$

The volumetric flowrate of the gas as it exits this openhole annulus section is

$$Q_{ga4} \quad \frac{\dot{w}_g}{\gamma_{ga4}}$$

$$Q_{ga4} \quad \frac{1.821}{4.142}$$

$$Q_{ga4} \quad 0.440\ \text{ft}^3/\text{sec}$$

The foam quality as it exits this openhole annulus section is

$$\Gamma_{sfa4} \quad \frac{Q_{ga4}}{Q_{ga4} \quad Q_w}$$

$$\Gamma_{sfa4} \quad \frac{0.440}{0.440 \quad 0.234}$$

$$\Gamma_{sfa4} \quad 0.653$$

Using Equation 10-5, the absolute viscosity of the foam as it exits this openhole annulus section is

$$\mu_{sfa4} \quad 0.00002089 \quad 1 \quad 3.6\ (0.653)$$

$$\mu_{sfa4} \quad 0.00006997 \quad \frac{\text{lb}\ \ \text{sec}}{\text{ft}^2}$$

The specific weight of the foam as it exits this openhole annulus section is approximated by

$$sfa4 \quad \frac{\dot{w}_g \quad \dot{w}_w}{\dfrac{P_{at}}{P_{a3}} \quad \dfrac{T_{av4}}{T_{at}} \quad Q_g \quad Q_w}$$

$$sfa4 \quad \frac{1.821 \quad 14.60}{\dfrac{1,826.6}{132,346} \quad \dfrac{598.79}{519.67} \quad (27.64) \quad 0.234}$$

$$sfa4 \quad 24.379 \ \text{lb/ft}^3$$

Using Equation 1-2, the density of the foam as it exits this openhole annulus is

$$sfa4 \quad \frac{24.379}{32.2}$$

$$sfa4 \quad 0.757 \ \frac{\text{lb} \quad \text{sec}^2}{\text{ft}^4}$$

From Equation 9-7, the kinematic viscosity of the foam as it exits this openhole annulus section is

$$sfa4 \quad \frac{0.00006997}{0.757}$$

$$sfa4 \quad 0.00009242 \ \frac{\text{ft}^2}{\text{sec}}$$

The average velocity of the foam as it exits this openhole annulus section is

$$V_{sfa4} \quad \frac{\dfrac{P_{at}}{P_{a3}} \quad \dfrac{T_{av4}}{T_{at}} \quad Q_g \quad Q_w}{\dfrac{}{4} \quad D_h^2 \quad D_3^2}$$

$$V_{sfa4} \quad \frac{\dfrac{1,826.6}{132,346} \quad \dfrac{598.79}{519.67} \quad (27.64) \quad 0.234}{\dfrac{}{4} \quad 0.656^{\ 2} \quad 0.552^{\ 2}}$$

V_{sfa4} 6.81 ft/sec

Using Equation 6-89 the Reynolds number of the foam as it exits this openhole annulus section is

$$N_{Rsfa4} \quad \frac{V_{sfa4} \; D_h \quad D_3}{sfa4}$$

$$N_{Rsfa4} \quad \frac{(6.81) \; (0.656 \quad 0.552)}{0.00009242}$$

$$N_{Rsfa4} \quad 7,679$$

The Reynolds number calculation above is greater than 4,000. This indicates that the flow condition is turbulent. Therefore, the empirical von Karman equation (i.e., Equation 6-92) must be used to determine the Fanning friction factor for the foam flow in this annulus section.

The surface roughness for the inside wall of a borehole in the example sandstone and limestone rock sequence, e_{oh}, is

e_{oh} 0.01 ft

The inner surface of this annulus section is the outer surface of the drill pipe tool joint lumped geometry has the surface roughness of commercial steel pipe, e_p. The surface roughness of commercial steel pipe is

e_p 0.00015 ft

Thus, using Equation 8-2, the average absolute surface roughness of this annulus section, e_{av4}, is

$$e_{av4} \quad \frac{(0.01) \quad \dfrac{}{4} \quad (0.656)^2 \quad (0.00015) \quad \dfrac{}{4} \quad (0.552)^2}{\dfrac{}{4} \quad (0.656)^2 \quad \dfrac{}{4} \quad (0.552)^2}$$

e_{av4} 0.0059 ft

Therefore, Equation 6-92 becomes

$$f_{a4} = \frac{1}{\left\{2 \ \log \left[\frac{0.656}{0.0059} \ 0.552\right] \ 1.14\right\}^2}$$

$$f_{a4} = 0.076$$

Equation 6-88 for the fourth increment in the annulus can be solved for the pressure at bottom of the increment, P_{a4}. This involves selecting this upper limit of the intergral by a trial and error procedure.   The magnitude of the upper limit pressure on the left side of the equation is selected to allow the left side integral to equal the right side integral. The integration can be carried out on the computer using one of the commercial analytic software programs.   The trial and error magnitude of the upper limit pressure that satisfies Equation 6-88 for this annulus section is

$$p_{a4} = 953.3 \text{ psia}$$

$$P_{a4} = p_{a4} \ 144$$

$$P_{a4} = 137,281 \text{ lb/ft}^2 \text{ abs}$$

Substituting the values of $\dot{w}_t$, Q_g, Q_w, P_g, P_{a3}, P_{a4}, T_g, T_{av4}, D_h, D_3, f_{a4}, and g into the left side of Equation 6-88 gives

$$\int_{132,346}^{137,281} \frac{dP}{\frac{17.37}{\frac{58,173.9}{P} \ 0.234} \ 1 \ \frac{0.076}{6.70} \ \left[\frac{\frac{58,173.9}{P} \ 0.234}{\frac{1}{4} \ 0.656^2 \ 0.552^2}\right]^2} = 125$$

Substituting the value of H_1, H_2, H_3 and H_4 into the right side of Equation 6-88 gives

$$\int_{6,650 \ 350 \ 2,375}^{6,650 \ 350 \ 2,375 \ 125} 1 \ dh = 125$$

As can be seen in the above, the right and left hand sides of Equation 6-88 yield the same answer. This shows that the upper limit pressure is correct.

The fifth annulus section increment is denoted by the length H_5.   The temperature at the bottom of the length H_5 in the openhole annulus section (bottom of the drill collar geometry), T_5, is

$$T_5 \quad T_r \quad 0.01\ (H_1 \quad H_2 \quad H_3 \quad H_4 \quad H_5)$$

$$T_5 \quad T_r \quad 0.01\ (6,650 \quad 350 \quad 2,375 \quad 125 \quad 500)$$

$$T_5 \quad 604.41°R$$

The average temperature of this openhole annulus section H_5 is

$$T_{av5} \quad \frac{T_4 \quad T_5}{2}$$

$$T_{av5} \quad 601.91°R$$

In order to obtain the approximate value of the Fanning friction factor for Equation 6-88, it is necessary to estimate the Reynolds number and, thus, the flow conditions in the openhole annulus section along H_5. This is accomplished by determining the Reynolds number at the exit end of this annulus section and assuming this Reynolds number approximates the flow conditions throughout the annulus section.

Using Equation 4-11, the approximate specific weight of the gas as it exits this cased annulus section is determined from P_{a4}. This is

$$_{a5} \quad \frac{(137,281)\ (1.0)}{(53.36)\ (601.91)}$$

$$_{a5} \quad 4.274\ \text{lb/ft}^3$$

The volumetric flowrate of the gas as it exits this openhole annulus section is

$$Q_{ga5} \quad \frac{\dot{w}_g}{_{ga5}}$$

$$Q_{ga5} \quad \frac{1.821}{4.274}$$

$$Q_{ga5} \quad 0.426\ \text{ft}^3/\text{sec}$$

The foam quality as it exits this openhole annulus section is

$$\mu_{sfa5} \approx \frac{Q_{ga5}}{Q_{ga5} + Q_w}$$

$$\mu_{sfa5} \approx \frac{0.426}{0.426 + 0.234}$$

$$\mu_{sfa5} \approx 0.646$$

Using Equation 10-5, the absolute viscosity of the foam as it exits this openhole annulus section is

$$\mu_{sfa5} \approx 0.00002089 \left[1 + 3.6 (0.646)\right]$$

$$\mu_{sfa5} \approx 0.00006943 \ \frac{\text{lb} \cdot \text{sec}}{\text{ft}^2}$$

The specific weight of the foam as it exits this openhole annulus section is approximated by

$$\gamma_{sfa5} \approx \frac{\dot{w}_g + \dot{w}_w}{\dfrac{P_{at}}{P_{a4}} \dfrac{T_{av5}}{T_{at}} Q_g + Q_w}$$

$$\gamma_{sfa5} \approx \frac{1.821 + 14.60}{\dfrac{1,826.6}{137,281} \dfrac{601.91}{519.67} (27.64) + 0.234}$$

$$\gamma_{sfa5} \approx 24.881 \ \text{lb/ft}^3$$

Using Equation 1-2, the density of the foam as it exits this openhole annulus is

$$\rho_{sfa5} \approx \frac{24.881}{32.2}$$

$$\rho_{sfa5} \approx 0.773 \ \frac{\text{lb} \cdot \text{sec}^2}{\text{ft}^4}$$

From Equation 9-7, the kinematic viscosity of the foam as it exits this openhole annulus section is

$$sfa5 \quad \frac{0.00006943}{0.773}$$

$$sfa5 \quad 0.00008986 \ \frac{\text{ft}^2}{\text{sec}}$$

The average velocity of the foam as it exits this openhole annulus section is

$$V_{sfa5} \quad \frac{\dfrac{P_{at}}{P_{a4}} \quad \dfrac{T_{av5}}{T_{at}} \quad Q_g \quad Q_w}{\overline{4} \quad D_h^2 \quad D_4^2}$$

$$V_{sfa5} \quad \frac{\dfrac{1,826.6}{137,281} \quad \dfrac{601.91}{519.67} \quad (27.64) \quad 0.234}{\overline{4} \quad 0.656^{\ 2} \quad 0.563^{\ 2}}$$

$$V_{sfa5} \quad 7.35 \ \text{ft/sec}$$

Using Equation 6-89 the Reynolds number of the foam as it exits this openhole annulus section is

$$\mathbf{N_{Rsfa5}} \quad \frac{V_{sfa5} \quad D_h \quad D_4}{sfa5}$$

$$\mathbf{N_{Rsfa5}} \quad \frac{(7.35) \ (0.656 \quad 0.563)}{0.00008986}$$

$$\mathbf{N_{Rsfa5}} \quad 7,672$$

The Reynolds number calculation above is greater than 4,000. This indicates that the flow condition is turbulent. Therefore, the empirical von Karman equation (i.e., Equation 6-92) must be used to determine the Fanning friction factor for the foam flow in this annulus section.

The inside surface of borehole roughness for a variety of rock formation types with those of known engineering pressure conduits. From this table the surface roughness for the inside wall of a borehole in the example sandstone and limestone rock sequence, e_{oh}, is

$$e_{oh} \quad 0.01 \ \text{ft}$$

The inner surface of this annulus section is the outer surface of the drill collar geometry has the surface roughness of commercial steel pipe, e_p.   The surface roughness of commercial steel pipe is

$$e_p \qquad 0.00015 \text{ ft}$$

Thus, using Equation 8-2, the average absolute surface roughness of this annulus section, e_{av5}, is

$$e_{av5} \qquad \dfrac{(0.01) \; \dfrac{-}{4} \; (0.656)^2 \quad (0.00015) \; \dfrac{-}{4} \; (0.563)^2}{\dfrac{-}{4} \; (0.656)^2 \quad \dfrac{-}{4} \; (0.563)^2}$$

$$e_{av5} \qquad 0.0058 \text{ ft}$$

Therefore, Equation 6-92 becomes

$$f_{a5} \qquad \dfrac{1}{\left[2 \; \log \; \dfrac{0.656 \quad 0.563}{0.0058} \quad 1.14 \right]^2}$$

$$f_{a5} \qquad 0.079$$

Equation 6-88 for the fifth increment in the annulus can be solved for the pressure at bottom of the increment, P_{a5}. This involves selecting this upper limit of the intergral by a trial and error procedure.   The magnitude of the upper limit pressure on the left side of the equation is selected to allow the left side integral to equal the right side integral. The integration can be carried out on the computer using one of the commercial analytic software programs.   The trial and error magnitude of the upper limit pressure that satisfies Equation 6-88 for this annulus section is

$$p_{a5} \qquad 1{,}116.2 \text{ psia}$$

$$P_{a5} \qquad p_{a5} \; 144$$

$$P_{a5} \qquad 160{,}728 \text{ lb/ft}^2 \text{ abs}$$

Substituting the values of $\dot{w}_t$, Q_g, Q_w, P_g, P_{a4}, P_{a5}, T_g, T_{av5}, D_h, D_4, f_{a5}, and g into the left side of Equation 6-88 gives

$$\int_{137,281}^{160,728} \frac{dP}{\cfrac{17.37}{\cfrac{58,477.0}{P}\,0.234}\left[1-\cfrac{0.079}{5.99}\cfrac{\left(\cfrac{58,477.0}{P}\,0.234\right)}{\cfrac{4}{}\,0.656^{2}\,0.563^{2}}\right]^{2}} = 500$$

Substituting the value of H_1, H_2, H_3, H_4 and H_5 into the right side of Equation 6-88 gives

$$\int_{6,650\ \ 350\ \ 2,375\ \ 125}^{6,650\ \ 350\ \ 2,375\ \ 125\ \ 500} 1\ dh \quad 500$$

As can be seen in the above, the right and left hand sides of Equation 6-88 yield the same answer. This shows that the upper limit pressure is correct.

At this point in the calculation process it is necessary check the two controlling criteria. These are the foam quality at the bottom of the annulus and the kinetic energy per unit volume of the flowing foam at a position just above the drill collars.

Using Equation 4-11, the approximate specific weight of the gas at the bottom of the annulus is determined from P_{a5}. This is

$$\gamma_{gbh} \quad \frac{(160,728)\ (1.0)}{(53.36)\ (604.41)}$$

$$\gamma_{gbh} \quad 4.984\ \text{lb/ft}^3$$

The volumetric flowrate of the gas at the bottom of the annulus is

$$Q_{gbh} \quad \frac{\dot{w}_g}{\gamma_{gbh}}$$

$$Q_{gbh} \quad \frac{1.821}{4.984}$$

$$Q_{gbh} \quad 0.365\ \text{ft}^3/\text{sec}$$

The foam quality at the bottom of the annulus is

$$\gamma_{sfbh} \quad \frac{Q_{gbh}}{Q_{gbh}\quad Q_w}$$

$$S_{fbh} = \frac{0.365}{0.365 + 0.234}$$

$$S_{fbh} = 0.610$$

The lumped geometry analysis provides a methodology for determining the approximate pressures in the annulus. These pressures can be used to determine the kinetic energy per unit volume value using the actual drill pipe outside diameter at the critical position just above the drill collars (where the kinetic energy per unit volume should be a minimum).

The specific weight of the foam as it exits the openhole drill collar annulus section was determined above to be

$$\gamma_{fa5} = 24.881 \ \text{lb/ft}^3$$

The average velocity of the foam just above the drill collar annulus section as it flows around the drill pipe body is

$$V_{sfake} = \frac{\frac{P_{at}}{P_{a4}} \frac{T_{av5}}{T_{at}} Q_g + Q_w}{\frac{\pi}{4} \left(D_h^2 - D_2^2 \right)}$$

$$V_{sfake} = \frac{\frac{1,826.6}{137,281} \frac{601.91}{519.67} (27.64) + 0.234}{\frac{\pi}{4} \left(0.656^2 - 0.375^2 \right)}$$

$$V_{sfake} = 2.90 \ \text{ft/sec}$$

Using Equation 1-2, the density of the foam at this position in the annulus is

$$\rho_{sfake} = \frac{\gamma_{fa5}}{g}$$

$$\rho_{sfake} = \frac{24.881}{32.2}$$

$$\rho_{sfake} = 0.773 \ \frac{\text{lb} \cdot \text{sec}^2}{\text{ft}^4}$$

Using Equation 1-1, the kinetic energy per unit volume at this position in the annulus is

$$KE_{sfake} = \frac{1}{2} \gamma_{sfake} V_{sfake}^2$$

$$KE_{sfake} = \frac{1}{2} (0.773)(2.90)^2$$

$$KE_{sfake} = 3.24 \frac{ft\text{-}lb}{ft^3}$$

The overall trial and error process has selected the approximate value of q_w that restricts the foam quality at the bottom of the annulus to slightly above 0.60 and restricts the minimum kinetic energy per unit volume in the annulus to slightly above 3.00 ft-lb/ft³. In this example the foam quality criteria appears to be the controlling criteria for the trial and error process since interative changes in q_w appear to approach the foam quality limit more rapidly than the kinetic energy per unit volume limit.

Drill Bit Nozzles

For this example the components of the stable foam (water and surfactant) are injected into the top of the inside of the drill string. The foam is generated at the bottom of the well when these components pass through the small drill bit nozzles. Therefore, the flow of these components down the drill string and through the drill bit nozzles is assumed to be aerated flow (as described in Chapter 9).

It is assumed that the 7 7/8 inch tri-cone roller cone drill bit is equipped with three 9/32 inch diameter jet nozzles. Therefore, the inside diameter of each nozzle D_n, is

$$d_n = 0.2813 \text{ inches}$$

$$D_n = \frac{d_n}{12}$$

$$D_n = 0.02344 \text{ ft}$$

From Equation 6-94, the equivalent single diameter for this drill bit, D_e, is

$$D_e = \sqrt{3 (0.02813)^2}$$

$$D_e = 0.0406 \text{ ft}$$

The approximate specific weight of the aerated fluid at the bottom of the annulus (just as it passes through the nozzles), γ_{mixbh}, is

$$\gamma_{mixbh} = \frac{\dot{w}_g + \dot{w}_w}{\dfrac{P_g}{P_{a5}}\dfrac{T_5}{T_g} Q_g + Q_w}$$

Substituting the values of $\dot{w}_g$, $\dot{w}_w$, P_g, P_{a5}, T_g, T_5, Q_g, and Q_w into the above equation gives, the specific weight of the aerated fluid mixture at the bottom of the annulus is

$$\gamma_{mixbh} = \frac{1.821 + 14.60}{\dfrac{1,826.6}{160,728}\dfrac{604.41}{519.67} (27.64) + 0.234}$$

$$\gamma_{mixbh} = 27.4 \ \text{lb/ft}^3$$

Using Equation 6-93, the pressure change in the aerated fluid through the drill bit, ΔP_b, can be approximated by

$$\Delta P_b = \frac{(1.821 + 14.60)^2}{2 (32.2) (27.4) (0.81)^2 \left(\dfrac{\pi}{4} 0.0406^2\right)^4}$$

$$\Delta P_b = 139,001 \ \text{lb/ft}^2$$

where the nozzle loss coefficient is taken to be 0.81 (see Chapter 6, Section 6.5).

Using Equation 6-95, the pressure in the aerated fluid just above the drill bit inside the drill string, P_{i5}, is

$$P_{i5} = P_{a5} + \Delta P_b$$

Using the above equation, the pressure in the aerated fluid just above the drill bit inside the drill string is

$$P_{i5} = 160,728 + 139,001$$

$$P_{i5} = 299,729 \ \text{lb/ft}^2 \ \text{abs}$$

$$p_{i5} = \frac{P_{i5}}{144}$$

$$p_{i5} = 2,082 \ \text{psia}$$

Geometry Inside the Drill String
Starting at the bottom of the drill string, the total length of the drill collars increment, H_5, in the openhole section is

$$H_5 \quad 500 \text{ ft}$$

The inside diameter of the drill collars length in this openhole section is

$$d_5 \quad 2.8125 \text{ inches}$$

$$D_5 \quad \frac{d_5}{12}$$

$$D_5 \quad 0.234 \text{ ft}$$

The total length of the drill pipe tool joints lumped geometry increment, H_4, in the openhole section is

$$H_4 \quad 125 \text{ ft}$$

The inside diameter of the drill pipe tool joints lumped geometry in this openhole section is

$$d_6 \quad 3.50 \text{ inches}$$

$$D_6 \quad \frac{d_6}{12}$$

$$D_6 \quad 0.292 \text{ ft}$$

The total length of the drill pipe body lumped geometry increment, H_3, in the openhole section is

$$H_3 \quad 2,375 \text{ ft}$$

The inside diameter of the drill pipe body lumped geometry in this openhole section is

$$d_7 \quad 3.826 \text{ inches}$$

$$D_7 \quad \frac{d_7}{12}$$

$$D_7 \quad 0.319 \text{ ft}$$

The total length of the lumped drill pipe tool joints geometry increment, H_2, in the cased section is

$$H_2 \qquad 350 \text{ ft}$$

The inside diameter of the drill pipe tool joints lumped geometry in this cased section is

$$D_6 \qquad 0.292 \text{ ft}$$

The total length of the lumped drill pipe body geometry increment, H_1, in the cased section is

$$H_1 \qquad 6,650 \text{ ft}$$

The inside diameter of the drill pipe body lumped geometry in this cased section is

$$D_7 \qquad 0.319 \text{ ft}$$

Inside the Drill String (10,000 ft to 7,000 ft)

The fifth drill string section increment is denoted by the length H_5. The temperature at the bottom of the drill collars (bottomhole temperature) in the openhole section is

$$T_5 \qquad 604.41°\text{R}$$

The average temperature of the drill collar length H_5 and, thus, the temperature of the aerated fluid flow inside the drill collars is

$$T_{av5} \qquad 601.91°\text{R}$$

In order to obtain the approximate value of the Fanning friction factor for Equation 6-102, it is necessary to estimate the Reynolds number and, thus, the flow conditions inside the drill collars along H_5. This is accomplished by determining the Reynolds number at the entrance end of the inside of the drill collar section and assuming this Reynolds number approximates the flow conditions throughout the inside of the drill collar section.

The absolute viscosity of the gas (air) at atmospheric conditions, $_g$, is

$$_g \qquad 0.012 \text{ cps}$$

$$_g \qquad (0.012)\ (0.001)\ (0.02089)$$

$$\mu_g \quad 0.000000251 \ \frac{\text{lb} \ \text{sec}}{\text{ft}^2}$$

Using Equation 4-11, the approximate specific weight of the gas as it enters this drill collar section is determined from P_{i5}. This is

$$\gamma_{gi5} \quad \frac{(299,729) \ (1.0)}{(53.36) \ (601.91)}$$

$$\gamma_{gi5} \quad 9.33 \ \text{lb/ft}^3$$

Using Equation 1-2, the density of the gas as it enters this drill collar section, ρ_{gi5}, is

$$\rho_{gi5} \quad \frac{9.33}{32.2}$$

$$\rho_{gi5} \quad 0.290 \ \frac{\text{lb} \ \text{sec}^2}{\text{ft}^4}$$

From Equation 9-7, the kinematic viscosity of the gas at this location, ν_{gi5}, is

$$\nu_{gi5} \quad \frac{0.000000251}{0.290}$$

$$\nu_{gi5} \quad 0.000000865 \ \frac{\text{ft}^2}{\text{sec}}$$

The absolute viscosity of the water (and surfactant), μ_w, is assumed to be approximately

$$\mu_w \quad 1 \ \text{cps}$$

$$\mu_w \quad (1.0) \ (0.001) \ (0.2089)$$

$$\mu_w \quad 0.00002089 \ \frac{\text{lb} \ \text{sec}}{\text{ft}^2}$$

Using Equation 1-2, the density of the incompressible fluid, ρ_w, is

$$\rho_w \quad \frac{62.4}{32.2}$$

$$\rho_w \quad 1.938 \quad \frac{\text{lb} \quad \text{sec}^2}{\text{ft}^4}$$

From Equation 9-7, the kinematic viscosity of the incompressible, ν_w, is

$$\nu_w \quad \frac{0.00002089}{1.938}$$

$$\nu_w \quad 0.00001078 \quad \frac{\text{ft}^2}{\text{sec}}$$

The average kinematic viscosity of the mixture as it enters this drill collar section, ν_{avi5}, is

$$\nu_{avi5} \quad \frac{(1.821)\,(0.000000865) \quad (14.60)\,(0.00001078)}{1.821 \quad 14.60}$$

$$\nu_{avi5} \quad 0.00000968 \ \text{ft}^2/\text{sec}$$

Using the inside diameter of the drill collars, D_5, the approximate average velocity of the aerated drilling fluid as it enters this drill collar section, V_{i5}, is

$$V_{i5} \quad \frac{\dfrac{1,826.6}{299,729} \quad \dfrac{601.91}{519.67} \quad (27.64) \quad 0.234}{\dfrac{\pi}{4} \quad 0.234^2}$$

$$V_{i5} \quad 9.94 \ \text{ft/sec}$$

Using Equation 6-103, the Reynolds number of the aerated drilling fluid as it enters this drill collar section, N_{Ri5}, is

$$N_{Ri5} \quad \frac{(9.94)\,(0.234)}{0.00000968}$$

$$N_{Ri5} \quad 240,763$$

The Reynolds number calculation above is greater than 4,000. This indicates that the flow condition is turbulent. Therefore, the empirical von Karman equation (i.e., Equation 6-106) is used to determine the approximate Fanning friction factor for the aerated fluid flow inside drill collars.

The inside surface of the drill collars is commercial steel with the surface roughness

e_p 0.00015 ft

With the above, Equation 6-106 becomes

$$f_{i5} \qquad \cfrac{1}{\left(2 \ \log \ \cfrac{0.234}{0.00015} \ \ 1.14 \right)^2}$$

f_{i5} 0.018

Equation 6-102 for the fifth increment inside the drill string can be solved for the pressure at the top of the increment, P_{i4}. This involves selecting this lower limit by a trial and error procedure. The magnitude of the lower limit pressure on the left side of the equation is selected to allow the left side integral to equal the right side integral.   The integration can be carried out on the computer using one of the commercial analytic software programs. The trial and error magnitude of the lower limit pressure is

p_{i4} 1,935.1 psia

P_{i4} p_{i4} 144

P_{i4} 278,659 lb/ft^2 abs

Substituting the values of $\dot{w}_g$, $\dot{w}_w$, Q_g, Q_w, P_g, P_{i4}, P_{i5}, T_g, T_{av5}, D_5, f_{i5}, and g into the left side of Equation 6-102 gives

$$\exists^{\,299,729}_{\substack{ \&\\ \&\\ \&\\ \&\\ \&\\ \&\\ \%278,659 }} \cfrac{dP}{\cfrac{16.42}{\cfrac{58,477.0}{P} \ \ 0.234} \ \ 1 \ \ \cfrac{0.018}{15.07} \ \ \cfrac{\left(\cfrac{58,477.0}{P} \ \ 0.234\right)^2}{\cfrac{}{4} \ \ 0.234^2}} \ \forall^{\,500}_{\ \#}$$

Substituting the values of H_1, H_2, H_3, H_4, and H_5 into the right side of Equation 6-102 gives

$$\int^{6,650 \ \ 350 \ \ 2.375 \ \ 125 \ \ 500}_{6,650 \ \ 350 \ \ 2,375 \ \ 125} \ 1 \ dh \qquad 500$$

As can be seen in the above, the right and left hand sides of Equation 6-102 yield the same answer. This shows that the lower limit pressure is correct.

The fourth drill string section increment is denoted by the length H_4. The temperature at the bottom of the drill pipe tool joints lumped geometry in the openhole section is

$$T_4 \quad 599.41°R$$

The average temperature of the drill pipe tool joints lumped geometry along H_4 and, thus, the temperature of the aerated fluid flow inside the drill string length is

$$T_{av4} \quad 598.79°R$$

In order to obtain the approximate value of the Fanning friction factor for Equation 6-102, it is necessary to estimate the Reynolds number and, thus, the flow conditions inside the drill pipe tool joints lumped geometry along H_4. This is accomplished by determining the Reynolds number at the entrance end of the inside of this drill string section and assuming this Reynolds number approximates the flow conditions throughout the inside this drill string section.

Using Equation 4-11, the approximate specific weight of the gas as it enters this drill string section is determined from P_{i4}. This is

$$\gamma_{gi4} \quad \frac{(278,659)\,(1.0)}{(53.36)\,(598.79)}$$

$$\gamma_{gi4} \quad 8.72 \ \text{lb/ft}^3$$

Using Equation 1-2, the density of the gas as it enters this drill string section, ρ_{gi4}, is

$$\rho_{gi4} \quad \frac{8.72}{32.2}$$

$$\rho_{gi4} \quad 0.271 \ \frac{\text{lb} \ \ \text{sec}^2}{\text{ft}^4}$$

From Equation 9-7, the kinematic viscosity of the gas at this location, ν_{gi4}, is

$$\nu_{gi4} \quad \frac{0.000000251}{0.271}$$

$$\nu_{gi4} \quad 0.000000926 \ \frac{\text{ft}^2}{\text{sec}}$$

The average kinematic viscosity of the mixture as it enters this drill string section, $_{avi4}$, is

$$_{avi4} \quad \frac{(1.821)\,(0.000000926) \quad (14.60)\,(0.00001078)}{1.821 \quad 14.60}$$

$$_{avi4} \quad 0.00000969 \ \text{ft}^2/\text{sec}$$

Using the inside diameter of the drill pipe tool joints, D_6, the approximate average velocity of the aerated drilling fluid as it enters this drill string section, V_{i4}, is

$$V_{i4} \quad \frac{\dfrac{1,826.6}{278,659} \quad \dfrac{598.79}{519.67}\ (27.64) \quad 0.234}{\dfrac{}{4}\ \ 0.292\ ^2}$$

$$V_{i4} \quad 6.63 \ \text{ft/sec}$$

Using Equation 6-103, the Reynolds number of the aerated drilling fluid as it enters this drill string section, N_{Ri4}, is

$$\mathbf{N_{Ri4}} \quad \frac{(6.63)\,(0.292)}{0.00000969}$$

$$\mathbf{N_{Ri4}} \quad 199,492$$

The Reynolds number calculation above is greater than 4,000. This indicates that the flow condition is turbulent. Therefore, the empirical von Karman equation (i.e., Equation 6-106) is used to determine the approximate Fanning friction factor for the aerated fluid flow inside this drill string section.

The inside surface of the drill pipe tool joints is commercial steel with the surface roughness

$$e_p \quad 0.00015 \ \text{ft}$$

With the above, Equation 6-106 becomes

$$f_{i4} \quad \frac{1}{\left(2\ \log\ \dfrac{0.292}{0.00015} \quad 1.14\right)^{2}}$$

$$f_{i4} \quad 0.017$$

Equation 6-102 for the fourth increment inside the drill string can be solved for the pressure at the top of the increment, P_{i3}. This involves selecting this lower limit by a trial and error procedure. The magnitude of the lower limit pressure on the left side of the equation is selected to allow the left side integral to equal the right side integral. The integration can be carried out on the computer using one of the commercial analytic software programs. The trial and error magnitude of the lower limit pressure is

$$p_{i3} \quad 1,901.8 \ \text{psia}$$

$$P_{i3} \quad p_{i3} \ 144$$

$$P_{i3} \quad 273,856 \ \text{lb/ft}^2 \ \text{abs}$$

Substituting the values of $\dot{w}_g$, $\dot{w}_w$, Q_g, Q_w, P_g, P_{i3}, P_{i4}, T_g, T_{av4}, D_6, f_{i4}, and g into the left side of Equation 6-102 gives

$$\int_{273,856}^{278,659} \frac{dP}{\frac{16.42}{\frac{58,173.9}{P} \ 0.234} \ 1 \ \frac{0.017}{18.80} \ \frac{\frac{58,173.9}{P} \ 0.234}{-\frac{}{4} \ 0.292} \ ^2} \quad 125$$

Substituting the values of H_1, H_2, H_3, and H_4 into the right side of Equation 6-102 gives

$$\int_{6,650 \ 350 \ 2,375}^{6,650 \ 350 \ 2.375 \ 125} 1 \ dh \quad 125$$

As can be seen in the above, the right and left hand sides of Equation 6-102 yield the same answer. This shows that the lower limit pressure is correct.

The third drill string section increment is denoted by the length H_3. The temperature at the bottom of the drill pipe body lumped geometry in the openhole section is

$$T_3 \quad 598.16°R$$

The average temperature of the drill pipe body lumped geometry along H_3 and, thus, the temperature of the aerated fluid flow inside the this drill string length is

$$T_{av3} \qquad 586.29°R$$

In order to obtain the approximate value of the Fanning friction factor for Equation 6-102, it is necessary to estimate the Reynolds number and, thus, the flow conditions inside the drill pipe body lumped geometry along H_3.   This is accomplished by determining the Reynolds number at the entrance end of the inside of this drill string section and assuming this Reynolds number approximates the flow conditions throughout the inside this drill string section.

Using Equation 4-11, the approximate specific weight of the gas as it enters this drill string section is determined from P_{i3}.   This is

$$\gamma_{gi3} \qquad \frac{(273,856)\ (1.0)}{(53.36)\ (586.29)}$$

$$\gamma_{gi3} \qquad 8.75\ \text{lb/ft}^3$$

Using Equation 1-2, the density of the gas as it enters this drill string section, γ_{gi3}, is

$$\gamma_{gi3} \qquad \frac{8.75}{32.2}$$

$$\gamma_{gi3} \qquad 0.272\ \frac{\text{lb}\quad\text{sec}^2}{\text{ft}^4}$$

From Equation 9-7, the kinematic viscosity of the gas at this location, γ_{gi3}, is

$$\gamma_{gi3} \qquad \frac{0.000000251}{0.272}$$

$$\gamma_{gi3} \qquad 0.000000922\ \frac{\text{ft}^2}{\text{sec}}$$

The average kinematic viscosity of the mixture as it enters this drill string section, γ_{avi3}, is

$$\gamma_{avi3} \qquad \frac{(1.821)\ (0.000000922)\qquad (14.60)\ (0.00001078)}{1.821 \qquad 14.60}$$

$$\gamma_{avi3} \qquad 0.00000969\ \text{ft}^2/\text{sec}$$

Using the inside diameter of the drill pipe tool body, D_7, the approximate average velocity of the aerated drilling fluid as it enters this drill string section, V_{i3}, is

$$V_{i3} \quad \frac{\dfrac{1,826.6}{273,856} \quad \dfrac{586.29}{519.67} \quad (27.64) \quad 0.234}{\dfrac{-}{4} \quad 0.319 \quad ^2}$$

$$V_{i3} \quad 5.54 \text{ ft/sec}$$

Using Equation 6-103, the Reynolds number of the aerated drilling fluid as it enters this drill string section, $\mathbf{N_{Ri3}}$, is

$$\mathbf{N_{Ri3}} \quad \frac{(5.54)\ (0.319)}{0.00000969}$$

$$\mathbf{N_{Ri3}} \quad 182,182$$

The Reynolds number calculation above is greater than 4,000. This indicates that the flow condition is turbulent. Therefore, the empirical von Karman equation (i.e., Equation 6-106) is used to determine the approximate Fanning friction factor for the aerated fluid flow inside this drill string section.

The inside surface of the drill pipe body is commercial steel with the surface roughness

$$e_p \quad 0.00015 \ ft$$

With the above, Equation 6-106 becomes

$$f_{i3} \quad \frac{1}{2\ \log \ \dfrac{0.319}{0.00015} \quad 1.14}^{\ 2}$$

$$f_{i3} \quad 0.016$$

Equation 6-102 for the third increment inside the drill string can be solved for the pressure at the top of the increment, P_{i2}. This involves selecting this lower limit by a trial and error procedure. The magnitude of the lower limit pressure on the left side of the equation is selected to allow the left side integral to equal the right side integral. The integration can be carried out on the computer using one of the

commercial analytic software programs. The trial and error magnitude of the lower limit pressure is

p_{i2} $1,323.3$ psia

P_{i2} p_{i2} 144

P_{i2} $190,555$ lb/ft^2 abs

Substituting the values of $\dot{w}_g$, $\dot{w}_w$, Q_g, Q_m, P_g, P_{i2}, P_{i3}, T_g, T_{av3}, D_7, f_{i3}, and g into the left side of Equation 6-102 gives

$$\int_{190,555}^{273,856} \frac{dP}{\dfrac{16.42}{\dfrac{56,959.5}{P} \ 0.234} \ 1 \ \dfrac{0.016}{20.54} \ \dfrac{\dfrac{56,959.5}{P} \ 0.234}{-\dfrac{0.319}{4} \ ^2} \ ^2} = 2,375$$

Substituting the values of H_1, H_2, and H_3 into the right side of Equation 6-102 gives

$$\int_{6,650 \ \ 350}^{6,650 \ \ 350 \ \ 2,375} 1 \ dh = 2,375$$

As can be seen in the above, the right and left hand sides of Equation 6-102 yield the same answer. This shows that the lower limit pressure is correct.

Inside the Drill String (7,000 ft to Surface)

The second drill string section increment is denoted by the length H_2. The temperature at the bottom of the drill pipe tool joints lumped geometry in the cased section is

T_2 $574.41°R$

The average temperature of the drill pipe tool joints lumped geometry along H_2 and, thus, the temperature of the aerated fluid flow inside the this drill string length is

T_{av2} $572.66°R$

In order to obtain the approximate value of the Fanning friction factor for Equation 6-102, it is necessary to estimate the Reynolds number and, thus, the flow conditions inside the drill pipe tool joints lumped geometry along H_2. This is accomplished by determining the Reynolds number at the entrance end of the inside

of this drill string section and assuming this Reynolds number approximates the flow conditions throughout the inside this drill string section.

Using Equation 4-11, the approximate specific weight of the gas as it enters this drill string section is determined from P_{i1}.   This is

$$\gamma_{gi2} \quad \frac{(190,555)\ (1.0)}{(53.36)\ (572.66)}$$

$$\gamma_{gi2} \quad 6.24 \ \text{lb/ft}^3$$

Using Equation 1-2, the density of the gas as it enters this drill string section, γ_{gi2}, is

$$\gamma_{gi2} \quad \frac{6.24}{32.2}$$

$$\gamma_{gi2} \quad 0.194 \ \frac{\text{lb} \ \text{sec}^2}{\text{ft}^4}$$

From Equation 9-7, the kinematic viscosity of the gas at this location, γ_{gi2}, is

$$\gamma_{gi2} \quad \frac{0.000000251}{0.194}$$

$$\gamma_{gi2} \quad 0.00000129 \ \frac{\text{ft}^2}{\text{sec}}$$

The average kinematic viscosity of the mixture as it enters this drill string section, γ_{avi2}, is

$$\gamma_{avi2} \quad \frac{(1.821)\ (0.00000129) \quad (14.60)\ (0.00001078)}{1.821 \quad 14.60}$$

$$\gamma_{avi2} \quad 0.00000973 \ \text{ft}^2/\text{sec}$$

Using the inside diameter of the drill pipe tool joints, D_6, the approximate average velocity of the aerated drilling fluid as it enters this drill string section, V_{i2}, is

$$V_{i2} \quad \cfrac{\cfrac{1,826.6}{190,555} \quad \cfrac{572.66}{519.67} \quad (27.64) \quad 0.234}{-\dfrac{}{4} \quad 0.292^{\,2}}$$

$$V_{i2} \quad 7.87 \;\; \text{ft/sec}$$

Using Equation 6-103, the Reynolds number of the aerated drilling fluid as it enters this drill string section, N_{Ri2}, is

$$\mathbf{N_{Ri2}} \quad \frac{(7.87)\,(0.292)}{0.00000973}$$

$$\mathbf{N_{Ri2}} \quad 235,987$$

The Reynolds number calculation above is greater than 4,000. This indicates that the flow condition is turbulent. Therefore, the empirical von Karman equation (i.e., Equation 6-106) is used to determine the approximate Fanning friction factor for the aerated fluid flow inside this drill string section.
The inside surface of the drill pipe tool joints is commercial steel with the surface roughness

$$e_p \quad 0.00015 \;\; \text{ft}$$

With the above, Equation 6-106 becomes

$$f_{i2} \quad \cfrac{1}{2\;\log \;\cfrac{0.292}{0.00015}\quad 1.14}^{\,2}$$

$$f_{i2} \quad 0.017$$

Equation 6-102 for the second increment inside the drill string can be solved for the pressure at the top of the increment, P_{i1}. This involves selecting this lower limit by a trial and error procedure. The magnitude of the lower limit pressure on the left side of the equation is selected to allow the left side integral to equal the right side integral. The integration can be carried out on the computer using one of the commercial analytic software programs. The trial and error magnitude of the lower limit pressure is

$$p_{i1} \quad 1,244.4 \;\; \text{psia}$$

$$P_{i1} \qquad p_{i1} \ 144$$

$$P_{i1} \qquad 179{,}196 \ \text{lb/ft}^2 \ \text{abs}$$

Substituting the values of $\dot{w}_g$, $\dot{w}_w$, Q_g, Q_m, P_g, P_{i1}, P_{i2}, T_g, T_{av2}, D_6, f_{i2}, and g into the left side of Equation 6-102 gives

$$\int_{179{,}196}^{190{,}555} \cfrac{dP}{\cfrac{16.42}{\cfrac{55{,}635.3}{P}^{0.234}} \left[1 + \cfrac{0.017}{18.80} \cfrac{\left(\cfrac{55{,}635.3}{P}\right)^{0.234}}{\cfrac{1}{4} \, 0.292^{2}} \right]^{2}} \qquad 350$$

Substituting the values of H_1, and H_2 into the right side of Equation 6-102 gives

$$\int_{6{,}650}^{6{,}650 \ 350} 1 \, dh \qquad 350$$

As can be seen in the above, the right and left hand sides of Equation 6-102 yield the same answer. This shows that the lower limit pressure is correct.

The first drill string section increment is denoted by the length H_1. The temperature at the bottom of the drill pipe body lumped geometry in the cased section is

$$T_1 \qquad 570.91°R$$

The average temperature of the drill pipe body lumped geometry along H_1 and, thus, the temperature of the aerated fluid flow inside the this drill string length is

$$T_{av1} \qquad 537.66°R$$

In order to obtain the approximate value of the Fanning friction factor for Equation 6-102, it is necessary to estimate the Reynolds number and, thus, the flow conditions inside the drill pipe body lumped geometry along H_1. This is accomplished by determining the Reynolds number at the entrance end of the inside of this drill string section and assuming this Reynolds number approximates the flow conditions throughout the inside this drill string section.

Using Equation 4-11, the approximate specific weight of the gas as it enters this drill string section is determined from P_{in}. This is

$$\rho_{gi1} \quad \frac{(179{,}196)\ (1.0)}{(53.36)\ (537.66)}$$

$$\rho_{gi1} \quad 6.25\ \text{lb/ft}^3$$

Using Equation 1-2, the density of the gas as it enters this drill string section, γ_{gi1}, is

$$\gamma_{gi1} \quad \frac{6.25}{32.2}$$

$$\gamma_{gi1} \quad 0.194\ \frac{\text{lb}\ \ \text{sec}^2}{\text{ft}^4}$$

From Equation 9-7, the kinematic viscosity of the gas at this location, ν_{gi1}, is

$$\nu_{gi1} \quad \frac{0.000000251}{0.194}$$

$$\nu_{gi1} \quad 0.00000129\ \frac{\text{ft}^2}{\text{sec}}$$

The average kinematic viscosity of the mixture as it enters this drill string section, ν_{avi1}, is

$$\nu_{avi1} \quad \frac{(1.821)\ (0.00000129)\quad (14.60)\ (0.00001078)}{1.821 \qquad 14.60}$$

$$\nu_{avi1} \quad 0.00000973\ \text{ft}^2/\text{sec}$$

Using the inside diameter of the drill pipe tool joints, D_7, the approximate average velocity of the aerated drilling fluid as it enters this drill string section, V_{i1}, is

$$V_{i1} \quad \frac{\dfrac{1{,}826.6}{179{,}196}\ \dfrac{537.66}{519.67}\ (27.64)\quad 0.234}{\dfrac{}{4}\ 0.319^{\,2}}$$

$$V_{i1} \quad 6.58\ \text{ft/sec}$$

Using Equation 6-103, the Reynolds number of the aerated drilling fluid as it enters this drill string section, N_{Ri2}, is

$$N_{Ri1} \quad \frac{(6.58)\ (0.319)}{0.00000973}$$

$$N_{Ril} \quad 215,692$$

The Reynolds number calculation above is greater than 4,000. This indicates that the flow condition is turbulent. Therefore, the empirical von Karman equation (i.e., Equation 6-106) is used to determine the approximate Fanning friction factor for the aerated fluid flow inside this drill string section.

The inside surface of the drill pipe tool joints is commercial steel with the surface roughness

$$e_p \quad 0.00015 \ \text{ft}$$

With the above, Equation 6-106 becomes

$$f_{i1} \quad \frac{1}{\left[2\ \log\ \dfrac{0.319}{0.00015}\ 1.14 \right]^2}$$

$$f_{i1} \quad 0.016$$

Equation 6-102 for the first increment inside the drill string can be solved for the pressure at the top of the increment, P_{in}. This involves selecting this lower limit by a trial and error procedure. The magnitude of the lower limit pressure on the left side of the equation is selected to allow the left side integral to equal the right side integral. The integration can be carried out on the computer using one of the commercial analytic software programs. The trial and error magnitude of the lower limit pressure is

$$p_{in} \quad 229.3 \ \text{psia}$$

$$P_{in} \quad p_{in}\ 144$$

$$P_{in} \quad 33,022 \ \text{lb/ft}^2 \ \text{abs}$$

Substituting the values of $\dot{w}_g$, $\dot{w}_w$, Q_g, Q_w, P_g, P_{in}, P_{i1}, T_g, T_{av1}, D_7, f_{i1}, and g into the left side of Equation 6-102 gives

$$179,196 = \left\{ \frac{dP}{\cfrac{16.42}{\left(\cfrac{52,235.0}{P}\right)^{0.234}} \left[1 - \cfrac{0.016}{20.54} \cfrac{\left(\cfrac{52,235.0}{P}\right)^{0.234}}{\cfrac{\pi}{4}(0.319)^2} (0.234)^2 \right]} \right\}_{33,022}^{6,650}$$

Substituting the values of H_1 into the right side of Equation 6-102 gives

$$\int_0^{6,650} 1 \, dh = 6,650$$

As can be seen in the above, the right and left hand sides of Equation 6-102 yield the same answer. This shows that the lower limit pressure is correct.

   The injection pressure while drilling at 10,000 ft of depth is approximately 229 psia. This is the approximate injection pressure for both the compressed air and the incompressible fluid (water and surfactant) as they enter the surface flow lines that lead to the top of the drill string. When drilling at a depth of 10,000 ft, the corresponding for the injection pressure above is an air volumetric flow rate of 1,658 acfm (with an incompressible fluid volumetric flow rate of 105 gal/hr). This compressed air injection pressure is the pressure the compressor output must match.

   Figure 10-3 shows the stable foam pressures in the annulus and the aerated fluid (both air and incompressible fluid) pressures inside the drill string as a function of depth for this illustrative example (while drilling at the depth of 10,000 ft). The figure shows the pressure at the bottom of the annulus is approximately 1,116 psia (p_{a5} above). If a target oil or natural gas rock formation pore pressure at the bottom of the borehole is above this value, the oil or natural gas will flow into the borehole as the drill bit is advanced into the producing rock formation. This would constitute an underbalanced drilling situation. If the pore pressure is less than this value, rock cuttings from the advance of the drill bit will be forced into the exposed pores around the bottom of the borehole resulting in formation damage. However, since there are two controlling criteria (in the annulus) for stable foam drilling (namely, maintaining foam quality in the annulus at 0.60 or greater and maintaining the kinetic energy per unit volume at 3.00 ft-lb/ft^3 or greater) the bottomhole pressure in the annulus cannot be held constant while drilling an interval.

   The anticipated drilling rate of penetration is estimated to be 60 ft/hr. The vertical interval section to be drilled is from a depth of 7,000 ft to a depth of 10,000 ft, or a 3,000 ft length of borehole. Therefore, the estimated actual drilling time to drill this interval is approximately 50 hours. Using similar calculations as those given above, the injection pressures as a function of drilling depth and, thus, drilling time can be obtained. Figure 10-4 shows the injection pressure as a function of drilling time for the interval from 7,000 ft to 10,000 ft. The maximum injection pressure is approximately 275 psia and occurs at the beginning of the interval at a

depth of 7,000 ft.   The minimum injection pressure is approximately 229 psia and occurs at the end of the interval at a depth of 10,000 ft.
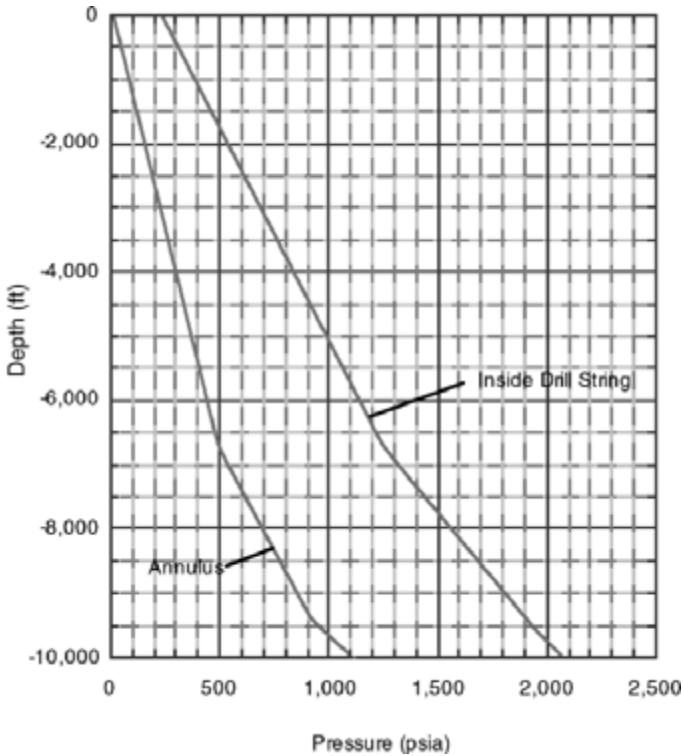
Figure 10-3: Pressure profile in the inside of the drill string and in the annulus for Illustrative Example 10.2 ($q_g = 1,658$ acfm and a drilling depth of 10,000 ft).

Figure 10-5 shows the water (and surfactant) injection volumetric flow rates as a function of drilling time for the interval from 7,000 ft to 10,000 ft.   The maximun volumetric flow rate of water (105 gal/min) occurs while drilling at a depth of 10,000 ft.   The minimum volumetric flow rate of water (78 gal/min) occurs while drilling at a depth of 7,000 ft.

Figure 10-6 shows the air injection volumetric flow rates as a function of drilling time for the interval from 7,000 ft to 10,000 ft.   The maximun volumetric flow rate of air (1,658 acfm) occurs while drilling at a depth of 10,000 ft.   The minimum volumetric flow rate of air (1,240 acfm) occurs while drilling at a depth of 7,000 ft.

Figure 10-7 shows the back pressure at the top of the annulus as a function of drilling time for the interval from 7,000 ft to 10,000 ft. The back pressure at the top of the annulus can be held constant at 17 psig while drilling the interval.
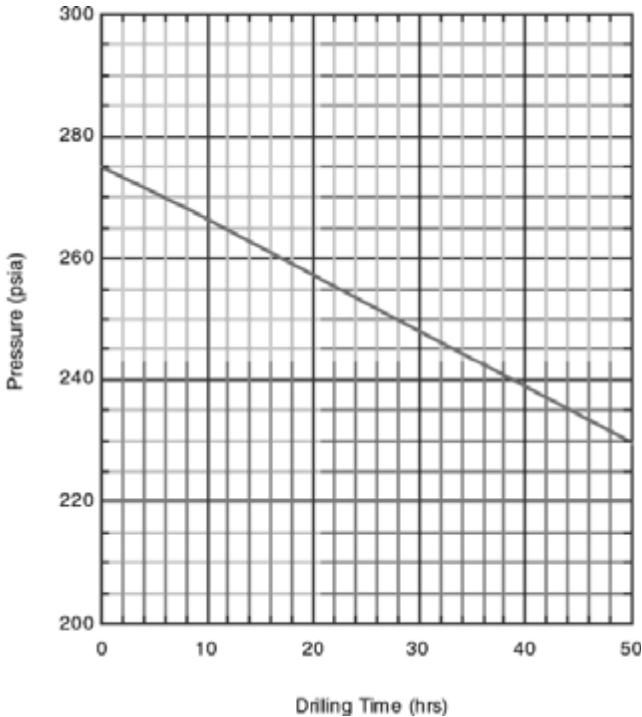
Figure 10-4: Drill string injection pressure as a function of drilling time (drilling depth) for Illustrative Example 10.2.

The data in Figures 10-4, 10-5, and 10-6 allow for the selection of the primary compressor unit to be used in the drilling operation. The primary compressor unit for a stable foam drilling operation is used in a different manner than its traditional use in an air drilling operation. As can be seen in Figures 10-5 and 10-6, the stable foam drilling operation requires varying both the water and air volumetric flow rates as the drilling progresses. These rates increase as the drilling depth is increased. Since primary compressors output a constant volumetric flow rate, it is necessary to measure (with a flow meter) the volumetric flow rate of air flowing to the top of the drill string and vent the remainder of the compressor output to the atmosphere through a vent line (assuming the required volumetric flow rate is less than the rated compressor output).

There are several possible candidate compressor units given in Section 4.7 of Chapter 4 that could be used to provide the compressed air for this example drilling operation. Since the volumetric flow rate of air required is from 1,240 acfm (drilling at 7,000 ft) to 1,658 acfm (drilling at 10,000 ft), the most appropriate is the semi-trailer mounted primary compressor unit with a Ingersoll Rand Model HHE, three stage, reciprocating piston primary compressor with a rated volumetric flow rate of 1,500 scfm (see Figure 4-26). This primary compressor has maximum pressure capability of 310 psig (at API Mechanical Equipment Standards standard conditions).
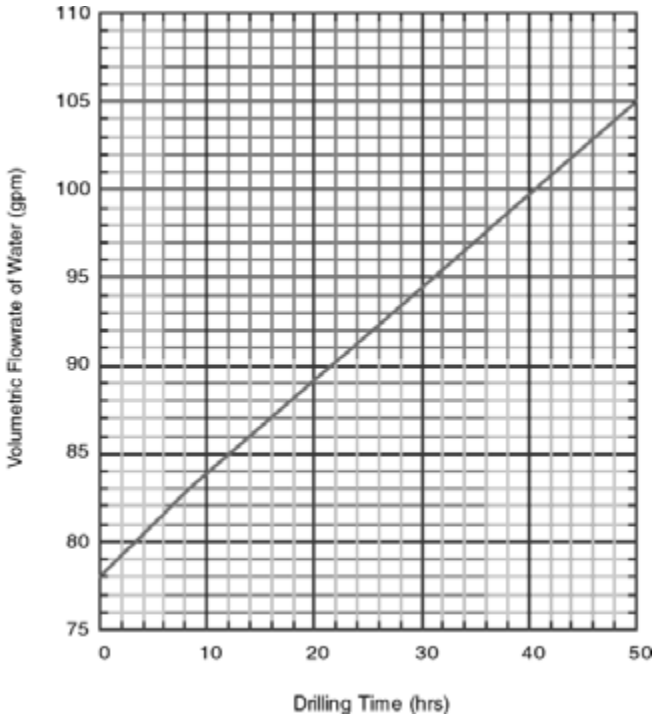
Figure 10-5: Drill string water (and surfactant) injection volumetric flow rate as a function of drilling time (drilling depth) for Illustrative Example 10.2.

The prime mover for this compressor unit is a diesel fueled, turbocharged, Caterpillar Model 3508 with a peak output of 644 horsepower at 1,000 rpm (at API standard conditions). One primary compressor unit can provide the stable foam drilling compressed air requirement for up to approximately 31 hours of drilling

(i.e., 1,860 ft of drilling interval or a depth of 8,860 ft, see Figure 10-6).   The primary compressor unit also has sufficient injection pressure capability to provide the injection pressure required by the foam drilling operation (see Figure 10-4). When the air volumetric flow rate requirement exceeds 1,500 acfm, a second primary compressor must be placed on line to provide the additional air to the foam operation.
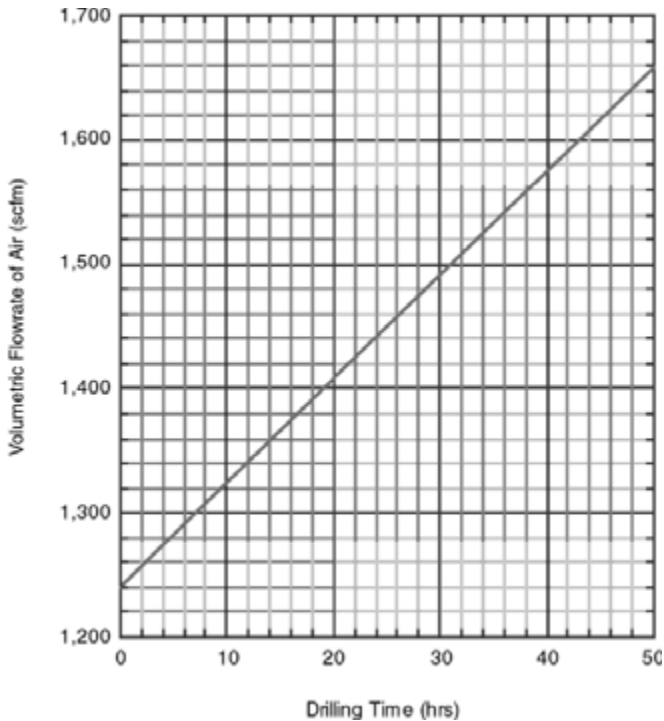
Figure 10-6: Drill string air injection volumetric flow rate as a function of drilling time (drilling depth) for Illustrative Example 10.2.

The last criteria is to check whether the prime mover of this primary compressor unit has the power to operate the compressor at the 4,000 ft surface elevation.   The highest injection pressure occurs while drilling out of the casing shoe at a depth of 7,000 ft.   This injection pressure is approximately 275 psia.   Even though the required air volumetric flow rate at this depth is approximately 1,240 acfm, the compressor must output the full 1,500 acfm (the remainder is vented).   The compressor is a three stage reciprocating piston compressor. Therefore,

$$n_s \qquad 3$$

The theoretical shaft horsepower, $\dot{W}_s$, required by the compressors is obtained from Equation 4-35a. Equation 4-35a becomes

$$\dot{W}_s \qquad \frac{(3)\,(1.4)}{(0.4)} \; \frac{(12.685)\;\;1,500}{229.17} \qquad \frac{275.0}{12.685} \,^{\frac{(0.4)}{(4)(1.4)}} \qquad 1$$

$$\dot{W}_s \qquad 296.8$$
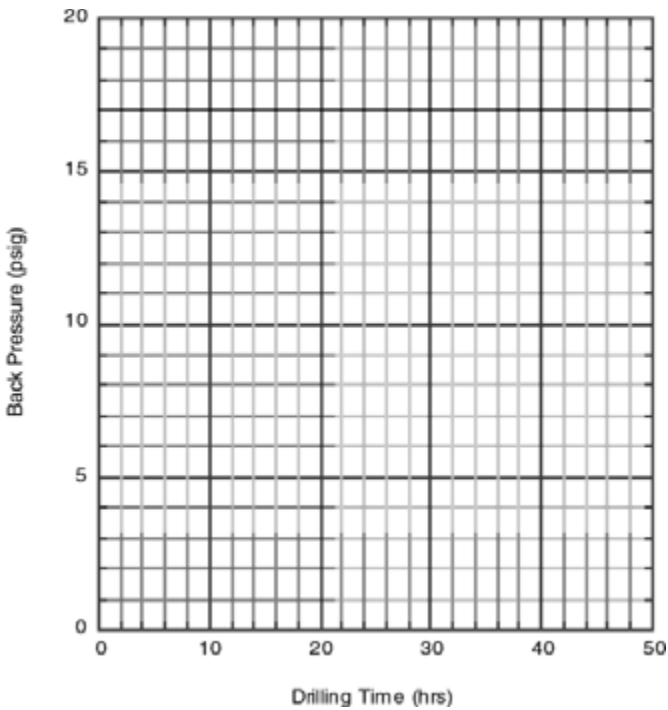
Figure 10-7: Back pressure at the top of the annulus as a function of drilling time (drilling depth) for Illustrative Example 10.2.

The mechanical efficiency, $\big(_m$, is

$$\gamma_m \quad 0.90$$

The first stage compressor ratio is

$$r_s \quad \left(\frac{275.0}{12.685}\right)^{\frac{1}{3}}$$

$$r_s \quad 2.79$$

The volumetric efficiency (only for the reciprocating piston compressor), γ_v, is determined from Equation 4-37. The compressor clearance volume ratio, c, is assumed to be 0.06. Equation 4-37 becomes

$$\gamma_v \quad 0.96 \quad 1 \quad 0.06 \quad 2.79^{\frac{1}{1.4}} \quad 1 \quad \overset{!}{\underset{\#}{\forall}}$$

$$\gamma_v \quad 0.899$$

From Equation 4-38, the actual shaft horsepower, $\dot{W}_{as}$, required by each compressor is

$$\dot{W}_{as} \quad \frac{296.8}{(0.90)\,(0.899)}$$

$$\dot{W}_{as} \quad 367.3$$

   The above determined 367.3 horsepower is the actual shaft power needed by each of the primary compressors to produce the 275 psia pressure output at the surface location elevation of 4,000 ft above sea level (while drilling at a depth of 7,000 ft).   At this surface location, the input horsepower available from the Caterpillar Model 3508 prime mover is a derated value (derated from the rated 644 horsepower available at 1,000 rpm). In order for the compressor unit to operate at this 4,000 ft surface location elevation, the derated input power available must be greater than the actual shaft power needed. Figure 4-15 shows that for 4,000 ft elevation the input power of a turbocharged prime mover must be derated by approximately 10 percent. The derated input horsepower, $\dot{W}_i$, available from the prime mover is

$$\dot{W}_i \quad 644\,(1 \quad 0.10)$$

$$\dot{W}_i \quad 579.6$$

For this illustrative example, the derated input power of the prime mover that operates the compressor is greater than the actual shaft horsepower needed by the compressor, thus, the selected compressor unit can be operated at this 4,000 ft surface location elevation (while drilling at a depth of 7,000 ft).

The volumetric flow rate of gas to create a stable foam drilling fluid is very dependent upon the flow resistance in the circulation system. This resistance is the sum of the major and minor flow friction losses in the flow system. This friction resistance creates choking of the circulation system and, therefore, generally increases the average pressure and in turn increases the average specific weight of the foam drilling fluid in the annulus and elsewhere in the circulation system. This can be seen by comparing the results from Illustrative Example 10.1 (non-friction) to those obtained from Illuatrative Example 10.2 (friction).

In general, foam drilling operations use a back pressure valve at or near the exit of the annulus. Thus, the main choking in the circulation system is the major and minor friction losses inside the drill string and in the annulus. However, by comparing the differences in the non-friction and friction results in Illustrative Examples 10.1 and 10.2 to the differences in the non-friction and friction results in Illustrative Examples 9.2 and 9.3 it can be seen that the differences are greater in the aerated drilling fluid examples. These larger differences are due to the fact that the aerated drilling fluid examples have used the natural flow resistance of the surface return flow line (which can be significant). The foam drilling fluid models have used a constant back pressure and, thus, the flow resistance of the surface return flow line has no effect on the calculations.

10.5 Prime Mover Fuel Consumption

In this section the fuel consumption of the prime mover for the compressor system will be discussed. Illustrative examples of the fuel consumption were discussed in detail in Chapter 4. In this section the illustrative example in this chapter will be completed with the calculation of the approximate fuel needed on the drilling location for the compressor system.

Illustrative Example 10.3 describes the implementation of the basic planning step No. 10 given in Section 10.1.

Illustrative Example 10.3 In Illustrative Example 10.2 the semi-trailer mounted unit with the Ingersoll Rand Model HHE, three-stage, reciprocating piston compressor system was selected for the drilling operation. In Illustrative Examples 10.2 the compressor unit was utilized to drill the interval from 7,000 ft to 10,000 ft. The compressor unit has a volumetric flow rate of 1,500 acfm. The compressed air flowing to the drilling operation varies over the drilled interval from 1,240 acfm to 1,658 acfm. But the compressor must output 1,500 acfm. The volumetric flow rate to the borehole must be varied as the interval is drilled and the excess is vented to the atmosphere. Therefore, to estimate the total diesel fuel needed by the compressor unit it is necessary to estimate the fuel consumption of the compressor units' Caterpillar Model 3508, diesel fueled, turbocharged, prime mover. The anticipated drilling rate of penetration is estimated to be 60 ft/hr. The vertical interval section to be drilled is from a depth of 7,000 ft to depth of 10,000 ft, or a 3,000 ft length of

borehole. Therefore, the estimated actual drilling time to drill this interval is approximately 50 hours.

The reciprocating piston compressor is not a fixed pressure ratio machine like the rotary compressor. As long as there is sufficient power available from the prime mover the reciprocating piston compressor will match the back pressure resistance. Thus, Figure 10-4 shows only one curve indicating the injection pressure is the same as the pressure output of the compressor unit.

In Illustrative Example 10.2 it was found that the actual shaft horsepower required by the reciprocating piston compressor unit to compress air to 275 psia was approximately 367.3 (at 7,000 ft of depth). Also in Illustrative Example 10.2 the derated horsepower available from the Caterpillar Model 3508 prime mover at the surface elevation of 4,000 ft was found to be 579.6. Drilling at a depth of 7,000 ft, the prime mover power ratio percent is

$$PR \quad \frac{367.3}{579.6} \ (100) \quad 63.4$$

Entering the abscissa of Figure 4-17 with the power ration percent, the approximate fuel consumption rate can be read on the ordinate using the diesel fuel curve. The approximate fuel consumption rate at this power level is 0.552 lb/hp-hr. The total weight of diesel fuel consumption per hour is

$$\dot{w}_f \quad 0.552 \ (367.3) \quad 202.8 \ \text{lb/hr}$$

The diesel fuel consumption rate (in United States gallons) for the drilling depth of 7,000 ft is

$$q_f \quad \frac{202.8}{(0.8156)(8.33)} \quad 29.8 \ \text{gal/hr}$$

Using the data in Figure 10-4 and similar calculations as those given above, the diesel fuel consumption rate as a function of drilling time (or drilling depth) can be obtained. Figure 10-8 shows the diesel fuel consumption rate as a function of drilling time (or drilling depth) for the reciprocating piston compressor unit. The approximate total diesel fuel needed for the compressor unit is obtained by the integration of the area under the curve in Figure 10-8. One compressor unit is used throughout the 50 hours of drilling. The fuel needed for this compressor is approximately 1,500 gallons. It is standard practice to assume a 20 percent addtional volume of fuel for circulating the well and other compressor operations on the rig. Therefore, the total diesel fuel consumption for this first compressor is about 1,800 gallons. The second compressor is place on line at 31 hours into the operation. The fuel needed for this compressor is 600 gallons. Adding the standard 20 percent gives a total diesel fuel consumption for this second compressor of about 720 gallons. Therefore, the total diesel fuel needed for the two compressor units is approximately 2,520 gallons.

Illustrative Examples 10-2 and 10-3 demonstrate the calculation procedures (step Nos. 1 to 10 given in Section 10.1) that can be used to plan a typical deep oil or natural gas well drilling operation.
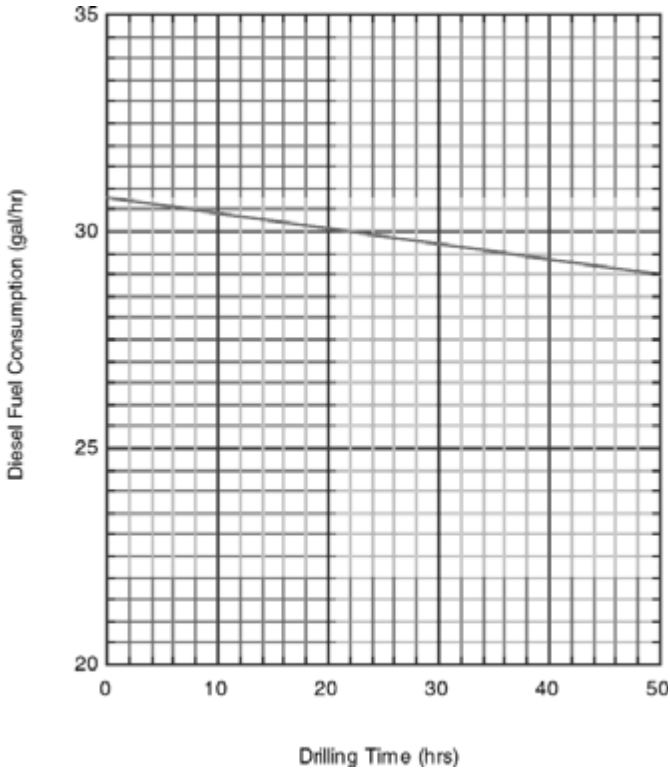
Figure 10-8: Fuel consumption rate as a function of drilling time for compressor used in Illustrative Example 10.2 ($q_g = 1,500$ acfm from the compressor).

10.6 Field Comparison

The following case history of vertical drilling operation demonstrates the accuracy of the planning calculation procedures discussed earlier that utilize complete major and minor friction loss terms.

Case History This was a vertical well drilled to a depth of 9,571 ft in an oil and natural gas producing basin in North Africa (Cambrian formation target).   The borehole profile is described by an 9 5/8 inch intermedicate casing run from surface to 7,632 ft. Below the intermediate casing is a 7 inch production liner that is tied

back to the 9 5/8 inch casing at 7,304 ft. The 7 inch liner was run from 7,304 ft to 8,859 ft. An openhole was drilled out of the bottom of the 7 inch liner to a depth of 9,571 ft. The stable foam was used to reduce the bottomhole pressure and allow underbalanced drilling. The openhole interval (from 8,859 ft to 9,571 ft) was drilled with an 6 inch tri-cone roller cutter drill bit.   The drill string while drilling at a depth of approximately 9,381 ft was made up of 5 inch drill pipe from surface to 7,361 ft, 3 1/2 inch drill pipe from 7,381 ft to 8,361 ft, 3 1/2 inch heavy weight drill pipe from 8,361 ft to 8,841 ft, and 4 3/4 inch drill collars from 8,841 ft to 9,381 ft. The incompressible fluid for the foam was 8.60 lb/gal treated water. The treated water was injected at a rate of 45 gal/min.   The drilling gas was inert atmospheric air (specific gravity of approximately 0.97) with an injection volumetric flow rate of approximately 1,500 acfm (surface elevation location of approximately 3,700 ft). Using the major and minor fluid flow lose calculations as described in this chapter, the predicted surface injection pressure for the stable foam drilling fluid was calculated to be 2,830 psig.   The actual field injection pressure was approximately 3,600 psig. The predicted bottomhole pressure was 1840 psig and the actual bottomhole pressure was approximately 2,000 psig (surface choke back pressure was approximately 600 psig). The predictions values are lower than the actual field recorded values. The stable foam calculations are not as accurate as those for air drilling operations or those for aerated drilling operations.

This comparison calculation was carried out using the same drill pipe body and drill pipe tool joints lumped geometry approximations as those in Illustrative Example 10.2 above. The success of these calculations depends upon the careful inclusion of all major and minor fluid flow friction losses.

10.7 Conclusions

The discussion in this chapter has concentrated on direct circulation operations. Stable foam drilling operations are generally restricted to direct circulation operations. Reverse circulation stable foam operations are used to carryout oil and natural gas well clean out (workover) maintenance.

The demonstration calcuations in this chapter have utilized lumped geometry approximations for the drill pipe body and drill pipe tool joints.   Such approximations appear to adequately model the overall friction resistance in the circulation system and give accurate results for bottomhole and injection pressures. An improvement to this drill string geometry approximation technique can be made by programming each tool joint indivdually at its proper location in the drill string. This type of program would be best carried out using a higher level computer language such as C++ or FORTRAN. Such a programmed solution would improve the detail pressure versus depth accuracy of the model. However, a comparison of this type of program gives very little change in bottomhole and injection pressures, and in the required volumetric flow rate of gas.

References

1. Hutchison, S. O., "New Approach for Producing and Repairing Wells," Proceedings 40th Annual California Region Meeting of the Society of Petroleum Engineerings of AIME, 1969.

2. Hutchison, S. O., "Foam Workovers Cut Costs 50%," *World Oil*, 1969.

3. Hutchison, S. O., and Anderson, G. W., "Preformed Stable Foam Aids Workover, Drilling," *Oil and Gas Journal*, 1972.

4. Mitchell, B. J., "Test Data Fill Theory Gap on Using Foam as a Drilling Fluid," *Oil and Gas Journal*, 1971.

5. Byer, A. H., Millhone, R. S., and Foote, R. W., "Flow Behavior of Foam as a Well Circulating Fluid," SPE 3986, Presented at the SPE 47th Annual Technical Conference and Exhibition, San Antonio, Texas, October 8-10, 1972.

6. Allan, P. D., "Nitrogen Drilling System for Gas Drilling Applications," SPE 28320, Presentation at the SPE 69th Annual Technical Conference and Exhibition, New Orleans, Louisiana, September 25-28, 1994.

7. *API Recommended Practice for Testing Foam Agents for Mist Drilling*, API RP-46, November 1966.

8. Abbott, W. K., *An Analysis of Slip Velocities of Spherical Particles in Foam Drilling Fluid*, Master of Science Thesis, Colorado School of Mines, Golden, Colorado, 1974.

9. Krug, J. A., and Mitchell, B. J., "Charts Help Find Volume, Pressure Needed for Foam Drilling," *Oil and Gas Journal*, February 7, 1972.

10. Lord, D. L., "Mathematical Analysis of Dynamic and Static Foam Behavior." SPE 7927, Presented at the SPE Symposium on Low-Permeability Gas Reservoirs, Denver, Colorado, May 20-22, 1979.

11. Okpobiri, G. A., and Ikoku, C. U., "Volumetric Requirements for Foam and Mist Drilling Operations," *SPEDE*, February 1986.

12. Daugherty, R. L., Franzini, J. B., and Finnemore, E. J., *Fluid Mechanics with Engineering Applications*, Eighth Edition, McGraw-Hill, 1985.

This page intentionally left blank.

Part 3: Deep Well Operations

This page intentionally left blank.

Eleven

Specialized Drilling Equipment

There are specialized surface and downhole equipment that either offer air and gas drilling operations unique operational advantages, or are specialized tools strictly for use in air and gas drilling operations. Some of this equipment is used only for shallow drilling (approximately less than 3,000 ft of vertical depth). However, most of the equipment discussed below can be used for a variety of depths and drilling objectives (e.g., monitoring wells, deep water wells, geothermal wells, or underbalanced oil and natural gas resource recovery wells).

11.1 Surface Equipment

Over the past three decades a number of rotary drilling surface equipment innovations have been introduced. These innovations have been directed at variety of applications from providing an increased capability to drill through more difficult, shallow, highly fractured, incompetent rock formations to enhancing the capability to drill long horizontal boreholes at a variety of depths. Such innovations have resulted in new types of rotary drilling rigs, new auxiliary rotary drilling equipment for convention drill rigs, and unique hoisting equipment that allows safe underbalance drilling operations.

11.1.1 *Specialized Drilling Rigs*

There are a variety of rotary drilling rigs on the market today. These rigs come in a variety of mechanical capabilities and sizes which in turn translates to a variety of vertical (and/or directional) capabilities. The key technology that has stimulated

rig development over the past three decades is the top head rotary drive. This is a hydraulically actuated device. A prime mover on the rig floor operates a hydraulic pump which pumps hydraulic fluid through hoses to a hydraulic motor (the reverse of a pump). The hydraulic motor is the rotating element of the top head rotary drive (see Chapter 1 for more discussion). The top head rotary drive is located on the drill rig mast and moves up and down on the mast in a track attached to the mast. The movement of the top head rotary drive can be actuated hydraulically or by a direct mechanical device such as a chain drive mechanism. This development was first introduced on small rotary drilling rigs that were capable of drilling only shallow wells (see Figure 1-3 for a typical example).   Since this introduction, the hydraulically actuated rotary device technology has been adapted for use on many new drilling rig designs that have greater depth directional capabilities.

Drill String and Casing Rotation Rigs

Figure 11-1 shows a typical dual rotary drilling rig. These very unique rotary drilling rig designs utilize hydraulically actuated rotary drives that can rotate both the drill pipe and the casing that is driven and advanced simultaneously with the advance of the drill string. This innovation allows these drilling rigs to drill shallow highly fractured, incompetent, unstable rock formations.

Figure 11-1: Dual rotary drilling rig used for shallow drilling (courtesy of Foremost Industries Incorporated).

The Foremost Model DR-24 drilling rig shown in Figure 11-1 has two rotary drive heads, a top rotary drive that rotates the drill string clockwise inside the casing, and a bottom rotary drive that rotates the casing counterclockwise (the sections of casing are welded together as the drilling advances). Figure 11-2 shows a view (looking up) of the two rotary drive heads.
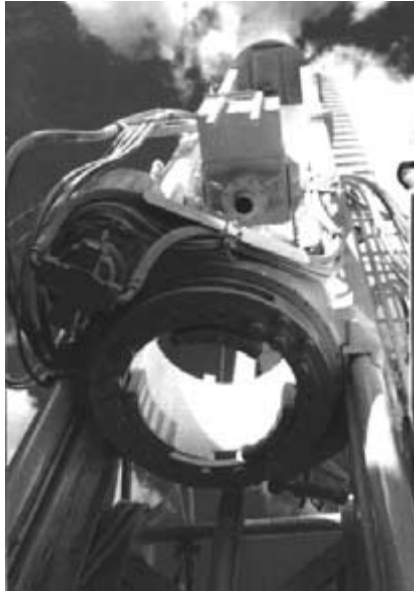
Figure 11-2: Dual rotary drive heads, at the top is the drill string rotary drive head, at the bottom is the casing rotary drive head (courtesy of Foremost Industries Incorporated).

A casing shoe ring drag type bit is welded to the bottom of the casing to give the casing rock destruction capability as it is advanced (see Figure 11-3).

These dual rotary drilling rigs are designed primarily for shallow drilling operations and can utilize drilling mud or a variety of air (or gas) drilling fluids. The rigs are used to drill monitoring wells, water wells, and mining and geotechnical boreholes. These dual rotary drilling rigs have only been in use for a little over a decade. The dual rotary drilling rig is characterized by two masts each having a track. Figure 11-1 shows these two masts. The taller narrower track has the head rotary drive for the drill sting and the lower wider track has the head rotary drive for the casing. The heads are moved on their respective tracks by hydraulic power.

These dual rotary drilling rigs are available in several rig sizes. The model number gives the capability of the rigs. Model DR 24 (shown in Figure 11-1) denotes a 24 ft downward stroke of the drill string rotary drive head (in its respective track). This model also has a 7 ft downward stroke of the casing rotary drive head

(in its respective track). These dual rotary rigs can handle a variety of drill string types and outside diameters (including dual wall pipe).   When simultaneously running casing while advancing the drill string, only internal/external flush welded joint casing can be used.
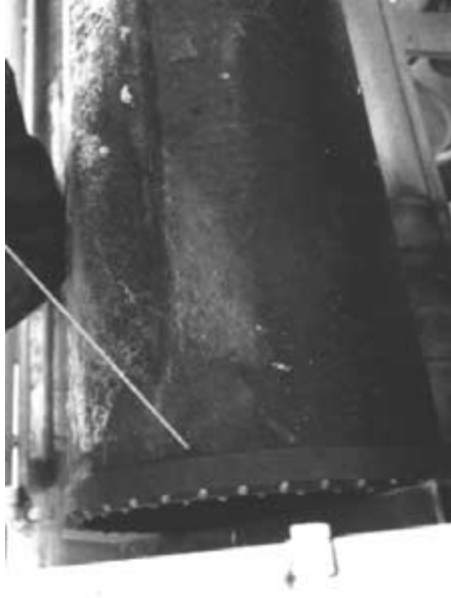
Figure 11-3: Casing shoe ring drag type bit (carbide studded) welded to the bottom of the casing (courtesy of Foremost Industries Incorporated).

Top Head Rotary Drive Slant Rigs

A variety of shallow drilling rigs can be used to drill a slant borehole. The slant capability of a drill rig refers to its ability to tilt the mast to an angle relative to the horizontal. Most slant capable rigs can slant their mast between 0˚ and 45˚ (relative to the vertical). The 0˚ angle is a vertical mast. Figure 1-1 is an example of a shallow drilling rig that has 0˚ to 45˚ slant capability. These slant capable small drill rigs are utilized in monitoring well construction, and in a variety of geotechnical and mining drilling operations.

Figure 11-4 shows a trailer mounted deep drilling rig that can be slanted to angles between 0˚ and 45˚. This rig design is known as the Sierra Model and is fabricated by the George E. Failing Supply Company, Limited (Canada). These rigs can utilize an integral top drive power swivel (similar to a top head rotary drive) that is hydraulically actuated, or a rotary table that can also be slanted to match the slant of the mast. The hoist system is of a conventional design with a crown block and track mounted traveling block. The can use a variety of drilling fluids (e.g., drilling mud, or air and gas drilling fluid technology). The rig in Figure 11-4 has a 73 ft

working clearance. This clearance allows the rig to be classified as a double (can pull a stand of two drill pipe, see Chapter 1). Figure 11-4 shows three hoses in the mast. One hose is the rotary hose that allows the drilling fluid to flow to the top drive power swivel mounted below the traveling block. The other two hoses are the hydraulic supply lines for the top drive power swivel.

These unique drill rigs are used throughout the world principally for oil and natural gas recovery drilling operations. These rigs can also be skid mounted for offshore platform operations.

Figure 11-4: Trailer mounted slant capable deep drilling rig (courtesy of George E. Failing Supply Company, Limited).

11.1.2 *Power Swivels*

The top drive power swivels are hung from the traveling block of a typical conventional drill rig. The power swivel is an auxiliary to the normal complement of drill rig equipment. The power swivel can be utilized on any conventional drill rig. When a power swivel is used, the rotary table must be removed. The power swivel works in much the same way as a top head rotary drive on smaller drill rigs. The power swivel is hydraulically actuated and can be used to rotate the drill string at speeds of a few rpm to normal drilling rotary speeds of about 100 rpm. Figure 11-5 shows a typical power swivel with an elevator bail at the top (attaches to the elevators on the traveling block) and the rotating stem at the bottom (which makes up to the top of the drill string). This example power swivel is a Bowen Tools Model S-1 with 30 ton lift, 0 to 75 rpm rotating, and 1,875 ft-lb torque capabilities.

The horizontal arm on the right side of the power swivel is supported at the far right end by a tight cable that is run the length of the rig working clearance. This arm and cable combination resists the internal torque generated by the power swivel as it rotates the drill string.

The main advantage to using a power swivel on a conventional rig is that the changes in rotary speed can be made smoothly. Also, the power swivel can be used to rotate the drill string in either a clockwise or counterclockwise direction. Further, the power swivel can rotate the drill string while lifting the drill string. These advantages combine to give very useful characteristics for directional drilling operations, particularly for long horizontal drilling operations.
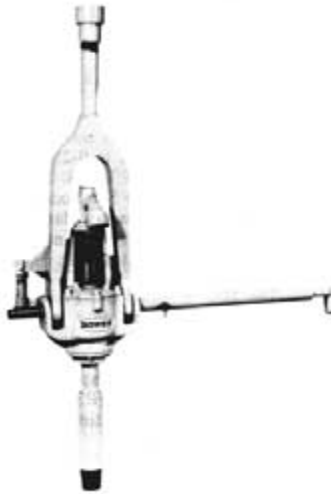
Figure 11-5: Typical power swivel (Model S-1) for conventional rotary drill rigs (courtesy of Bowen Tools, Incorporated).

When drilling long a near horizontal section (of the order of 1,000 ft or greater) the rock cuttings tend to fall to the low side of the borehole. This is particularly true when a directional course correction is being made. During course corrections, the drill string is not rotated and is slid along the low side of the borehole. The downhole motor rotates the drill bit. This allows the bent sub above the downhole motor to dictate the direction of the correction. While sliding the drill string, the rock cuttings entrained in the drilling fluid tend to accumulate between the drill pipe tool joints. The drilling fluid will seek the least resistance to flow and move through the high side of the borehole above the drill sting. To clean this accumulation from the bottom of the borehole, it is necessary to periodically cease drilling forward and lift and rotate the drill string with the power swivel. It is not possible to lift and rotate the drill string when drilling with a conventional rotary

table. When a course correction has been completed, the power swivel can be used to rotate the drill string at a low speed (approximately 10 rpm or less). The slow rotation of the drill string averages out the effect of the bent sub and allows straight hole drilling. Under these drilling conditions, the rotating drill string stirs the rock cutting off the low side of the borehole and more complete cleaning is accomplished. But here again, periodic lifting of the drill string is usually necessary to eliminate any cuttings accumulations. Here again, most conventional drill rig rotary tables cannot rotate at speeds less than 30 rpm. Rotating at 30 rpm or greater with a bent sub near the bottom of the drill string sharply increases the possibility of BHA damage and a drill string mechanical failure which could result in a fishing job.

Figure 11-6 shows the basic components and dimensions of the Bowen Tools Model S-1. The elevator bail at the top of this model will fit 2 3/8 inch and 2 7/8 inch elevators. The rotary hose box connection on the left side of the drawing on the right of the figure mates to a 2 inch national pipe thread (NPT) pin connection. The output shaft of the power swivel has a 2 3/8 inch API internal flush (IF) pin connection. In oil and natural gas recovery drilling operations, this output shaft is made up to the upward facing box of a kelly sub valve (for blowout protection, see Chapter 3). Such a sub also protects the treads on the power swivel output shaft from excessive wear due to repeated connections while making trips. Looking at the drawing on the right, on the right side of this drawing are the hydraulic hose connections (lined up one behind the other). These connections are for the hydraulic hoses that connect the power swivel to its hydraulic pump unit (usually on a skid next to the drill rig). The hydraulic pump is actuated by a prime mover. The pump unit provides the hydraulic fluid power that actuates the power swivel.
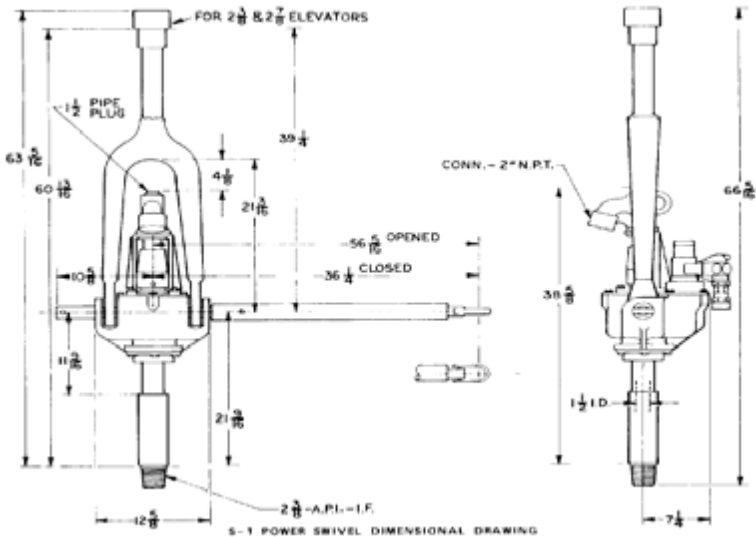
Figure 11-6: Components of the Model S-1 power swivel (courtesy of Bowen Tools, Incorporated).

11.1.3 *Snubbing Units*

In oil and natural gas recovery drilling, there are special operational situations that require the insertion of a drill string or a liner into a well that has been shut-in and is under high internal gas pressure. These situations are usually either the result of an unexpected subsurface blowout, or due to the operational desire to complete a well without damaging the natural gas production zone (i.e., underbalanced drilling and completion). Inserting tubulars into a shut-in high pressure well is a potentially dangerous operation and requires unique surface equipment to accomplish. If sufficient gas is released from the well to the atmosphere to compensate for the tubulars volume, then the insertion operation is known as a snubbing operation. If, on the other hand, the well is allowed to flow through the blooey line to the atmosphere as the tubulars are inserted, the operation is known as a stripping operation. Stripping operations are usually designed for low wellhead pressures and, thus, do not require snubbing units. Inserting a tubular against the static pressure of a well requires the assistance of the snubbing unit to force the tubular into the well.

Figure 11-7 shows a schematic of a typical snubbing operation. The snubbing unit shown utilizes the lifting capability of the drilling rig hoist system to force a tubular string into a pressurized well. The snubbing unit platform is secured to the top of the BOP stack and the traveling slips made up to the top of the tubular working string to be inserted into the well.
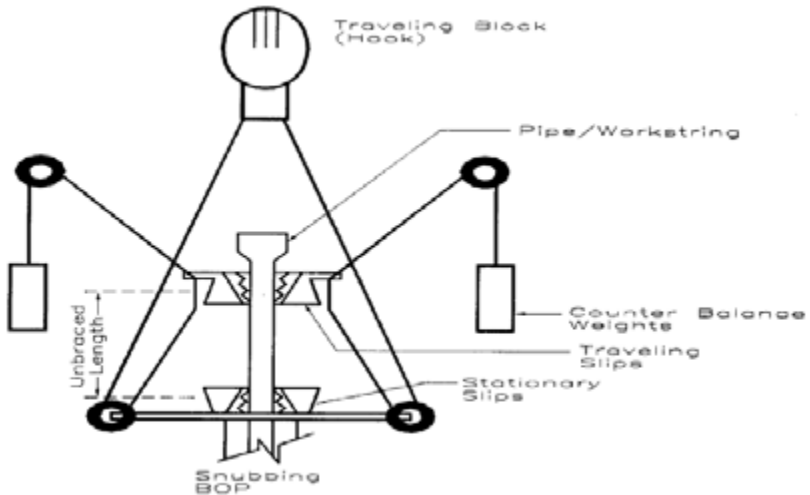
Figure 11-7: Snubbing unit schematic (courtesy of Cudd Pressure Control, Incorporated).

A set of sheaves with cables are rigged up to the top of the BOP stack (sheaves attached to the unit platform) and the traveling slips in such a manner as to allow the traveling slips to be forced downward as the traveling block is raised. Additional

tubulars are attached to the top of the working string and the process repeated until the entire working string is inserted.

Figure 11-8 shows a BOP stack with the snubbing unit equipment attached. This combination is called the snubbing stack. Because of safety considerations, the BOP stack for any snubbing operation must have at the minimum a double BOP configuration. This has a safety pipe ram on top (to fit the pipe being inserted) and a blind ram on the bottom to secure the well when no pipe is in the well. The example shown in Figure 11-8 shows an annular BOP on the top of the BOP stack above the double BOP configuration. The annular BOP working together with the pipe ram allows a working string with tool joints to be safely inserted during the snubbing operation. The pipe ram BOP and the annular BOP seal gas from escaping around the working string outside surface.
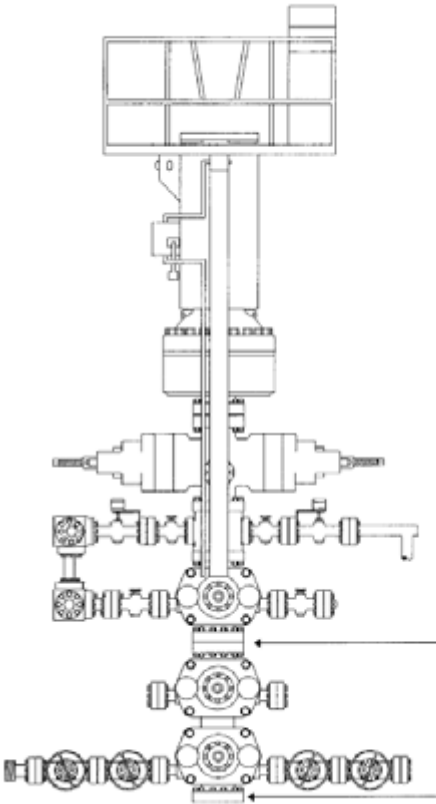
Figure 11-8: Snubbing stack rig up. The arrows show where the double ram type BOPs are located on the stack (courtesy of Cudd Pressure Control, Incorporated).

11.2 Downhole Equipment

There are several downhole drilling devices that are unique to air and gas drilling operations. These are the downhole air hammer, the progressive cavity positive displacement motor (modified for compressed gas drilling fluids), the downhole pneumatic turbine motor, and the sliding vane positive displacement motor.

11.2.1 *Downhole Air Hammers*

There are two basic designs for the downhole air hammer. One design utilizes a flow path of the compressed air through a control rod (or feed tube) down the center hammer piston (or through passages in the piston) and then through the hammer bit. The other design utilizes a flow path through a housing annulus passage (around the piston) and then through the hammer bit. Figure 11-9 shows a schematic of a typical control rod flow design downhole air hammer. The hammer action of the piston on the top of the drill bit shank provides a impact force that is transmitted down the shank to the bit studs which in turn crush the rock at the rock face. In shallow boreholes where there is little annulus back pressure, the piston impacts the top of the bit shank at a rate of from about 600 to 1,700 strikes per minute (depending on volumetric flow rate of gas). However, in deep boreholes where the annulus back pressure is usually high, impacts can be as low as 100 to 300 strikes per minute. This unique air drilling device requires that the drill string with the air hammer be rotated so that the drill bit studs impact over the entire rock face. In this manner an entire layer of the rock face can be destroyed and the drill bit advanced.

Figure 11-9 shows the air hammer suspended from a drill string lifted off the bottom (the shoulder of the bit is not in contact with the shoulder of the driver sub). In this position, compressed air flows through the pin connection at the top of the hammer to the bit without actuating the piston action (i.e., to blow the borehole clean). When the hammer is placed on the bottom of the borehole and weight placed on the hammer, the bit shank will be pushed up inside the hammer housing until the bit shoulder is in contact with the shoulder of the driver sub. This action aligns one of the piston ports (of one of the flow passage through the piston) with one of the control rod windows. This allows the compressed air to flow to the space below the piston which in turn forces the piston upward in the hammer housing. During this upward stroke of the piston, no air passes through the bit shank to the rock face. In essence, rock cuttings transport is suspended during this upward stroke of the piston.

When the piston reaches the top of its stroke, another one of the piston ports aligns with one of the control rod windows and supplies compressed air to the open space above the piston. This air flow forces the piston downward until it impacts the top of the bit shank. At the same instant the air flows to the space above the piston, the foot valve at the bottom of the control rod opens and air inside the drill string is exhaust through the control rod, bit shank, and the bit orifices to the rock face. This compressed air exhaust entrains the rock cuttings created by the drill bit for transport up the annulus to the surface. This impact force on the bit allows the rotary action of the drill bit to be very effective in destroying rock at the rock face. This in turn allows the air hammer to drill with low WOB. Typically for a 6 3/4 inch outside diameter air hammer drilling with a 7 7/8 inch air hammer bit, the WOB can be as low as 1,500 lbs. Downhole air hammers must have an oil type

lubricant injected into the injected air during the drilling operation. This lubricant is needed to lubricate the piston surfaces as it moves in the hammer housing. Air hammers are used exclusively for vertical drilling operations.

This piston cycle is repeated as the drill string (and thus the drill bit) is rotated and in this manner continuous layers of rock on the rock face are crushed and the cuttings removed. The air flow through the air hammer is not continuous. When the piston is being lifted in the hammer, air is not being exhausted through the drill bit. For example, at a piston impact rate of 600 strikes per minute the air is shut down for about 0.050 seconds per cycle. This is so short a time that the air flow rate through the annulus can be assumed as a continuous flow.
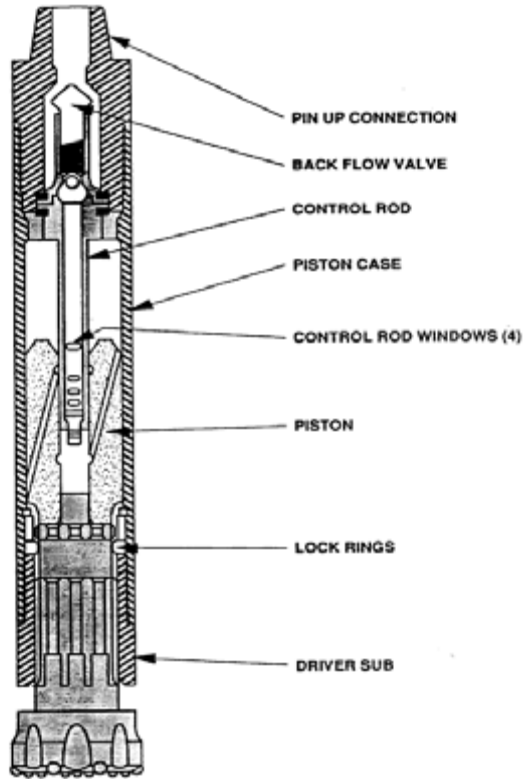
Figure 11-9: Schematic cutaway of a typical air hammer (courtesy of Diamond Air Drilling Services, Incorporated).

Downhole air hammers are available in housing outside diameters from 3 inches to 16 inches. The 3 inch housing outside diameter hammer can drill a borehole as

small as 3 5/8 inches. The 16 inch housing outside diameter hammer can drill a boreholes from 17 1/2 inches to 33 inches. For shallow drilling operations, conventional air hammer bits are adequate. For deep drilling operations (usually oil and gas recovery wells), higher quality oil field quality drill bits are required (see Figure 3-11).

There are a variety of manufacturers of downhole air hammers. These manufacturers use several different designs for their respective products. The air hammer utilizes very little power in moving the piston inside the hammer housing. For example, a typical 6 3/4 inch outside diameter air hammer with a 77 lb piston operating at about 600 strikes per minute, will use less than 2 horsepower driving the piston. This is a very small amount of power relative to the total needed for the actual rotary drilling operation. Thus, it is clear that the vast majority of the power to the drill string is provided by the rotary table. Therefore, any pressure loss (i.e., energy loss) due to the piston lifting effort can usually be ignored. The major pressure loss in the flow through an air hammer is due to the flow energy losses from the constrictions in the flow path when the air is allowed to exit the hammer (on the down stroke of the piston). All air hammer designs have internal flow constrictions. These flow constrictions can be used to model the flow losses through the hammer. In most designs these constrictions can be approximately represented by a set of internal orifice diameters in the flow passages to the drill bit. These internal orifices are usually the ports (and associated channels) through the piston and the orifice at the open foot valve.

Illustrative Example 11.1 Determine the injection pressure and resulting compressor fuel consumption when an air hammer is utilized to drill the openhole interval from 7,000 ft to 10,000 ft of the Illustrative Example 8.3 series in Chapter 8. In this illustrative example it is assumed that an 6 3/4 inch outside diameter Halco Model D750 air hammer with a 7 7/8 inch diameter air hammer bit is used to drill at 10,000 ft. This is a feed tube type design downhole air hammer. The internal constrictions in this air hammer can be represented as compressed air flow through a 1.60 inch inside diameter feed tube, then three 5/8 inch inside diameter passages each approximately 8.0 inches in length through the hammer piston, then through 1.4375 inch inside diameter passage approximately 11.0 inches in length through the hammer bit, and then through three 1.125 inch inside diameter passages each approximately 3.0 inches in length from the bottom of the main passage through the bit to the exit orifices in the bit to the bottom of the borehole. The air hammer piston is estimated to be operating at about 216 strokes per minute. In the Illustrative Example 8.3 series two semi-trailer mounted Dresser Clark Model CFB-4, four-stage, reciprocating piston compressors were selected. Each of these compressors were driven by a Caterpillar Model D398 diesel fueled prime mover. These two compressor units provide a total of 2,400 acfm to the borehole. The drilling location is at 4,000 ft above sea level. The annulus solution given in Illustrative Example 8.3b will be used as the starting point for this example.

In Illustrative Example 8.3b the bottomhole annulus pressure was determined. This annulus bottomhole pressure was found to be

$$p_{a5} \qquad 204.5 \text{ psia}$$

$$P_{a5} \qquad p_{a5} \ 144$$

$$P_{a5} \qquad 29,448 \ \text{lb/ft}^2 \ \text{abs}$$

Using the air hammer to drill the borehole does not alter the annulus solution obtained in Illustrative Example 8.3b.   However, it will alter the pressure calculations from the bottom of the annulus to the top of the inside of the drill string (the injection pressure).

Air Hammer Bit Orifice Passages

As discussed above, the air flow through an air hammer is curtailed over approximately one half of the cycle time period of the piston motion.   Therefore, since the weight rate of flow of compressed air being injected into the inside of the top of the drill string is constant and must be the same as the weight rate of flow exiting the blooey line, then the flow through the air hammer over half the cycle period must be twice the flow rate through the overall circulation system.   Thus, the pressure should be determined in the various air hammer constrictions with twice the flow rate.

The air hammer bit used in this example operation has three open orifice passages, each with an inside diameter of 1.125 inches and length of 3.0 inches. Thus, the inside diameter of the open orifice, D_{op}, is

$$d_{op} \qquad 1.125 \ \text{inches}$$

$$D_{op} \qquad \frac{d_{op}}{12}$$

$$D_{op} \qquad 0.0938 \ \text{ft}$$

The length of the orifice passages, L_{op}, is

$$l_{op} \qquad 3.0 \ \text{inches}$$

$$L_{op} \qquad \frac{l_{op}}{12}$$

$$L_{op} \qquad 0.250 \ \text{ft}$$

Equations 6-67, 6-68, 6-72, and 6-73 can be used altered and used to evaluate the flow through the three orifice passages in the air hammer bit.   The inside surface of these orifice passages have the surface roughness of commercial steel.   Therefore, over the length of the passages the surface roughness is

$$e_p \qquad 0.00015 \ \text{ft}$$

With the above, Equation 6-73 becomes

$$f_{iop} = \left[\cfrac{1}{2 \, \log \cfrac{0.0938}{0.00015} + 1.14} \right]^2$$

$$f_{iop} = 0.022$$

Equations 6-67 and 6-68 become, respectively,

$$a_{iop} = \frac{1.0}{53.36}$$

$$a_{iop} = 0.019$$

and

$$b_{iop} = \frac{0.022}{2 \, (32.2)} \left(\frac{53.36}{1.0} \right)^2 \left[\cfrac{\cfrac{2}{3} \, (2.635)}{-\cfrac{2}{4} \, (0.0938)^5} \right]^2$$

$$b_{iop} = 673{,}900$$

Equation 6-72 becomes

$$P_{iop} = \cfrac{(29{,}448)^2 + (673{,}900) \, (604.41)^2 \left[e^{\frac{2 \, (0.019) \, (0.250)}{604.41}} - 1 \right]}{e^{\frac{2 \, (0.019) \, (0.250)}{604.41}}}^{0.5}$$

$$P_{iop} = 29{,}520 \ \text{lb/ft}^2 \ \text{abs}$$

$$p_{iop} = \frac{P_{iop}}{144}$$

$$p_{iop} = 205.0 \ \text{psia}$$

Air Hammer Bit Shank Passage

The air hammer bit shank passage has an inside diameter of 1.4375 inches and a length of 11.0 inches. Thus, the inside diameter of the shank passage, D_{sp}, is

$$d_{sp} \quad 1.4375 \text{ inches}$$

$$D_{sp} \quad \frac{d_{sp}}{12}$$

$$D_{sp} \quad 0.120 \text{ ft}$$

The length of the shank passage, L_{sp}, is

$$l_{sp} \quad 11.0 \text{ inches}$$

$$L_{sp} \quad \frac{l_{sp}}{12}$$

$$L_{sp} \quad 0.917 \text{ ft}$$

Over the length of the bit shank passage the surface roughness is

$$e_p \quad 0.00015 \text{ ft}$$

With the above, Equation 6-73 becomes

$$f_{isp} \quad \frac{1}{\left(2 \ \log \dfrac{0.120}{0.00015} \quad 1.14 \right)^2}$$

$$f_{isp} \quad 0.021$$

Equations 6-67 and 6-68 become, respectively,

$$a_{isp} \quad \frac{1.0}{53.36}$$

$$a_{isp} \quad 0.019$$

and

$$b_{isp} \quad \frac{0.021}{2\,(32.2)} \quad \frac{53.36}{1.0}^{\,2} \quad \frac{(2)\,(2.635)^{\,2}}{\frac{}{4}\,(0.120)^5}$$

$$b_{isp} \quad 1,673,000$$

Equation 6-72 becomes

$$P_{isp} \quad \frac{(29,520)^2 \quad (1,673,000)\,(604.41)^2 \quad e^{\frac{2\,(0.019)\,(0.917)}{604.41}} \quad 1}{e^{\frac{2\,(0.019)\,(0.917)}{604.41}}}^{\,0.5}$$

$$P_{isp} \quad 30,100 \ \text{lb/ft}^2 \ \text{abs}$$

$$p_{isp} \quad \frac{P_{isp}}{144}$$

$$p_{isp} \quad 209.0 \ \text{psia}$$

Air Hammer Bit Piston Passages

The air hammer bit used in this example operation has three passages in the piston that allow the compressed air to flow to the chamber below the piston, each with an inside diameter of 0.625 inches and length of 8.0 inches. Thus, the inside diameter of the passage, D_{pp}, is

$$d_{pp} \quad 0.625 \ \text{inches}$$

$$D_{pp} \quad \frac{d_{pp}}{12}$$

$$D_{pp} \quad 0.0521 \ \text{ft}$$

The length of the piston passages, L_{pp}, is

$$l_{pp} \quad 8.0 \ \text{inches}$$

$$L_{pp} \qquad \frac{l_{pp}}{12}$$

$$L_{pp} \qquad 0.667 \text{ ft}$$

Over the length of the passages the surface roughness is

$$e_p \qquad 0.00015 \text{ ft}$$

With the above, Equation 6-73 becomes

$$f_{ipp} \qquad \frac{1}{\left[2 \ \log \dfrac{0.0521}{0.00015} \quad 1.14 \right]^2}$$

$$f_{ipp} \qquad 0.026$$

Equations 6-67 and 6-68 become, respectively,

$$a_{ipp} \qquad \frac{1.0}{53.36}$$

$$a_{ipp} \qquad 0.019$$

and

$$b_{ipp} \qquad \frac{0.026}{2 \ (32.2)} \left[\frac{53.36}{1.0}\right]^2 \frac{\left[\dfrac{2}{3} \ (2.635)\right]^2}{\left[\dfrac{}{4} \ (0.0521)^5\right]}$$

$$b_{ipp} \qquad 14,910,000$$

Equation 6-72 becomes

$$P_{ipp} \quad \frac{(30,100)^2 \quad (14,910,000)\,(604.41)^2 \quad e^{\frac{2\,(0.019)\,(0.667)}{604.41}} \quad 1}{e^{\frac{2\,(0.019)\,(0.667)}{604.41}}}^{0.5}$$

$$P_{ipp} \quad 31,470 \ \text{lb/ft}^2 \ \text{abs}$$

$$p_{ipp} \quad \frac{P_{ipp}}{144}$$

$$p_{ipp} \quad 218.6 \ \text{psia}$$

On-Off Action of Air Hammer

Using Equation 4-11, the approximate specific weight of the air inside the drill collars as it enters the air hammer is determined from P_{ipp}. This is

$$_{ah} \quad \frac{(31,470)\,(1.0)}{(53.36)\,(604.41)}$$

$$_{ah} \quad 0.976 \ \text{lb/ft}^3$$

The inside diameter of the drill collars above the air hammer entrance is

$$d_5 \quad 2.8125 \ \text{inches}$$

$$D_5 \quad \frac{d_5}{12}$$

$$D_5 \quad 0.234 \ \text{ft}$$

The cross-section area of the inside of the drill collars is

$$A_{dci} \quad \frac{}{4} \quad 0.234^{\ 2}$$

$$A_{dci} \quad 0.0430 \ \text{ft}^2$$

The approximate velocity of the compressed air inside the drill collars is

$$V_{dci} \qquad \frac{2.635}{(0.976)\ (0.0430)}$$

$$V_{dci} \qquad 62.6\ \text{ft/sec}$$

For drilling at 10,000 ft, the estimated number of piston cycles is

$$N_p \qquad 216\ \text{strikes/minute}$$

The period of a single cycle of the piston is

$$p \qquad \frac{60}{216}$$

$$p \qquad 0.278\ \text{sec}$$

The flow to the air hammer is stopped for approximately one half of the cycle period. Thus, distance the air flow is compressed inside the drill collars above the hammer is approximately

$$L_c \qquad \frac{0.278}{2} \quad (62.6)$$

$$L_c \qquad 8.70\ \text{ft}$$

The length of a cubic foot of the compressed air in the drill collars prior to the stop is

$$L \qquad \frac{1}{0.0430}$$

$$L \qquad 23.18\ \text{ft}$$

The length of a cubic foot of the compressed air in the drill collars after the stop is

$$L_c \qquad 23.18 \qquad 8.70$$

$$L_c \qquad 14.49\ \text{ft}$$

The new compressed volume of the compressed air in the drill collars after the stop is

$$Vol_c \qquad (14.49)\ (0.0430)$$

$$Vol_c \quad 0.625 \ \text{ft}^3$$

But the weight inside this new volume is that of the specific weight determined above. Therefore, the new specific weight of the compressed air in the drill collars after the stop is

$$\gamma_{cdci} \quad \frac{0.976}{0.625}$$

$$\gamma_{cdci} \quad 1.561 \ \text{lb/ft}^3$$

Using Equation 4-11, the pressure due to the stop action of the air hammer is

$$P_{cdci} \quad \frac{(1.561) \ (53.36) \ (604.41)}{(1.0)}$$

$$P_{cdci} \quad 50,360 \ \text{lb/ft}^2 \ \text{abs}$$

$$p_{cdci} \quad \frac{P_{cdci}}{144}$$

$$p_{cdci} \quad 349.7 \ \text{psia}$$

Geometry Inside the Drill String
Starting at the bottom of the drill string, the total length of the drill collars length increment, H_5, in the openhole section is

$$H_5 \quad 500 \ \text{ft}$$

The inside diameter of the drill collars length in this openhole section is

$$d_5 \quad 2.8125 \ \text{inches}$$

$$D_5 \quad \frac{d_5}{12}$$

$$D_5 \quad 0.234 \ \text{ft}$$

The total length of the drill pipe tool joints lumped geometry increment, H_4, in the openhole section is

$$H_4 \quad 125 \ \text{ft}$$

The inside diameter of the drill pipe tool joints lumped geometry in this openhole section is

d_6 3.50 inches

D_6 $\dfrac{d_6}{12}$

D_6 0.292 ft

The total length of the lumped drill pipe body geometry increment, H_3, in the openhole section is

H_3 2,375 ft

The inside diameter of the drill pipe body lumped geometry in this openhole section is

d_7 3.826 inches

D_7 $\dfrac{d_7}{12}$

D_7 0.319 ft

The total length of the lumped drill pipe tool joints geometry increment, H_2, in the cased section is

H_2 350 ft

The inside diameter of the drill pipe tool joints lumped geometry in this cased section is

D_6 0.292 ft

The total length of the lumped drill pipe body geometry increment, H_1, in the cased section is

H_1 6,650 ft

The inside diameter of the drill pipe body lumped geometry in this cased section is

D_7 0.319 ft

Inside the Drill String (10,000 ft to 7,000 ft)
    The fifth drill string section increment is denoted by the length H_5.   The temperature at the bottom of the drill collars (bottomhole temperature) in the openhole section is

$$T_5 \qquad 604.41°R$$

The average temperature of the drill collar length H_5 and, thus, the temperature of the gas flow inside the drill collars is

$$T_{av5} \qquad 601.91°R$$

The inside surface of the drill collars has the surface roughness of commercial steel. Therefore, over this drill collar length the surface roughness is

$$e_p \qquad 0.00015 \ \text{ft}$$

With the above, Equation 6-73 becomes

$$f_{i5} \qquad \cfrac{1}{\left[2 \ \log \cfrac{0.234}{0.00015} \quad 1.14 \right]^2}$$

$$f_{i5} \qquad 0.018$$

Equations 6-67 and 6-68 become, respectively,

$$a_{i5} \qquad \frac{1.0}{53.36}$$

$$a_{i5} \qquad 0.019$$

and

$$b_{i5} \qquad \frac{0.018}{2 \ (32.2)} \left(\frac{53.36}{1.0} \right)^2 \frac{(2.635)^2}{\left(\dfrac{}{4} \ (0.234)^5 \right)}$$

$$b_{i5} \qquad 12,420$$

Equation 6-72 becomes

$$P_{i4} = \frac{(50,360)^2 - (12,420)(601.91)^2 \; e^{\frac{2\,(0.019)\,(500)}{601.91}} - 1}{e^{\frac{2\,(0.019)\,(500)}{601.91}}}^{0.5}$$

$$P_{i4} = 50,950 \; \text{lb/ft}^2 \; \text{abs}$$

$$p_{i4} = \frac{P_{i4}}{144}$$

$$p_{i4} = 353.8 \; \text{psia}$$

The pressure given above is the flowing air pressure at the top of the drill collar length inside the drill string in the openhole section of the borehole.

The fourth drill string section increment is denoted by the length H_4. The temperature at the bottom of the drill pipe tool joints lumped geometry length in the openhole section is

$$T_4 = 599.41°\text{R}$$

The average temperature of the drill pipe tool joints lumped length along H_4 and, thus, the temperature of the gas flow inside this drill string length is

$$T_{av4} = 598.79°\text{R}$$

The inside surface of the drill pipe tool joint has the surface roughness of commercial steel. Therefore, over this lumped drill pipe tool joint length the surface roughness is

$$e_p = 0.00015 \; \text{ft}$$

With the above, Equation 6-73 becomes

$$f_{i4} = \frac{1}{\left(2 \; \log \frac{0.292}{0.00015} + 1.14\right)^2}$$

$$f_{i4} = 0.017$$

Equations 6-67 and 6-68 become, respectively,

$$a_{i4} \quad \frac{1.0}{53.36}$$

$$a_{i4} \quad 0.019$$

and

$$b_{i4} \quad \frac{0.017}{2\ (32.2)} \quad \frac{53.36}{1.0}^2 \quad \frac{(2.635)^2}{-\dfrac{}{4}\ (0.292)^5}$$

$$b_{i4} \quad 3,958$$

Equation 6-72 becomes

$$P_{i3} \quad \frac{(50,950)^2 \quad (3,958)\ (598.79)^2 \quad e^{\frac{2\ (0.019)\ (125)}{598.79}} \quad 1}{e^{\frac{2\ (0.019)\ (125)}{598.79}}}^{0.5}$$

$$P_{i3} \quad 50,860 \ \text{lb/ft}^2 \ \text{abs}$$

$$p_{i3} \quad \frac{P_{i3}}{144}$$

$$p_{i3} \quad 353.2 \ \text{psia}$$

The pressure given above is the flowing air pressure at the top of the lumped drill pipe tool joint length inside the drill string in the openhole section of the borehole.

The third drill string section increment is denoted by the length H_3. The temperature at the bottom of the drill pipe body lumped geometry length in the openhole section is

$$T_3 \quad 598.16°\text{R}$$

The average temperature of the drill pipe body lumped geometry length along H_3 and, thus, the temperature of the gas flow inside this drill string length is

$$T_{av3} \quad 586.29°\text{R}$$

The inside surface of the drill pipe body has the surface roughness of commercial steel. Therefore, over this lumped drill pipe body length the surface roughness is

$$e_p \qquad 0.00015 \ \text{ft}$$

With the above, Equation 6-73 becomes

$$f_{i3} \qquad \frac{1}{\left(2 \ \log \dfrac{0.319}{0.00015} \quad 1.14 \right)^2}$$

$$f_{i3} \qquad 0.016$$

Equations 6-67 and 6-68 become, respectively,

$$a_{i3} \qquad \frac{1.0}{53.36}$$

$$a_{i3} \qquad 0.019$$

and

$$b_{i3} \qquad \frac{0.016}{2 \ (32.2)} \left(\frac{53.36}{1.0} \right)^2 \frac{(2.635)^2}{\left(\dfrac{}{4} \right)^2 (0.319)^5}$$

$$b_{i3} \qquad 2,486$$

Equation 6-72 becomes

$$P_{i2} \qquad \frac{(50,860)^2 \quad (2,486) \ (586.29)^2 \left(e^{\frac{2 \ (0.019) \ (2,375)}{586.29}} \quad 1 \right)}{e^{\frac{2 \ (0.019) \ (2,375)}{586.29}}}^{0.5}$$

$$P_{i2} \qquad 48,402 \ \text{lb/ft}^2 \ \text{abs}$$

$$p_{i2} \qquad \frac{P_{i2}}{144}$$

$$p_{i2} \qquad 336.1 \text{ psia}$$

The pressure given above is the flowing air pressure at the top of the lumped drill pipe body length inside the drill string in the openhole section of the borehole.

Inside the Drill String (7,000 ft to Surface)

The second drill string section increment is denoted by the length H_2. The temperature at the bottom drill pipe tool joints lumped geometry length in the cased section is

$$T_2 \qquad 574.41°R$$

The average temperature of the drill pipe tool joints lumped geometry along H_2 and, thus, the temperature of the gas flow inside this drill string length is

$$T_{av2} \qquad 572.66°R$$

The inside surface of the drill pipe body has the surface roughness of commercial steel. Therefore, over this lumped drill pipe body length the surface roughness is

$$e_p \qquad 0.00015 \text{ ft}$$

With the above, Equation 6-73 becomes

$$f_{i2} \qquad \frac{1}{\left(2 \ \log \ \dfrac{0.292}{0.00015} \quad 1.14 \right)^2}$$

$$f_{i2} \qquad 0.017$$

Equations 6-67 and 6-68 become, respectively,

$$a_{i2} \qquad \frac{1.0}{53.36}$$

$$a_{i2} \qquad 0.019$$

and

$$b_{i2} \quad \frac{0.017}{2\,(32.2)} \quad \frac{53.36}{1.0}^2 \quad \frac{(2.635)^2}{\dfrac{-}{4}\,(0.292)^5}$$

$$b_{i2} \quad 3,958$$

Equation 6-72 becomes

$$P_{i1} \quad \frac{(48,402)^2 \quad (3,958)\,(572.66)^2 \quad e^{\frac{2\,(0.019)\,(350)}{572.66}} \quad 1}{e^{\frac{2\,(0.019)\,(350)}{572.66}}}^{0.5}$$

$$P_{i1} \quad 48,157 \ \text{lb/ft}^2 \ \text{abs}$$

$$p_{i1} \quad \frac{P_{i1}}{144}$$

$$p_{i1} \quad 334.4 \ \text{psia}$$

The pressure given above is the flowing air pressure at the top of the lumped drill pipe tool joints length inside the drill string in the cased section of the borehole.

The first drill string section increment is denoted by the length H_1. The temperature at the bottom drill pipe body lumped geometry length in the cased section is

$$T_1 \quad 570.91°\text{R}$$

The average temperature of the drill pipe body lumped geometry along H_1 and, thus, the temperature of the gas flow inside this drill string length is

$$T_{av1} \quad 537.66°\text{R}$$

The inside surface of the drill pipe body has the surface roughness of commercial steel. Therefore, over this lumped drill pipe body length the surface roughness is

$$e_p \quad 0.00015 \ \text{ft}$$

With the above, Equation 6-73 becomes

$$f_{i1} = \left[\frac{1}{2 \, \log \dfrac{0.319}{0.00015} + 1.14} \right]^2$$

$$f_{i1} = 0.016$$

Equations 6-67 and 6-68 become, respectively,

$$a_{i1} = \frac{1.0}{53.36}$$

$$a_{i1} = 0.019$$

and

$$b_{i1} = \frac{0.016}{2 \, (32.2)} \left[\frac{53.36}{1.0} \right]^2 \frac{(2.635)^2}{\left[\dfrac{\pi}{4} \right]^2 (0.319)^5}$$

$$b_{i1} = 2,486$$

Equation 6-72 becomes

$$P_{in} = \left[\frac{(48,157)^2 - (2,486) \, (537.66)^2 \left[e^{\frac{2 \, (0.019) \, (6,650)}{537.66}} - 1 \right]}{e^{\frac{2 \, (0.019) \, (6,650)}{537.66}}} \right]^{0.5}$$

$$P_{in} = 41,537 \ \text{lb/ft}^2 \ \text{abs}$$

$$p_{in} = \frac{P_{in}}{144}$$

$$p_{in} = 288.5 \ \text{psia}$$

   The injection pressure given above is the flowing air pressure at the top of the lumped drill pipe body length inside the drill string in the cased section of the borehole while drilling at a depth of 10,000 ft. This is the approximate injection at the top of the drill string required to force a volumetric flow rate of 2,400 acfm

through the circulation system.   This injection pressure is the pressure the compressor output must match.

Compressor Unit Prime Mover Capability

Knowing the injection pressure, it is necessary to ascertain whether the prime mover of this primary compressor unit has the power to operate at the 4,000 ft surface elevation.   The prime mover for this compressor is a diesel fueled, turbocharged, Caterpillar Model D398 with a peak output of 760 horsepower at 900 rpm (at API standard conditions) (see Section 4.7 in Chapter 4).   The theoretical shaft horsepower, $\dot{W}_s$, required by each of the two compressors is obtained from Equation 4-35a.   Equation 4-35a becomes

$$\dot{W}_s \quad \frac{(4)\,(1.4)}{(0.4)} \quad \frac{(12.685) \; \dfrac{2,400}{2}}{229.17} \quad \frac{288.5}{12.685} \; {}^{\frac{(0.4)}{(4)(1.4)}} \quad 1$$

$$\dot{W}_s \quad 232.5$$

The mechanical efficiency, $_m$, is

$$_m \quad 0.90$$

This is a four-stage reciprocating piston compressor.   Therefore,

$$n_s \quad 4$$

The first stage compressor ratio is

$$r_s \quad \frac{232.5}{12.685} \; {}^{\frac{1}{4}}$$

$$r_s \quad 2.18$$

The volumetric efficiency (only for the reciprocating piston compressor), $_v$, is determined from Equation 4-38.   The compressor clearance volume ratio, c, is assumed to be 0.06.   Equation 4-38 becomes

$$_v \quad 0.96 \quad 1 \quad 0.06 \quad 2.18 \; {}^{\frac{1}{1.4}} \quad 1$$

$$_v \quad 0.917$$

From Equation 4-39, the actual shaft horsepower, $\dot{W}_{as}$, required by each compressor is

$$\dot{W}_{as} \quad \frac{232.5}{(0.90)\ (0.917)}$$

$$\dot{W}_{as} \quad 281.7$$

The above determined 281.7 horsepower is the actual shaft power needed by each of the two compressors to produce the 288.5 psia pressure output at the surface location elevation of 4,000 ft above sea level (while drilling at a depth of 10,000 ft). At this surface location, the input horsepower available from the Caterpillar Model D398 prime mover is a derated value (derated from the rated 760 horsepower available at 900 rpm). In order for the compressor units to operate at this 4,000 ft surface location elevation, the derated input power available must be greater than the actual shaft power needed. Figure 4-15 shows that for 4,000 ft elevation the input power of a turbocharged prime mover must be derated by approximately 10 percent. The derated input horsepower, $\dot{W}_i$, available from the prime mover is

$$\dot{W}_i \quad 760\ (1 \quad 0.10)$$

$$\dot{W}_i \quad 684.0$$

For this illustrative example, the prime mover of each of the two compressor units derated input power is greater than the actual shaft horsepower needed, thus, the selected compressor units can be operated at this 4,000 ft surface location elevation (while drilling at a depth of 10,000 ft).

Compressor Unit Fuel Consumption

The reciprocating piston compressor is not a fixed pressure ratio machine like the rotary compressor. As long as there is sufficient power available from the prime mover the reciprocating piston compressor will match the back pressure resistance. It was found above that the actual shaft horsepower required by each of the two reciprocating piston compressor units to compress air to 288.4 psia was approximately 281.7 (while drilling at 10,000 ft of depth). Also above it was found that the derated horsepower available from the Caterpillar Model D398 prime mover at the surface elevation of 4,000 ft was 684.0. Drilling at a depth of 10,000 ft, the prime mover power ratio is

$$PR \quad \frac{281.7}{684.0}\ (100) \quad 41.2$$

Using Figure 4-17 the diesel fuel consumption rate for a power level of 41.2 percent is 0.680 lb/hp-hr of diesel fuel. The total weight rate of diesel fuel consumption per hour is

$\dot{w}_f$ 0.680 (281.7)   191.6 lb/hr

The diesel fuel consumption rate (in United States gallons) for the drilling depth of 10,000 ft is

$$q_f \quad \frac{191.6}{(0.8156)\ (8.33)} \quad 28.2 \ \text{gal/hr}$$

Since there are two compressor units providing compressed air to this example air hammer drilling operation, the total diesel fuel consumption rate while drilling at the 10,000 ft of depth is approximately 57 gal/hr.

11.2.2 *Converted Downhole Positive Displacement Mud Motors*

Only one commercially successful positive displacement fluid motor has been developed. These motors are known as helical or capsular motors.   These are based on the work of French engineer Rene Moineau who patented numerous variants of these devices for hydraulic (incompressible fluid) pumps (and hydraulic motors) between 1930 and 1948. The driving stage of these motors is composed of a rigid shaft made up of continuous (or progressive) helical lobe cavities. This rigid helical lobe shaft is inserted into a flexible helical lobe cavity sheath (tight fitting).   The outside surface of the sheath is affixed to the inside surface of a rigid cylindrical housing. As fluid is pumped under pressure into one end of this device, the rigid shaft is forced to rotate as the fluid passes through the cavities between the rigid shaft lobes and the flexible lobe cavities in the sheath.   Figure 11-10 shows a cutaway view of the helical lobe section of a typical downhole positive displacement mud motor based on this Moineau design [1].

In Figure 11-10 the rigid helical lobe shaft is denoted as the rotor and the flexible helical lobe cavity sheath is denoted as the stator. In this figure, the drill string would be made up to the top of the motor and the drilling mud pumped under pressure into the motor through the drill string connection. The flow of the drilling mud through the motor would force the rotor to rotate. The bottom end of the rotor is connected to a flexible universal joint coupling and shaft with a bearing assembly and drive sub. Through this connection the drill bit is turned at the same rotational speed as the rotor. The drilling mud exits the motor at the bottom end and flows through the drill bit open orifices (or nozzles). In the bottom of the annulus, the drilling mud entrains the rock cuttings generated by the drill bit and carries these cuttings to the surface in the annulus [2].

The example positive displacement motor shown in Figure 11-10 has a 5 lobe rigid helical shaft and a 6 lobe flexible helical cavity sheath configuration. A cross-section view of this configuration is shown in Figure 11-11 together with several other typical configurations [1].

Assuming the same downhole motor size and fluid volumetric flow rate through the motor (same hydraulic power), the basic differences between the five typical lobe configurations given in Figure 11-11 are
  • The higher the lobe configuration, the higher the rotor shaft output torque,
  • The higher the lobe configuration, the lower the rotor shaft output speed.

Depending on the drilling applications, a motor size and lobe configuration may be more effective than another.
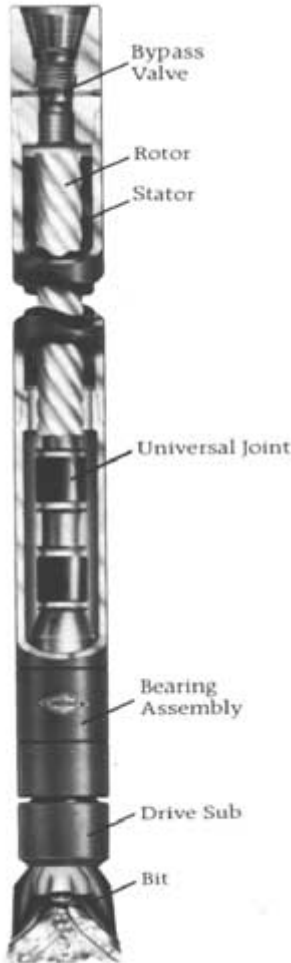
Figure 11-10: Cutaway view of a typical 5:6 lobe configuration positive displacement mud motor (courtesy of Baker Oil Tools).

Downhole positive displacement motors have been very useful in directional drilling operations. For directional drilling operations, the downhole positive displacement motor is made up to a bent sub directly above the motor with an

MWD system made up above the bent sub. The conventional drill string is made up to the top of the MWD.
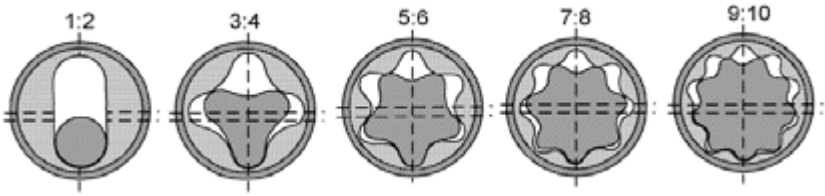
Figure 11-11: Different lobe configurations for the progressive helical lobe positive displacement motors.

These drilling mud actuated positive displacement motors have been adapted for use in air and gas drilling operations. Positive displacement motors converted for air and gas drilling operations usually involve replacing the conventional mud motor bearing assembly (which uses the drilling mud as the lubricant) with a sealed grease lubricated bearing assembly. Also, the dimensional tolerances between the rigid helical lobe shaft and the helical lobe flexible sheath are relaxed to provide a looser fit between these elements. To operate these downhole motors in an air drilling operation, a liquid lubricant must be injected into the compressed air flow being injected into the top of the drill string. These downhole motors can be operated with aerated drilling fluids (usually drilling mud with air or gas aeration) or with stable foam with little or no special motor preparations.

The primary operational concern when drilling with a downhole positive displacement motor using compressed air (or gas) is the tendency of the rotor shaft to rotate at too high a speed and, thus, destroy (with friction heat) the elastomer flexible helical cavity sheath of the motor. One operational situation where this can occur is when there is excessive expansion of the air as it passes through the progressive cavities of the motor. Such excessive expansion can allow run away rotor speeds which can only be controlled by inserting appropriately sized nozzles into the drill bit (or a single nozzle inside motor flow passage above the drill bit connection) [3]. The small diameter nozzles choke the air flow from the motor and provide a back pressure at the bottom of the positive displacement motor (above the drill bit). This back pressure controls the air expansion and, thereby, controls output rotational speed of the rotor.

Another run away speed situation can occur when the drilling load is taken off the motor by lifting the drill string. Under these conditions, the rotor can again go to high speeds and destroy the elastomer flexible sheath. This must be controlled by installing a by-pass valve above the motor section. This by-pass valve is actuated when weight is taken off the drill bit. When the weight is removed the valve is opened and most of the flow down the inside of the drill string is diverted directly to the annulus. Little fluid flow goes through the motor cavity and, therefore, the speed of the rotor is kept under control.

The downhole positive displacement motor is actuated by the volumetric flow rate of the fluid passing through it. The output speed of the motor rotor shaft is

directly proportional to the volumetric flow rate of the fluid. The torque that the rotor shaft can produce is nearly directly proportional to the pressure drop through the motor. Thus, the power the motor can generate is also directly proportional to the pressure drop through the motor. Figure 11-12 shows the torque and power outputs versus pressure drop plots for a typical 6 3/4 inch outside diameter, 5:6 lobe, downhole positive displacement motor with a volumetric flow rate of 400 gal/min of drilling mud or other incompressible drilling fluid.

The plots in Figure 11-12 are for the drilling fluid volumetric flow rate of 400 gal/min. This volumetric flow rate gives a nearly constant motor rotor rotation speed of 200 rpm (the drill bit speed). There are a similar family of plots that can be prepared for this motor for other drilling fluid volumetric flow rates. Higher volumetric flow rates yield higher drill bit speeds and lower volumetric flow rates yield lower drill bit speeds. The torque and power plots are similarly altered for increases and decreases in volumetric flow rates.

Illustrative Example 11.2 Determine the injection pressure and resulting compressor fuel consumption when a Baker Oil Tools Model Mach 1, 6 3/4 inch outside diameter, 5:6 lobe, downhole positive displacement motor is utilized to drill the openhole interval from 7,000 ft to 10,000 ft of the Illustrative Example 8.3 series in Chapter 8. The positive displacement motor is to use a 7 7/8 inch tri-cone roller cutter drill bit to drill at 10,000 ft. It is required that the downhole motor develop 25 horsepower when drilling under load. In the Illustrative Example 8.3 series two semi-trailer mounted Dresser Clark Model CFB-4, four-stage, reciprocating piston compressors where selected. Each of these compressors where driven by a Caterpillar Model D398 diesel fueled prime mover. These two compressor units provide a total of 2,400 acfm to the borehole. The drilling location is at 4,000 ft above sea level. The annulus solution given in Illustrative Example 8.3b will be used as the starting point for this example.

In Illustrative Example 8.3b the bottomhole annulus pressure was determined. This annulus bottomhole pressure was found to be

$$p_{a5} \quad 204.5 \ \text{psia}$$

$$P_{a5} \quad p_{a5} \ 144$$

$$P_{a5} \quad 29,448 \ \text{lb/ft}^2 \ \text{abs}$$

Using the positive displacement motor to drill the borehole does not alter the annulus solution obtained in Illustrative Example 8.3b. However, it will alter the pressure calculations from the bottom of the annulus to the top of the inside of the drill string (the injection pressure).

Drill Bit Nozzles

The tri-cone roller cutter drill bit used in this example operation has three nozzles. The nozzle inside diameter is selected by trial and error. Figure 11-12 shows that for a drilling mud flow rate of 400 gal/min, the drill bit speed will be 200 rpm. Thus, the nozzles inside diameter must be selected to give a simulated

flow rate of compressed air through the motor of approximately 400 gal/min.   Using a nozzle inside diameter of 10/32 inches (for all three nozzles) yields a drill bit speed of approximately 200 rpm. The inside diameter of the nozzles, D_n, is

$$d_n \quad 0.3125 \text{ inches}$$

$$D_n \quad \frac{d_n}{12}$$

$$D_n \quad 0.0260 \text{ ft}$$

Circulation Rate 400 gpm
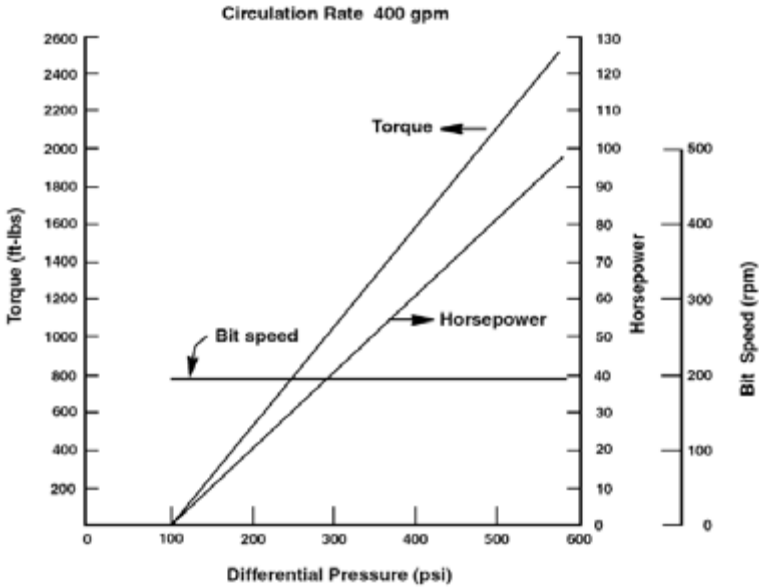
Figure 11-12: Horsepower and torque rotor shaft output versus pressure drop across a Baker Oil Tools Model Mach 1, 6 3/4 inch outside diameter positive displacement motor. For a volumetric flow rate of 400 gal/min (courtesy of Baker Oil Tools).

The total cross-sectional area of flow through the drill bit nozzles, A_n, is

$$A_n \quad 3 \quad \frac{}{4} \quad (0.0260)^2$$

$$A_n \quad 0.00160 \text{ ft}^2$$

Equation 6-62 is used to determine the pressure inside the drill bit just above the nozzles. The flow through nozzles is sonic. Therefore, Equation 6-62 must be used to determine the pressure upstream of bottomhole annulus pressure. Thus, Equation 6-62 becomes

$$P_{iab} \quad \frac{(2.635)\,(604.41)^{0.5}}{(0.00160)\quad \dfrac{(32.2)\,(1.4)\,(1.0)}{53.36}\quad \dfrac{2}{2.4}\,^{\frac{2.4}{0.4}}\quad ^{0.5}}$$

$$P_{iab} \quad 76{,}220 \ \text{lb/ft}^2 \ \text{abs}$$

$$p_{iab} \quad \frac{P_{iab}}{144}$$

$$p_{iab} \quad 529.3 \ \text{psia}$$

Positive Displacement Motor Performance

Positive displacement pumps and motors are characterized by their displacement volume. From the basic data in Figure 11-12, the motor displacement can be obtained. The displacement, *s*, is [2]

$$s \quad \frac{(231.016)\,(400)}{(200)}$$

$$s \quad 462.032 \ \text{in}^3$$

Using Figure 11-12, a pressure drop across the motor of 220 psi will give 25 horsepower (at the drill bit speed of 200 rpm). The pressure at the bottom of the motor cavity, p_{bm}, is approximately equal to p_{iab}. Therefore,

$$p_{bm} \quad 529.3 \ \text{psia}$$

$$P_{bm} \quad p_{bm} \ 144$$

$$P_{bm} \quad 76{,}219 \ \text{lb/ft}^2 \ \text{abs}$$

The pressure above the motor, p_{am}, is

$$p_{am} \quad p_{bm} \quad 220$$

$$p_{am} \quad 749.3 \ \text{psia}$$

$$P_{am} \qquad p_{am} \ 144$$

$$P_{am} \qquad 107,899 \ \text{lb/ft}^2 \ \text{abs}$$

The average pressure in the motor, p_{mav}, is approximately

$$p_{mav} \qquad \frac{p_{bm} \qquad p_{am}}{2}$$

$$p_{mav} \qquad \frac{529.3 \qquad 729.3}{2}$$

$$p_{mav} \qquad 639.3 \ \text{psia}$$

$$P_{mav} \qquad p_{mav} \ 144$$

$$P_{mav} \qquad 92,060 \ \text{lb/ft}^2 \ \text{abs}$$

Using Equation 4-11 the average specific weight of the air in the motor cavity, $_{mav}$, is approximately

$$_{mav} \qquad \frac{(92,060) \ (1.0)}{(53.36) \ (604.41)}$$

$$_{mav} \qquad 2.854 \ \text{lb/ft}^3$$

The average volumetric flow rate of the air through the motor cavity, Q_{mav}, is approximately

$$Q_{mav} \qquad \frac{\dot{w}_g}{_{mav}}$$

$$Q_{mav} \qquad \frac{2.635}{2.854}$$

$$Q_{mav} \qquad 0.923 \ \text{ft}^3/\text{sec}$$

$$q_{mav} \qquad \frac{(0.923) \ (12^3) \ (60)}{231.016}$$

$$q_{mav} \qquad 414.3 \ \text{gal/min}$$

The drill bit speed of the motor, N_m, when operating on air is approximately

$$N_m \quad \frac{231.016 \ q_{mav}}{s}$$

$$N_m \quad \frac{(231.016) \ (414.3)}{462.032}$$

$$N_m \quad 207.2 \ \text{rpm}$$

The above drill bit speed is quite close to the 200 rpm required. If 9/32 inch nozzles are placed in the drill bit, the bit speed would be lower. And if 11/32 inch nozzles are placed in the drill bit, the bit speed would be higher.

The use of the 10/32 inch nozzles in the drill bit controls the drill bit speed and the expansion of the air inside the motor when the motor is under load (with WOB). When the load is removed from the motor (no WOB), the motor will go to run away speeds and damage of the elastomer flexible sheath will result. Thus, when the motor load is removed, either the air flow to the drill string must be shut down, or a weight actuated by-pass must be used to divert the air to the annulus when the weight on bit is removed.

Geometry Inside the Drill String

Starting at the bottom of the drill string, the total length of the drill collars length increment, H_5, in the openhole section is

$$H_5 \quad 500 \ \text{ft}$$

The inside diameter of the drill collars length in this openhole section is

$$d_5 \quad 2.8125 \ \text{inches}$$

$$D_5 \quad \frac{d_5}{12}$$

$$D_5 \quad 0.234 \ \text{ft}$$

The total length of the drill pipe tool joints lumped geometry increment, H_4, in the openhole section is

$$H_4 \quad 125 \ \text{ft}$$

The inside diameter of the drill pipe tool joints lumped geometry in this openhole section is

$$d_6 \quad 3.50 \ \text{inches}$$

$$D_6 \quad \frac{d_6}{12}$$

$$D_6 \quad 0.292 \text{ ft}$$

The total length of the lumped drill pipe body geometry increment, H_3, in the openhole section is

$$H_3 \quad 2,375 \text{ ft}$$

The inside diameter of the drill pipe body lumped geometry in this openhole section is

$$d_7 \quad 3.826 \text{ inches}$$

$$D_7 \quad \frac{d_7}{12}$$

$$D_7 \quad 0.319 \text{ ft}$$

The total length of the lumped drill pipe tool joints geometry increment, H_2, in the cased section is

$$H_2 \quad 350 \text{ ft}$$

The inside diameter of the drill pipe tool joints lumped geometry in this cased section is

$$D_6 \quad 0.292 \text{ ft}$$

The total length of the lumped drill pipe body geometry increment, H_1, in the cased section is

$$H_1 \quad 6,650 \text{ ft}$$

The inside diameter of the drill pipe body lumped geometry in this cased section is

$$D_7 \quad 0.319 \text{ ft}$$

Inside the Drill String (10,000 ft to 7,000 ft)
The fifth drill string section increment is denoted by the length H_5. The temperature at the bottom of the drill collars (bottomhole temperature) in the openhole section is

$$T_5 \qquad 604.41°R$$

The average temperature of the drill collar length H_5 and, thus, the temperature of the gas flow inside the drill collars is

$$T_{av5} \qquad 601.91°R$$

The inside surface of the drill collars has the surface roughness of commercial steel. Therefore, over this drill collar length the surface roughness is

$$e_p \qquad 0.00015 \ \text{ft}$$

With the above, Equation 6-73 becomes

$$f_{i5} \qquad \left[\frac{1}{2 \ \log \dfrac{0.234}{0.00015} \quad 1.14} \right]^2$$

$$f_{i5} \qquad 0.018$$

Equations 6-67 and 6-68 become, respectively,

$$a_{i5} \qquad \frac{1.0}{53.36}$$

$$a_{i5} \qquad 0.019$$

and

$$b_{i5} \qquad \frac{0.018}{2 \ (32.2)} \left[\frac{53.36}{1.0} \right]^2 \frac{(2.635)^2}{-\dfrac{2}{4} \ (0.234)^5}$$

$$b_{i5} \qquad 12,420$$

The pressure above the motor, P_{am}, is the approximate pressure at the bottom of the inside of the drill string. Thus, Equation 6-72 becomes

$$P_{i4} \qquad \frac{(107,899)^2 \qquad (12,420)\,(601.91)^2 \quad e^{\frac{2\,(0.019)\,(500)}{601.91}} \qquad 1}{e^{\frac{2\,(0.019)\,(500)}{601.91}}}^{0.5}$$

$$P_{i4} \qquad 106,877 \ \text{lb/ft}^2 \ \text{abs}$$

$$p_{i4} \qquad \frac{P_{i4}}{144}$$

$$p_{i4} \qquad 742.2 \ \text{psia}$$

The pressure given above is the flowing air pressure at the top of the drill collar length inside the drill string in the openhole section of the borehole.

The fourth drill string section increment is denoted by the length H_4. The temperature at the bottom of the drill pipe tool joints lumped geometry length in the openhole section is

$$T_4 \qquad 599.41°\text{R}$$

The average temperature of the drill pipe tool joints lumped length along H_4 and, thus, the temperature of the gas flow inside this drill string length is

$$T_{av4} \qquad 598.79°\text{R}$$

The inside surface of the drill pipe tool joint has the surface roughness of commercial steel. Therefore, over this lumped drill pipe tool joint length the surface roughness is

$$e_p \qquad 0.00015 \ \text{ft}$$

With the above, Equation 6-73 becomes

$$f_{i4} \qquad \frac{1}{\left(2 \ \log \dfrac{0.292}{0.00015} \quad 1.14\right)^2}$$

$$f_{i4} \qquad 0.017$$

Equations 6-67 and 6-68 become, respectively,

$$a_{i4} \quad \frac{1.0}{53.36}$$

$$a_{i4} \quad 0.019$$

and

$$b_{i4} \quad \frac{0.017}{2\ (32.2)} \quad \frac{53.36}{1.0}^2 \quad \frac{(2.635)^2}{\dfrac{}{4}\ (0.292)^5}$$

$$b_{i4} \quad 3{,}958$$

Equation 6-72 becomes

$$P_{i3} \quad \frac{(106{,}877)^2 \quad (3{,}958)\ (598.79)^2\ e^{\frac{2\ (0.019)\ (125)}{598.79}} \quad 1}{e^{\frac{2\ (0.019)\ (125)}{598.79}}}^{0.5}$$

$$P_{i3} \quad 106{,}511 \ \text{lb/ft}^2 \ \text{abs}$$

$$p_{i3} \quad \frac{P_{i3}}{144}$$

$$p_{i3} \quad 739.7 \ \text{psia}$$

The pressure given above is the flowing air pressure at the top of the lumped drill pipe tool joint length inside the drill string in the openhole section of the borehole.

The third drill string section increment is denoted by the length H_3. The temperature at the bottom of the drill pipe body lumped geometry length in the openhole section is

$$T_3 \quad 598.16°\text{R}$$

The average temperature of the drill pipe body lumped geometry length along H_3 and, thus, the temperature of the gas flow inside this drill string length is

$$T_{av3} \quad 586.29°\text{R}$$

The inside surface of the drill pipe body has the surface roughness of commercial steel. Therefore, over this lumped drill pipe body length the surface roughness is

$$e_p \quad 0.00015 \text{ ft}$$

With the above, Equation 6-73 becomes

$$f_{i3} \quad \left[\frac{1}{2 \log \dfrac{0.319}{0.00015} \quad 1.14} \right]^2$$

$$f_{i3} \quad 0.016$$

Equations 6-67 and 6-68 become, respectively,

$$a_{i3} \quad \frac{1.0}{53.36}$$

$$a_{i3} \quad 0.019$$

and

$$b_{i3} \quad \frac{0.016}{2 \ (32.2)} \left[\frac{53.36}{1.0}\right]^2 \quad \frac{(2.635)^2}{\dfrac{}{4} (0.319)^5}$$

$$b_{i3} \quad 2,486$$

Equation 6-72 becomes

$$P_{i2} \quad \frac{(106,511)^2 \quad (2,486) \ (586.29)^2 \quad e^{\frac{2 \ (0.019) \ (2,375)}{586.29}} \quad 1}{e^{\frac{2 \ (0.019) \ (2,375)}{586.29}}}^{0.5}$$

$$P_{i2} \quad 99,332 \text{ lb/ft}^2 \text{ abs}$$

$$p_{i2} \quad \frac{P_{i2}}{144}$$

$$p_{i2} \quad 689.8 \text{ psia}$$

The pressure given above is the flowing air pressure at the top of the lumped drill pipe body length inside the drill string in the openhole section of the borehole.

Inside the Drill String (7,000 ft to Surface)

The second drill string section increment is denoted by the length H_2. The temperature at the bottom drill pipe tool joints lumped geometry length in the cased section is

$$T_2 \quad 574.41°R$$

The average temperature of the drill pipe tool joints lumped geometry along H_2 and, thus, the temperature of the gas flow inside this drill string length is

$$T_{av2} \quad 572.66°R$$

The inside surface of the drill pipe body has the surface roughness of commercial steel. Therefore, over this lumped drill pipe body length the surface roughness is

$$e_p \quad 0.00015 \text{ ft}$$

With the above, Equation 6-73 becomes

$$f_{i2} \quad \frac{1}{\left[2 \ \log \ \dfrac{0.292}{0.00015} \ \ 1.14 \right]^2}$$

$$f_{i2} \quad 0.017$$

Equations 6-67 and 6-68 become, respectively,

$$a_{i2} \quad \frac{1.0}{53.36}$$

$$a_{i2} \quad 0.019$$

and

$$b_{i2} \quad \frac{0.017}{2\,(32.2)} \quad \frac{53.36}{1.0}^2 \quad \frac{(2.635)^2}{-\frac{}{4}\,(0.292)^5}$$

$$b_{i2} \quad 3,958$$

Equation 6-72 becomes

$$P_{i1} \quad \frac{(99,332)^2 \quad (3,958)\,(572.66)^2 \; e^{\frac{2\,(0.019)\,(350)}{572.66}} \quad 1}{e^{\frac{2\,(0.019)\,(350)}{572.66}}}^{0.5}$$

$$P_{i1} \quad 98,350 \ \mathrm{lb/ft}^2 \ \mathrm{abs}$$

$$p_{i1} \quad \frac{P_{i1}}{144}$$

$$p_{i1} \quad 683.0 \ \mathrm{psia}$$

The pressure given above is the flowing air pressure at the top of the lumped drill pipe tool joints length inside the drill string in the cased section of the borehole.

The first drill string section increment is denoted by the length H_1.   The temperature at the bottom drill pipe body lumped geometry length in the cased section is

$$T_1 \quad 570.91°R$$

The average temperature of the drill pipe body lumped geometry along H_1 and, thus, the temperature of the gas flow inside this drill string length is

$$T_{av1} \quad 537.66°R$$

The inside surface of the drill pipe body has the surface roughness of commercial steel.   Therefore, over this lumped drill pipe body length the surface roughness is

$$e_p \quad 0.00015 \ \mathrm{ft}$$

With the above, Equation 6-73 becomes

$$f_{i1} \quad \frac{1}{\left[2 \ \log \ \left(\frac{0.319}{0.00015}\right) \quad 1.14\right]^2}$$

$$f_{i1} \quad 0.016$$

Equations 6-67 and 6-68 become, respectively,

$$a_{i1} \quad \frac{1.0}{53.36}$$

$$a_{i1} \quad 0.019$$

and

$$b_{i1} \quad \frac{0.016}{2 \ (32.2)} \ \left(\frac{53.36}{1.0}\right)^2 \ \frac{(2.635)^2}{\left(\frac{}{4}\right)^2 (0.319)^5}$$

$$b_{i1} \quad 2,486$$

Equation 6-72 becomes

$$P_{in} \quad \frac{(98,350)^2 \quad (2,486) \ (537.66)^2 \ \left[e^{\frac{2 \ (0.019) \ (6,650)}{537.66}} \quad 1\right]}{e^{\frac{2 \ (0.019) \ (6,650)}{537.66}}}^{0.5}$$

$$P_{in} \quad 79,693 \ \text{lb/ft}^2 \ \text{abs}$$

$$p_{in} \quad \frac{P_{in}}{144}$$

$$p_{in} \quad 553.4 \ \text{psia}$$

The injection pressure given above is the flowing air pressure at the top of the lumped drill pipe body length inside the drill string in the cased section of the borehole while drilling at a depth of 10,000 ft. This is the approximate injection at the top of the drill string required to force a volumetric flow rate of 2,400 acfm

through the circulation system.   This injection pressure is the pressure the compressor output must match.

Compressor Unit Prime Mover Capability

Knowing the injection pressure, it is necessary to ascertain whether the prime mover of this primary compressor unit has the power to operate at the 4,000 ft surface elevation.   The prime mover for this compressor is a diesel fueled, turbocharged, Caterpillar Model D398 with a peak output of 760 horsepower at 900 rpm (at API standard conditions) (see Section 4.7 in Chapter 4).   The theoretical shaft horsepower, $\dot{W}_s$, required by each of the two compressors is obtained from Equation 4-35a. Equation 4-35a becomes

$$\dot{W}_s \quad \frac{(4)\ (1.4)}{(0.4)}\ \frac{(12.685)\ \dfrac{2,400}{2}}{229.17}\ \frac{553.4}{12.685}^{\frac{(0.4)}{(4)(1.4)}} \quad 1$$

$$\dot{W}_s \quad 287.9$$

The mechanical efficiency, $_m$, is

$$_m \quad 0.90$$

This is a four-stage reciprocating piston compressor. Therefore,

$$n_s \quad 4$$

The first stage compressor ratio is

$$r_s \quad \frac{553.4}{12.685}^{\frac{1}{4}}$$

$$r_s \quad 2.57$$

The volumetric efficiency (only for the reciprocating piston compressor), $_v$, is determined from Equation 4-38.   The compressor clearance volume ratio, c, is assumed to be 0.06. Equation 4-38 becomes

$$_v \quad 0.96 \quad 1 \quad 0.06 \quad 2.57^{\frac{1}{1.4}} \quad 1$$

$$_v \quad 0.905$$

From Equation 4-39, the actual shaft horsepower, $\dot{W}_{as}$, required by each compressor is

$$\dot{W}_{as} \quad \frac{287.9}{(0.90)\ (0.905)}$$

$$\dot{W}_{as} \quad 353.6$$

The above determined 353.6 horsepower is the actual shaft power needed by each of the two compressors to produce the 553.4 psia pressure output at the surface location elevation of 4,000 ft above sea level (while drilling at a depth of 10,000 ft). At this surface location, the input horsepower available from the Caterpillar Model D398 prime mover is a derated value (derated from the rated 760 horsepower available at 900 rpm). In order for the compressor units to operate at this 4,000 ft surface location elevation, the derated input power available must be greater than the actual shaft power needed. Figure 4-15 shows that for 4,000 ft elevation the input power of a turbocharged prime mover must be derated by approximately 10 percent. The derated input horsepower, $\dot{W}_i$, available from the prime mover is

$$\dot{W}_i \quad 760\ (1 \quad 0.10)$$

$$\dot{W}_i \quad 684.0$$

For this illustrative example, the prime mover of each of the two compressor units derated input power is greater than the actual shaft horsepower needed, thus, the selected compressor units can be operated at this 4,000 ft surface location elevation (while drilling at a depth of 10,000 ft).

Compressor Unit Fuel Consumption

The reciprocating piston compressor is not a fixed pressure ratio machine like the rotary compressor. As long as there is sufficient power available from the prime mover the reciprocating piston compressor will match the back pressure resistance. It was found above that the actual shaft horsepower required by each of the two reciprocating piston compressor units to compress air to 553.4 psia was approximately 353.6 (while drilling at 10,000 ft of depth). Also above it was found that the derated horsepower available from the Caterpillar Model D398 prime mover at the surface elevation of 4,000 ft was 684.0. Drilling at a depth of 10,000 ft, the prime mover power ratio is

$$PR \quad \frac{353.6}{684.0}\ (100) \quad 51.7$$

Using Figure 4-17 the diesel fuel consumption rate for a power level of 51.7 percent is 0.630 lb/hp-hr of diesel fuel. The total weight rate of diesel fuel consumption per hour is

$$\dot{w}_f \quad 0.630\ (353.6) \quad 222.8\ \text{lb/hr}$$

The diesel fuel consumption rate (in United States gallons) for the drilling depth of 10,000 ft is

$$q_f \quad \frac{222.8}{(0.8156)(8.33)} \quad 32.8 \text{ gal/hr}$$

Since there are two compressor units providing compressed air to this example air hammer drilling operation, the total diesel fuel consumption rate while drilling at the 10,000 ft of depth is approximately 66 gal/hr.

11.2.3 *Downhole Pneumatic Turbine Motors*

The downhole pneumatic turbine motor is a rather new innovation in air drilling downhole equipment. This motor was developed in the early 1980's and was first used in the Geysers geothermal fields in Northern California [4, 5]. Figure 11-13 shows a schematic of the typical downhole pneumatic turbine motor. These downhole motors are actuated by a single stage aerodynamic turbine device. The turbine speed is controlled by a governor which is attached to the top of the turbine shaft. The aerodynamic turbine runs at high speed when exposed to a high weight rate of flow of compressed air or other gases. The high weight rate of flow of compressed air (or gas) is needed to carry the drill bit generated cuttings to the surface in the annulus.

The downhole turbine motor develops power mainly from the kinetic energy of the weight rate of flow through the turbine stator and rotor. There is a small pressure drop through the turbine, but with the high weight rate of flow through the turbine the pressure drop does not contribute greatly to the power. The single stage turbine converts the air flow energy to high speed mechanical shaft energy. This high mechanical shaft speed must be reduced to operate the drill bit. The downhole turbine motor has a sealed small compact gear reduction system that is directly coupled to the bottom of the turbine output shaft (i.e., the high speed coupling). The downhole motor can be fitted with several gear box configurations which can give reductions from 40 to 1 to as high as 120 to 1. The gears are grease lubricated and, therefore, their speed is limited. The governor on the turbine provides protection for the gears by controlling the input to the gear box from the turbine.

The output shaft of the gear box is directly coupled to the main drive shaft (with thrust and radial bearing assembly) with a high torque capability coupling. The high torque coupling allows high non-transient torque to be transferred from the output shaft of the gear box to the main drive shaft and, thus, to the tri-cone drill bit. Any transient impact torques are absorbed by the flexible spring system in the coupling, thus, protecting the gear teeth in the gear box from damaging impact forces.

In general, the downhole pneumatic turbine motor is used with roller cone drill bits. The motors can be actuated on compressed air and other compressed gases and the motors do not require any lubricant to be injected into the air or gas flowing to the motor. In essence, the motor can be run with dry air or gas. On the other hand, the motor can also be operated with unstable foam (misting).
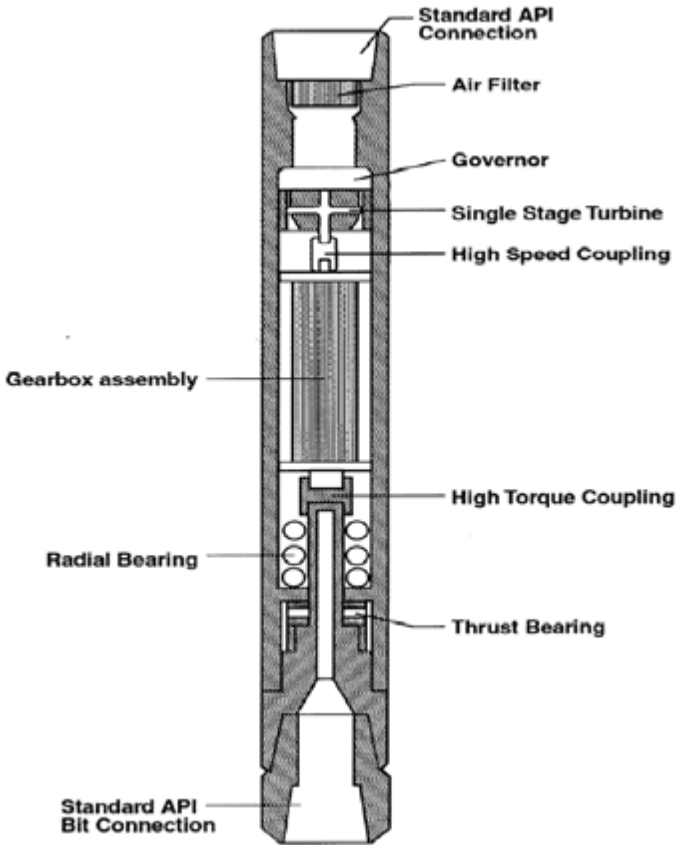
Figure 11-13: Schematic cutaway of a downhole pneumatic turbine motor (courtesy of Rift Pneumatics Incorporated).

The downhole pneumatic turbine motors must be operated with a junk screen above the turbine section when drilling deep wells. This screen will catch any large particles of pipe scale or other foreign matter before they can lodge in the turbine stator and rotor.

These downhole turbine motors are more mechanically complicated than either the downhole air hammer or the downhole positive displacement motor. Therefore, it is necessary to manage the various drillings string forces on the BHA (including the motor) in order to prevent motor damage.

Like the downhole positive displacement motor the downhole turbine motor may require drill bit nozzles to choke the exhaust of the turbine device [3]. This is

particularly the case when drilling at shallow depth with high volumetric flow rates of air or gas. At shallow depth the bottomhole annulus pressure is low and the turbine must be choked in order to limit the torque and power in the gear box and at the drill bit.

Illustrative Example 11.3 Determine the injection pressure and resulting compressor fuel consumption when a Rift Pneumatics Model 650, 6 1/2 inch outside diameter, downhole pneumatic turbine motor is utilized to drill the openhole interval from 7,000 ft to 10,000 ft of the Illustrative Example 8.3 series in Chapter 8. The gear box for this motor has a 112.5 to 1 reduction ratio. The positive displacement motor is to use a 7 7/8 inch tri-cone roller cutter drill bit to drill at 10,000 ft. It is required that the downhole motor develop approximately 28 horsepower when drilling under load. In the Illustrative Example 8.3 series two semi-trailer mounted Dresser Clark Model CFB-4, four-stage, reciprocating piston compressors where selected. Each of these compressors where driven by a Caterpillar Model D398 diesel fueled prime mover. These two compressor units provide a total of 2,400 acfm to the borehole. The drilling location is at 4,000 ft above sea level. The annulus solution given in Illustrative Example 8.3b will be used as the starting point for this example.

Figure 11-14 shows the power performance plot of the Model 650, 6 1/2 inch outside diameter, downhole pneumatic turbine motor actuated with a flow rate of 2,400 acfm (at a surface location of 4,000 ft, i.e., 2.635 lb/sec). In order to obtain a 28 horsepower output at the drive shaft, the governor is set to give a drive shaft speed of about 40 rpm. This would limit the turbine rotor speed to 4,500 rpm. It should be noted that a higher weight rate of flow of air or gas will result in a larger power parabola than that shown in Figure 11-14. The larger power parabola will have a higher peak power (that occurs at a higher drill bit speed) and a higher theoretical runaway speed (where there is no load on the motor). Likewise, a lower weight rate of flow of air or gas will result in a smaller power parabola.

In Illustrative Example 8.3b the bottomhole annulus pressure was determined. This annulus bottomhole pressure was found to be

$$p_{a5} \quad 204.5 \text{ psia}$$

$$P_{a5} \quad p_{a5} \ 144$$

$$P_{a5} \quad 29,448 \text{ lb/ft}^2 \text{ abs}$$

Using the downhole pneumatic turbine motor to drill the borehole does not alter the annulus solution obtained in Illustrative Example 8.3b. However, it will alter the pressure calculations from the bottom of the annulus to the top of the inside of the drill string (the injection pressure).

Drill Bit Open Orifices

The downhole pneumatic turbine motor is being used to drill a deep borehole. Therefore, the bottomhole pressure is high and drill bit nozzles are not needed to choke the motor. The inside diameter of the open orifices, D_o, is

$$d_o \qquad 0.70 \ \text{inches}$$

$$D_o \qquad \frac{d_o}{12}$$

$$D_o \qquad 0.0583 \ \text{ft}$$
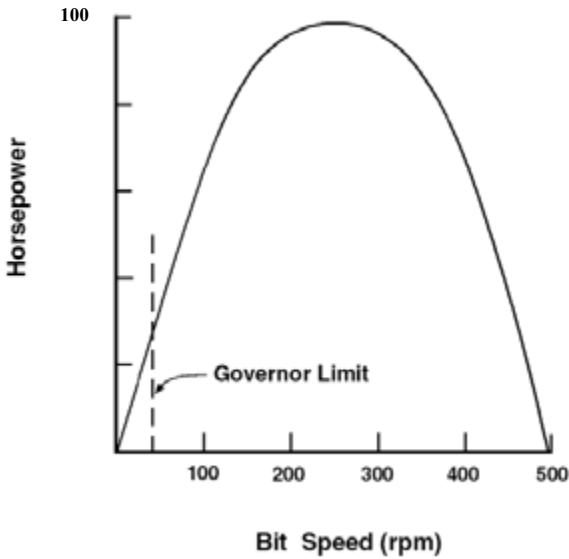
Figure 11-14: Power versus drill bit speed for a Rift Pneumatics, Model 650, 6 1/2 inch outside diameter, downhole pneumatic turbine motor operating by a 2.635 lb/sec weight rate of flow. The motor is fitted with gear box with a 112.5 to 1 reduction ratio. (courtesy of Rift Pneumatics Incorporated).

The total cross-sectional area of flow through the drill bit open orifices, A_o, is

$$A_o \qquad 3 \ \frac{}{4} \ (0.0583)^2$$

$$A_o \qquad 0.00802 \ \text{ft}^2$$

Using Equation 4-11 the specific weight of the air flow at the bottom of the annulus, $_{a5}$, is

$$\rho_{a5} \quad \frac{(29,448)\,(1.0)}{(53.36)\,(604.41)}$$

$$\rho_{a5} \quad 0.913 \text{ lb/ft}^3$$

Equation 6-63 is used to determine the pressure inside the drill bit just above the nozzles. The flow through nozzles is subsonic. Therefore, Equation 6-63 must be used to determine the pressure upstream of bottomhole annulus pressure. Equation 6-63 becomes

$$P_{iab} \quad (29,448) \quad \left[\frac{\dfrac{2.635}{0.00802}^2}{2\,(32.2)\,\dfrac{1.4}{0.4}\,(29,448)\,(0.913)} \quad 1 \right]^{\frac{1.4}{0.4}}$$

$$P_{iab} \quad 31,330 \text{ lb/ft}^2 \text{ abs}$$

$$p_{iab} \quad \frac{P_{iab}}{144}$$

$$p_{iab} \quad 217.6 \text{ psia}$$

Drive Shaft Passage

The pneumatic turbine motor drive shaft passage has an inside diameter of 1.50 inches and a length of 21.0 inches. Thus, the inside diameter of the drive shaft passage, D_{sp}, is

$$d_{sp} \quad 1.50 \text{ inches}$$

$$D_{sp} \quad \frac{d_{sp}}{12}$$

$$D_{sp} \quad 0.125 \text{ ft}$$

The length of the drive shaft passage, L_{sp}, is

$$l_{sp} \quad 21.0 \text{ inches}$$

$$L_{sp} \quad \frac{l_{sp}}{12}$$

$$L_{sp} \quad 1.750 \text{ ft}$$

Over the length of the drive shaft passage the surface roughness is

$$e_p \quad 0.00015 \text{ ft}$$

With the above, Equation 6-73 becomes

$$f_{isp} \quad \cfrac{1}{\left[2 \, \log \left(\cfrac{0.125}{0.00015}\right) \quad 1.14\right]^2}$$

$$f_{isp} \quad 0.021$$

Equations 6-67 and 6-68 become, respectively,

$$a_{isp} \quad \frac{1.0}{53.36}$$

$$a_{isp} \quad 0.019$$

and

$$b_{isp} \quad \frac{0.021}{2 \, (32.2)} \left(\frac{53.36}{1.0}\right)^2 \frac{(2.635)^2}{\left(\cfrac{}{4}\right)^2 (0.125)^5}$$

$$b_{isp} \quad 334,500$$

Equation 6-72 becomes

$$P_{isp} \quad \left[\cfrac{(31,330)^2 \quad (334,500) \, (604.41)^2 \quad e^{\frac{2 \, (0.019) \, (1.750)}{604.41}} \quad 1}{e^{\frac{2 \, (0.019) \, (1.750)}{604.41}}}\right]^{0.5}$$

$$P_{isp} \quad 31,540 \text{ lb/ft}^2 \text{ abs}$$

$$p_{isp} \qquad \frac{P_{isp}}{144}$$

$$p_{isp} \qquad 219.0 \ \text{psia}$$

Annulus Passage Around the Gear Box

The pneumatic turbine motor annulus passage around the gear box has an annulus outside surface diameter of 5.50 inches and an inside surface diameter of 4.70 inches. The length of the annulus section is 15.0 inches. Thus, the annulus outside diameter, D_{ano}, is

$$d_{ano} \qquad 5.50 \ \text{inches}$$

$$D_{ano} \qquad \frac{d_{ano}}{12}$$

$$D_{ano} \qquad 0.458 \ \text{ft}$$

The annulus inside diameter, D_{ani}, is

$$d_{ani} \qquad 4.70 \ \text{inches}$$

$$D_{ani} \qquad \frac{d_{ani}}{12}$$

$$D_{ani} \qquad 0.392 \ \text{ft}$$

The length of the annulus passage, L_{anp}, is

$$l_{anp} \qquad 15.0 \ \text{inches}$$

$$L_{anp} \qquad \frac{l_{anp}}{12}$$

$$L_{anp} \qquad 1.250 \ \text{ft}$$

Over the length of the annulus passage the surface roughness is

$$e_{p} \qquad 0.00015 \ \text{ft}$$

With the above, Equation 6-73 becomes

$$f_{ianp} = \left[\cfrac{1}{2 \, \log \cfrac{0.458 + 0.392}{0.00015} + 1.14} \right]^2$$

$$f_{ianp} = 0.024$$

Equations 6-67 and 6-68 become, respectively,

$$a_{ianp} = \frac{1.0}{53.36}$$

$$a_{ianp} = 0.019$$

and

$$b_{ianp} = \frac{0.024}{2 \, (32.2) \, (0.458 + 0.392)} \, \frac{53.36}{1.0}^2 \, \frac{(2.635)^2}{\frac{}{4}(0.458)^2 \, (0.392)^2{}^2}$$

$$b_{ianp} = 56,130$$

Equation 6-72 becomes

$$P_{ianp} = \left[\frac{(31,540)^2 + (56.130)(604.41)^2 \left(e^{\frac{2 \, (0.019) \, (1.250)}{604.41}} - 1 \right)}{e^{\frac{2 \, (0.019) \, (1.250)}{604.41}}} \right]^{0.5}$$

$$P_{ian\,p} = 31,560 \ \text{lb/ft}^2 \ \text{abs}$$

$$p_{ian\,p} = \frac{P_{ian\,p}}{144}$$

$$p_{ian\,p} = 219.2 \ \text{psia}$$

Turbine Motor Performance

The downhole pneumatic turbine motor Model 650 has a single stage axial flow turbine device. There are 23 stator gas flow orifices around the periphery of the

turbine stator.   Each turbine stator orifice is small converging-diverging nozzle. Figure 11-15 shows a schematic cutaway of the stator converging-diverging nozzle and the flow interaction to the rotor.   The throat of the each nozzle is 0.136 inches and the radial peripheral depth of each nozzle is 0.280 inches.   The diameter of the turbine rotor to the centerline of the stator nozzles and the rotor buckets is 4.97 inches.   The stall torque generated by the turbine device, $Torque_{sr}$, is

$$Torque_{sr} = 2 \left(\frac{\dot{w}_g \ V_n}{g} \right) \left(\frac{D_{cl}}{2} \right) \cos 30° \qquad (11\text{-}1)$$

where $\dot{w}_g$ is the weight rate of flow of the gas (lb/sec),

$\quad$ V_n is the velocity of the gas at the exit from the nozzle (ft/sec),

$\quad$ D_{cl} is the diameter to the centerline of the nozzles (ft).

   In order to develop full power in the turbine, the velocity of the gas at the throat of each nozzle should be sonic velocity.   Thus, the pressure drop across each nozzle should be at the critical pressure ratio or less (see Equation 6-62).   This insures that the velocity at the exit of each nozzle will be at sonic velocity or greater.   Sonic velocity, V_s, is

$$V_s = \sqrt{k \ g \ \mathbf{R} \ T_{bh}} \qquad (11\text{-}2)$$

Using Equation 11-2 and assuming the pressure drop across the nozzles is critical or less, the velocity of the air flow from each active nozzle will be at least

$$V_s = \sqrt{(1.4) \ (32.2) \ (53.36) \ (604.41)}$$

$$V_s = 1,206 \ \text{ft/sec}$$

The diameter to the centerline of the nozzles on the periphery of the rotor is

$$d_{cl} = 4.97 \ \text{inches}$$

$$D_{cl} = \frac{d_{cl}}{12}$$

$$D_{cl} = 0.414 \ \text{ft}$$

Using Equation 11-1, the stall torque of the turbine rotor (i.e., the maximum torque developed) is

$$Torque_{sr} = 2 \left(\frac{(2.635) \ (1,206)}{32.2} \right) \left(\frac{0.414}{2} \right) (0.8660)$$

$$\text{Torque}_{sr} \quad 35.38 \text{ ft} \quad \text{lb}$$

The stall torque of the drive shaft (drill bit), Torque_{sb}, is

$$\text{Torque}_{sb} \quad (35.38)(112.5)$$

$$\text{Torque}_{sb} \quad 3,980 \text{ ft} \quad \text{lb}$$
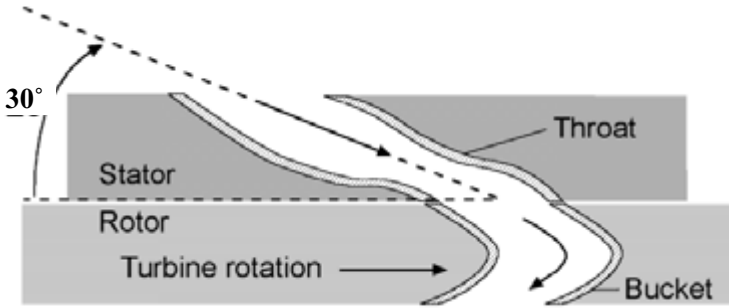
Figure 11-15: Cutaway of the a typical compressible flow stator nozzle and rotor bucket configuration.

The periphery speed of the turbine rotor is determined by the gas velocity at the exit of each nozzle. When there is no load on the drill bit, the tip speed of the turbine rotor will approach the velocity of the gas exiting each nozzle. Thus, the theoretical runaway speed of the rotor, N_{rr}, is

$$N_{rr} \quad \frac{V_s (60)}{\frac{D_{cl}}{2} \quad 2}$$

$$N_{rr} \quad \frac{(1,206)(60)}{\frac{0.414}{2} \quad 2}$$

$$N_{rr} \quad 55,642 \text{ rpm}$$

The runaway speed of the motor drive shaft (drill bit), N_{rb}, is

$$N_{rb} \quad \frac{N_{rr}}{G_r} \tag{11-3}$$

where G_r is the gear box reduction ratio. Using Equation 11-3, the runaway speed of the drive shaft (drill bit) is

$$N_{rb} \quad \frac{55,642}{112.5}$$

$$N_{rb} \quad 494.6 \text{ rpm}$$

The torque developed by the motor at any drive shaft (drill bit) speed is

$$\text{Torque}_b \quad \text{Torque}_{sb} \quad 1 \quad \frac{N_b}{N_{rb}} \tag{11-4}$$

where N_b is the drive shaft (drill bit) speed (rpm). Using Equation 11-4, the torque at the drive shaft (drill bit) speed of 40 rpm is

$$\text{Torque}_b \quad (3,980) \quad 1 \quad \frac{40}{494.6}$$

$$\text{Torque}_b \quad 3,658 \text{ ft} \quad \text{lb}$$

The drive shaft (drill bit) horsepower developed at any drive shaft (drill bit) speed is

$$\text{HP}_b \quad \frac{\text{Torque}_b \; N_b}{5,252}$$

$$\text{HP}_b \quad \frac{(3,658)\;(40)}{5,252}$$

$$\text{HP}_b \quad 27.86$$

Maintaining Sonic Velocity in Nozzle Throat

In order to maintain sonic gas flow in the throat in each active nozzle, the ratio of the pressure below the turbine device to the pressure above the turbine device must be less than the critical ratio as defined by Equation 6-62. To obtain this condition, several of the 23 nozzles in the stator must be plugged. Plugging these nozzles restricts the flow of gas to only a few nozzles and, thus, increases the pressure above the turbine stator.

The nozzle throat opening, L_t, is

$$l_t \quad 0.136 \text{ inches}$$

$$L_t \qquad \frac{l_t}{12}$$

$$L_t \qquad 0.0113 \ \text{ft}$$

The nozzle depth along the periphery of the stator, L_d, is

$$l_d \qquad 0.280 \ \text{inches}$$

$$L_d \qquad \frac{l_d}{12}$$

$$L_d \qquad 0.0233 \ \text{ft}$$

Assuming that 16 of the nozzles are plugged, then the total nozzle flow area, A_{tn}, is

$$A_{tn} \qquad (23 \qquad 16) \ (0.0113) \ (0.0233)$$

$$A_{tn} \qquad 0.00185 \ \text{ft}^2$$

Assuming sonic gas flow conditions at the throats of each of the remaining 7 nozzles in the stator, Equation 6-62 can be used to determine the pressure above the turbine stator. Equation 6-62 becomes

$$P_{ias} \qquad \frac{(2.635) \ (604.41)^{0.5}}{(0.00185) \ \dfrac{(32.2) \ (1.4) \ (1.0)}{53.36} \ \left(\dfrac{2}{2.4}\right)^{\frac{2.4}{0.4}} \ ^{0.5}}$$

$$P_{ias} \qquad 65,790 \ \text{lb/ft}^2 \ \text{abs}$$

$$p_{ias} \qquad \frac{P_{ias}}{144}$$

$$p_{ias} \qquad 456.9 \ \text{psia}$$

The ratio of the pressure below the turbine to the pressure above the turbine (stator) is

$$\frac{p_{ianp}}{p_{ias}} \qquad \frac{219.2}{456.9}$$

$$\frac{p_{ianp}}{p_{ias}} \qquad 0.480$$

The critical pressure ratio for air is 0.528. The ratio of the pressure below the turbine to the pressure above the turbine is less than the critical pressure ratio, therefore, the flow conditions in the active nozzles are sonic.

Geometry Inside the Drill String

Starting at the bottom of the drill string, the total length of the drill collars length increment, H_5, in the openhole section is

$$H_5 \qquad 500 \text{ ft}$$

The inside diameter of the drill collars length in this openhole section is

$$d_5 \qquad 2.8125 \text{ inches}$$

$$D_5 \qquad \frac{d_5}{12}$$

$$D_5 \qquad 0.234 \text{ ft}$$

The total length of the drill pipe tool joints lumped geometry increment, H_4, in the openhole section is

$$H_4 \qquad 125 \text{ ft}$$

The inside diameter of the drill pipe tool joints lumped geometry in this openhole section is

$$d_6 \qquad 3.50 \text{ inches}$$

$$D_6 \qquad \frac{d_6}{12}$$

$$D_6 \qquad 0.292 \text{ ft}$$

The total length of the lumped drill pipe body geometry increment, H_3, in the openhole section is

$$H_3 \qquad 2,375 \text{ ft}$$

The inside diameter of the drill pipe body lumped geometry in this openhole section is

$$d_7 \qquad 3.826 \text{ inches}$$

$$D_7 \qquad \frac{d_7}{12}$$

$$D_7 \qquad 0.319 \text{ ft}$$

The total length of the lumped drill pipe tool joints geometry increment, H_2, in the cased section is

$$H_2 \qquad 350 \text{ ft}$$

The inside diameter of the drill pipe tool joints lumped geometry in this cased section is

$$D_6 \qquad 0.292 \text{ ft}$$

The total length of the lumped drill pipe body geometry increment, H_1, in the cased section is

$$H_1 \qquad 6,650 \text{ ft}$$

The inside diameter of the drill pipe body lumped geometry in this cased section is

$$D_7 \qquad 0.319 \text{ ft}$$

Inside the Drill String (10,000 ft to 7,000 ft)
The fifth drill string section increment is denoted by the length H_5. The temperature at the bottom of the drill collars (bottomhole temperature) in the openhole section is

$$T_5 \qquad 604.41°R$$

The average temperature of the drill collar length H_5 and, thus, the temperature of the gas flow inside the drill collars is

$$T_{av5} \qquad 601.91°R$$

The inside surface of the drill collars has the surface roughness of commercial steel. Therefore, over this drill collar length the surface roughness is

$$e_p \qquad 0.00015 \text{ ft}$$

With the above, Equation 6-73 becomes

$$f_{i5} \quad \left[\frac{1}{2 \ \log \ \dfrac{0.234}{0.00015} \quad 1.14} \right]^2$$

$$f_{i5} \quad 0.018$$

Equations 6-67 and 6-68 become, respectively,

$$a_{i5} \quad \frac{1.0}{53.36}$$

$$a_{i5} \quad 0.019$$

and

$$b_{i5} \quad \frac{0.018}{2 \ (32.2)} \quad \left[\frac{53.36}{1.0} \right]^2 \quad \frac{(2.635)^2}{\left[\dfrac{}{4} \ (0.234)^5 \right]^2}$$

$$b_{i5} \quad 12,420$$

The pressure above the motor, P_{am}, is the approximate pressure at the bottom of the inside of the drill string. Thus, Equation 6-72 becomes

$$P_{i4} \quad \left[\frac{(65,790)^2 \quad (12,420) \ (601.91)^2 \quad e^{\frac{2 \ (0.019) \ (500)}{601.91}} \quad 1}{e^{\frac{2 \ (0.019) \ (500)}{601.91}}} \right]^{0.5}$$

$$P_{i4} \quad 65,830 \ \text{lb/ft}^2 \ \text{abs}$$

$$p_{i4} \quad \frac{P_{i4}}{144}$$

$$p_{i4} \quad 457.2 \ \text{psia}$$

The pressure given above is the flowing air pressure at the top of the drill collar length inside the drill string in the openhole section of the borehole.

The fourth drill string section increment is denoted by the length H_4. The temperature at the bottom of the drill pipe tool joints lumped geometry length in the openhole section is

$$T_4 \quad 599.41°R$$

The average temperature of the drill pipe tool joints lumped length along H_4 and, thus, the temperature of the gas flow inside this drill string length is

$$T_{av4} \quad 598.79°R$$

The inside surface of the drill pipe tool joint has the surface roughness of commercial steel. Therefore, over this lumped drill pipe tool joint length the surface roughness is

$$e_p \quad 0.00015 \text{ ft}$$

With the above, Equation 6-73 becomes

$$f_{i4} \quad \frac{1}{\left[2 \ \log \left(\dfrac{0.292}{0.00015} \right) \ 1.14 \right]^2}$$

$$f_{i4} \quad 0.017$$

Equations 6-67 and 6-68 become, respectively,

$$a_{i4} \quad \frac{1.0}{53.36}$$

$$a_{i4} \quad 0.019$$

and

$$b_{i4} \quad \frac{0.017}{2\ (32.2)} \left(\frac{53.36}{1.0} \right)^2 \frac{(2.635)^2}{\left(\dfrac{-}{4} \ (0.292)^5 \right)}$$

$$b_{i4} \quad 3,958$$

Equation 6-72 becomes

$$P_{i3} = \frac{(65,830)^2 - (3,958)\,(598.79)^2\left[e^{\frac{2\,(0.019)\,(125)}{598.79}} - 1\right]}{e^{\frac{2\,(0.019)\,(125)}{598.79}}}\Bigg.^{0.5}$$

$$P_{i3} = 65,660 \text{ lb/ft}^2 \text{ abs}$$

$$p_{i3} = \frac{P_{i3}}{144}$$

$$p_{i3} = 456.0 \text{ psia}$$

The pressure given above is the flowing air pressure at the top of the lumped drill pipe tool joint length inside the drill string in the openhole section of the borehole.

The third drill string section increment is denoted by the length H_3.   The temperature at the bottom of the drill pipe body lumped geometry length in the openhole section is

$$T_3 = 598.16°R$$

The average temperature of the drill pipe body lumped geometry length along H_3 and, thus, the temperature of the gas flow inside this drill string length is

$$T_{av3} = 586.29°R$$

The inside surface of the drill pipe body has the surface roughness of commercial steel. Therefore, over this lumped drill pipe body length the surface roughness is

$$e_p = 0.00015 \text{ ft}$$

With the above, Equation 6-73 becomes

$$f_{i3} = \left[\frac{1}{2\,\log\left(\dfrac{0.319}{0.00015}\right) + 1.14}\right]^2$$

$$f_{i3} = 0.016$$

Equations 6-67 and 6-68 become, respectively,

$$a_{i3} = \frac{1.0}{53.36}$$

$$a_{i3} = 0.019$$

and

$$b_{i3} = \frac{0.016}{2\,(32.2)} \left(\frac{53.36}{1.0}\right)^2 \frac{(2.635)^2}{\left(\dfrac{-}{4}\right)^2 (0.319)^5}$$

$$b_{i3} = 2,486$$

Equation 6-72 becomes

$$P_{i2} = \frac{(65,660)^2 - (2,486)\,(586.29)^2 \left[e^{\frac{2\,(0.019)\,(2,375)}{586.29}} - 1\right]}{e^{\frac{2\,(0.019)\,(2,375)}{586.29}}}^{0.5}$$

$$P_{i2} = 61,184 \ \text{lb/ft}^2 \ \text{abs}$$

$$p_{i2} = \frac{P_{i2}}{144}$$

$$p_{i2} = 429.4 \ \text{psia}$$

The pressure given above is the flowing air pressure at the top of the lumped drill pipe body length inside the drill string in the openhole section of the borehole.

   Inside the Drill String (7,000 ft to Surface)
   The second drill string section increment is denoted by the length H_2. The temperature at the bottom drill pipe tool joints lumped geometry length in the cased section is

$$T_2 = 574.41°\text{R}$$

The average temperature of the drill pipe tool joints lumped geometry along H_2 and, thus, the temperature of the gas flow inside this drill string length is

$$T_{av2} \quad 572.66°R$$

The inside surface of the drill pipe body has the surface roughness of commercial steel. Therefore, over this lumped drill pipe body length the surface roughness is

$$e_p \quad 0.00015 \text{ ft}$$

With the above, Equation 6-73 becomes

$$f_{i2} \quad \frac{1}{\left(2 \ \log \ \dfrac{0.292}{0.00015} \ 1.14 \right)^2}$$

$$f_{i2} \quad 0.017$$

Equations 6-67 and 6-68 become, respectively,

$$a_{i2} \quad \frac{1.0}{53.36}$$

$$a_{i2} \quad 0.019$$

and

$$b_{i2} \quad \frac{0.017}{2 \ (32.2)} \ \left(\frac{53.36}{1.0}\right)^2 \ \frac{(2.635)^2}{\left(\dfrac{}{4}\right)^2 (0.292)^5}$$

$$b_{i2} \quad 3,958$$

Equation 6-72 becomes

$$P_{i1} \quad \frac{(61,184)^2 \quad (3,958) \ (572.66)^2 \ e^{\frac{2 \ (0.019) \ (350)}{572.66}} \ 1}{e^{\frac{2 \ (0.019) \ (350)}{572.66}}}^{0.5}$$

$$P_{i1} \quad 61,370 \text{ lb/ft}^2 \text{ abs}$$

$$p_{i1} \qquad \frac{P_{i1}}{144}$$

$$p_{i1} \qquad 426.2 \;\; \text{psia}$$

The pressure given above is the flowing air pressure at the top of the lumped drill pipe tool joints length inside the drill string in the cased section of the borehole.

The first drill string section increment is denoted by the length H_1. The temperature at the bottom drill pipe body lumped geometry length in the cased section is

$$T_1 \qquad 570.91°\text{R}$$

The average temperature of the drill pipe body lumped geometry along H_1 and, thus, the temperature of the gas flow inside this drill string length is

$$T_{av1} \qquad 537.66°\text{R}$$

The inside surface of the drill pipe body has the surface roughness of commercial steel. Therefore, over this lumped drill pipe body length the surface roughness is

$$e_p \qquad 0.00015 \;\; \text{ft}$$

With the above, Equation 6-73 becomes

$$f_{i1} \qquad \frac{1}{\left(2 \; \log \; \dfrac{0.319}{0.00015} \; 1.14 \right)^2}$$

$$f_{i1} \qquad 0.016$$

Equations 6-67 and 6-68 become, respectively,

$$a_{i1} \qquad \frac{1.0}{53.36}$$

$$a_{i1} \qquad 0.019$$

and

$$b_{i1} \quad \frac{0.016}{2\,(32.2)} \quad \frac{53.36}{1.0}^{\,2} \quad \frac{(2.635)^2}{-\!\frac{}{4}\,(0.319)^5}$$

$$b_{i1} \quad 2,486$$

Equation 6-72 becomes

$$P_{in} \quad \frac{(61,370)^2 \quad (2,486)\,(537.66)^2 \; e^{\frac{2\,(0.019)\,(6,650)}{537.66}} \quad 1}{e^{\frac{2\,(0.019)\,(6,650)}{537.66}}}^{0.5}$$

$$P_{in} \quad 51,340 \; \text{lb/ft}^2 \; \text{abs}$$

$$p_{in} \quad \frac{P_{in}}{144}$$

$$p_{in} \quad 356.5 \; \text{psia}$$

The injection pressure given above is the flowing air pressure at the top of the lumped drill pipe body length inside the drill string in the cased section of the borehole while drilling at a depth of 10,000 ft. This is the approximate injection at the top of the drill string required to force a volumetric flow rate of 2,400 acfm through the circulation system. This injection pressure is the pressure the compressor output must match.

Compressor Unit Prime Mover Capability

Knowing the injection pressure, it is necessary to ascertain whether the prime mover of this primary compressor unit has the power to operate at the 4,000 ft surface elevation. The prime mover for this compressor is a diesel fueled, turbocharged, Caterpillar Model D398 with a peak output of 760 horsepower at 900 rpm (at API standard conditions) (see Section 4.7 in Chapter 4). The theoretical shaft horsepower, $\dot{W}_s$, required by each of the two compressors is obtained from Equation 4-35a. Equation 4-35a becomes

$$\dot{W}_s \quad \frac{(4)\,(1.4)}{(0.4)} \quad \frac{(12.685)\,\frac{2,400}{2}}{229.17} \quad \frac{356.5}{12.685}^{\frac{(0.4)}{(4)(1.4)}} \quad 1$$

$$\dot{W}_s \quad 250.2$$

The mechanical efficiency, η_m, is

$$\eta_m \quad 0.90$$

This is a four-stage reciprocating piston compressor. Therefore,

$$n_s \quad 4$$

The first stage compressor ratio is

$$r_s \quad \left(\frac{356.5}{12.685}\right)^{\frac{1}{4}}$$

$$r_s \quad 2.30$$

The volumetric efficiency (only for the reciprocating piston compressor), η_v, is determined from Equation 4-38.   The compressor clearance volume ratio, c, is assumed to be 0.06. Equation 4-38 becomes

$$\eta_v \quad 0.96 \quad 1 \quad 0.06 \quad \left(2.30^{\frac{1}{1.4}} \quad 1\right)$$

$$\eta_v \quad 0.913$$

From Equation 4-39, the actual shaft horsepower, $\dot{W}_{as}$, required by each compressor is

$$\dot{W}_{as} \quad \frac{250.2}{(0.90)\ (0.913)}$$

$$\dot{W}_{as} \quad 304.5$$

The above determined 304.5 horsepower is the actual shaft power needed by each of the two compressors to produce the 356.5 psia pressure output at the surface location elevation of 4,000 ft above sea level (while drilling at a depth of 10,000 ft). At this surface location, the input horsepower available from the Caterpillar Model D398 prime mover is a derated value (derated from the rated 760 horsepower available at 900 rpm). In order for the compressor units to operate at this 4,000 ft surface location elevation, the derated input power available must be greater than the actual shaft power needed. Figure 4-15 shows that for 4,000 ft elevation the input power of a turbocharged prime mover must be derated by approximately 10 percent.

The derated input horsepower, $\dot{W}_i$, available from the prime mover is

$$\dot{W}_i \quad 760\ (1 \quad 0.10)$$

$$\dot{W}_i \quad 684.0$$

For this illustrative example, the prime mover of each of the two compressor units derated input power is greater than the actual shaft horsepower needed, thus, the selected compressor units can be operated at this 4,000 ft surface location elevation (while drilling at a depth of 10,000 ft).

Compressor Unit Fuel Consumption

The reciprocating piston compressor is not a fixed pressure ratio machine like the rotary compressor. As long as there is sufficient power available from the prime mover the reciprocating piston compressor will match the back pressure resistance. It was found above that the actual shaft horsepower required by each of the two reciprocating piston compressor units to compress air to 356.5 psia was approximately 304.5 (while drilling at 10,000 ft of depth). Also above it was found that the derated horsepower available from the Caterpillar Model D398 prime mover at the surface elevation of 4,000 ft was 684.0. Drilling at a depth of 10,000 ft, the prime mover power ratio is

$$PR \quad \frac{304.5}{684.0}\ (100) \quad 44.5$$

Using Figure 4-17 the diesel fuel consumption rate for a power level of 44.5 percent is 0.670 lb/hp-hr of diesel fuel. The total weight rate of diesel fuel consumption per hour is

$$\dot{w}_f \quad 0.670\ (304.5) \quad 204.0\ \text{lb/hr}$$

The diesel fuel consumption rate (in United States gallons) for the drilling depth of 10,000 ft is

$$q_f \quad \frac{204.0}{(0.8156)(8.33)} \quad 30.0\ \text{gal/hr}$$

Since there are two compressor units providing compressed air to this example air hammer drilling operation, the total diesel fuel consumption rate while drilling at the 10,000 ft of depth is approximately 60 gal/hr.

11.2.4 *Downhole Pneumatic Sliding Vane Motors*

In the late 1950s Reed Tool Company developed and field tested the first downhole air motor [6]. This downhole air motor was a two stage sliding vane design (a positive displacement motor design) with a two stage planetary gear reduction gear box with a reduction ratio of 32 to 1. The field testing of the motor revealed that the sliding vane cavities where prone to filling up with pipe scale and other foreign particles in the compressed air flow. Also, the non-metal sliding vanes

had a tendency to be damaged and worn by the pipe scale flowing into the sliding vane cavities of the motor. Due to these problems this early downhole air motor based on the sliding vane design was abandoned.

In the past decade, several new downhole air motors based on the sliding vane design have been offered for commercial use. The cross section of these new sliding vane motors are similar to that shown in Figure 11-16 [1]. The reports on the performance of these new sliding vane downhole air motors are not available. Therefore, these motor designs have not been analyzed in examples.

11.3 Conclusions

The specialized surface equipment discussed has general applications to vertical and directional drilling operations. The specialized downhole air hammer is only used for straight hole drilling. Therefore, most air hammer drilling is in vertical boreholes. However, there are some very shallow (near surface) applications where air hammers are used to drill slant or horizontal boreholes. In these applications require specialized directional control techniques that usually rely on drill through or "daylight" drilling (i.e., where the drill bit will exit to the surface).

The specialized downhole rotary motors are nearly always used to drill directional boreholes. These downhole rotary motors are used in shallow and deep drilling operations. It is clear that the converted downhole positive displacement mud motors will require the greatest compressor injection pressures and, therefore, require the most fuel for the compressors that supply the compressed air.   The downhole pneumatic turbine motors are not pressure driven motors and, therefore, do not generally require a much greater fuel consumption for the compressors than conventional air drilling.
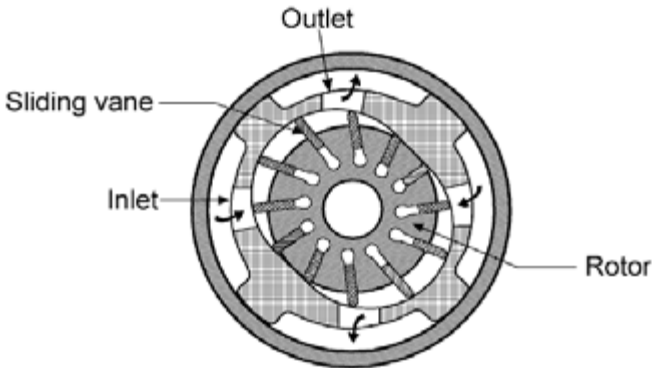
Figure 11-16: Typical sliding vane motor cross section.

An important issue for the specialized downhole equipment is that of lubrication. There are some environmental drilling applications that require no lubricants be injected into the compressed air flow to the drill string. Also, there are underbalanced oil and natural gas recovery drilling applications that do not allow

water to be injected into the compressed air or gas flow to the drill string.   The downhole pneumatic turbine motors are the only specialized downhole drilling equipment that can be used with dry compressed air (or other drilling gases).

References

1. Tiraspolsky, W., *Hydraulic Downhole Drilling Motors*, Gulf Publishing, 1981.

2. Bourgoyne, A. T., Millheim, K. K., Chenevert, M. E., and Young, F. S., *Applied Drilling Engineering*, SPE, First Printing, 1986.

3. Lyons, W. C., U. S. Patent No. 4,553,611; Issued November 19, 1985; "Pressure Regulator for Downhole Turbine."

4. Lyons, W. C., Miska, S., and Johnson, P. W., "Downhole Pneumatic Turbine Motor: Testing and Simulation Results," *SPE Drilling Engineering*, September 1990.

5. Johnson, P. W., and Lyons, W. C., "Development and Validation of a Model for Predicting the Performance of a Downhole Pneumatic Turbine Powered Drilling Engine," *Journal of Petroleum Science and Engineering*, July 1992.

6. Magner, H. J., "Air Motor Drill," *Petroleum Engineer*, October 1960.

This page intentionally left blank.

Chapter

Twelve

Directional Drilling Operations

Planning is the most important factor in any directional or horizontal drilling project. All directionally drilled wells have to accurately placed in a three-dimensional target area. These directional drilling projects depend upon providing the operation with drilling fluids that will adequately clean the borehole of drill bit generated rock cuttings. This is especially the case when drilling a horizontal section in a directional well. Directional wells have been drilled using compressed air and natural gas, aerated (or gasified) incompressible drilling fluids, and stable foam drilling fluids.

12.1 Introduction

Directional drilling is generally categorized by the build angle rate of the directional portion of the borehole. These categories are stated in borehole angle build rate from the vertical per 100 ft (or per ft). Figure 12-1 shows a schematic of the three generally accepted categories of directional drilling. The figure shows three boreholes drilled to the ultimate high angle of approximately 90˚ from the vertical. These three categories are long-radius boreholes, medium-radius boreholes, and short-radius boreholes. All three of these directional drilling build rate categories have unique downhole and surface equipment.

12.1.1 *Long-Radius Drilling*

In the early years of rotary drilling (i.e., the late 1920's), long-radius directional operations was the only directional method available for drilling controlled deviated

(from the vertical) boreholes. Much of the early constraint on build rate was due to the availability of high quality steel tubulars for downhole operations.   Early directional drilling operations (long-radius) utilized crude directional control technology. Since those early years, great technological advances have taken place. Present long-radius technology can place the drill bit in a 3 ft diameter target sphere located at a depth of 15,000 ft and 5,000 ft of horizontal displacement from the vertical. It is generally accepted that long-radius boreholes are drilled with a build rate of approximately 2° to 6° per 100 ft of borehole length from a kick-off depth (the depth where the deviated portion of the well is initiated). This build rate translates to radii of curvature of boreholes of approximately 1,000 ft to 3,000 ft. Long-radius boreholes can usually be kicked-off at nearly any depth (in a vertical well). Today, long-radius boreholes are most frequently applied to offshore drilling operations. This type of directional drilling is often denoted as "extended reach" drilling. This is mainly due to the fact that long-radius directional operations can usually construct wells that are deviated as much as 5,000 ft (projected on the horizontal) or more from the vertical axis of the initial vertical section of the well.

12.1.2 *Medium-Radius Drilling*

Medium-radius directional drilling is characterized by a build rate of approximately 6° to 40° per 100 ft of borehole arc length drilled. This build rate translates to radii of curvature of boreholes of approximately 300 ft to 700 ft. The development of medium-radius drilling technology in the mid 1980's was the direct result of improved high quality tubulars and sophisticated downhole gyroscopic surveying equipment.   Medium-radius directional drilling technology is mostly applied to land directional drill operations. Medium-radius directional boreholes can be initiated at nearly any depth in a vertical well. Here again, present medium-radius technology can place the drill bit in a 3 ft diameter target sphere located at a depth of 15,000 ft and 3,000 ft of horizontal displacement form the vertical. Today, this type of directional well is the most used in land drilling operations.

12.1.3 *Short-Radius Drilling*

Short-radius directional drilling is characterized by a build rate of approximately 40° to 70° per 100 ft and approximately 70° to 150° per 100 ft for the ultra short-radius technology (short-radius is sometimes given in degrees per ft). This build rate translates to radii of curvature of boreholes of approximately 82 ft to 140 ft for the intermediate short-radius technology, and 40 ft to 82 ft for the ultra short-radius technology.   The development of the short-radius technology preceded the development of the medium-radius technology. In the late 1930's articulated drill collars were designed, fabricated, and used on a number of wells around the world to drill "drainhole" completions. These were curved open boreholes in the producing formations in the well and were drilled with a conventional rotary rig (i.e., rotation of the drill string from the surface). These early drainholes could be drilled in the well as part of its original completion, or drilled as sidetracks sometime later in the life of the well to aid in enhancing the recovery the oil or gas.   The original drainhole technology allowed for orientation of the kick-off direction in the well, but could only be used to drill a continuous curved section of borehole about 90 ft in arc length. In the late 1970's these drainhole tools were modernized and provided with the capability to drill both a curved section of openhole and a follow-on straight

(usually horizontal) section of openhole. Early field test demonstrated that these new modernized articulated drill string could drill horizontals out to 500 ft. These were some of the earliest horizontal wells ever drilled. These early field tests and operations were drilled using both drilling mud and air and gas drilling fluid technologies. In the late 1980's downhole positive displacement motors (PDMs) were used to extend the capability of the ultra short-radius technology to horizontals out to 1,000 ft. The intermediate short-radius drilling tools with PDMs are capable of horizontals out to 3,000 ft. Short-radius technology is used exclusively for land drilling operations. Short-radius drilling was used extensively in the 1980's, but have generally been replaced by the more flexible medium-radius directional drilling technology. Short-radius directional drilling technology does not have the target accuracy that long-radius and medium-radius drilling technologies have. This comes from the fact that MWD technology is not very compatible with the short-radius technology. A rough estimate is that typical short-radius tools can place the drill bit in a 10 ft diameter target sphere located at a depth of 5,000 ft and 1,000 ft of horizontal displacement from the vertical.

Table 12-1 gives the basic specifications of the various long-radius, medium-radius, and short-radius drilling tools and auxiliary equipment in commercial use.

Table 12-1: Directional drilling technology specification (Baker Tool Company)

	Tool Sizes (in)	**Bit Sizes (in)**	**Radius (ft)**
Long-radius	4 3/4	6 to 8 1/2	1000 to 1900
	6 3/4	8 1/2 to 9 7/8	1000 to 1900
Medium-radius	3 3/4	4 1/2 to 4 3/4	286
	4 3/4	6 to 8 1/2	286 to 300
	6 3/4	8 1/2 to 9 7/8	400 to 716
	8	12 1/4	400 to 716
Short-radius	3 3/4	4 1/2 to 4 3/4	19 to 25
	4 3/4	5 7/8 to 6	32 to 38
	4 3/4	6 1/4 to 6 1/2	38 to 42

12.2 Directional Control

Many technologies have been developed through the past seven decades directed at improving commercial directional drilling using conventional incompressible drilling fluids (e.g., water-based drilling muds and oil -based drilling muds). Air and gas drilling technology has been a small niche area of the drilling industry. Therefore, up until the late 1980's little attention was given to the development of directional drilling technologies for air and gas drilling operations. Although there has been some recent development activities to develop air and gas directional drilling technologies, these have not been entirely successful or accepted commercially.
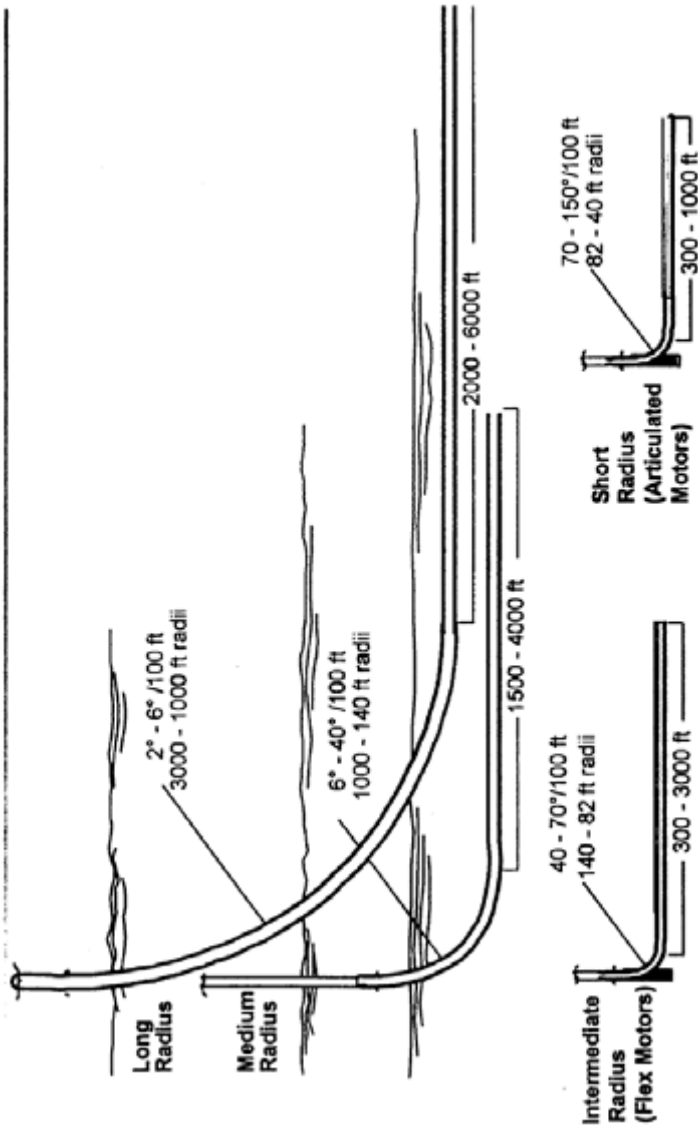
Figure 12-1: Directional drilling technology build rate (radius of curvature) categories (courtesy Baker Tool Company).

In general, present day commercial air and gas drilling directional operations have relied heavily on existing conventional directional technologies for their respective operations. Field operations over the past twenty years has shown that there are few directional control technologies that are successful in air and gas drilled directional boreholes.

12.2.1 *Downhole Survey Equipment*

In 1929, John Eastman began performing acid-bottle surveys for drilling operations in California. In the next two years Eastman designed and introduced the first magnetic single-shot and multiple-shot downhole survey instruments. Also, about the same time, Eastman developed and field tested the first retrievable whipstock. These early developments initiated controlled directional drilling operations. It is mandatory that any directional drilling operation be controlled by sophisticated downhole borehole survey equipment.

The control of a directional drilling operation is dependent on durability and accuracy of the survey equipment used to plot the borehole path as drilling progresses. It is a basic requirement for both vertical and directional drilling operations that the borehole be tracked as a well is drilled.

In conventional vertical well drilling the plotting of the borehole is usually carried out using simple downhole instruments and technician analysis techniques. Most local government agencies require an operating company to submit three-dimensional graphic proof of where even a simple vertical borehole is located once a well has been completed. For sophisticated directional drilling operations, the survey data obtained should be of such quality as to allow the future projection of a borehole path as the drill bit is advanced. In general, directional drilling operations require complicated downhole survey equipment and associated analysis techniques. There are two downhole equipment systems in commercial use today that are used to obtain basic downhole borehole survey data.

Magnetic Instruments

These downhole survey instruments were introduced in the oil field in the mid-1930's. Magnetic downhole instruments make use a simple compass and a simple pendulum to give azimuth angles and deviation (from the vertical) angles. The compass detects the earth's magnetic field to give azimuth angles of the downhole platform position relative to magnetic north. The pendulum uses the earth's gravitational field to give deviation angles of the downhole platform position relative to vertical. The magnetic instruments cannot be used in the cased section of a borehole. These instruments have to be run into nonmagnetic tubulars (in the openhole section) in order to obtain reliable survey data. This is accomplished by using 90 ft or so of nonmagnetic (i.e., nickel alloy) drill collars in the BHA of the drill string.

These magnetic instruments are available in single-shot or multiple-shot systems. The single-shot system has a single photographic film camera and a timing mechanism on-board the instrument (operated by batteries). When the single-shot is lowered on a wire line (slick line) to the appropriate depth where the survey is to be conducted, the timer actuates the camera. The camera takes a picture of the compass/pendulum positions. The instrument is then pulled from the well and the film retrieved from the instrument and developed. This provides the drilling operation with a single data point defining the path of the borehole. Most drill rigs

have their own single-shot system and take position readings every few hundred feet of drilled depth (measured depth) (most governmental agencies require survey data at 500 ft intervals or less). These single readings can be plotted to show the three-dimensional location of the borehole.

The multiple-shot instrument is operated very much like the single-shot instrument except that it takes many photographs of the compass/pendulum. The time intervals for the multiple camera shots can be pre-set in the instrument. Thus, if a continuous set of position points are needed, the instrument can be lowered (on a slick line) to the bottom location in the drill string and instrument slowly pulled out of the well so that the camera can take photos of the compass/pendulum at pre-determined depths. In this manner, a reliable three-dimensional location of the surveyed borehole section can be prepared.

Magnetic survey instruments are durable downhole tools and if properly "hardened," can survive high vibration environments.

Gyroscopic Instruments

Conventional gyroscopic survey instruments are designed to take stationary readings referenced to an initial directional gyroscopic alignment. This initial directional gyroscopic alignment is set at the surface prior to running the instrument into the well. This alignment is preserved by using mechanical gimbals.

Gyroscopic instruments are designed either to take stationary readings based on the rate gyroscopic response to the earth's rotation, or to take readings of the sensor outputs as the tool moves through the borehole. These sensor outputs are referenced to the original sensor alignment (e.g., the tool face and bent sub) to calculate tool attitude.

There is a special class of high end gyroscopic survey instrumentation that are available on a limited basis. These gyroscopic instruments utilize three ring-laser gyroscopes and three accelerometers in combination with precision depth measurement to achieve high speed, high accuracy, real-time borehole position surveys. These newer class of gyroscopic survey instrument is the basis of most new MWD systems.

Air and Gas Drilling Applications

The magnetic single-shot and multishot instruments are not used while drilling is progressing. These instruments are run in the well when all drilling operations have ceased. Thus, when used simply as survey tools, these downhole instruments are not subjected to the high drill string vibrations that characterize compressed air (or other gas) drilling operations. The magnetic downhole instruments are usually used to obtain a three-dimensional plot of the borehole at drilling stoppage intervals. Once the magnetic instruments are retrieved, the photos developed (usually at the rig site) and the position readings entered into a computer, calculations are made and the borehole trajectory plotted. This borehole trajectory plot can be used by a directional driller to make the appropriate mechanical corrections to the drill string (i.e., orientation of the tool face of the bent sub) to improve the accuracy of a directional drill operation. However, when using magnetic instruments such corrections cannot be made rapidly (as in an MWD system). Using magnetic survey instruments in a directional drilling operation is not a real-time process. But in some directional drilling operations, particularly small diameter boreholes, the use of magnetic survey instruments to control borehole trajectory is quite cost-effective. In these drilling situations, even the single-shot instrument can be used to give position data that can

be plotted with a computer to give a good quality borehole trajectory. This trajectory can then be used to make tool face corrections to improve subsurface target intercept accuracy.

The basic downhole gyroscopic survey instrument can be used in much the same manner as the magnetic survey instruments discussed above. These instruments can be run into the well when drilling has ceased and borehole attitude versus depth readings taken as the instrument is withdrawn from the well. These simple gyroscopic survey instruments are hard wired to the surface with an active wire line. Thus, the data coming from the well can be used in real-time to update a borehole trajectory plot. Once the trajectory is known, appropriate mechanical corrections can be made to the drill string by the directional driller to improve the accuracy of the directional drilling operation. The main advantage of the gyroscopic survey instruments is that they can be used in any part of the well (cased and openhole) and do not require nonmagnetic drill collars in the drill string.

12.2.2 *MWD Equipment*

MWD downhole and surface equipment utilize survey data in a real-time analysis process to give an updated trajectory of a directional borehole and, with appropriate software, a prediction of the future borehole path. This knowledge allows the directional driller to make appropriate mechanical corrections in drill string orientation (called "steering" the drill string) that will allow the advancing drill bit to hit an intended subsurface target area. An MWD requires that the downhole survey instrument operate in the drill string as drilling progresses. Both the magnetic and gyroscopic survey instruments can be used as the basic survey tools for MWD systems. Once the survey data has been obtained (either by magnetic or gyroscopic), the MWD system must provide a way to get this information to the surface where the directional driller can act on the information and make appropriate drill string orientation adjustments.

Conventional drilling mud operations have MWD systems that make use of an acoustic mud pulse signal communication systems that provides nearly real-time survey information to the surface operators (via a pulse generated binary code). However, this mud pulse system does not work in compressed air (or other gas) drilling fluids, in aerated mud drilling fluids, or in stable foam drilling fluids. The compressed gas dampens and scatters any acoustic signals generated at the bottom of the drill string by these pulse systems.

Also, particularly in compressed air (or other gas) drilling, the rather delicate gyroscopic survey instruments on-board most MWD systems are easily damaged in the high drill string vibration environment characterized by air and gas drilling operations. Some attempts to "harden" these instruments to survive these forces have been successful, particularly for the larger diameter downhole instruments. But this remains a problem for smaller diameter downhole instruments. The magnetic survey instruments are generally harder and, thus, more survivable in high drill string vibration environments.

Steering Tools

The steering tool is an early type of MWD system. Steering tools have a hard wire connection which runs from the downhole survey instrument package in the BHA to surface computer and output printer and plotter. Figure 12-2 shows a schematic of this type of system. The active hard wire is run down the outside of

the drill pipe near the surface (secured to the drill pipe) to a side-entry sub. The side-entry sub is in the drill string near its top. The hard wire plugs into a plug connection in the side-entry sub. In the inside of the side-entry sub is a similar plug connection that connects to another active wire line that runs inside the drill string to the survey instruments in the BHA. The steering tool shown in Figure 12-2 uses magnetic survey instruments to give compass/pendulum readings to the surface in real-time. The survey package in the BHA is located just above the bent housing (sub) and is referenced to the tool face of the bent housing. Since this is a magnetic survey instrument, the survey package must be in a nonmagnetic (Monel alloy) drill collars. With the survey package referenced to the bent housing tool face, the surface operator always knows how the compass/pendulum readings relate to the position of the bent sub. The steering tool example in Figure 12-2 makes use of a PDM to rotate the drill bit. The downhole motor together with the bent housing allows the housing tool face to be oriented. When the tool face is properly oriented, the entire drill string can be slid along the low side of the borehole as the drill bit is advanced in a pre-determined direction. Figure 12-2 shows an example of a side track operation where a cement plug is used to force the drill bit to drill into the rock formation on the side of the borehole. When it is necessary to drill straight after the direction corrections have been made and the directional portion of the well completed, the drill string can be raised to the side-entry sub and the hard wire section on the outside of the drill string removed. The drill string can then be lowered into the well and the drill string slowly rotated as the combined PDM and drill string rotation advance the drill bit. In this manner, the effect of the bent housing can be averaged-out and the borehole advanced along a more or less straight directional course. Obviously, any downhole motor that can operate on compressed air (or other gas), aerated drilling mud, or stable foam can be used with a steering tool to provide a directional drilling capabilities for air and gas drilling operations.

Steering tools have had moderate success in providing directional drilling capabilities for air and gas drilling operations. These successes have generally been confined to larger diameter borehole directional operations. Steering tools are available in tool outside diameters from 9 1/2 inches to 3 3/8 inches in diameter (i.e., for borehole diameters from 17 1/2 inches to 4 3/4 inches).

Electromagnetic MWD

The electromagnetic MWD downhole tool transmits its downhole survey measurements by emitting electromagnetic waves which are received at a surface antenna, processed by a computer, and outputted as printouts and trajectory plots that can be used by the directional driller to make drill string corrections. The electromagnetic waves carrying the survey data transmits through the rock formations between the downhole tool and the surface (see Figure 12-3). The electromagnetic transmission does depend on the rock types being traversed by the waves, thus, the operational capability of this MWD system can be depth limited. This electromagnetic telemetry system does not depend on a particular type of drilling fluid being in the well, thus, the system can be used with any rotary drilling fluid system. The electromagnetic telemetry system operates on a long-life battery subsystem, therefore, no drilling fluid driven on-board generator is needed.
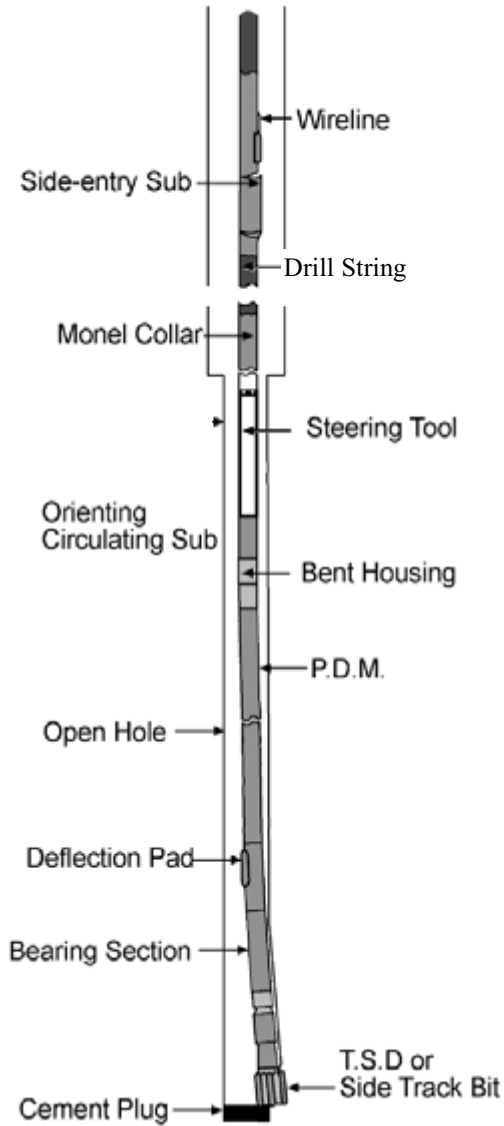
Figure 12-2: Schematic of a steering tool system.

These electromagnetic MWD tools are available with either magnetometer/accelerometer-based survey subsystems or with gyroscope based survey subsystems.   The three-axis magnetometer and accelerometer survey subsystem must utilize nonmagnetic housings and drill collars in much the same manner as the downhole magnetic survey instruments discussed above.   The alternative gyroscope based survey subsystem utilizes two, two-axis gyroscopes, and three-axis accelerometers.   This gyroscope based subsystem does not require nonmagnetic housings or drill collars.
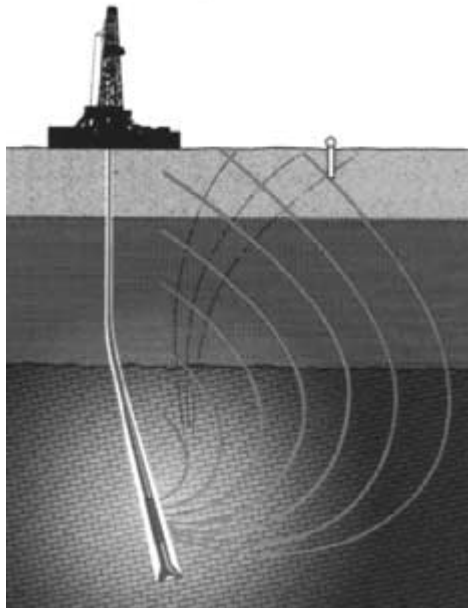
Figure 12-3: Schematic of an electromagnetic MWD transmission of data to a surface antenna (courtesy Geoservices Inc.).

Air and Gas Drilling Applications

The electromagnetic MWD system has incorporated several other important downhole logging features that are of particular use in underbalanced drilling operations.   These are bottomhole annulus pressure, gamma ray, and resistivity measurements.   The mud pulse transmission based MWD systems have all but totally replaced the steering tools.   Since steering tools still have limited use in larger diameter borehole air and gas directional drilling operations.   Therefore, steering tools have not generally been upgraded to carry out auxiliary logging operations (e.g., bottomhole pressure, etc).

Both the steering tool system and the electromagnetic MWD system have durability problems related to the drill string high vibration environments that characterizes compressed air (or other gas) drilling operations.   This is basically a

hardening problem and time and experience should provide solutions for both systems.

The most serious problem is the depth transmission limitation of the electromagnetic system. This can be somewhat relieved by using relay subs placed in the drill string at strategic intervals to boost the transmission signal from the MWD to the surface antenna. It is not clear this signal boosting technique will be feasible in the small diameter boreholes that are most often used in compressed air (or other gas) drilling operations.

12.3 Horizontal Drilling with Inert Atmospheric Air

The very recent development of the membrane filter units to reduce the oxygen percentage in atmospheric air has been driven by the need to eliminate the risk of downhole fires and explosions when drilling boreholes in rock formations containing hydrocarbons. This problem was recognized in the early years of the development of air and gas drilling technology. In those early years, the solution was to use natural gas as the drilling fluid. But using natural gas as a drilling fluid increased the risk of surface fire or explosions in and around the drill rig. Also, although in early years natural gas was inexpensive, today natural gas has a sizable share of the energy market and the cost of using natural gas for drilling operations has become prohibitive.

The risk of downhole fires and explosions exists for both vertical and horizontal drilling operations. However, this risk is far more acute for horizontal drilling operations. This is due to the fact that during a typical horizontal drilling operation, the horizontal interval drilled in the hydrocarbon bearing rock formations is several times longer than in typical vertical interval drilled in a vertical drilling operation (assuming similar hydrocarbon bearing rock formations). Further, the drilling rate of penetration for a horizontal drilling operation will be about half that of vertical drilling (assuming the similar rock type).

12.3.1 *Allowable Oxygen Concentrations*

For the past two decades membrane technologies have been used to separate oxygen (and some other molecules) for gas mixtures, particularly atmospheric air. Because of the high cost, high fire and explosive risk, and potential for high profitability of horizontal wells, membrane technology has been developed that can provide high volumetric flow rates of inert atmospheric air for drilling operations (with oxygen content reduced below the fire/explosive ignition level). Membrane filter technology for drilling operations has been incorporated in portable skid mounted units that can be placed in series in the gas flow line between the primary compressor(s) and the drill rig. Figure 12-4 shows a schematic of a basic drilling location plan that utilizes a membrane filter unit to provide the drilling operation with inert atmospheric air.

Drilling operations membrane units are available in input flow rate capacities that are rated as 750 scfm, 1,500 scfm. and 3,000 scfm. This is the same rating system as that used for primary compressors. As can be seen in Figure 12-4, the membrane units are fed compressed air from the primary compressor. Thus, the flow rate capacities of the membrane units should closely match the flow rate capacities of the primary compressor(s) being used to supply the membrane unit.
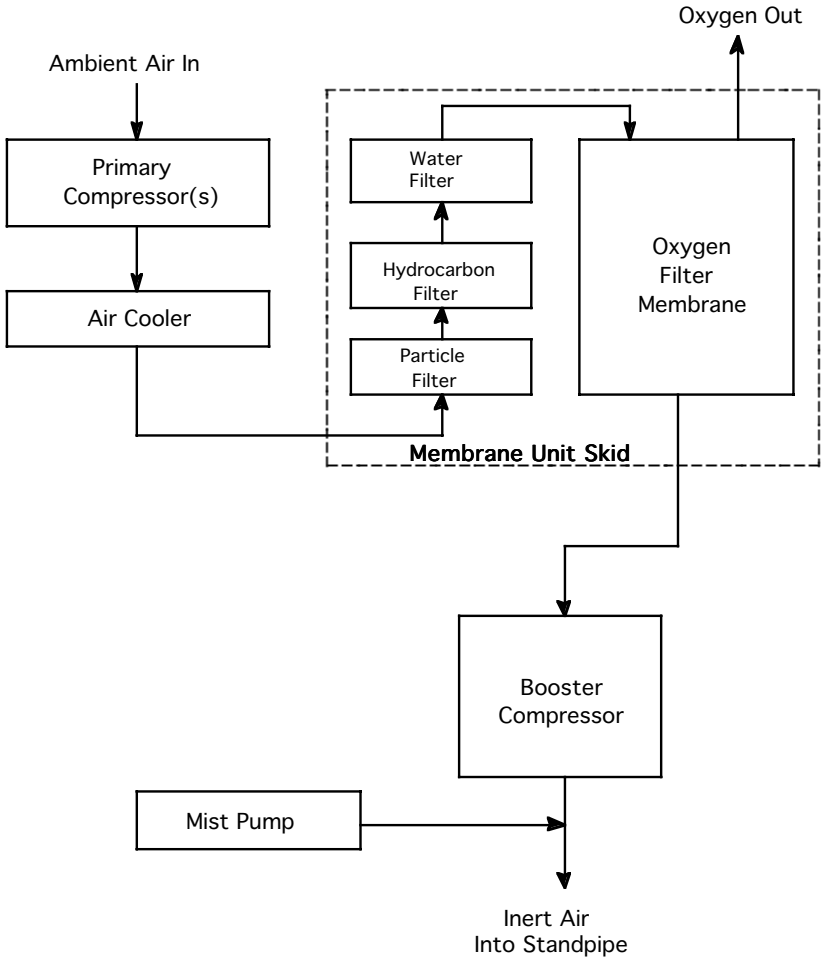
Figure 12-4: Schematic of location plan utilizing membrane filter unit [1].

12.3.2 *Membrane Unit Efficiencies*

It is not necessary for these membrane filter units to filter all the oxygen from the atmospheric air in order to render the injected drilling gas inert to downhole hydrocarbon ignition. Filtering oxygen down to approximately five percent (by volume) of the resulting gas will make the gas inert [2, 3]. When the membrane filter units were introduced, Burlington Resources Incorporated (San Juan Division) carried out field tests to evaluate the efficiency of the units. Figure 12-5 gives the approximate results of these tests. Thus, if the drilling operation requires that the oxygen content in atmospheric air be reduced to approximately five percent (by

volume) level, Figure 12-5 shows that the efficiency of the unit will be approximately fifty percent. Therefore, if a primary compressor unit rated at 1,500 scfm (or acfm) is used to supply a membrane filter unit also rated at 1,500 scfm (or acfm), then the output from the filter unit will only be 750 scfm (or acfm) of inert atmospheric air (i.e., going to the drill rig).
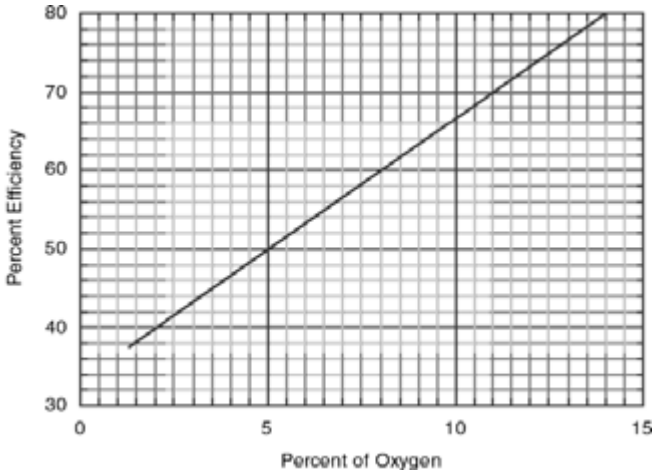
Figure 12-5: Membrane filter unit volumetric flow rate efficiency versus percent of oxygen (by volume) remaining in output [1].

12.4 Minimum Volumetric Flow Rates for Horizontal Boreholes

There is general confusion regarding the determination of the minimum volumetric flow rates for drilling operations that include a final long horizontal borehole increment. There are two different operational situations that affect how the minimum volumetric flow rate for a particular horizontal well situation is determined.

12.4.1 *Rotating Drill String While Drilling*

Drilling a horizontal interval at the bottom of a well is usually accomplished by using a downhole motor that is used in conjunction with some type of downhole drilling control equipment. This downhole drilling control equipment can be either a sophisticated MWD system referenced to a bent sub above the downhole motor, or a simple single-shot survey referenced to the bent sub tool face. Regardless of the drilling control method used, when direction corrections are not being made, the entire drill string is slowly rotated to average out the effect of the bent sub to allow "straight" drilling. When drilling a horizontal borehole, the drill bit cuttings generated by the bit advance will have a tendency to fall and accumulate on the low side of the hole. The rotation of the drill string mechanically agitates these

accumulated rock cuttings.   This agitation will force the rock cuttings into the drilling fluid return flow stream in the annulus. Thus, drill string rotation promotes more efficient horizontal borehole cleaning.

12.4.2 *Sliding Drill String While Drilling*

When directional corrections are being made, rotation is stopped, the drill string is oriented so that the bent sub can be effective in correcting the directions of drilling, and the drill string is slid along the low side of the borehole as the downhole motor rotates the drill bit (allowing the drill bit to advance).   Under this operational situation the rock cuttings that might accumulate on the low side of the hole will not be mechanically agitated and forced into the return flow stream above the drill string. This operational situation is probably the worst case from the view point of horizontal borehole cleaning.   To analyze this particular operational situation it will be necessary to draw on the pneumatic conveying literature [4].   For horizontal pneumatic conveying, saltation occurs when the conveyed solids fall to the low side of the hole. To further understand saltation, Figure 12-6 shows the solids flow characteristics for horizontal pneumatic conveying.
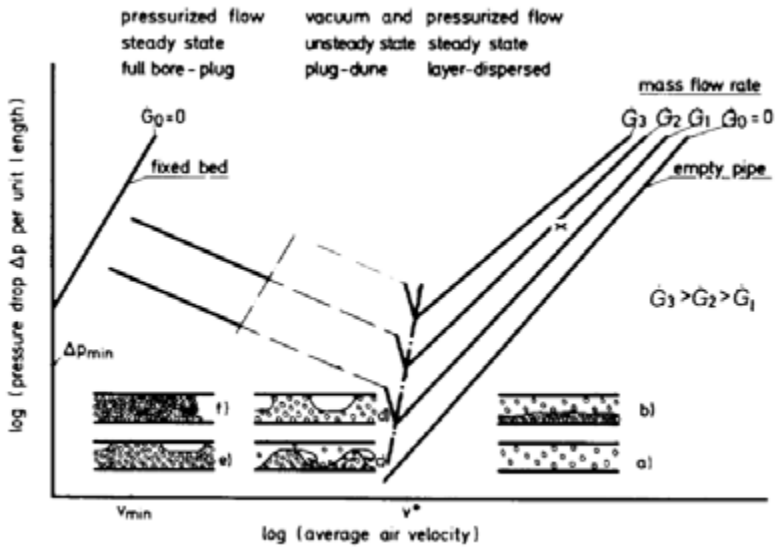
Figure 12-6: Solids flow characteristics in horizontal pneumatic conveying.   Note that the units of $\dot{G}$ is lb/sec [4].

The nearly vertical dashed line in the center of Figure 12-6 shows the saltation velocity of the air flow for various solid flow rates ($\dot{G}$).   The right side of the saltation line is the dilute phase flow and left of the saltation line is dense phase flow (see Section 8.2).   Schematics a) and b) in Figure 12-6 show different air/solids flow situations for the dilute phase flow.   Schematic a) shows all solids entrained in

the air flow. Schematic b) shows a small volume of the solids lying on the low side of the horizontal flow duct, but the air flow with entrained solids flowing at steady state conditions above slower moving low side steady state solids/air flow. Schematics c), d), e), and f) show various stages of unsteady dense solids/air flow.

Clearly the minimum volumetric flow rate for the sliding drill string situation in horizontal drilling should attempt to avoid excessive saltation. Sliding of the drill string in the horizontal borehole is complicated by the actual borehole cross-section geometry. When sliding the drill string will lay on the low side of the borehole. Thus, the return flow in the borehole is not flow in an annulus. To give some perspective, Figure 12-7 shows an example of the borehole cross-section geometry for a 7 7/8 inch borehole with API 4 1/2 inch, 16.60 lb/ft nominal, EU-S135, NC50(IF) drill pipe. This drill pipe has tool joints with a 6 5/8 inch outside diameter. As can be seen in Figure 12-7, the tool joint larger diameter holds the drill pipe body off the bottom of the borehole (the tool joint is the dashed circle).
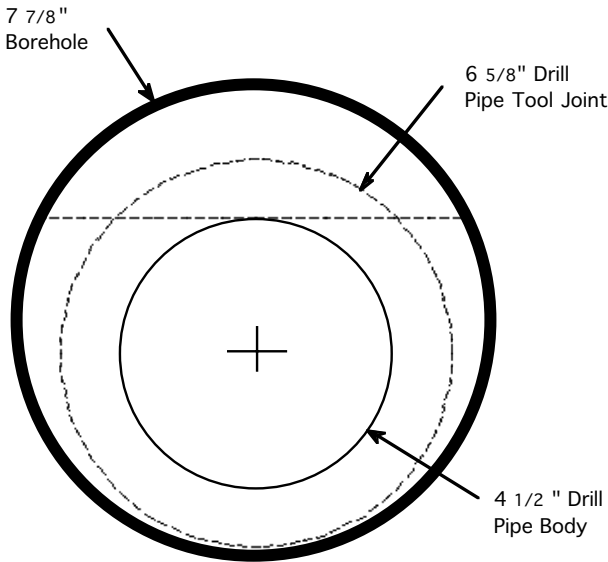
Figure 12-7: Cross-section geometry of a 7 7/8 inch borehole with a sliding 4 1/2 inch drill pipe on low side of hole.

The actual return flow of the gas with entrained rock cuttings will take the path of less resistance around the drill string. This means most of the flow will be above the horizontal dashed line in Figure 12-7.

Illustrative Example 12.1   Determine the cross-section area and the hydraulic diameter of the assumed flow path opening described above for the drill pipe borehole geometry shown in Figure 12-7. Ignore the protrusion of the drill pipe tool joints into this flow area.

The hydraulic radius is defined for this flow path opening (area above the horizontal dashed line) as [5]

$$R_h = \frac{\text{flow cross - section area}}{\text{wetted perimeter}} \qquad (12\text{-}1)$$

Note, the hydraulic radius term is not a true geometric radius.
The flow path opening cross-section area is

$$a_{fp} = 11.965 \text{ in}^2$$

The wetted perimeter is

$$s_{wp} = 16.147 \text{ inches}$$

Equation 12-1 becomes

$$R_h = \frac{11.970}{16.147}$$

$$R_h = 0.742 \text{ inches}$$

The effective hydraulic diameter of the is flow path opening is [5]

$$d_h = 4 \; R_h$$

$$d_h = 4 \; (0.742)$$

$$d_h = 2.965 \text{ inches}$$

If the return flow were channeled to the annulus space above the drill string, then the flow velocity would be higher than if the flow were channeled through an ideal annulus space with equal openings on all sides of the drill string (assuming constant volumetric flow rate). Thus, the carrying capacity of this higher velocity channel above the drill string should be high.   But there are protrusions of tool joints into this "path of least resistance" which will cause cuttings to be dropped into the low side of the borehole in spaces that do not have high velocity flows. Therefore, saltation of cuttings into the low side of the borehole is unavoidable. Thus, the only way to avoid unmanageable saltation accumulations in the low side of the borehole will be to drill (directionally by sliding the drill string) for a drill pipe joint, then pull the drill string back a stand of joints in the mast and blow the hole clean before going back to bottom and continuing sliding and drilling.   This careful cleaning process while sliding the drill string appears to unavoidable.

12.4.3 *Equations for Radius and Slant (or Horizontal) Drilling*

Direct circulation equations have been developed for air or gas drilling operations that can be used to model the radius segment and the horizontal (or slant) segment of a directionally drilled borehole [6]. These equations have been developed using the basic equations given in Chapter 6, namely, Equations 6-57 (annulus flow) and 6-72 (inside drill string flow).

The equations that model the radius and straight sections of a directional borehole neglect the column weight of the air or gas in these borehole segments.

Annulus Flow

The equation for the pressure at the bottom of the radius segment, P_{br}, in the annulus is

$$P_{br} = \left[P_{tr}^2 + 2\ a_a\ b_a\ T_{av}\ L\ e^{\frac{2\ a_a\ R}{T_{av}}} \right]^{0.5} \qquad (12\text{-}2)$$

where P_{tr} is the pressure at the top of the radius segment (lb/ft^2 abs),

    R is the radius of the curved segment (ft).

The values of a_a and b_a are given by Equations 6-55 and 6-56, respectively. The arc length of the curved segment, L, is

$$L = \theta_m\ R \qquad (12\text{-}3)$$

where θ_m is the maximum angle the borehole axis makes with vertical (radians).

The equation for the pressure at the bottom of the horizontal segment, P_{ex}, in the annulus is

$$P_{ex} = \left[P_{en}^2 + 2\ a_a\ b_a\ T_{av}\ L \right]^{0.5} \qquad (12\text{-}4)$$

where P_{en} is the pressure at the entrance to the horizontal segment (lb/ft^2 abs),

    L is the length of the horizontal segment (ft).

Inside Drill String Flow

The equation for the pressure at the top of the radius segment, P_{tr}, inside the drill string is

$$P_{tr} = \left[P_{br}^2 + 2\ a_i\ b_i\ T_{av}\ L\ e^{\frac{2\ a_i\ R}{T_{av}}} \right]^{0.5} \qquad (12\text{-}5)$$

where P_{br} is the pressure at the bottom of the radius segment (lb/ft^2 abs). The values of a_i and b_i are given by Equations 6-70 and 6-71, respectively.

The equation for the pressure at the bottom of the horizontal segment, P_{en}, inside the drill string is

$$P_{en} = \left[P_{ex}^2 \ + \ 2 \ a_i \ b_i \ T_{av} \ L \ \right]^{0.5} \tag{12-7}$$

where P_{ex} is the pressure at the exit to the horizontal segment (lb/ft^2 abs).

Minimum Volumetric Flow Rate

In the illustrative example below, the minimum volumetric flow rate of inert atmospheric air will be discussed for the two directional drilling operational situations, rotating the drill string and sliding the drill string.

Illustrative Example 12.2   Figure 12-8 gives a well profile for a directionally drilled borehole that is to be initiated at a kickoff point (KOP) of approximately 7,000 ft. This well profile is similar to that given in Illustrative Example series 8.1, 8.2, and 8.3. However, in this example the well will be drilled directionally in the 3,000 ft of openhole drilling below the casing shoe at 7,000 ft. It is planned that the directional segments of the well below the casing shore are to be drilled with the PDM used in Illustrative Example 11.2. The curved segment of the openhole will be a 318 ft medium radius borehole. The curved segment will be drilled to an angle of 90° to the vertical. This will give an arc length of approximately 500 ft. At the end of the curved segment, a 2,500 ft horizontal is to be drilled. The drill string in the vertical cased section of the well is to be 4 1/2 inch, heavy-weight drill pipe (see Table 3-3).   The drill string in the openhole section of the well (curved and horizontal segments) is to be API 4 1/2 inch, 16.60 lb/ft nominal, EU-S135, NC50 (IF) drill pipe. The MWD, bent sub, and PDM with a 7 7/8 inch drill bit will make up the BHA. The anticipated rate of penetration for the directional drilling operation is 30 ft/hr. The drilling operation surface location is at 4,000 ft above mean sea level. The openhole section of the well is to be drilled with inert atmospheric air (i.e., $S_g = 0.97$). Determine the approximate minimum volumetric flow rate required to clean the well when drilling at the end of the 2,500 ft horizontal (or 3,000 ft of openhole drilling).

In Illustrative Example 12.3 below, the major and minor losses solution is presented using the lumped geometry approximations introduced in the Illustrative Example series 8.3a and 8.3b, and also used in Illustrative Example 11.2.   This solution can be used to determine the minimum volumetric flow rate of inert atmospheric air while drilling at the end of the openhole section.   This is accomplished via a trial and error process that determines the volumetric flow rate that will give an annulus minimum kinetic energy per unit volume of approximately 3.0 ft-lb/ft^3.

Rotating the Drill String

It is assumed that when the drill string is rotated in a directional well the flow geometry in the annulus space can be adequately approximated as an annulus flow. Therefore, assuming an annulus geometry of flow, it was found that the approximate volumetric flow rate of inert atmospheric air that will give an annulus kinetic energy per unit volume of 3.0 ft-lb/ft^3 is 1,630 acfm. This critical annulus cross-section where the minimum kinetic energy per unit volume occurs is just up-hole from the

top of the lumped geometry tool joints that is above the BHA (i.e., approximately 150 ft from the bottom of the openhole section of the well).

Sliding the Drill String

As was discussed above, when the drill string is slid in the openhole (when a directional correction must be made), the drill string will lay on the low side of the horizontal openhole. If the flow area at the top of the drill string in the horizontal segment of the openhole is assumed to have the geometry discussed in Illustrative Example 12.1, then the flow velocity and the kinetic energy per unit volume will be high in this space. Thus, the minimum kinetic energy per unit volume will shift to a new critical annulus cross-section. This new critical annulus cross-section is just up-hole from the top of the lumped geometry tool joints in the cased section of the well (i.e., approximately 350 ft from the bottom of the cased section of the well). The approximate volumetric flow rate of inert atmospheric air that will give an annulus kinetic energy per unit volume of 3.0 ft-lb/ft^3 at this new critical cross-section is 1,350 acfm.
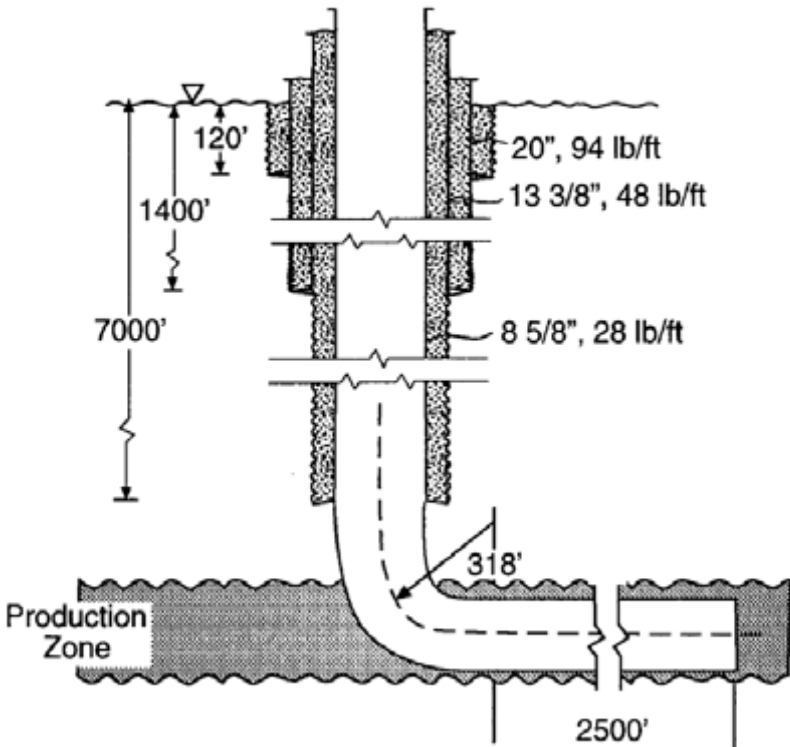
Figure 12-8: Directional well profile for Illustrative Examples 12.2 and 12.3.

Comparing the above two directional drilling situations, it is clear that the higher minimum volumetric flow rate is the appropriate selection (i.e., 1,630 acfm). This is true for two important reasons. First, even though the sliding situation gives a lower minimum volumetric flow rate, cuttings will accumulate in the low side of the borehole and there is no mechanism for getting them up into the flow stream since there is no rotation of the drill string (the lower flow rate is a false minimum). Second, the 1,630 acfm value ensures that all critical cross-sections in the annulus have a kinetic energy per unit volume of 3.0 ft-lb/ft^3 or greater.

12.5 Injection Pressure and Selection of Compressor Equipment

Air and gas technology directional wells for the oil and natural gas recovery operations are often drilled using inert atmospheric air as the drilling fluid. Thus, when selecting the type and number of compressor units for a directional drilling operation, the number and capacity of the accompanying membrane units must also be determined.

Illustrative Example 12.3 For the planned directional drilling operation given in Illustrative Example 12.2 above, determine the number of semi-trailer mounted, Dresser Clark Model CFB-4, four stage, reciprocating piston compressor units (see Figure 4-25) required to drill the 3,000 ft of directional openhole shown in Figure 12-8. The compressor units are rated at 1,200 acfm each. Also, determine the number of skid mounted membrane filter units rated at 1,500 acfm each that will be needed to supply the drilling operation with inert atmospheric air. It is required that the inert atmospheric air have only 5 percent oxygen content.

As determined in Illustrative Example 12.2 above, the minimum volumetric flow rate while drilling at the end of the 3,000 ft directional borehole is approximately 1,630 acfm. Figure 12-5 shows that the membrane filter units are about 50 percent efficient when producing inert atmospheric air with 5 percent oxygen content. Therefore, four compressor units and four membrane units will be required to provide the compressed inert atmospheric air. The approximate volumetric flow rate to the drill string during the directional drilling operation will be 2,400 acfm. The factor of safety in volumetric flow rate will be

$$FS \ = \ \frac{2,400}{1,630}$$

$$FS \ = \ 1.47$$

Illustrative Example 12.4 For the planned directional drilling operation given in Illustrative Examples 12.2 and 12.3 above, determine the bottomhole annulus pressure drill string injection pressure while drilling at the end of the 3,000 ft directional borehole. Also, determine the total fuel consumption rate for the compressors when drilling at the end of the 3,000 ft directional borehole.

This solution is very similar to that given in Illustrative Example 11.2 except the drilling rate for this directional drilling operation is anticipated to be 30 ft/hr (as opposed to 60 ft/hr in Illustrative Example 11.2). The PDM downhole motor is the same and the required power and drill bit speed outputs are the same (i.e., 25

horsepower and 200 rpm). Table 12-2 gives a summary of the pressures as a function of true vertical depth (TVD) and measured depth (MD).

Table 12-2: Summary of pressures for Illustrative Example 12.4.

TVD (ft)	MD (ft)	Annulus Space (psia)	Inside Drill String (psia)
0	0	12.7	640.3
6650	6650	58.1	729.4
7000	7000	66.2	735.0
7318	7500	71.3	734.0
7318	9850	91.2	730.0
7318	10000	111.6	730.0

The bottomhole pressure in the annulus is 111.6 psia. The bottomhole pressure in the vertical well (with the same PDM) was 204.5 psia. A small part of the difference is due to the different anticipated penetration rates for the two problems. But most of the difference is due to less friction resistance in the directional borehole. The directional borehole is to be drilled with 4 1/2 inch drill pipe in the drill string. The vertical borehole problem had 500 ft of 6 3/4 inch drill collars in the BHA. The injection pressure for the directional drilling problem is 640.3 psia. This is greater than the 553.4 psia for the vertical drilling problem. This reflects the contribution of the additional 3,000 ft of gas column weight in the vertical drilling problem.

The diesel fuel consumption rate for each of the four semi-trailer mounted compressor units is approximately 33 gals/hr when drilling at the end of the 3,000 ft directional section of the well. Thus, the total fuel consumption for all four compressors will be approximately 132 gals/hr while drilling at the end of the directional section.

12.6 Field Operations Comparisons

The following case histories of directional drilling operations demonstrate the accuracy of the planning calculation procedures discussed in earlier chapters and in this chapter that utilize complete major and minor friction loss terms.

Case History No. 1 This well was drilled in the San Juan Basin in northwestern New Mexico. This was directional borehole drilled to a MD of 7,240 ft and a TVD of 5,568 ft. The well was cased to a MD of 5,173 ft with API 7 inch casing. The KOP was at 5,183 ft. A 4 3/4 inch diameter PDM with a 6 1/4 inch drill bit was used to drill a medium radius curved segment of the borehole with an arc length of 310 ft. An PDM was also used to drill the horizontal segment of the borehole to a length of 1,428 ft in the Dakota sand formation. The drill string was made up of 3 1/2 inch heavy weight drill pipe in the vertical section of the well and API 3 1/2 inch drill pipe in the curved and horizontal section of the well. The drilling rate in the horizontal segment of the borehole was 23 ft/hr. Inert atmospheric air was used as the drilling fluid. The volumetric flow rate injected into the well was 2,400 acfm (the surface location elevation was approximately 6,100 ft). The predicted surface injection pressure was 492 psig and the actual injection pressure was 500 psig

Case History No. 2 This well was also drilled in the San Juan Basin in northwestern New Mexico. This was directional borehole drilled to a MD of 8,065 ft and a TVD of 5,800 ft. The well was cased to a MD of 5,461 ft with API 7 inch

casing. The cased hole was kicked off at a MD of 5,557 ft so that the bottom of the casing had a build angle of 20˚ to vertical. A 4 3/4 inch diameter PDM with a 6 1/4 inch drill bit was used to drill a medium radius curved segment of the borehole with an arc length of 666 ft to a final angle to vertical of 88˚. Also in this well an PDM was used to drill the horizontal segment of the borehole to a length of 1,937 ft in the Dakota sand formation. The drill string was made up of 3 1/2 inch heavy weight drill pipe in the vertical section of the well and API 3 1/2 inch drill pipe in the curved and horizontal section of the well. The drilling rate in the horizontal segment of the borehole was 25 ft/hr. Inert atmospheric air was used as the drilling fluid. The volumetric flow rate injected into the well was 2,800 acfm (the surface location elevation was approximately 6,200 ft). The predicted surface injection pressure was 539 psig and the actual injection pressure was 550 psig.

12.7 Conclusions

The analytic models developed in Chapter 8 for vertical wells and in this chapter for directional wells appear to be accurate in predicting injection pressures and likely bottomhole pressures for air (and other gases) operations.

As in preceding chapters, the demonstration calculations in this chapter have utilized lumped geometry approximations for the drill pipe body and drill pipe tool joints.   Such approximations appear to adequately model the overall friction resistance in the circulation system and give accurate results for bottomhole and injection pressures. An improvement to this drill string geometry approximation technique can be made by programming each tool joint individually at its proper location in the drill string. This type of program would be best carried out using a higher level computer language such as C++ or FORTRAN. Such a programmed solution would improve the detail pressure versus depth accuracy of the model. However, a comparison of this type of program gives very little change in bottomhole and injection pressures, and in the required volumetric flow rate of gas.

References

1. Allan, P. D., "Nitrogen Drilling System for Gas Drilling Applications," SPE 28320. Presented at the SPE 69th Annual Technical Conference and Exhibition, New Orleans, Louisiana, 25-28 September 1994.

2. Zabetakis, M. G., "Flammability Characteristics of Combustible Gases and Vapors," *Bureau of Mines Bulletin 627*, Washington D. C., 1964.

3. Coward, H. F., and Jones, G. W., "Limits of Flammability of Gases and Vapors," *Bureau of Mines Bulletin 503*, Washington D. C., 1952.

4. Marcus, R. D., Leung, L. S. , Klinzing, G. E., and Rizk, F., *Pneumatic Conveying of Solids*, Chapman and Hall, 1990.

5. Daugherty, R. L., Franzini, J. B., and Finnemore, E. J., *Fluid Mechanics with Engineering Applications*, Eighth Edition, McGraw-Hill, 1985.

6. Guo, B., Miska, S. Z., and Lee, R. Volume Requirements for Directional Air Drilling," IADC/SPE 27510, Presented at the 1994 IADC/SPE Drilling Conference, Dallas, Texas, 15 to 18 February 1994.

This page intentionally left blank.

Appendices

This page intentionally left blank.

Dimensions and Units,
Conversion Factors

The systems of dimensions and units used in mechanics are based on Newton's second law of motion, which is force equals mass mutiplied by acceleration, or

$$F = m\,a \tag{A-1}$$

for consistent systems of units.

In the English unit system, engineers define a pound of force as the force required to accelerate one slug of mass at the rate of one foot per second per second. One slug of mass has a weight of approximately 32.2 lb when acted upon by the acceleration of gravity present at the surface of the earth. Thus, Equation A-1 in the English units is

$$1 \text{ lb } = (1 \text{ slug}) (1 \text{ ft/sec}^2)$$

In the International System of Units (or SI metric), engineers define a newton of force as the force required to accelerate one kilogram of mass at the rate of one meter per second per second. Thus, Equation A-1 in the SI metric is

$$1 \text{ N } = (1 \text{ kg}) (1 \text{ m/sec}^2)$$

The physicists, on the other hand, utilize a version of the SI metric that defines a dyne of force as the force required to accelerate one gram of mass at the rate of one centimeter per second per second.

Unfortunately, these different systems tend to create confusion. In many parts of the world engineers use the kilogram for both force and mass units. With universal adoption of metric SI, however, this confusion should gradually disappear.

Any system based on length (L), mass (M), and time (T) is absolute because it is independent of the gravitational acceleration g. A system based on length (L), weight, i.e., force (F), and time (T) is referred to as a gravitational system, since weight depends on the value of g which in turn varies with location (i.e., altitude and latitude). Hence the weight (W) of a certain mass varies with its location. This variation is not generally considered in this text as the variation in the value of g is

small as long as we are analyzing a problem on or quite near the earth's surface. Fluid mechanics problems for other locations, such as the moon where g is very different than on the earth, can be handled by the methods presented in this text if proper consideration is given to the value of g.

The metric SI is known as a mass system, since mass is not dependent on the gravitational system. Indeed, the gravitational acceleration g at the location either on the earth's surface on moon's surface needs to be known in order to handle specific problems.

Table A-1: Definitions of English system quantities

Force	1 lb =	1 slug-ft/sec^2
Area	1 acre =	43,560 ft^2
Energy	1 Btu =	778 ft-lb
Flowrate	1 cfs =	448.83 gpm
Length	1 ft =	12 inches
	1 yd =	3 ft
	1 statute mile =	5,280 ft
	1 nautical mile =	6,000 ft
Mass	1 slug =	1 lb-sec^2/ft
Power	1 hp =	550 ft-lb/sec = 0.708 Btu/sec
Velocity	1 mph =	1.467 ft/sec
	1 knot =	1.689 ft/sec = 1.152 mph
Volume	1 ft^3 =	7.48 U.S. gal
	1 U.S. gal =	231 in^3 = 0.1337 ft^3 (8.34 lb of water)
	1 British imperial gal =	1.2 U.S. gal (10 lb of water)
Weight	1 U.S. (short) ton =	2,000 lb
	1 British (long) ton =	2,240 lb

Table A-2: Definitions of metric SI quantities

Force	1 N =	1 kg-m/sec^2
Area	1 Hectare (ha) =	$10^4 \text{ m}^2 = 100$ m square
Energy (or work)	1 Joule (J) =	1 N-m
Flowrate	$\text{m}^3/\text{sec }$ =	60,000 lpm
Length	1 centimeter =	10 millimeter
	1 m =	100 centimeter
	1 kilometer =	1,000 m
Mass	1 kg =	1,000 gram
	1 metric ton =	1,000 kg
Power	1 Watt =	1 N-m/sec
Velocity	1 kph =	1,000 m/hr = 0.277 m/sec
Volume	1 m^3 =	1,000 liter
	1 liter =	10^3 cm
Weight	See Force above	

Table A-3: Basic quantities English to metric SI conversions

	English unit	SI unit
Acceleration of gravity	32.2 ft/sec^2	9.81 m/sec^2
Density of water (at 39.4˚F or 4˚C)	1.94 slug/ft^3	$1,000 \text{ kg/m}^3$
Specific weight of water	62.4 lb/ft^3	$9,810 \text{ N/m}^3$
Standard sea level atmospheric pressure		
API (at 60˚F)	14.966 psia	
ASME (at 68˚F)	14.7 psia	
UK (at 60˚F)	30.00 inches of Hg	
Continental Europe (at 15˚C)		750 mm of Hg

Table A-4: Other important English and metric SI quantities and conversions

Engineering gas constant **R**
    English   **R** = 53.36 ft-lb/lb-° R
    Metric   **R** = 29.28 N-m/N-K

Energy
    English   1 ft-lb = 1 lb-ft
    Metric SI   1 N-m = 1 joule (J)

Heat
    English   1 Btu = 252 cal (heat reqired to raise 1.0 lb of
                                water 1.0° R)
    Metric   1 cal = 4.187 J (heat required to raise 1.0 g of
                                water 1.0 K)

Temperature
    English   ° R = 459.67° + ° F
    Metric SI   K = 273.15° + ° C

Pressure
    English   1 lb/ft^2 = 144 psi
    Metric SI 1 Pascal (Pa) = N/m^2

Power
    English   1 horsepower = 550 ft-lb/sec
    Metric SI   1 watt (W) = 1 J/sec (or 1 N-m/sec)

Absolute Viscosity
    English   1 lb-sec/ft^2 = 47.88 N-sec/m^2
    Metric SI   1 Poise (P) = 10^{-1} N-sec/m^2

Kinematic Viscosity
    English   1 ft^2/sec = 0.0929 m^2/sec
    Metric SI   1 Stoke (St) = 10^{-4} m^2/sec

Table A-5: Commomly used prefixes for metric SI units

Factor by which unit is multiplied	Prefix	Symbol
10^9	giga	G
10^6	mega	M
10^3	kilo	k
10^{-2}	centi	c
10^{-3}	milli	m
10^{-6}	micro	μ
10^{-9}	nano	n

Table A-6: Conversion Factors (English to metric SI)

	To convert English units	Multiply by	To obtain metric (SI) units
Acceleration	ft/sec^2	0.3048	m/sec^2
Area	ft^2	0.0929	m^2
	Acre (43,560 ft^2)	0.4047	Hectare (100 m^2)
Density	slug/ft^3	515.4	kg/m^3
Energy (work or quantity of heat)	ft-lb	1.356	N-m (joule)
	ft-lb	3.77 x 10^{-7}	kWh
	Btu (778 ft-lb)	1,055	N-m (joule)
Flowrate	ft^3/sec	0.02832	m^3/sec (10^3 L/sec)
Force	lb	4.448	N
Length	in	25.4	mm
	ft	0.3048	m
	mile (5,280 ft)	1.609	km
Mass	slug	14.59	kg
Power	ft-lb/sec	1.356	W (N-m/sec)
	hp (550 ft-lb/sec)	745.7	W (N-m/sec)
Pressure	psi	6,895	N/m^2 (pascal)
	lb/ft^2	47.88	N/m^2 (pascal)
Specific heat	ft-lb/slug-° R	0.1672	N-m/kg-K
Specific weight	lb/ft^3	157.1	N/m^3
Velocity	ft/sec	0.3048	m/sec
Viscosity			
Absolute	lb-sec/ft^2	47.88	N-sec/m^2
Kinematic	ft^2/sec	0.0929	m^2/sec (10^4 St)
Volume	ft^3	0.02832	m^3
	gallon (US)	3.785	L (10^{-3} m^3)

Table A-7: Conversion Factors (metric SI to English)

	To convert metric SI units	Multiply by	To obtain English units
Acceleration	m/sec^2	3.281	ft/sec^2
Area	m^2	10.76	ft^2
	Hectare (100 m^2)	2.471	Acre (43,560 ft^2)
Density	kg/m^3	0.001940	slug/ft^3
Energy (work or quantity of heat)	N-m (joule)	0.7376	ft-lb
	kWh	2.650 x 10^6	ft-lb
	N-m (joule)	0.0009480	Btu (778 ft-lb)
Flowrate	m^3/sec (10^3 L/sec)	35.31	ft^3/sec
Force	N	0.2248	lb
Length	mm	0.03937	in
	m	3.281	ft
	km	0.6215	mile (5,280 ft)
Mass	kg	0.06854	slug
Power	W (N-m/sec)	0.7375	ft-lb/sec
	W (N-m/sec)	0.001341	hp (550 ft-lb/sec)
Pressure	N/m^2 (pascal)	0.0001450	psi
	N/m^2 (pascal)	0.02089	lb/ft^2
Specific heat	N-m/kg-K	5.981	ft-lb/slug-° R
Specific weight	N/m^3	0.006365	lb/ft^3
Velocity	m/sec	3.281	ft/sec
Viscosity			
Absolute	N-sec/m^2	0.02089	lb-sec/ft^2
Kinematic	m^2/sec (10^4 St)	10.76	ft^2/sec
Volume	m^3	35.31	ft^3
	L (10^{-3} m^3)	0.2642	gallons (US)

This page intentionally left blank.

B

API Drill Collar and Drill Pipe Properties

This appendix gives the basic geometric and physical properties of API drill collars and API drill pipe.

B.1 API Drill Collars

Table B-1 gives the dimensions and weight per unit length for API drill collars. Table B-2 gives the possible rotary shoulder connections and recommended make-up torque for the various drill collar sizes with API connections.

B.2 API Drill Pipe

Table B-3 gives the dimensions and the weight per unit length for the API drill pipe body. Table B-4 gives the dimensions of the tool joints, actual weight per unit length, and mechanical properties for new Grade E drill pipe. Table B-5 gives the dimensions of the tool joints, actual weight per unit length, and mechanical properties for new Grades X, G and S drill pipe (known as high strength drill pipe). Table B-6 gives the API rotary shouldered connection interchange list.

Table B-1:   API Drill Collar Weight (Steel) (pounds per foot)

(1)	(2)	(3)	(4)	(5)	(6)	(7)	(8)	(9)	(10)	(11)	(12)	(13)	(14)
Drill Collar OD, inches	Drill Collar ID, Inches												
	1	$1^1/_4$	$1^1/_2$	$1^3/_4$	2	$2^1/_4$	$2^1/_2$	$2^3/_4$	3	$3^1/_4$	$3^1/_2$	$3^3/_4$	4
$2^7/_8$	19	18	16										
3	21	20	18										
$3^1/_8$	22	22	20										
$3^1/_4$	26	24	22										
$3^1/_2$	30	29	27										
$3^3/_4$	35	33	32										
4	40	39	37	35	32	29							
$4^1/_8$	43	41	39	37	35	32							
$4^1/_4$	46	44	42	40	38	35							
$4^1/_2$	51	50	48	46	43	41							
$4^3/_4$			54	52	50	47	44						
5			61	59	56	53	50						
$5^1/_4$			68	65	63	60	57						
$5^1/_2$			75	73	70	67	64	60					
$5^3/_4$			82	80	78	75	72	67	64	60			
6			90	88	85	83	79	75	72	68			
$6^1/_4$			98	96	94	91	88	83	80	76	72		
$6^1/_2$			107	105	102	99	96	91	89	85	80		
$6^3/_4$			116	114	111	108	105	100	98	93	89		
7			125	123	120	117	114	110	107	103	98	93	84
$7^1/_4$			134	132	130	127	124	119	116	112	108	103	93
$7^1/_2$			144	142	139	137	133	129	126	122	117	113	102
$7^3/_4$			154	152	150	147	144	139	136	132	128	123	112
8			165	163	160	157	154	150	147	143	138	133	122
$8^1/_4$			176	174	171	168	165	160	158	154	149	144	133
$8^1/_2$			187	185	182	179	176	172	169	165	160	155	150
9			210	208	206	203	200	195	192	188	184	179	174
$9^1/_2$			234	232	230	227	224	220	216	212	209	206	198
$9^3/_4$			248	245	243	240	237	232	229	225	221	216	211
10			261	259	257	254	251	246	243	239	235	230	225
11			317	315	313	310	307	302	299	295	291	286	281
12			379	377	374	371	368	364	361	357	352	347	342

Notes:
1.   See API Specification 7, Table 13 for API standard drill collar dimensions.
2.   For special configurations of drill collars, consult manufacturer for reduction in weight.

Table B-2: API Recommended Make-up Torque[1] for Rotary Shouldered Drill Collar Connections (See footnotes for use of this table.)

(1)	(2)	(3)	(4)	(5)	(6)	(7)	(8)	(9)	(10)	(11)	(12)	(13)
Connection		OD, in.	Minimum Make-up Torque ft-lb[2] — Bore of Drill Collar, inches									
Size, in.	Type		1	1¼	1½	1¾	2	2¼	2½	2 13/16	3	3¾
API	NC23	3	*2,508	*2,508	*2,508							
		3⅛	*3,330	*3,330	2,647							
		3¼	4,000	3,387	2,647							
2⅜	Regular	3		*2,241	*2,241	1,749						
		3⅛		*3,028	2,574	1,749						
		3¼		3,285	2,574	1,749						
2⅞	PAC[3]	3		*3,797	*3,797	2,926						
		3⅛		*4,966	4,151	2,926						
		3¼		5,206	4,151	2,926						
2⅜ API	API IF NC 26	3½		*4,606	*4,606	3,697						
		3¾		5,501	4,668	3,697						
2⅞	Regular	3½		*3,838	*3,838	*3,838						
		3¾		5,766	4,951	4,002						
		3⅞		5,766	4,951	4,002						
2⅞	Slim Hole											
2⅞	Extra Hole	3¾		*4,089	*4,089	*4,089						
3⅛	Double Streamline	3⅞		*5,352	*5,352	*5,352						
2⅞	Mod. Open	4⅛		8,059	8,059	7,433						
2⅞ API	API IF NC 31	3⅞		*4,640	*4,640	*4,640	*4,640					
		4⅛		*7,390	*7,390	*7,390	6,853					
3½	Regular	4⅛		*6,466	*6,466	*6,466	*6,466	5,685				
		4¼		*7,886	*7,886	*7,886	7,115	5,685				
		4½		10,471	9,514	8,394	7,115	5,685				
3½	Slim Hole	4¼		*8,858	*8,858	8,161	6,853	5,391				
		4½		10,286	9,307	8,161	6,853	5,391				
API	NC 35	4½				*9,038	*9,038	*9,038	7,411			
		4¾				12,273	10,826	9,202	7,411			
		5				12,273	10,826	9,202	7,411			
3½	Extra Hole	4¼				*5,161	*5,161	*5,161	*5,161			
4	Slim Hole	4½				*8,479	*8,479	*8,479	8,311			
3½	Mod. Open	4¾				*12,074	11,803	11,803	8,311			
		5				13,283	11,803	10,144	8,311			
		5¼				13,283	11,803	10,144	8,311			

Table B-2: *(Continued)*

(1)	(2)	(3)	(4)	(5)	(6)	(7)	(8)	(9)	(10)	(11)	(12)	(13)
3½	API IF	4¾				9,986	*9,986	*9,986	*9,986	8,315		
API	NC 38	5				*13,949	*13,949	12,907	10,977	8,315		
4½	Slim Hole	5¼				16,207	14,643	12,097	10,977	8,315		
		5½				16,207	14,643	12,907	10,977	8,315		
3½	H-90[4]	4¾				*8,786	*8,786	*8,786	*8,786	*8,786		
		5				*12,794	*12,794	*12,794	*12,794	10,408		
		5¼				*17,094	16,929	15,137	13,151	10,408		
		5½				18,522	16,929	15,137	13,151	10,408		
4	Full Hole	5				*10,910	*10,910	*10,910	*10,910	*10,910		
API	NC 40	5¼				*15,290	*15,290	*15,290	14,969	12,125		
4	Mod. Open	5½				*19,985	18,886	17,028	14,969	12,125		
4½	Double Streamline	5¾				20,539	18,886	17,028	14,969	12,125		
		6				20,539		17,028	14,969	12,125		
	H-90[4]	5¼				*12,590	*12,590	*12,590	*12,590	*12,590		
		5½				*17,401	*17,401	*17,401	*17,401	16,536		
		5¾				*22,531	*22,531	21,714	19,543	16,536		
		6				25,408	23,671	21,714	19,543	16,536		
		6¼				25,408	23,671	21,714	19,543	16,536		
4½	API Regular	5½				*15,576	*15,576	*15,576	*15,576	*15,576		
		5¾				*20,609	*20,609	20,609	19,601	16,629		
		6				25,407	23,686	21,749	19,601	16,629		
		6¼				25,407	23,686	21,749	19,601	16,629		
API	NC44	5¾				*20,895	*20,895	*20,895	*20,895	18,161		
		6				*26,453	25,510	23,493	21,257	18,161		
		6¼				27,300	25,510	23,493	21,257	18,161		
		6½				27,300	25,510	23,493	21,257	18,161		
4½	API Full Hole	5½					*12,973	*12,973	*12,973	*12,973	*12,973	
		5¾					*18,119	*18,119	*18,119	*18,119	17,900	
		6					*23,605	23,028	23,028	19,921	17,900	
		6¼					27,294	25,272	22,028	19,921	17,900	
		6½					27,294	25,272	22,028	19,921	17,900	
4½	Extra Hole	5¾						*17,738	*17,738	*17,738	*17,738	
API	NC 46	6						*23,422	*23,422	22,426	20,311	
4	API IF	6¼						28,021	25,676	22,426	20,311	
4	Semi IF	6½						28,021	25,676	22,426	20,311	
5⁻	Double Streamline	6¾						28,021	25,676	22,426	20,311	
4½	Mod. Open											
4½	H-90[4]	5¾						*18,019	*18,019	*18,019	*18,019	
		6						*23,681	*23,681	23,159	21,051	
		6¼						28,732	26,397	23,159	21,051	
		6½						28,732	26,397	23,159	21,051	
		6¾						28,732	26,397	23,159	21,051	

Table B-2: *(Continued)*

(1)	(2)	(3)	(4)	(5)	(6)	(7)	(8)	(9)	(10)	(11)	(12)	(13)
5	H-90⁴	6¼	*25,360	*25,360	*25,360	*25,360	23,988					
		6½	*31,895	*31,895	29,400	27,167	23,988					
		6¾	35,292	32,825	29,400	27,167	23,988					
		7	35,292	32,825	29,400	27,167	23,988					
4½ API	API IF	6¼	*23,004	*23,004	*23,004	*23,004	*23,004					
	NC50	6½	*29,679	*29,679	*29,679	*29,679	26,675					
5	Extra Hole	6¾	*36,742	35,824	32,277	29,966	26,675					
5	Mod. Open	7	38,379	35,824	32,277	29,966	26,675					
5½	Double Streamline	7¼	38,379	35,824	32,277	29,966	26,675					
5	Semi-IF	7½	38,379	35,824	32,277	29,966	26,675					
5½	H-90⁴	6¾	*34,508	*34,508	*34,508	34,142	30,781					
		7	*41,993	40,117	36,501	34,142	30,781					
		7¼	42,719	40,117	36,501	34,142	30,781					
		7½	42,719	40,117	36,501	34,142	30,781					
5½	API Regular	6¼	*31,941	*31,941	*31,941	*31,941	30,495					
		7	*39,419	*39,419	36,235	33,868	30,495					
		7¼	42,481	39,866	36,235	33,868	30,495					
		7½	42,481	39,866	36,235	33,868	30,495					
5½	API Full Hole	7	*32,762	*32,762	*32,762	*32,762	*32,762					
		7¼	*40,998	*40,998	*40,998	*40,998	*40,998					
		7½	*49,661	*49,661	47,756	45,190	41,533					
		7¾	54,515	51,687	47,756	45,190	41,533					
		7¾	54,515	51,687	47,756	45,190	41,533					
API	NC 56	7¼		*40,498	*40,498	*40,498	*40,498					
		7½		*49,060	48,221	45,680	42,058					
		7¾		52,115	48,221	45,680	42,058					
		8		52,115	48,221	45,680	42,058					
6⅜	API Regular	7½		*46,399	*46,399	*46,399	*46,399					
		7¾		*55,627	53,346	50,704	46,936					
		8		57,393	53,346	50,704	46,936					
		8¼		57,393	53,346	50,704	46,936					
6⅝	H-90⁴	7½		*46,509	*46,509	*46,509	*46,509					
		7¾		*55,708	*55,708	53,629	49,855					
		8		60,321	56,273	53,629	49,855					
		8¼		60,321	56,273	53,629	49,855					
API	NC 61	8		*55,131	*55,131	*55,131	*55,131					
		8¼		*65,438	*65,438	*65,438	61,624					
		8½		72,670	68,398	65,607	61,624					
		8¾		72,670	68,398	65,607	61,624					
		9		72,670	68,398	65,607	61,624					

Table B-2:   *(Continued)*

(1)	(2)	(3)	(4)	(5)	(6)	(7)	(8)	(9)	(10)	(11)	(12)	(13)
5½	API IF	8		*56,641	*56,641	*56,641	*56,641	*56,641				
		8¼		*67,133	*67,133	*67,133	63,381	59,027				
		8½		74,626	70,227	67,436	63,381	59,027				
		8¾		74,626	70,227	67,436	63,381	59,027				
		9		74,626	70,227	67,436	63,381	59,027				
		9¼		74,626	70,227	67,436	63,381	59,027				
6⅝	API Full Hole	8½		*67,789	*67,789	*67,789	*67,789	*67,789	67,184			
		8¾		*79,544	*79,544	*79,544	76,706	72,102	67,184			
		9		88,582	83,992	80,991	76,706	72,102	67,184			
		9¼		88,582	83,992	80,991	76,706	72,102	67,184			
		9½		88,582	83,992	80,991	76,706	72,102	67,184			
API	NC70	9		*75,781	*75,781	*75,781	*75,781	*75,781	*75,781			
		9¼		*88,802	*88,802	*88,802	*88,802	*88,802	*88,802			
		9½		*102,354	*102,354	*102,354	101,107	96,214	90,984			
		9¾		113,710,	108,841	105,657	101,107	96,214	90,984			
		10		113,710,	108,841	105,657	101,107	96,214	90,984			
		10½		113,710,	108,841	105,657	101,107	96,214	90,984			
API	NC77	10		*108,194	*108,194	*108,194	*108,194	*108,194	*108,194			
		10¼		*124,051	*124,051	*124,051	*124,051	*124,051	*124,051			
		10½		*140,491	140,491	140,491	140,488	135,119	129,375			
		10¾		154,297	148,965	145,476	140,488	135,119	129,375			
		11		154,297	148,965	145,476	140,488	135,119	129,375			
7	H-90[4]	8		*53,454	*53,454	*53,454	*53,454	*53,454	*53,454			
		8¼		*63,738	*63,738	*63,738	*63,738	60,971	56,382			
		8½		*74,478	72,066	69,265	65,267	60,971	56,382			
7⅜	API Regular	8½		*60,402	*60,402	*60,402	*60,402	*60,402	*60,402			
		8¾		*72,169	*72,169	*72,169	*72,169	*72,169	*72,169			
		9		*84,442	*84,442	*84,442	84,221	79,536	74,529			
		9¼		96,301	91,633	88,580	84,221	79,536	74,529			
		9½		96,301	91,633	88,580	84,221	79,536	74,529			
7⅝	H-90[4]	9		*73,017	*73,017	*73,017	*73,017	*73,017	*73,017			
		9¼		*86,006	*86,006	*86,006	*86,006	*86,006	*86,006			
		9½		*99,508	*99,508	*99,508	*99,508	*99,508	*96,285			
8⅜	API Regular	10		*109,345	*109,345	*109,345	*109,345	*109,345	*109,345			
		10¼		*125,263	*125,263	*125,263	*125,263	*125,263	125,034			
		10½		*141,767	*141,767	141,134	136,146	130,777	125,034			
8⅝	H-90[4]	10¼		*113,482	*113,482	*113,482	*113,482	*113,482	*113,482			
		10½		*130,063	*130,063	*130,063	*130,063	*130,063	*130,063			
7	H-90[4] (with low torque face)	8¾			*68,061	*68,061	67,257	62,845	58,131			
		9			74,235	71,361	67,257	62,845	58,131			

Table B-2: *(Continued)*

(1)	(2)	(3)	(4)	(5)	(6)	(7)	(8)	(9)	(10)	(11)	(12)	(13)
7⅞	API Regular (with low torque face)	9¼ 9½ 9¾ 10				*73,099 *86,463 91,789 91,789	*73,099 *86,463 87,292 87,292	*73,099 82,457 82,457 82,457	*73,099 77,289 77,289 77,289			
7⅞	H-90[4] (with low torque face)	9¾ 10 10¼ 10½			*91,667 *106,260 117,112 117,112	*91,667 *106,260 113,851 113,851	*91,667 *106,260 109,188 109,188	*91,667 104,171 104,171 104,171	*91,667 98,804 98,804 98,804			
8⅝	API Regular (with low torque face)	10¾ 11 11¼				*112,883 *130,672 147,616	*112,883 *130,672 142,430	*112,883 *130,672 136,846	*112,883 *130,672 130,871			
8⅝	H-90[4] (with low torque face)	10¾ 11 11¼				*92,960 *110,781 *129,203	*92,960 *110,781 *129,203	*92,960 *110,781 *129,203	*92,960 *110,781 *129,203			

*Notes:

1. Torque figures preceded by an asterisk (*) indicate that the weaker member for the corresponding outside diameter (OD) and bore is the BOX; for all other torque values, the weaker member is the PIN.

2. In each connection size and type group, torque values apply to all connection types in the group, when used with the same drill collar outside diameter and bore, i.e. 2³/₈ API IF, API NC 26, and 2⁷/₈ Slim Hole connections used with 3¹/₂x1¹/₄ drill collars all have the same minimum make-up torque of 4600 ft. lb., and the BOX is the weaker member.

3. Stress-relief features are disregarded for make-up torque.

[1]Basis of calculations for recommended make-up torque assumed the use of a thread compound containing 40-60 percent by weight of finely powdered metallic zinc or 60 percent by weight of finely powdered metallic lead, with not more than 0.3 percent total active sulfur (reference the caution regarding the use of hazardous materials in Appendix G of specification 7) applied thoroughly to all threads and shoulders and using the modified Screw Jack formula in A.8, and a unit stress of 62,500 psi in the box or pin, whichever is weaker.

[2]Normal torque range is tabulated value plus 10 percent. Higher torque values may be used under extreme conditions.

[3]Make-up torque for 2⁷/₈ PAC connection is based on 87,500 psi stress and other factors listed in footnote 1.

[4]Make-up torque for H-90 connection is based on 56,200 psi stress and other factors listed in footnote 1.

Table B-3:   API New Drill Pipe Dimensional Data

(1)	(2)	(3)	(4)	(5)	(6)	(7)
Size OD in. D	Nominal Weight Threads and Couplings lb/ft	Plain End Weight[1] lb/ft	Wall Thickness in.	ID in. d	Section Area Body of Pipe[2] sq. in. A	Polar Sectional Modulus[3] cu. in. Z
$2^3/_8$	4.85	4.43	0.190	1.995	1.3042	1.321
	6.65	6.26	0.280	1.815	1.8429	1.733
$2^7/_8$	6.85	6.16	0.217	2.441	1.8120	2.241
	10.40	9.72	0.362	2.151	2.8579	3.204
$3^1/_2$	9.50	8.81	0.254	2.992	2.5902	3.923
	13.30	12.31	0.368	2.764	3.6209	5.144
	15.50	14.63	0.449	2.602	4.3037	5.847
4	11.85	10.46	0.262	3.476	3.0767	5.400
	14.00	12.93	0.330	3.340	3.8048	6.458
	15.70	14.69	0.380	3.240	4.3216	7.157
$4^1/_2$	13.75	12.24	0.271	3.958	3.6004	7.184
	16.60	14.98	0.337	3.826	4.4074	8.543
	20.00	18.69	0.430	3.640	5.4981	10.232
	22.82	21.36	0.500	3.500	6.2832	11.345
5	16.25	14.87	0.296	4.408	4.3743	9.718
	19.50	17.93	0.362	4.276	5.2746	11.415
	25.60	24.03	0.500	4.000	7.0686	14.491
$5^1/_2$	19.20	16.87	0.304	4.892	4.9624	12.221
	21.90	19.81	0.361	4.778	5.8282	14.062
	24.70	22.54	0.415	4.670	6.6296	15.688
$6^5/_8$	25.20	22.19	0.330	5.965	6.5262	19.572
	27.20	24.22	0.362	5.901	7.1227	21.156

[1] lb/ft = 3.3996 x A (col. 6)
[2] $A = 0.7854 \, (D^2 - d^2)$
[3] $Z = 0.19635 \, \dfrac{(D^2 - d^2)}{D}$

Table B-4: API Mechanical Properties of New Tool Joints and New Grade E75 Drill Pipe

(1)	(2)	(3)	(4)	(5)	(6)	(7)	(8)	(9)	(10)	(11)	(12)
										Mechanical Properties	
	Drill Pipe Data			**Tool Joint Data**				**Tensile Yield, lb**		**Torsional Yield, ft-lb**	
Nominal Size In.	Nominal Weight lb/ft	Approx. Weight¹ lb/ft	Type Upset	Conn.	OD in.	ID in.	Drift Diameter² in.	Pipe³	Tool Joint⁴	Pipe⁵	Tool Joint⁶
2 3/8	4.85	5.26	EU	NC26(IF)	3 3/8	1 3/4	1.625	97817.	313681.	4763.	6875.b
		4.95	EU	OH	3 1/8	2	1.807	97817.	206416.	4763.	4521.p
		5.05	EU	SLH90	3 1/4	2	1.850	97817.	202670.	4763.	5129.p
		5.15	EU	WO	3 3/8	2	1.807	97817.	205369.	4763.	4311.p
	6.65	6.99	EU	NC26(IF)	3 3/8	1 3/4	1.625	138214.	313681.	6250.	6875.b
		6.89	EU	OH	3 1/4	1 3/4	1.625	138214.	294620.	6250.	6484.b
		6.71	IU	PAC	2 7/8	1 3/8	1.250	138214.	238504.	6250.	4688.P
		6.78	EU	SLH90	3 1/4	2	1.670	138214.	202850.	6250.	5129.p
2 7/8	6.85	7.50	EU	NC31(IF)	4 1/8	2 1/8	2.000	135902.	447130.	8083.	12053.p
		6.93	EU	OH	3 3/4	2 7/16	2.253	135902.	223937.	8083.	5585.P
		7.05	EU	SLH90	3 7/8	2 7/16	2.296	135902.	260783.	8083.	7628.p
		7.31	EU	WO	4 1/8	2 7/16	2.253	135902.	289264.	8083.	7197.p
	10.40	10.87	EU	NC31(IF)	4 1/8	2 1/8	1.963	214344.	447130.	11554.	12053.p
		10.59	EU	OH	3 7/8	2 5/32	1.963	214344.	345566.	11554.	8814.P
		10.27	IU	PAC	3 1/8	1 1/2	1.375	214344.	272938.	11554.	5730.P
		10.59	EU	SLH90	3 7/8	2 5/32	2.006	214344.	382765.	11554.	11288.p
		11.19	IU	XH	4 1/4	1 7/8	1.750	214344.	505054.	11554.	13282.p
		10.35	IU	NC26(SH)	3 3/8	1 3/4	1.625	214344.	313681.	11554.	6875.B
3 1/2	9.50	10.58	EU	NC38(IF)	4 3/4	2 11/16	2.563	194264.	587308.	14146.	18107.p
		9.84	EU	OH	4 1/2	3	2.804	194264.	392071.	14146.	11870.p
		9.99	EU	SLH90	4 5/8	3	2.847	194264.	366705.	14146.	12650.p
		10.14	EU	WO	4 3/4	3	2.804	194264.	419797.	14146.	12878.p
3 1/2	13.30	14.37	EU	H90	5 1/4	2 3/4	2.619	271569.	664050.	18551.	23847.p
		13.93	EU	NC38(IF)	4 3/4	2 11/16	2.457	271569.	587308.	18551.	18107.p
		13.75	EU	OH	4 3/4	2 11/16	2.414	271569.	559582.	18551.	17305.p
		13.40	IU	NC31(SH)	4 1/4	2 1/8	2.000	271569.	447130.	18551.	11869.P
		13.91	EU	XH	4 3/4	2 7/16	2.313	271569.	570939.	18551.	17493.p
	15.50	16.54	EU	NC38(IF)	5	2 9/16	2.414	322775.	649158.	21086.	20326.p
4	11.85	13.00	IU	H90	5 1/2	2 13/16	2.688	230755.	913708.	19474.	35374.p
		13.52	EU	NC46(IF)	6	3 1/4	3.125	230755.	901164.	19474.	33625.p
		12.10	EU	OH	5 1/4	3 3/32	3.287	230755.	621357.	19474.	21976.p
		12.91	EU	WO	5 1/4	3 7/16	3.313	230755.	782987.	19474.	28809.p
	14.00	15.04	IU	NC40(FH)	5 1/4	2 11/16	2.688	285359.	711611.	23288.	23487.p
		15.43	IU	H90	5 1/2	2 13/16	2.688	285359.	913708.	23288.	35374.p
		15.85	EU	NC46(IF)	6	3 1/4	3.125	285359.	901164.	23288.	33625.p
4	14.00	15.02	EU	OH	5 1/2	3 1/4	3.125	285359.	759875.	23288.	27289.p
		14.35	IU	SH	4 5/8	2 9/16	2.438	285359.	512035.	23288.	15170.P

Table B-4: *(Continued)*

(1)	(2)	(3)	(4)	(5)	(6)	(7)	(8)	(9)	(10)	(11)	(12)
	15.70	16.80	IU	NC40(FH)	$5\frac{1}{4}$	$2\frac{11}{16}$	2.563	324118.	776406.	25810.	25673.p
		17.09	IU	H90	$5\frac{1}{2}$	$2\frac{13}{16}$	2.688	324118.	913708.	25810.	35374.p
		17.54	EU	NC46(IF)	6	$3\frac{1}{4}$	3.095	324118.	901164.	25810.	33625.p
$4\frac{1}{2}$	13.75	15.23	IU	H90	6	$3\frac{1}{4}$	3.125	270034.	938403.	25907.	38925.p
		15.36	EU	NC50(IF)	$6\frac{5}{8}$	$3\frac{3}{4}$	3.625	270034.	939096.	25907.	37676.p
		14.04	EU	OH	$5\frac{3}{4}$	$3\frac{31}{32}$	3.770	270034.	554844.	25907.	20939.p
		14.77	EU	WO	$6\frac{1}{8}$	$3\frac{7}{8}$	3.750	270034.	849266.	25907.	33651.p
	16.60	18.14	IEU	FH	6	3	2.875	330558.	976156.	30807.	34780.p
		17.92	IEU	H90	6	$3\frac{1}{4}$	3.125	330558.	938403.	30807.	38925.p
		17.95	EU	NC50(IF)	$6\frac{3}{8}$	$3\frac{3}{4}$	3.625	330558.	939096.	30807.	37676.p
		17.07	EU	OH	$5\frac{7}{8}$	$3\frac{1}{4}$	3.625	330558.	713979.	30807.	27243.p
		16.79	IEU	NC38(SH)	5	$2\frac{11}{16}$	2.563	330558.	587308.	30807.	18346.P
		18.37	IEU	NC46(XH)	$6\frac{1}{4}$	$3\frac{1}{4}$	3.125	330558.	901164.	30807.	33993.p
	20.00	21.64	IEU	FH	6	3	2.875	412358.	976156.	36901.	34780.p
		21.64	EU	H90	6	3	2.875	412358.	1085665.	36901.	45152.p
		21.59	EU	NC50(IF)	$6\frac{3}{8}$	$3\frac{3}{8}$	3.452	412358.	1025980.	36901.	41235.p
		22.09	IEU	NC46(XH)	$6\frac{1}{4}$	3	2.875	412358.	1048426.	36901.	39659.p
	22.82	24.11	EU	NC50(IF)	$6\frac{5}{8}$	$3\frac{5}{8}$	3.452	471239.	1025980.	40912.	41235.p
		24.56	IEU	NC46(XH)	$6\frac{1}{4}$	3	2.875	471239.	1048426.	40912.	39659.p
5	19.50	22.28	IEU	$5\frac{1}{2}$ FH	7	$3\frac{3}{4}$	3.625	395595.	1448407.	41167.	60338.b
		20.85	IEU	NC50(XH)	$6\frac{5}{8}$	$3\frac{3}{4}$	3.625	395595.	939095.	41167.	37676.p
	25.60	28.27	IEU	$5\frac{1}{2}$ FH	7	$3\frac{1}{2}$	3.375	530144.	1619231.	52257.	60338.b
		26.85	IEU	NC50(XH)	$6\frac{5}{8}$	$3\frac{1}{2}$	3.375	530144.	1109920.	52257.	44673.p
$5\frac{1}{2}$	21.90	23.78	IEU	FH	7	4	3.875	437116.	1265802.	50710.	56045.p
	24.70	26.30	IEU	FH	7	4	3.875	497222.	1265802.	56574.	56045.p
$6\frac{5}{8}$	25.20	27.28	IEU	FH	8	5	4.875	489464.	1447697.	70580.	73620.p
$6\frac{5}{8}$	27.70	29.06	IEU	FH	8	5	4.875	534198.	1447697.	76295.	73620.p

[1]Tool Joint plus drill pipe, for Range 2 steel pipe (see Appendix A for method of calculation).

[2]See Section 4.4.

[3]The tensile yield strength of Grade E drill pipe is based on 75,000 psi minimum yield strength.

[4]The tensile strength of the tool joint pin is based on 120,000 psi minimum yield and the cross sectional area at the root of the thread＿inch from the shoulder.

[5]The torsional yield strength is based on a shear strength of 57.7 percent of the minimum yield strength.

[6]p = pin limited yield; b = box limited yield; P or B indicates that tool joint could not meet 80 percent of tube torsion yield.

Table B-5: API Mechanical Properties of New Tool Joints and New High Strength Drill Pipe

(1)	(2)	(3)	(4)	(5)	(6)	(7)	(8)	(9)	(10)	(11)	(12)
		Drill Pipe Data			Tool Joint Data			Tensile Yield, lb		Torsional Yield, ft-lb	
Nominal Size In.	Nominal Weight lb/ft	Approx. Weight[1] lb/ft	Type Upset	Conn.	OD in.	ID in.	Drift Diameter[2] in.	Pipe[3]	Tool Joint[4]	Pipe[3]	Tool Joint[5]
$2^{3}/_{8}$	6.65	7.11	EU-X95	NC26(IF)	$3^{3}/_{8}$	$1^{3}/_{4}$	1.625	175072.	313681.	7917.	6875.b
		6.99	EU-X95	SLH90	$3^{1}/_{4}$	$1^{13}/_{16}$	1.670	175072.	270223.	7917.	6884.p
	6.65	7.11	EU-G105	NC26(IF)	$3^{3}/_{8}$	$1^{3}/_{4}$	1.625	193500.	313681.	8751.	6875.b
		6.99	EU-G105	SLH90	$3^{1}/_{4}$	$1^{13}/_{16}$	1.670	193500.	270223.	8751.	6884.P
$2^{7}/_{8}$	10.40	11.09	EU-X95	NC31(IF)	$4^{1}/_{8}$	2	1.875	271503.	495726.	14635.	13389.p
		10.95	EU-X95	SLH90	4	2	1.875	271503.	443971.	14635.	13218.p
	10.40	11.09	EU-G105	NC31(IF)	$4^{1}/_{8}$	2	1.875	300082.	495726.	16176.	13389.p
		10.95	EU-G105	SLH90	4	2	1.875	300082.	443971.	16176.	13218.p
	10.40	11.55	EU-S135	NC31(IF)	$4^{3}/_{8}$	$1^{5}/_{8}$	1.500	385820.	623844.	20798.	17170.p
		11.26	EU-S135	SLH90	$4^{1}/_{8}$	$1^{5}/_{8}$	1.500	385820.	572089.	20798.	17213.p
$3^{1}/_{2}$	13.30	14.60	EU-X95	NC38(IF)	$5^{1}/_{4}$	$2^{1}/_{4}$	2.619	343988.	664050.	23498.	23833.p
		14.62	EU-X95	NC38(IF)	5	$2^{9}/_{16}$	2.438	343988.	649158.	23498.	20326.p
		14.06	EU-X95	SLH90	$4^{3}/_{4}$	$2^{9}/_{16}$	2.438	343988.	596066.	23498.	20879.p
	13.30	14.71	EU-G105	NC38(IF)	5	$2^{7}/_{16}$	2.313	380197.	708063.	25972.	22213.p
		14.06	EU-G105	SLH90	$4^{3}/_{4}$	$2^{7}/_{16}$	2.438	380197.	596066.	25972.	20879.p
	13.30	14.92	EU-S135	NC38(IF)	5	$2^{1}/_{8}$	2.000	488825.	842440.	33392.	26515.P
		14.65	EU-S135	SLH90	5	$2^{1}/_{8}$	2.000	488825.	789348.	33392.	28078.p
		15.13	EU-S135	NC40(4FH)	$5^{3}/_{8}$	$2^{7}/_{16}$	2.313	488825.	897161.	33392.	29930.p
	15.50	16.82	EU-X95	NC38(IF)	5	$2^{7}/_{16}$	2.313	408848.	708063.	26708.	22213.p
	15.50	17.03	EU-G105	NC38(IF)	5	$2^{1}/_{8}$	2.000	451885.	842440.	29520.	26515.p
		16.97	EU-G105	NC40(4FH)	$5^{1}/_{4}$	$2^{9}/_{16}$	2.438	451885.	838257.	29520.	27760.p
	15.50	17.57	EU-S135	NC40(4FH)	$5^{1}/_{2}$	$2^{1}/_{4}$	2.125	580995.	979996.	37954.	32943.p
4	14.00	15.34	IU-X95	NC40(FH)	$5^{1}/_{4}$	$2^{11}/_{16}$	2.563	361454.	776406.	29498.	25673.p
		15.63	IU-X95	H90	$5^{1}/_{2}$	$2^{13}/_{16}$	2.688	361454.	913708.	29498.	35374.p
		16.19	EU-X95	NC46(IF)	6	$3^{1}/_{4}$	3.125	361454.	901164.	29498.	33625.p
	14.00	15.91	IU-G105	NC40(FH)	$5^{1}/_{2}$	$2^{7}/_{16}$	2.313	399502.	897161.	32603.	30114.p
		15.63	IU-G105	H90	$5^{1}/_{2}$	$2^{13}/_{16}$	2.688	399502.	913708.	32603.	35374.p
		16.19	EU-G105	NC46(IF)	6	$3^{1}/_{4}$	3.125	399502.	901164.	32603.	33625.p
	14.00	16.19	IU-S135	NC40(FH)	$5^{1}/_{2}$	2	1.875	513646.	1080135.	41918.	36363.p
		15.63	IU-S135	H90	$5^{1}/_{2}$	$2^{13}/_{16}$	2.688	513646.	913708.	41918.	35374.p
		16.42	EU-S135	NC46(IF)	6	3	2.875	513646.	1048426.	41918.	39229.p

Table B-5: *(Continued)*

(1)	(2)	(3)	(4)	(5)	(6)	(7)	(8)	(9)	(10)	(11)	(12)
	15.70	17.52	IU-X95	NC40(FH)	5 1/2	2 13/16	2.313	410550.	897161.	32692.	30114.p
		17.23	IU-X95	H90	5 1/2	2 13/16	2.688	410550.	913708.	32692.	35374.p
		17.80	EU-X95	NC46(IF)	6	3 1/4	3.125	410550.	901164.	32692.	33625.p
	15.70	17.52	IU-G105	NC40(FH)	5 1/2	2 13/16	2.313	453765.	897161.	36134.	30114.p
		17.23	IU-G105	H90	5 1/2	2 13/16	2.688	453765.	913708.	36134.	35374.p
		17.80	EU-G105	NC46(IF)	6	3 1/4	3.125	453765.	901164.	36134.	33625.p
	15.70	18.02	EU-S135	NC46(IF)	6	3	2.875	583413.	1048426.	46458.	39229.p
4 1/2	16.60	18.33	IEU-X95	FH	6	3	2.875	418707.	976156.	39022.	34780.p
		18.11	IEU-X95	H90	6	3 1/4	3.125	418707.	938403.	39022.	38925.p
		18.36	EU-X95	NC50(IF)	6 5/8	3 3/4	3.625	418707.	939095.	39022.	37676.p
		18.79	IEU-X95	Nc46(XH)	6 1/4	3	2.875	418707.	1048426.	39022.	39659.p
4 1/2	16.60	18.33	IEU-G105	FH	6	3	2.625	462781.	976156.	43130.	34780.p
		18.33	IEU-G105	H90	6	3	3.125	462781.	1085665.	43130.	45152.p
		18.36	EU-G105	NC50(IF)	6 5/8	3 3/4	3.625	462781.	939095.	43130.	37676.p
		18.79	IEU-G105	NC46(XH)	6 1/4	3	2.875	462781.	1048426.	43130.	39659.p
	16.60	19.19	IEU-S135	FH	6 1/4	2 1/2	2.375	595004.	1235337.	55453.	44769.p
4 1/2	16.60	18.33	IEU-S135	H90	6	3	2.875	595004.	1085665.	55453.	45152.p
		18.62	EU-S135	NC50(IF)	6 5/8	3 1/2	3.375	595004.	1109920.	55453.	44673.p
		19.00	IEU-S135	NC46(XH)	6 1/4	2 3/4	2.625	595004.	1183908.	55453.	44871.p
	20.00	22.39	IEU-X95	FH	6	2 1/2	2.375	522320.	1235337.	46741.	44265.p
		21.78	IEU-X95	H90	6	3 1/4	3.125	522320.	938403.	46741.	38925.p
		22.08	EU-X95	NC50(IF)	6 5/8	3 1/2	3.375	522320.	1109920.	46741.	44673.p
		22.67	IEU-X95	NC46(XH)	6 1/4	2 3/4	2.625	522320.	1183908.	46741.	44871.p
	20.00	22.39	IEU-G105	FH	6	2 1/2	2.375	577301.	1235337.	51661.	44265.p
		22.00	IEU-G105	H90	6	3	2.875	577301.	1085665.	51661.	45152.p
		22.08	EU-G105	NC50(IF)	6 5/8	3 1/4	3.375	577301.	1109920.	51661.	44673.p
		22.86	IEU-G105	NC46(XH)	6 1/4	2 1/2	2.375	577301.	1307608.	51661.	49630.p
	20.00	23.03	EU-S135	NC50(IF)	6 5/8	3	2.875	742244.	1416225.	66421.	57800.p
		23.03	IEU-S135	NC46(XH)	6 1/4	2 1/4	2.125	742244.	1419527.	66421.	53936.p
	22.82	25.13	EU-X95	FH	6 1/4	2 1/4	2.125	596903.	1347256.	51821.	48912.p
		24.24	EU-X95	NC50(IF)	6 5/8	3 1/2	3.375	596903.	1109920.	51821.	44673.p
		24.77	IEU-X95	NC46(XH)	6 5/8	2 3/4	2.625	596903.	1183908.	51821.	44871.p
	22.82	24.72	EU-G105	NC50(IF)	6 5/8	3 1/4	3.125	659735.	1268963.	57276.	51447.p
		24.96	IEU-G105	NC46(XH)	6 1/4	2 1/2	2.375	659735.	1307608.	57276.	46930.p
	22.82	25.41	EU-S135	NC50(IF)	6 5/8	2 1/4	2.625	848230.	1551706.	73641.	63406.p
5	19.50	22.62	IEU-X95	5_FH	7	3 3/4	3.625	501087.	1448407.	52144.	60338.b
		21.93	IEU-X95	H90	6 1/2	3 1/4	3.125	501087.	1176265.	52144.	51807.p
		21.45	IEU-X95	NC50(XH)	6 5/8	3 1/2	3.375	501087.	1109920.	52144.	44673.p

Table B-5: *(Continued)*

(1)	(2)	(3)	(4)	(5)	(6)	(7)	(8)	(9)	(10)	(11)	(12)
	19.50	22.62	IEU-G105	5_FH	7	3¾	3.625	553833.	1448407.	57633.	60338.b
		22.15	IEU-G105	H90	6½	3	2.875	553833.	1323527.	57633.	58398.p
		21.93	IEU-G105	NC50(XH)	6⅝	3¼	3.125	553833.	1268963.	57633.	51447.p
	19.50	23.48	IEU-S135	5_FH	7¼	3½	3.375	712070.	1619231.	74100.	72627.p
		22.61	IEU-S135	NC50(XH)	6⅝	2¾	2.625	712070.	1551706.	74100.	63406.p
	25.60	28.59	IEU-X95	5_FH	7	3½	3.375	671515.	1619231.	66192.	60338.b
		27.87	IEU-X95	NC50(XH)	6⅝	3	2.875	671515.	1416225.	66192.	56984.b
	25.60	29.16	IEU-G105	5_FH	7¼	3½	3.375	742201.	1619231.	73159.	72627.p
		28.32	IEU-G105	NC50(XH)	6⅝	2¾	2.625	742201.	1551706.	73159.	63406.b
	25.60	29.43	IEU-S135	5_FH	7¼	3¼	3.125	954259.	1778274.	94062.	76156.b
5½	21.90	24.53	IEU-X95	FH	7	3¾	3.625	553681.	1448407.	64233.	60338.b
		24.80	IEU-X95	H90	7	3½	3.125	553681.	1268877.	64233.	59091.p
	21.90	25.38	IEU-G105	FH	7¼	3½	3.375	611963.	1619231.	70994.	72627.p
	21.90	26.50	IEU-S135	FH	7½	3	2.875	786809.	1925536.	91278.	87341.p
	24.70	27.85	IEU-X95	FH	7¼	3½	3.375	629814.	1619231.	71660.	72627.p
5½	24.70	27.85	IEU-G105	FH	7¼	3½	3.375	696111.	1619231.	79204.	72627.p
	24.70	27.77	IEU-S135	FH	7½	3	2.875	894999.	1925536.	101833.	87341.p
6⅝	25.20	27.15	IEU-X95	FH	8	5	4.875	619988.	1448416.	89402.	73661.p
	25.20	28.20	IEU-G105	FH	8¼	4¾	4.625	685250.	1678145.	98812.	86237.p
	25.20	29.63	IEU-S135	FH	8½	4¼	4.125	881035.	2102260.	127044.	109226.p
	27.70	30.11	IEU-X95	FH	8¼	4¾	4.625	676651.	1678145.	96640.	86237.p
	27.70	30.11	IEU-G105	FH	8¼	4¾	4.625	747250.	1678145.	106813.	86237.p
	27.70	31.54	IEU-S135	FH	8½	4¼	4.125	961556.	2102260.	137330.	109226.P

[1] Tool Joint plus drill pipe, for Range 2 steel pipe (See Appendix A for method of calculation).

[2] See Section 4.4.

[3] The torsional yield strength is based on a shear strength of 5737 percent of the minimum yield strength.

[4] The tensile strength of the tool joint pin is based on 120,000 psi yield and the cross sectional area at the root of the thread _ inch from the shoulder.

[6] p = pin limited yield; b = box limited yield; P or B indicates that tool joint could not meet 80 percent of tube torsion yield.

Table B-6:   API Rotary Shouldered Connection Interchange List

Common Name		Pin Base Diameter (Tapered)	Threads per in.	Taper In/ft	Thread Form[1]	Same as or Interchanges With
Style	Size					
Internal Flush (I.F.)	2³/₈"	2.876	4	2	V-0.065 (V-0.038 rad)	2⁷/₈" Slim Hole N.C. 26[2]
	2⁷/₈"	3.391	4	2	V-0.065 (V-0.038 rad)	3¹/₂" Slim Hole N.C. 31[2]
	3¹/₂"	4.016	4	2	V-0.065 (V-0.038 rad)	4¹/₂" Slim Hole N.C. 38[2]
	4"	4.834	4	2	V-0.065 (V-0.038 rad)	4¹/₂" Extra Hole N.C. 46[2]
	4¹/₂"	5.250	4	2	V-0.065 (V-0.038 rad)	5" Extra Hole N.C. 50[2] 5¹/₂" Double Streamline
Full Hole (F/H.)	4"	4.280	4	2	V-0.065 (V-0.038 rad)	4¹/₂" Double Streamline N.C. 40[2]
Extra Hole (X.H.) (E.H.)	2⁷/₈"	3.327	4	2	V-0.065 (V-0.038 rad)	3¹/₂" Double Streamline
	3¹/₂"	3.812	4	2	V-0.065 (V-0.038 rad)	4" Slim Hole 4¹/₂" External Flush
	4¹/₂"	4.834	4	2	V-0.065 (V-0.038 rad)	4" Internal Flush N.C. 46[2]
	5"	5.250	4	2	V-0.065 (V-0.038 rad)	4¹/₂" Internal Flush N.C. 50[2] 5¹/₂" Double Streamline
Slim Hole (S.H.)	2⁷/₈"	2.876	4	2	V-0.065 (V-0.038 rad)	2³/₈" Internal Flush N.C. 26[2]
	3¹/₂"	3.391	4	2	V-0.065 (V-0.038 rad)	2⁷/₈" Internal Flush N.C. 31[2]
	4"	3.812	4	2	V-0.065 (V-0.038 rad)	3¹/₂" Extra Hole 4¹/₂" External Flush
	4¹/₂"	4.016	4	2	V-0.065 (V-0.038 rad)	3¹/₂" Internal Flush N.C. 38[2]
Double Streamline (DSL)	3¹/₂"	3.327	4	2	V-0.065 (V-0.038 rad)	2⁷/₈" Extra Hole
	4¹/₂"	4.280	4	2	V-0.065 (V-0.038 rad)	4" Full Hole N.C. 40[2]
	5¹/₂"	5.250	4	2	V-0.065 (V-0.038 rad)	4¹/₂" Internal Flush 5" Extra Hole N.C. 50[2]
Numbered Connection (N.C.)	26	2.876	4	2	V-0.038 rad	2³/₈" Internal Flush 2⁷/₈" Slim Hole
	31	3.391	4	2	V-0.038 rad	2⁷/₈" Internal Flush 3¹/₂" Slim Hole
	38	4.016	4	2	V-0.038 rad	3¹/₂" Internal Flush 4¹/₂" Slim Hole
	40	4.280	4	2	V-0.038 rad	4" Full Hole 4¹/₂" Double Streamline
	46	4.834	4	2	V-0.038 rad	4" Internal Flush 4¹/₂" Extra Hole
	50	5.250	4	2	V-0.038 rad	4¹/₂" Internal Flush 5"Extra Hole
External Flush (E.F.)	4¹/₂"	3.812	4	2	V-0.065 (V-0.038 rad)	4" Slim Hole 3¹/₂" Extra Hole

[1]Connections with two thread forms shown may be machined with either thread form without affecting gauging or interchangeability.

[2]Numbered connections (N.C.) may be machined only with the V-0.038 radius thread form.

This page intentionally left blank.

Casing Properties

This appendix gives the basic geometric and mechanical properties of API steel casing, water well steel casing, stainless steel well casing and other non-metal well casing.

C.1 Steel Well Casing

Table C-1 gives the dimensions, weight per unit length and mechanical properties for API casing. Table C-2 gives the dimensions, weight per unit length and mechanical properties for water well steel casing. Table C-3 gives the dimensions, weight per unit length and mechanical properties for stainless steel well casing.

C.2 Non-Metal Well Casing

Table C-4 gives the dimensions, weight per unit length and mechanical properties for PVC well casing. Table C-5 gives the dimensions, weight per unit length and mechanical properties for ABS well casing. Table C-6 gives the dimensions, weight per unit length and mechanical properties for SR well casing.

Table C-1:   API Minimum Performance Properties of Casing

1	2	3	4	5	6	7	8	9	10
						Threaded and Coupled			
Size Outside Diameter in.	Nominal Weight. Threads And Coupling lb. per ft.	Grade	Wall Thickness	Inside Diameter	Drift Diameter	Outside Diameter of Coupling	Outside Diameter Special Clearance Coupling	Collapse Resistance	Pipe Body Yield Strength
D			in. t	in. d	in.	in. W.	in. W.	psi.	1000 lbs.
$4^1/_2$	9.50	H-40	0.205	4.090	3.965	5.000	—	2,760	111
	9.50	J-55	0.205	4.090	3.965	5.000	—	3,310	152
	10.50	J-55	0.224	4.052	3.927	5.000	4.875	4,010	165
	11.60	J-55	0.250	4.000	3.875	5.000	4.875	4,960	184
	9.50	K-55	0.205	4.090	3.965	5.000	—	3,310	152
	10.50	K-55	0.224	4.052	3.927	5.000	4.875	4,010	165
	11.60	K-55	0.250	4.000	3.875	5.000	4.875	4,960	184
	11.60	C-75	0.250	4.000	3.875	5.000	4.875	6,100	250
	13.50	C-75	0.290	3.920	3.795	5.000	4.875	8,140	288
	11.60	L-80	0.250	4.000	3.875	5.000	4.875	6,350	267
	13.50	L-80	0.290	3.920	3.795	5.000	4.875	8,540	307
	11.60	N-80	0.250	4.000	3.875	5.000	4.875	6,350	267
	13.50	N-80	0.290	3.920	3.795	5.000	4.875	8,540	307
	11.60	C-90	0.250	4.000	3.875	5.000	4.875	6,820	300
	13.50	C-90	0.290	3.920	3.795	5.000	4.875	9,300	345
	11.60	C-95	0.250	4.000	3.875	5.000	4.875	7,030	317
	13.50	C-95	0.290	3.920	3.795	5.000	4.875	9,660	364
	11.60	P-110	0.250	4.000	3.875	5.000	4.875	7,580	367
	13.50	P-110	0.290	3.920	3.795	5.000	4.875	10,680	422
	15.10	P-110	0.337	3.826	3.701	5.000	4.875	14,350	485
	15.10	Q125	0.337	3.826	3.701	5.000	—	15,840	551
5	11.50	J-55	0.220	4.560	4.435	5.563	—	3,060	182
	13.00	J-55	0.253	4.494	4.369	5.563	5.375	4,140	208
	15.00	J-55	0.296	4.408	4.283	5.563	5.375	5,560	241
	11.50	K-55	0.220	4.560	4.435	5.563	—	3,060	182
	13.00	K-55	0.253	4.494	4.369	5.563	5.375	4,140	208
	15.00	K-55	0.296	4.408	4.283	5.563	5.375	5,560	241
	15.00	C-75	0.296	4.408	4.283	5.563	5.375	6,940	328
	18.00	C-75	0.362	4.276	4.151	5.563	5.375	9,960	396
	21.40	C-75	0.437	4.126	4.001	5.563	5.375	11,970	470
	23.20	C-75	0.478	4.044	3.919	5.563	5.375	12,970	509
	24.10	C-75	0.500	4.000	3.875	5.563	5.375	13,500	530
	15.00	L-80	0.296	4.408	4.283	5.563	5.375	7,250	350
	18.00	L-80	0.362	4.276	4.151	5.563	5.375	10,500	422
	21.40	L-80	0.437	4.126	4.001	5.563	5.375	12,760	501
	23.20	L-80	0.478	4.044	3.919	5.563	5.375	13,830	543
	24.10	L-80	0.500	4.000	3.875	5.563	5.375	14,400	566
	15.00	N-80	0.296	4.408	4.283	5.563	5.375	7,250	350
	18.00	N-80	0.362	4.276	4.151	5.563	5.375	10,500	422
	21.40	N-80	0.437	4.126	4.001	5.563	5.375	12,760	501
	23.20	N-80	0.478	4.044	3.919	5.563	5.375	13,830	543
	24.10	N-80	0.500	4.000	3.875	5.563	5.375	14,400	566

Table C-1:   *(Continued)*

1	2	3	4	5	6	7	8	9	10
	15.00	C-90	0.296	4.408	4.283	5.563	5.375	7,840	394
	18.00	C-90	0.362	4.276	4.151	5.563	5.375	11,530	475
	21.40	C-90	0.437	4.126	4.001	5.563	5.375	14,360	564
	23.20	C-90	0.478	4.044	3.919	5.563	5.375	15,560	611
	24.10	C-90	0.500	4.000	3.875	5.563	5.375	16,200	636
	15.00	C-95	0.296	4.408	4.283	5.563	5.375	8,110	416
	18.00	C-95	0.362	4.276	4.151	5.563	5.375	12,030	501
	21.40	C-95	0.437	4.126	4.001	5.563	5.375	15,160	595
	23.20	C-95	0.478	4.044	3.919	5.563	5.375	16,430	645
	24.10	C-95	0.500	4.000	3.875	5.563	5.375	17,100	672
	15.00	P-110	0.296	4.408	4.283	5.563	5.375	8,850	481
	18.00	P-110	0.362	4.276	4.151	5.563	5.375	13,470	580
	21.40	P-110	0.437	4.126	4.001	5.563	5.375	17,550	689
	23.20	P-110	0.478	4.044	3.919	5.563	5.375	19,020	747
	24.10	P-110	0.500	4.000	3.875	5.563	5.375	19,800	778
	18.00	Q-125	0.362	4.276	4.151	5.563	—	14,830	659
	21.40	Q-125	0.437	4.126	4.001	5.563	—	19,940	783
	23.20	Q-125	0.478	4.044	3.919	5.563	—	21,620	849
	24.10	Q-125	0.500	4.000	3.875	5.563	—	22,500	884
$5^1/_2$	14.00	H-40	0.244	5.012	4.887	6.050	—	2,620	161
	14.00	J-55	0.244	5.012	4.887	6.050	—	3,120	222
	15.50	J-55	0.275	4.950	4.825	6.050	5.875	4,040	248
	17.00	J-55	0.304	4.892	4.767	6.050	5.875	4,910	273
	14.00	K-55	0.244	5.012	4.887	6.050	—	3,120	222
	15.50	K-55	0.275	4.950	4.825	6.050	5.875	4,040	248
	17.00	K-55	0.304	4.892	4.767	6.050	5.875	4,910	273
	17.00	C-75	0.304	4.892	4.767	6.050	5.875	6,040	372
	20.00	C-75	0.361	4.778	4.653	6.050	5.875	8,410	437
	23.00	C-75	0.415	4.670	4.545	6.050	5.875	10,470	497
	17.00	L-80	0.304	4.892	4.767	6.050	5.875	6,280	397
	20.00	L-80	0.361	4.778	4.653	6.050	5.875	8,830	466
	23.00	L-80	0.415	4.670	4.545	6.050	5.875	11,160	530
	17.00	N-80	0.304	4.892	4.767	6.050	5.875	6,280	397
	20.00	N-80	0.361	4.778	4.653	6.050	5.875	8,830	466
	23.00	N-80	4.415	4.670	4.545	6.050	5.875	11,160	530
	17.00	C-90	0.304	4.892	4.767	6.050	5.875	6,740	447
	20.00	C-90	0.361	4.778	4.653	6.050	5.875	9,630	525
	23.00	C-90	0.415	4.670	4.545	6.050	5.875	12,380	597
	26.00	C-90	0.476	4.548	4.423	6.050	5.875	14,240	676
	35.00	C-90	0.650	4.200	4.075	6.050	5.875	18,760	891
	17.00	C-95	0.304	4.892	4.767	6.050	5.875	6,940	471
	20.00	C-95	0.361	4.778	4.653	6.050	5.875	10,010	554
	23.00	C-95	0.415	4.670	4.545	6.050	5.875	12,940	630
	17.00	P-110	0.304	4.892	4.767	6.050	5.875	7,480	546
	20.00	P-110	0.361	4.778	4.653	6.050	5.875	11,100	641
	23.00	P-110	0.415	4.670	4.545	6.050	5.875	14,540	729
	23.00	Q-125	0.415	4.670	4.545	6.050	—	16,070	829
$6^5/_8$	20.00	H-40	0.288	6.049	5.924	7.390	—	2,520	229
	20.00	J-55	0.288	6.049	5.924	7.390	7.000	2,970	315
	24.00	J-55	0.352	5.921	5.796	7.390	7.000	4,560	382
	20.00	K-55	0.288	6.049	5.924	7.390	7.000	2,970	315
	24.00	K-55	0.352	5.921	5.796	7.390	7.000	4,560	382
	24.00	C-75	0.352	5.921	5.796	7.390	7.000	5,550	520
	28.00	C-75	0.417	5.791	5.666	7.390	7.000	7,790	610
	32.00	C-75	0.475	5.675	5.550	7.390	7.000	9,800	688

Table C-1: *(Continued)*

1	2	3	4	5	6	7	8	9	10
	24.00	L-80	0.352	5.921	5.796	7.390	7.000	5,760	555
	28.00	L-80	0.417	5.791	5.666	7.390	7.000	8,170	651
	32.00	L-80	0.475	5.675	5.550	7.390	7.000	10,320	734
	24.00	N-80	0.352	5.921	5.796	7.390	7.000	5,760	555
	28.00	N-80	0.417	5.791	5.666	7.390	7.000	8,170	651
	32.00	N-80	0.475	5.675	5.550	7.390	7.000	10,320	734
	24.00	C-90	0.352	5.921	5.796	7.390	7.000	6,140	624
	28.00	C-90	0.417	5.791	5.666	7.390	7.000	8,880	732
	32.00	C-90	0.475	5.675	5.550	7.390	7.000	11,330	826
	24.00	C-95	0.352	5.921	5.796	7.390	7.000	6,310	659
	28.00	C-95	0.417	5.791	5.666	7.390	7.000	9,220	773
	32.00	C-95	0.475	5.675	5.550	7.390	7.000	11,810	872
	24.00	P-110	0.352	5.921	5.796	7.390	7.000	6,730	763
	28.00	P-110	0.417	5.791	5.666	7.390	7.000	10,160	598
	32.00	P-110	0.475	5.675	5.550	7.390	7.000	13,220	1,009
	32.00	Q125	0.475	5.675	5.550	7.390	—	14,530	1,147
7	17.00	H-40	0.231	6.538	6.413	7.656	—	1,420	196
	20.00	H-40	0.272	6.456	6.331	7.656	—	1,970	230
	20.00	J-55	0.272	6.456	6.331	7.656	—	2,270	316
	23.00	J-55	0.317	6.366	6.241	7.656	7.375	3,270	366
	26.00	J-55	0.362	6.276	6.151	7.656	7.375	4,320	415
	20.00	K-55	0.272	6.456	6.331	7.656	—	2,270	316
	23.00	K-55	0.317	6.366	6.241	7.656	7.375	3,270	366
	26.00	K-55	0.362	6.276	6.151	7.656	7.375	4,320	415
	23.00	C-75	0.317	6.366	6.241	7.656	7.375	3,750	499
	26.00	C-75	0.362	6.276	6.151	7.656	7.375	5,220	566
	29.00	C-75	0.408	6.184	6.059	7.656	7.375	6,730	634
	32.00	C-75	0.453	6.094	5.969	7.656	7.375	8,200	699
	35.00	C-75	0.498	6.004	5.879	7.656	7.375	9,670	763
	38.00	C-75	0.540	5.920	5.795	7.656	7.375	10,680	822
	23.00	L-80	0.317	6.366	6.241	7.656	7.375	3,830	532
	26.00	L-80	0.362	6.276	6.151	7.656	7.375	5,410	604
	29.00	L-80	0.408	6.184	6.059	7.656	7.375	7,020	676
	32.00	L-80	0.453	6.094	5.969	7.656	7.375	8,610	745
	35.00	L-80	0.498	6.004	5.879	7.656	7.375	10,180	814
	38.00	L-80	0.540	5.920	5.795	7.656	7.375	11,390	877
	23.00	N-80	0.317	6.366	6.241	7.656	7.375	3,830	532
	26.00	N-80	0.362	6.276	6.151	7.656	7.375	5,410	604
	29.00	N-80	0.408	6.184	6.059	7.656	7.375	7,020	676
	32.00	N-80	0.453	6.094	5.969	7.656	7.375	8,610	745
	35.00	N-80	0.498	6.004	5.879	7.656	7.375	10,180	814
	38.00	N-80	0.540	5.920	5.795	7.656	7.375	11,390	877
	23.00	C-90	0.317	6.366	6.241	7.656	7.375	4,030	599
	26.00	C-90	0.362	6.276	6.151	7.656	7.375	5,740	679
	29.00	C-90	0.408	6.184	6.059	7.656	7.375	7,580	760
	32.00	C-90	0.453	6.094	5.969	7.656	7.375	9,380	839
	35.00	C-90	0.498	6.004	5.879	7.656	7.375	11,170	915
	38.00	C-90	0.540	5.920	5.795	7.656	7.375	12,820	986
	23.00	C-95	0.317	6.366	6.241	7.656	7.375	4,140	632
	26.00	C-95	0.362	6.276	6.151	7.656	7.375	5,880	717
	29.00	C-95	0.408	6.184	6.059	7.656	7.375	7,830	803
	32.00	C-95	0.453	6.094	5.969	7.656	7.375	9,750	885
	35.00	C-95	0.498	6.004	5.879	7.656	7.375	11,650	966
	38.00	C-95	0.540	5.920	5.795	7.656	7.375	13,440	1,041

Table C-1:   *(Continued)*

1	2	3	4	5	6	7	8	9	10
	26.00	P-110	0.362	6.276	6.151	7.656	7.375	6,230	830
	29.00	P-110	0.408	6.184	6.059	7.656	7.375	8,530	929
	32.00	P-110	0.453	6.094	5.969	7.656	7.375	10,780	1,025
	35.00	P-110	0.498	6.004	5.879	7.656	7.375	13,020	1,119
	38.00	P-110	0.540	5.920	5.795	7.656	7.375	15,140	1,205
	35.00	Q125	0.498	6.004	5.879	7.656	—	14,310	1,272
	38.00	Q125	0.540	5.920	5.795	7.656	—	16,750	1,370
7⅝	24.00	H-40	0.300	7.025	6.900	8.500	—	2,030	276
	26.40	J-55	0.328	6.969	6.844	8.500	8.125	2,890	414
	26.40	K-55	0.328	6.969	6.844	8.500	8.125	2,890	414
	26.40	C-75	0.328	6.969	6.844	8.500	8.125	3,280	564
	29.70	C-75	0.375	6.875	6.750	8.500	8.125	4,650	641
	33.70	C-75	0.430	6.765	6.640	8.500	8.125	6,300	729
	39.00	C-75	0.500	6.625	6.500	8.500	8.125	8,400	839
	42.80	C-75	0.562	6.501	6.376	8.500	8.125	10,240	935
	45.30	C-75	0.595	6.435	6.310	8.500	8.125	10,790	986
	47.10	C-75	0.625	6.375	6.250	8.500	8.125	11,290	1,031
7⅝	26.40	L-80	0.328	6.969	6.844	8.500	8.125	3,400	602
	29.70	L-80	0.375	6.875	6.750	8.500	8.125	4,790	683
	33.70	L-80	0.430	6.765	6.640	8.500	8.125	6,560	778
	39.00	L-80	0.500	6.625	6.500	8.500	8.125	8,820	895
	42.80	L-80	0.562	6.501	6.376	8.500	8.125	10,810	998
	45.30	L-80	0.595	6.435	6.310	8.500	8.125	11,510	1,051
	47.10	L-80	0.625	6.375	6.250	8.500	8.125	12,040	1,100
	26.40	N-80	0.328	6.969	6.844	8.500	8.125	3,400	602
	29.70	N-80	0.375	6.875	6.750	8.500	8.125	4,790	683
	33.70	N-80	0.430	6.765	6.640	8.500	8.125	6,560	778
	39.00	N-80	0.500	6.625	6.500	8.500	8.125	8,820	895
	42.80	N-80	0.562	6.501	6.376	8.500	8.125	10,810	998
	45.30	N-80	0.595	6.435	6.310	8.500	8.125	11,510	1,051
	47.10	N-80	0.625	6.375	6.250	8.500	8.125	12,040	1,100
	26.40	C-90	0.328	6.969	6.844	8.500	8.125	3,610	677
	29.70	C-90	0.375	6.875	6.750	8.500	8.125	5,040	769
	33.70	C-90	0.430	6.765	6.640	8.500	8.125	7,050	875
	39.00	C-90	0.500	6.625	6.500	8.500	8.125	9,620	1,007
	42.80	C-90	0.562	6.501	6.376	8.500	8.125	11,890	1,122
	45.30	C-90	0.595	6.435	6.310	8.500	8.125	12,950	1,183
	47.10	C-90	0.625	6.375	6.250	8.500	8.125	13,540	1,237
	26.40	C-95	0.328	6.969	6.844	8.500	8.125	3,710	714
	29.70	C-95	0.375	6.875	6.750	8.500	8.125	5,140	811
	33.70	C-95	0.430	6.765	6.640	8.500	8.125	7,280	923
	39.00	C-95	0.500	6.625	6.500	8.500	8.125	10,000	1,063
	42.80	C-95	0.562	6.501	6.376	8.500	8.125	12,410	1,185
	45.30	C-95	0.595	6.435	6.310	8.500	8.125	13,660	1,248
	47.10	C-95	0.625	6.375	6.250	8.500	8.125	14,300	1,306
	29.70	P-110	0.375	6.875	6.750	8.500	8.125	5,350	940
	33.70	P-110	0.430	6.765	6.640	8.500	8.125	7,870	1,069
	39.00	P-110	0.500	6.625	6.500	8.500	8.125	11,080	1,231
	42.80	P-110	0.562	6.501	6.376	8.500	8.125	13,920	1,372
	45.30	P-110	0.595	6.435	6.310	8.500	8.125	15,430	1,446
	47.10	P-110	0.625	6.375	6.250	8.500	8.125	16,550	1,512
	39.00	Q125	0.500	6.625	6.500	8.500	—	12,060	1,399
	42.80	Q125	0.562	6.501	6.376	8.500	—	15,350	1,559
	45.30	Q125	0.595	6.435	6.310	8.500	—	17,090	1,643
	47.10	Q125	0.625	6.375	6.250	8.500	—	18,700	1,718

Table C-1:   *(Continued)*

1	2	3	4	5	6	7	8	9	10
8⅝	28.00	H-40	0.304	8.017	7.892	9.625	—	1,610	318
	32.00	H-40	0.352	7.921	7.796	9.625	—	2,200	366
	24.00	J-55	0.265	8.097	7.972	9.625	—	1,370	381
	32.00	J-55	0.352	7.921	7.796	9.625	9.125	2,530	503
	36.00	J-55	0.400	7.825	7.700	9.625	9.125	3,450	568
	24.00	K-55	0.264	8.097	7.972	9.625	—	1,370	381
	32.00	K-55	0.352	7.921	7.796	9.625	9.125	2,530	503
	36.00	K-55	0.400	7.825	7.700	9.625	9.125	3,450	568
	36.00	C-75	0.400	7.825	7.700	9.625	9.125	4,000	775
	40.00	C-75	0.450	7.725	7.600	9.625	9.125	5,330	867
	44.00	C-75	0.500	7.625	7.500	9.625	9.125	6,660	957
	49.00	C-75	0.557	7.511	7.386	9.625	9.125	8,180	1,059
	36.00	L-80	0.400	7.825	7.700	9.625	9.125	4,100	827
	40.00	L-80	0.450	7.725	7.600	9.625	9.125	5,520	925
	44.00	L-80	0.500	7.625	7.500	9.625	9.125	6,950	1,021
	49.00	L-80	0.557	7.511	7.386	9.625	9.125	8,580	1,129
	36.00	N-80	0.400	7.825	7.700	9.625	9.125	4,100	827
	40.00	N-80	0.450	7.725	7.600	9.625	9.125	5,520	925
	44.00	N-80	0.500	7.625	7.500	9.625	9.125	6,950	1,021
	49.00	N-80	0.557	7.511	7.386	9.625	9.125	8,580	1,129
	36.00	C-90	0.400	7.825	7.700	9.625	9.125	4,250	930
	40.00	C-90	0.450	7.725	7.600	9.625	9.125	5,870	1,040
	44.00	C-90	0.500	7.625	7.500	9.625	9.125	7,490	1,149
	49.00	C-90	0.557	7.511	7.386	9.625	9.125	9,340	1,271
	36.00	C-95	0.400	7.825	7.700	9.625	9.125	4,350	982
	40.00	C-95	0.450	7.725	7.600	9.625	9.125	6,020	1,098
	44.00	C-95	0.500	7.625	7.500	9.625	9.125	7,740	1,212
	49.00	C-95	0.557	7.511	7.386	9.625	9.125	9,710	1,341
	40.00	P-110	0.450	7.725	7.600	9.625	9.125	6,390	1,271
	44.00	P-110	0.500	7.625	7.500	9.625	9.125	8,420	1,404
	49.00	P-110	0.557	7.511	7.386	9.625	9.125	10,740	1,553
	49.00	Q125	0.557	7.511	7.386	9.625	—	11,660	1,765
9⅝	32.30	H-40	0.312	9.001	8.845	10.625	—	1,370	365
	36.00	H-40	0.352	8.921	8.765	10.625	—	1,720	410
	36.00	J-55	0.352	8.921	8.765	10.625	10.125	2,020	564
	40.00	J-55	0.395	8.835	8.679	10.625	10.125	2,570	630
	36.00	K-55	0.352	8.921	8.765	10.625	10.125	2,020	564
	40.00	K-55	0.395	8.835	8.679	10.625	10.125	2,570	630
	40.00	C-75	0.395	8.835	8.679	10.625	10.125	2,990	859
	43.50	C-75	0.435	8.755	8.599	10.625	10.125	3,730	942
	47.00	C-75	0.472	8.681	8.525	10.625	10.125	4,610	1,018
	53.50	C-75	0.545	8.535	8.379	10.625	10.125	6,350	1,166
	40.00	L-80	0.395	8.835	8.679	10.625	10.125	3,090	916
	43.50	L-80	0.435	8.755	8.599	10.625	10.125	3,810	1,005
	47.00	L-80	0.472	8.681	8.525	10.625	10.125	4,760	1,086
	53.50	L-80	0.545	8.535	8.379	10.625	10.125	6,620	1,244
	40.00	N-80	0.395	8.835	8.679	10.625	10.125	3,090	916
	43.50	N-80	0.435	8.755	8.599	10.625	10.125	3,810	1,005
	47.00	N-80	0.472	8.681	8.525	10.625	10.125	4,760	1,086
	53.50	N-80	0.545	8.535	8.379	10.625	10.125	6,620	1,244
	40.00	C-90	0.395	8.835	8.679	10.625	10.125	3,250	1,031
	43.50	C-90	0.435	8.755	8.599	10.625	10.125	4,010	1,130
	47.00	C-90	0.472	8.681	8.525	10.625	10.125	5,000	1,221
	53.50	C-90	0.545	8.535	8.379	10.625	10.125	7,120	1,399

Table C-1:   *(Continued)*

1	2	3	4	5	6	7	8	9	10
	40.00	C-95	0.395	8.835	8.679	10.625	10.125	3,320	1,088
	43.50	C-95	0.435	8.755	8.599	10.625	10.125	4,120	1,193
	47.00	C-95	0.472	8.681	8.525	10.625	10.125	5,090	1,289
	53.50	C-95	0.545	8.535	8.379	10.625	10.125	7,340	1,477
	43.50	P-110	0.435	8.755	8.599	10.625	10.125	4,420	1,381
	47.00	P-110	0.472	8.681	8.525	10.625	10.125	5,300	1,493
	53.50	P-110	0.545	8.535	8.379	10.625	10.125	7,950	1,710
	47.00	Q125	0.472	8.681	8.525	10.625	—	5,640	1,697
	53.50	Q125	0.545	8.535	8.379	10.625	—	8,440	1,943
$10^3/_4$	32.75	H-40	0.279	10.192	10.036	11.750	—	840	367
	40.50	H-40	0.350	10.050	9.894	11.750	—	1,390	457
	40.50	J-55	0.350	10.050	9.894	11.750	11.250	1,580	629
	45.50	J-55	0.400	9.950	9.794	11.750	11.250	2,090	715
	51.00	J-55	0.450	9.850	9.694	11.750	11.250	2,700	801
	40.50	K-55	0.350	10.050	9.894	11.750	11.250	1,580	629
	45.50	K-55	0.400	9.950	9.794	11.750	11.250	2,090	715
	51.00	K-55	0.450	9.850	9.694	11.750	11.250	2,700	801
	51.00	C-75	0.450	9.850	9.694	11.750	11.250	3,110	1,092
	55.50	C-75	0.495	9.760	9.604	11.750	11.250	3,920	1,196
	51.00	L-80	0.450	9.850	9.694	11.750	11.250	3,220	1,165
	55.50	L-80	0.495	9.760	9.604	11.750	11.250	4,020	1,276
	51.00	N-80	0.450	9.850	9.694	11.750	11.250	3,220	1,165
	55.50	N-80	0.495	9.760	9.604	11.750	11.250	4,020	1,276
	51.00	C-90	0.450	9.850	9.694	11.750	11.250	3,400	1,310
	55.50	C-90	0.495	9.760	9.604	11.750	11.250	4,160	1,435
	51.00	C-95	0.450	9.850	9.694	11.750	11.250	3,480	1,383
	55.50	C-95	0.495	9.760	9.604	11.750	11.250	4,290	1,515
	51.00	P-110	0.450	9.850	9.694	11.750	11.250	3,660	1,602
	55.50	P-110	0.495	9.760	9.604	11.750	11.250	4,610	1,754
	60.70	P-110	0.545	9.660	6.504	11.750	11.250	5,880	1,922
	65.70	P-110	0.595	9.560	9.404	11.750	11.250	7,500	2,088
	60.70	Q125	0.545	9.660	6.504	11.250	—	6,080	2,184
	65.70	Q125	0.595	9.560	9.404	11.250	—	7,920	2,373
$11^3/_4$	42.00	H-40	0.333	11.084	10.928	12.750	—	1,040	478
	47.00	J-55	0.375	11.000	10.844	12.750	—	1,510	737
	54.00	J-55	0.435	10.880	10.724	12.750	—	2,070	850
	60.00	J-55	0.489	10.772	10.616	12.750	—	2,660	952
	47.00	K-55	0.375	11.000	10.844	12.750	—	1,510	737
	54.00	K-55	0.435	10.880	10.724	12.750	—	2,070	850
	60.00	K-55	0.489	10.772	10.616	12.750	—	2,660	952
	60.00	C-75	0.489	10.772	10.616	12.750	—	3,070	1,298
	60.00	L-80	0.489	10.772	10.616	12.750	—	3,180	1,384
	60.00	N-80	0.489	10.772	10.616	12.750	—	3,180	1,384
	60.00	C-90	0.489	10.772	10.616	12.750	—	3,360	1,557
	60.00	C-95	0.489	10.772	10.616	12.750	—	3,440	1,644
	60.00	P-110	0.489	10.772	10.616	12.750	—	3,610	1,903
	60.00	Q125	0.489	10.772	10.616	12.750	—	3,680	2,162

Table C-1: *(Continued)*

1	2	3	4	5	6	7	8	9	10
13³/₈	48.00	H-40	0.330	12.715	12.559	14.375	—	740	541
	54.50	J-55	0.380	12.615	12.459	14.375	—	1,130	853
	61.00	J-55	0.430	12.515	12.359	14.375	—	1,540	962
	68.00	J-55	0.480	12.415	12.259	14.375	—	1,950	1,069
	54.50	K-55	0.380	12.615	12.459	14.375	—	1,130	853
	61.00	K-55	0.430	12.515	12.359	14.375	—	1,540	962
	68.00	K-55	0.480	12.415	12.259	14.375	—	1,950	1,069
	68.00	C-75	0.480	12.415	12.259	14.375	—	2,220	1,458
	72.00	C-75	0.514	12.347	12.191	14.375	—	2,600	1,558
	68.00	L-80	0.480	12.415	12.259	14.375	—	2,260	1,556
	72.00	L-80	0.514	12.347	12.191	14.375	—	2,670	1,661
	68.00	N-80	0.480	12.415	12.259	14.375	—	2,260	1,556
	72.00	N-80	0.514	12.347	12.191	14.375	—	2,670	1,661
	68.00	G-90	0.480	12.415	12.259	14.375	—	2,320	1,750
	72.00	G-90	0.514	12.347	12.191	14.375	—	2,780	1,869
	68.00	C-95	0.480	12.415	12.259	14.375	—	2,330	1,847
	72.00	C-95	0.514	12.347	12.191	14.375	—	2,820	1,973
	68.00	P-110	0.480	12.415	12.259	14.375	—	2,330	2,139
	72.00	P-110	0.514	12.347	12.191	14.375	—	2,890	2,284
	72.00	Q125	0.514	12.347	12.191	14.375	—	2,880	2,596
16	65.00	H-40	0.375	15.250	15.062	17.000	—	630	736
	75.00	J-55	0.438	15.124	14.936	17.000	—	1,020	1,178
	84.00	J-55	0.495	15.010	14.822	17.000	—	1,410	1,326
	75.00	K-55	0.438	15.124	14.936	17.000	—	1,020	1,178
	84.00	K-55	0.495	15.010	14.822	17.000	—	1,410	1,326
18⁵/₈	87.50	H-40	0.435	17.755	17.567	20.000	—	*630	994
	87.50	J-55	0.435	17.755	17.567	20.000	—	*630	1,367
	87.50	K-55	0.435	17.755	17.567	20.000	—	*630	1,367
20	94.00	H-40	0.438	19.124	18.936	21.000	—	*520	1,077
	94.00	J-55	0.438	19.124	18.936	21.000	—	*520	1,480
	106.50	J-55	0.500	19.000	18.812	21.000	—	*770	1,685
	133.00	J-55	0.635	18.730	18.542	21.000	—	1,500	2,125
	94.00	K-55	0.438	19.124	18.936	21.000	—	*520	1,480
	106.50	K-55	0.500	19.000	18.812	21.000	—	*770	1,685
	133.00	K-55	0.635	18.730	18.542	21.000	—	1,500	2,125

Some joint strengths listed in Col. 20 through 27 are greater than the corresponding pipe body yield strength listed in Col. 12.

* Collapse resistance values calculated by elastic formula.

† Internal pressure resistance is the lowest of the internal yield pressure of the pipe, the internal yield pressure of the coupling, or the internal pressure leak resistance at the E_1 or E- plane.

‡ For J55 and K55 casing the next higher grade is N80.
For N80 casing the next higher grade is P110.
For P1110 casing the next higher grade is 150 YS, a non-API steel grade having a minimum yield strength of 150,000 psi.
No higher grades have been established for 5AC casing.

Table C-2: Physical Properties of Water-Well Steel Casing

Outside Diameter (in.)	Inside Diameter (in.)	Wall Thickness (in.)	Weight (lb/ft)	Collapsing Strength		Axial Compression Strength (tons)	Tensile Strength (tons)
				(psi)	(ft/water)		
6.625	6.406	0.1094	7.61	199	459	39.2	67.2
6.625	6.344	0.1406	9.74	371	857	50.1	85.9
6.625	6.281	0.1719	11.85	593	1369	61.0	104.5
6.625	6.250	0.1875	12.81	720	1662	66.4	113.7
6.625	6.125	0.2500	17.02	1288	2974	87.6	150.1
8.625	8.406	0.1094	9.95	99	229	51.2	87.8
8.625	8.344	0.1406	12.74	192	444	65.6	112.4
8.625	8.281	0.1719	15.52	319	736	79.9	137.0
8.625	8.250	0.1875	16.79	393	908	87.0	149.1
8.625	8.125	0.2500	22.36	756	1745	115.1	197.3
10.750	10.375	0.1875	21.15	228	528	108.9	186.7
10.750	10.250	0.2500	28.04	461	1065	144.3	247.4
10.750	10.125	0.3125	34.71	760	1756	179.3	307.4
12.750	12.375	0.1875	25.16	147	340	129.5	222.0
12.750	12.250	0.2500	33.38	306	707	171.8	294.5
12.750	12.125	0.3125	41.52	521	1203	213.7	366.3
12.750	12.000	0.3750	49.57	795	1835	262.4	437.4
14.000	13.625	0.1875	27.73	115	265	142.4	244.1
14.000	13.500	0.2500	36.71	242	560	189.0	324.0
14.000	13.375	0.3125	45.68	419	967	235.2	403.1
14.000	13.250	0.3750	54.57	636	1469	280.9	481.6
14.500	14.125	0.1875	28.66	105	242	147.5	252.9
14.500	14.000	0.2500	38.05	222	512	195.9	335.8
14.500	13.875	0.3125	47.36	385	890	243.8	417.9
14.500	13.750	0.3750	56.57	588	1359	291.2	499.2
16.000	15.625	0.1875	31.67	80	185	163.0	279.4
16.000	15.500	0.2500	42.05	172	398	216.5	371.1
16.000	15.375	0.3125	52.36	303	700	269.5	462.0
16.000	15.250	0.3750	62.58	470	1085	322.1	552.2
16.625	16.250	0.1875	32.29	72	167	169.4	290.5
16.625	16.125	0.2500	43.73	156	360	225.1	385.8
16.625	16.000	0.3125	54.45	276	637	280.3	480.4
16.625	15.875	0.3750	65.09	429	991	335.0	574.3
18.000	17.625	0.1875	35.67	58	134	183.6	314.8
18.000	17.500	0.2500	47.39	126	292	244.0	418.2
18.000	17.375	0.3125	59.03	226	521	303.9	520.9
18.000	17.250	0.3750	70.59	355	820	363.4	622.9
18.625	18.250	0.1875	36.92	53	122	190.1	325.8
18.625	18.125	0.2500	49.07	116	267	252.6	433.0
18.625	18.000	0.3125	61.33	207	478	314.6	539.4
18.625	17.875	0.3750	73.10	327	755	376.3	645.0
20.000	19.625	0.1875	39.68	43	100	204.2	350.1
20.000	19.500	0.2500	52.73	95	221	271.5	465.4
20.000	19.375	0.3125	65.71	172	398	338.2	579.8
20.000	19.250	0.3750	78.60	274	633	404.6	693.6
20.625	20.250	0.1875	40.93	40	92	210.7	361.2
20.625	20.125	0.2500	54.41	88	203	280.0	480.1

Table C-2: *(Continued)*

20.625	20.000	0.3125	67.80	159	367	349.0	598.3
20.625	19.875	0.3750	81.11	254	586	417.5	715.7
22.000	21.500	0.2500	58.07	74	170	298.9	512.5
22.000	21.375	0.3125	72.38	134	310	372.6	638.8
22.000	21.250	0.3750	86.61	215	498	445.8	764.3
22.500	22.000	0.2500	59.41	69	160	305.8	524.2
22.500	21.875	0.3125	74.05	126	292	381.2	653.5
22.500	21.750	0.3750	88.61	203	470	456.1	782.0
24.000	23.500	0.2500	63.41	58	134	326.4	559.6
24.000	23.375	0.3125	79.06	107	246	407.0	697.7
24.000	23.250	0.3750	94.62	172	398	487.1	835.0
24.500	24.000	0.2500	64.75	55	127	333.3	571.4
24.500	23.875	0.3125	80.73	101	233	415.6	712.4
24.500	23.750	0.3750	96.62	163	377	497.4	852.7
26.000	25.500	0.2500	68.75	47	108	353.9	606.7
26.000	25.375	0.3125	85.73	86	198	441.3	756.6
26.000	25.250	0.3750	102.63	140	323	528.3	905.7
26.500	26.000	0.2500	70.09	44	102	360.8	618.5
26.500	25.875	0.3125	87.40	82	188	449.9	771.3
26.500	25.750	0.3750	104.63	133	307	538.6	923.3
28.000	27.500	0.2500	74.09	38	88	381.4	653.8
28.000	27.375	0.3125	92.41	70	162	475.7	815.5
28.000	27.250	0.3750	110.64	115	265	569.5	976.4
28.500	28.000	0.2500	75.43	36	83	388.3	665.6
28.500	27.875	0.3125	94.08	67	155	484.3	830.2
28.500	27.750	0.3750	112.64	110	253	597.8	994.0
30.000	29.500	0.2500	79.43	31	72	408.9	701.0
30.000	29.375	0.3125	99.08	58	134	510.1	874.4
30.000	29.250	0.3750	118.65	95	221	610.8	1047.0
30.500	30.000	0.2500	80.77	30	69	415.8	712.8
30.500	29.875	0.3125	100.75	56	128	518.6	889.1
30.500	29.750	0.3750	120.65	91	211	621.1	1064.7

Note: Collapse strength values are based upon Timoshenko's formula with 1% as a value of ellipticity and 35,000 psi as the steel yield point. Strengths are based upon 35,000 psi yield strength and 60,000 psi ultimate strength steel.

Table C-3:   API-Hydraulic Collapse and Burst Pressure and Unit Weight of Stainless Steel Well Casing

Nom. Size Inches	Schedule Number	Outside Diameter Inches	Wall Thickness Inches	Inside Diameter Inches	Internal Cross-Sectional Area Sq. In.	Internal Pressure psi		External Pressure psi Collapsing	Weight Pounds per Foot
						Test	Bursting		
2	5	2.375	0.065	2.245	3.958	820	4,105	896	1.619
	10	2.375	0.109	2.157	3.654	1,375	6,884	2,196	2.663
	40	2.375	0.154	2.067	3.356	1,945	9,726	3,526	3.087
	80	2.375	0.218	1.939	2.953	2,500	13,768	5,419	5.069
2½	5	2.875	0.083	2.709	5.761	865	4,330	1,081	2.498
	10	2.875	0.120	2.635	5.450	1,250	6,260	1,905	3.564
	40	2.875	0.203	2.469	4.785	2,118	10,591	3,931	6.347
3	5	3.500	0.063	3.334	8.726	710	3,557	639	3.057
	10	3.500	0.120	3.260	8.343	1,030	5,142	1,375	4.372
	40	3.500	0.216	3.068	7.389	1,851	9,257	3,307	7.647
3½	5	4.000	0.083	3.834	11.54	620	3,112	431	3.505
	10	4.000	0.120	3.760	11.10	900	4,500	1,081	5.019
	40	4.000	0.226	3.548	9.887	1,695	8,475	2,941	9.194
4	5	4.500	0.083	4.334	14.75	555	2,766	316	3.962
	10	4.500	0.120	4.260	14.25	800	4,000	845	5.666
	40	4.500	0.237	4.026	12.72	1,580	7,900	2,672	10.891
5	5	5.563	0.109	5.345	22.43	587	2,949	350	6.409
	10	5.563	0.134	5.295	22.01	722	3,613	665	7.842
	40	5.563	0.258	5.047	20.00	1,391	6,957	2,231	14.754
6	5	6.625	0.109	6.407	32.22	494	2,467	129	7.656
	10	6.625	0.134	6.357	31.72	606	3,033	394	9.375
	40	6.625	0.280	6.065	28.89	1,268	6,340	1,942	19.152

Table C-4: API Hydraulic Collapse Pressure and Unit Weight of PVC Well Casing

Outside Diameter (in.) Nominal	Actual	SDR/SCH	Wall Thickness (Minimum in.)	DR	Weight in Air (lb/100 ft) PVC 12454	PVC 14333	Weight in Water (lb/100 ft) PVC 12454	PVC 14333	Hydraulic Collapse Pressure (psi) PVC 12454	PVC 14333
2	2.375	SCH-80	0.218	10.9	94	91	27	24	947	758
		SDR-13.5	0.176	13.5	78	75	22	19	470	376
		SCH-40	0.154	15.4	69	66	20	17	307	246
		SDR-17	0.140	17.0	63	61	18	16	224	179
		SDR-21	0.113	21.0	51	47	14	12	115	92
2½	2.875	SCH-80	0.276	10.4	144	139	41	36	1,110	885
		SDR-13.5	0.213	13.5	114	110	32	28	470	376
		SCH-40	0.203	14.2	109	105	31	27	400	320
		SDR-17	0.169	17.0	92	89	26	23	224	179
		SDR-21	0.137	21.0	76	73	22	19	115	92
3	3.500	SCH-80	0.300	11.7	193	186	55	48	750	600
		SDR-13.5	0.259	13.5	169	163	48	42	470	376
		SCH-40	0.216	16.2	143	138	41	36	262	210
		SDR-17	0.206	17.0	136	132	39	34	224	179
		SDR-21	0.167	21.0	112	108	32	28	115	92
3½	4.000	SCH-80	0.318	12.6	235	227	67	59	589	471
		SDR-13.5	0.296	13.5	220	212	63	55	470	376
		SDR-17	0.235	17.0	178	172	51	44	224	179
		SCH-40	0.226	17.7	176	172	49	43	197	158
		SDR-21	0.190	21.0	146	141	42	36	115	92
4	4.500	SCH-80	0.337	13.3	282	272	80	70	494	395
		SDR-13.5	0.333	13.5	279	269	80	70	470	376
		SDR-17	0.265	17.0	226	218	64	56	224	179
		SCH-40	0.237	19.0	203	196	58	51	158	126
		SDR-21	0.214	21.0	185	178	53	46	115	92
		SDR-26	0.173	26.0	151	145	43	38	59	47
		SDR-32.5	0.138	32.5	121	117	34	30	29	23
		SDR-41	0.110	41.0	97	94	28	24	14	11
4½	4.950	—	0.248	20.0	235	226	67	58	134	107
		—	0.190	26.0	182	176	52	46	59	47
5	5.563	SDR-13.5	0.412	13.5	427	411	122	106	470	376
		SCH-80	0.375	14.8	391	377	112	98	350	280
		SDR-17	0.327	17.0	345	332	99	86	224	179
		SDR-21	0.265	21.0	283	273	81	71	115	92
		SCH-40	0.258	21.6	276	266	79	69	105	84
5	5.563	SDR-26	0.214	26.0	231	222	66	58	59	47
		—	0.190	29.3	206	198	59	51	40	32
		SDR-32.5	0.171	32.5	186	179	52	46	29	23
		SDR-41	0.136	41.0	149	144	43	37	14	11

Table C-4:   *(Continued)*

6	6.140	SDR-32.5	0.189	32.5	227	218	65	56	29	23
		SDR-41	0.150	41.0	181	175	52	45	14	11
6	6.625	SDR-13.5	0.491	13.5	605	584	173	151	470	376
		SCH-80	0.432	15.3	538	519	154	134	314	171
		SDR-17	0.390	17.0	489	472	140	122	224	179
		SDR-21	0.316	21.0	402	387	115	100	115	92
		SCH-40	0.280	23.7	358	345	102	89	78	62
		SDR-26	0.255	26.0	327	316	93	82	59	47
		SDR-32.5	0.204	32.5	264	255	75	66	29	23
		—	0.190	34.9	246	238	70	62	23	18
		SDR-41	0.162	41.0	211	204	60	53	14	11
7	7.000	—	0.300	28.3	405	390	116	101	83	66
8	8.160	SDR-32.5	0.251	32.5	400	386	114	100	29	23
		SDR-41	0.199	41.0	320	308	91	80	14	11
	8.625	SDR-17	0.508	17.0	830	800	237	207	224	179
		SCH-80	0.500	17.2	818	788	234	204	216	173
		SDR-21	0.410	21.0	678	654	194	170	115	92
		SDR-26	0.332	26.0	555	535	159	139	59	47
		SCH-40	0.322	26.8	539	520	154	135	54	43
		SDR-32.5	0.265	32.5	447	431	128	109	29	23
		SDR-41	0.210	41.0	356	343	102	89	14	11
10	10.200	SDR-32.5	0.314	32.5	626	604	179	156	29	23
		SDR-41	0.249	41.0	500	482	143	125	14	11
10	10.750	SDR-17	0.632	17.0	1290	1240	368	322	224	179
		SCH-80	0.593	18.1	1210	1170	346	303	184	147
		SDR-21	0.511	21.0	1050	1020	301	263	115	92
		SDR-26	0.413	26.0	860	830	246	215	59	47
		SCH-40	0.365	29.4	764	737	218	191	40	32
		SDR-32.5	0.331	32.5	695	670	199	173	29	23
		SDR-41	0.262	41.0	557	537	159	139	14	11
12	12.750	SDR-17	0.750	17.0	1810	1760	517	453	224	179
		SCH-80	0.687	18.6	1670	1610	476	417	168	134
		SDR-21	0.606	21.0	1480	1430	423	370	115	92
		SDR-26	0.490	26.0	1210	1170	346	302	59	47
		SCH-40	0.406	31.4	1010	974	288	252	33	26
		SDR-32.5	0.392	32.5	977	942	279	244	29	23
		SDR-41	0.311	41.0	780	752	223	195	14	11
14	14.000	SCH-80	0.750	18.7	2000	1930	572	500	166	133
		SDR-21	0.667	21.0	1790	1730	512	448	115	92
		SDR-26	0.539	26.0	1460	1410	418	366	59	47
		SCH-40	0.437	32.0	1200	1150	341	299	31	25
		SDR-32.5	0.430	32.5	1180	1140	336	294	29	23
		SDR-41	0.342	41.0	942	908	269	235	14	11

Table C-5: Hydraulic Collapse Pressure and Unit Weight and ABS Well Casing

Outside Diameter (in.) Nominal	Actual	SDR/SC	Wall Thickness (Minimum in.)	DR	Weight in Air (lb/100 ft) ABS 434	ABS 533	Weight in Water (lb/100 ft) ABS 434	ABS 533	Hydraulic Collapse Pressure (psi) ABS 434	ABS 533
2	2.375	SCH-80	0.218	10.9	71	70	3.4	2.7	829	592
		SDR-13.5	0.176	13.5	59	58	2.8	2.2	412	294
		SCH-40	0.154	15.4	52	51	2.5	2.0	269	192
		SDR-17	0.140	17.0	47	47	2.2	1.8	196	140
		SDR-21	0.113	21.0	39	38	1.8	1.5	100	71
2½	2.875	SCH-80	0.276	10.4	108	107	5.1	4.1	968	691
		SDR-13.5	0.213	13.5	85	85	4.0	3.3	412	294
		SCH-40	0.203	14.2	82	81	3.9	3.1	350	250
		SDR-17	0.169	17.0	69	68	3.3	2.6	196	140
		SDR-21	0.137	21.0	57	56	2.7	2.1	100	71
3	3.500	SCH-80	0.300	11.7	145	144	6.9	5.5	656	468
		SDR-13.5	0.259	13.5	126	125	6.0	4.8	412	294
		SCH-40	0.216	16.2	107	106	5.1	4.1	229	164
		SDR-17	0.206	17.0	103	102	4.9	3.9	196	140
		SDR-21	0.167	21.0	84	83	4.0	3.2	100	71
3½	4.000	SCH-80	0.318	12.6	176	175	8.4	6.7	515	368
		SDR-13.5	0.296	13.5	165	164	7.8	6.3	412	294
		SDR-17	0.235	17.0	134	133	6.4	5.1	196	140
		SCH-40	0.226	17.7	129	128	6.1	4.9	173	124
		SDR-21	0.190	21.0	109	108	5.2	4.1	100	71
4	4.500	SCH-80	0.337	13.3	211	209	10.0	8.0	432	308
		SDR-13.5	0.333	13.5	209	207	10.0	8.0	412	294
		SDR-17	0.265	17.0	169	168	8.0	6.5	196	140
		SCH-40	0.237	19.0	152	151	7.2	5.8	138	98
		SDR-21	0.214	21.0	138	137	6.6	5.3	100	71
		SDR-26	0.173	26.0	113	112	5.4	4.3	51	36
5	5.563	SDR-13.5	0.412	13.5	320	317	15.2	12.2	412	294
		SCH-80	0.375	14.8	294	291	14.0	11.2	306	218
		SDR-17	0.327	17.0	258	256	12.3	9.8	196	140
		SDR-21	0.265	21.0	212	210	10.0	8.1	100	71
		SCH-40	0.258	21.6	207	205	9.8	7.9	92	66
		SDR-26	0.214	26.0	173	171	8.2	6.6	51	36
6	6.625	SDR-13.5	0.491	13.5	454	450	21.7	17.3	412	294
		SCH-80	0.432	15.3	404	400	19.2	15.4	275	196
		SDR-17	0.390	17.0	367	364	17.4	14.0	196	140
		SDR-21	0.316	21.0	301	298	14.3	11.5	100	71
		SCH-40	0.280	23.7	268	266	12.8	10.2	69	49
		SDR-26	0.255	26.0	246	243	11.7	9.3	51	36
8	8.625	SDR-17	0.508	17.0	622	616	29.6	23.7	196	140
		SCH-80	0.500	17.2	613	607	29.2	23.3	189	135
		SDR-21	0.410	21.0	509	504	24.2	19.4	100	71
		SDR-26	0.332	26.0	416	412	19.8	15.8	51	36
		SCH-40	0.322	26.8	404	400	19.2	15.4	47	34

Table C-5: *(Continued)*

10	10.750	SDR-17	0.632	17.0	965	956	46.0	36.8	196	140
		SCH-80	0.593	18.1	909	901	43.3	34.6	161	115
		SDR-21	0.511	21.0	790	738	37.6	30.0	100	71
		SDR-26	0.413	26.0	645	639	30.7	24.6	51	36
		SCH-40	0.365	29.4	573	568	27.3	21.8	35	25
12	12.750	SDR-17	0.750	17.0	1360	1350	64.7	51.8	196	140
		SCH-80	0.687	18.6	1250	1240	59.6	47.6	148	106
		SDR-21	0.606	21.0	1110	1100	52.9	42.3	100	71
		SDR-26	0.490	26.0	908	899	43.2	34.6	51	36
		SCH-40	0.406	31.4	758	751	36.1	28.9	29	20
14	14.000	SDR-21	0.667	21.0	1340	1330	64.0	51.2	100	71
		SDR-26	0.539	26.0	1100	1090	52.2	41.8	51	36
16	16.000	SDR-21	0.762	21.0	1750	1740	83.5	66.8	100	71
		SDR-26	0.616	26.0	1430	1420	68.2	54.6	51	36

Note: SDR = standard dimension ratio; SCH – schedule, DR – dimension ratio (actual OD/wall thickness)
Sources: *Manual on the Selection and Installation of Thermoplastic Water Well Casing*, National Water Well Association, 500 West Wilson Bridge Road, Worthington, OH 43085. ASTM F 480-88a.

Table C-6: Hydraulic Collapse Pressure and Weight of SR Well Casing

Outside Diameter (in.) Nominal	Actual	SDR	Wall Thickness (Minimum in.)	DR	Weight in Air (lb/100 ft)	Weight in Water (lb/100 ft)	Hydraulic Collapse Pressure (psi)
2	2.375	SDR-13.5	0.176	13.5	58	2.8	376
		SDR-17	0.140	17.0	47	2.2	180
		SDR-21	0.113	21.0	39	1.8	92
2½	2.875	SDR-13.5	0.213	13.5	85	4.0	376
		SDR-17	0.169	17.0	69	3.3	180
		SDR-21	0.137	21.0	57	2.7	92
3	3.500	SDR-13.5	0.259	13.5	126	6.0	376
		SDR-17	0.206	17.0	102	4.8	180
		SDR-21	0.167	21.0	84	4.0	92
3½	4.000	SDR-13.5	0.296	13.5	165	7.8	376
		SDR-17	0.234	17.0	134	6.4	180
		SDR-21	0.190	21.0	109	5.2	92
4	4.500	SDR-13.5	0.330	13.5	209	10.0	376
		SDR-17	0.265	17.0	169	8.0	180
		—	0.250	18.0	160	7.6	150
		SDR-21	0.214	21.0	138	6.6	92
		—	0.200	22.5	130	6.2	74
		—	0.175	25.7	114	5.4	49
4½	4.886	—	0.230	21.2	162	7.7	89
		—	0.200	24.4	142	6.8	57
5	5.300	—	0.320	16.6	240	11.4	194
		—	0.250	21.2	191	9.1	89
		—	0.200	26.5	154	7.3	44
		—	0.174	30.3	136	6.5	29
5	5.563	SDR-13.5	0.412	13.5	320	15.2	376
		SDR-17	0.327	17.0	258	12.3	180
		SDR-21	0.265	21.0	212	10.0	92
		—	0.225	24.7	182	8.7	55
		SDR-26	0.214	26.0	173	8.2	47

Table C-6: *(Continued)*

6	6.275	—	0.320	19.6	288	13.7	114
		—	0.250	25.1	228	10.9	52
		—	0.200	31.4	184	8.8	26
		—	0.175	35.8	161	7.7	17
6	6.625	SDR-13.5	0.491	13.5	454	21.6	376
		SDR-17	0.390	17.0	367	17.5	180
		—	0.320	20.7	305	14.5	86
		SDR-26	0.255	26.0	246	11.7	47
		—	0.250	26.5	241	11.5	44
7	7.000	—	0.250	28.0	255	12.1	37
8	8.625	SDR-17	0.508	17.0	622	29.6	180
		SDR-21	0.410	21.0	509	24.2	92
		SDR-26	0.332	26.0	416	19.8	47
		—	0.250	34.5	317	15.1	20
10	10.750	SDR-17	0.632	17.0	965	46.0	180
		SDR-21	0.511	21.0	790	37.6	92
		SDR-26	0.413	26.0	645	30.7	47
12	12.750	SDR-17	0.750	17.0	360	64.7	180
		SDR-21	0.606	21.0	1110	52.9	92
		SDR-26	0.490	26.0	908	43.2	47
14	14.000	SDR-21	0.667	21.0	1340	64.0	92
		SDR-26	0.539	26.0	1100	52.2	47
16	16.000	SDR-21	0.762	21.0	1750	83.5	92
		SDR-26	0.616	26.0	1432	68.2	47

Note: SDR = standard dimension ratio, DR = dimension ratio (actual OD/Wall Thickness).
Sources: *Manual on the Selection and Installation of Thermoplastic Water Well Casing*, written and produced by the National Water Well Association, 500 West Wilson Bridge Road, Worthington, OH 3085. ASTM F 480-88a.

This page intentionally left blank.

D

Average Annual Atmospheric Conditions

This appendix gives the graphic representation of the average atmospheric conditions for mid-latitudes (30˚ N to 60˚ N) of the North American continent.

Figure D-1 gives the average annual atmospheric pressure of air for mid-latitudes of the North American continent as a function of surface elevation location above mean sea level. These average annual atmospheric pressures are of critical importance in predicting the actual weight rate of flow of air (or other gases) at an actual drilling location (see Chapters 5, 8, 9 and 10).

Figure D-2 gives the average annual atmospheric temperature of air for mid-latitudes of the North American continent as a function of surface elevation location above mean sea level. These average annual atmospheric temperatures are of critical importance in predicting the approximate geothermal temperature at an actual drilling location (see Chapters 5, 8, 9 and 10).

Figure D-3 gives the specific weight of atmospheric air for the average annual atmospheric pressures and temperatures given in Figures D-1 and D-2 as a function of surface elevation location above mean sea level.

Figure D-4 gives the specific weight of air at the average annual atmospheric pressures given in Figure D-1 for various actual atmospheric temperatures (i.e., 20˚ F, 40˚F, 60˚F, 80˚F) as a function of surface elevation location above mean sea level. These values are very useful for determining the adjusted minimum volumetric flowrate for air (or other gases) for surface elevations above mean sea level (see Chapters 4, 5, 8, 9 and 10).
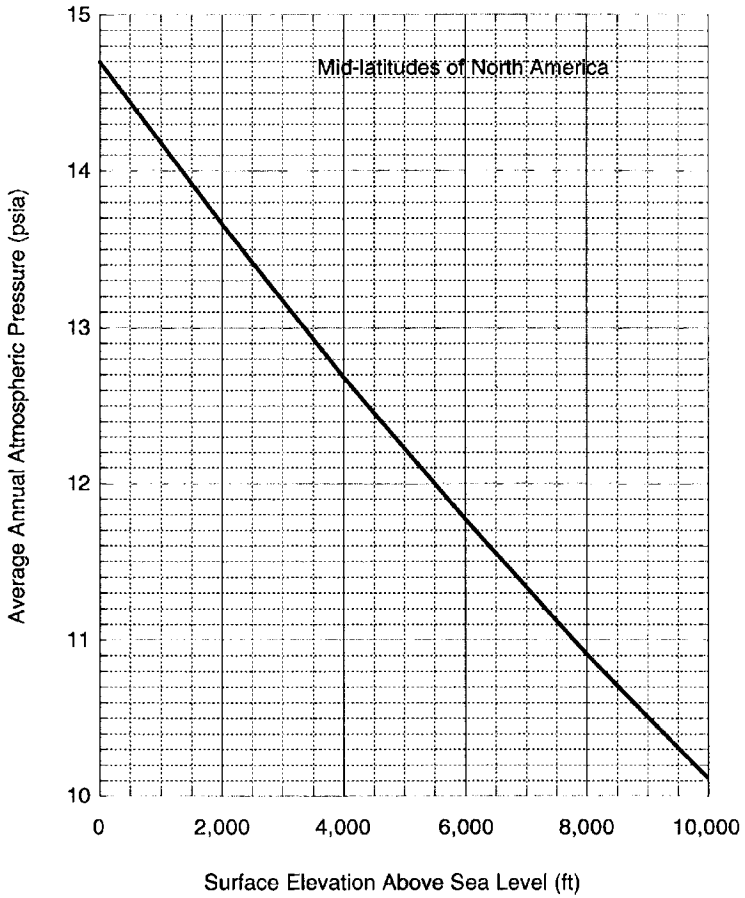
Figure D-1: Average annual atmospheric pressures versus surface elevation above mean sea level.
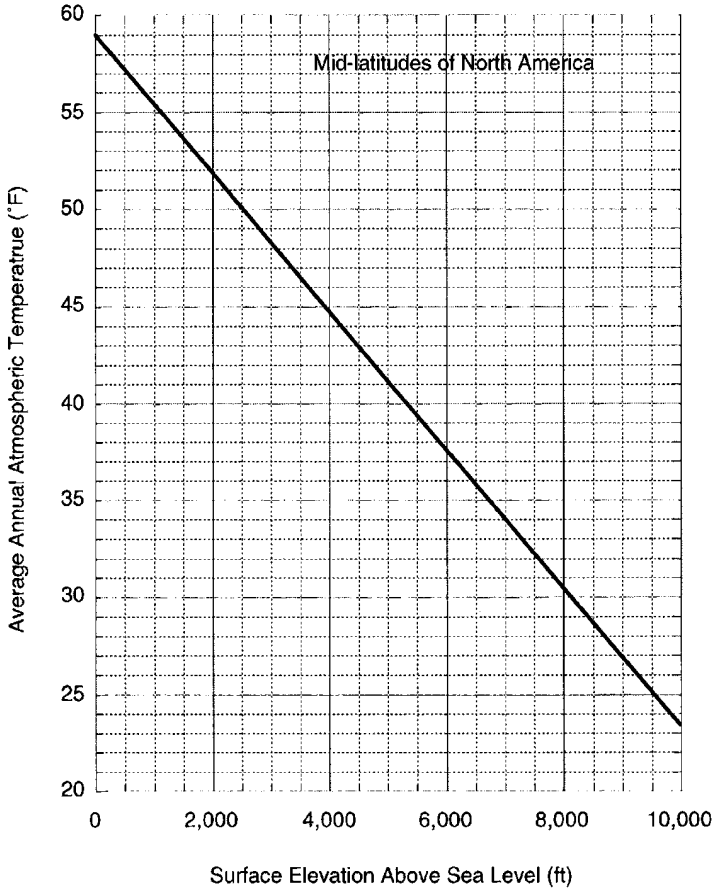
Figure D-2: Average annual atmospheric temperatures versus surface elevation above mean sea level.
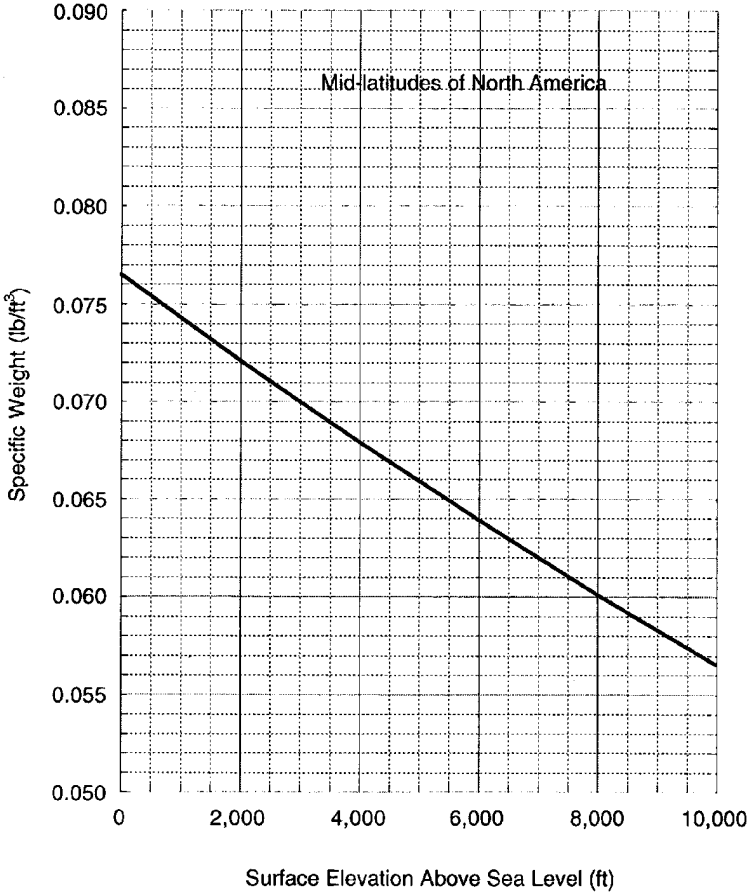
Figure D-3: Specific weight of atmospheric air for average annual pressures and temperatures in Figures D-1 and D-2 versus surface elevation above mean sea level.
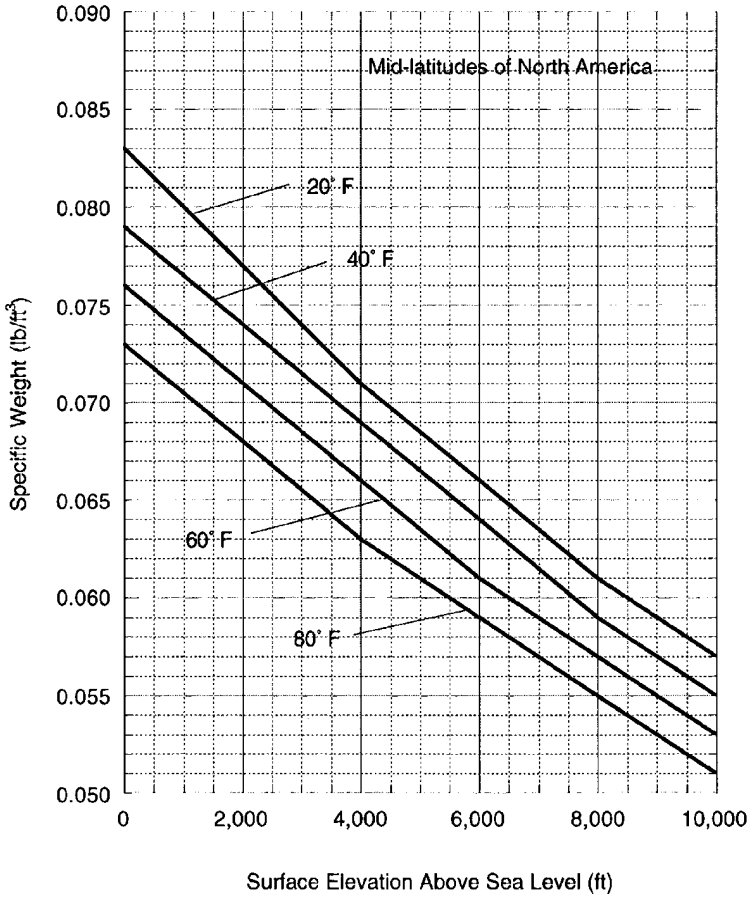
Figure D-4: Specific weights of atmospheric air versus surface elevation above mean sea level (for various atmospheric temperatures).

This page intentionally left blank.

Direct Circulation Minimum Volumetric Flow rates

This appendix gives the direct circulation minimum volumetric flow rates for deep air drilled boreholes. For API Mechanical Equipment standard conditions the figures that follow give the minimum volumetric flow rates as a function of drilling depth for the drilling rates of 0 ft/hr, 30 ft/hr, 60 ft/hr, 90 ft/hr, and 120 ft/hr. These figures are developed from the calculations presented in Chapter 8. The calculations are carried out assuming sedimentary rock formations.

Figure E-1:   Borehole 4 1/2 inches, drill pipe 2 3/8 inches.
Figure E-2:   Borehole 4 3/4 inches, drill pipe 2 3/8 inches.
Figure E-3:   Borehole 6 1/4 inches, drill pipe 2 7/8 inches.
Figure E-4:   Borehole 6 3/4 inches, drill pipe 2 7/8 inches.
Figure E-5:   Borehole 7 3/8 inches, drill pipe 2 7/8 inches.
Figure E-6:   Borehole 6 1/4 inches, drill pipe 3 1/2 inches.
Figure E-7:   Borehole 6 3/4 inches, drill pipe 3 1/2 inches.
Figure E-8:   Borehole 7 3/8 inches, drill pipe 3 1/2 inches.
Figure E-9:   Borehole 7 7/8 inches, drill pipe 3 1/2 inches.
Figure E-10: Borehole 7 3/8 inches, drill pipe 4 inches.
Figure E-11: Borehole 7 7/8 inches, drill pipe 4 inches.
Figure E-12: Borehole 8 3/4 inches, drill pipe 4 inches.
Figure E-13: Borehole 7 7/8 inches, drill pipe 4 1/2 inches.
Figure E-14: Borehole 8 3/4 inches, drill pipe 4 1/2 inches.
Figure E-15: Borehole 9 inches, drill pipe 4 1/2 inches.
Figure E-16: Borehole 8 3/4 inches, drill pipe 5 inches.
Figure E-17: Borehole 9 inches, drill pipe 5 inches.
Figure E-18: Borehole 9 7/8 inches, drill pipe 5 inches.
Figure E-19: Borehole 11 inches, drill pipe 5 inches.
Figure E-20: Borehole 9 7/8 inches, drill pipe 5 1/2 inches.
Figure E-21: Borehole 11 inches, drill pipe 5 1/2 inches.
Figure E-22: Borehole 12 1/4 inches, drill pipe 5 1/2 inches.
Figure E-23: Borehole 11 inches, drill pipe 6 5/8 inches.
Figure E-24: Borehole 12 1/4 inches, drill pipe 6 5/8 inches.
Figure E-25: Borehole 15 inches, drill pipe 6 5/8 inches.
Figure E-26: Borehole 17 1/2 inches, drill pipe 6 5/8 inches.
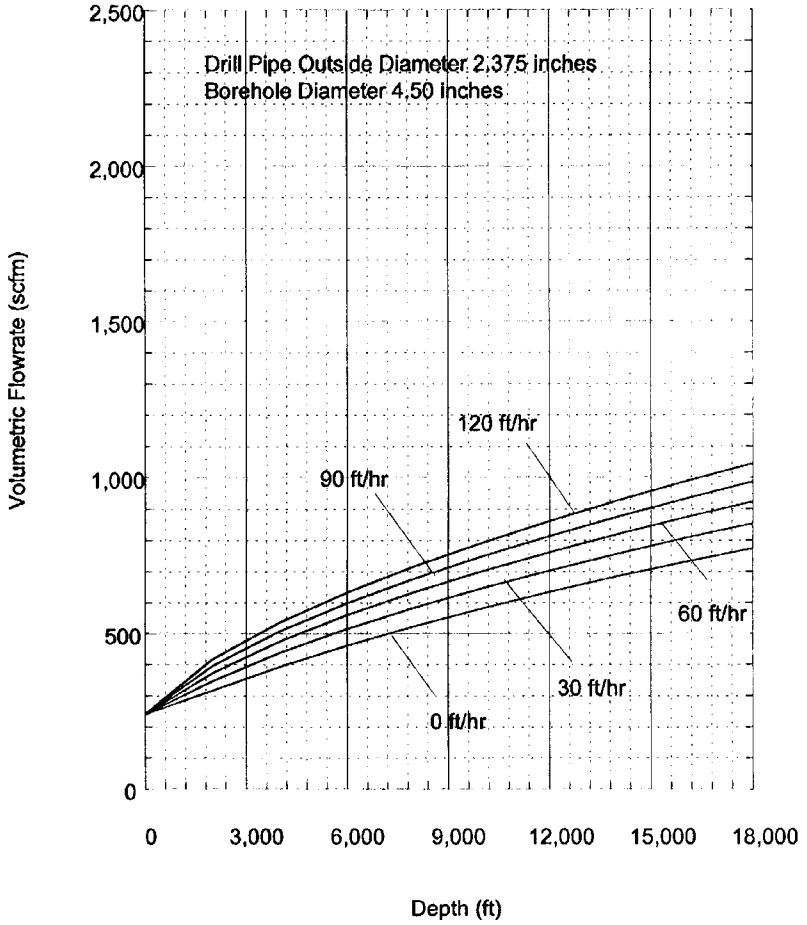
Figure E-1: Minimum volumetric flow rate of air at API standard conditions for 2 3/8 inch drill pipe and 4 1/2 inch borehole.
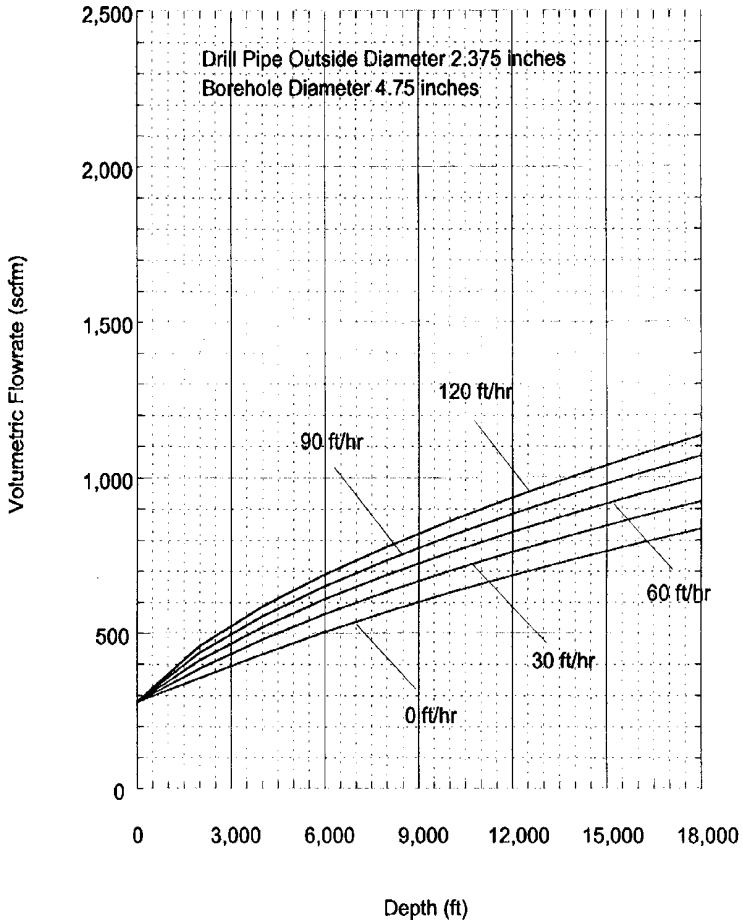
Figure E-2: Minimum volumetric flow rate of air at API standard conditions for 2 3/8 inch drill pipe and 4 3/4 inch borehole.
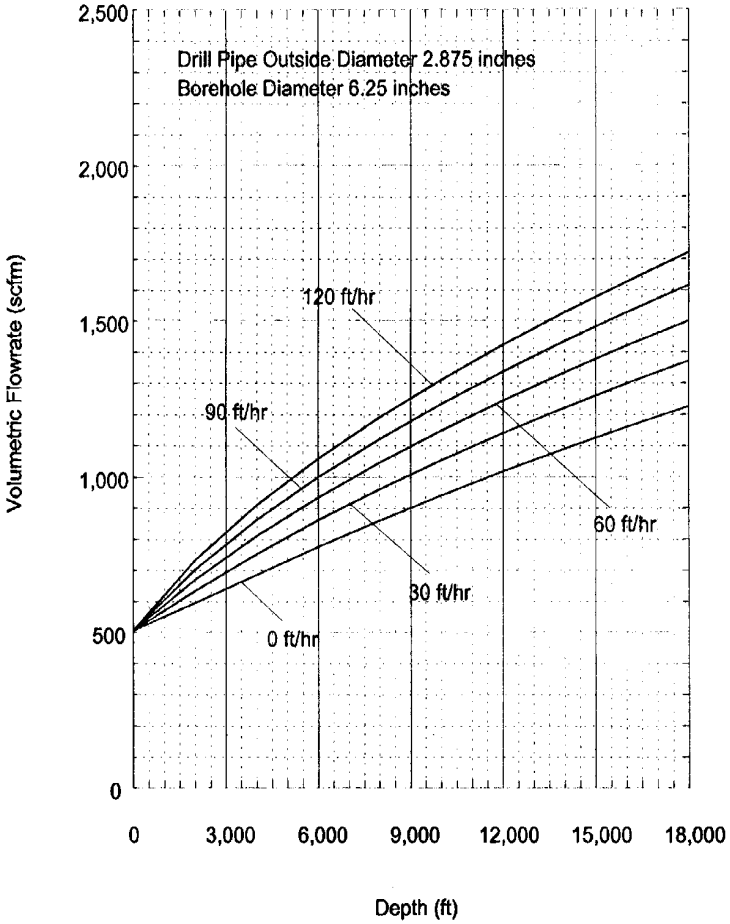
Figure E-3: Minimum volumetric flow rate of air at API standard conditions for 2 7/8 inch drill pipe and 6 1/4 inch borehole.
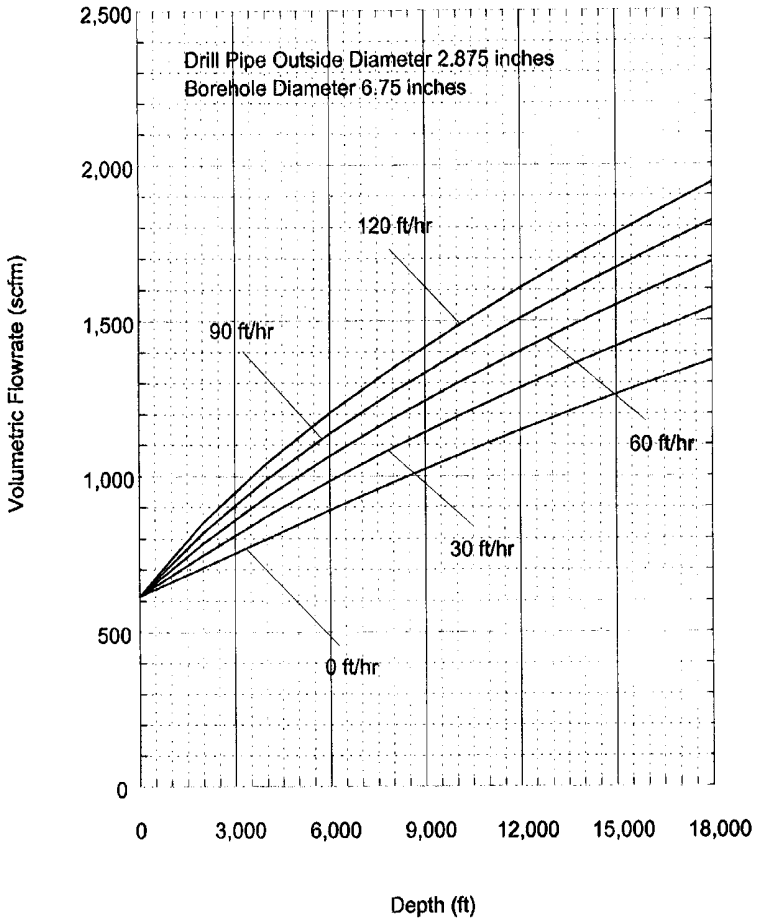
Figure E-4: Minimum volumetric flow rate of air at API standard conditions for 2 7/8 inch drill pipe and 6 3/4 inch borehole.
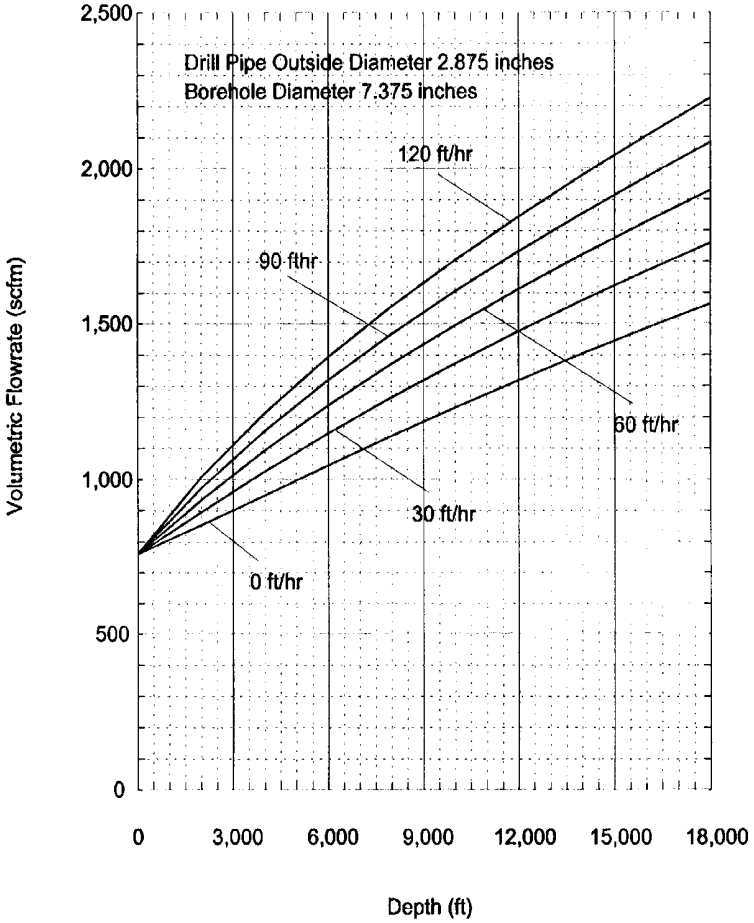
Figure E-5: Minimum volumetric flow rate of air at API standard conditions for 2 7/8 inch drill pipe and 7 3/8 inch borehole.
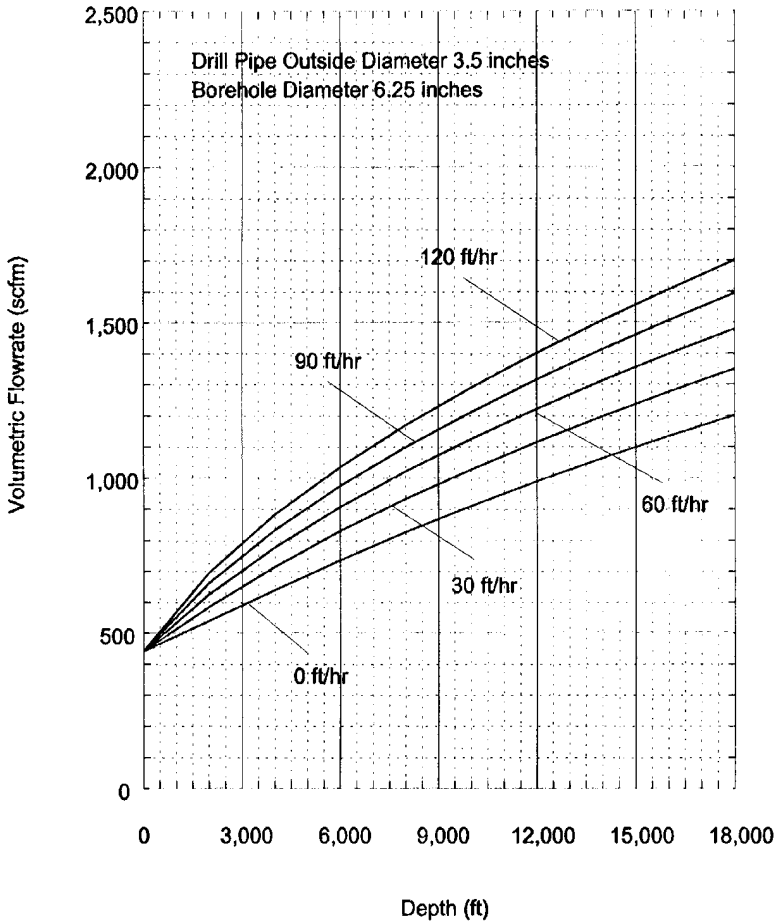
Figure E-6: Minimum volumetric flow rate of air at API standard conditions for 3 1/2 inch drill pipe and 6 1/4 inch borehole.
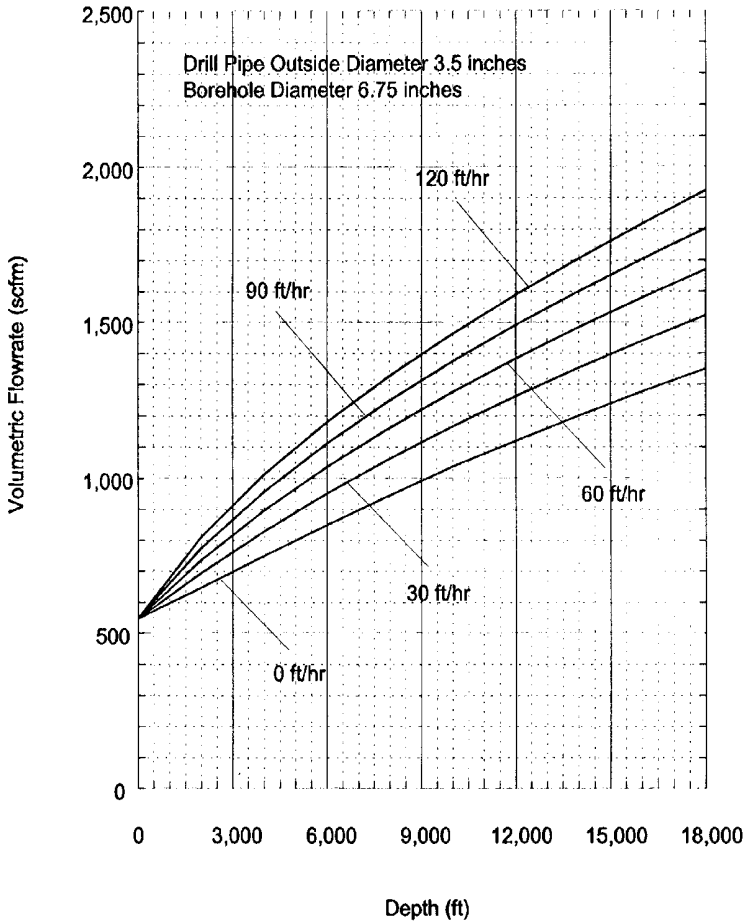
Figure E-7: Minimum volumetric flow rate of air at API standard conditions for 3 1/2 inch drill pipe and 6 3/4 inch borehole.
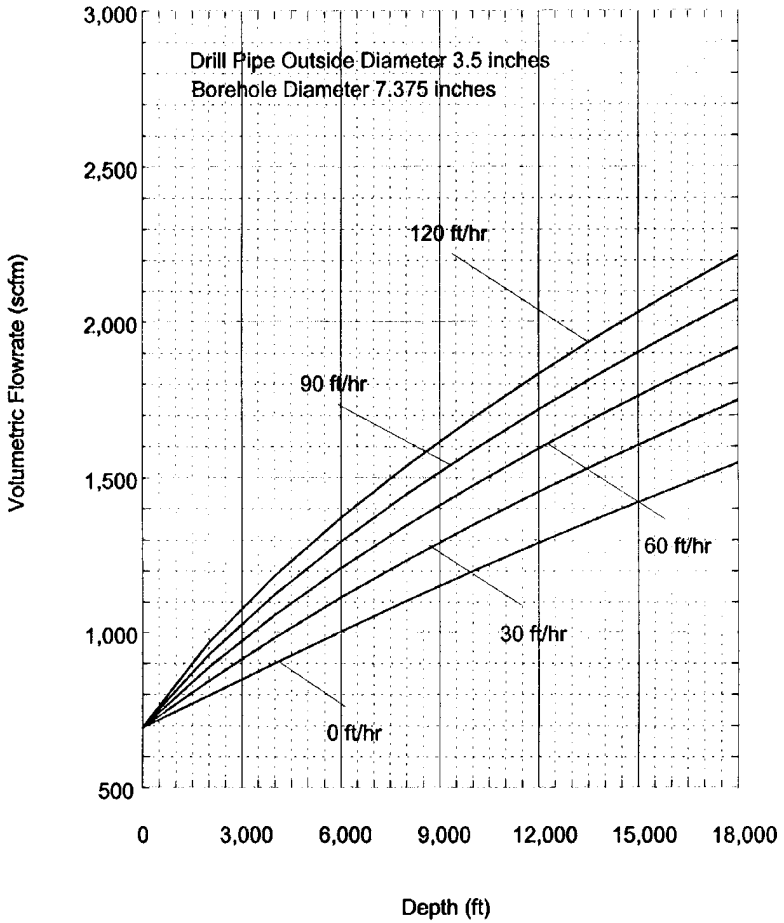
Figure E-8: Minimum volumetric flow rate of air at API standard conditions for 3 1/2 inch drill pipe and 7 3/8 inch borehole.
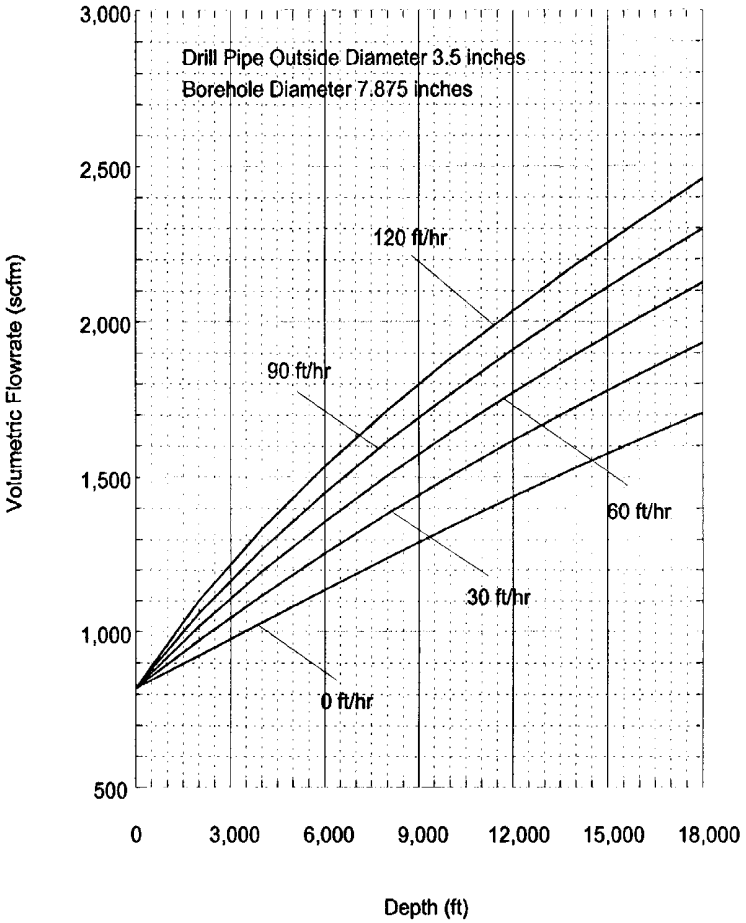
Figure E-9: Minimum volumetric flow rate of air at API standard conditions for 3 1/2 inch drill pipe and 7 7/8 inch borehole.
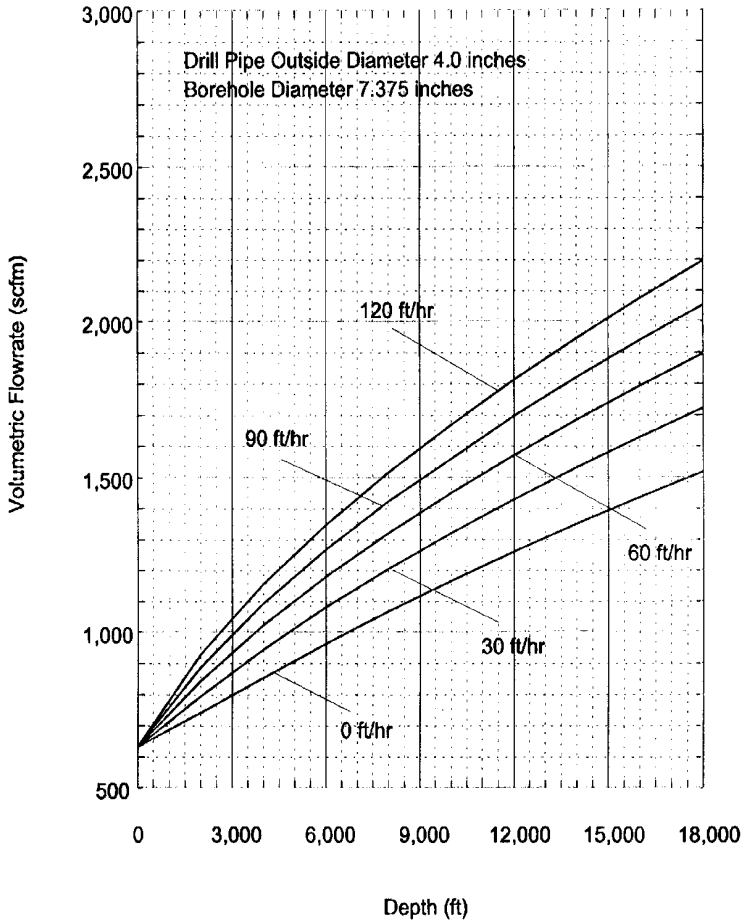
Figure E-10: Minimum volumetric flow rate of air at API standard conditions for 4 inch drill pipe and 7 3/8 inch borehole.
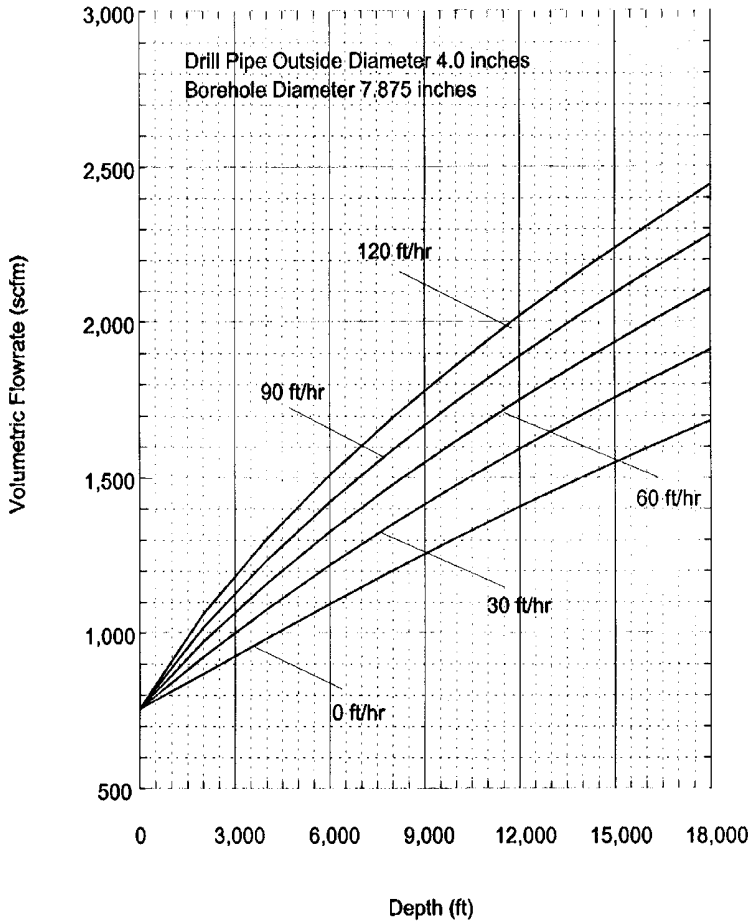
Figure E-11: Minimum volumetric flow rate of air at API standard conditions for 4 inch drill pipe and 7 7/8 inch borehole.
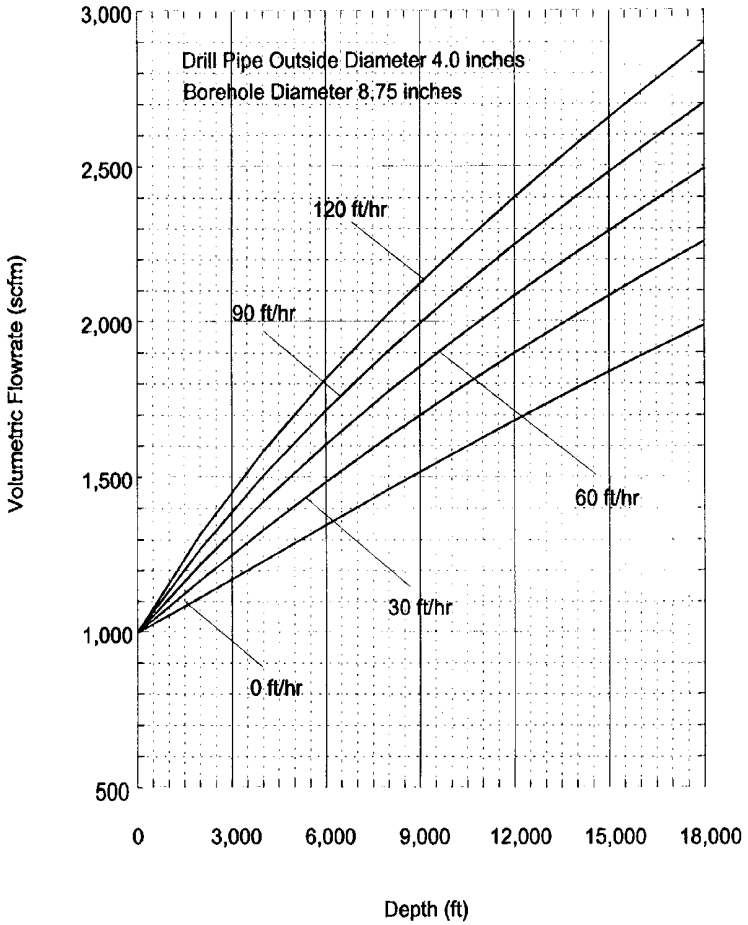
Figure E-12: Minimum volumetric flow rate of air at API standard conditions for 4 inch drill pipe and 8 3/4 inch borehole.
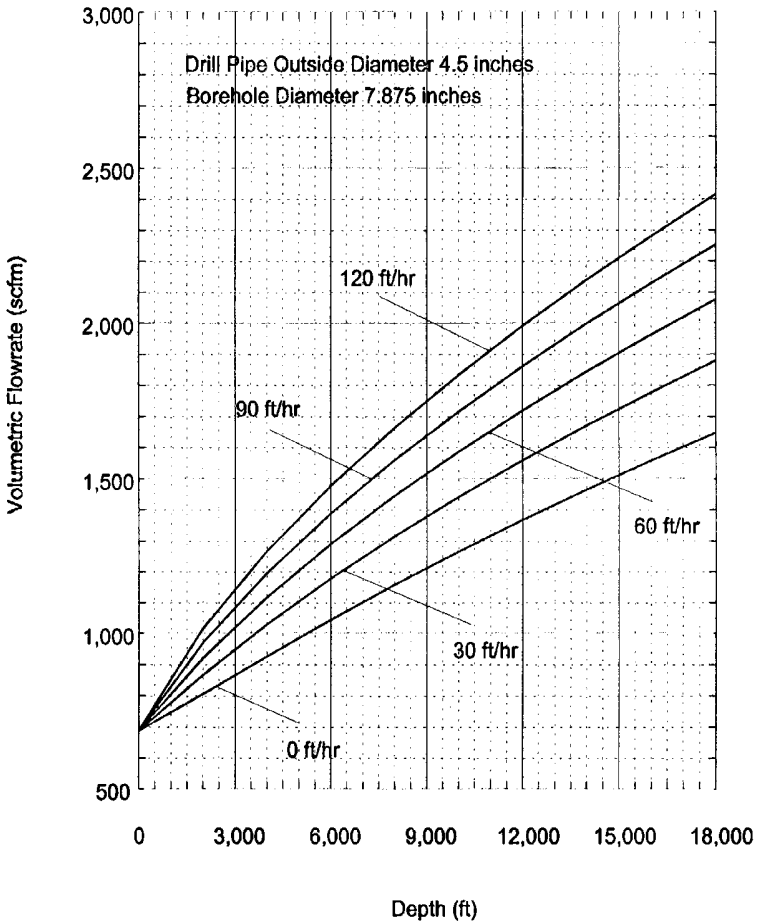
Figure E-13: Minimum volumetric flow rate of air at API standard conditions for 4 1/2 inch drill pipe and 7 7/8 inch borehole.
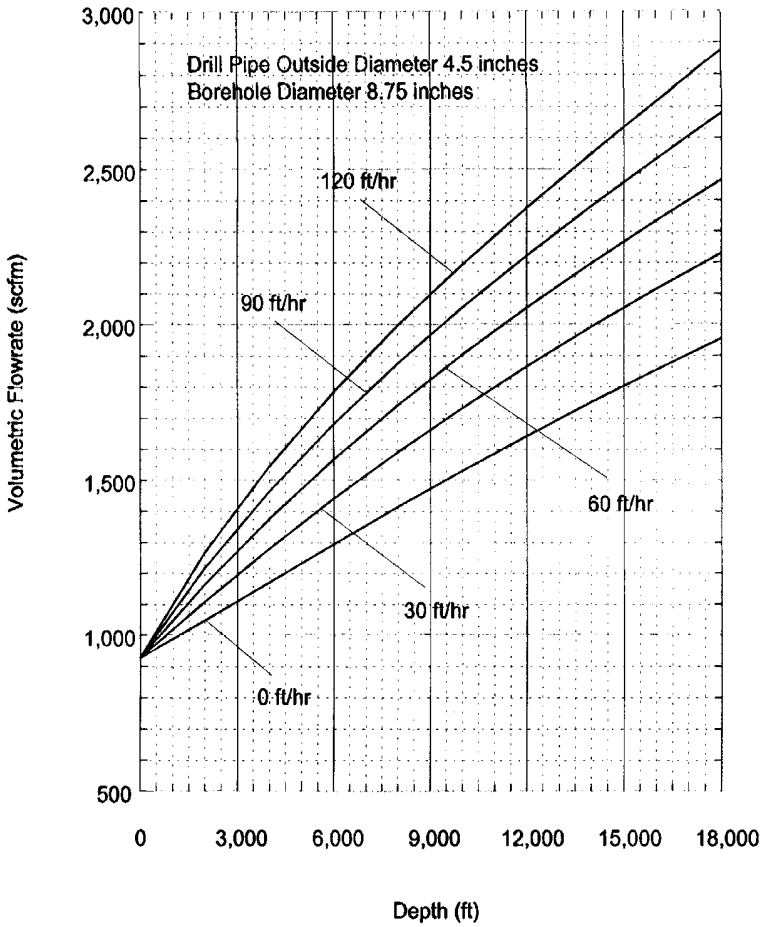
Figure E-14: Minimum volumetric flow rate of air at API standard conditions for 4 1/2 inch drill pipe and 8 3/4 inch borehole.
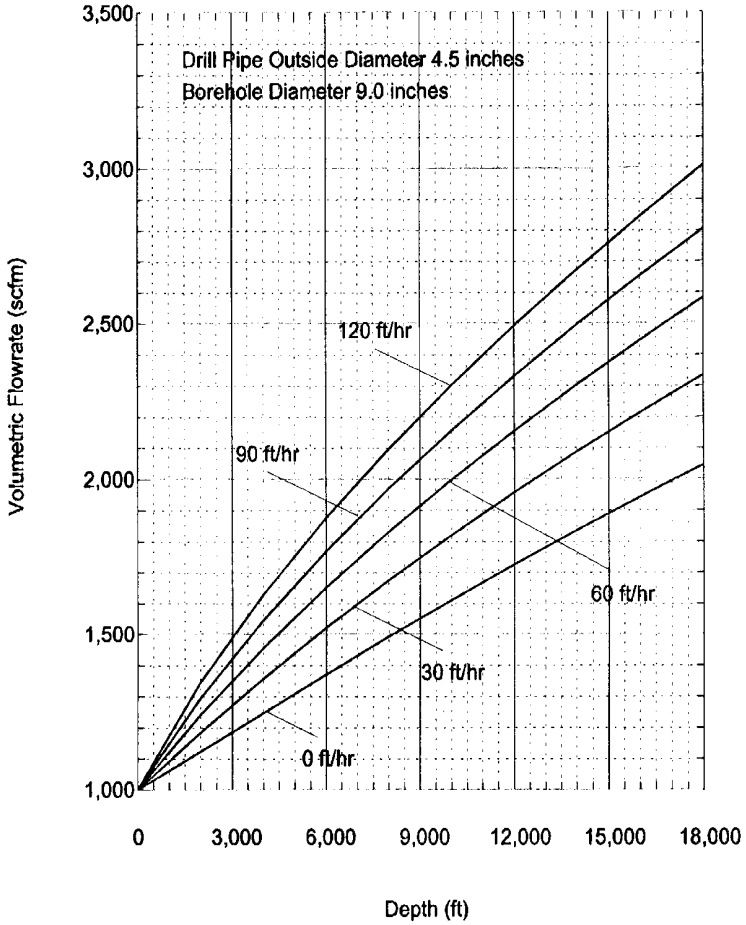
Figure E-15: Minimum volumetric flow rate of air at API standard conditions for 4 1/2 inch drill pipe and 9 inch borehole.
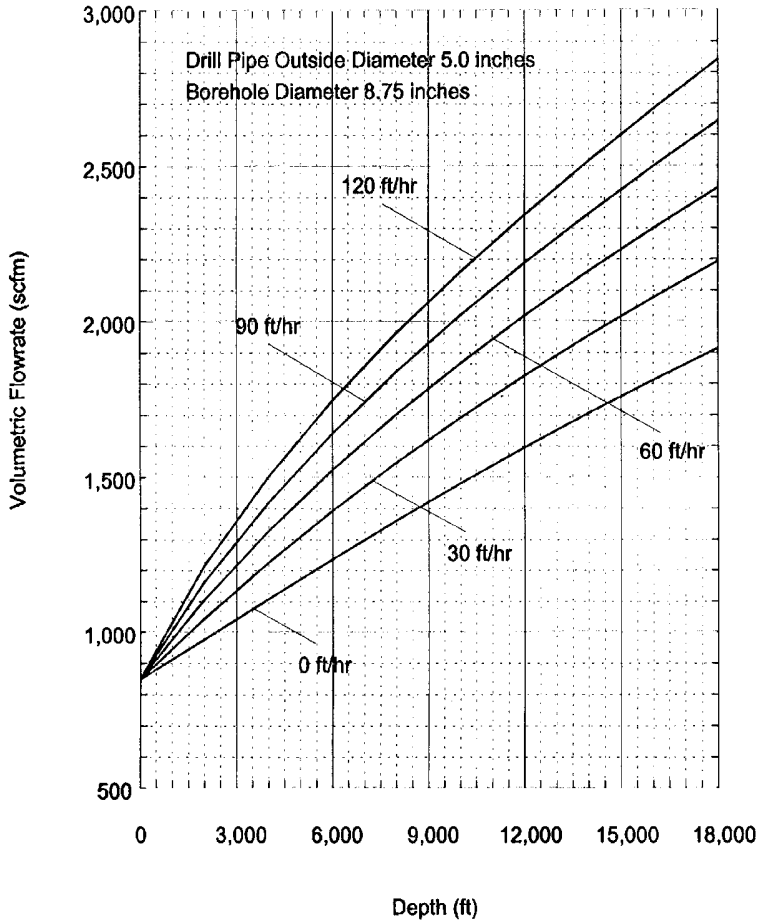
Figure E-16: Minimum volumetric flow rate of air at API standard conditions for 5 inch drill pipe and 8 3/4 inch borehole.
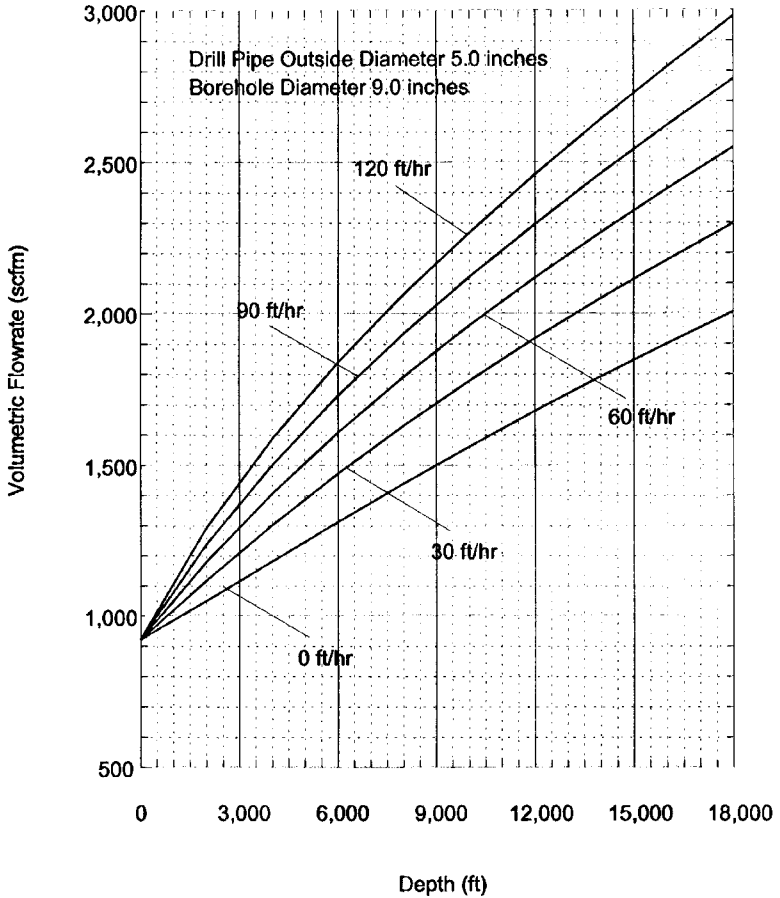
Figure E-17: Minimum volumetric flow rate of air at API standard conditions for 5 inch drill pipe and 9 inch borehole.
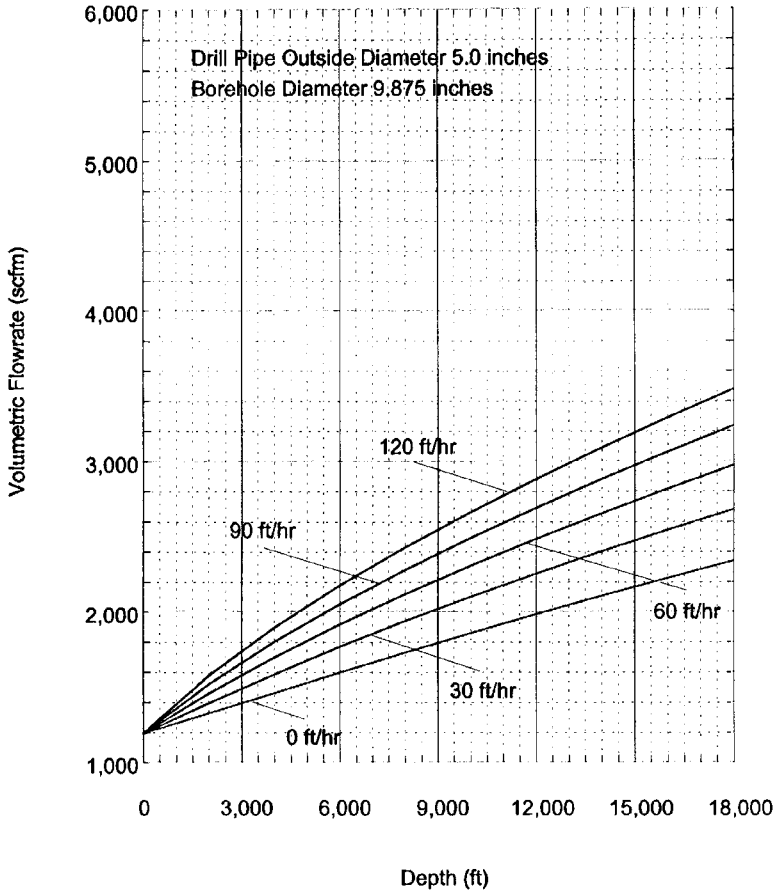
Figure E-18: Minimum volumetric flow rate of air at API standard conditions for 5 inch drill pipe and 9 7/8 inch borehole.
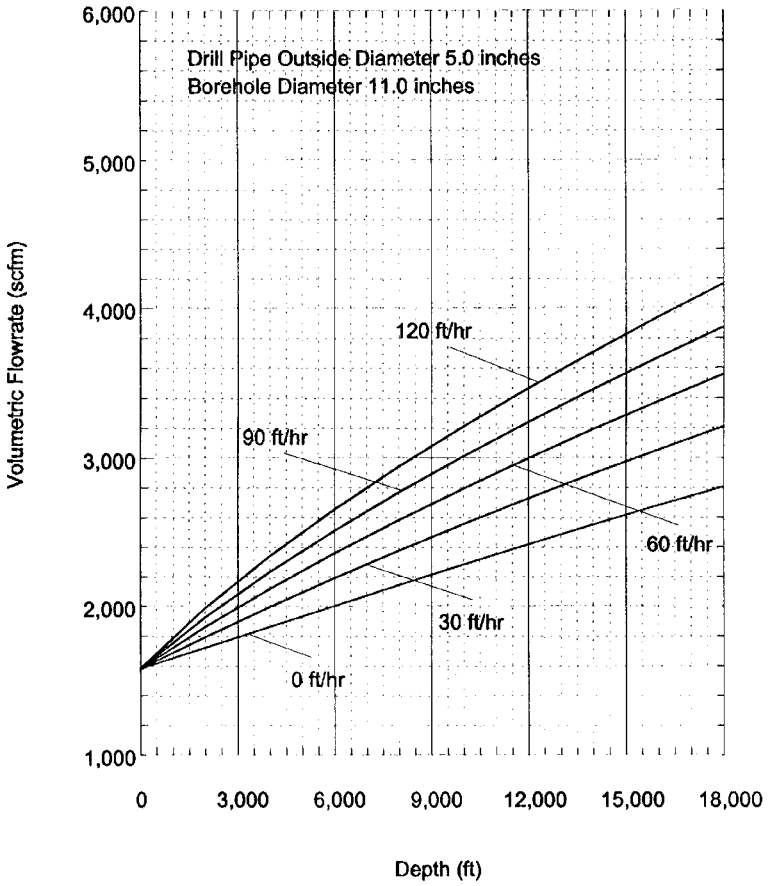
Figure E-19: Minimum volumetric flow rate of air at API standard conditions for 5 inch drill pipe and 11 inch borehole.
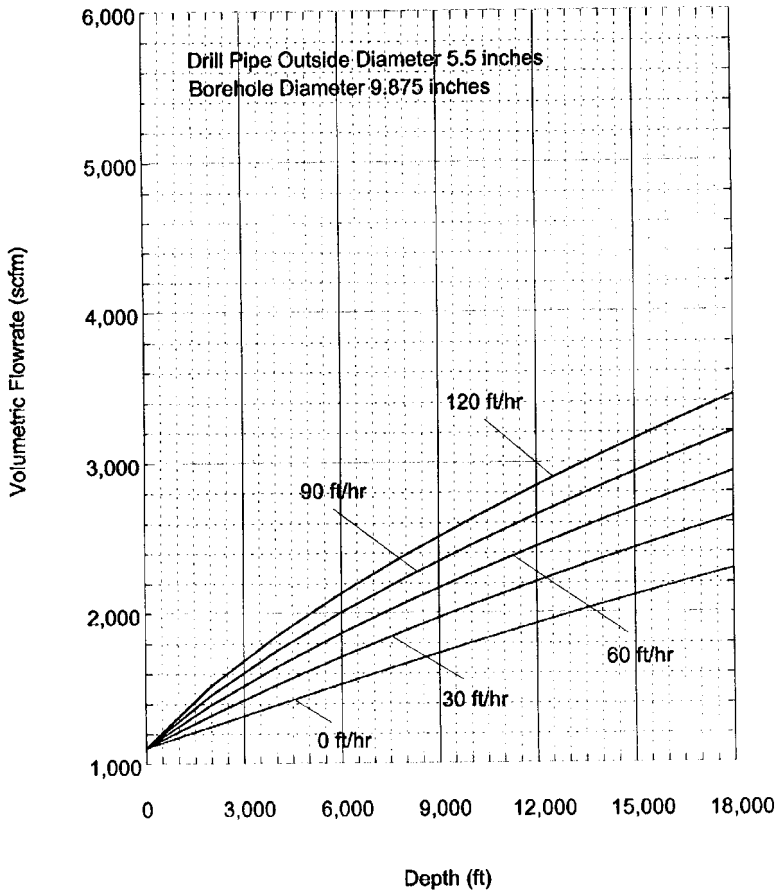
Figure E-20: Minimum volumetric flow rate of air at API standard conditions for 5 1/2 inch drill pipe and 9 7/8 inch borehole.
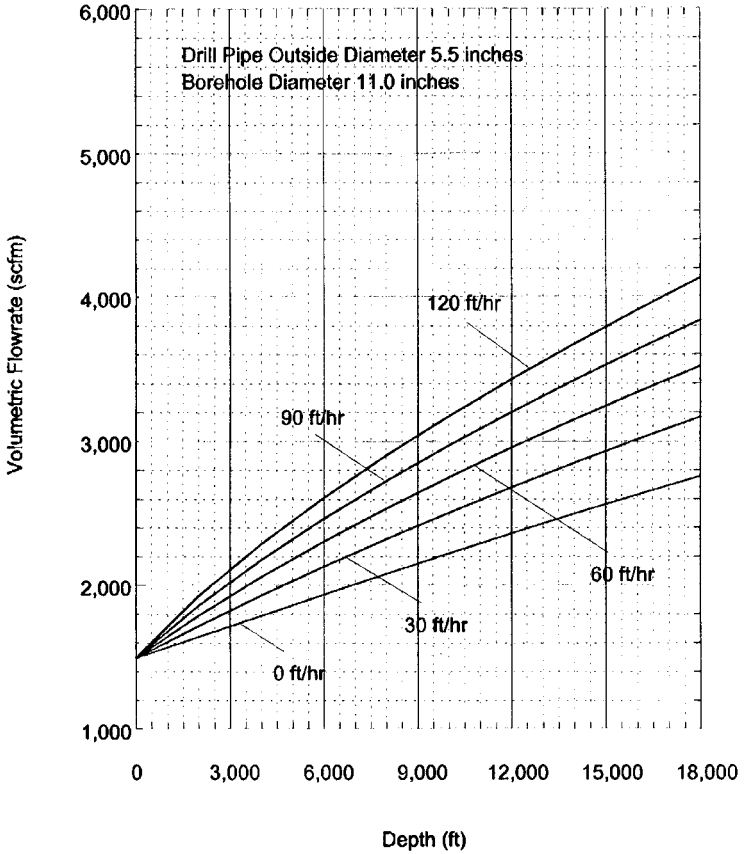
Figure E-21: Minimum volumetric flow rate of air at API standard conditions for 5 1/2 inch drill pipe and 11 inch borehole.
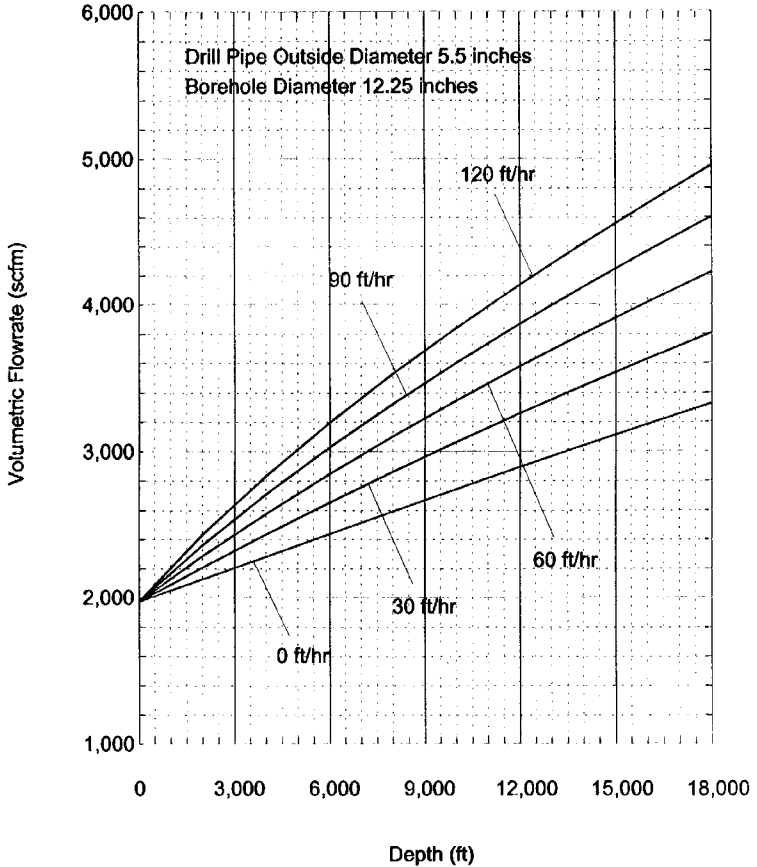
Figure E-22: Minimum volumetric flow rate of air at API standard conditions for 5 1/2 inch drill pipe and 12 1/4 inch borehole.
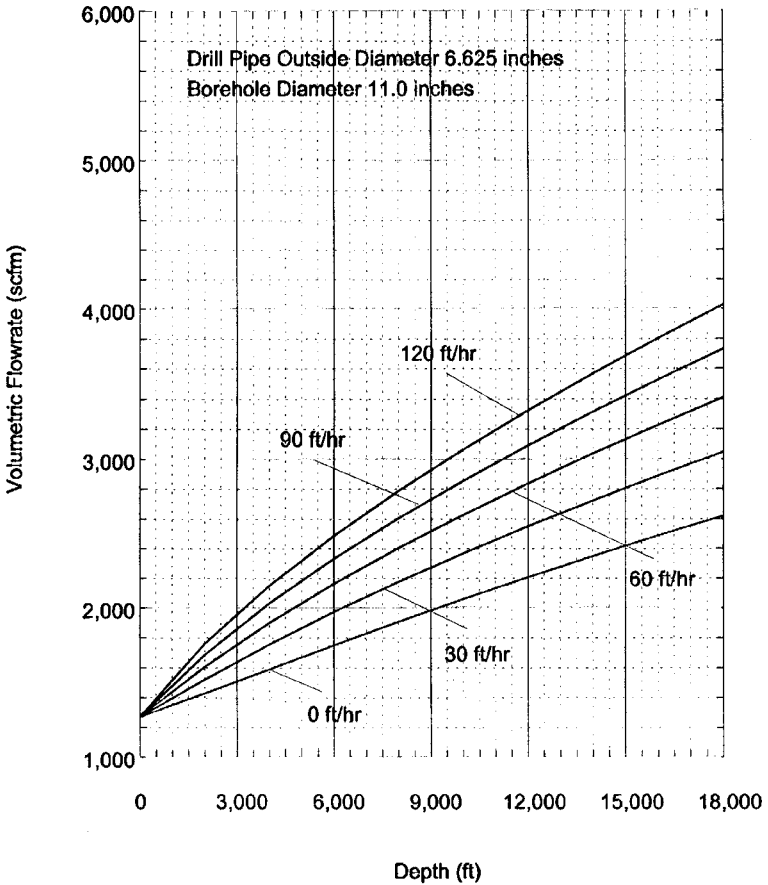
Figure E-23: Minimum volumetric flow rate of air at API standard conditions for 6 5/8 inch drill pipe and 11 inch borehole.
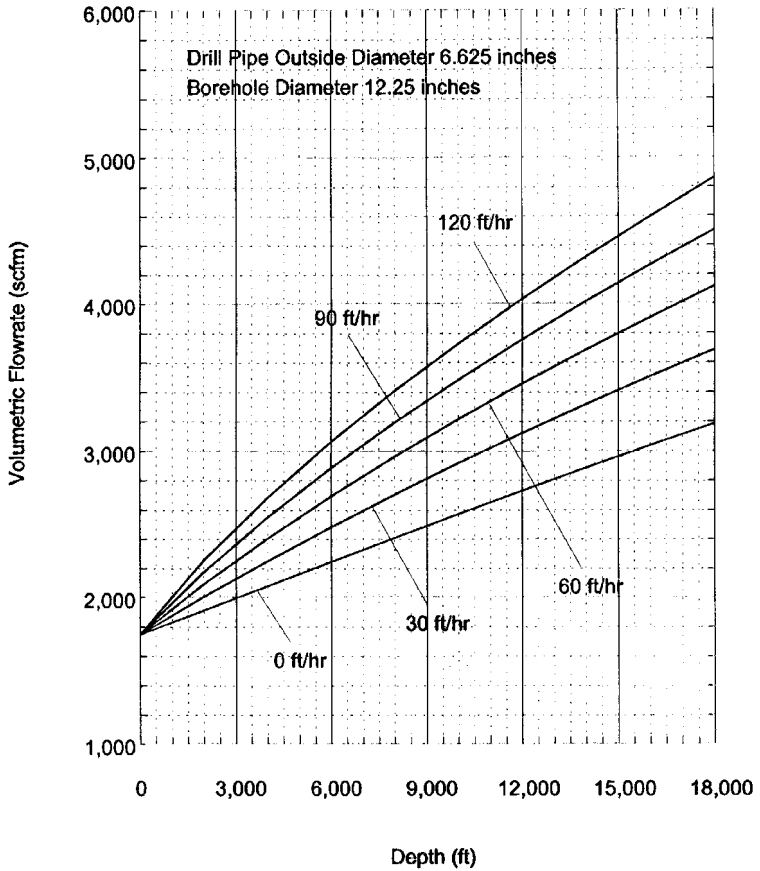
Figure E-24: Minimum volumetric flow rate of air at API standard conditions for 6 5/8 inch drill pipe and 12 1/4 inch borehole.
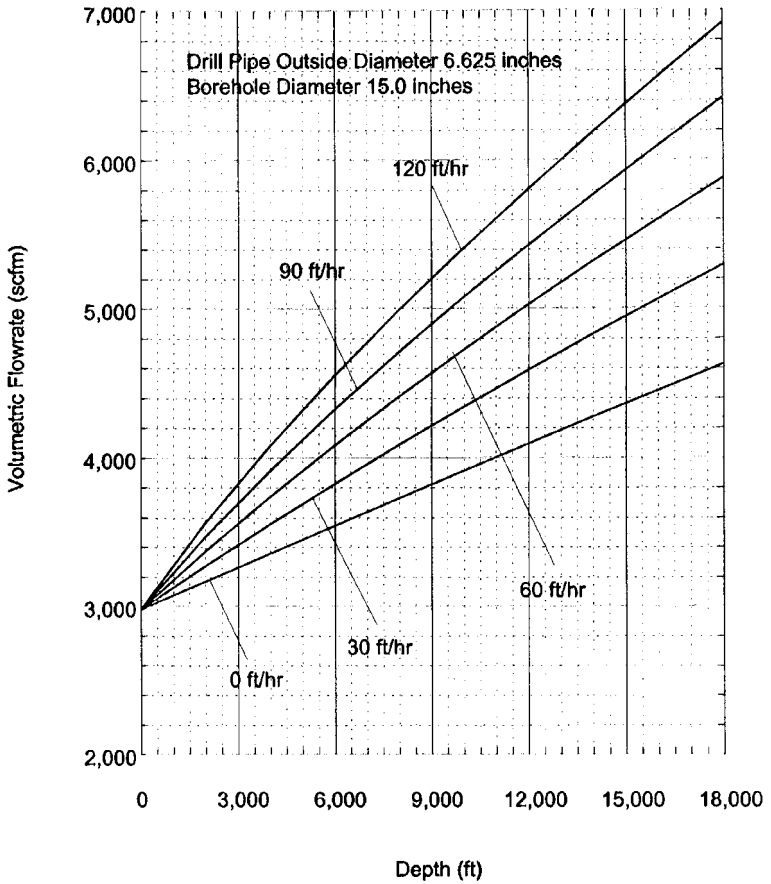
Figure E-25: Minimum volumetric flow rate of air at API standard conditions for 6 5/8 inch drill pipe and 15 inch borehole.
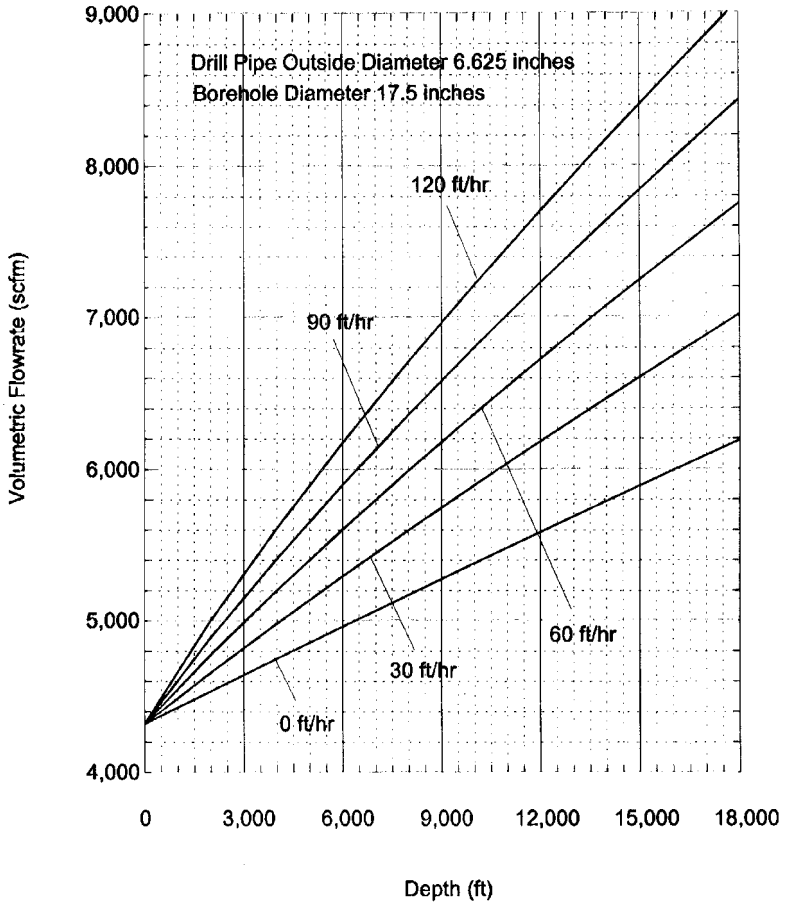
Figure E-26: Minimum volumetric flow rate of air at API standard conditions for 6 5/8 inch drill pipe and 17 1/2 inch borehole.

This page intentionally left blank.

Index

Absolute roughness, 6-10, 6-28, 7-10,
    7-15, 8-12
Absolute roughness for commercial pipe,
    6-28, 7-15
Absolute surface roughness, 9-29, 10-47
Absolute viscosity, 10-24
Actual shaft power, 4-26, 4-30, 8-50,
    8-56, 8-57, 9-71, 10-79
Actual cubic feet per minute (acfm), 4-5,
Aerated flow, 10-55
Aerated fluid drilling model, 6-21, 7-20
Aerated fluid procedure, 8-73
Air, 6-1, 7-1
Air and gas drilling model, 6-16, 7-15
Air hammer bits, 3-6, 3-12
Air injection volumetric flow rate, 10-77
Air stripped of oxygen, 6-1, 7-1
Air volumetric flow rate, 2-6, 9-69
AISI grade classifications of steel, 3-23
American Iron and Steel Institute (AISI),
    3-19
Annulus, 1-7
Annulus injection, 9-5
API drill pipe steel grades, 3-23
API Mechanical Equipment Standards
    standard atmospheric conditions, 4-4
API threaded shoulder connections, 3-3
Ariel Model JG-4, 4-42
Ariel Model JGJ/2, 4-39, 8-53
ASME standard atmospheric conditions,
    4-4, 8-53
Atmosphere at elevation, 4-5
Atmospheric pressure, 8-8
Atmospheric temperature, 8-9

Average absolute surface roughness,
    5-7, 8-14, 8-33, 8-35, 10-43
Average kinematic viscosity, 9-28, 9-36
Axial flow compressors, 4-6

Back pressure, 10-11, 10-20, 10-24,
    10-78
Bleed-down, 10-5
Bleed-off line, 2-4
Blind shear ram, 2-13
Blind tee, 8-24
Blooey line, 2-17, 8-24
Blowout prevention equipment, 2-13
Blowout preventor stack (BOP), 2-8,
    2-13, 11-9
Booster compressor, 4-23, 8-55
Bottomhole assembly (BHA), 3-17,
    3-18, 3-22
Bottomhole foam quality, 6-26,
    10-16, 10-53
Bottomhole pressure conditions, 10-17
Bottomhole temperature conditions,
    10-17
Bowen Tools Model S-1, 11-7
Bubble structure, 10-2
Bubbles, 9-1
Burlington Resources Incorporated,
    12-12
Burn pit, 2-17
Butane, 4-23, 4-33

This page intentionally left blank.

BE THE ONE WITH THE KNOW-HOW IN DRILLING'S HOTTEST TREND

Develop expertise in the technology that's the fastest-growing in the drilling industry. By 2005, 30% of all wells will be drilled using gas and air, according to a U.S. Department of Energy estimate. This comprehensive guide, written by an internationally known expert and holder of nine drilling patents, lays out absolutely everything you need to design and apply air and gas drilling to all kinds of operations, from the most basic to the most complex, and for the shallowest to the deepest.

The AIR AND GAS DRILLING MANUAL shows you how to:

■ Master the air and gas drilling techniques in vital industries: construction and development of water wells, monitoring wells, geotechnical boreholes, mining operations boreholes, and more

■ Calculate volumetric flow and compressor requirements

■ Drill with stable foam, unstable foam, and aerated liquids (as well as gas and air)

■ Handle the special considerations of deep hole drilling

■ Perform direct and reverse-flow circulation calculations

■ Specify drills, collars, and casings

■ Engineer and operate specialized downhole projects

■ Plan operations and choose air package contractors

■ Typical air packages utilized

Whether you're a geologist, environmentalist, or a petroleum, mining, drilling, groundwater, or other engineer, this definitive, applications-based resource is poised to increase your expertise in this critical new area of drilling technology.

CONSTRUCTION

WATER WELLS

ENVIRONMENTAL MONITORING AND REMEDIATION

GEOTECH BOREHOLES

HORIZONTAL

MINING

NATURAL GAS

PETROLEUM

VERTICAL

WATER WELLS

McGraw-Hill
A Division of The McGraw-Hill Companies

www.books.mcgraw-hill.com

Cover Design: Mary McDonnell